frontiers | Research Topics

Abdominal aortic aneurysms: Advancements in diagnosis, biomarkers, drug therapeutics, surgical and endovascular treatment

Edited by
Zhenjie Liu, Weiguo Fu, Wei Wang, Morgan Salmon and Ho Pei

Published in
Frontiers in Cardiovascular Medicine

FRONTIERS EBOOK COPYRIGHT STATEMENT

The copyright in the text of individual articles in this ebook is the property of their respective authors or their respective institutions or funders. The copyright in graphics and images within each article may be subject to copyright of other parties. In both cases this is subject to a license granted to Frontiers.

The compilation of articles constituting this ebook is the property of Frontiers.

Each article within this ebook, and the ebook itself, are published under the most recent version of the Creative Commons CC-BY licence. The version current at the date of publication of this ebook is CC-BY 4.0. If the CC-BY licence is updated, the licence granted by Frontiers is automatically updated to the new version.

When exercising any right under the CC-BY licence, Frontiers must be attributed as the original publisher of the article or ebook, as applicable.

Authors have the responsibility of ensuring that any graphics or other materials which are the property of others may be included in the CC-BY licence, but this should be checked before relying on the CC-BY licence to reproduce those materials. Any copyright notices relating to those materials must be complied with.

Copyright and source acknowledgement notices may not be removed and must be displayed in any copy, derivative work or partial copy which includes the elements in question.

All copyright, and all rights therein, are protected by national and international copyright laws. The above represents a summary only. For further information please read Frontiers' Conditions for Website Use and Copyright Statement, and the applicable CC-BY licence.

ISSN 1664-8714
ISBN 978-2-8325-2386-5
DOI 10.3389/978-2-8325-2386-5

About Frontiers

Frontiers is more than just an open access publisher of scholarly articles: it is a pioneering approach to the world of academia, radically improving the way scholarly research is managed. The grand vision of Frontiers is a world where all people have an equal opportunity to seek, share and generate knowledge. Frontiers provides immediate and permanent online open access to all its publications, but this alone is not enough to realize our grand goals.

Frontiers journal series

The Frontiers journal series is a multi-tier and interdisciplinary set of open-access, online journals, promising a paradigm shift from the current review, selection and dissemination processes in academic publishing. All Frontiers journals are driven by researchers for researchers; therefore, they constitute a service to the scholarly community. At the same time, the *Frontiers journal series* operates on a revolutionary invention, the tiered publishing system, initially addressing specific communities of scholars, and gradually climbing up to broader public understanding, thus serving the interests of the lay society, too.

Dedication to quality

Each Frontiers article is a landmark of the highest quality, thanks to genuinely collaborative interactions between authors and review editors, who include some of the world's best academicians. Research must be certified by peers before entering a stream of knowledge that may eventually reach the public - and shape society; therefore, Frontiers only applies the most rigorous and unbiased reviews. Frontiers revolutionizes research publishing by freely delivering the most outstanding research, evaluated with no bias from both the academic and social point of view. By applying the most advanced information technologies, Frontiers is catapulting scholarly publishing into a new generation.

What are Frontiers Research Topics?

Frontiers Research Topics are very popular trademarks of the *Frontiers journals series*: they are collections of at least ten articles, all centered on a particular subject. With their unique mix of varied contributions from Original Research to Review Articles, Frontiers Research Topics unify the most influential researchers, the latest key findings and historical advances in a hot research area.

Find out more on how to host your own Frontiers Research Topic or contribute to one as an author by contacting the Frontiers editorial office: frontiersin.org/about/contact

Abdominal aortic aneurysms: Advancements in diagnosis, biomarkers, drug therapeutics, surgical and endovascular treatment

Topic editors

Zhenjie Liu — The Second Affiliated Hospital of Zhejiang University School of Medicine, China

Weiguo Fu — Fudan University, China

Wei Wang — Central South University, China

Morgan Salmon — University of Michigan, United States

Ho Pei — National University of Singapore, Singapore

Topic coordinator

Bowen Wang — University of Virginia, United States

Citation

Liu, Z., Fu, W., Wang, W., Salmon, M., Pei, H., eds. (2023). *Abdominal aortic aneurysms: Advancements in diagnosis, biomarkers, drug therapeutics, surgical and endovascular treatment*. Lausanne: Frontiers Media SA.

doi: 10.3389/978-2-8325-2386-5

Table of contents

frontiers | Frontiers in Cardiovascular Medicine

TYPE Editorial
PUBLISHED 02 June 2023
DOI 10.3389/fcvm.2023.1218335

Check for updates

OPEN ACCESS

EDITED AND REVIEWED BY
Pietro Enea Lazzerini,
University of Siena, Italy

*CORRESPONDENCE:
Zhenjie Liu
lawson4001@zju.edu.cn

RECEIVED 07 May 2023
ACCEPTED 15 May 2023
PUBLISHED 02 June 2023

CITATION
Liu Z (2023) Editorial: Abdominal aortic aneurysms: advancements in diagnosis, biomarkers, drug therapeutics, surgical and endovascular treatment.
Front. Cardiovasc. Med. 10:1218335.
doi: 10.3389/fcvm.2023.1218335

COPYRIGHT
© 2023 Liu. This is an open-access article distributed under the terms of the Creative Commons Attribution License (CC BY). The use, distribution or reproduction in other forums is permitted, provided the original author(s) and the copyright owner(s) are credited and that the original publication in this journal is cited, in accordance with accepted academic practice. No use, distribution or reproduction is permitted which does not comply with these terms.

Editorial: Abdominal aortic aneurysms: advancements in diagnosis, biomarkers, drug therapeutics, surgical and endovascular treatment

Zhenjie Liu

Department of Vascular Surgery, The Second Hospital of Zhejiang University School of Medicine, Hangzhou, China

KEYWORDS

abdominal aortic aneurysm, diagnose, biomarker, drug therapeutic, surgical and endovascular treatment

Editorial on the Research Topic
Abdominal aortic aneurysms: advancements in diagnosis, biomarkers, drug therapeutics, surgical and endovascular treatment

An abdominal aortic aneurysm (AAA) is a dilated aorta with the diameter 1.5 times the normal one, involving all three anatomical layers. AAAs mostly remain asymptomatic until the aneurysm ruptures, which can be unpredictable and fatal, with a mortality rate of over 50% (1). Current guidelines recommend watchful waiting and lifestyle adjustment for smaller, slow-growing aneurysms, while elective/prophylactic surgical repairs are recommended for larger aneurysms that have grown beyond certain thresholds (55 mm for males and 50 mm for females) (2, 3).

Considerable advancements have been made in the management of AAA, specifically in endovascular treatment, through the development of novel stent grafts and synthetic grafts that cater to intricate and challenging aortic anatomies. Unfortunately, there are no effective medical therapies for AAA, especially for newly diagnosed patients who do not have surgical indications (4). Despite the fact that many drugs, such as Doxycycline and Rapamycin, demonstrated efficacy in animal models, the outcomes of clinical trials are disappointing (5–7). For asymptomatic AAAs, aortic ruptures are life-threatening. Early detection for impending rupture of AAA is still inaccessible.

An increasing number of researchers are dedicating their efforts to studying AAA, resulting in significant progress in the field. In this research topic, an international selection of researchers contributed original research, case reports, and up-to-date reviews to enhance our current understanding of AAA. These studies have focused on various aspects of this disease, including improved methods of diagnosis, predictable biomarkers, drug therapeutics, and surgical and endovascular treatments.

1. Basic research works

Several contributions in this research topic focused on identifying biomarkers and potential treatment options. Lowis et al. reviewed the mechanosignals involved in AAA

development, including divergent mechanosignal, endothelial, and smooth muscle cell mechanosensors, mechanical stress, inflammation, and redox stress circuits. They also briefly reviewed intraluminal thrombus and mechanosensing in AAA, highlighting the manipulation of mechano-machinery as a potential avenue for future research in AAA. Another review article discussed the roles of extracellular vesicles (EV) in the pathological process of AAA and their potential clinical applications. Lu et al. reviewed the EV-based biomarkers for AAA diagnosis and the therapeutic potential of stem cell-derived EVs. With advancements in EV display technology and membrane hybrid technology, researchers have been able to equip EVs with desirable functions, making these vesicles a promising tool for the treatment of AAA.

While some researchers reviewed biomarkers in AAA, others have focused on gene expression changes as a potential avenue for understanding the development and progression of AAA. Chen et al. conducted a study that focused on immune infiltration patterns in AAA by constructing a competing endogenous RNA network. They obtained expression profiles of circRNAs and mRNAs from Gene Expression Omnibus (GEO) to build a ceRNA network and validated key genes expressions and immune cell infiltration using clinical specimens. Their study identified significant roles of PPARG, FOXO1, RAB5C, and HSPA8, as well as the involvement of M1 macrophages and resting CD4 memory T cells. Another work by Chen et al. identified the biomarkers and analyzed infiltrated immune cells in stable and ruptured abdominal aortic aneurysms. Unlike the result in AAA vs. healthy aorta, this study showed that NFKB1 might be an important transcription factor mediating the inflammatory response of AAA and aortic rupture, and CD19, SELL, and CCR7 were selected as hub genes for AAA, whereas OAS3, IFIT1, and IFI44l were identified as hub genes for aortic rupture in a predictive model constructed. However, experimental evidence is still necessary since the result varies from databases and different statistical methods.

Animal models play a crucial role in investigating the pathophysiology of AAA and developing new therapeutic and diagnostic approaches. So far, the three most widely adopted AAA-inducing methods are angiotensin II (AngII) infusion (8), porcine pancreatic elastase intraluminal perfusion (9), and calcium salt topical application (10), featuring varying incidence rates, anatomical locations, lesion sizes, and disease courses. With the emerging interest and research efforts dedicated to the propagation phase of AAA, it is of significant mechanistic and translational value to identify the appropriate experimental models that recapitulate the progressive AAA progression into rupture (11). Yin et al. reviewed the progress in murine models of RAAA. The ideal RAAA model should provide consistent aneurysm formation in the appropriate anatomical location (i.e., infrarenal aortic segment) and consistent AAA rupture over a chronic course. Although few of the existing models could faithfully recapitulate the clinical features of RAAA, some models, such as β-aminopropionitrile combined with topical application of elastase, and AngII combined with elastase intraluminal perfusion model, have the potential to be modified to an RAAA model.

In addition to reviews, original research studies are published on this research topic. Griepke et al. demonstrated the effectiveness of selectively inhibiting soluble tumor necrosis factor signaling in reducing abdominal aortic aneurysm progression in a rat AAA model. Chinese researchers shared their study which specially focused on traditional Chinese medicine therapy in cardiovascular diseases. Hong et al. found that Xin'an famous prescription Ershen Zhenwu Decoction (ESZWD) significantly reduced left ventricular end-diastolic diameter, decreased N-terminal pro-brain natriuretic peptide (NT-proBNP), angiotensinII, aldosterone, reactive oxygen species, and malondialdehyde, and increased serum superoxide dismutase, without significantly affecting inflammatory factors. They investigated thirty components of ESZWD and identified salsolinol, aconitine, paeoniflorin, and miltrione as the potential pharmacodynamic substances for ESZWD in treating CHF-HKYd. This work suggests a potential application of traditional Chinese medicine therapy in other cardiovascular diseases, including AAA.

2. Laboratory and CTA assisted diagnose

In addition to their foundational research endeavors, colloquially known as bench work, several clinical scientists presented their research projects based on clinical-oriented understandings.

Cai et al. compared the laboratory test results of 320 patients with peripheral artery diseases and 320 patients with abdominal aortic aneurysms. They found that levels of bilirubin and D-dimer increased in AAA-only patients compared to PAD-only patients ($P < 0.001$). Further analysis confirmed a differential distribution of bilirubin, D-dimer, fibrinogen, and platelet count between AAA patients and PAD patients ($P < 0.05$), and suggested a cutoff value of 0.675 mg/L for D-dimer, which could be used to predict AAA in PAD patients.

Computed tomography (CT) scan is an essential diagnostic tool in AAA patients. Liu et al. attempted to measure the maximum transverse diameter (MTD) of and CT values of ILT by using multi-spiral computed tomography angiography (MSCTA) to investigate the predictive value of MTD with different CT values of thrombus on the risk of AAA rupture. Their study 45 intact AAA and 17 ruptured AAA MSCTA results. The median of maximum CT value of thrombus at the plane of MTD was higher in RAAA (107.0 HU) than the median in IAAA (84.5 HU) ($P < 0.001$). The maximum CT value was also a significant risk factor for RAAA ($P < 0.001$). High-density ILT shown on MSCTA in AAAs was associated with aneurysm rupture, and its maximum transverse diameter combined with the maximum CT value in its plane is a better predictor of RAAA.

To diagnose AAA using CT, it's important to have appropriate reference values for a given population. Therefore, it is important to establish reference values specific to the population being

studied to ensure accurate and reliable diagnosis. A study by Wang et al. provided valuable information on the size of normal abdominal aortas in different segments among Chinese adults (>18 years) without abdominal aortic disease, using enhanced CT. The study measured the inner-to-inner areas of the subphrenic, suprarenal, infrarenal, and distal segments of the abdominal aorta in 1,066 patients. The median areas of the subphrenic abdominal aorta, suprarenal abdominal aorta, infrarenal abdominal aorta, and distal abdominal aorta were 412.1 mm^2, 308.0 mm^2, 242.2 mm^2 and 202.2 mm^2 in Chinese male population, and the median areas of the subphrenic abdominal aorta, suprarenal abdominal aorta, infrarenal abdominal aorta, and distal abdominal aorta were 327.7 mm^2, 243.4 mm^2, 185.4 mm^2 and 159.6 mm^2 in female Chinese population. These reference values can be useful in the diagnosis and management of abdominal aortic diseases in the Chinese population.

3. Research focused on non-surgical management of AAA

The management of AAA poses a challenge when dealing with smaller aneurysms without surgical indications as there is no established way to slow down the progression of the aneurysm's dilation (4). The management of AAA poses a challenge when dealing with smaller aneurysms that do not require surgery, as there is currently no established approach to impede the progression of their dilation. Consequently, numerous researchers are committed to discovering effective techniques and medications to enhance the current watchful observation strategy for small aneurysms.

A comprehensive understanding of the natural history of AAA is crucial for developing effective ways to slow down the dilation of the aorta. To this end, Wu et al. conducted a prospective cohort study on the natural history of isolated abdominal aortic dissection, which shared some similar pathophysiological changes with AAA. The study included 68 patients who were followed up for up to 5.5 years. The findings suggested a more aggressive treatment regimen for IAAD, with EVAR being the first choice, especially for those with persistent symptoms and patent false lumen, regardless of sex, age, or aortic size. This study may indicate a more aggressive treatment strategy for AAA with dissection.

In recent years, there has been a growing interest in lifestyle changes as a means of managing small abdominal aortic aneurysms (AAA), in light of the "watchful and wait" strategy. Although smoking cessation and physical exercise both have shown promising benefits in reducing AAA risks, few studies concerned the role of healthy dietary patterns, at both clinical and preclinical levels (12–14). With an increasing benefits of various dietary regimens against cardiovascular diseases recently, understanding the therapeutic and mechanistic implications of certain dietary patterns would hold significant value in informing the future guideline of AAA management (15). Herein, Yin et al. summarized the recent progress in dietary therapies for AAA based on epidemiological and experimental evidence. Additionally, they discussed perspectives of emerging dietary regimens and potential molecular basis. Further investigations are still pending in selected emerging dietary regimens as well as diet-mediated mechanisms. And it can be envisioned that future research efforts will be increasingly dedicated to a better understanding of as well as translational development of the first non-surgical management of AAA in the form of dietary therapies.

Despite growing interest in lifestyle interventions for AAA management, pharmacological approaches remain more commonly explored. Niu et al. conducted a meta-analysis reviewing the association between metformin and abdominal aortic aneurysm, which include 10 cohort studies and 85,050 patients. The findings suggest metformin may limit the expansion of AAA and reduce the incidence of AAA and postoperative mortality. However, given the limited number of trials included, further biological experiments and clinical trials are still necessary to validate these results and establish metformin's role in AAA management.

Besides the potential benefits of drug therapies, the effects of different drugs on AAA treatment and adverse outcomes remain a critical area of research. A review by Chen et al. focused on the role of fluoroquinolones (FQs) in aortic aneurysms and dissections incidence and mortality. They summarized relevant clinical trials and found that FQs were associated with an increased incidence of AAD in the general population and a higher risk of adverse outcomes in patients with pre-existing AAD. Although the authors noted that the results may be affected by unmeasured confounding factors, it should be considered by physicians contemplating using FQs in patients with aortic dilation and those at high risk of AAD.

4. Surgical and endovascular treatment

Endovascular aneurysm repair (EVAR) has been established as a viable alternative to open repair surgery for treating AAA (2, 3). However, secondary aneurysm ruptured caused by endoleaks and a high rate of secondary intervention limite EVAR's survival benefit (16, 17). Type II endoleak (T2EL) is the most common type of endoleaks (18, 19). To address this issue, several strategies for pre-emptive embolization have been developed, including embolization of aneurysm sac side branches (ASSB) and aneurysm sac coil embolization (ASCE) (20–22). Wu et al. conducted a network meta-analysis to compare the effectiveness of different preventive interventions for T2EL in the suppression of aneurysm sac expansion and reducing the need for re-intervention with 31 studies involving 18,542 patients. The study found that all prophylactic embolization strategies improved the clinical outcomes of EVAR, with pre-emptive embolization of the inferior mesenteric artery (IMA-ASSB) showing the best clinical effect in suppressing aneurysm sac expansion and reducing the need for re-intervention, while non-selective embolization of ASSB (NS-ASSB) was found to be more effective in reducing the incidence of T2EL. IMA-ASSB alone or in combination with ASCE demonstrated benefits in clinical outcomes of EVAR. However, it should be noted that network

meta-analysis is still an indirect method based on existing data, and more studies are needed to establish more credible conclusions.

In addition to endoleaks, other patient-related factors can impact the outcomes of EVAR. Wang et al. developed and compared multi-modal models based on morphological, deep learning (DL) and radiomics features to predict outcomes after EVAR. The result showed that the radiomic model based on logistics regression had a better predictive performance for patient status after EVAR than the optimized morphological feature model and the DL model. The morphological feature model and DL model have their own advantages and could also be used to predict outcomes after EVAR. These findings provide valuable insights into EVAR treatment and post-operation follow-up.

RAAAs, known as the life-threatening complication of AAA, have up to an 85% mortality rate (23). Ruptured endovascular aneurysm repair (rEVAR) is now considered as an alternative to operative treatment for RAAAs (2, 3). Meanwhile, the discussion about the role of rEVAR has been sustained during the past two decades due to the discrepancy between randomized controlled trials (RCTs) and real-life studies (24–27). In the retrospective study conducted by Fang et al., the efficacy and safety of EVAR-selected and EVAR-only strategies in the management of RAAA were evaluated. Results showed no difference in third-day mortality and long-term outcomes between the EVAR-only strategy and the EVAR-selected strategy, while the EVAR-only strategy was associated with a more simplified algorithm, less influence on hemodynamics, and a shorter operation and recovery time, indicating a non-inferior feasibility of EVAR-only strategy to EVAR-selected strategy.

The surgical strategy for infected abdominal aortic aneurysms poses another significant challenge. Li et al. reported their cases about *in situ* repair or reconstruction of the abdominal aorta-iliac artery using autologous fascia-peritoneum with posterior rectus sheath for the treatment of the infected abdominal aortic and iliac artery aneurysms. They repaired the aneurysms using autologous peritoneal fascial tissue, supplemented with grafts when necessary. After 2–19 months follow-up, five out of seven patients survived. While long-term follow-up and a larger sample size are necessary to establish the efficacy of this treatment, the *in situ* repair or reconstruction with autologous peritoneal fascial tissue with rectus sheath appears to be a promising and feasible option for infected aneurysm patients without adequate autologous venous substitutes.

In addition to studies focused directly on AAA, we also collect researches in other related areas that may also contribute to the management of AAA. Huang et al. designed a modular multifunctional left heart bypass (LHB) circuit integrated with ultrafiltration and reserved pipelines for cardiopulmonary bypass in thoracoabdominal aortic aneurysm repair. This circuit made the assembly of the LHB circuit more easily, and more efficient, which may contribute to the TAAA repair operation performed in lower volume centers easily. Another study by Luo et al. provided us with some concerns about in-hospital care for AAA patients. Their study highlighted the significance of elevated blood creatinine and urea nitrogen levels at ICU admission and their correlation with the risk of in-hospital death and 1-year mortality in patients with intracranial hemorrhage. This is especially relevant for elderly AAA patients who are at higher risk of intracranial hemorrhage. By monitoring these biomarkers and providing timely interventions, healthcare providers can potentially improve patient outcomes and reduce mortality rates. This study highlights the importance of comprehensive and personalized care for AAA patients, which takes into account individual risk factors and biomarkers.

In conclusion, the diverse and high-quality contributions of this Research Topic enriched our understanding of diagnosis, biomarkers, drug therapeutics, surgical and endovascular treatment in AAA. Moreover, these studies have opened up potential avenues for further research in this field, while also providing novel insights that may lead to improved management and outcomes for patients with AAA.

Author contributions

ZL contributed to all parts of the manuscript.

Conflict of interest

The author declares that the research was conducted in the absence of any commercial or financial relationships that could be construed as a potential conflict of interest.

Publisher's note

All claims expressed in this article are solely those of the authors and do not necessarily represent those of their affiliated organizations, or those of the publisher, the editors and the reviewers. Any product that may be evaluated in this article, or claim that may be made by its manufacturer, is not guaranteed or endorsed by the publisher.

References

1. Karthikesalingam A, Holt PJ, Vidal-Diez A, Ozdemir BA, Poloniecki JD, Hinchliffe RJ, et al. Mortality from ruptured abdominal aortic aneurysms: clinical lessons from a comparison of outcomes in England and the USA. *Lancet*. (2014) 383(9921):963–9. doi: 10.1016/S0140-6736(14)60109-4

2. Chaikof EL, Dalman RL, Eskandari MK, Jackson BM, Lee WA, Mansour MA, et al. The society for vascular surgery practice guidelines on the care of patients with an abdominal aortic aneurysm. *J Vasc Surg*. (2018) 67(1):2–77. e2. doi: 10.1016/j.jvs.2017.10.044

3. Wanhainen A, Verzini F, Van Herzeele I, Allaire E, Bown M, Cohnert T, et al. Editor's choice—european society for vascular surgery (ESVS) 2019 clinical practice guidelines on the management of abdominal aorto-iliac artery aneurysms. *Eur J Vasc Endovasc Surg*. (2019) 57(1):8–93. doi: 10.1016/j.ejvs.2018.09.020

4. Lindeman JH, Matsumura JS. Pharmacologic management of aneurysms. *Circ Res*. (2019) 124(4):631–46. doi: 10.1161/CIRCRESAHA.118.312439

5. Meijer CA, Stijnen T, Wasser MN, Hamming JF, van Bockel JH, Lindeman JH, et al. Doxycycline for stabilization of abdominal aortic aneurysms: a randomized trial. *Ann Intern Med*. (2013) 159(12):815–23. doi: 10.7326/0003-4819-159-12-201312170-00007

6. Baxter BT, Matsumura J, Curci JA, McBride R, Larson L, Blackwelder W, et al. Effect of doxycycline on aneurysm growth among patients with small infrarenal abdominal aortic aneurysms: a randomized clinical trial. *JAMA*. (2020) 323 (20):2029–38. doi: 10.1001/jama.2020.5230

7. Rouer M, Xu BH, Xuan HJ, Tanaka H, Fujimura N, Glover KJ, et al. Rapamycin limits the growth of established experimental abdominal aortic aneurysms. *Eur J Vasc Endovasc Surg*. (2014) 47(5):493–500. doi: 10.1016/j.ejvs.2014.02.006

8. Daugherty A, Manning MW, Cassis LA. Angiotensin II promotes atherosclerotic lesions and aneurysms in apolipoprotein E-deficient mice. *J Clin Invest*. (2000) 105 (11):1605–12. doi: 10.1172/JCI7818

9. Pyo R, Lee JK, Shipley JM, Curci JA, Mao D, Ziporin SJ, et al. Targeted gene disruption of matrix metalloproteinase-9 (gelatinase B) suppresses development of experimental abdominal aortic aneurysms. *J Clin Invest*. (2000) 105(11):1641–9. doi: 10.1172/JCI8931

10. Longo GM, Xiong W, Greiner TC, Zhao Y, Fiotti N, Baxter BT. Matrix metalloproteinases 2 and 9 work in concert to produce aortic aneurysms. *J Clin Invest*. (2002) 110(5):625–32. doi: 10.1172/JCI0215334

11. Lu HS, Owens AP, 3rd, Liu B, Daugherty A. Illuminating the importance of studying interventions on the propagation phase of experimental mouse abdominal aortic aneurysms. *Arterioscler Thromb Vasc Biol*. (2021) 41(4):1518–20. doi: 10.1161/ATVBAHA.121.316070

12. Aune D, Schlesinger S, Norat T, Riboli E. Tobacco smoking and the risk of abdominal aortic aneurysm: a systematic review and meta-analysis of prospective studies. *Sci Rep*. (2018) 8(1):14786. doi: 10.1038/s41598-018-32100-2

13. Aune D, Sen A, Kobeissi E, Hamer M, Norat T, Riboli E. Physical activity and the risk of abdominal aortic aneurysm: a systematic review and meta-analysis of prospective studies. *Sci Rep*. (2020) 10(1):22287. doi: 10.1038/s41598-020-76306-9

14. Weston M, Batterham AM, Tew GA, Kothmann E, Kerr K, Nawaz S, et al. Patients awaiting surgical repair for large abdominal aortic aneurysms can exercise at moderate to hard intensities with a low risk of adverse events. *Front Physiol*. (2016) 7:684. doi: 10.3389/fphys.2016.00684

15. Brandhorst S, Longo VD. Dietary restrictions and nutrition in the prevention and treatment of cardiovascular disease. *Circ Res*. (2019) 124(6):952–65. doi: 10.1161/CIRCRESAHA.118.313352

16. Patel R, Sweeting MJ, Powell JT, Greenhalgh RM, investigators Et. Endovascular versus open repair of abdominal aortic aneurysm in 15-years' follow-up of the UK endovascular aneurysm repair trial 1 (EVAR trial 1): a randomised controlled trial. *Lancet*. (2016) 388(10058):2366–74. doi: 10.1016/S0140-6736(16)31135-7

17. De Bruin JL, Baas AF, Buth J, Prinssen M, Verhoeven EL, Cuypers PW, et al. Long-term outcome of open or endovascular repair of abdominal aortic aneurysm. *N Engl J Med*. (2010) 362(20):1881–9. doi: 10.1056/NEJMoa0909499

18. Dijkstra ML, Zeebregts CJ, Verhagen HJM, Teijink JAW, Power AH, Bockler D, et al. Incidence, natural course, and outcome of type II endoleaks in infrarenal endovascular aneurysm repair based on the ENGAGE registry data. *J Vasc Surg*. (2020) 71(3):780–9. doi: 10.1016/j.jvs.2019.04.486

19. Sidloff DA, Gokani V, Stather PW, Choke E, Bown MJ, Sayers RD. Type II endoleak: conservative management is a safe strategy. *Eur J Vasc Endovasc Surg*. (2014) 48(4):391–9. doi: 10.1016/j.ejvs.2014.06.035

20. Dosluoglu HH, Rivero M, Khan SZ, Cherr GS, Harris LM, Dryjski ML. Pre-emptive nonselective perigraft aortic sac embolization with coils to prevent type II endoleak after endovascular aneurysm repair. *J Vasc Surg*. (2019) 69(6):1736–46. doi: 10.1016/j.jvs.2018.10.054

21. Natrella M, Rapellino A, Navarretta F, Iob G, Cristoferi M, Castagnola M, et al. Embo-EVAR: a technique to prevent type II endoleak? A single-center experience. *Ann Vasc Surg*. (2017) 44:119–27. doi: 10.1016/j.avsg.2017.01.028

22. Fabre D, Fadel E, Brenot P, Hamdi S, Gomez Caro A, Mussot S, et al. Type II endoleak prevention with coil embolization during endovascular aneurysm repair in high-risk patients. *J Vasc Surg*. (2015) 62(1):1–7. doi: 10.1016/j.jvs.2015.02.030

23. Force USPST, Owens DK, Davidson KW, Krist AH, Barry MJ, Cabana M, et al. Screening for abdominal aortic aneurysm: uS preventive services task force recommendation statement. *JAMA*. (2019) 322(22):2211–8. doi: 10.1001/jama.2019.18928

24. Li Y, Li Z, Wang S, Chang G, Wu R, Hu Z, et al. Endovascular versus open surgery repair of ruptured abdominal aortic aneurysms in hemodynamically unstable patients: literature review and meta-analysis. *Ann Vasc Surg*. (2016) 32:135–44. doi: 10.1016/j.avsg.2015.09.025

25. Investigators IT, Powell JT, Sweeting MJ, Thompson MM, Ashleigh R, Bell R, et al. Endovascular or open repair strategy for ruptured abdominal aortic aneurysm: 30 day outcomes from IMPROVE randomised trial. *Br Med J*. (2014) 348:f7661. doi: 10.1136/bmj.f7661

26. Reimerink JJ, Hoornweg LL, Vahl AC, Wisselink W, van den Broek TA, Legemate DA, et al. Endovascular repair versus open repair of ruptured abdominal aortic aneurysms: a multicenter randomized controlled trial. *Ann Surg*. (2013) 258 (2):248–56. doi: 10.1097/SLA.0b013e31828d4b76

27. Hinchliffe RJ, Bruijstens L, MacSweeney ST, Braithwaite BD. A randomised trial of endovascular and open surgery for ruptured abdominal aortic aneurysm—results of a pilot study and lessons learned for future studies. *Eur J Vasc Endovasc Surg*. (2006) 32(5):506–13. discussion 14-5. doi: 10.1016/j.ejvs.2006.05.016

frontiers | Frontiers in Cardiovascular Medicine

ORIGINAL RESEARCH
published: 26 April 2022
doi: 10.3389/fcvm.2022.870132

Development and Comparison of Multimodal Models for Preoperative Prediction of Outcomes After Endovascular Aneurysm Repair

Yonggang Wang, Min Zhou, Yong Ding, Xu Li, Zhenyu Zhou, Zhenyu Shi and Weiguo Fu**

Department of Vascular Surgery, Zhongshan Hospital, Institute of Vascular Surgery, Fudan University, National Clinical Research Center for Interventional Medicine, Shanghai, China

OPEN ACCESS

Edited by:
Zhenjie Liu,
The Second Affiliated Hospital of Zhejiang University School of Medicine, China

Reviewed by:
Konstantinos Spanos,
University of Thessaly, Greece
Jiang Xiong,
People's Liberation Army General Hospital, China
Ding Yuan,
Sichuan University, China
Li Lubin,
Yantai Yuhuangding Hospital, China

***Correspondence:**
Zhenyu Shi
shizhenyumax@163.com
Weiguo Fu
fu.weiguo@zs-hospital.sh.cn

Specialty section:
This article was submitted to General Cardiovascular Medicine, a section of the journal Frontiers in Cardiovascular Medicine

Received: *05 February 2022*
Accepted: *23 March 2022*
Published: *26 April 2022*

Citation:
Wang Y, Zhou M, Ding Y, Li X, Zhou Z, Shi Z and Fu W (2022) Development and Comparison of Multimodal Models for Preoperative Prediction of Outcomes After Endovascular Aneurysm Repair. Front. Cardiovasc. Med. 9:870132. doi: 10.3389/fcvm.2022.870132

Objective: The aim of this study was to develop and compare multimodal models for predicting outcomes after endovascular abdominal aortic aneurysm repair (EVAR) based on morphological, deep learning (DL), and radiomic features.

Methods: We retrospectively reviewed 979 patients (January 2010—December 2019) with infrarenal abdominal aortic aneurysms (AAAs) who underwent elective EVAR procedures. A total of 486 patients (January 2010–December 2015) were used for morphological feature model development and optimization. Univariable and multivariable analyses were conducted to determine significant morphological features of EVAR-related severe adverse events (SAEs) and to build a morphological feature model based on different machine learning algorithms. Subsequently, to develop the morphological feature model more easily and better compare with other modal models, 340 patients of AAA with intraluminal thrombosis (ILT) were used for automatic segmentation of ILT based on deep convolutional neural networks (DCNNs). Notably, 493 patients (January 2016–December 2019) were used for the development and comparison of multimodal models (optimized morphological feature, DL, and radiomic models). Of note, 80% of patients were classified as the training set and 20% of patients were classified as the test set. The area under the curve (AUC) was used to evaluate the predictive abilities of different modal models.

Results: The mean age of the patients was 69.9 years, the mean follow-up was 54 months, and 307 (31.4%) patients experienced SAEs. Statistical analysis revealed that short neck, angulated neck, conical neck, ILT, ILT percentage $\geq$51.6%, luminal calcification, double iliac sign, and common iliac artery index $\geq$1.255 were associated with SAEs. The morphological feature model based on the support vector machine had a better predictive performance with an AUC of 0.76, an accuracy of 0.76, and an F1 score of 0.82. Our DCNN model achieved a mean intersection over union score of more than 90.78% for the segmentation of ILT and AAA aortic lumen. The multimodal model result showed that the radiomic model based on logistics regression had better predictive performance (AUC 0.93, accuracy 0.86, and F1 score 0.91) than

the optimized morphological feature model (AUC 0.62, accuracy 0.69, and F1 score 0.81) and the DL model (AUC 0.82, accuracy 0.85, and F1 score 0.89).

Conclusion: The radiomic model has better predictive performance for patient status after EVAR. The morphological feature model and DL model have their own advantages and could also be used to predict outcomes after EVAR.

Keywords: abdominal aortic aneurysm, endovascular repair (EVAR), multimodal, morphologic features, deep learning, radiomics

INTRODUCTION

Endovascular aneurysm repair (EVAR) for abdominal aortic aneurysm (AAA) has some advantages in the minimal invasion, rapid postoperative recovery, shorter hospital stay, and low mortality and morbidity. However, long-term follow-up results reveal a high risk of postoperative complications and re-intervention, when compared with open surgical repair (OSR). Thus, for patients who undergo EVAR, lifetime follow-up is recommended by guidelines (1–4). However, close follow-up may result in unexpected side effects, such as renal function impairment, radiation exposure, and economic and time costs. Therefore, an individualized follow-up protocol is needed (5–9).

Morphological features have been widely used to evaluate risk after EVAR. The operators first treat patients they do not make an estimation of individual patient risk through these adverse morphological features, such as the short neck, angulated neck, intraluminal thrombosis (ILT), calcification, and iliac artery tortuosity (9–11). Recently, Karthikesalingam Alan used preoperative morphological features and artificial neural network (ANN) to predict endograft complications, and Ali Kordzadeh applied 26 preoperative attributes and ANN for the detection of endoleaks (types I–III, respectively). However, the limited number of patients with different complications may have influenced the prediction performance. Moreover, the above studies did not fully exploit the morphological features and did not compare the differences between different machine learning (ML) algorithms, and the feature extraction process was time-consuming (12, 13).

Convolutional neural networks (CNNs) extract non-linear, entangled, and representative features from massive and high-dimensional data from medical images. Benefiting from its strong feature-learning ability, the deep learning (DL) model has shown human expert-level performance in diagnosis, detection, prognosis, and treatment selection (14–16). Unfortunately, preoperative computed tomography angiography (CTA) DL feature stratification methods for EVAR were still unavailable. Radiomics has been widely used in the study of oncology (17). Texture analysis, as a part of radiomics, has gradually been used in AAA, such as predicting expansion, endotension, regression of endoleaks, and aneurysm progression after EVAR (18–21). Compared with texture analysis, radiomics can obtain more features, which may potentially improve prognostic and predictive accuracy in EVAR (22–24). Recently, Charalambous Stavros used radiomics and support vector machines (SVM) trained on 1-month and 6-month radiomic data after EVAR to predict Type 2 endoleaks (T2ELs) leading sac expansion at 1 year (25). Similarly, at present, preoperative CTA radiomic feature stratification methods for EVAR were unavailable.

In this study, we first determined the significant morphological features and developed a morphological feature model based on different ML algorithms. We then used DL algorithms to make the model development more convenient. Subsequently, we studied the relationship between DL features, radiomic features, and EVAR-related severe adverse events (SAEs), to develop models and compare them with an optimized morphological feature model.

MATERIALS AND METHODS

Data and Computed Tomography Collection

From January 2010 to December 2019, 1,523 patients with infrarenal AAAs who underwent elective EVAR at our single center were retrospectively reviewed. Patients with preoperative and postoperative CTA were enrolled in this study. The exclusion criteria were abdominal aortic dissecting aneurysm, ruptured AAA, isolated iliac artery aneurysm, history of aortic surgery, fenestration, and chimney technique. A total of 979 patients were included in this study. Ethical approval was obtained from the ethics committee of our hospital (B2021-063). The need to obtain informed consent from patients was waived due to the retrospective nature of the study.

Contrast-enhanced computed tomography (CT) was performed using Toshiba Aquilion One-64 (Version 3.1; Toshiba Medical Systems, Otawara, Japan) with 1-mm thickness slices. Triple-phase CT was performed, which included a plain scan, arterial phase, and portal venous phase. Arterial phase images were acquired 20–30 s after injection of contrast agent (Ultravist, Bayer Schering Pharma, Berlin, Germany).

End Points

Patients were scheduled for follow-up at 3, 6, and 12 months and annually thereafter. CTA and color Doppler ultrasound were routinely performed. Follow-up data were collected until June 2021. The primary end points were EVAR-related SAEs, including type I/III endoleaks, persistent type II endoleaks (persist longer than 6 months), re-intervention,

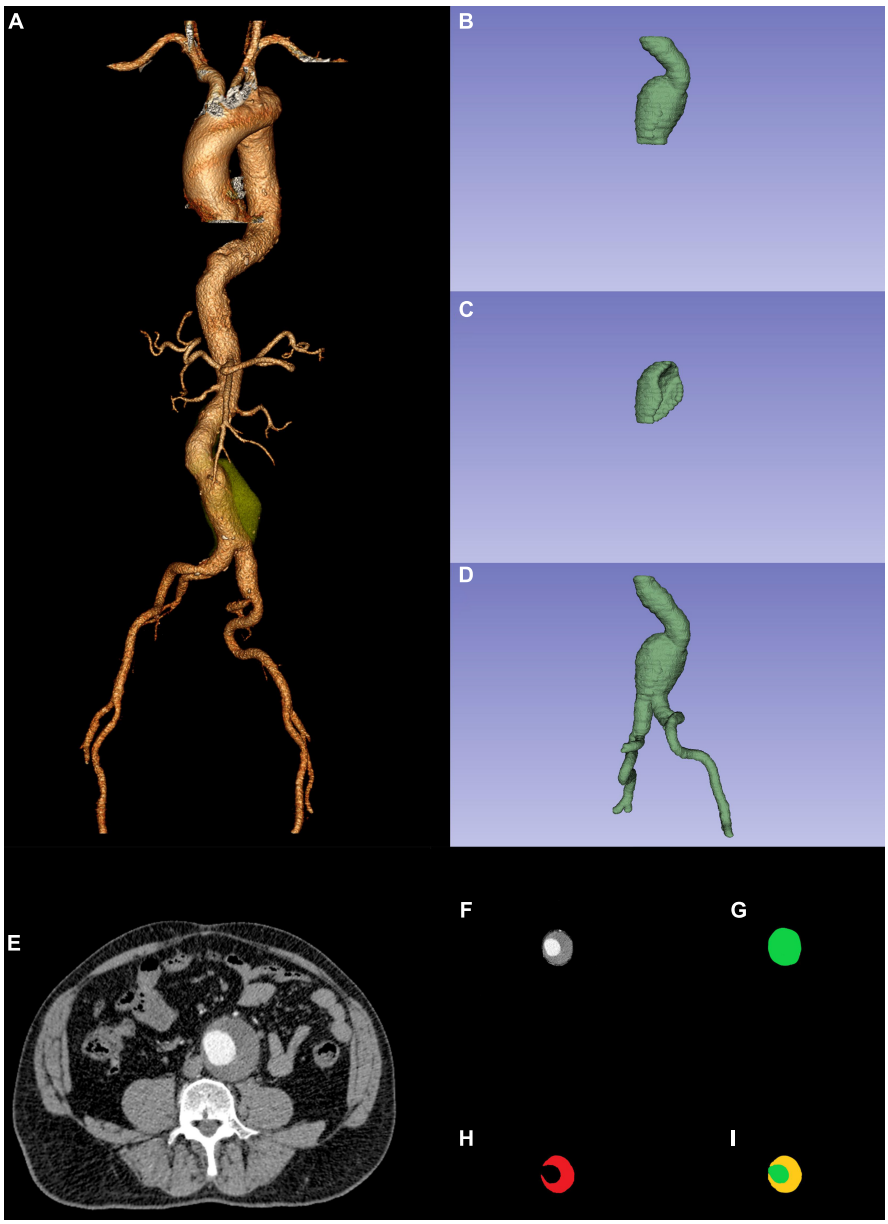

FIGURE 1 | Preoperative CTA reconstruction **(A)**; AAA sac ROI **(B)**; ILT ROI **(C)**; AAA ROI **(D)**; AAA original ROI CTA slice **(F)** was the combination between AAA ROI CTA slicer **(G)** and original ROI CTA slice **(E)**; CTA slicer **(I)** was the combination between AAA sac ROI CTA slicer **(G)** and ILT ROI CTA slicer **(H)**. CTA, computed tomography angiography; AAA, abdominal aortic aneurysm; ROI, region of interest; ILT, intraluminal thrombosis.

iliac limb occlusion or restenosis, stent-graft migration (≥5 mm), stent-graft fracture, aneurysm sac enlargement (≥5 mm), AAA rupture, and aneurysm-related mortality (3, 4).

Morphological Feature Model Development

Among the 979 patients, 486 patients (from January 2010 to December 2015) were used for morphological feature model development. Morphological features were extracted from the preoperative CTA images (**Figure 1A**). All of these morphological features were conducted with centerlines of flow by two investigators in a Vitrea Workstation, with disagreements resolved by a third one. All investigators were blinded to EVAR outcomes. A total of 32 morphological features were used in this study. The major morphological features included short neck (less than 15 mm), conical neck (neck dilation over 10% within 15 mm below the most caudal renal artery), angulated neck (at least 60° between the long axis of the aneurysm sac and juxtarenal aorta), obvious thrombus (the widest part of thrombus (≥2 mm thick) covering at least 50% of the circumference

of the proximal neck), calcified neck (calcification accounting for more than or equal to 50% of the proximal neck), ILT, ILT percentage, common iliac artery index (CAI), and double iliac sign (DIS) (26–28). The significant morphological features were used to build a morphological feature model based on different ML algorithms.

Morphological Feature Model Optimization

To create a morphological feature model easier and compare it with other modal models, we used deep convolutional neural networks (DCNNs) to fully automatically segment ILT in preoperative CTA and realized automatic computation of ILT percentage (29, 30). To apply the DCNN model, AAA segmentation was performed in the preoperative CTA using ITK-SNAP (version 3.8.0[1]). The AAA sac region of interest (ROI: from the lowest renal artery to the aortic bifurcation) and ILT ROI were manually segmented by a junior vascular surgeon and adjusted by a senior vascular surgeon. We then combined the AAA sac ROI (**Figures 1B,G**) and the ILT ROI (**Figures 1C,H**). The combined ROI (**Figure 1I**) was resized to 512 × 512 pixels by third-order spline interpolation in each CTA slice and fed into the DCNN model. The software MATLAB (Version 2021a; MathWorks, Natick, Massachusetts) based on NVIDIA GeForce RTX 3090 was used to create the DCNN model.

We designed the relevant parameters and used a fully convolutional network named DeepLabv3+ semantic segmentation model (31) combined with a backbone convolutional feature extractor, the ResNet-50 network for transfer learning (32, 33), with the aim of automatic segmentation of the ILT and AAA aortic lumen (AL). A 4-fold cross-validation was employed to provide more robustness (34).

Development and Comparison of Multimodal Models

The remaining 493 patients, from January 2016 to December 2019, were used for the development and comparison of multimodal models. To fully determine the nature of the training set and build a reliable classification model for further prediction, we used a 5-fold cross-validation technique (34).

An Optimized Morphological Feature Model

Based on previous statistical analysis results (significant morphological features) and the DCNN model (fully automatic segmentation ILT and realized automatic computation ILT percentage), in this section, we created a morphological feature model based on different ML algorithms, which became easier and more convenient.

Deep Learning Model Development

Segmentation of the AAA ROI (ROI: from the renal artery to the common femoral artery bifurcation) was performed in the same manner as the AAA sac ROI and ILT ROI. Since the AAA ROI (**Figures 1D,G**) represented less of the entire image, we normalized the non-ROI of the original images (**Figure 1E**) using MATLAB to obtain better predictions. Later, the AAA original ROI CTA slices (**Figure 1F**) were resized to 224 × 224 pixels by third-order spline interpolation in each CTA slice and fed into the DL model. The DL model development had the same environment as that of the DCNN model.

The ResNet-50 network was used for transfer learning (32, 33), and we only needed to modify the last number class to 2 and add the Sigmoid activation function after the fully connected layer. To make a robust prediction, each patient's CTA slices of the AAA original ROI CTA slices were fed into the DL model, and the average probability was treated as the result of the probability of EVAR-related SAEs.

Radiomic Model Development

Radiomic features were extracted using Python (version 3.8.5[2]) through preoperative CTA images and the AAA ROI (**Figure 1D**). The Python packages used were SimpleITK (2.0.0), Sklearn (0.24.2), Pyradiomics (3.0.1), and PyWavelets (1.1.1). First, the Pearson correlation analysis excluded radiomic features with high reproducibility. We then used analysis of variance (ANOVA) to exclude features that had no significant influence on EVAR-related SAEs. Finally, the least absolute shrinkage and selection operator (LASSO) regression was used to determine the features related to SAEs after EVAR. The selected radiomic features were used to build models using different ML algorithms.

TABLE 1 | Clinical characteristics and outcomes of patients with EVAR.

Variable	Patients (*n* = 979)
Age (years)	69.9 ± 8.1
Male sex *n* (%)	779 (79.6)
Coronary heart disease *n* (%)	168 (17.2)
Hypertension *n* (%)	698 (71.3)
Hyperlipidemia *n* (%)	501 (51.2)
Diabetes mellitus *n* (%)	87 (8.9)
Chronic obstructive pulmonary disease *n* (%)	275 (28.1)
Chronic renal failure *n* (%)	59 (12.1)
Peripheral artery disease *n* (%)	115 (11.7)
Endurant *n* (%)	457 (46.7)
Excluder *n* (%)	281 (28.7)
Zenith *n* (%)	241 (24.6)
Maximal aneurysm diameter (mm)	56.9 ± 15.3
Type Ia endoleak *n* (%)	35 (3.6)
Type Ib endoleak *n* (%)	37 (3.8)
Type III endoleak *n* (%)	7 (0.7)
Persistent type II endoleak *n* (%)	78 (8.0)
Iliac limb occlusion or restenosis *n* (%)	82 (8.4)
Sac enlargement *n* (%)	47 (4.8)
Aneurysm-related mortality *n* (%)	21 (2.1)

EVAR, endovascular aneurysm repair.

[1]http://www.itksnap.org

[2]http://www.python.org

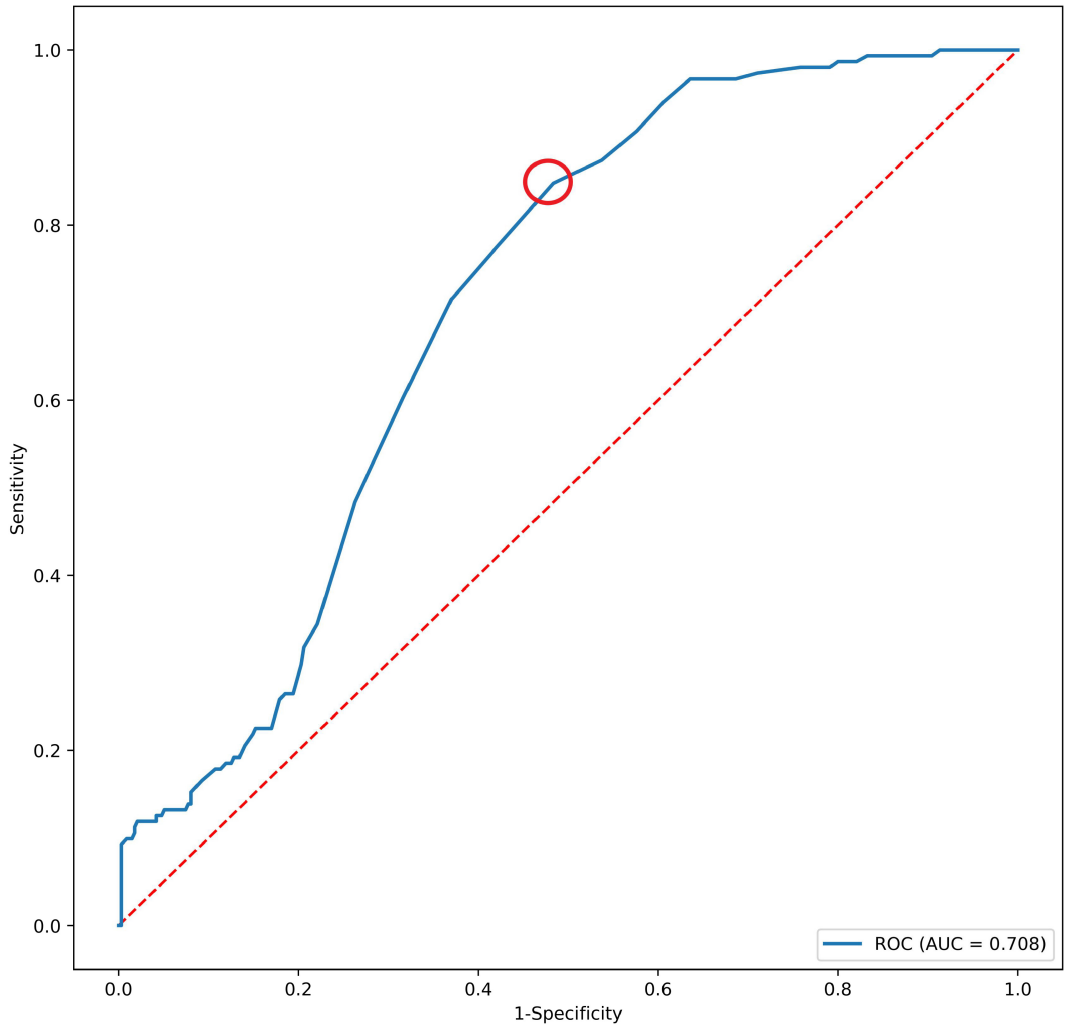

FIGURE 2 | The AUC of CAI and SAEs after EVAR. The red dotted circle represents the optimal cutoff point. AUC, area under the curve; CAI, common iliac artery index; SAEs, severe adverse events.

TABLE 2 | Predictors of SAEs after EVAR by multivariate analyses and predictive performance of different models.

Predictors of SAEs after EVAR by multivariate analyses				**Predictive performance of different model in training set and test set**					
Variable	**OR**	**95% CI**	***P*-value**		**AUC**	**Accuracy**	**Precision**	**Recall**	**F1 score**
Age	1.005	0.978–1.033	0.714	LR Training set	0.79	0.76	0.90	0.79	0.84
Neck length	1.009	0.995–1.022	0.214	Test set	0.79	0.73	0.90	0.73	0.81
Short neck	0.598	0.364–0.983	0.042	KNN Training set	0.78	0.76	0.95	0.76	0.84
Angulated neck	1.079	1.020–1.142	0.009	Test set	0.75	0.69	0.98	0.67	0.80
Conical neck	2.440	1.465–4.064	0.001	DT Training set	0.78	0.74	0.92	0.77	0.84
ILT	0.425	0.206–0.874	0.020	Test set	0.72	0.68	0.90	0.68	0.77
ILT percentage ≥ 51.6%	8.024	2.715–23.71	0.000	SVM Training set	0.78	0.76	0.91	0.79	0.85
Luminal calcification	0.542	0.344–0.852	0.008	**Test set**	**0.76**	**0.76**	**0.90**	**0.75**	**0.82**
DSI	0.334	0.161–0.692	0.003	RF Training set	0.88	0.81	0.90	0.84	0.87
Common iliac calcification	0.573	0.296–1.109	0.099	Test set	0.66	0.66	0.83	0.68	0.75
CAI max	0.981	0.912–1.141	0.501	AdaBoost Training set	0.81	0.76	0.89	0.79	0.84
CAI (≥1.255)	2.404	1.394–4.148	0.002	Test set	0.79	0.73	0.88	0.74	0.80

SAEs, severe adverse events; EVAR, endovascular aneurysm repair. The SVM had better predictive performance in the test set.

TABLE 3 | The segmentation performance in the validation set and test set.

	Validation set	Test set
ILT IOU (mean ± SD)	0.8791 ± 0.0028	0.8650 ± 0.0033
AAA AL IOU (mean ± SD)	0.9108 ± 0.0050	0.8595 ± 0.0085
Mean IOU (mean ± SD)	0.9298 ± 0.0022	0.9078 ± 0.0029
ILT weight IOU (mean ± SD)	0.9981 ± 0.0001	0.9976 ± 0.0001

Statistics Analysis

Descriptive analyses were performed to assess the clinical characteristics and outcomes of the cohort. Values are presented as frequencies or percentages for categorical features and as mean ± SD for continuous variables. Univariable and multivariable analyses were conducted to determine the significant morphological features of EVAR-related SAEs and to build a morphological feature model based on different ML algorithms. Based on the presence of EVAR-related SAEs, patients were randomly divided, 80% were used as the training set and 20% as the test set. The morphological feature model and radiomic model development were based on ML using Python. ML algorithms include logistics regression (LR), Naive Bayes (NB), k-nearest neighbors (KNN), decision tree (DT), SVM, random forest (RF), AdaBoost, Xgboost, and LightGBM. The DCNNs and DL models were developed using MATLAB software. The area under the curve (AUC) from the receiver-operating characteristic (ROC) curve was used to evaluate the predictive effect and select the best performing model in the training set. Applying the selected model, the AUC from the ROC curve was used to evaluate the predictive effect in the test set. Statistical significance was set at $P < 0.05$. Statistical analyses were performed using SPSS (Version 23, IBM, Armonk, NY, United States), Python, and MATLAB.

RESULTS

Patient Characteristics and Outcomes

The mean age of the patients was 69.9 years (range: 41–89 years), and 779 of them were men (79.6%). Comorbidities included coronary heart disease (17.2%), hypertension (71.3%), hyperlipidemia (51.2%), and diabetes mellitus (8.9%). Of note, three types of modular devices were used in these patients, namely, 457 Endurant (Medtronic, Santa Rosa, CA, United States), 281 Excluder (W. L. Gore & Associates, Flagstaff, AZ, United States), and 241 Zenith (Cook Medical, Bloomington, IN, United States). The baseline demographic data were summarized in **Table 1**.

The mean follow-up was 54 months, including 307 (31.4%) patients who had EVAR-related SAEs, including 35 (3.6%) type Ia endoleak; 37 (3.8%) type Ib endoleak; 7 (0.7%) type III endoleak; 78 (8.0%) persistent type II endoleak; 82 (8.4%) iliac limb occlusion or restenosis; 47 (4.8%) sac enlargement; and 21 (2.1%) aneurysm-related mortality (**Table 1**).

Morphological Feature Model Development and Test

In a total of 486 patients with a maximal Youden's index of 0.364 (sensitivity: 0.848 and specificity: 0.484), the optimal cutoff value of the CAI was 1.255 (**Figure 2**). Multivariate analyses showed that short neck, angulated neck, conical neck, ILT, ILT percentage ≥51.6%, luminal calcification, DSI, and CAI (≥1.255) were significant morphological features of EVAR-related SAEs (**Table 2**).

A total of 388 patients were randomly assigned to the training set (No SAEs, 269; SAEs, 119); 98 patients were collected to the test set (No SAEs, 66; SAEs, 32). The AUC of the morphological

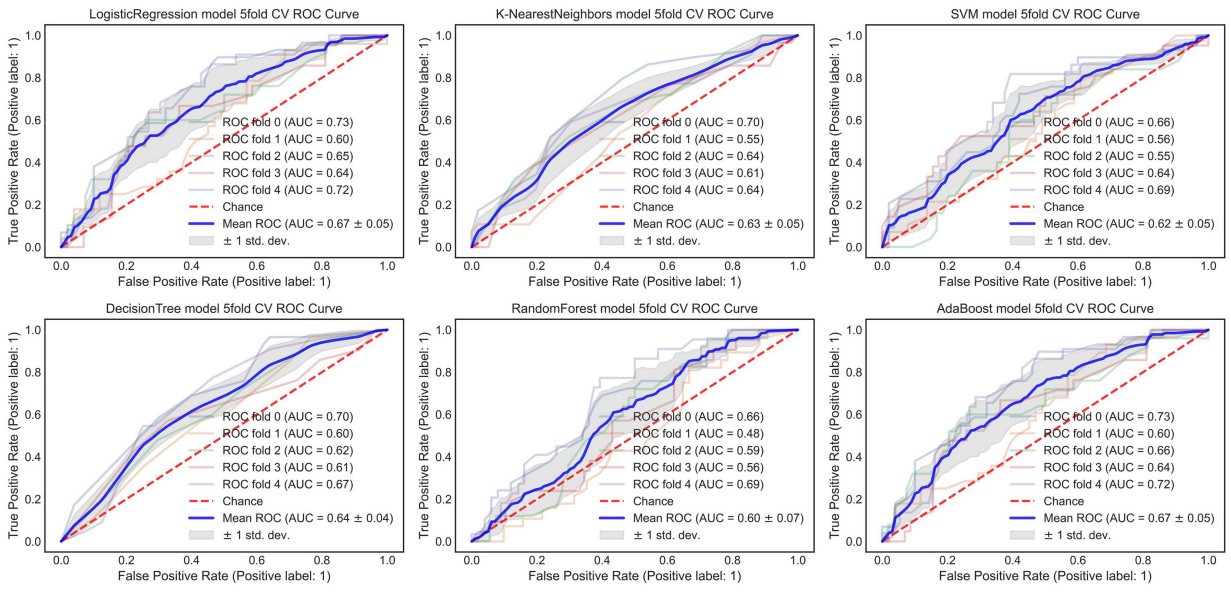

FIGURE 3 | The AUC of the optimized morphological feature model for predicting EVAR-related SAEs in the training set. AUC, area under the curve; SAEs, severe adverse events; EVAR, endovascular aneurysm repair.

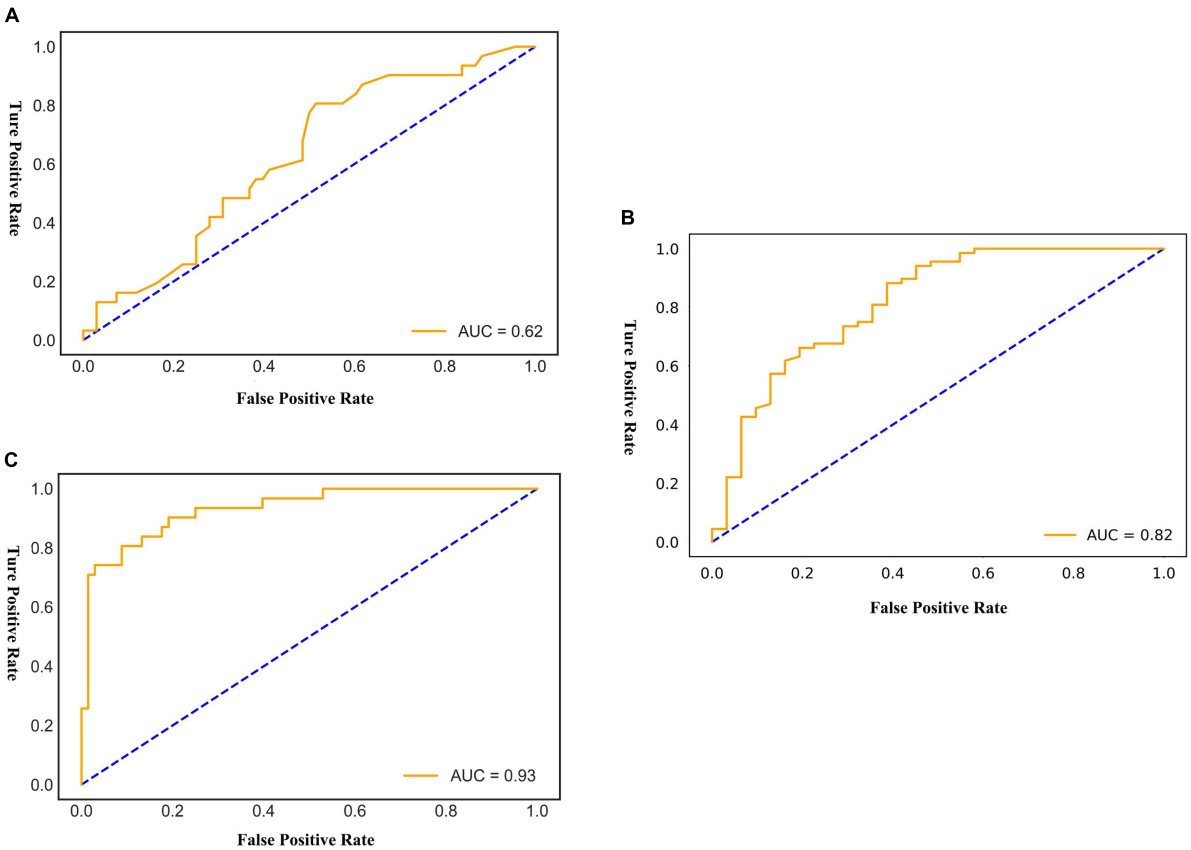

FIGURE 4 | The AUC of the multimodal models for predicting EVAR-related SAEs in the test set. AUC, area under the curve; SAEs, severe adverse events; EVAR, endovascular aneurysm repair. **(A)** AdaBoost ROC curve with test dataset. **(B)** Fold 3 ROC curve with test dataset. **(C)** LogisticRegression ROC curve with test dataset.

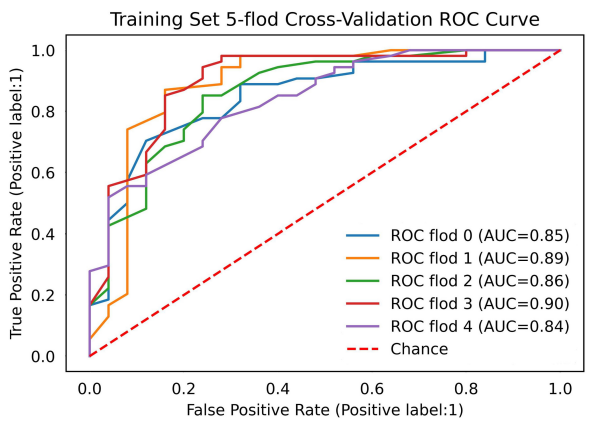

FIGURE 5 | The AUC of the DL model for predicting EVAR-related SAEs in the training set. AUC, area under the curve; DL, deep learning; SAEs, severe adverse events; EVAR, endovascular aneurysm repair.

feature model for predicting EVAR-related SAEs in the test set was as follows: LR 0.79, KNN 0.75, DT 0.72, SVM 0.76, RF 0.66, and AdaBoost 0.79. The accuracy for the test set was LR 0.73, KNN 0.69, DT 0.68, SVM 0.76, RF 0.66, and AdaBoost 0.73. The F1 scores in the test set were LR 0.81, KNN 0.80, DT 0.77, SVM 0.82, RF 0.75, and AdaBoost 0.80. The quantitative performance indicated that the morphological feature model based on SVM had a better predictive performance with an AUC of 0.76, an accuracy of 0.76, and an F1 score of 0.82 (**Table 2**).

Morphological Feature Model Optimization

From January 2010 to December 2015, 340 patients of infrarenal AAAs with ILT were used for morphological feature model optimization. By training in 34,760–35,652 CTA images (n = 204) and validation in 6,968–7,860 CTA images (n = 68), our DCNN model achieved a mean intersection over union (IOU) more than 90.78% for ILT and AAA AL in test set (**Table 3**). The manual segmentation of ILT volume, AAA AL volume, and ILT percentage were 48.6 ± 9.779 cm^3, 112.5 ± 77.63 cm^3, and 30.18 ± 11.32%, respectively. Our DCNN model results were 46.8 ± 12.11 cm^3, 107.1 ± 99.25 cm^3, and 34.29 ± 10.70%. The ILT volume, AAA AL volume, and ILT percentage differences were less than 5% (3.81, 4.81, and 4.11%).

TABLE 4 | The predictive performance of multimodal models in the training set and test set.

		Training set		Test set				
		AUC	Accuracy	AUC	Accuracy	Precision	Recall	F1 score
Optimized morphological feature model	LR	0.67 ± 0.05 (0.60–0.73)	0.63 ± 0.05 (0.56–0.69)	0.63	0.60	0.75	0.62	0.68
	KNN	0.62 ± 0.04 (0.55–0.67)	0.67 ± 0.05 (0.59–0.73)	0.56	0.71	0.71	0.99	0.82
	DT	0.64 ± 0.04 (0.60–0.70)	0.68 ± 0.04 (0.62–0.72)	0.56	0.68	0.69	0.97	0.80
	SVM	0.62 ± 0.05 (0.55–0.69)	0.59 ± 0.05 (0.51–0.65)	0.58	0.55	0.74	0.51	0.61
	RF	0.59 ± 0.07 (0.48–0.70)	0.58 ± 0.05 (0.51–0.65)	0.53	0.56	0.70	0.62	0.66
	AdaBoost	**0.67 ± 0.05 (0.60–0.74)**	**0.68 ± 0.02 (0.65–0.71)**	**0.62**	**0.69**	**0.70**	**0.94**	**0.81**
Deep learning model	Fold 0	0.85	0.86	0.81	0.83	0.90	0.84	0.87
	Fold 1	0.89	0.89	0.81	0.84	0.89	0.87	0.88
	Fold 2	0.86	0.87	0.79	0.79	0.86	0.82	0.84
	Fold 3	**0.90**	**0.90**	**0.82**	**0.85**	**0.88**	**0.90**	**0.89**
	Fold 4	0.85	0.84	0.81	0.81	0.86	0.87	0.86
Radiomics model	**LR**	**0.93 ± 0.02 (0.90–0.95)**	**0.87 ± 0.03 (0.82–0.91)**	**0.93**	**0.86**	**0.94**	**0.89**	**0.91**
	NB	0.80 ± 0.03 (0.76–0.84)	0.77 ± 0.04 (0.73–0.83)	0.77	0.76	0.78	0.85	0.81
	SVM	0.93 ± 0.02 (0.89–0.95)	0.87 ± 0.04 (0.82–0.92)	0.92	0.86	0.93	0.88	0.90
	RF	0.93 ± 0.04 (0.87–0.97)	0.86 ± 0.04 (0.80–0.91)	0.90	0.89	0.96	0.89	0.92
	Xgboost	0.94 ± 0.03 (0.88–0.97)	0.87 ± 0.04 (0.81–0.92)	0.90	0.85	0.88	0.90	0.89
	LightGBM	0.94 ± 0.03 (0.89–0.97)	0.87 ± 0.04 (0.80–0.91)	0.90	0.86	0.88	0.91	0.89

The AdaBoost, Fold 3 and LR had better predictive performance in the test set.

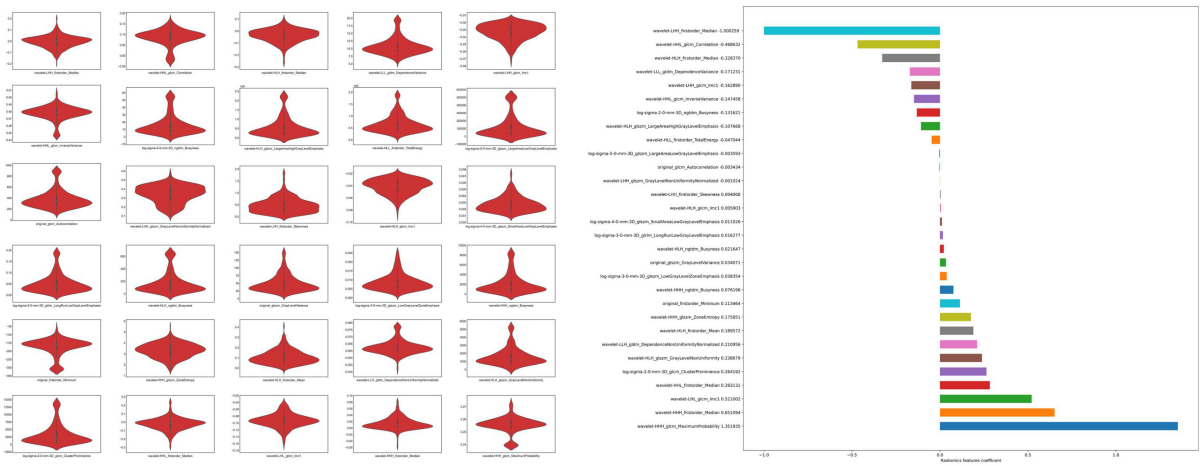

FIGURE 6 | Significant radiomic features and feature coefficients.

Development and Comparison of Multimodal Models

A total of 493 patients were used for the development of multimodal models, 394 patients were allocated to the training set (No SAEs, 269; SAEs, 125), and 99 patients were allocated to the test set (No SAEs, 68; SAEs, 31). Multimodal models include optimized morphological features, DL, and radiomic models.

An Optimized Morphological Feature Model

The AUC of the optimized morphological feature model for predicting EVAR-related SAEs in the test set was as follows: LR 0.63, KNN 0.56, DT 0.56, SVM 0.58, RF 0.53, and AdaBoost 62. The accuracy for the test set was LR 0.60, KNN 0.71, DT 0.68, SVM 0.55, RF 0.56, and AdaBoost 0.69. The F1 score for the test set was LR 0.68, KNN 0.82, DT 0.80, SVM 0.61, RF 0.66, and AdaBoost 0.81. The ROC curves (**Figures 3**, **4A**) and quantitative performance (**Table 4**) indicated that the optimized morphological feature model based on AdaBoost had a better predictive performance with an AUC of 0.62, an accuracy of 0.69, and an F1 score of 0.81.

Deep Learning Model

By training in 92012-93925 CTA images (n = 315), the DL model showed excellent predictive performance in validation

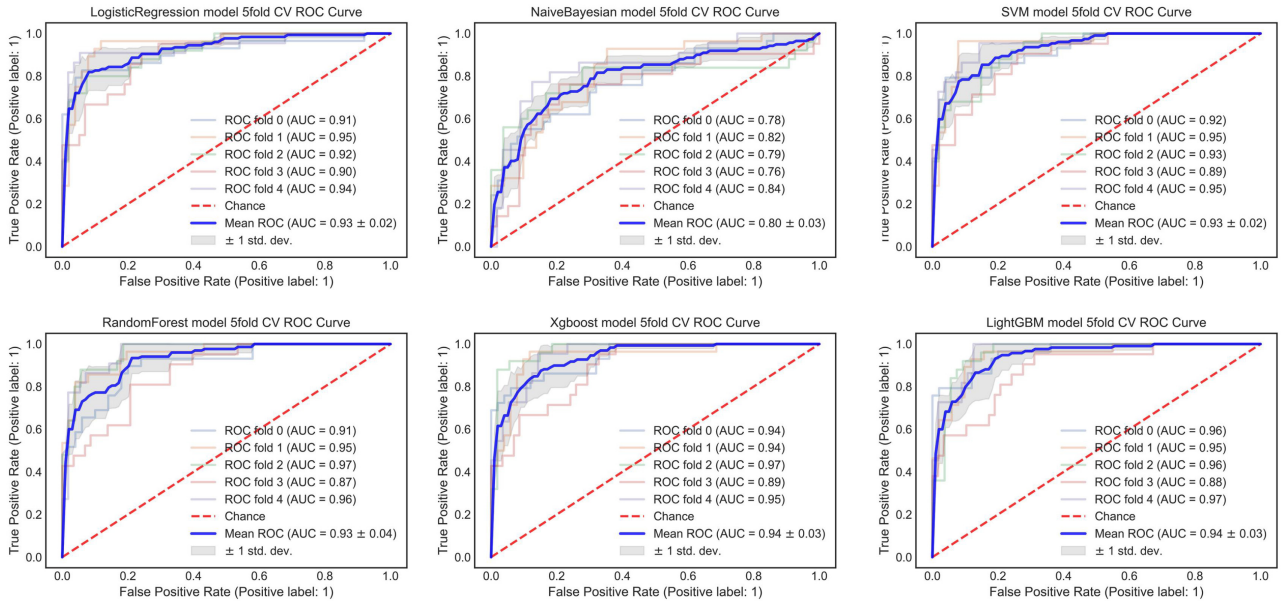

FIGURE 7 | The AUC of the radiomic model for predicting EVAR-related SAEs in the training set. AUC, area under the curve; SAEs, severe adverse events; EVAR, endovascular aneurysm repair.

set (n = 79) by 5-fold cross-validation with an AUC of 0.87 ± 0.03, accuracy of 0.87 ± 0.02, and F1 score of 0.90 ± 0.02. This performance was further confirmed in the test set (n = 79) with an AUC of 0.81 ± 0.01, an accuracy of 0.82 ± 0.02, and an F1 score of 0.87 ± 0.02. The ROC curves (**Figures 4**, **5**) and quantitative performance (**Table 4**) indicated that the DL model (Fold 3) had a better predictive performance with an AUC of 0.82, an accuracy of 0.85, and an F1 score of 0.89.

Radiomic Model

We extracted 1,223 radiomic features from each patient, and 30 features were preserved and used for radiomic model development. The significant radiomic features and feature coefficients are shown in **Figure 6**. The AUC of the radiomic model for predicting EVAR-related SAEs in the test set was as follows: LR 0.93, NB 0.77, SVM 0.92, RF 0.90, Xgboost 0.90, and LightGBM 0.90. The accuracy for the test set was LR 0.86, NB 0.76, SVM 0.86, RF 0.89, Xgboost 0.88, and LightGBM 0.88. The F1 score for the test set was LR 0.91, NB 0.81, SVM 0.90, RF 0.92, Xgboost 0.89, and LightGBM 0.89. The ROC curves (**Figures 4**, **7**) and the quantitative performance (**Table 4**) indicated that the radiomic model based on LR had a better predictive performance with an AUC of 0.93, an accuracy of 0.86, and an F1 score of 0.91.

DISCUSSION

Existing risk score models, such as the Glasgow Aneurysm Score (GAS), Vascular Biochemical and Hematological Outcome Model (VBHOM), the National Surgical Quality Improvement Project (NSQIP), the Vascular Study Group of New England (VSGNE), the Vascular Governance North West model (VGNW), the Medicare model, and the EVAR Risk Assessment (ERA) model, cannot accurately predict complications and re-intervention in the era of EVAR (35–41). Fortunately, when studying the risk factors for model development, we found that morphological features were highly correlated with complications and re-intervention after EVAR. In addition, we also found that conventional statistical models could not fully exploit complex and subtle relationships between features for prediction. These findings were confirmed by Karthikesalingam Alan and Ali Kordzadeh. Karthikesalingam Alan applied ANN and 19 preoperative morphological features to predict endograft complications, and in external validation, the 5-year rates of freedom from aortic complications, limb complications, and mortality in low- and high-risk groups were 95.9 vs. 67.9%, 99.3 vs. 92.0%, and 87.9 vs. 79.3%, respectively (10). Ali Kordzadeh used ANN and 26 preoperative attributes (of which five morphological features) for the detection of endoleaks (types I–III, respectively), and the overall accuracy of the model was >86% (11). To avoid the limited number of patients with different complications that influenced the prediction performance and fully exploited morphological features, the prediction performance between different ML algorithms and model development was easier. A total of 486 patients were used for morphological feature model development, of which 151(31.1%) patients had SAEs. We identified 8 significant morphological features from 32 morphological features and developed a morphological feature model based on different ML algorithms. Our morphological feature model based on SVM had better performance than other ML algorithms, with an AUC of 0.76, an accuracy of 0.76, and an F1 score of

0.82. Later, we proposed the DCNN model for fully automatic segmentation of the ILT in preoperative CTA images. Distinct from traditional thrombus segmentation methods, which have been addressed with intensity-based semiautomatic algorithms combined with shape priors (42, 43). Our DCNN model fully automatically segmented ILT and achieved a mean IOU score of more than 90.78% for segmentation of ILT and AAA AL. The volume difference between the segmentation obtained with the proposed DCNNs and the ground truths was within the experienced human observer variance ($P > 0.05$). Both the ILT segmentation performance and ILT volume difference were better than the currently available models (44, 45).

Development and comparison of multimodal models showed that the optimized morphological feature model based on AdaBoost had a better predictive performance with an AUC of 0.62, an accuracy of 0.69, and an F1 score of 0.81. The AUC, accuracy, and F1 score decreased when compared with our previous studies (AUC 0.76, accuracy 0.76, and F1 score 0.82). We assumed that the main reason was that, in this section, we performed a 5-fold cross-validation, and the limited amount of data affected the model prediction performance (30). However, it did not prevent the morphological feature model as a useful adjunct tool for predicting outcomes after EAVR under the condition of sufficient data. In addition, the morphological feature model may be more acceptable for clinicians.

Based on DL algorithms and graphics processing units (GPUs) that power their training, the DL model has shown human expert-level performance in prognosis (12, 25). Our proposed DL model (Fold 3) predicts the outcome after EVAR with an AUC of 0.82, an accuracy of 0.85, and an F1 score of 0.89. Through a hierarchical neural network structure, the DL model extracted multilevel features from visual characteristics to abstract mappings that were directly related to SAEs after EVAR (29). The DL model was fast and easy to use. Since our method was an end-to-end pipeline that requires only the manually selected AAA region and image preprocessing, the CTA slice was input to predict the status after EVAR directly without further human input. It was easier than the morphological feature model and radiomic method. Besides, the DL model only required CTA images, without increasing the cost. In addition, CTA was easy to acquire throughout the course of treatment; therefore, this model could be used multiple times.

Radiomic methods used CT images to quantify AAA information at the macroscopic level, and radiomic analysis provides quantitative features to mine high-dimensional information and may build the relationship between AAA images and EVAR-related SAEs (20–22). Reviewing the current literature, few radiomic studies have been carried out in patients with AAA. However, there have been many studies about texture analysis, and Carl W. Kotze used CT texture analysis and 18F-fluorodeoxyglucose positron emission tomography to predict AAA dilatation (16). García G developed a computer-supported endotension detection method based on texture analysis for EVAR (17). García G also evaluated the texture features and classification of AAA endoleak after EVAR, gray-level co-occurrence matrix (GLCM), gray-level run-length matrix (GLRLM), and gray-level dependence matrix (GLDM) were able to distinguish favorable or unfavorable regression with an accuracy of 93.41 ± 0.024%, 90.17 ± 0.077%, and 81.98 ± 0.045%, respectively (18). Ding N applied GLCM, GLRLM, and GLDM for predicting aneurysm expansion after EVAR with accuracy (85.17, 87.23, and 86.09%) and AUC (0.90, 0.86, and 0.83) (19). Recently, Charalambous Stavros used radiomics and the SVM classifier trained on 6-month radiomic features to predict T2ELs leading sac expansion at 1 year with an AUC of 89.3%, and the SVM classifier developed with 6-month radiomic features showed an AUC of 95.5% at 1 year (23). Our radiomic model is based on LR to preoperative prediction outcomes after EVAR with AUC 0.93, accuracy 0.86, and F1 score 0.91. Although, compared with other modal models, the radiomic model had better prediction performance. We suggest that the morphological feature, DL, and radiomic models all can be used to predict outcomes after EVAR.

Our study has some limitations. First, due to the retrospective single-center nature of the study, selective bias could not be avoided. Despite internal validation and testing, it was necessary to estimate these multimodal models at other institutions. Second, the limited data affected the prediction performance for the development of multimodal models. Besides, the relatively small sample size limited the possibility of conducting a subgroup predicting different SAEs after EVAR. Third, the morphological feature model development was still time-consuming under the condition of fully automatically segmenting ILT and computing ILT percentage. The DL model showed effective performance for predicting outcomes after EVAR. A high environment was required for DL model development. At present, radiomics lacks a standardized methodology for radiomic analyses, a universal lexicon to denote features that are semantically equivalent, and lists of feature values alone do not sufficiently capture the details of feature extraction that might nonetheless strongly affect feature values (43, 44). Finally, the combination of morphological features, DL, and radiomic features was unclear. In the future study, we will aim to improve prediction performance by combining different modal models.

CONCLUSION

Applying morphological features, DL, and radiomic models, we can evaluate the risk of postoperative outcomes after EVAR. Using these models, operators can more accurately estimate individual patient risk after EVAR and identify subgroups of patients who require more intensive follow-up. This might affect both patient selection and surveillance after EVAR, which remained important for prognosis after EVAR.

DATA AVAILABILITY STATEMENT

The original contributions presented in the study are included in the article/**Supplementary Material**, further inquiries can be directed to the corresponding author/s.

ETHICS STATEMENT

The studies involving human participants were reviewed and approved by Zhongshan Hospital Fudan University Ethic Committee. Written informed consent for participation was not required for this study in accordance with the national legislation and the institutional requirements.

AUTHOR CONTRIBUTIONS

ZS and WF contributed to the conception and design. MZ, YD, and XL performed the data collection and interpretation. YW, ZZ, and ZS performed ROI segmentation and images preprocessing. YW analyzed the datasets and wrote this manuscript. ZS obtained the funding. All authors read and approved the final manuscript.

FUNDING

We acknowledge that the present research was sponsored by the National Natural Science Foundation of China (grant number 81870342).

SUPPLEMENTARY MATERIAL

The Supplementary Material for this article can be found online at: https://www.frontiersin.org/articles/10.3389/fcvm.2022.870132/full#supplementary-material

REFERENCES

1. Patel R, Sweeting MJ, Powell JT, Greenhalgh RM. Endovascular versus open repair of abdominal aortic aneurysm in 15-years' follow-up of the UK endovascular aneurysm repair trial 1 (EVAR trial 1): a randomised controlled trial. *Lancet.* (2016) 388:2366–74. doi: 10.1016/S0140-6736(16)31135-7
2. Lederle FA, Kyriakides TC, Stroupe KT, Freischlag JA, Padberg FT Jr., Matsumura JS, et al. Open versus endovascular repair of abdominal aortic aneurysm. *N Engl J Med.* (2019) 380:2126–35. doi: 10.1056/NEJMoa1715955
3. Chaikof EL, Dalman RL, Eskandari MK, Jackson BM, Lee WA, Mansour MA, et al. The society for vascular surgery practice guidelines on the care of patients with an abdominal aortic aneurysm. *J Vasc Surg.* (2018) 67:2–77. doi: 10.1016/j.jvs.2017.10.044
4. Wanhainen A, Verzini F, Van Herzeele I, Allaire E, Bown M, Cohnert T, et al. Editor's choice – European society for vascular surgery (ESVS) 2019 clinical practice guidelines on the management of abdominal aorto-iliac artery aneurysms. *Eur J Vasc Endovasc Surg.* (2019) 57:8–93. doi: 10.1016/j.ejvs.2018.09.020
5. Nana P, Kouvelos G, Brotis A, Spanos K, Giannoukas A, Matsagkas M. The effect of endovascular aneurysm repair on renal function in patients treated for abdominal aortic aneurysm. *Curr Pharm Des.* (2019) 25:4675–85. doi: 10.2174/1381612825666191129094923
6. Harbron RW, Abdelhalim M, Ainsbury EA, Eakins JS, Alam A, Lee C, et al. Patient radiation dose from x-ray guided endovascular aneurysm repair: a Monte Carlo approach using voxel phantoms and detailed exposure information. *J Radiol Prot.* (2020) 40:704–26. doi: 10.1088/1361-6498/ab944e
7. Burgers LT, Vahl AC, Severens JL, Wiersema AM, Cuypers PW, Verhagen HJ, et al. Cost-effectiveness of elective endovascular aneurysm repair versus open surgical repair of abdominal aortic aneurysms. *Eur J Vasc Endovasc Surg.* (2016) 52:29–40. doi: 10.1016/j.ejvs.2016.03.001
8. Steuer J, Lachat M, Veith FJ, Wanhainen A. Endovascular grafts for abdominal aortic aneurysm. *Eur Heart J.* (2016) 37:145–51. doi: 10.1093/eurheartj/ehv593
9. Oliveira NFG, Gonçalves FB, Hoeks SE, Josee van Rijn M, Ultee K, Pinto JP, et al. Long-term outcomes of standard endovascular aneurysm repair in patients with severe neck angulation. *J Vasc Surg.* (2018) 68:1725–35. doi: 10.1016/j.jvs.2018.03.427
10. Fujii T, Banno H, Kodama A, Sugimoto M, Akita N, Tsuruoka T, et al. Aneurysm sac thrombus volume predicts aneurysm expansion with type II endoleak after endovascular aneurysm repair. *Ann Vasc Surg.* (2020) 66:85–94. doi: 10.1016/j.avsg.2019.11.045
11. Mascoli C, Faggioli G, Gallitto E, Longhi M, Abualhin M, Pini R, et al. Planning and endograft related variables predisposing to late distal type I endoleaks. *Eur J Vasc Endovasc Surg.* (2019) 58:334–42. doi: 10.1016/j.ejvs.2019.03.036
12. Karthikesalingam A, Attallah O, Ma X, Bahia SS, Thompson L, Vidal-Diez A, et al. An artificial neural network stratifies the risks of re-intervention and mortality after endovascular aneurysm repair; a retrospective observational study. *PLoS One.* (2015) 10:e0129024. doi: 10.1371/journal.pone.0129024
13. Kordzadeh A, Hanif MA, Ramirez MJ, Railton N, Prionidis I, Browne T. Prediction, pattern recognition and modelling of complications post-endovascular infra renal aneurysm repair by artificial intelligence. *Vascular.* (2021) 29:171–82. doi: 10.1177/1708538120949658
14. Tran KA, Kondrashova O, Bradley A, Williams ED, Pearson JV, Waddell N. Deep learning in cancer diagnosis, prognosis and treatment selection. *Genome Med.* (2021) 13:152. doi: 10.1186/s13073-021-00968-x
15. Gao R, Zhao S, Aishanjiang K, Cai H, Wei T, Zhang Y, et al. Deep learning for differential diagnosis of malignant hepatic tumors based on multi-phase contrast-enhanced CT and clinical data. *J Hematol Oncol.* (2021) 14:154. doi: 10.1186/s13045-021-01167-2
16. Esteva A, Kuprel B, Novoa RA, Ko J, Swetter SM, Blau HM, et al. Dermatologist-level classification of skin cancer with deep neural networks. *Nature.* (2017) 542:115–8. doi: 10.1038/nature21056
17. Bera K, Braman N, Gupta A, Velcheti V, Madabhushi A. Predicting cancer outcomes with radiomics and artificial intelligence in radiology. *Nat Rev Clin Oncol.* (2022) 19:132–46. doi: 10.1038/s41571-021-00560-7
18. Kotze CW, Rudd JHF, Ganeshan B, Menezes LJ, Brookes J, Agu O, et al. CT signal heterogeneity of abdominal aortic aneurysm as a possible predictive biomarker for expansion. *Atherosclerosis.* (2014) 233:510–7. doi: 10.1016/j.atherosclerosis.2014.01.001
19. García G, Tapia A, De Blas M. Computer-supported diagnosis for endotension cases in endovascular aortic aneurysm repair evolution. *Comput Methods Programs Biomed.* (2014) 115:11–9. doi: 10.1016/j.cmpb.2014.03.004
20. García G, Maiora J, Tapia A, De Blas M. Evaluation of texture for classification of abdominal aortic aneurysm after endovascular repair. *J Digit Imaging.* (2012) 25:369–76. doi: 10.1007/s10278-011-9417-7
21. Ding N, Hao Y, Wang Z, Xuan X, Kong L, Xue H, et al. CT texture analysis predicts abdominal aortic aneurysm post-endovascular aortic aneurysm repair progression. *Sci Rep.* (2020) 10:12268. doi: 10.1038/s41598-020-69226-1
22. Lambin P, Rios-Velazquez E, Leijenaar R, Carvalho S, van Stiphout RG, Granton P, et al. Radiomics: extracting more information from medical images using advanced feature analysis. *Eur J Cancer.* (2012) 48:441–6. doi: 10.1016/j.ejca.2011.11.036
23. Kumar V, Gu Y, Basu S, Berglund A, Eschrich SA, Schabath MB, et al. Radiomics: the process and the challenges. *Magn Reson Imaging.* (2012) 30:1234–48. doi: 10.1016/j.mri.2012.06.010
24. Gillies RJ, Kinahan PE, Hricak H. Radiomics: images are more than pictures. They are data. *Radiology.* (2016) 278:563–77. doi: 10.1148/radiol.2015151169
25. Charalambous S, Klontzas ME, Kontopodis N, Ioannou CV, Perisinakis K, Maris TG, et al. Radiomics and machine learning to predict aggressive type 2 endoleaks after endovascular aneurysm repair: a proof of concept. *Acta Radiol.* (2021) 27:2841851211032443. doi: 10.1177/02841851211032443
26. Brownrigg JR, de Bruin JL, Rossi L, Karthikesalingam A, Patterson B, Holt PJ, et al. Endovascular aneurysm sealing for infrarenal abdominal aortic aneurysms: 30-day outcomes of 105 patients in a single centre. *Eur J Vasc Endovasc Surg.* (2015) 50:157–64. doi: 10.1016/j.ejvs.2015.03.024

27. Ding Y, Shan Y, Zhou M, Cai L, Li X, Shi Z, et al. Amount of intraluminal thrombus correlates with severe adverse events in abdominal aortic aneurysms after endovascular aneurysm repair. *Ann Vasc Surg.* (2020) 67:254–64. doi: 10.1016/j.avsg.2020.02.011
28. Taudorf M, Jensen LP, Vogt KC, Grønvall J, Schroeder TV, Lönn L. Endograft limb occlusion in EVAR: iliac tortuosity quantified by three different indices on the basis of preoperative CTA. *Eur J Vasc Endovasc Surg.* (2014) 48:527–33. doi: 10.1016/j.ejvs.2014.04.018
29. LeCun Y, Bengio Y, Hinton G. Deep learning. *Nature.* (2015) 521:436–44. doi: 10.1038/nature14539
30. Shelhamer E, Long J, Darrell T. Fully convolutional networks for semantic segmentation. *IEEE Trans Pattern Anal Mach Intell.* (2017) 39:640–51. doi: 10.1109/TPAMI.2016.2572683
31. Chen L-C, Zhu Y, Papandreou G, Schroff F, Adam H. Encoder-decoder with atrous separable convolution for semantic image segmentation. In: Ferrari V, Hebert M, Sminchisescu C, Weiss Y editors. *Computer Vision – ECCV 2018. Lecture Notes in Computer Science*. Cham: Springer (2018).
32. Raghu S, Sriraam N, Temel Y, Rao SV, Kubben PL. EEG based multi-class seizure type classification using convolutional neural network and transfer learning. *Neural Netw.* (2020) 124:202–12. doi: 10.1016/j.neunet.2020.01.017
33. Joshi V, Le Gallo M, Haefeli S, Boybat I, Nandakumar SR, Piveteau C, et al. Accurate deep neural network inference using computational phase-change memory. *Nat Commun.* (2020) 11:2473. doi: 10.1038/s41467-020-16108-9
34. Qin LX, Huang HC, Begg CB. Cautionary note on using cross-validation for molecular classification. *J Clin Oncol.* (2016) 34:3931–8. doi: 10.1200/JCO.2016.68.1031
35. Patterson BO, Karthikesalingam A, Hinchliffe RJ, Loftus IM, Thompson MM, Holt PJ. The glasgow aneurysm score does not predict mortality after open abdominal aortic aneurysm in the era of endovascular aneurysm repair. *J Vasc Surg.* (2011) 54:353–7. doi: 10.1016/j.jvs.2011.01.029
36. Patterson BO, Holt PJ, Hinchliffe R, Nordon IM, Loftus IM, Thompson MM. Existing risk prediction methods for elective abdominal aortic aneurysm repair do not predict short-term outcome following endovascular repair. *J Vasc Surg.* (2010) 52:25–30. doi: 10.1016/j.jvs.2010.01.084
37. Eslami MH, Rybin DV, Doros G, Farber A. Description of a risk predictive model of 30-day postoperative mortality after elective abdominal aortic aneurysm repair. *J Vasc Surg.* (2017) 65:65–74. doi: 10.1016/j.jvs.2016.07.103
38. Eslami MH, Rybin D, Doros G, Kalish JA, Farber A. Comparison of a Vascular Study Group of New England risk prediction model with established risk prediction models of in-hospital mortality after elective abdominal aortic aneurysm repair. *J Vasc Surg.* (2015) 62:1125–33. doi: 10.1016/j.jvs.2015.06.051
39. Grant SW, Grayson AD, Purkayastha D, Wilson SD, McCollum C. Logistic risk model for mortality following elective abdominal aortic aneurysm repair. *Br J Surg.* (2011) 98:652–8. doi: 10.1002/bjs.7463
40. Giles KA, Schermerhorn ML, O'Malley AJ, Cotterill P, Jhaveri A, Pomposelli FB, et al. Risk prediction for perioperative mortality of endovascular vs open repair of abdominal aortic aneurysms using the Medicare population. *J Vasc Surg.* (2009) 50:256–62. doi: 10.1016/j.jvs.2009.01.044
41. Barnes M, Boult M, Maddern G, Fitridge R. A model to predict outcomes for endovascular aneurysm repair using preoperative variables. *Eur J Vasc Endovasc Surg.* (2008) 35:571–9. doi: 10.1016/j.ejvs.2007.12.003
42. Lalys F, Yan V, Kaladji A, Lucas A, Esneault S. Generic thrombus segmentation from pre- and post-operative CTA. *Int J Comput Assist Radiol Surg.* (2017) 12:1501–10. doi: 10.1007/s11548-017-1591-8
43. Zohios C, Kossioris G, Papaharilaou Y. Geometrical methods for level set based abdominal aortic aneurysm thrombus and outer wall 2D image segmentation. *Comput Methods Programs Biomed.* (2012) 107:202–17. doi: 10.1016/j.cmpb.2011.06.009
44. López-Linares K, Aranjuelo N, Kabongo L, Maclair G, Lete N, Ceresa M, et al. Fully automatic detection and segmentation of abdominal aortic thrombus in post-operative CTA images using deep convolutional neural networks. *Med Image Anal.* (2018) 46:202–14. doi: 10.1016/j.media.2018.03.010
45. Caradu C, Spampinato B, Vrancianu AM, Bérard X, Ducasse E. Fully automatic volume segmentation of infrarenal abdominal aortic aneurysm computed tomography images with deep learning approaches versus physician controlled manual segmentation. *J Vasc Surg.* (2021) 74:246.e–56.e6. doi: 10.1016/j.jvs.2020.11.036
46. Shi Z, Traverso A, van Soest J, Dekker A, Wee L. Technical Note: ontology-guided radiomics analysis workflow (O-RAW). *Med Phys.* (2019) 46:5677–84. doi: 10.1002/mp.13844qrPlease cite Refs. (46, 47) inside the text.
47. van Timmeren JE, Cester D, Tanadini-Lang S, Alkadhi H, Baessler B. Radiomics in medical imaging-"how-to" guide and critical reflection. *Insights Imaging.* (2020) 11:91. doi: 10.1186/s13244-020-00887-2

Conflict of Interest: The authors declare that the research was conducted in the absence of any commercial or financial relationships that could be construed as a potential conflict of interest.

The handling editor ZL is currently organizing a Research Topic with WF.

Publisher's Note: All claims expressed in this article are solely those of the authors and do not necessarily represent those of their affiliated organizations, or those of the publisher, the editors and the reviewers. Any product that may be evaluated in this article, or claim that may be made by its manufacturer, is not guaranteed or endorsed by the publisher.

Copyright © 2022 Wang, Zhou, Ding, Li, Zhou, Shi and Fu. This is an open-access article distributed under the terms of the Creative Commons Attribution License (CC BY). The use, distribution or reproduction in other forums is permitted, provided the original author(s) and the copyright owner(s) are credited and that the original publication in this journal is cited, in accordance with accepted academic practice. No use, distribution or reproduction is permitted which does not comply with these terms.

frontiers | Frontiers in Cardiovascular Medicine

SYSTEMATIC REVIEW
published: 23 May 2022
doi: 10.3389/fcvm.2022.908747

Association Between Metformin and Abdominal Aortic Aneurysm: A Meta-Analysis

Wenqiang Niu[1†], Juan Shao[2†], Benxiang Yu[1], Guolong Liu[1], Ran Wang[3], Hengyang Dong[1], Haijie Che[1] and Lubin Li[1*]*

[1] Department of Vascular Surgery, Yantai Yuhuangding Hospital, Yantai, China, [2] Department of Dermatology, Yantai Yuhuangding Hospital, Yantai, China, [3] Nursing Department, Heze Medical College, Heze, China

Objective: To systematically examine the association between metformin and abdominal aortic aneurysm (AAA) and provide a basis for the treatment of AAA.

Methods: Pubmed, Embase, Cochrane Library, and Ovid databases were searched by computer to identify the literature related to metformin and AAA published until February 2022. The literature was screened according to the inclusion and exclusion criteria, data were extracted, and a quality assessment was conducted. The meta-analysis was performed using Stata 16.0 and RevMan 5.3 software.

Results: Seven articles containing a total of 10 cohort studies (85,050 patients) met the inclusion criteria and were included in the review. Meta-analysis showed that metformin can limit the expansion of AAA (MD = – 0.72, 95% CI: – 1.08 ∼ –0.37, $P < 0.00001$), as well as reduce AAA repair or AAA rupture-related mortality (OR = 0.80, 95% CI:0.66 ∼ 0.96, $P = 0.02$). The difference was statistically significant ($P < 0.05$).

Conclusion: Metformin can limit the expansion of AAA and reduce the incidence of AAA and postoperative mortality. However, further biological experiments and clinical trials still need to be conducted to support this.

Keywords: metformin, abdominal aortic aneurysm, expansion, mortality, meta-analysis

OPEN ACCESS

Edited by:
Zhenjie Liu,
The Second Affiliated Hospital of Zhejiang University School of Medicine, China

Reviewed by:
Lei Peng,
North Sichuan Medical College, China
Santosh Karnewar,
University of Virginia, United States

***Correspondence:**
Haijie Che
chj1437@163.com
Lubin Li
lubinhuanghe@163.com

[†]These authors have contributed equally to this work and share first authorship

Specialty section:
This article was submitted to General Cardiovascular Medicine, a section of the journal Frontiers in Cardiovascular Medicine

Received: *31 March 2022*
Accepted: *04 May 2022*
Published: *23 May 2022*

Citation:
Niu W, Shao J, Yu B, Liu G, Wang R, Dong H, Che H and Li L (2022) Association Between Metformin and Abdominal Aortic Aneurysm: A Meta-Analysis. Front. Cardiovasc. Med. 9:908747. doi: 10.3389/fcvm.2022.908747

INTRODUCTION

Abdominal aortic aneurysm (AAA) is a common asymptomatic disease with a prevalence of 1.2–4% in people over the age of 50 (1–4). If left untreated, AAA can progress to aneurysm rupture and seriously threaten the patient's life. Despite significant advances in research on the genetic, metabolic, and environmental risks associated with aortic aneurysms and population-based disease screening programs, thousands of patients die prematurely due to aneurysm-related events. Studies have reported that the average annual mortality rate from aortic aneurysms worldwide is 2.8/100,000, which has increased by 12% over the past 20 years (5).

AAA remains a significant preventable cause of death in the early twenty-first century. According to the guidelines, aggressive surgical intervention is recommended for larger diameter AAA or symptomatic AAA. However, with improved screening and appropriate examination equipment, many cases of AAA can be detected at a very young age when they are asymptomatic. However, regular imaging can only monitor this type of AAA. Relevant studies have reported that up to 70% of this type of AAA will eventually grow to the size requiring surgical repair (6, 7).

Currently, there is no medical treatment that can inhibit the growth of small AAA. Therefore, in recent years, domestic and international researchers have been committed to exploring the non-surgical treatment of AAA, hoping to limit the further expansion of AAA in a non-invasive fashion and achieve the goal of avoiding surgical treatment or delaying the time of operation.

Despite the fact that numerous clinical trials have proven that pharmacological interventions are ineffective in limiting the AAA enlargement or disease progression, studies in various population groups have demonstrated a negative correlation between diabetes and the prevalence, growth, and rupture of AAA (8–10). The causal mechanism behind this correlation is not yet precisely understood but may be related to hyperglycemia, the effect of antidiabetic drugs, or other factors of the diabetic environment (11, 12). It is well-known that metformin is one of the most commonly used drugs for the treatment of diabetes. Experimental studies have shown that it inhibits the proliferation of aortic smooth muscle cells and the expression of extracellular matrix metalloproteinase (MMP)-2. It also reduces oxidative stress (13–16). Therefore, metformin could potentially become a drug that will be used in the future to treat AAA.

Nevertheless, the association between metformin and AAA remains unclear. To help clarify the available epidemiological evidence, we conducted a meta-analysis of the literature on metformin and AAA published until February 2022 to further explore the relationship between metformin and AAA.

METHODS

Search Strategy

This meta-analysis was performed in accordance with the Preferred Reporting Items for Systematic Reviews and Meta-Analyses (PRISMA) (17, 18). The literature on metformin and AAA was systematically searched in Pubmed, Embase, Cochrane Library, and Ovid databases until February 2022. The search terms included "Metformin (Dimethylbiguanidine, Dimethylguanylguanidine, Glucophage, Metformin Hydrochloride, Hydrochloride, Metformin, Metformin HCl, HCl, Metformin)," "Aortic aneurysm (Aneurysms, Aortic, Aortic Aneurysms, Aneurysm, Aortic)," "Aortic dilatation," and "Cohort Study." Two reviewers (RW and HD) independently browsed all articles and selected only cohort studies to be included in this review. There were no language restrictions for the included studies. The analysis was based on published articles and conference abstracts with available statistical data and charts. Authors were contacted to provide additional data from their studies, if necessary. The relevant literature from the reference lists of the included articles was also manually searched, screened, and reviewed.

Criteria for Inclusion and Exclusion

In our opinion, if these studies were cohort studies in adult diabetic patients with a minimum duration of 8 weeks of metformin pharmacologic intervention, the article clearly demonstrates the effect of metformin pharmacologic therapy on change in aortic aneurysm diameter or on events related to aortic dilation as outcome results, we consider these studies eligible for inclusion. The cohort study articles contained risk estimates of OR, RR, or HR with a corresponding 95% CI.

We excluded (1) observational and retrospective studies; and (2) Studies with Intervention Duration <8 Weeks, and (3) reviews, case reports, comments, recommendations, letters, ongoing trials, protocols, conference abstracts, consensus or statements, and articles lacking applicable data; and (4) studies that could not be utilized, such as duplicate reports, as well as studies of poor quality, of an inconsistent type, or with too little information, and (5) studies with inappropriate statistical methods and insufficient data.

Data Extraction

Two researchers (RW and HD) searched for relevant articles, screened eligible articles based on the inclusion and exclusion criteria, and independently extracted data using a standardized datasheet. Disagreements were resolved by discussion with a third researcher (GL). We extracted basic information (author, year, country), type of study, inclusion criteria, participants and their number, interventions (metformin), and results. We compared treatment strategies for aortic changes with or without metformin medication in patients with aortic aneurysms, without the limitation of treatment history. The results of evaluation were as follows: trends in aortic diameter and AAA repair or AAA rupture related mortality.

Quality Assessment

The Newcastle-Ottawa Scale (NOS) was used to evaluate the quality of all studies (19). The NOS checklist contains three quality parameters: (1) selected population, (2) comparability, and (3) assessment of exposure or outcome in cohort studies. Each study was scored from zero to nine. Studies that scored $\geq$ seven were considered high-quality articles.

Data Analysis

Statistical analyses were performed using Stata16.0 and Review Manager 5.3 software. We used MD and the corresponding 95% CI to account for continuous data and OR to account for dichotomous results (20). $P < 0.05$ indicated statistical significance. The I^2 statistic, which reflects the proportion of heterogeneity, was used to analyze inconsistency in the results. With $I^2 < 50\%$ and insignificant heterogeneity, the fixed-effects model was used. With $I^2 \geq 50\%$ and significant heterogeneity, the sensitivity analysis was performed to identify the source of heterogeneity (21). The random-effects model was used if the cause of heterogeneity could not be determined (22).

RESULTS

Study Inclusion

By searching the relevant literature, 91 articles were retrieved and screened according to the established inclusion and exclusion criteria, and a total of seven articles were included in the review (**Figure 1**). The seven articles contained a total of 10 cohort studies with 85,050 participants. The relevant characteristics of the included literature are displayed in **Table 1**.

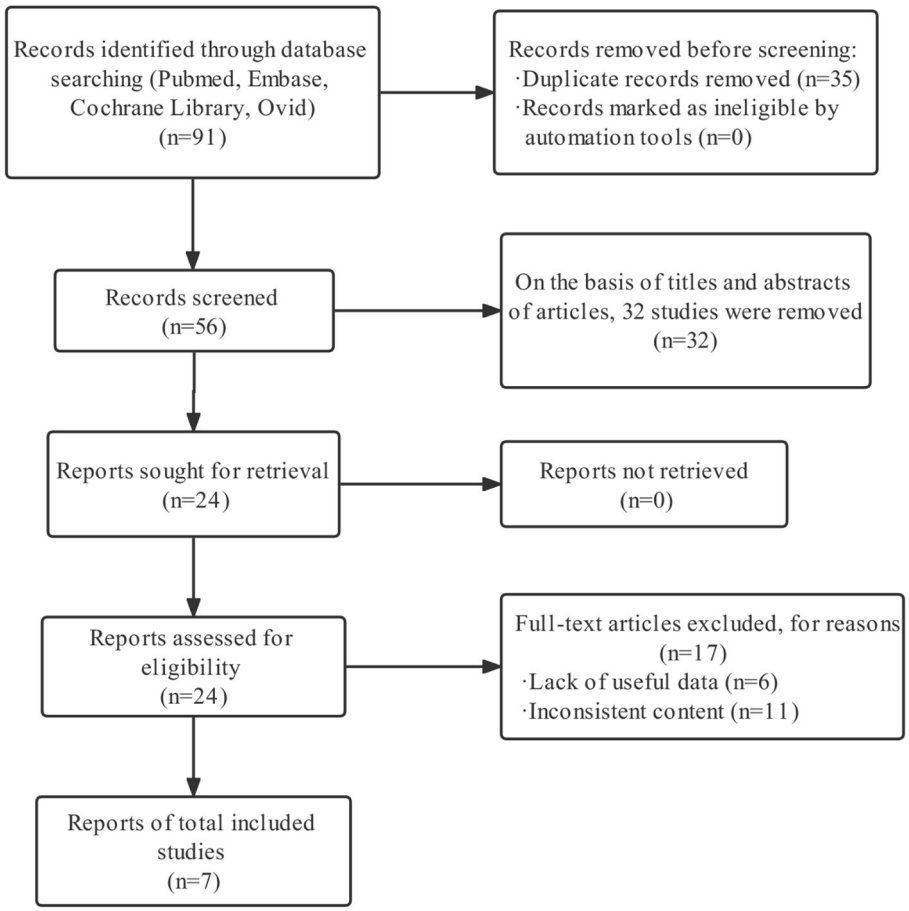

FIGURE 1 | Flow chart presenting the screening process.

Study Quality

According to the NOS scale, the quality evaluation scores of seven cohort study articles were ≥ 7, and the quality was high (**Table 2**).

Result of the Meta-Analysis

Association Between Metformin and Enlargement of Abdominal Aortic Diameter

We analyzed eight cohort studies that enrolled 16,111 patients (prescribe metformin: 5,984 participants; not prescribe metformin: 10,127 participants) to assess the association between metformin and abdominal aortic diameter enlargement. The analysis showed significant heterogeneity among the studies ($I^2 = 83\%$, $P < 0.00001$). Forest plots showed that metformin inhibited the enlargement of abdominal aortic diameter compared to patients not treated with metformin drugs (MD $= -0.72$, 95% CI: – 1.08 ~ -0.37, $P < 0.00001$) (**Figure 2**).

The Egger test was subsequently performed. The results showed $t = -3.03$ ($P = 0.023$), indicating that the meta-analysis findings were subject to publication bias (30, 31). To identify the source of heterogeneity, we further performed the sensitivity analysis and re-did the meta-analysis, removing studies using the item-by-item method. After excluding Fujimura et al., the meta-analysis showed significantly reduced heterogeneity among the studies ($I^2 = 39\%$, $P < 0.00001$) (**Figure 3**).

AAA Repair or AAA Rupture-Related Mortality

Five cohort studies with 75,593 patients analyzed AAA repair or AAA rupture-related mortality changes. There was significant heterogeneity among the cohort studies ($I^2 = 76\%$, $P = 0.002$). The results showed that AAA repair or AAA rupture-related mortality was significantly lower in the group taking metformin than in the group not taking metformin (OR $= 0.80$, 95%*CI*: 0.66 ~ 0.96, $P = 0.02$). Further, the Egger test showed $t = -2.12$ ($P = 0.124$) (**Figure 4**).

DISCUSSION

In this study, a meta-analysis of seven included cohort studies was conducted, in which the relationship between metformin and AAA was examined using the degree of abdominal aortic diameter enlargement as an index. The results showed that metformin limited the enlargement of AAA diameter. At the

TABLE 1 | Characteristics of the included studies.

Study authors and country	Publication year	Study design	Participants	Follow-up duration (mean years)	Outcomes	Adjusted OR (95% CI)/ rates of enlargement (mm/year)	Quality scores
Fujimura et al. (23), America	(2016)	Cohort studies	Elderly patients with diabetes with untreated AAA ($n = 58$)	2.6	Maximum aortic diameter growth measured by contrast-enhanced CT	Patients with AAA prescribed metformin, 0.4 ± 0.6 ($n = 15$) Patients with AAA not prescribed metformin, 1.7 ± 0.5 ($n = 43$)	7
Golledge et al. (24), Australia and New Zealand	(2017)	Cohort studies 1	Elderly patients with AAA (infrarenal aortic diameter ≥ 30 mm) ($n = 1,357$)	3.6	Maximum aortic diameter growth measured by ultrasound	Patients with AAA prescribed metformin, 1.03 ± 2.68 ($n = 118$) Patients with AAA not prescribed metformin, 1.62 ± 2.45 ($n = 1,239$)	8
Golledge et al. (24), Australia and New Zealand	(2017)	Cohort studies 2	Elderly patients with AAA (infrarenal aortic diameter ≥ 30 mm) ($n = 287$)	2.9	Maximum aortic diameter growth measured by contrast enhanced CT	Patients with AAA prescribed metformin, 1.40 ± 2.99 ($n = 39$) Patients with AAA not prescribed metformin,2.55 ± 3.04 ($n = 248$)	8
Golledge et al. (24), Australia and New Zealand	(2017)	Cohort studies 3	Elderly patients with AAA (infrarenal aortic diameter ≥ 30 mm) ($n = 53$)	1	Maximum aortic diameter growth measured by Philips Medical Systems	Patients with AAA prescribed metformin, 0.37 ± 1.28 ($n = 16$) Patients with AAA not prescribed metformin, 1.46 ± 1.52 ($n = 37$)	8
Itoga et al. (25), America	(2018)	Cohort studies	Elderly patients with diabetes and a diagnosis of AAA without rupture ($n = 13,843$)	4.2	Maximum aortic diameters growth determined from radiographic reports	Patients with AAA prescribed metformin, 1.2 ± 1.9 ($n = 5,496$) Patients with AAA not prescribed metformin, 1.5 ± 2.2 ($n = 8,347$)	8
Golledge et al. (26), Australia	(2019)	Cohort studies 1	Patients with asymptomatic unrepaired AAA of any diameter ≥ 30 mm ($n = 1,080$)	3.2	The combined incidence of AAA repair (open or endovascular) or mortality due to AAA rupture (defined as AAA events)	Patients with AAA prescribed metformin, 0.63 ± 1.42 ($n = 129$) Patients with AAA not prescribed metformin,1.15 ± 1.99 ($n = 105$)	8
Golledge et al. (26), Australia	(2019)	Cohort studies 2	Patients with asymptomatic unrepaired AAA of any diameter ≥50 mm ($n = 763$)	3.6	The combined incidence of AAA repair (open or endovascular) or mortality due to AAA rupture (defined as AAA events)	Patients with AAA prescribed metformin, 0.48 ± 1.58 ($n = 106$) Patients with AAA not prescribed metformin, 1.16 ± 2.72 ($n = 75$)	8
Unosson et al. (27), Sweden	(2021)	Cohort studies	Patients with initial abdominal aortic diameter ≥30 mm ($n = 98$)	3.2	Maximum aortic diameter growth measured by ultrasound	Patients with AAA prescribed metformin, 1.1 ± 1.1 ($n = 65$) Patients with AAA not prescribed metformin, 1.6 ± 1.4 ($n = 33$)	8
Sutton et al. (28), American	(2020)	Cohort studies	Male patients with AAA ($n =$ 67,434)	5	Surgery and/or death after the diagnosis of AAA	Death 0.88 (0.85 to 0.91) Death after surgery 0.93 (0.84 to 1.04)	8
Turowicz et al. (29), Poland	(2021)	Cohort studies	Patients undergoing AAA repair ($n = 77$)	0.1	Maximum aortic diameter growth measured by contrast enhanced CT	0.09 (0.02 to 0.47)	7

same time, metformin also reduced AAA repair or AAA rupture-related mortality.

Over the past 20 years, significant progress has been made in the open or endovascular surgical treatment of large, symptomatic, and ruptured AAA. However, there is still a gap in the pharmacological inhibition of minor AAA enlargement. Although numerous clinical trials have shown that pharmacological interventions are ineffective in limiting AAA expansion or disease progression, the available evidence suggests that patients with diabetes are less likely to develop AAA. When an aneurysm is present, they also have a slower rate of aneurysm progression or expansion. Despite the many common risk factors for the development of aneurysmal and cardiovascular diseases, the paradoxical relationship between diabetes and aneurysmal disease remains controversial and insufficiently substantiated for interpretation (32, 33).

In one of the largest studies on the association between diabetes and AAA, which involved 5,697 patients, the results showed that AAA increased by an average of 2.2 mm per year. However, patients with diabetes had an average decrease in AAA growth of 0.5 mm per year compared to patients without diabetes (34). A study by Kristensen et al. (35) reported that AAA patients with high hemoglobin A1c had a slower rate of increase in the aortic vessel diameter than patients with low hemoglobin A1c, regardless of whether the patients had diabetes. A prolonged hyperglycemic environment leads to glycosylation of the extracellular matrix, which further leads to cross-linking of collagen and elastin in the aortic wall. Compared to non-cross-linked collagen, the cross-linked extracellular matrix is more difficult for proteases to cleave, which reduces the release of matrix metalloproteinases and cytokines from inflammatory cells such as monocytes (8, 36). However, a study conducted in 2017 involving 628,264 people who were screened for vascular disease reported that among people without diabetes, the risk of developing an aortic aneurysm increased with higher blood glucose levels in the non-diabetic range, while patients diagnosed with diabetes had a lower risk of aortic aneurysm (37). From this report, we can suggest that the negative association between diabetes and the prevalence and growth of an aortic aneurysm may be due to treatment rather than the presence of diabetes.

In the pharmacological treatment of diabetes, metformin is the drug used for the longest treatment. In cardiovascular disease, there is increasing evidence that metformin protects blood vessels by inhibiting the production of reactive oxygen species, the activity of inflammatory nuclear factor-kB, targets of the mammalian rapamycin (antifungal antibiotic) pathway, autophagy, and mural angiogenesis (38). In rodent studies, it has been reported that metformin inhibits pathological mechanisms of aortic inflammation, extracellular matrix remodeling, and oxidative stress involved in AAA (23, 39).

Metformin is one of the most commonly used drugs for the treatment of diabetes. To support our results, researchers have conducted animal experiments with metformin and modeled an AAA model with porcine pancreatic elastase in normoglycemic mice. The results showed that the incidence and growth rate of AAA were significantly decreased in mice taking metformin. At the same time, it was also shown that in the AAA mouse model

TABLE 2 | The Newcastle-Ottawa Scale (NOS).

Study authors	Quality evaluation	Representativeness of the exposed cohort (1)	Selection of the non-exposed cohort (1)	Ascertainment of exposure (1)	Demonstration that the outcome of interest was not present at the start of the study (1)	Comparison of the ability of cohorts based on the design or analysis (2)	Assessment of the outcome (1)	Was follow-up long enough for the outcomes to occur (1)	Adequacy of the cohort follow-up (1)
Fujimura et al. (23)	7	1	1	1	1	1	0	1	1
Golledge et al. (24)	8	1	1	1	1	2	1	0	1
Itoga et al. (25)	8	1	1	1	1	1	1	1	1
Golledge et al. (26)	8	1	1	1	1	1	1	1	1
Unosson et al. (27)	8	1	1	1	1	1	1	1	1
Sutton et al. (28)	8	1	1	1	1	1	1	1	1
Turowicz et al. (29)	7	1	1	1	1	1	1	0	1

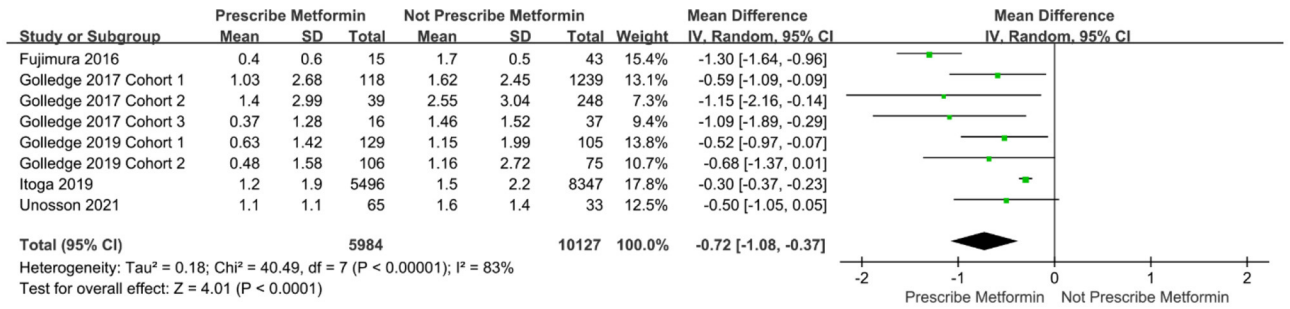

FIGURE 2 | Forest plot for the enlargement of abdominal aortic diameter.

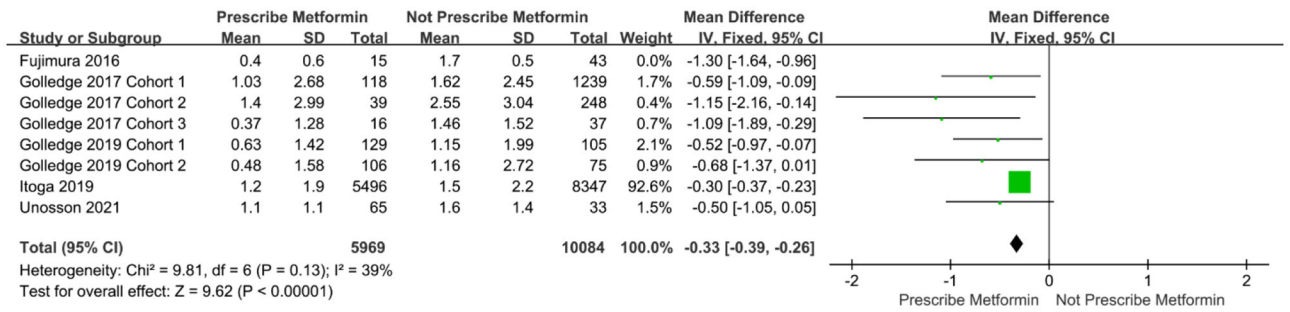

FIGURE 3 | Forest plot after excluding the data on the enlargement of abdominal aortic diameter by Fujimura et al.

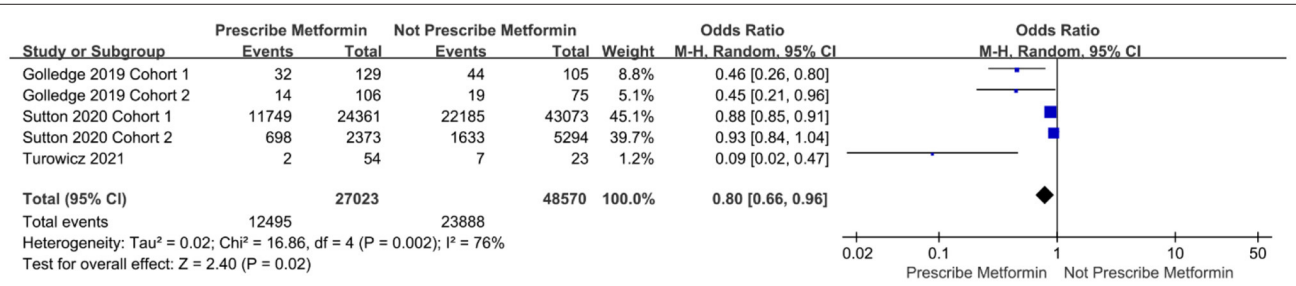

FIGURE 4 | Forest plot for AAA repair or AAA rupture-related mortality.

modeled by angiotensin II, metformin had a protective effect on aneurysms, and this protective mechanism was associated with its ability to activate the AMP-activated protein kinase (AMPK) pathway (39). In addition, as oral hypoglycemic drugs, thiazolidinediones (e.g., pyrazine, rosiglitazone, etc.) regulate peroxisome proliferator-activated receptor-γ (a nuclear hormone receptor family transcription factor), thereby affecting the activity of matrix metalloprotein−9 (MMP-9) and the release of cytokines. Dipeptidyl peptidase—4 (DPP-4) inhibitors (e.g., salbutamol, sitagliptin, etc.) can also reduce the production of reactive oxygen species (ROS) by mitochondria.

A study by Hsu et al. (40) on the relationship between the use of oral hypoglycemic drugs and the risk for aortic aneurysm showed that in patients with diabetes, that risk was lower in patients taking metformin than in those not taking it. Another study by Kristensen et al. (41) showed that patients who took metformin for a prolonged period of time had a lower rate of abdominal aortic aneurysm enlargement relative to those who took metformin for a long time. This also supports the finding that metformin limits the expansion of abdominal aortic aneurysms. Eight additional meta-analyses, including 29,587 patients, reported that metformin significantly inhibited aortic aneurysm enlargement in patients with abdominal aortic aneurysms (95% CI: $-1.38 \sim -0.28$) (42). A recent meta-analysis of 10 studies reported that in patients with type 2 diabetes, metformin drugs reduced the rate of aneurysm diameter growth ($MD = -0.67$, 95% CI: – 1.20 $\sim$ −0.15) and the probability of AAA occurrence (OR = 0.61, 95% *CI*: 0.4 $\sim$ 0.92) (43). This is similar to the results of our review, in which we included more experimental studies that were cohort-based, potentially

reducing selection bias. The results indicated that metformin inhibits the progression of aortic aneurysm diameter and reduces the incidence of abdominal aortic aneurysm and associated mortality after abdominal aortic aneurysm surgery.

Relevant studies have shown that atherosclerosis and AAA share common risk factors, including gender, advanced age, hypertension, and smoking. Therefore, atherosclerosis may be considered a potential pathophysiological mechanism of AAA (44, 45). Vessels are constantly stimulated by hemodynamic perturbations, which lead to changes in vascular smooth muscle cells and promote the release of matrix remodeling enzymes, resulting in vascular structure remodeling. At the same time, due to atherosclerosis, vascular smooth muscle cells get destroyed and lose their function, which promotes the expansion of the intima and ultimately leads to localized medial thinning and rupture of the aortic wall. Sarajlić et al. (46) speculated that hereditary diseases might correlate with diabetes, limiting the progression of AAA. The authors noted that multiple effector kinases are involved in both the AAA and atherosclerotic pathways, which may only be affected by genetic mutations that disrupt the aneurysm pathway. Chen et al. (47) have shown that metformin drugs are feasible for treating cardiovascular disease due to their anti-atherosclerotic and lipid-lowering effects. Some studies suggest that the anti-atherosclerosis effect of metformin may be related to its own effect, further reducing carotid intima-media thickness (CIMT) (48). Another explanation is that metformin drugs are able to inhibit macrophage apoptosis to a certain extent, reduce lipid deposition, and block the process of vascular atherosclerosis development (49).

Metformin has an omnidirectional mode of action, and although it has been used in the treatment of diabetes for more than 60 years, its exact mechanism of action in therapy is still not fully understood (50). According to the findings of *in vitro* studies and animal models, metformin may inhibit the pathological progression of AAA through a variety of mechanisms, including limiting aortic inflammation and reducing extracellular matrix remodeling and oxidative stress (23, 51). It has also been shown that an aneurysm enlargement that metformin inhibits may be associated with decreased secretion of matrix metalloproteinases (MMPs) and interleukin-6 (IL-6) (8). Despite this, there is no uniform consensus regarding the mechanism by which metformin limits the AAA enlargement, which warrants further experimental studies in this area.

In the included literature, studies on the relationship between metformin and AAA were confounded by multiple factors, including age, race, region, and other drugs used to treat diabetes. This may have biased the results of our meta-analysis. In general, we concluded that metformin limited the expansion of AAA, however, there was large variability in the studies. Through the sensitivity analysis, we were able to identify that the source of heterogeneity was likely in the Fujimura et al. (23) study. In that study, the dilatation rate of the abdominal aorta was much higher than in other included studies, and the follow-up time was also longer. However, the quality score for that study was high, its content was sufficient, and the experimental design was reasonable. Based on these quality assessment criteria, there was no reason to exclude the study from the meta-analysis, and its results also show that metformin limits the expansion of AAA.

The limitation of this meta-analysis is that there are only a few existing studies on the relationship between metformin and aortic aneurysm, so the number of articles included in the review is small. At the same time, some studies had smaller sample sizes and shorter follow-up times. Larger samples and longer follow-ups are still needed for further long-term exploration of the association between metformin and AAA. In addition, there is no uniform clinical standard for measuring and reporting AAA, which contributes to differences in accuracy and leads to heterogeneity.

CONCLUSIONS

In summary, we performed a meta-analysis on the association between metformin and AAA. We found that metformin limits the expansion of AAA to a certain extent and reduces the incidence of AAA and postoperative mortality. However, since the mechanism by which metformin inhibits AAA is not precise, further biological experiments and clinical trials are needed to fully elucidate its mode of action.

DATA AVAILABILITY STATEMENT

The original contributions presented in the study are included in the article/supplementary material, further inquiries can be directed to the corresponding authors.

AUTHOR CONTRIBUTIONS

LL and WN: conception and design. GL, RW, and HD: collection and assembly of data. WN, JS, and BY: data analysis and interpretation and manuscript writing. LL and HC: revision of manuscript. All authors contributed to the article and approved the submitted version.

REFERENCES

1. Alund M, Mani K, Wanhainen A. Selective screening for abdominal aortic aneurysm among patients referred to the vascular laboratory. *Eur J Vasc Endovasc Surg.* (2008) 35:669–74. doi: 10.1016/j.ejvs.2007.12.014
2. Baumgartner I, Hirsch AT, Abola MT, Cacoub PP, Poldermans D, Steg PG, et al. Cardiovascular risk profile and outcome of patients with abdominal aortic aneurysm in out-patients with atherothrombosis: data from the Reduction of Atherothrombosis for Continued Health (REACH) registry. *J Vasc Surg.* (2008) 48:808–14. doi: 10.1016/j.jvs.2008.05.026
3. Lederle FA, Johnson GR, Wilson SE, Chute EP, Hye RJ, Makaroun MS, et al. The aneurysm detection and management study screening program: validation cohort and final results. Aneurysm Detection and Management Veterans Affairs Cooperative Study Investigators. *Arch Intern Med.* (2000) 160:1425–30. doi: 10.1001/archinte.160.10.1425

4. Lindholt JS, Juul S, Fasting H, Henneberg EW. Screening for abdominal aortic aneurysms: single centre randomised controlled trial. *BMJ*. (2005) 330:750. doi: 10.1136/bmj.38369.620162.82
5. Sampson UK, Norman PE, Fowkes FG, Aboyans V, Yanna Song, Harrell FE Jr, et al. Global and regional burden of aortic dissection and aneurysms: mortality trends in 21 world regions, 1990 to 2010. *Glob Heart*. (2014) 9:171–80. doi: 10.1016/j.gheart.2013.12.010
6. Erbel R, Aboyans V, Boileau C, Bossone E, Bartolomeo RD, Eggebrecht H, et al. 2014 ESC guidelines on the diagnosis and treatment of aortic diseases: document covering acute and chronic aortic diseases of the thoracic and abdominal aorta of the adult the task force for the diagnosis and treatment of aortic diseases of the European Society of Cardiology (ESC) *Eur Heart J*. (2014) 35:2873–926. doi: 10.1093/eurheartj/ehu281
7. Cao P, De Rango P, Verzini F, Parlani G, Romano L, Cieri E, et al. Comparison of surveillance versus aortic endografting for small aneurysm repair (CAESAR): results from a randomised trial. *Eur J Vasc Endovasc Surg*. (2011) 41:13–25. doi: 10.1016/j.ejvs.2010.08.026
8. Golledge J, Karan M, Moran CS, Muller J, Clancy P, Dear AE, et al. Reduced expansion rate of abdominal aortic aneurysms in patients with diabetes may be related to aberrant monocyte-matrix interactions. *Eur Heart J*. (2008) 29:665–72. doi: 10.1093/eurheartj/ehm557
9. Takagi H, Umemoto T, ALICE. (All-Literature Investigation of Cardiovascular Evidence) group. negative association of diabetes with rupture of abdominal aortic aneurysm. *Diab Vasc Dis Res*. (2016) 13:341–7. doi: 10.1177/1479164116651389
10. Theivacumar NS, Stephenson MA, Mistry H, Valenti D. Diabetes mellitus and aortic aneurysm rupture: a favorable association? *Vasc Endovascular Surg*. (2014) 48:45–50. doi: 10.1177/1538574413505921
11. Dua MM, Miyama N, Azuma J, Schultz GM, Sho M, Morser J, et al. Hyperglycemia modulates plasminogen activator inhibitor-1 expression and aortic diameter in experimental aortic aneurysm disease. *Surgery*. (2010) 148:429–35. doi: 10.1016/j.surg.2010.05.014
12. Thompson A, Cooper JA, Fabricius M, Humphries SE, Ashton HA, Hafez H. An analysis of drug modulation of abdominal aortic aneurysm growth through 25 years of surveillance. *J Vasc Surg*. (2010) 52:55–61. doi: 10.1016/j.jvs.2010.02.012
13. Vasamsetti SB, Karnewar S, Kanugula AK, Thatipalli AR, Kumar JM, Kotamraju S. Metformin inhibits monocyte-to-macrophage differentiation via AMPK-mediated inhibition of STAT3 activation: potential role in atherosclerosis. *Diabetes*. (2015) 64:2028–41. doi: 10.2337/db14-1225
14. Li L, Mamputu JC, Wiernsperger N, Renier G. Signaling pathways involved in human vascular smooth muscle cell proliferation and matrix metalloproteinase-2 expression induced by leptin: inhibitory effect of metformin. *Diabetes*. (2005) 54:2227–34. doi: 10.2337/diabetes.54.7.2227
15. Kim SA, Choi HC. Metformin inhibits inflammatory response via AMPK-PTEN pathway in vascular smooth muscle cells. *Biochem Biophys Res Commun*. (2012) 425:866–72. doi: 10.1016/j.bbrc.2012.07.165
16. Isoda K, Young JL, Zirlik A, MacFarlane LA, Tsuboi N, Gerdes N, et al. Metformin inhibits proinflammatory responses and nuclear factor-kappaB in human vascular wall cells. *Arterioscler Thromb Vasc Biol*. (2006) 26:611–7. doi: 10.1161/01.ATV.0000201938.78044.75
17. Moher D, Liberati A, Tetzlaff J, Altman DG, PRISMA group. Preferred reporting items for systematic reviews and meta-analyses: the PRISMA statement. *J Clin Epidemiol*. (2009) 62:1006–12. doi: 10.1016/j.jclinepi.2009.06.005
18. McInnes MDF, Moher D, Thombs BD. Preferred reporting items for a systematic review and meta-analysis of diagnostic test accuracy studies: the PRISMA-DTA statement. *JAMA*. (2018) 319:388–96. doi: 10.1001/jama.2017.19163
19. Wells G, Shea B, O'Connell D, Robertson J, Peterson J, Welch V, et al. *The Newcastle-Ottawa Scale (NOS) for Assessing the Quality of Nonrandomised Studies in Meta-Analyses[J]*. Ottawa: Ottawa Hospital Research Institute, (2011) 2:1–12.
20. DerSimonian R, Laird N. Meta-analysis in clinical trials revisited. *Contemp Clin Trials*. (2015) 45:139–45. doi: 10.1016/j.cct.2015.09.002
21. Cordero CP, Dans AL. Key concepts in clinical epidemiology: detecting and dealing with heterogeneity in meta-analyses. *J Clin Epidemiol*. (2021) 130:149–51. doi: 10.1016/j.jclinepi.2020.09.045
22. Kriston L. Dealing with clinical heterogeneity in meta-analysis. *Assumptions, Methods, Interpretation Int J Methods Psychiatr Res*. (2013) 22:1–15. doi: 10.1002/mpr.1377
23. Fujimura N, Xiong J, Kettler EB, Xuan H, Glover KJ, Mell MW, et al. Metformin treatment status and abdominal aortic aneurysm disease progression. *J Vasc Surg*. (2016) 64:46–54. doi: 10.1016/j.jvs.2016.02.020
24. Golledge J, Moxon J, Pinchbeck J, Anderson G, Rowbotham S, Jenkins J, et al. Association between metformin prescription and growth rates of abdominal aortic aneurysms. *Br J Surg*. (2017) 104:1486–93. doi: 10.1002/bjs.10587
25. Itoga NK, Rothenberg KA, Suarez P, Ho TV, Mell MW, Xu B. et al. Metformin prescription status and abdominal aortic aneurysm disease progression in the ***US***. *J Vasc Surg*. (2019) 69:710–6. doi: 10.1016/j.jvs.2018.06.194
26. Golledge J, Morris DR, Pinchbeck J, Rowbotham S, Jenkins J, Bourke M, et al. Metformin prescription is associated with a reduction in the combined incidence of surgical repair and rupture related mortality in patients with abdominal aortic aneurysm. *Eur J Vasc Endovasc Surg*. (2019) 57:94–101. doi: 10.1016/j.ejvs.2018.07.035
27. Unosson J, Wågsäter D, Bjarnegård N, De Basso R, Welander M, Mani K, et al. Metformin prescription associated with reduced abdominal aortic aneurysm growth rate and reduced chemokine expression in a Swedish cohort. *Ann Vasc Surg*. (2021) 70:425–33. doi: 10.1016/j.avsg.2020.06.039
28. Sutton SS, Magagnoli J, Cummings TH, Hardin JW. Association between metformin and abdominal aortic aneurysm in diabetic and non-diabetic US veterans. *J Investig Med*. (2020) 68:1015–8. doi: 10.1136/jim-2019-001177
29. Turowicz A, Kobecki J, Laskowska A, Wojciechowski J, Swiatkowski F, Chabowski M. Association of metformin and abdominal aortic aneurysm repair outcomes. *Ann Vasc Surg*. (2021) 75:390–6. doi: 10.1016/j.avsg.2021.02.048
30. Room R. Dealing with publication bias: two possible steps forward. *Drug Alcohol Rev*. (2008) 27:343–4. doi: 10.1080/09595230802090063
31. Jackson D. The implications of publication bias for meta-analysis' other parameter. *Stat Med*. (2006) 25:2911–21. doi: 10.1002/sim.2293
32. Lederle FA. The strange relationship between diabetes and abdominal aortic aneurysm. *Eur J Vasc Endovasc Surg*. (2012) 43:254–6. doi: 10.1016/j.ejvs.2011.12.026
33. De Rango P, Farchioni L, Fiorucci B, Lenti M. Diabetes and abdominal aortic aneurysms. *Eur J Vasc Endovasc Surg*. (2014) 47:243–61. doi: 10.1016/j.ejvs.2013.12.007
34. Sweeting MJ, Thompson SG, Brown LC, Powell JT, RESCAN. collaborators. meta-analysis of individual patient data to examine factors affecting growth and rupture of small abdominal aortic aneurysms *Br J Surg*. (2012) 99:655–65. doi: 10.1002/bjs.8707
35. Kristensen KL, Dahl M, Rasmussen LM, Lindholt JS. Glycated hemoglobin is associated with the growth rate of abdominal aortic aneurysms: a substudy from the VIVA (Viborg Vascular) randomized screening trial. *Arterioscler Thromb Vasc Biol*. (2017) 37:730–6. doi: 10.1161/ATVBAHA.116.308874
36. Dattani N, Sayers RD, Bown MJ. Diabetes mellitus and abdominal aortic aneurysms: a review of the mechanisms underlying the negative relationship. *Diab Vasc Dis Res*. (2018) 15:367–74. doi: 10.1177/1479164118780799
37. Morris D R, Sherliker P, Clack R, Lam H, Carter J, Halliday A, et al. The association of blood glucose and diabetes with peripheral arterial disease involving different vascular territories: results from 628 246 people who attended vascular screening. *Eur Heart J*. (2017) 38:654–654.
38. Diaz-Morales N, Rovira-Llopis S, Bañuls C, Lopez-Domenech S, Escribano-Lopez I, Veses S, et al. Does metformin protect diabetic patients from oxidative stress and leukocyte-endothelium interactions? *Antioxid Redox Signal*. (2017) 27:1439–45. doi: 10.1089/ars.2017.7122
39. Yang L, Shen L, Gao P, Li G, He Y, Wang M, et al. Effect of AMPK signal pathway on pathogenesis of abdominal aortic aneurysms. *Oncotarget*. (2017) 8:92827–40. doi: 10.18632/oncotarget.21608
40. Hsu CY, Su YW, Chen YT, Tsai SH, Chang CC, Li SY, et al. Association between use of oral-antidiabetic drugs and the risk of aortic aneurysm: a nested case-control analysis. *Cardiovasc Diabetol*. (2016) 15:125. doi: 10.1186/s12933-016-0447-9
41. Kristensen KL, Pottegård A, Hallas J, Rasmussen LM, Lindholt JS. Metformin treatment does not affect the risk of ruptured abdominal aortic aneurysms. *J Vasc Surg*. (2017) 66:768–74. doi: 10.1016/j.jvs.2017.01.070

42. Yu X, Jiang D, Wang J, Wang R, Chen T, Wang K, et al. Metformin prescription and aortic aneurysm: systematic review and meta-analysis. *Heart.* (2019) 105:1351–7. doi: 10.1136/heartjnl-2018-314639
43. Yuan Z, Heng Z, Lu Y, Wei J, Cai Z. The protective effect of metformin on abdominal aortic aneurysm: a systematic review and meta-analysis. *Front Endocrinol (Lausanne).* (2021) 12:721213. doi: 10.3389/fendo.2021.721213
44. Shantikumar S, Ajjan R, Porter KE, Scott DJ. Diabetes and the abdominal aortic aneurysm. *Eur J Vasc Endovasc Surg.* (2010) 39:200–7. doi: 10.1016/j.ejvs.2009.10.014
45. Golledge J, Norman PE. Atherosclerosis and abdominal aortic aneurysm: cause, response, or common risk factors? *Arterioscler Thromb Vasc Biol.* (2010) 30:1075–7. doi: 10.1161/ATVBAHA.110.206573
46. Sarajlić A, Gligorijević V, Radak D, PrŽulj N. Network wiring of pleiotropic kinases yields insight into protective role of diabetes on aneurysm. *Integr Biol (Camb).* (2014) 6:1049–57. doi: 10.1039/c4ib00125g
47. Chen Y, Li H, Ye Z, Găman MA, Tan SC, Zhu F. The effect of metformin on carotid intima-media thickness (CIMT): a systematic review and meta-analysis of randomized clinical trials. *Eur J Pharmacol.* (2020) 886:173458. doi: 10.1016/j.ejphar.2020.173458
48. Eilenberg W, Stojkovic S, Piechota-Polanczyk A, Kaider A, Kozakowski N, Weninger WJ, et al. Neutrophil gelatinase associated lipocalin (NGAL) is elevated in type 2 diabetics with carotid artery stenosis and reduced under metformin treatment. *Cardiovasc Diabetol.* (2017) 16:98. doi: 10.1186/s12933-017-0579-6
49. Huangfu N, Wang Y, Cheng J, Xu Z, Wang S. Metformin protects against oxidized low density lipoprotein-induced macrophage apoptosis and inhibits lipid uptake. *Exp Ther Med.* (2018) 15:2485–91. doi: 10.3892/etm.2018.5704
50. Pierotti MA, Berrino F, Gariboldi M, Melani C, Mogavero A, Negri T, et al. Targeting metabolism for cancer treatment and prevention: metformin, an old drug with multi-faceted effects. *Oncogene.* (2013) 32:1475–87. doi: 10.1038/onc.2012.181
51. Hinchliffe RJ. Metformin and abdominal aortic aneurysm. *Eur J Vasc Endovasc Surg.* (2017) 54:679–80. doi: 10.1016/j.ejvs.2017.08.016

Conflict of Interest: The authors declare that the research was conducted in the absence of any commercial or financial relationships that could be construed as a potential conflict of interest.

Publisher's Note: All claims expressed in this article are solely those of the authors and do not necessarily represent those of their affiliated organizations, or those of the publisher, the editors and the reviewers. Any product that may be evaluated in this article, or claim that may be made by its manufacturer, is not guaranteed or endorsed by the publisher.

Copyright © 2022 Niu, Shao, Yu, Liu, Wang, Dong, Che and Li. This is an open-access article distributed under the terms of the Creative Commons Attribution License (CC BY). The use, distribution or reproduction in other forums is permitted, provided the original author(s) and the copyright owner(s) are credited and that the original publication in this journal is cited, in accordance with accepted academic practice. No use, distribution or reproduction is permitted which does not comply with these terms.

frontiers | Frontiers in Cardiovascular Medicine

REVIEW
published: 31 May 2022
doi: 10.3389/fcvm.2022.927542

Applications of Extracellular Vesicles in Abdominal Aortic Aneurysm

Shan Lu[1,2,3†], *Ruihan Wang*[1,2,3†], *Weiguo Fu*[1,2,3*] *and Yi Si*[1,2,3*]

[1] Department of Vascular Surgery, Zhongshan Hospital, Fudan University, Shanghai, China, [2] Vascular Surgery Institute of Fudan University, Shanghai, China, [3] National Clinical Research Center for Interventional Medicine, Shanghai, China

Abdominal aortic aneurysm (AAA) is a localized expansion of the abdominal aorta which can lead to lethal complication as the rupture of aortic wall. Currently there is still neither competent method to predict the impending rupture of aneurysm, nor effective treatment to arrest the progression of small and asymptomatic aneurysms. Accumulating evidence has confirmed the crucial role of extracellular vesicles (EVs) in the pathological course of AAA, acting as important mediators of intercellular communication. Given the advantages of intrinsic targeting properties, lower toxicity and fair stability, EVs show great potential to serve as biomarkers, therapeutic agents and drug delivery carriers. However, EV therapies still face several major challenges before they can be applied clinically, including off-target effect, low accumulation rate and rapid clearance by mononuclear phagocyte system. In this review, we first illustrate the roles of EV in the pathological process of AAA and evaluate its possible clinical applications. We also identify present challenges for EV applications, highlight different strategies of EV engineering and constructions of EV-like nanoparticles, including EV display technology and membrane hybrid technology. These leading-edge techniques have been recently employed in multiple cardiovascular diseases and their promising application in the field of AAA is discussed.

Keywords: aortic abdominal aneurysm, extracellular vesicle, biomarker, therapeutic, engineering

OPEN ACCESS

Edited by:
Zhenjie Liu,
The Second Affiliated Hospital of Zhejiang University School of Medicine, China

Reviewed by:
Li Yin,
University of Virginia, United States
Doran Mix,
University of Rochester, United States

***Correspondence:**
Yi Si
si.yi@zs-hospital.sh.cn
Weiguo Fu
fu.weiguo@zs-hospital.sh.cn

†These authors share first authorship

Specialty section:
This article was submitted to General Cardiovascular Medicine, a section of the journal Frontiers in Cardiovascular Medicine

Received: *24 April 2022*
Accepted: *12 May 2022*
Published: *31 May 2022*

Citation:
Lu S, Wang R, Fu W and Si Y (2022) Applications of Extracellular Vesicles in Abdominal Aortic Aneurysm. Front. Cardiovasc. Med. 9:927542. doi: 10.3389/fcvm.2022.927542

INTRODUCTION

Abdominal aortic aneurysm (AAA) is mainly characterized with immune cell infiltration, extracellular matrix (ECM) degradation and apoptosis of vascular smooth muscle cells (VSMCs), leading to the weakening of vascular wall and dilation of abdominal aorta. The prevalence of AAA reached up to 8% among males aged over 65 years old, and the major complication of AAA is aortic rupture, of which the mortality rate exceeds 80% and causes 150,000–200,000 deaths annually across the world (1, 2). Although computed tomography angiography (CTA) and other advanced imaging techniques can provide accurate anatomic information of AAA such as its location and size, most patients of AAA are asymptomatic before the rupture occurs and the progression of AAA toward rupture is not linear but unpredictable for medical imaging techniques, so sensitive and specific biomarkers are needed to assess the condition of AAA and prevent impending rupture. According to current guidelines, large asymptomatic AAAs (>55 mm diameter in men and >50 mm diameter in women) and symptomatic AAAs are recommended for open repair surgery or endovascular aortic repair (EVAR) (3). In contrast, there are no available therapy options for small asymptomatic AAAs except for regular follower-up and monitoring of the change of AAAs. Currently no convictable evidence can support that commonly used drugs for AAA, such as β-blockers, angiotensin-converting enzyme inhibitors and antiplatelet agents, are beneficial to

the limitation of AAA growth or rupture (4). In such a scenario, the need to identify alternative approaches should be prioritized.

Extracellular vesicle (EV), an important medium for intercellular communication, has drawn researcher's attention in the last few decades and been placed in the limelight in different fields of diseases. EV was first identified in differentiated reticulocytes by Pan et al. (5) in the 1980s but was only regarded as "cellular garbage bags" for expired and degenerative proteins until 2007, when Hadi Valadi et al. (6) discovered that EV contains both mRNA and microRNA (miRNA) that can be transferred to and act on other cells. Since then, a series of studies have reported that EV plays an important role in various stages of the pathogenesis of atherosclerosis, myocardial infarction (MI), ischemia-reperfusion and other cardiovascular diseases (7–9). Exosome is derived from the fusion of intracellular endosomes with the plasma membrane and represents the smallest kind of EV, which is generally 30–150 nm in diameter (10). Despite its small size, exosome is the most important subtype of EV, playing a vital role in mediating cell-to-cell communication. The current review aims to summarize the crucial role and clinical transformation value of exosome/EV in AAAs as a promising source of biomarkers, therapeutic agents and drug delivery carriers.

THE BIOGENESIS AND PERFORMANCE OF EVs IN AAA DEVELOPMENT

EVs consist of a phospholipid bilayer envelope structure with a characteristic cup-shaped appearance, and they can be secreted by almost all types of cells and distributed throughout body fluids, including plasma, saliva, cerebrospinal fluid, lymphatic fluid and urine (11–14). The biogenesis of EVs is generally initiated in the endosome system, in which case they are referred to as exosomes. First, the plasma membrane buds inward and fuses with the primary endocytic vesicles to form early endosomes. Then, the endosome membrane invaginates and sprouts to form multivesicular bodies (MVBs) which contain multiple intraluminal vesicles (ILVs). Exosomes are considered as ILVs that are released to the extracellular environment after the fusion of MVBs with the plasma membrane (12, 15) (**Figure 1**).

After EVs are secreted from cells, they can stably exist in the interstitial fluid, owing to their lipid bilayer structure, which can not only protect EVs themselves from degradation but also ensure the integrity and security of the cargoes carried within. During the process of EV biogenesis, a series of molecular contents with cell biological activity are encapsulated into EVs, such as proinflammatory and anti-inflammatory cytokines, nucleic acids (DNA, RNA, mRNA, miRNA), enzymes and many other proteins (16, 17). The composition of regulatory substances carried by EVs largely depends on the cell type and state of the secretory cells (18). When cells are exposed to hypoxia, inflammation or other stressors, the components of regulatory substances will change, eventually leading to high heterogeneity in the content and types of regulatory substances in EVs. Therefore, changes in the type and quantity of regulatory substances in EVs may reflect the physiological or pathological status of parent cells (6).

EVs involve in multiple pathological processes by modulating cell-cell interaction, which significantly contributes to the progression of AAA. As mentioned above, immune cell infiltration is one of the major characteristics of AAA, and macrophages are found to account for the largest proportion of the infiltrated cells according to a recent single-cell RNA sequencing results (19). These macrophages are recruited mainly to the adventitia and media of the aortic wall and most of them will switch to M1 phenotype (20). The M1 polarization of macrophages will enhance inflammatory response and deteriorate vasculature remodeling by secreting matrix metalloproteinase (MMP), pro-inflammatory cytokines and EVs. Wang et al. (21) revealed that VSMCs incorporate these EVs and implement the messages received from macrophages. The stimulated VSMCs promote the expression of MMP-2, which would degrade surrounding ECM and further vitiate the aortic wall. However, the administration of GW4869, a widely used blocker of EV secretion, can reverse the disruptive effect of dilated aortic, which again verifies that EVs play an important part in the development of AAA. Besides, T cells are another major subset in human AAA, and a positive relationship has been observed between the T cells infiltration and AAA size (22). Dang et al. (23) found that T cell-derived EVs can promote the macrophage migration from circulatory system to aortic wall and subsequently potentiate AAA. In spite of the discovery of the roles of EVs in macrophage-VSMC and T cell-macrophage communication, the functional materials inside EVs, their relevant signal pathways and many other types of involved EVs still remain unclear and need further investigations.

EV-BASED BIOMARKERS AND THERAPIES IN AAA

At present, the diameter of the aorta measured by CTA is considered as the golden standard for AAA diagnosis, and regular follow-ups are required to monitor potential changes of AAA diameter. However, the progression of AAA follows a discontinuous pattern, which may accelerate unexpected between adjacent two follow-ups and cause serious adverse events. In such condition, the identification of effective biomarkers may help to predict the rupture of AAA and avoid potential death. EVs appear to be an intriguing source of biomarkers, for the changes of their circulatory numbers and contents can convey important information and reflect the pathological status of diseases. Martinez-Pinna et al. (24) performed a differential proteomic study based on human plasma-derived EVs and compared the differential expression of proteins in EVs between AAA population and normal population. The number of identified proteins in EVs is higher in AAA group than in normal group, which may indicate a hyper-secretive condition in AAA disease. And the study observed a series of proteins with enhanced expression level including ferritin, mitochondrial Hsp60, c-reactive protein and platelet factor 4, which are all closely related to AAA-relevant pathological mechanisms. Ferritin and Hsp60

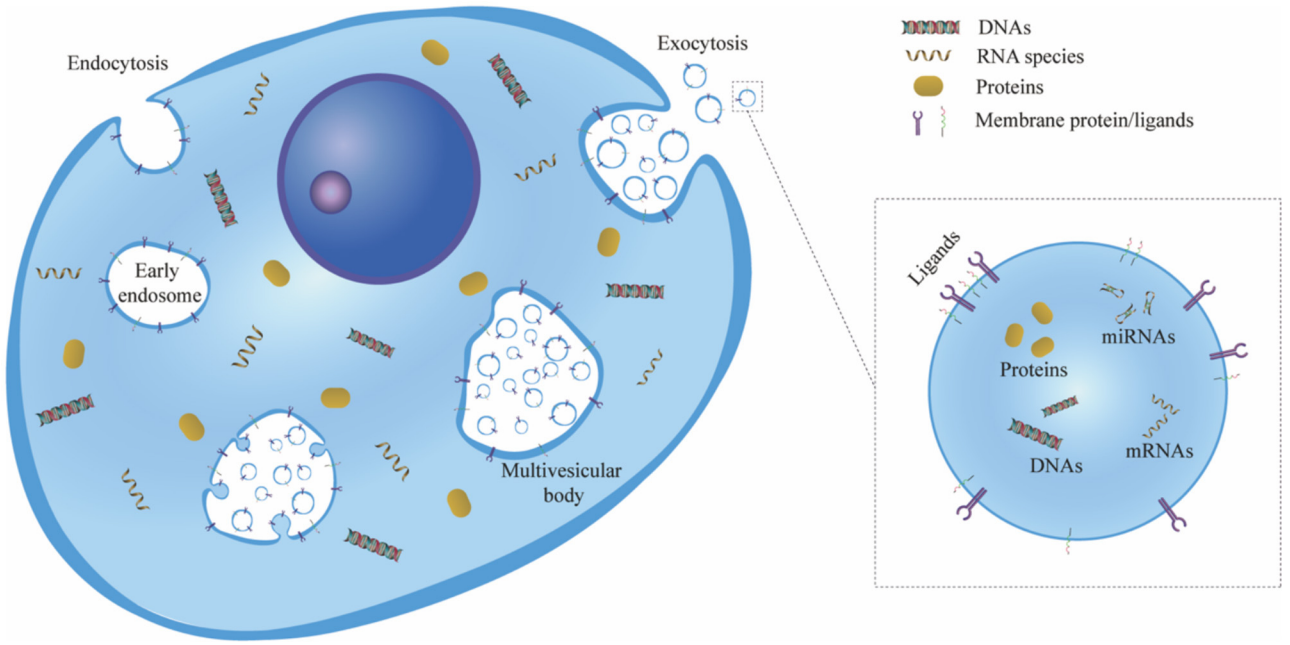

FIGURE 1 | Schematic representation of exosome biogenesis. First, the cell plasma membrane buds inward to form early endosomes via endocytosis. Then, the endosome membrane invaginates and sprouts to form ILVs, and the early endosomes mature and become MVBs. Exosomes are considered ILVs that are released to the extracellular environment owing to the exocytosis of MVBs. ILV, intraluminal vesicle; MVB, multivesicular body.

involve in the oxidative stress and iron deposition in lesion area (25, 26), while c-reactive protein and platelet factor 4 are important participators in the process of inflammatory response and intraluminal thrombogenesis. Fernandez-García et al. (27) also found that ficolin-3, a crucial recognition molecule in the lectin pathway of the complement system, has an increased expression level in EVs separated from AAA patients' serum (28). Moreover, the expression level of ficolin-3 is also found upregulated in EVs isolated from the aortic wall of aneurysm and intraluminal thrombus (ILT) compared to normal aortic wall. This discovery indicates that enhanced ficolin-3 expression in serum is a result of active production and secretion in lesion tissues. Apart from proteins, miRNA is another critical cargo of EVs. It can interact with mRNAs to regulate the protein synthesis activity. Diverse miRNAs can be selectively packed into EVs and transferred from cells to cells to modulate disease-related processes. Recent research enriched EVs from serum of AAA patients and performed small RNA-sequencing to identify potential miRNA biomarkers (29). It turns out that the expressions of miR-122-5p, miR-2110 and miR-483-5p are upregulated in AAA patients' serum. However, to date no individual biomarker has been proven to be sufficient to predict such a complex disease as AAA, so the use of a combination of multiple biomarkers can be a promising approach for clinical application (30).

As in many other cardiovascular diseases, inflammatory response plays a vital role in the development of most AAAs. Chronic AAA is featured with recruitment of large amounts of immune cells, particularly macrophages and T cells, and subsequent ECM degradation and destruction of the aortic wall. The potential of stem cell therapies in AAA treatment has aroused great interest. By injecting stem cells from multiple sources (such as bone marrow, adipose and placenta) intravenously or directly to the adventitia of aortic wall, the development of AAA is evidently restricted (31–34). Further studies suggest the therapeutic effect of stem cell administration comes from the secreted EVs which convey complicated paracrine signals. Growing evidence has confirmed that EV therapy is superior to cell-based treatment in several aspects. While low retention and survival rates limit the progression of stem cell administration, the EV membrane derived from their parent cells ensures high efficiency of transmission (35). EVs can be locally transplanted in the demanded time and space with a defined and accurate dosage, whereas implanted stem cells may undergo apoptosis and subsequently have a low arrival rate to the target area (36). In addition, EVs are more stable for *in vitro* conservation and transportation as non-vital vesicles and more durable for long-term cryopreservation and freeze-thaw processes with little change in their biochemical activities (37). Most importantly, EV therapy prevails over cell-based treatment based on the principle of safety assurance. Burgeoning awareness and concern have been discussed with regard to the safety issues that arise from cell-based treatments, such as tumorigenicity, immunological rejection and occurrence of embolism (38, 39). By contrast, EVs have higher safety and better tolerability due to their low mutagenicity and low immunogenicity. Sun et al. (40) transplanted EVs derived from human umbilical cord mesenchymal stem cells (MSC) into rabbits, guinea pigs and

rats, and no adverse effect were observed with respect to liver or renal function, hemolysis, vascular and muscle stimulation, systemic anaphylaxis, pyrogen or hematology indexes. Clinical trials of EV administration in cancer patients also revealed positive therapeutic outcomes without adverse effects (41, 42).

The therapeutic potential of stem cell-derived EVs has been extensively explored in multiple cardiovascular diseases, especially in myocardial infarction and atherosclerosis (43–47). However, there is currently only a few researches about the application of EV in AAA treatment. Sajeesh et al. (48) investigated the effects of EVs derived from bone marrow-derived MSC (BM-MSC) in the context of AAA rat model. It appears that EVs can tip the balance of the aortic lesion from a proteolytic milieu to an anti-proteolytic one, mainly by suppressing the expression of elastolytic MMP2 and enhancing the expression of natural tissue inhibitor of MMP2 (TIMP-2). Intriguingly, it's reported that MMP2 is primarily overexpressed in small AAAs, whereas large, rupture-prone AAAs mainly exhibit up-regulation of MMP-9 (49, 50). This indicates potential therapeutic value of BM-MSC-derived EVs in the early treatment of small AAAs. Intravenous injection or local administration of therapeutic EVs may help to slow down the course of AAA. As mentioned above, miRNA is a principal cargo of EVs and is closely involved in AAA development. EVs from different cells have diverse miRNA expression profiles and multiple miRNAs have been reported to exert different effects on disease progression. Spinosa et al. (51) defined the critical role of MSC-derived EVs in attenuating the aortic dilation and relieving inflammatory response via miR-147. And the transfection of miR-147 inhibitor in MSC abrogates such therapeutic effect, which in turn confirms the critical role of miR-147. Contrariwise, some miRNAs contribute to the progression of AAA formation. For example, miR-106a is found to down-regulate the expression of TIMP-2 and accelerate VSMC cell apoptosis and ECM degradation (52). Similarly, overexpression of miR-29b appears to augment AAA expansion in a mice model, while the administration of anti-miR-29b triggers a fibrotic response and retards AAA growth (53). And in human AAA tissue samples, a reduction of miR-29b expression is also observed, which may suggest the down regulation of miR-29b is a physiological protective response of the aortic wall to expansion. Local delivery of anti-miRNA drugs via expandable balloons and drug-eluting stents can be innovative avenues for small AAA treatment (54).

Altogether, as important mediators of intercellular communication, EVs can incorporate bioactive molecules and are endowed with intrinsic targeting properties and low immunogenicity because of their inherited membrane from parent cells (55). These characteristics make EVs a more promising drug delivery system than traditional synthetic delivery system (56). However, there are several disadvantages hindering further utilization of EVs in a therapeutic context. Innate EVs lack of specific molecules to exclusively bind with target tissue or cells and their low accumulation rate also adds to the off-target effect (57). Another major challenge is the noteworthy loss rate of circulating EVs due to mononuclear phagocytosis, which leads to rapid clearance and maldistribution of EVs (58). Therefore, different strategies for EV engineering are developed and constructions of bioinspired EV-like nanoparticles are elaborately designed to obtain higher delivery efficiency and better therapeutic effect.

RECENT ADVANCEMENT IN THE ENGINEERING OF THERAPEUTIC EVs

This section will highlight the current promising strategies of EV engineering technologies. Because only very few researches have focused on EV engineering in the field of AAA treatment, we will first broaden our outlook and introduce engineering strategies applied in cardiovascular diseases, and then proposed feasible utilizations in the area of AAA.

EV Display Technology

Although the many advantages of EV bring it further attention as a drug delivery vehicle, an unsatisfactory targeting rate still hinders the clinical use of EV therapies. Natural unmodified EVs are enriched in and cleared by the liver, spleen, kidney and other organs after systematic administration, making it difficult to achieve effective therapeutic concentrations in target organs (59). Selecting an efficient engineering strategy is a necessary step to further improve EV-based therapies. EV display technology, which allows re-engineering of the membrane protein composition, has been extensively studied in the last decade (60).

A popular application of EV display technology is to add targeting ligands via transfection of parent cells with fusion genes of targeting peptides and EV membrane proteins. The overexpression of the fusion protein on the surface of EV membrane can steer the engineered EVs directly toward target area. Lysosomal-associated membrane protein 2 (Lamp2b) is expressed abundantly on the surface of EV, which is extensively chosen as a component of the designed fusion protein (61). Wang et al. (62) engineered Lamp2b fused with ischemic myocardium-targeting peptide CSTSMLKAC (IMTP) to treat myocardial infarction. They found the bioengineered EVs can specifically target ischemic myocardium and exert therapeutic effects on acute myocardial infarction. Similarly, cardiac-targeting peptide (CTP)-Lamp2b is generated and expressed on the EV membrane and it can enhance EV delivery to heart cells and tissue without toxicity (63). In the context of AAA, the features of aneurysm lesions can be utilized as potential targets, involving inflammatory cell infiltration, MMP overexpression, ECM degradation and VSMC apoptosis. Elastin constitutes the tunica media of aortic wall, which is always found degraded in the pathological progression of AAA. Elastin fiber is mainly composed of two components, which are a core of amorphous cross-linked elastin protein and peripheral fibrils (64). Before the degradation of elastin protein, MMPs will first break down the peripheral glycoproteins and thus expose the hydrophobic core of elastin (65). Sinha et al. (66) took advantage of this pathological feature and developed an elastin antibody tethered nanoparticle (EL-NP) to target degraded elastic lamina. They observed in rat AAA model that the EL-NPs can specifically target AAA after systematic administration, and accumulate in the degraded

elastic lamina rather than healthy aorta. Inspired by this, it is plausible to fuse the genes of elastin antibody with Lamp2b, and the overexpressed fusion protein can guide the therapeutic EVs toward target tissue and cells in the dilated aorta. Besides elastin, other characteristic molecules and cells such as collagen, MMP, VSMC and macrophages can also be considered as potential delivery targets for EV engineering (67, 68).

Targeting molecules can also be added to the surface of the EV membrane via a direct chemical engineering approach. Membrane coating technology can provide an excellent platform for the insertion of targeting peptides into EV membrane (69). Polymeric materials, such as polylactic-co-glycolic acid (PLGA) and polyethylene glycol (PEG), are first cocultured with targeting peptides. Then parent cells or EVs are incubated with the polymeric materials-peptide mixture. Polymeric materials can self-assemble to form the membrane-coated structure with anchored targeting peptides, which provide EVs with extended circulation time and promoted targeting ability (70). Wang et al. (71) attached the Arg-Gly-Asp (RGD) peptide to the surface of EVs via linkage to PEG-lipid, which self-assembles into the EV membrane. Since the RGD peptide can specifically bind to integrin $\alpha_V\beta_3$ expressed on the surface of angiogenic blood vessels, RGD can guide bioengineered EVs to blood vessels and promote therapeutic angiogenesis. Likewise, Vandergriff et al. (72) conjugated cardiac homing peptide (CHP) with dioleoylphpatidylethanolamine N-hydroxysuccinimide (DOPE-NHS) and incubated the DOPE-CHP complex with isolated EVs. The lipophilic tails of DOPE-CHP can spontaneously insert into the EV membrane, thus coating EVs with the CHP peptide. The results demonstrated that the engineered EVs exhibit improved viability and elevated targeting ability, which lead to reductions in fibrosis and scar size at the infarcted site and promotion of cellular proliferation and angiogenesis. Similar strategy can be applied to the implantation of elastin antibody or other targeting peptides on EV membrane in AAA treatment. This chemical-based engineering approach elicits a similar effect on the promotion of delivery efficiency compared to the parnet-cell-based methods (73). However, the risk of a possible immune response to synthetic polymers concerns researchers. Despite the surface functionalization provided by the inserted peptides, it's difficult to accurately simulate the complex interfaces of the natural cell membrane merely by adding certain targeting proteins or peptides. More recently, researchers have shifted their interests to utilizing natural cell membrane components as EV coating materials.

In addition to targeting proteins or peptides, other specific compounds, such as magnetic nanoparticles and nucleic acid aptamers, can also be applied to direct exosomes toward target cells and tissues (74–76). Taken together, above-mentioned strategies enhance the targeting abilities of EVs by displaying or modifying specific molecules on the surface of EV membrane (**Figure 2**). However, EV display technology is not without issues. For example, targeting peptides displayed on the surface of EV membrane are sometimes degraded by proteases in the cells or body fluids, resulting in a loss of their targeting ability. Moreover, if the relative molecular weight of targeting peptide is too high, the expression or correct folding of the fusion protein could be disrupted, thereby restricting its effect on EV functions. Therefore, it is of great significance to enhance the durability of targeting peptides to biodegradation and reduce their relative molecular weight to further develop EV display technology.

Membrane Hybrid Technology

As we discussed above, most naturally secreted EVs lack sufficient targeting capability. To achieve a desired therapeutic effect, a higher dosage of EVs is used, but this creates another dilemma in which large amounts of EVs injected in the circulatory system will accumulate in the liver and kidney and cause a series of toxic responses (77). Although adding targeting proteins or peptides on the surface of EV membrane can largely enhance homing efficiency, this approach might be suboptimal since these modifications are often highly labor-intensive and time-consuming processes. Besides, the addition of several functional membrane proteins can hardly simulate the complex interface of the natural cell membrane and the protein-protein interaction network. Cell membrane-camouflaged nanoparticles, which combine the versatile functionalities of different types of cellular membranes with therapeutic nanomaterials, have recently gained increasing attention (78). Membranes from various kinds of cells, such as erythrocytes, leukocytes, platelets, stem cells and even cancer cells, are exploited as carriers to transport drugs to treat a multitude of diseases (70, 74, 78–81). Cell membrane-camouflaged technology has emerged as an interesting biomimetic strategy to imbue nanomaterial with the inherent functions and properties of natural cells for various biomedical applications. Inspired by the cell membrane-camouflaged strategy, biomimetic engineering has been shown to hybridize EV membrane with different cell membranes, which has recently emerged as a novel research avenue to promote the efficiency of EV delivery in various cardiovascular diseases.

Leukocyte infiltration is often a hallmark of inflammatory response in cardiovascular diseases, and monocytes from the circulatory system are the main cell type that infiltrate lesion area and orchestrate tissue remodeling (82). After they are recruited to the injury site, monocytes then differentiate into macrophages and localize to the lesion, playing an important role in ECM remodeling and removal of dead cell debris (20, 83). Multiple adhesive molecules collectively regulate the migration of monocytes, including macrophage receptor 1 (Mac1; also known as integrin αMβ2), P-selectin glycoprotein ligand 1 (PSGL1), very late antigen 4 (VLA4; also known as integrin α4β1) and C-C motif chemokine receptor 2 (CCR2) (84, 85). To utilize their chemotaxis wandering ability, monocytes are processed by cell lysis, differential centrifugation and homogenization to form monocyte membrane vesicles, which are later hybridized with prepared EVs via an incubation-extrusion process. Besides *in vivo* homing ability, monocyte membrane also contains an important signaling protein, CD47, which can act against opsonization and reticuloendothelial system (RES) clearance, thus providing membrane-hybrid EVs with immune evasion ability (86). Zhang et al. (87) constructed monocyte-membrane-hybrid MSC-EVs (Mon-EVs) in a mouse myocardial ischemia-reperfusion injury model. Mon-EVs had a longer circulation time and higher accumulation rate at the lesion than unmodified EVs did, and

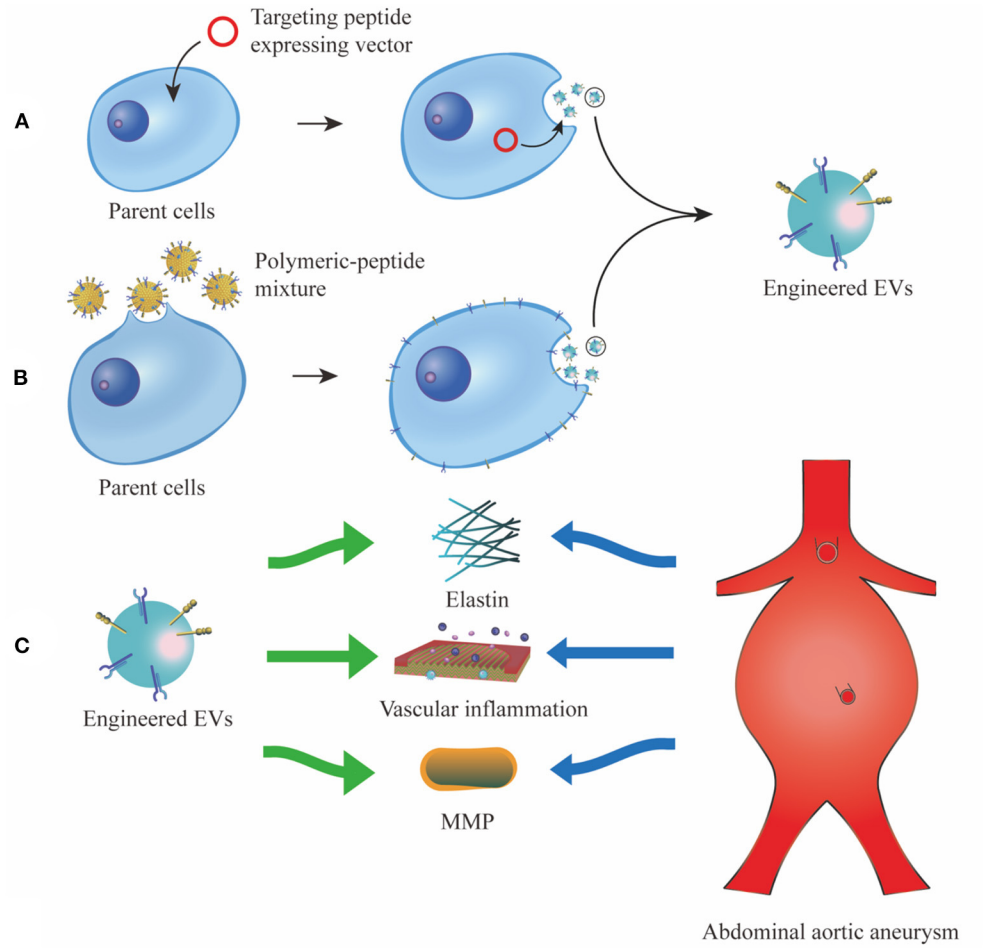

FIGURE 2 | Different strategies of EV display technology. **(A)**, vectors which convey fusion genes of targeting peptides and EV membrane proteins are transfected into the parent cells. The targeting peptides are overexpressed and enriched on the surface of EV membrane. **(B)**, targeting peptides are first cocultured with polymeric material, then the polymeric-peptide mixture self-assembles to the membrane of parent cells and their derived EVs. **(C)**, the engineered EVs can specifically target characteristic tissue and cells in AAA, such as elastin, vascular inflammation and MMP. EV, extracellular vesicle; MMP, matrix metalloproteinase.

Mon-EVs treatment exhibited a more favorable effects on cardiac function and remodeling, neovascularization and endothelial maturation. In the context of human AAA, proinflammatory macrophages are mainly found in the adventitial layer of aortic aneurysm (88). The recruitment of circulatory macrophages to the lesion area largely relies on selectins and multiple chemokine-receptor pathways, especially CCL2/CCR2 axis (89–91). Deficiency of any signaling receptor or ligand has been proved to decrease macrophage accumulation in the aortic wall and reduce aneurysm formation (92–94). The fusion of MSC-derived EVs with monocyte membranes can theoretically endow the hybridized products with an enhanced active targeting efficiency toward the adventitial lesion of AAA, and subsequently achieve a better therapeutic effect.

Platelets are unique anucleate cell fragments which involve in many pathophysiological processes, including atherosclerosis, tumor development and inflammation (95). In circulation, platelets can rapidly adhere to location of vascular lesion and aggregate to form hemostatic plugs. The lipid bilayer of platelet membrane is festooned with transmembrane proteins and other glycoprotein integrins, including membrane binding molecules such as GPIIb/IIIa and CD62P, and immunomodulatory proteins such as CD47 and CD55 (96, 97). The GPIIb/IIIa complex, also known as integrin αIIbβ3, is one of the most abundant receptors expressed on the platelet membrane and plays a pivotal role in mediating platelet aggregation (98). Given the advantages of platelet membrane, Hu et al. (99) constructed platelet-membrane-hybrid exosomes (P-XOs) in the treatment of MI mouse model. Compared to non-modified EVs, P-XOs showed remarkably enhanced cardiac targeting ability because of transmembrane proteins GPIV and GPIX, and integrin-associated tetraspanins CD9 and CD81 on the platelet membrane. Immunomodulatory proteins such as CD47 and CD59 help P-XOs bypass macrophagic clearance, leading to extended circulation time. Consequently, P-XOs exhibited improved therapeutic capacity to promote angiogenesis, inhibit

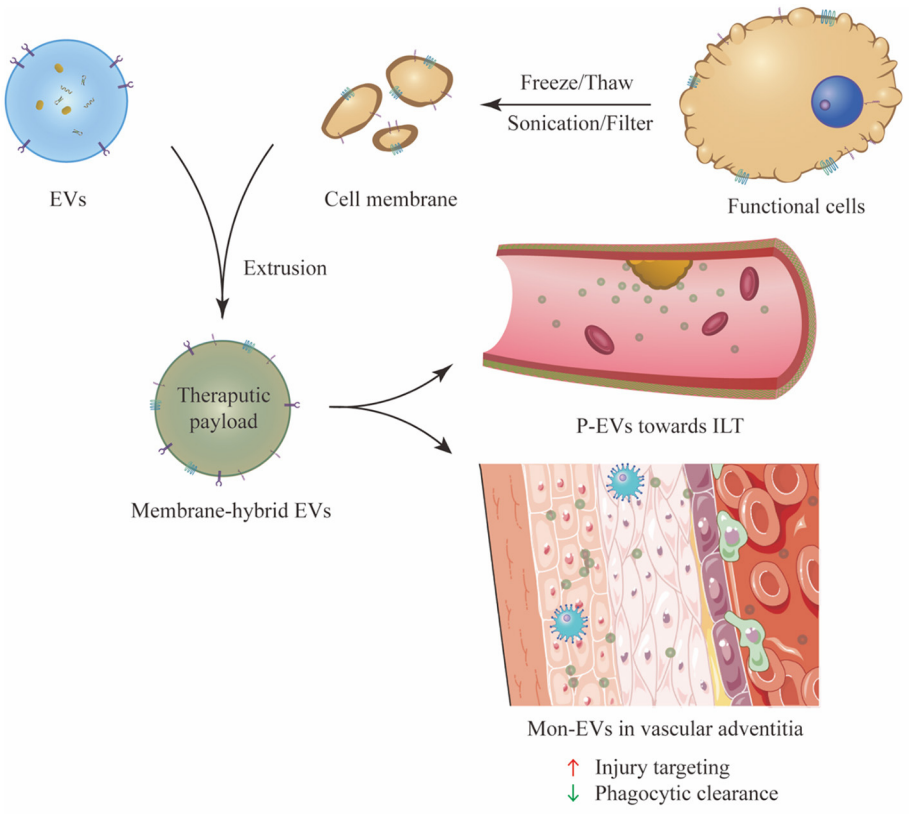

FIGURE 3 | Preparation and experimental application of membrane hybrid technology. P-EVs can actively target the ILT which adheres to the AAA wall, while Mon-EVs mainly accumulate in the adventitia of aortic wall and exert therapeutic effect. The membrane-hybridized EVs exhibit enhanced injury targeting ability and immune evasion ability. P-EV, platelet-membrane-hybrid EV; ILT, intraluminal thrombus; Mon-EVs, monocyte-membrane-hybrid EV.

oxidant injury in cardiomyocytes and ameliorate cardiac function. In the context of AAA, ILT is present in about 75% of all AAAs, which may have both accelerative effect and protective effect on AAA growth and its potential rupture (100). On one hand, ILT is found to harbor large quantities of inflammatory cells and proteases, which degrade AAA matrix and further weaken the aortic wall (101, 102). On the other hand, ILT provides physical cushioning for AAA wall from high hemodynamic stresses, thus protecting patients from abrupt AAA rupture (103, 104). Based on these factors, it's important to steadily dissolve ILT to reduce its proteolytic effect while stabilizing its mechanical shielding structure to protect AAA wall. Sivaraman et al. (105) encapsulated tissue plasminogen activator inside PLGA-nanoparticles and found the slow release of tissue plasminogen activator can gradually lyse ILT without damaging its general structure. Also, the porous structure of ILT facilitates the penetration of therapeutic drugs from circulation toward AAA wall. Further, Pawlowski et al. (106) developed platelet microparticle-inspired nanovesicles, which mimic the membrane interface structure of platelet-derived EVs. These engineered nanovesicles turned to specifically anchor onto thrombus via active platelet integrin GPIIb/IIIa and P-selectin, and then accurately release their thrombolytic payload. Since the platelet membrane can supply targeting ability toward thrombus, it's a plausible approach to load MSC-derived EVs with thrombolytic drugs and hybridize them with platelet membranes, in order to achieve a therapeutic effect at both the ILT and AAA wall.

Membrane hybrid technology has emerged as a novel and versatile strategy to endow EVs with desirable functions and a complex surface interface similar to cell membranes, thereby providing improved drug delivery efficiency; this would otherwise be unachievable via peptide conjugation technology. This method is generalizable to all kinds of EVs with simple procedures of membrane fusion, and it may advance engineered EVs as a promising and preferable tool in the treatment of AAA (**Figure 3**).

CONCLUSIONS

The onset mechanism and different treatments for AAA have gradually been studied in depth, yet to date the mainstream therapies only involve surgical or endovascular repair applied for large or symptomatic AAAs. Effective treatments for small AAAs are absent, and a sensitive monitoring method is needed to predict potential AAA rupture and disease progression. As an important mediator of intercellular communication, EVs offer exciting promise for monitoring and treatment in AAA and possess various advantages, such as membrane stability,

biocompatibility and intrinsic targeting properties. The bioactive molecules inside EVs, including cytokines, enzymes and nucleic acids, especially miRNAs, play a vital role in mediating immune cell infiltration, MMP expression, EMC degradation and VSMC apoptosis. Different drugs can be loaded into EVs or EV-like nanoparticles and delivered toward the lesion to slow, arrest or even reverse the AAA growth (107–109). However, natural EVs lack sufficient targeting ability to specifically bind to the site of injury, and they are easily eliminated by the mononuclear phagocyte system. To overcome these limitations, scientists have developed different strategies, including EV display technology and membrane hybrid technology, to promote targeting ability and immune evasion ability of engineered EVs. But still, the research of EV applications for AAA is in its infancy. Current knowledge regarding the spatial and temporal release of EVs from various cells in the pathogenesis of AAA still largely remains inadequate. Different experiments are required to specify the accurate dosage and frequency of EV administration. And important issues about *in vivo* pharmacokinetic properties, mode of administration and medication safety await comprehensive assessments. To answer these questions, extensive EV research of AAA diagnosis and treatment is essential for the future translation from bench to bedside.

AUTHOR CONTRIBUTIONS

SL and RW conducted the literature review, drafted the manuscript, and prepared the figures. WF and YS edited and revised the manuscript. All authors have substantially contributed to the article and approved the submitted version.

FUNDING

This work was supported by the National Natural Science Foundation of China (Grant 82070497 to YS).

ACKNOWLEDGMENTS

We thank the laboratory affiliated to the Department of Vascular Surgery of Zhongshan Hospital for the core support.

REFERENCES

1. Nordon IM, Hinchliffe RJ, Loftus IM, Thompson MM. Pathophysiology and epidemiology of abdominal aortic aneurysms. *Nat Rev Cardiol.* (2011) 8:92–102. doi: 10.1038/nrcardio.2010.180
2. Golledge J. Abdominal aortic aneurysm: update on pathogenesis and medical treatments. *Nat Rev Cardiol.* (2019) 16:225–42. doi: 10.1038/s41569-018-0114-9
3. Gloviczki P, Lawrence PF, Forbes TL. Update of the society for vascular surgery abdominal aortic aneurysm guidelines. *J Vasc Surg.* (2018) 67:1. doi: 10.1016/j.jvs.2017.11.022
4. Lederle FA, Noorbaloochi S, Nugent S, Taylor BC, Grill JP, Kohler TR, et al. Multicentre study of abdominal aortic aneurysm measurement and enlargement. *Br J Surg.* (2015) 102:1480–7. doi: 10.1002/bjs.9895
5. Pan BT, Teng K, Wu C, Adam M, Johnstone RM. Electron microscopic evidence for externalization of the transferrin receptor in vesicular form in sheep reticulocytes. *J Cell Biol.* (1985) 101:942–8. doi: 10.1083/jcb.101.3.942
6. Valadi H, Ekström K, Bossios A, Sjöstrand M, Lee JJ, Lötvall JO. Exosome-Mediated transfer of mRNAs and microRNAs is a novel mechanism of genetic exchange between cells. *Nat Cell Biol.* (2007) 9:654–9. doi: 10.1038/ncb1596
7. Boulanger CM, Loyer X, Rautou PE, Amabile N. Extracellular vesicles in coronary artery disease. *Nat Rev Cardiol.* (2017) 14:259–72. doi: 10.1038/nrcardio.2017.7
8. Sluijter JPG, Davidson SM, Boulanger CM, Buzás EI, de Kleijn DPV, Engel FB, et al. Extracellular vesicles in diagnostics and therapy of the ischaemic heart: position paper from the working group on cellular biology of the heart of the European society of cardiology. *Cardiovasc Res.* (2018) 114:19–34. doi: 10.1093/cvr/cvx211
9. Loyer X, Zlatanova I, Devue C, Yin M, Howangyin KY, Klaihmon P, et al. Intra-Cardiac release of extracellular vesicles shapes inflammation following myocardial infarction. *Circ Res.* (2018) 123:100–6. doi: 10.1161/CIRCRESAHA.117.311326
10. Helwa I, Cai J, Drewry MD, Zimmerman A, Dinkins MB, Khaled ML, et al. A Comparative study of serum exosome isolation using differential ultracentrifugation and three commercial reagents. *PLoS ONE.* (2017) 12:e0170628. doi: 10.1371/journal.pone.0170628
11. Pathan M, Fonseka P, Chitti SV, Kang T, Sanwlani R, Van Deun J, et al. Vesiclepedia 2019: a compendium of RNA, proteins, lipids and metabolites in extracellular vesicles. *Nucleic Acids Res.* (2019) 47:D516–d9. doi: 10.1093/nar/gky1029
12. van Niel G, D'Angelo G, Raposo G. Shedding light on the cell biology of extracellular vesicles. *Nat Rev Mol Cell Biol.* (2018) 19:213–28. doi: 10.1038/nrm.2017.125
13. Sun Y, Xia Z, Shang Z, Sun K, Niu X, Qian L, et al. Facile preparation of salivary extracellular vesicles for cancer proteomics. *Sci Rep.* (2016) 6:24669. doi: 10.1038/srep24669
14. Ranghino A, Dimuccio V, Papadimitriou E, Bussolati B. Extracellular vesicles in the urine: markers and mediators of tissue damage and regeneration. *Clin Kidney J.* (2015) 8:23–30. doi: 10.1093/ckj/sfu136
15. Hessvik NP, Llorente A. Current knowledge on exosome biogenesis and release. *Cell Mol Life Sci.* (2018) 75:193–208. doi: 10.1007/s00018-017-2595-9
16. Mathivanan S, Ji H, Simpson RJ. Exosomes: extracellular organelles important in intercellular communication. *J Proteomics.* (2010) 73:1907–20. doi: 10.1016/j.jprot.2010.06.006
17. Xu R, Rai A, Chen M, Suwakulsiri W, Greening DW, Simpson RJ. Extracellular vesicles in cancer - implications for future improvements in cancer care. *Nat Rev Clin Oncol.* (2018) 15:617–38. doi: 10.1038/s41571-018-0036-9
18. Vizoso FJ, Eiro N, Cid S, Schneider J, Perez-Fernandez R. Mesenchymal stem cell secretome: toward cell-free therapeutic strategies in regenerative medicine. *Int J Mol Sci.* (2017) 18:1852. doi: 10.3390/ijms18091852
19. Zhao G, Lu H, Chang Z, Zhao Y, Zhu T, Chang L, et al. Single-cell RNA sequencing reveals the cellular heterogeneity of aneurysmal infrarenal abdominal aorta. *Cardiovasc Res.* (2021) 117:1402–16. doi: 10.1093/cvr/cvaa214
20. Raffort J, Lareyre F, Clément M, Hassen-Khodja R, Chinetti G, Mallat Z. Monocytes and macrophages in abdominal aortic aneurysm. *Nat Rev Cardiol.* (2017) 14:457–71. doi: 10.1038/nrcardio.2017.52
21. Wang Y, Jia L, Xie Y, Cai Z, Liu Z, Shen J, et al. Involvement of macrophage-derived exosomes in abdominal aortic aneurysms development. *Atherosclerosis.* (2019) 289:64–72. doi: 10.1016/j.atherosclerosis.2019.08.016
22. Sagan A, Mikolajczyk TP, Mrowiecki W, MacRitchie N, Daly K, Meldrum A, et al. T Cells are dominant population in human abdominal aortic aneurysms and their infiltration in the perivascular tissue correlates with disease severity. *Front Immunol.* (2019) 10:1979. doi: 10.3389/fimmu.2019.01979
23. Dang G, Li T, Yang D, Yang G, Du X, Yang J, et al. T lymphocyte-derived extracellular vesicles aggravate abdominal aortic aneurysm by promoting macrophage lipid peroxidation and migration via pyruvate kinase muscle isozyme 2. *Redox Biol.* (2022) 50:102257. doi: 10.1016/j.redox.2022.102257
24. Martinez-Pinna R, Gonzalez de. Peredo A, Monsarrat B, Burlet-Schiltz O, Martin-Ventura JL. Label-free quantitative proteomic

analysis of human plasma-derived microvesicles to find protein signatures of abdominal aortic aneurysms. *Proteomics Clin Appl.* (2014) 8:620–5. doi: 10.1002/prca.201400010
25. Nchimi A, Defawe O, Brisbois D, Broussaud TK, Defraigne JO, Magotteaux P, et al. MR imaging of iron phagocytosis in intraluminal thrombi of abdominal aortic aneurysms in humans. *Radiology.* (2010) 254:973–81. doi: 10.1148/radiol.09090657
26. Ghosh JC, Siegelin MD, Dohi T, Altieri DC. Heat shock protein 60 regulation of the mitochondrial permeability transition pore in tumor cells. *Cancer Res.* (2010) 70:8988–93. doi: 10.1158/0008-5472.CAN-10-2225
27. Fernandez-García CE, Burillo E, Lindholt JS, Martinez-Lopez D, Pilely K, Mazzeo C, et al. Association of ficolin-3 with abdominal aortic aneurysm presence and progression. *J Thromb Haemost.* (2017) 15:575–85. doi: 10.1111/jth.13608
28. Hummelshoj T, Fog LM, Madsen HO, Sim RB, Garred P. Comparative study of the human ficolins reveals unique features of Ficolin-3 (Hakata antigen). *Mol Immunol.* (2008) 45:1623–32. doi: 10.1016/j.molimm.2007.10.006
29. Hildebrandt A, Kirchner B, Meidert AS, Brandes F, Lindemann A, Doose G, et al. Detection of atherosclerosis by small RNA-sequencing analysis of extracellular vesicle enriched serum samples. *Front Cell Dev Biol.* (2021) 9:729061. doi: 10.3389/fcell.2021.729061
30. Folsom AR, Yao L, Alonso A, Lutsey PL, Missov E, Lederle FA, et al. Circulating biomarkers and abdominal aortic aneurysm incidence: the Atherosclerosis Risk in Communities (ARIC) Study. *Circulation.* (2015) 132:578–85. doi: 10.1161/CIRCULATIONAHA.115.016537
31. Yamawaki-Ogata A, Fu X, Hashizume R, Fujimoto KL, Araki Y, Oshima H, et al. Therapeutic potential of bone marrow-derived mesenchymal stem cells in formed aortic aneurysms of a mouse model. *Eur J Cardiothorac Surg.* (2014) 45:e156–65. doi: 10.1093/ejcts/ezu018
32. Xie J, Jones TJ, Feng D, Cook TG, Jester AA Yi R, et al. Human adipose-derived stem cells suppress elastase-induced murine abdominal Aortic Inflammation and Aneurysm Expansion Through Paracrine Factors. *Cell Transplant.* (2017) 26:173–89. doi: 10.3727/096368916X692212
33. Blose KJ, Ennis TL, Arif B, Weinbaum JS, Curci JA, Vorp DA. Periadventitial adipose-derived stem cell treatment halts elastase-induced abdominal aortic aneurysm progression. *Regen Med.* (2014) 9:733–41. doi: 10.2217/rme.14.61
34. Sharma AK, Lu G, Jester A, Johnston WF, Zhao Y, Hajzus VA, et al. Experimental abdominal aortic aneurysm formation is mediated by IL-17 and attenuated by mesenchymal stem cell treatment. Circulation. 2012;126(11 Suppl. 1):S38-45. doi: 10.1161/CIRCULATIONAHA.111.083451
35. Wang X, Tang Y, Liu Z, Yin Y, Li Q, Liu G, et al. The application potential and advance of mesenchymal stem cell-derived exosomes in myocardial infarction. *Stem Cells Int.* (2021) 2021:5579904. doi: 10.1155/2021/5579904
36. Phinney DG, Prockop DJ. Concise review: mesenchymal stem/multipotent stromal cells: the state of transdifferentiation and modes of tissue repair–current views. *Stem Cells.* (2007) 25:2896–902. doi: 10.1634/stemcells.2007-0637
37. Yu B, Zhang X, Li X. Exosomes derived from mesenchymal stem cells. *Int J Mol Sci.* (2014) 15:4142–57. doi: 10.3390/ijms15034142
38. Fleury A, Martinez MC, Le Lay S. Extracellular vesicles as therapeutic tools in cardiovascular diseases. *Front Immunol.* (2014) 5:370. doi: 10.3389/fimmu.2014.00370
39. Jung JW, Kwon M, Choi JC, Shin JW, Park IW, Choi BW, et al. Familial occurrence of pulmonary embolism after intravenous, adipose tissue-derived stem cell therapy. *Yonsei Med J.* (2013) 54:1293–6. doi: 10.3349/ymj.2013.54.5.1293
40. Sun L, Xu R, Sun X, Duan Y, Han Y, Zhao Y, et al. Safety evaluation of exosomes derived from human umbilical cord mesenchymal stromal cell. *Cytotherapy.* (2016) 18:413–22. doi: 10.1016/j.jcyt.2015.11.018
41. Dai S, Wei D, Wu Z, Zhou X, Wei X, Huang H, et al. Phase I clinical trial of autologous ascites-derived exosomes combined with GM-CSF for colorectal cancer. *Mol Ther.* (2008) 16:782–90. doi: 10.1038/mt.2008.1
42. Morse MA, Garst J, Osada T, Khan S, Hobeika A, Clay TM, et al. A phase I study of dexosome immunotherapy in patients with advanced non-small cell lung cancer. *J Transl Med.* (2005) 3:9. doi: 10.1186/1479-5876-3-9
43. Zhang CS, Shao K, Liu CW Li CJ, Yu BT. Hypoxic preconditioning BMSCs-exosomes inhibit cardiomyocyte apoptosis after acute myocardial infarction by upregulating microRNA-24. *Eur Rev Med Pharmacol Sci.* (2019) 23:6691–9. doi: 10.26355/eurrev_201908_18560
44. Pan J, Alimujiang M, Chen Q, Shi H, Luo X. Exosomes derived from miR-146a-modified adipose-derived stem cells attenuate acute myocardial infarction-induced myocardial damage via downregulation of early growth response factor 1. *J Cell Biochem.* (2019) 120:4433–43. doi: 10.1002/jcb.27731
45. Ju C, Shen Y, Ma G, Liu Y, Cai J, Kim IM, et al. Transplantation of cardiac mesenchymal stem cell-derived exosomes promotes repair in ischemic myocardium. *J Cardiovasc Transl Res.* (2018) 11:420–8. doi: 10.1007/s12265-018-9822-0
46. Wang D, Gao B, Yue J, Liu F, Liu Y, Fu W, et al. Exosomes from mesenchymal stem cells expressing miR-125b inhibit neointimal hyperplasia via myosin IE. *J Cell Mol Med.* (2019) 23:1528–40. doi: 10.1111/jcmm.14060
47. Li J, Xue H, Li T, Chu X, Xin D, Xiong Y, et al. Exosomes derived from mesenchymal stem cells attenuate the progression of atherosclerosis in ApoE(-/-) mice via miR-let7 mediated infiltration and polarization of M2 macrophage. *Biochem Biophys Res Commun.* (2019) 510:565–72. doi: 10.1016/j.bbrc.2019.02.005
48. Sajeesh S, Broekelman T, Mecham RP, Ramamurthi A. Stem cell derived extracellular vesicles for vascular elastic matrix regenerative repair. *Acta Biomater.* (2020) 113:267–78. doi: 10.1016/j.actbio.2020.07.002
49. Goodall S, Crowther M, Hemingway DM, Bell PR, Thompson MM. Ubiquitous elevation of matrix metalloproteinase-2 expression in the vasculature of patients with abdominal aneurysms. *Circulation.* (2001) 104:304–9. doi: 10.1161/01.CIR.104.3.304
50. Sivaraman B, Ramamurthi A. Multifunctional nanoparticles for doxycycline delivery towards localized elastic matrix stabilization and regenerative repair. *Acta Biomater.* (2013) 9:6511–25. doi: 10.1016/j.actbio.2013.01.023
51. Spinosa M, Lu G, Su G, Bontha SV, Gehrau R, Salmon MD, et al. Human mesenchymal stromal cell-derived extracellular vesicles attenuate aortic aneurysm formation and macrophage activation via microRNA-147. *FASEB J.* (2018) 32:fj201701138RR. doi: 10.1096/fj.201701138RR
52. Han ZL, Wang HQ, Zhang TS, He YX, Zhou H. Up-regulation of exosomal miR-106a may play a significant role in abdominal aortic aneurysm by inducing vascular smooth muscle cell apoptosis and targeting TIMP-2, an inhibitor of metallopeptidases that suppresses extracellular matrix degradation. *Eur Rev Med Pharmacol Sci.* (2020) 24:8087–95. doi: 10.26355/eurrev_202008_22493
53. Maegdefessel L, Azuma J, Toh R, Merk DR, Deng A, Chin JT, et al. Inhibition of microRNA-29b reduces murine abdominal aortic aneurysm development. *J Clin Invest.* (2012) 122:497–506. doi: 10.1172/JCI61598
54. San Juan A, Bala M, Hlawaty H, Portes P, Vranckx R, Feldman LJ, et al. Development of a functionalized polymer for stent coating in the arterial delivery of small interfering RNA. *Biomacromolecules.* (2009) 10:3074–80. doi: 10.1021/bm900740g
55. Lu M, Xing H, Yang Z, Sun Y, Yang T, Zhao X, et al. Recent advances on extracellular vesicles in therapeutic delivery: Challenges, solutions, and opportunities. *Eur J Pharm Biopharm.* (2017) 119:381–95. doi: 10.1016/j.ejpb.2017.07.010
56. Chong SY, Lee CK, Huang C, Ou YH, Charles CJ, Richards AM, et al. Extracellular vesicles in cardiovascular diseases: alternative biomarker sources, therapeutic agents, and drug delivery carriers. *Int J Mol Sci.* (2019) 20:3272. doi: 10.3390/ijms20133272
57. Wiklander OP, Nordin JZ, O'Loughlin A, Gustafsson Y, Corso G, Mäger I, et al. Extracellular vesicle *in vivo* biodistribution is determined by cell source, route of administration and targeting. *J Extracell Vesicles.* (2015) 4:26316. doi: 10.3402/jev.v4.26316
58. Wan Z, Zhao L, Lu F, Gao X, Dong Y, Zhao Y, et al. Mononuclear phagocyte system blockade improves therapeutic exosome delivery to the myocardium. *Theranostics.* (2020) 10:218–30. doi: 10.7150/thno.38198
59. O'Loughlin AJ, Woffindale CA, Wood MJ. Exosomes and the emerging field of exosome-based gene therapy. *Curr Gene Ther.* (2012) 12:262–74. doi: 10.2174/156652312802083594
60. Vakhshiteh F, Atyabi F, Ostad SN. Mesenchymal stem cell exosomes: a two-edged sword in cancer therapy. *Int J Nanomedicine.* (2019) 14:2847–59. doi: 10.2147/IJN.S200036

61. Alvarez-Erviti L, Seow Y, Yin H, Betts C, Lakhal S, Wood MJ. Delivery of siRNA to the mouse brain by systemic injection of targeted exosomes. *Nat Biotechnol.* (2011) 29:341–5. doi: 10.1038/nbt.1807
62. Wang X, Chen Y, Zhao Z, Meng Q, Yu Y, Sun J, et al. Engineered exosomes with ischemic myocardium-targeting peptide for targeted therapy in myocardial infarction. *J Am Heart Assoc.* (2018) 7:e008737. doi: 10.1161/JAHA.118.008737
63. Kim H, Yun N, Mun D, Kang JY, Lee SH, Park H, et al. Cardiac-specific delivery by cardiac tissue-targeting peptide-expressing exosomes. *Biochem Biophys Res Commun.* (2018) 499:803–8. doi: 10.1016/j.bbrc.2018.03.227
64. Rosenbloom J, Abrams WR, Mecham R. Extracellular matrix 4: the elastic fiber. *FASEB J.* (1993) 7:1208–18. doi: 10.1096/fasebj.7.13.8405806
65. Sluijter JP, de Kleijn DP, Pasterkamp G. Vascular remodeling and protease inhibition–bench to bedside. *Cardiovasc Res.* (2006) 69:595–603. doi: 10.1016/j.cardiores.2005.11.026
66. Sinha A, Shaporev A, Nosoudi N, Lei Y, Vertegel A, Lessner S, et al. Nanoparticle targeting to diseased vasculature for imaging and therapy. *Nanomedicine.* (2014) 10:1003–12. doi: 10.1016/j.nano.2014.02.002
67. Yin L, Zhang K, Sun Y, Liu Z. Nanoparticle-Assisted diagnosis and treatment for abdominal aortic aneurysm. *Front Med (Lausanne).* (2021) 8:665846. doi: 10.3389/fmed.2021.665846
68. Cheng J, Zhang R, Li C, Tao H, Dou Y, Wang Y, et al. A targeting nanotherapy for abdominal aortic aneurysms. *J Am Coll Cardiol.* (2018) 72:2591–605. doi: 10.1016/j.jacc.2018.08.2188
69. Fang RH, Kroll AV, Gao W, Zhang L. Cell membrane coating nanotechnology. *Adv Mater.* (2018) 30:e1706759. doi: 10.1002/adma.201706759
70. Fang RH, Hu CM, Luk BT, Gao W, Copp JA, Tai Y, et al. Cancer cell membrane-coated nanoparticles for anticancer vaccination and drug delivery. *Nano Lett.* (2014) 14:2181–8. doi: 10.1021/nl500618u
71. Wang J, Li W, Lu Z, Zhang L, Hu Y, Li Q, et al. The use of RGD-engineered exosomes for enhanced targeting ability and synergistic therapy toward angiogenesis. *Nanoscale.* (2017) 9:15598–605. doi: 10.1039/C7NR04425A
72. Vandergriff A, Huang K, Shen D, Hu S, Hensley MT, Caranasos TG, et al. Targeting regenerative exosomes to myocardial infarction using cardiac homing peptide. *Theranostics.* (2018) 8:1869–78. doi: 10.7150/thno.20524
73. Antes TJ, Middleton RC, Luther KM, Ijichi T, Peck KA, Liu WJ, et al. Targeting extracellular vesicles to injured tissue using membrane cloaking and surface display. *J Nanobiotechnology.* (2018) 16:61. doi: 10.1186/s12951-018-0388-4
74. Wang H, Wu J, Williams GR, Fan Q, Niu S, Wu J, et al. Platelet-membrane-biomimetic nanoparticles for targeted antitumor drug delivery. *J Nanobiotechnology.* (2019) 17:60. doi: 10.1186/s12951-019-0494-y
75. Wang Y, Chen X, Tian B, Liu J, Yang L, Zeng L, et al. Nucleolin-Targeted extracellular vesicles as a versatile platform for biologics delivery to breast cancer. *Theranostics.* (2017) 7:1360–72. doi: 10.7150/thno.16532
76. Sivaraman B, Swaminathan G, Moore L, Fox J, Seshadri D, Dahal S, et al. Magnetically-responsive, multifunctional drug delivery nanoparticles for elastic matrix regenerative repair. *Acta Biomater.* (2017) 52:171–86. doi: 10.1016/j.actbio.2016.11.048
77. Wang J, Lee CJ, Deci MB, Jasiewicz N, Verma A, Canty JM, et al. MiR-101a loaded extracellular nanovesicles as bioactive carriers for cardiac repair. *Nanomedicine.* (2020) 27:102201. doi: 10.1016/j.nano.2020.102201
78. Luk BT, Zhang L. Cell membrane-camouflaged nanoparticles for drug delivery. *J Control Release.* (2015) 220:600–7. doi: 10.1016/j.jconrel.2015.07.019
79. Liu W, Ruan M, Wang Y, Song R, Ji X, Xu J, et al. Light-Triggered biomimetic nanoerythrocyte for tumor-targeted lung metastatic combination therapy of malignant melanoma. *Small.* (2018) 14:e1801754. doi: 10.1002/smll.201801754
80. Xuan M, Shao J, Dai L, He Q, Li J. Macrophage cell membrane camouflaged mesoporous silica nanocapsules for *in vivo* cancer therapy. *Adv Healthc Mater.* (2015) 4:1645–52. doi: 10.1002/adhm.201500129
81. Hu CM, Zhang L, Aryal S, Cheung C, Fang RH, Zhang L. Erythrocyte membrane-camouflaged polymeric nanoparticles as a biomimetic delivery platform. *Proc Natl Acad Sci U S A.* (2011) 108:10980–5. doi: 10.1073/pnas.1106634108
82. Nahrendorf M, Swirski FK, Aikawa E, Stangenberg L, Wurdinger T, Figueiredo JL, et al. The healing myocardium sequentially mobilizes two monocyte subsets with divergent and complementary functions. *J Exp Med.* (2007) 204:3037–47. doi: 10.1084/jem.20070885
83. Honold L, Nahrendorf M. Resident and monocyte-derived macrophages in cardiovascular disease. *Circ Res.* (2018) 122:113–27. doi: 10.1161/CIRCRESAHA.117.311071
84. Meisel SR, Shapiro H, Radnay J, Neuman Y, Khaskia AR, Gruener N, et al. Increased expression of neutrophil and monocyte adhesion molecules LFA-1 and Mac-1 and their ligand ICAM-1 and VLA-4 throughout the acute phase of myocardial infarction: possible implications for leukocyte aggregation and microvascular plugging. *J Am Coll Cardiol.* (1998) 31:120–5. doi: 10.1016/S0735-1097(97)00424-5
85. Imhof BA, Aurrand-Lions M. Adhesion mechanisms regulating the migration of monocytes. *Nat Rev Immunol.* (2004) 4:432–44. doi: 10.1038/nri1375
86. Stachelek SJ, Finley MJ, Alferiev IS, Wang F, Tsai RK, Eckells EC, et al. The effect of CD47 modified polymer surfaces on inflammatory cell attachment and activation. *Biomaterials.* (2011) 32:4317–26. doi: 10.1016/j.biomaterials.2011.02.053
87. Zhang N, Song Y, Huang Z, Chen J, Tan H, Yang H, et al. Monocyte mimics improve mesenchymal stem cell-derived extracellular vesicle homing in a mouse MI/RI model. *Biomaterials.* (2020) 255:120168. doi: 10.1016/j.biomaterials.2020.120168
88. Boytard L, Spear R, Chinetti-Gbaguidi G, Acosta-Martin AE, Vanhoutte J, Lamblin N, et al. Role of proinflammatory CD68(+) mannose receptor(-) macrophages in peroxiredoxin-1 expression and in abdominal aortic aneurysms in humans. *Arterioscler Thromb Vasc Biol.* (2013) 33:431–8. doi: 10.1161/ATVBAHA.112.300663
89. Soehnlein O, Lindbom L, Weber C. Mechanisms underlying neutrophil-mediated monocyte recruitment. *Blood.* (2009) 114:4613–23. doi: 10.1182/blood-2009-06-221630
90. Combadière C, Potteaux S, Rodero M, Simon T, Pezard A, Esposito B, et al. Combined inhibition of CCL2, CX3CR1, and CCR5 abrogates Ly6C(hi) and Ly6C(lo) monocytosis and almost abolishes atherosclerosis in hypercholesterolemic mice. *Circulation.* (2008) 117:1649–57. doi: 10.1161/CIRCULATIONAHA.107.745091
91. Ishibashi M, Egashira K, Zhao Q, Hiasa K, Ohtani K, Ihara Y, et al. Bone marrow-derived monocyte chemoattractant protein-1 receptor CCR2 is critical in angiotensin II-induced acceleration of atherosclerosis and aneurysm formation in hypercholesterolemic mice. *Arterioscler Thromb Vasc Biol.* (2004) 24:e174–8. doi: 10.1161/01.ATV.0000143384.69170.2d
92. Moehle CW, Bhamidipati CM, Alexander MR, Mehta GS, Irvine JN, Salmon M, et al. Bone marrow-derived MCP1 required for experimental aortic aneurysm formation and smooth muscle phenotypic modulation. *J Thorac Cardiovasc Surg.* (2011) 142:1567–74. doi: 10.1016/j.jtcvs.2011.07.053
93. Tieu BC, Lee C, Sun H, Lejeune W, Recinos A. 3rd, Ju X, et al. An adventitial IL-6/MCP1 amplification loop accelerates macrophage-mediated vascular inflammation leading to aortic dissection in mice. *J Clin Invest.* (2009) 119:3637–51. doi: 10.1172/JCI38308
94. Hannawa KK, Eliason JL, Woodrum DT, Pearce CG, Roelofs KJ, Grigoryants V, et al. L-selectin-mediated neutrophil recruitment in experimental rodent aneurysm formation. *Circulation.* (2005) 112:241–7. doi: 10.1161/CIRCULATIONAHA.105.535625
95. Garraud O, Cognasse F. Are platelets cells? and if yes, are they immune cells? *Front Immunol.* (2015) 6:70. doi: 10.3389/fimmu.2015.00070
96. Olsson M, Bruhns P, Frazier WA, Ravetch JV, Oldenborg PA. Platelet homeostasis is regulated by platelet expression of CD47 under normal conditions and in passive immune thrombocytopenia. *Blood.* (2005) 105:3577–82. doi: 10.1182/blood-2004-08-2980
97. Li Z, Hu S, Huang K, Su T, Cores J, Cheng K. Targeted anti-IL-1β platelet microparticles for cardiac detoxing and repair. *Sci Adv.* (2020) 6:eaay0589. doi: 10.1126/sciadv.aay0589
98. Bose RJ, Ha K, McCarthy JR. Bio-inspired nanomaterials as novel options for the treatment of cardiovascular disease. *Drug Discov Today.* (2021) 26:1200–11. doi: 10.1016/j.drudis.2021.01.035

99. Hu S, Wang X, Li Z, Zhu D, Cores J, Wang Z, et al. Platelet membrane and stem cell exosome hybrid enhances cellular uptake and targeting to heart injury. *Nano Today*. (2021) 39:101210. doi: 10.1016/j.nantod.2021.101210
100. Sun N, Leung JH, Wood NB, Hughes AD, Thom SA, Cheshire NJ, et al. Computational analysis of oxygen transport in a patient-specific model of abdominal aortic aneurysm with intraluminal thrombus. *Br J Radiol*. (2009) 82 Spec No 1:S18-23. doi: 10.1259/bjr/89466318
101. Kazi M, Thyberg J, Religa P, Roy J, Eriksson P, Hedin U, et al. Influence of intraluminal thrombus on structural and cellular composition of abdominal aortic aneurysm wall. *J Vasc Surg.* (2003) 38:1283–92. doi: 10.1016/S0741-5214(03)00791-2
102. Fontaine V, Jacob MP, Houard X, Rossignol P, Plissonnier D, Angles-Cano E, et al. Involvement of the mural thrombus as a site of protease release and activation in human aortic aneurysms. *Am J Pathol.* (2002) 161:1701–10. doi: 10.1016/S0002-9440(10)64447-1
103. Mower WR, Quiñones WJ, Gambhir SS. Effect of intraluminal thrombus on abdominal aortic aneurysm wall stress. *J Vasc Surg.* (1997) 26:602–8. doi: 10.1016/S0741-5214(97)70058-2
104. Wang DH, Makaroun MS, Webster MW, Vorp DA. Effect of intraluminal thrombus on wall stress in patient-specific models of abdominal aortic aneurysm. *J Vasc Surg.* (2002) 36:598–604. doi: 10.1067/mva.2002.126087
105. Sivaraman B, Sylvester A, Ramamurthi A. Fibrinolytic PLGA nanoparticles for slow clot lysis within abdominal aortic aneurysms attenuate proteolytic loss of vascular elastic matrix. *Mater Sci Eng C Mater Biol Appl.* (2016) 59:145–56. doi: 10.1016/j.msec.2015.09.056
106. Pawlowski CL Li W, Sun M, Ravichandran K, Hickman D, Kos C, et al. Platelet microparticle-inspired clot-responsive nanomedicine for targeted fibrinolysis. *Biomaterials.* (2017) 128:94–108. doi: 10.1016/j.biomaterials.2017.03.012
107. Nosoudi N, Nahar-Gohad P, Sinha A, Chowdhury A, Gerard P, Carsten CG, et al. Prevention of abdominal aortic aneurysm progression by targeted inhibition of matrix metalloproteinase activity with batimastat-loaded nanoparticles. *Circ Res.* (2015) 117:e80–9. doi: 10.1161/CIRCRESAHA.115.307207
108. Sylvester A, Sivaraman B, Deb P, Ramamurthi A. Nanoparticles for localized delivery of hyaluronan oligomers towards regenerative repair of elastic matrix. *Acta Biomater.* (2013) 9:9292–302. doi: 10.1016/j.actbio.2013.07.032
109. Jennewine B, Fox J, Ramamurthi A. Cathepsin K-targeted sub-micron particles for regenerative repair of vascular elastic matrix. *Acta Biomater.* (2017) 52:60–73. doi: 10.1016/j.actbio.2017.01.032

Conflict of Interest: The authors declare that the research was conducted in the absence of any commercial or financial relationships that could be construed as a potential conflict of interest.

Publisher's Note: All claims expressed in this article are solely those of the authors and do not necessarily represent those of their affiliated organizations, or those of the publisher, the editors and the reviewers. Any product that may be evaluated in this article, or claim that may be made by its manufacturer, is not guaranteed or endorsed by the publisher.

Copyright © 2022 Lu, Wang, Fu and Si. This is an open-access article distributed under the terms of the Creative Commons Attribution License (CC BY). The use, distribution or reproduction in other forums is permitted, provided the original author(s) and the copyright owner(s) are credited and that the original publication in this journal is cited, in accordance with accepted academic practice. No use, distribution or reproduction is permitted which does not comply with these terms.

frontiers | Frontiers in Cardiovascular Medicine

ORIGINAL RESEARCH
published: 03 June 2022
doi: 10.3389/fcvm.2022.890228

D-Dimer Is a Diagnostic Biomarker of Abdominal Aortic Aneurysm in Patients With Peripheral Artery Disease

Huoying Cai[1†], Baihong Pan[1†], Jie Xu[2], Shuai Liu[1], Lei Wang[1], Kemin Wu[1], Pu Yang[1], Jianhua Huang[1] and Wei Wang[1,3]*

[1] Department of General and Vascular Surgery, Xiangya Hospital, Central South University, Changsha, China, [2] Department of Epidemiology and Health Statistics, School of Public Health, Central South University, Changsha, China, [3] National Clinical Research Center for Geriatric Disorders, Xiangya Hospital, Central South University, Changsha, China

OPEN ACCESS

Edited by:
Zhenjie Liu,
The Second Affiliated Hospital of Zhejiang University School of Medicine, China

Reviewed by:
Jinwei Xie,
Sichuan University, China
Jianing Yue,
Fudan University, China
Li Yin,
Zhejiang University, China

***Correspondence:**
Wei Wang
wangweicsu@126.com

[†]*These authors have contributed equally to this work and share first authorship*

Specialty section:
This article was submitted to General Cardiovascular Medicine, a section of the journal Frontiers in Cardiovascular Medicine

Received: *05 March 2022*
Accepted: *22 April 2022*
Published: *03 June 2022*

Citation:
Cai H, Pan B, Xu J, Liu S, Wang L, Wu K, Yang P, Huang J and Wang W (2022) D-Dimer Is a Diagnostic Biomarker of Abdominal Aortic Aneurysm in Patients With Peripheral Artery Disease. Front. Cardiovasc. Med. 9:890228. doi: 10.3389/fcvm.2022.890228

Background: Etiology and risk factors of peripheral artery disease (PAD) include age, smoking, and hypertension, etc. , which are shared by an abdominal aortic aneurysm (AAA). Concomitance with AAA in patients with PAD is not rare but is easily overlooked in the clinical situation, though management strategies are altered totally. This study aims to investigate diagnostic biomarkers for the prediction of AAA in patients with PAD.

Methods: A total of 684 patients diagnosed with AAA and/or PAD were enrolled and analyzed retrospectively. Each patient with PAD and AAA was gender and age-matched. Demographic data, medical history, and serum laboratory test profiles were obtained. Statistical analysis was performed to determine diagnostic biomarkers of AAA in patients with PAD.

Results: Firstly, 320 patients with PAD-only and 320 patients with AAA-only were compared. Levels of bilirubin and D-Dimer were decreased, while the incidence of diabetes mellitus, levels of fibrinogen, and platelet count were increased significantly in patients with PAD-only compared with those in patients with AAA-only ($P < 0.001$). Next, 364 patients with PAD (44 patients with AAA) and 364 patients with AAA (44 patients with PAD) were compared. Multivariate logistic regression analysis confirmed the differential distribution of bilirubin, D-dimer, fibrinogen, and platelet count between patients with AAA and patients with PAD ($P < 0.05$). Receiver operator curves (ROC) showed that the area under the curve (AUC) of total bilirubin, direct bilirubin, D-dimer, fibrinogen, and platelet count was 0.6113, 0.5849, 0.7034, 0.6473, and 0.6785, respectively. Finally, to further validate the predictive efficacy of mentioned markers, a multivariable logistics regression analysis was performed between the PAD only group and the PAD with AAA group. The results suggested increased levels of D-dimer in the PAD with AAA group compared to the PAD only group (OR: 2.630, 95% CI:1.639–4.221; $P < 0.001$). In particular, the Youden index suggested that the cut-off value of D-dimer for predicting AAA in patients with PAD was 0.675 mg/L with a sensitivity of 76.9% and a specificity of 84.9% (AUC = 0.8673; 95% CI, 0.8106–0.9240, $P < 0.001$). In all 364 patients with PAD, 41.46% patients were diagnosed AAA when D-dimer

is >0.675 mg/L, while only 3.55% patients were diagnosed AAA when D-dimer ≤0.675 mg/L.

Conclusions: PAD and AAA exert different clinical and serum profiles; D-dimer (>0.675 mg/L) is a reliable biomarker for the prediction of AAA in patients with PAD.

Keywords: abdominal aortic aneurysm, peripheral artery disease, D-dimer, fibrinogen, platelet count

INTRODUCTION

Abdominal aortic aneurysm (AAA) is defined as the dilation of the abdominal aortic artery (≥30 mm, ≥50% normal size) (1, 2). With the aging of the population, the incidence of AAA has been rising significantly, which has become a serious problem threatening health conditions (3, 4). In particular, mortality of ruptured AAA ∼90% if untreated and 40% if treated (5, 6). Early diagnosis and careful monitoring are key to better managing the issue.

Peripheral arterial disease (PAD) is a chronic atherosclerotic disease. PAD leads to chronic ischemia of the lower extremity, manifesting as intermittent claudication or critical limb ischemia. PAD occurs mainly in elderly male patients (7). The prevalence of PAD was up to 10% around the world and is associated with increased mortality and morbidity (8).

Risk factors of PAD include age, gender (male), smoking, hypertension, abnormal blood lipid (8–14), and others, which are shared by AAA. The etiology of these two diseases is also atherosclerosis (15, 16), meaning it is clinically possible that patients with the mentioned risk factors can have PAD and AAA simultaneously (12.1% in the present study), which is easily overlooked by clinicians given that AAA is mostly asymptomatic. However, therapeutic options may vary among those patients. For example, patients with PAD may need first to receive surgical repair of AAA if the diameter is ≥55 mm or careful monitoring of the aorta if the diameter is ≤55 mm.

Therefore, markers to predict AAA in patients with PAD are needed to facilitate health care providers to better screen out AAA in patients with PAD. To date, relatively few studies have specifically investigated the potential value of a blood marker-based approach.

Aim

The aim of this study is to: (1) investigate the similarity and differentia of risk factors of the two diseases, and (2) to explore serum-based diagnostic biomarkers to predict AAA in patients with PAD.

MATERIALS AND METHODS

Enrollment of Study Objects

Six hundred and eighty-four patients who were diagnosed with AAA and/or PAD at the department of vascular surgery, Xiangya Hospital, Central South University from January 2010 to May 2019 were enrolled in this study. Patients can be divided into different groups based on diagnosis: including the AAA only group ($n = 320$), in which patients were diagnosed with AAA, but not with PAD; the PAD only group ($n = 320$); in which patients were diagnosed with PAD but not with AAA; and the PAD + AAA group ($n = 44$), in which patients were diagnosed with both AAA and PAD (**Figure 1**). All procedures were approved by the Institute Review Board of Xiangya Hospital, Central South University (IRB No. 201905267). Patients were informed, and consent forms were obtained for research purposes.

Including criteria for AAA: (1) Age >40 years old; (2) AAA was confirmed by CTA or MRA.

The exclusion criteria are as follows: (1) infectious AAA; (2) secondary AAA with certain causes (such as injury); (3) severe mental illness leading to incapability of cooperation; (4) severe infectious or autoimmune diseases; (5) pregnancy or malignant tumor; and (6) thrombotic diseases such as venous thromboembolism.

The inclusion criteria for PAD were: (1) Age > 40 years; (2) High-risk factors such as smoking, diabetes, hypertension, hyperlipidemia, and others; (3) Symptoms of the ischemic lower extremity; (4) The pulse of the distal arteries of the ischemic limb is weakened or disappeared; (5) Ankle-brachial index (ABI) of ≤0.9; (6) Artery stenosis or occlusion were confirmed by CTA or ultrasound. The clinical diagnosis of PAD can be made if four of the above diagnostic criteria were met.

The exclusion criteria of PAD are as follows: (1) severe infectious or connective tissue diseases; (2) pregnancy or malignant tumor; (3) severe mental illness leading to the incapability of cooperation; and (4) thrombotic diseases such as venous or arterial thromboembolism.

Information Collection

Demographic characteristics, history, and personal history were recorded. Peripheral blood was collected at the time of administration. Specifically, levels of D-dimer were obtained at the time of admission by enzyme-linked immunosorbent assay. Laboratory tests were performed and data were collected.

Statistical Analysis

Kolmogorov-Smirnov test was used to determine whether quantitative data were normally distributed. Quantitative data are shown as a mean ± standard deviation (SD) for normally distributed variables or median (interquartile range) for non-normally distributed variables. Qualitative data are presented as relative frequencies. Chi-square test or Fisher exact test was performed among qualitative data, and Student's *t*-test or Mann Whitney *U*-test was conducted among quantitative data. Multivariate logistic regression analysis was utilized to determine

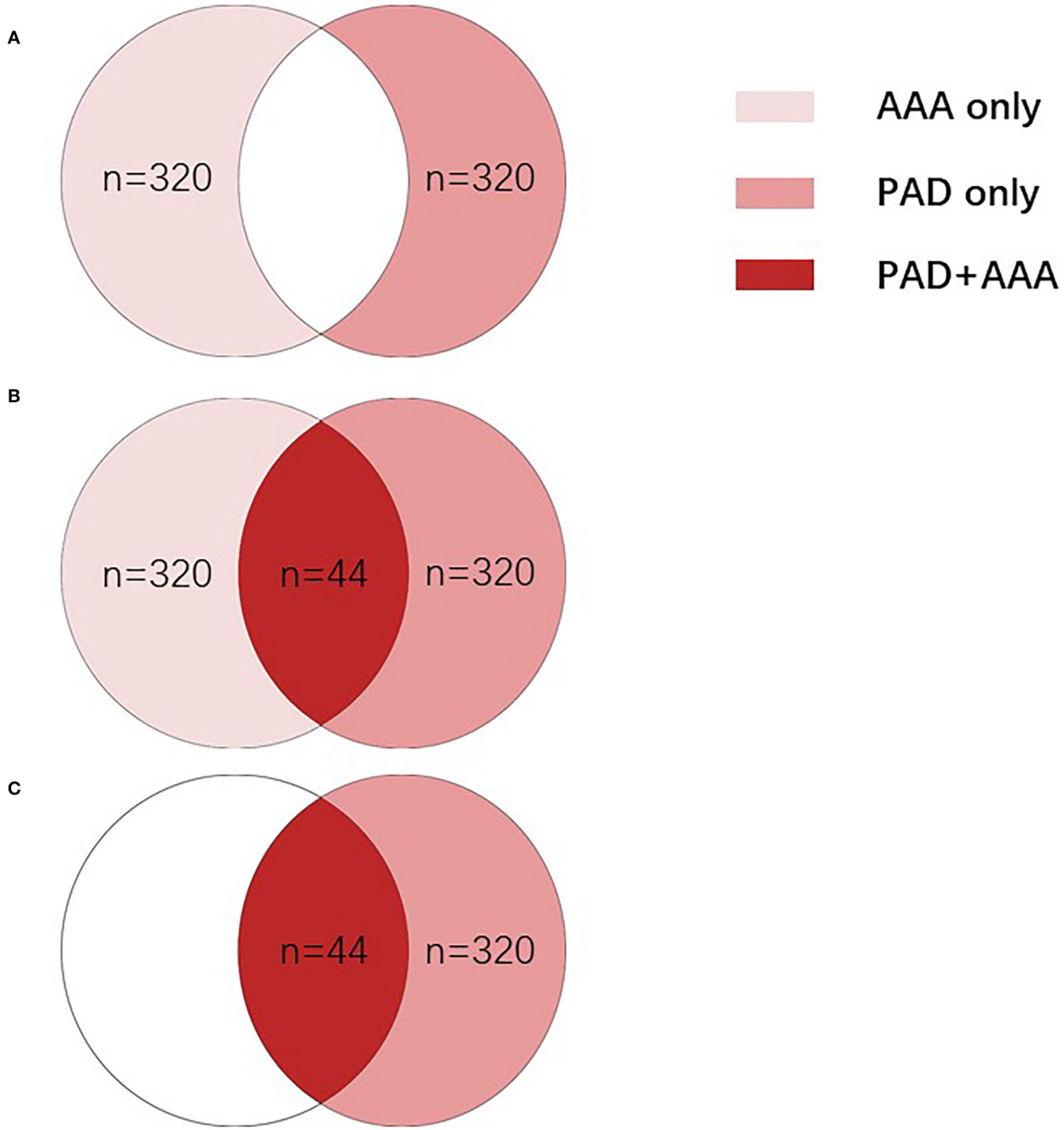

FIGURE 1 | All patients were divided into different groups based on diagnosis. **(A)** To compare the difference between the PAD group and AAA group, AAA only group ($n = 320$), in which patients were diagnosed with AAA without PAD, and the PAD only group ($n = 320$), in which patients were diagnosed with PAD without AAA were enrolled. **(B)** To evaluate whether different indicators can be used to distinguish patients with PAD and patients with AAA, all 684 patients were divided into two groups: the AAA group ($n = 364$), in which patients were diagnosed with AAA only ($n = 320$) or both AAA and PAD ($n = 44$); and the PAD group ($n = 364$), in which patients were diagnosed with PAD only ($n = 320$) or both PAD and AAA ($n = 44$). **(C)** To evaluate whether d-dimer can clinically distinguish patients with PAD with and without AAA, 364 patients were enrolled, including the PAD only group ($n = 320$), in which patients were diagnosed with AAA without PAD and the PAD + AAA group ($n = 44$), in which patients were diagnosed with both AAA and PAD. AAA, abdominal aortic aneurysm; PAD, peripheral arterial disease.

the differential distribution of biomarkers. Receiver operating characteristics (ROC) curves and the area under the curve (AUC) were performed to further assess the diagnostic efficacy of biomarkers. All statistical analyses were performed using the Statistical Product and Service Solutions (SPSS) 22.0 statistical software package (IBM Analytics, Armonk, NY, USA).

RESULTS

Incidence of Diabetes Mellitus and Levels of D-Dimer, Fibrinogen, and Platelet Count Are Differentially Distributed Among Patients With PAD and AAA

Demographic and medical history were recorded. To screen the potential differentially distributed parameters in patients with AAA and patients with PAD, statistical analysis was performed in AAA only group ($n = 320$) and PAD only group ($n = 320$). As shown in **Table 1**, the incidence of diabetes mellitus decreased significantly in AAA only group compared to PAD only group (11.25 vs. 31.56%, $P < 0.01$). No obvious difference in age, gender, hypertension, dyslipidemia, coronary heart disease, cerebral infarction, smoking, or drinking was founded between AAA only group and PAD only group ($P > 0.05$).

To screen the potential differentially distributed serum markers among patients with PAD and patients with AAA, peripheral blood samples were collected at the time of admission, and laboratory tests were performed (liver function, renal function, lipids, coagulation, and platelet count). As shown in **Table 2**, levels of total bilirubin, direct bilirubin, and D-dimer were increased, while levels of fibrinogen and platelet were decreased significantly in AAA only group when compared with those in PAD only group ($P < 0.001$). No obvious difference in TBA, BUN, SCR, uric acid, fasting glucose, low-density lipoprotein cholesterol, high-density lipoprotein cholesterol, triglyceride, total cholesterol, PT, or hemoglobin were found between AAA only group and PAD only group ($P > 0.05$). This suggests that patients with AAA may experience relatively high levels of bilirubin and D-dimer, while patients with PAD may show relatively high levels of fibrinogen and platelet.

The absolute value of circulating parameters in **Table 2** cannot fully reflect the health status of patients since whether those markers are in the normal range is more clinically relevant. Thus, patients in the AAA only group and PAD only group are sub-grouped into a normal or abnormal group (**Table 3**). Statistical analysis was carried out to validate the association of variables with AAA and PAD. As shown in **Table 3**, patients with AAA-only manifested a higher possibility of having an abnormal status of D-dimer, fibrinogen, and platelet count, and a lower possibility

TABLE 1 | Demographic and Clinical Characteristics of patients in AAA only and PAD only group.

Parameter	AAA only $n = 320$	PAD only $n = 320$	*P*-value
Age (years)	67.66 ± 7.96	68.23 ± 7.95	n.s.
Male, *n* (%)	266 (83.1%)	266 (83.1%)	n.s.
Hypertension, *n* (%)	197 (62.56%)	197 (62.56%)	n.s.
Dyslipidemia, *n* (%)	109 (64.50%)	113 (63.66%)	n.s.
DM, *n* (%)	36 (11.25%)	101 (31.56%)	<0.01
CAD, *n* (%)	98 (30.52%)	87 (27.19%)	n.s.
CI, *n* (%)	30 (9.37%)	42 (13.12%)	n.s.
Smoking, *n* (%)	214 (66.87%)	224 (70.00%)	n.s.
Drinking, *n* (%)	114 (35.62%)	120 (37.5%)	n.s.

Quantitative data are presented as mean ± standard deviation or median (interquartile) and are compared with the Student's t-test or Mann Whitney U-test. Qualitative data are presented as relative frequencies and are compared with Chi-square test or Fisher exact test. AAA, abdominal aortic aneurysm; PAD, peripheral artery disease; DM, diabetes mellitus; CAD, coronary artery disease; CI, cerebral infarction; n.s., not significant (p > 0. 05).

TABLE 2 | Blood Laboratory test profiles of patients in AAA only and PAD only group.

Parameter	AAA only $n = 320$	PAD only $n = 320$	*P*-value
Total bilirubin (umol/L)	9.80 (7.12/13.10)	7.90 (5.50/10.57)	<0.001
Direct bilirubin (umol/L)	3.90 (2.90/5.40)	3.35 (2.40/4.40)	<0.001
TBA (umol/L)	4.20 (2.40/6.82)	3.95 (2.50/7.07)	0.936
BUN (mmol/L)	5.64 (4.56/7.18)	5.58 (4.28/7.45)	0.327
SCR (umol/L)	94.00 (81.00/112.90)	91.00 (77. 25/110.75)	0.077
Uric acid (umol/L)*	349.43 ± 104.15	347.09 ± 102.80	0.775
Fasting glucose(mmol/L)	5.17 (4.70/5.97)	5.22 (4.51/6.08)	0.852
TG (mmol/L)	1.35 (0. 93/1.91)	1.50 (1.11/2.44)	0.463
TC (mmol/L)	4.59 (3.83/5.44)	4.52 (3.73/5.19)	0.090
HDL-C(mmol/L)*	1.10 ± 0.32	1.19 ± 0.25	0.501
LDL-C (mmol/L)	2.92 (2.33/3.54)	3.70 (2.85/4.35)	0.118
PT(s)	13.00 (12.50/13.80)	13.00 (12.40/13.80)	0.381
Fibrinogen (g/L)	3.46 (2.73/4.37)	4.45 (4.02/5.75)	<0.001
D-dimer (mg/L)	0.80 (0.45/1.52)	0.280 (0.18/0.46)	<0.001
Hemoglobin(g/L)*	123.80 ± 18.77	123.70 ± 20.82	0.949
Platelet count, $*10^9$/L	168.00 (138.25/213.50)	221.00 (168.00/294.00)	<0.001

*Data is presented as medians (interquartile range, Q1/Q3) or mean ± standard deviation and are compared with the Student's t-test (marked with *) or Mann Whitney U-test. AAA, abdominal aortic aneurysm; PAD, peripheral artery disease; TBA, total bile acid; BUN, blood urea nitrogen; SCR, serum creatinine; TG, triglyceride; TC, total cholesterol; HDL, high-density lipoprotein; LDL, low-density lipoprotein.*

TABLE 3 | Differential distribution of clinical and blood laboratory test parameters in AAA only and PAD only group.

Parameters	Status	AAA only *n* (%)	PAD only *n* (%)	*P*-value	OR (95% CI)
Diabetes mellitus	Yes	36 (26.3)	101 (73.7)	<0.001	0.275 (0.181–0.418)
	No	284 (56.5)	219 (43.5)		
Total bilirubin	normal	33 (55.9)	26 (44.1)	>0.05	1.300 (0.758–2.229)
	abnormal	287 (49.4)	294 (50.6)		
Direct bilirubin	normal	34 (54.0)	29 (46.0)	>0.05	1.193 (0.708–2.010)
	abnormal	286 (49.6)	291 (50.4)		
D-dimer	*normal*	93 (26.9)	253 (73.1)	<0.001	9.217 (6.420–13.232)
	abnormal	227 (77.2)	67 (22.8)		
Fibrinogen	normal	107 (37.4)	179 (62.6)	<0.001	0.396 (0.287–0.545)
	abnormal	213 (60.2)	141 (39.8)		
Platelet count	normal	284 (48.1)	306 (51.9)	0.001	0.361 (0.191–0.683)
	abnormal	36 (72.0)	14 (28.0)		

Data is compared with the Chi-square test or Fisher exact test. Normal range of total bilirubin, direct bilirubin, D-dimer, fibrinogen and platelet count, provided by the Department of Laboratory Medicine, is ≤17.1, ≤6.8, ≤0.5, ≤4, and ≥100, respectively. AAA, abdominal aortic aneurysm; PAD, peripheral artery disease; CI, confidence interval; OR, odds ratio.

of diabetes mellitus when compared with patients with PAD-only ($P < 0.001$). No obvious difference in the abnormal status of total bilirubin and direct bilirubin was identified between AAA only group and PAD only group ($P > 0.05$), which is reasonable due to the median (Q1/Q3) value of total bilirubin and direct bilirubin in **Table 2** are in the normal range (normal range for total bilirubin and is ≤17.1 and ≤6.8, respectively).

Together, the above results suggested that diabetes mellitus, D-dimer, fibrinogen, and platelet count were differentially distributed in patients with AAA when compared to patients with PAD.

D-Dimer, Fibrinogen, and Platelet Count Can Be Used to Distinguish Between Patients With AAA and Patients With PAD

The AAA and PAD share common risk factors including atherosclerosis, age, gender (male), smoking and hypertension, and others. This makes it clinically realistic that a patient with PAD is concomitant with AAA, which is easily overlooked by clinicians, although management strategies are altered totally. To find out variants to distinguish between patients with AAA and patients with PAD, multivariable logistics regression analysis was performed in the AAA group ($n = 364$, **Figure 1B**) and PAD group ($n = 364$, **Figure 1B**). Results in **Table 4** indicated that total bilirubin, direct bilirubin, D-dimer, fibrinogen, and platelet count could be used to distinguish between patients with AAA and patients with PAD ($P < 0.05$).

To further evaluate the diagnostic efficacy of the mentioned markers, the receiver operating characteristic (ROC) curve of the five risk factors mentioned above was performed in the AAA group ($n = 364$, **Figure 1B**) and PAD group ($n = 364$, **Figures 1B**, **2**). **Figure 2F** summarizes detailed information on ROC curves in **Figure 2**. As indicated in **Figure 2F**, D-dimer may be the most optimal biomarker for the distinction between patients with AAA and patients with PAD with the area under the curve (AUC) of 0.7034.

TABLE 4 | Risk factors in AAA group and PAD group.

Risk factors	OR (95% CI)	*P*-value
Total bilirubin (umol/L)	1.159 (1.038–1.295)	0.009
Direct bilirubin (umol/L)	0.778 (0.613–0.987)	0.038
Fibrinogen (g/L)	0.838 (0.726–0.968)	0.016
D-dimer (mg/L)	1.531 (1.244–1.885)	<0.001
Platelet count, $*10^9$/L	0.995 (0.992–0.997)	<0.001

Multivariable logistics regression analysis was performed in AAA group and PAD group. AAA, abdominal aortic aneurysm; PAD, peripheral arterial disease; CI, confidence interval; OR, odds ratio.

D-Dimer Is a Reliable Diagnostic Biomarker of AAA in Patients With PAD Patients

As mentioned above, the main objective of this study was to find out ideal biomarkers for the prediction of AAA in patients with PAD. Total bilirubin, direct bilirubin, D-dimer, fibrinogen, and platelet may potentially be predictive biomarkers of AAA, though OR value or AUC was not that promising between patients with AAA ($n = 364$) and patients with PAD ($n = 364$). To further validate the efficacy of these biomarkers in a more clinically realistic condition, statistical analysis was performed again between the AAA + PAD group ($n = 44$) and the PAD group ($n = 364$).

As shown in **Table 5**, multivariate logistic regression analysis showed that the serum levels of D-dimer increased in AAA + PAD group compared with the PAD group (OR: 2.630, 95% CI:1.639–4.221; $P < 0.001$). No significant difference in fibrinogen and platelet count was found between the AAA + PAD group and the PAD group ($P > 0.05$).

Furthermore, the ROC curve of the D-dimer was carried out (**Figure 3**), and AUC was 0.867. The Youden index suggested that the best cutoff value of D-dimer was 0.675 mg/L (**Table 6** with partial data provided).

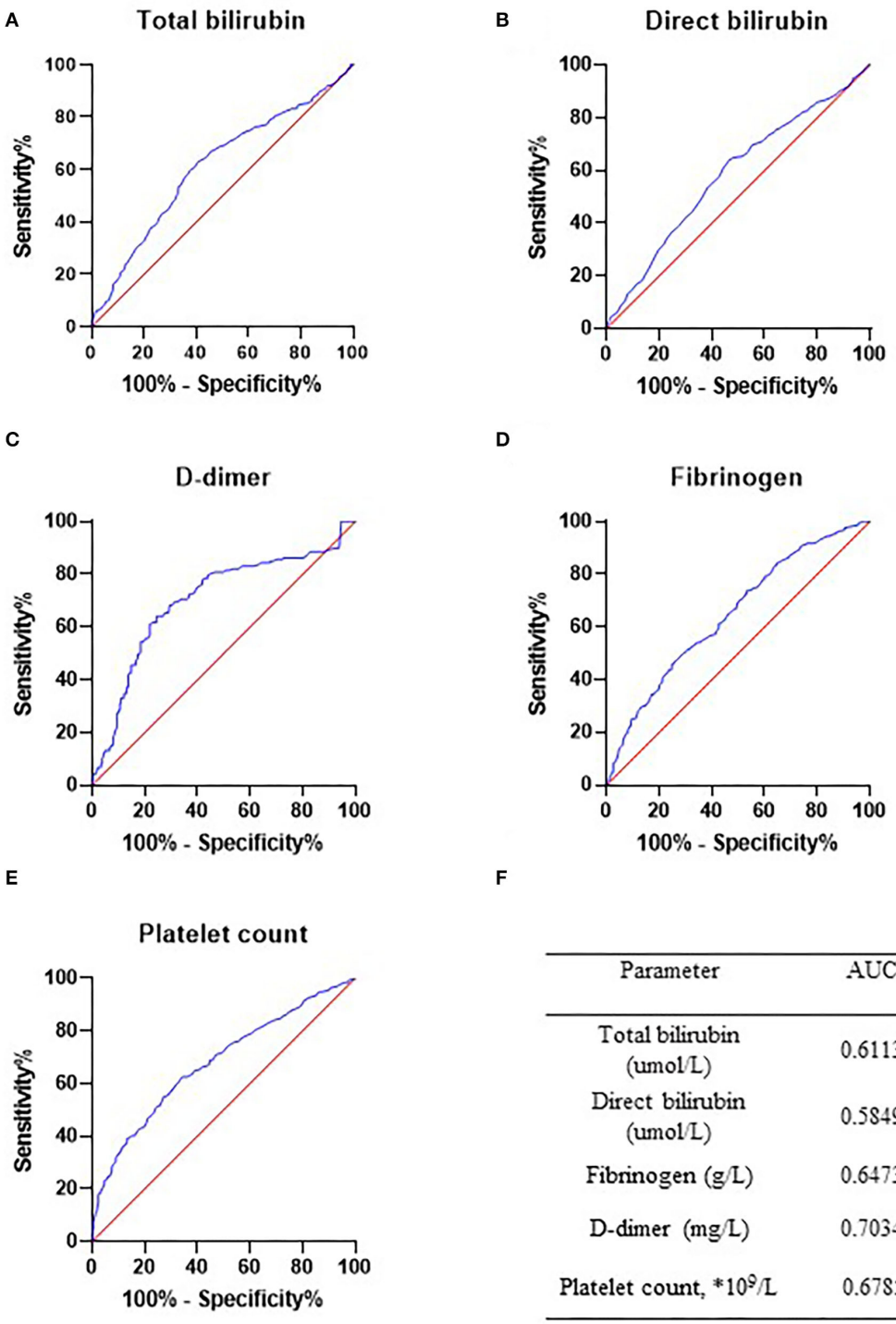

F

Parameter	AUC	95% confidence limit
Total bilirubin (umol/L)	0.6113	0.5703–0.6523
Direct bilirubin (umol/L)	0.5849	0.5436–0.6263
Fibrinogen (g/L)	0.6473	0.6075–0. 6870
D-dimer (mg/L)	0.7034	0.6510–0.7558
Platelet count, $*10^9$/L	0.6785	0.6398–0.7171

FIGURE 2 | Receiver operator characteristic curve in abdominal aortic aneurysm (AAA) group and peripheral arterial disease (PAD) group. Receiver operator characteristic curve of total bilirubin **(A)**, direct bilirubin **(B)**, D-dimer **(C)**, fibrinogen **(D)**, and platelet count **(E)** was drawn in PAD only and AAA only patients. Diagnostic efficacy of these markers was determined. **(F)** Detailed information of ROC curves. AAA, abdominal aortic aneurysm; PAD, peripheral arterial disease.

To better visualize the predictive efficacy of D-dimer for AAA, the 364 patients with PAD were divided into two groups based on D-dimer: D-dimer > 0.65 mg/L, and D-dimer ≤ 0.65 mg/L. As shown in **Figure 4**, 41.46% of patients with PAD were concomitant with AAA when D-dimer was > 0.65 mg/L, while only 3.55% of patients

TABLE 5 | Multivariable logistics regression analysis in AAA+PAD group and PAD group.

Risk factors	OR (95% CI)	*P*-value
Total bilirubin (umol/L)	1.189 (0.947–1.493)	0.136
Direct bilirubin (umol/L)	0.692 (0.408–1.174)	0.172
Fibrinogen (g/L)	0.793 (0.584–1.075)	0.136
D-dimer (mg/L)	2.63 (1.639–4.211)	<0.001
Platelet count, $*10^9$/L	0.997 (0.992–1.002)	0.279

CI, confidence interval; OR, odds ratio; AAA, abdominal aortic aneurysm; PAD, peripheral arterial disease.

with PAD were concomitant with AAA when D-dimer was ≤0.65 mg/L.

DISCUSSION

In this study, we demonstrated that AAA and PAD share a group of risk factors, such as hypertension, dyslipidemia, smoking, and drinking. However, patients with AAA experienced a decreased incidence of diabetes mellitus, lowered levels of fibrinogen and platelet count, and upregulated levels of D-dimer and bilirubin. Our study further validates the diagnostic efficacy of these markers for the prediction of AAA and suggests that D-dimer is a promising biomarker with satisfying sensitivity and specificity. Patients with PAD with D-dimer of ≥0.675 indicated a highly possible presence of AAA.

Studies have revealed that hypertension, smoking, cardiovascular diseases, dyslipidemia, cerebrovascular disease, and renal insufficiency are well-defined risk factors for AAA (17–22). Researchers have also suggested that hypertensive, smoking, and dyslipidemia individuals have a higher risk of PAD (14, 23, 24). The dominant etiology of PAD and AAA is arterial atherosclerosis. Thus, it is clinically realistic that patients with PAD are concomitant with AAA (**Figure 1**). To date, relatively few studies have specifically focused on the potential value of a blood marker-based approach for clinicians to screen whether patients have PAD combined with AAA. Our results show that D-dimer helps predict AAA in patients with PAD in a time- and cost-effective manner over ultrasound-based screening of AAA. Coagulation status test, including D-dimer is routine, at least in China, prior to surgical treatment of PAD, thus, clinicians are less likely to ignore the dramatic increase of D-dimer in patients with PAD. The likelihood of neglecting AAA in patients with PAD is decreased significantly without the extra costs of time and money.

As is well-demonstrated, a large volume of intraluminal aortic thrombus is common in patients with AAA (25, 26), resulting from activated coagulation status inside an aneurysm. D-dimer is the degradative product of fibrin, and increased levels of D-dimer indicate the presence of coagulation procedure and secondary hyperfibrinolysis. Thus, circulating D-dimer in patients with AAA originates from fibrinolysis of intraluminal thrombus, which explains increased levels of D-dimer in patients with AAA (**Table 2**). Our finding is consistent with previous studies, which have confirmed the diagnostic value of D-dimer for AAA (27–30). However, control group in those studies is non-atherosclerotic population even healthy subjects. The conclusions obtained from these studies may not be applicable among athero-thrombosis diseases, for example, PAD, since AAA and PAD share common risk factors and etiologies. Our research has filled gaps in knowledge and the inclusion of patients with PAD in this study is important in distinguishing patients with AAA from PAD not only in the general population, but serum D-dimer also facilitates the diagnosis of AAA in symptomatic PAD individuals.

Currently, D-dimer is widely used as an exclusion of venous thrombo-embolism and is regarded as cost- and time-effective. As shown in **Figure 4**, only 3.55% of patients with PAD were

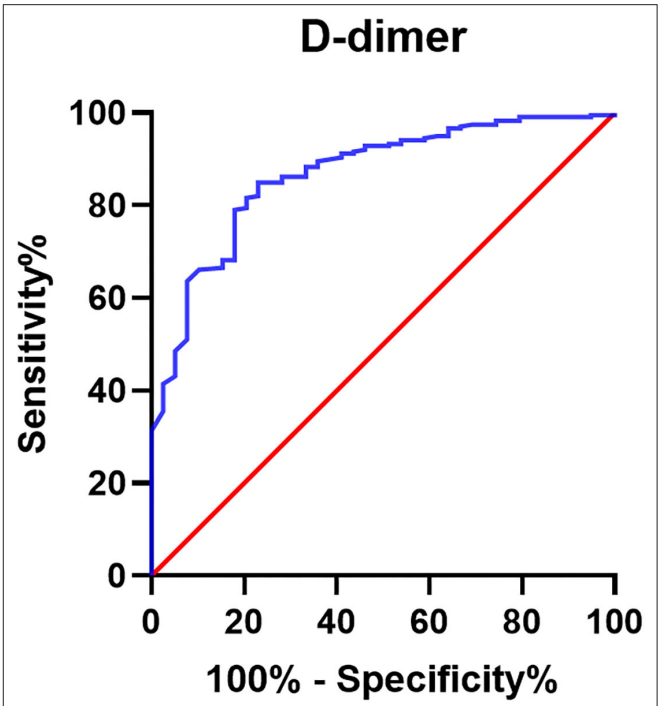

FIGURE 3 | Receiver operator characteristic curve of D-dimer for prediction of AAA in PAD group. Receiver operator characteristic curve of D-dimer was drawn for the prediction of AAA in patients with PAD ($n = 364$). The AUC of D-dimer is 0.867.

TABLE 6 | Diagnostic efficacy of D-dimer for AAA determined by Youden index.

D-dimer	Sensitivity	Specificity	Youden index
0.6750	0.769	0.849	0.619
0.6600	0.769	0.845	0.614
0.5050	0.821	0.791	0.611
0.5550	0.795	0.816	0.611
0.6450	0.769	0.841	0.610
0.5400	0.795	0.812	0.607
0.4950	0.821	0.782	0.603

Youden index was determined to evaluate diagnostic efficacy of D-dimer.

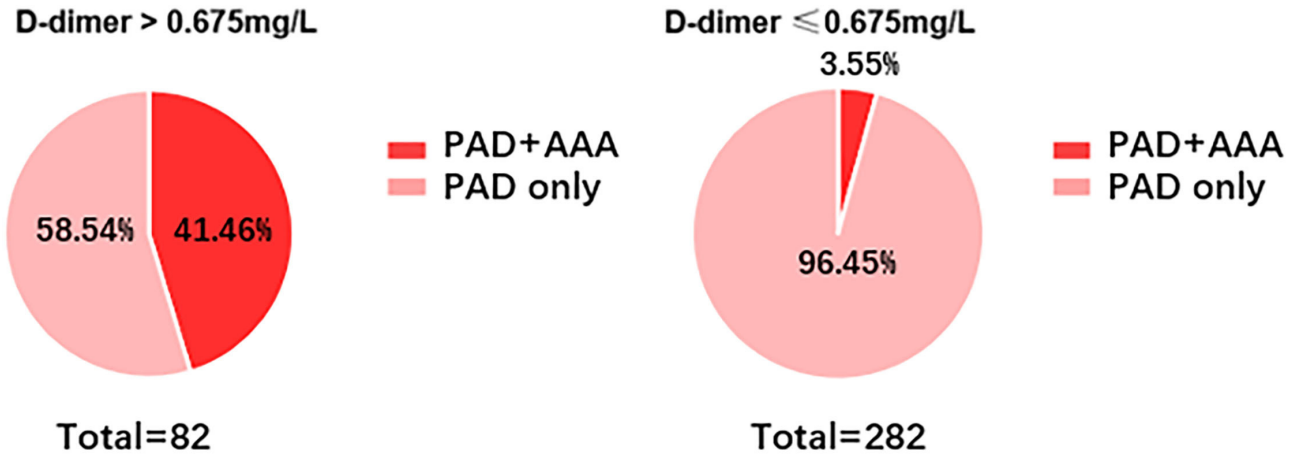

FIGURE 4 | Incidence of AAA in patients with PAD with different levels of D-dimer. Incidence of AAA was determined in patients with PAD when D-dimer is ≤0.675 mg/L or ≥0.675 mg/L.

diagnosed with AAA. Therefore, we can similarly take advantage of D-dimer ≤0.675 mg/L as an exclusion biomarker of AAA in patients with PAD.

As we know, platelet and fibrinogen are fundamental materials for coagulation, and conversion of fibrinogen to fibrin and platelet aggression are key steps in the coagulation procedure. Thus, constant coagulation will lead to the consumption of platelet and fibrinogen. This may explain the findings of the present study, that patients with AAA exerted decreased levels of platelet and fibrinogen compared with patients with PAD (**Tables 2–4**). These observations are consistent with previous publications (31–33).

In accordance with others, the prevalence of diabetes is decreased in patients with AAA and increased significantly in patients with PAD (**Tables 1**, **3**). Some epidemiological studies indicate that diabetes is a protective factor for AAA and can inhibit the occurrence and progression of AAA (34, 35). The underlying mechanism may be that metformin prescription is associated with decreased AAA enlargement (36). Diabetes is also a well-recognized risk factor for PAD.

Our study has several limitations. First, the study was performed in a single-center with a limited sample size. A large scale and multicenter study is a necessity to further validate the conclusions. Second, diagnostic accuracy can be compromised when patients with PAD are experiencing atherosclerotic thrombosis due to active coagulation and fibrinolysis processes in the lower extremities.

CONCLUSION

Our study has revealed differentially distributed serum markers (bilirubin, D-dimer, fibrinogen, and platelet) and the prevalence of diabetes among patients with AAA and patients with PAD. Particularly, the serum level of D-dimer is a promising biomarker for the presence of AAA in patients with PAD. A patient with PAD with a D-dimer of ≥0.675 mg/L requires further evaluation for the presence of AAA.

DATA AVAILABILITY STATEMENT

The original contributions presented in the study are included in the article/supplementary material, further inquiries can be directed to the corresponding author.

ETHICS STATEMENT

The studies involving human participants were reviewed and approved by Ethics Committee of Xiangya Hospital, Central South University. The patients/participants provided their written informed consent to participate in this study.

AUTHOR CONTRIBUTIONS

WW and JH conceived and designed the study. HC, LW, SL, KW, and PY collected the data. HC, BP, JX, LW, SL, and WW analyzed the data. HC and BP wrote the manuscript. BP, KW, PY, JH, and WW provided a substantial revision of the manuscript. WW obtained funding. All authors have read and approved the final manuscript.

FUNDING

This study was funded by the National Natural Science Foundation of China (No. 81873525), the Clinical Research Project of Xiangya hospital, CSU, and the project was sponsored by the Scientific Research Foundation for the Returned Overseas Chinese Scholars, State Education Ministry.

REFERENCES

1. LeFevre ML. Screening for abdominal aortic aneurysm: U.S. preventive services task force recommendation statement annals of internal medicine. *Ann Intern Med.* (2014) 161:281–90. doi: 10.7326/M14-1204
2. Alcorn HG, Wolfson SK Jr, Sutton-Tyrrell K, Kuller LH, O'Leary D. Risk factors for abdominal aortic aneurysms in older adults enrolled in the cardiovascular health study. *Arterioscler Thromb Vasc Biol.* (1996) 16:963–70. doi: 10.1161/01.ATV.16.8.963
3. Huang T, Liu S, Huang J, Xu B, Bai Y, Wang W. Meta-analysis of the growth rates of abdominal aortic aneurysm in the Chinese population. *BMC Cardiovasc Disord.* (2019) 19:204. doi: 10.1186/s12872-019-1160-x
4. Yu J, Liu S, Huang J, Wang W. Current theories and clinical trial evidence for limiting human abdominal aortic aneurysm growth. *Curr Drug Targets.* (2018) 19:1302–8. doi: 10.2174/1389450118666171113114310
5. Sampson UK, Norman PE, Fowkes FG, Aboyans V, Song Y, Harrell FE Jr, et al. Estimation of global and regional incidence and prevalence of abdominal aortic aneurysms 1990 to 2010. *Glob Heart.* (2014) 9:159–70. doi: 10.1016/j.gheart.2013.12.009
6. Huang J, Li G, Wang W, Wu K, Le T. 3D printing guiding stent graft fenestration: a novel technique for fenestration in endovascular aneurysm repair. *Vascular.* (2017) 25:442–6. doi: 10.1177/1708538116682913
7. Hamur H, Onk OA, Vuruskan E, Duman H, Bakirci EM, Kucuksu Z, et al. Determinants of chronic total occlusion in patients with peripheral arterial occlusive disease. *Angiology.* (2017) 68:151–8. doi: 10.1177/0003319716641827
8. Norgren L, Hiatt WR, Dormandy JA, Nehler MR, Harris KA, Fowkes FG, et al. Inter-society consensus for the management of peripheral arterial disease (Tasc II). *J Vasc Surg.* (2007) 45:S5–67. doi: 10.1016/j.jvs.2006.12.037
9. Folsom AR, Yao L, Alonso A, Lutsey PL, Missov E, Lederle FA, et al. Circulating biomarkers and abdominal aortic aneurysm incidence: the Atherosclerosis Risk in Communities (ARIC) study. *Circulation.* (2015) 132:578–85. doi: 10.1161/CIRCULATIONAHA.115.016537
10. Guirguis-Blake JM, Beil TL, Senger CA. Whitlock EP. Ultrasonography screening for abdominal aortic aneurysms: a systematic evidence review for the U.S. preventive services task force. *Ann Intern Med.* (2014) 160:321–9. doi: 10.7326/M13-1844
11. Barba A, Vega de. Ceniga M, Estallo L, de la Fuente N, Viviens B, Izagirre M. Prevalence of abdominal aortic aneurysm is still high in certain areas of Southern Europe. *Ann Vasc Surg.* (2013) 27:1068–73. doi: 10.1016/j.avsg.2013.01.017
12. Kent KC, Zwolak RM, Egorova NN, Riles TS, Manganaro A, Moskowitz AJ, et al. Analysis of risk factors for abdominal aortic aneurysm in a cohort of more than 3 million individuals. *J Vasc Surg.* (2010) 52:539–48. doi: 10.1016/j.jvs.2010.05.090
13. Forsdahl SH, Singh K, Solberg S, Jacobsen BK. Risk factors for abdominal aortic aneurysms: a 7-year prospective study: the tromso study, 1994–2001. *Circulation.* (2009) 119:2202–8. doi: 10.1161/CIRCULATIONAHA.108.817619
14. Mascarenhas JV, Albayati MA, Shearman CP, Jude EB. Peripheral arterial disease. *Endocrinol Metab Clin North Am.* (2014) 43:149–66. doi: 10.1016/j.ecl.2013.09.003
15. Wang W, Xu B, Xuan H, Ge Y, Wang Y, Wang L, et al. Hypoxia-inducible factor 1 in clinical and experimental aortic aneurysm disease. *J Vasc Surg.* (2018) 68:1538–50 e2. doi: 10.1016/j.jvs.2017.09.030
16. Yu J, Liu R, Huang J, Wang L, Wang W. Inhibition of phosphatidylinositol 3-kinase suppresses formation and progression of experimental abdominal aortic aneurysms. *Sci Rep.* (2017) 7:15208. doi: 10.1038/s41598-017-15207-w
17. Golledge J. Abdominal aortic aneurysm: update on pathogenesis and medical treatments. *Nat Rev Cardiol.* (2019) 16:225–42. doi: 10.1038/s41569-018-0114-9
18. Li X, Zhao G, Zhang J, Duan Z, Xin S. Prevalence and trends of the abdominal aortic aneurysms epidemic in general population—a meta-analysis. *PLoS ONE.* (2013) 8:e81260. doi: 10.1371/journal.pone.0081260
19. Golledge J, Muller J, Daugherty A, Norman P. Abdominal aortic aneurysm: pathogenesis and implications for management. *Arterioscler Thromb Vasc Biol.* (2006) 26:2605–13. doi: 10.1161/01.ATV.0000245819.32762.cb
20. Singh K, Bonaa KH, Jacobsen BK, Bjork L, Solberg S. Prevalence of and risk factors for abdominal aortic aneurysms in a population-based study: the tromso study. *Am J Epidemiol.* (2001) 154:236–44. doi: 10.1093/aje/154.3.236
21. Jamrozik K, Norman PE, Spencer CA, Parsons RW, Tuohy R, Lawrence-Brown MM, et al. Screening for abdominal aortic aneurysm: lessons from a population-based study. *Med J Aust.* (2000) 173:345–50. doi: 10.5694/j.1326-5377.2000.tb125684.x
22. Lederle FA, Johnson GR, Wilson SE, Chute EP, Littooy FN, Bandyk D, et al. Prevalence and associations of abdominal aortic aneurysm detected through screening. Aneurysm Detection and Management (ADAM) veterans affairs cooperative study group. *Ann Internal Med.* (1997) 126:441–9. doi: 10.7326/0003-4819-126-6-199703150-00004
23. Selvin E, Erlinger TP. Prevalence of and risk factors for peripheral arterial disease in the United States: results from the national health and nutrition examination survey, 1999–2000. *Circulation.* (2004) 110:738–43. doi: 10.1161/01.CIR.0000137913.26087.F0
24. Murabito JM, D'Agostino RB, Silbershatz H, Wilson WF. Intermittent claudication. A risk profile from the Framingham heart study. *Circulation.* (1997) 96:44–9. doi: 10.1161/01.CIR.96.1.44
25. Golledge J, Wolanski P, Parr A, Buttner P. Measurement and determinants of infrarenal aortic thrombus volume. *Eur Radiol.* (2008) 18:1987–94. doi: 10.1007/s00330-008-0956-3
26. Fan YN, Ke X, Yi ZL, Lin YQ, Deng BQ, Shu XR, et al. Plasma D-dimer as a predictor of intraluminal thrombus burden and progression of abdominal aortic aneurysm. *Life Sci.* (2020) 240:117069. doi: 10.1016/j.lfs.2019.117069
27. Sidloff DA, Stather PW, Choke E, Bown MJ, Sayers RD. A systematic review and meta-analysis of the association between markers of hemostasis and abdominal aortic aneurysm presence and size. *J Vasc Surg.* (2014) 59:528–35.e4. doi: 10.1016/j.jvs.2013.10.088
28. Golledge J, Muller R, Clancy P, McCann M, Norman PE. Evaluation of the diagnostic and prognostic value of plasma D-dimer for abdominal aortic aneurysm. *Eur Heart J.* (2011) 32:354–64. doi: 10.1093/eurheartj/ehq171
29. Takagi H, Manabe H, Kawai N, Goto S, Umemoto T. Plasma fibrinogen and D-dimer concentrations are associated with the presence of abdominal aortic aneurysm: a systematic review and meta-analysis. *Eur J Vasc Endovasc Surg.* (2009) 38:273–7. doi: 10.1016/j.ejvs.2009.05.013
30. Yamazumi K, Ojiro M, Okumura H, Aikou T. An activated state of blood coagulation and fibrinolysis in patients with abdominal aortic aneurysm. *Am J Surg.* (1998) 175:297–301. doi: 10.1016/S0002-9610(98)00014-2
31. Monaco M, Di Tommaso L, Stassano P, Smimmo R, De Amicis V, Pantaleo A, et al. Impact of blood coagulation and fibrinolytic system changes on early and mid term clinical outcome in patients undergoing stent endografting surgery. *Interact Cardiovasc Thorac Surg.* (2006) 5:724–8. doi: 10.1510/icvts.2006.136507
32. Milne AA, Adam DJ, Murphy WG, Ruckley CV. Effects of asymptomatic abdominal aortic aneurysm on the soluble coagulation system, platelet count and platelet activation. *Eur J Vasc Endovasc Surg.* (1999) 17:434–7. doi: 10.1053/ejvs.1998.0790
33. Bradbury A, Adam D, Garrioch M, Brittenden J, Gillies T, Ruckley CV. Changes in platelet count, coagulation and fibrinogen associated with elective repair of asymptomatic abdominal aortic aneurysm and aortic reconstruction for occlusive disease. *Eur J Vasc Endovasc Surg.* (1997) 13:375–80. doi: 10.1016/S1078-5884(97)80079-2
34. De Rango P, Farchioni L, Fiorucci B, Lenti M. Diabetes and abdominal aortic aneurysms. *Eur J Vasc Endovasc Surg.* (2014) 47:243–61. doi: 10.1016/j.ejvs.2013.12.007
35. Lederle FA. The strange relationship between diabetes and abdominal aortic aneurysm. *Eur J Vasc Endovasc Surg.* (2012) 43:254–6. doi: 10.1016/j.ejvs.2011.12.026
36. Itoga NK, Rothenberg KA, Suarez P, Ho TV, Mell MW, Xu B, et al. Metformin prescription status and abdominal aortic aneurysm disease

progression in the U.S. veteran population. *J Vasc Surg.* (2019) 69:710–6 e3. doi: 10.1016/j.jvs.2018.06.194

Conflict of Interest: The authors declare that the research was conducted in the absence of any commercial or financial relationships that could be construed as a potential conflict of interest.

The handling editor ZL is currently organizing a Research Topic with the WW.

Publisher's Note: All claims expressed in this article are solely those of the authors and do not necessarily represent those of their affiliated organizations, or those of the publisher, the editors and the reviewers. Any product that may be evaluated in this article, or claim that may be made by its manufacturer, is not guaranteed or endorsed by the publisher.

Copyright © 2022 Cai, Pan, Xu, Liu, Wang, Wu, Yang, Huang and Wang. This is an open-access article distributed under the terms of the Creative Commons Attribution License (CC BY). The use, distribution or reproduction in other forums is permitted, provided the original author(s) and the copyright owner(s) are credited and that the original publication in this journal is cited, in accordance with accepted academic practice. No use, distribution or reproduction is permitted which does not comply with these terms.

frontiers | Frontiers in Cardiovascular Medicine

TYPE Systematic Review
PUBLISHED 22 July 2022
DOI 10.3389/fcvm.2022.947809

Check for updates

OPEN ACCESS

EDITED BY
Wei Wang,
Central South University, China

REVIEWED BY
Bao Liu,
Peking Union Medical College Hospital (CAMS), China
Sabine Steiner,
Leipzig University, Germany

*CORRESPONDENCE
Zhang Hongpeng
zhanghongpeng@vip.sina.com
Guo Wei
guoweiplagh@sina.com

SPECIALTY SECTION
This article was submitted to General Cardiovascular Medicine, a section of the journal Frontiers in Cardiovascular Medicine

RECEIVED 19 May 2022
ACCEPTED 29 June 2022
PUBLISHED 22 July 2022

CITATION
Wu Y, Yin J, Hongpeng Z and Wei G (2022) Systematic review and network meta-analysis of pre-emptive embolization of the aneurysm sac side branches and aneurysm sac coil embolization to improve the outcomes of endovascular aneurysm repair. *Front. Cardiovasc. Med.* 9:947809. doi: 10.3389/fcvm.2022.947809

COPYRIGHT
© 2022 Wu, Yin, Hongpeng and Wei. This is an open-access article distributed under the terms of the Creative Commons Attribution License (CC BY). The use, distribution or reproduction in other forums is permitted, provided the original author(s) and the copyright owner(s) are credited and that the original publication in this journal is cited, in accordance with accepted academic practice. No use, distribution or reproduction is permitted which does not comply with these terms.

Systematic review and network meta-analysis of pre-emptive embolization of the aneurysm sac side branches and aneurysm sac coil embolization to improve the outcomes of endovascular aneurysm repair

Ye Wu[1,2], Jianhan Yin[1,3], Zhang Hongpeng[1]* and Guo Wei[1]*

[1]Department of Vascular Surgery, First Medical Center, Chinese PLA General Hospital, Beijing, China, [2]Medical College of Chinese PLA, Beijing, China, [3]Nankai University, Tianjin, China

Objective: Previous reports have revealed a high incidence of type II endoleak (T2EL) after endovascular aneurysm repair (EVAR). The incidence of T2EL after EVAR is reduced by pre-emptive embolization of aneurysm sac side branches (ASSB) and aneurysm sac coil embolization (ASCE). This study aimed to investigate whether different preventive interventions for T2EL were correlated with suppression of aneurysm sac expansion and reduction of the re-intervention rate.

Methods: The PubMed, Web of Science, MEDLINE and Embase databases, and conference proceedings were searched to identify articles on EVAR with or without embolization. The study was developed in line with the Participants, Interventions, Comparisons, Outcomes, and Study design principles and was conducted and reported in accordance with the Preferred Reporting Items for Systematic reviews and Meta-Analyses guidelines. We used network meta-analysis based on multivariate random-effects meta-analysis to indirectly compare outcomes of different strategies for embolization during EVAR.

Results: A total of 31 studies met all inclusion criteria and were included in the qualitative and quantitative syntheses. The included studies were published between 2001 and 2022 and analyzed a total of 18,542 patients, including 1,882 patients who received prophylactic embolization treatment during EVAR (experimental group) and 16,660 who did not receive prophylactic embolization during EVAR (control group). The effect of pre-emptive embolization of the inferior mesenteric artery (IMA) (IMA-ASSB) in preventing T2EL was similar (relative risk [RR] 1.01, 95% confidence interval [CI] 0.38–2.63) to the effects of non-selective embolization of ASSB (NS-ASSB) and ASCE (RR 0.88, 95% CI 0.40–1.96). IMA-ASSB showed a better clinical

effect in suppressing the aneurysm sac expansion (RR 0.27, 95% CI 0.09–2.25 compared with NS-ASSB; RR 0.93, 95% CI 0.16–5.56 compared with ASCE) and reducing the re-intervention rate (RR 0.34, 95% CI 0.08–1.53 compared with NS-ASSB; RR 0.66, 95% CI 0.19–2.22 compared with ASCE). All prophylactic embolization strategies improved the clinical outcomes of EVAR.

Conclusion: Prophylactic embolization during EVAR effectively prevents T2EL, suppresses the aneurysm sac expansion, and reduces the re-intervention rate. IMA embolization demonstrated benefits in achieving long-term aneurysm sac stability and lowering the risk of secondary surgery. NS-ASSB more effectively reduces the incidence of T2EL, while IMA embolization alone or in combination with ASCE enhances the clinical benefits of EVAR. In addition, as network meta-analysis is still an indirect method based on a refinement of existing data, more studies and evidence are still needed in the future to establish more credible conclusions.

KEYWORDS

prophylactic embolization, inferior mesenteric artery, type II endoleak, meta-analysis, abdominal aortic aneurysm

Introduction

Endovascular aneurysm repair (EVAR) has become the accepted standard therapy for abdominal aortic aneurysm (AAA) because of its low perioperative mortality and minimal invasiveness (1). However, the long-term outcomes of EVAR have not been fully elucidated and remain controversial. Recent clinical trials have shown that EVAR no longer achieves an early survival benefit compared with open surgery, because of a significant increase in death from secondary aneurysm rupture mostly caused by endoleaks (2) and a higher rate of secondary intervention (3).

Among several types of endoleaks, the most common is type II endoleak (T2EL) (4, 5). T2EL occurs because of retrograde perfusion of the AAA sac from the inferior mesenteric artery (IMA), lumbar arteries (LAs), middle sacral artery, or aberrant renal arteries (6). Most T2ELs resolve spontaneously with time and it remains debatable whether T2ELs requires aggressive therapy that may be associated with adverse late outcomes (7–11). A previous study demonstrated that 9.8% of aortic ruptures after EVAR were caused by T2EL (12), while a meta-analysis of 32 studies and 21,744 patients showed that 0.9% of patients with an isolated T2EL had a ruptured AAA (13). A reduction in the incidence of T2EL may improve the prognosis and decrease the psychological and economic burden of patients undergoing EVAR (14).

The role of pre-emptive embolization of aneurysm sac side branches (ASSB) in preventing T2EL has been debated for the past two decades. Early evidence in 2001 suggested that additional ASSB is unnecessary because of the uncertain incidence of T2EL during follow-up (15). However, recent progress in preoperative optimization, medical devices, and high-quality supportive care has led to significantly improved clinical outcomes of ASSB. Despite the lack of high-quality evidence, the latest meta-analysis suggests that ASSB aids in preventing T2EL, aneurysm sac enlargement, and re-intervention (16). The other prophylactic embolization treatment implemented during EVAR is aneurysm sac coil embolization (ASCE). To date, there is still no generalized and commonly accepted standard method of ASCE (11). However, studies have shown that ASCE effectively prevents T2EL, particularly during the mid-term follow-up of high-risk patients (17–20). A meta-analysis of 17 studies with 2,084 participants also demonstrated the safety and effectiveness of ASCE in preventing T2EL (21).

The most common sources of T2EL are the IMA and LAs. However, there is still a lack of clinical trials directly comparing the efficacy of non-selective embolization of patent aortic side branches versus embolization of the IMA alone. Furthermore, few studies have directly compared ASSB and ASCE. There was no recording and follow-up of other arteries such as accessory renal arteries in the studies that we consulted and incorporated. In the present study, we aimed to perform a network meta-analysis to compare the efficacy and basic outcomes of different prophylactic embolization treatments in IMA, Las, and sac embolization during EVAR.

Methods

Study design

The study was developed in line with the Participants, Interventions, Comparisons, Outcomes, Study design principles and was conducted and reported in accordance with the Preferred Reporting Items for Systematic reviews and Meta-Analyses guidelines (22).

Participants

The participants were patients of any age with AAA who underwent EVAR with or without prophylactic embolization comprising either ASSB or ASCE. ASSB was divided into preoperative pre-emptive embolization of the IMA (IMA-ASSB) and non-selective preoperative embolization of the IMA and LAs (NS-ASSB). Few studies reported embolization of the median sacral artery or accessory renal artery.

Interventions

EVAR with IMA-ASSB, NS-ASSB, or ASCE.

Comparison intervention

EVAR without prophylactic embolization treatment.

Outcomes

Primary outcomes

a. Incidence of T2EL during follow-up. The presence of T2EL was defined as the temporary or permanent appearance of T2EL during postoperative follow-up examination.

b. Incidence of enlargement of the diameter or size of the aneurysm sac during follow-up.

Secondary outcomes

a. Late all-cause-related mortality.

b. Rate of re-intervention during follow-up.

One thing to note, only a few studies mentioned their observation and follow-up of complications which was not sufficient for statistical analysis.

Eligibility criteria

1. Inclusion criteria: retrospective or prospective studies evaluating the effect of ASSB or ASCE during EVAR compared with a control group or not that underwent no preventive intervention measures and had the patent collateral arteries retained; no date or limit on patients or publications; follow-up period of not less than 6 months; outcome indicators included the occurrence of T2EL diagnosed by contrast-enhanced CT, CTA, MRA, or other appropriate imaging examination.

2. Clinical exclusion criteria: flawed study design, implementation process, or statistical methods; funding organization influenced the study design or the implementation, analysis, or interpretation of data; incomplete data in original articles that could not be refined; case report or studies about embolization of other arteries, such as the median sacral artery or accessory renal artery which without intervention to IMA or LAs; prophylactic embolization in animals; fewer than 10 patients per group; Embolization performed in second operations.

3. Non-clinical exclusion criteria: overlapping series (only the latest publication of serial reports of a certain cohort was included); non-original article (i.e., review, case report, editorial).

Information sources

Multiple electronic health databases (MEDLINE, Embase, PubMed, and Web of Science) were searched to identify relevant articles published from 1 October 2001 to 11 May 2022.

Search strategy

The MEDLINE, Embase, PubMed, and Web of Science databases were searched with an unrestricted search strategy that applied a combination of Medical Subject Headings and keywords combined with the Boolean operators AND or OR to retrieve relevant reports. The following terms were used: ["aortic aneurysm abdominal" (Title/ Abstract) OR "abdominal aortic aneurysms" (Title/ Abstract) OR "aneurysms abdominal aortic" (Title/Abstract) OR "aortic aneurysms abdominal" (Title/Abstract) OR "abdominal aortic aneurysm" (Title/Abstract) OR "aneurysm abdominal aortic" (Title/Abstract)] AND ["embolization" (Title/Abstract) OR "embolism" (Title/Abstract) OR "embolizations" (Title/Abstract)]. Controlled trials comparing prophylactic embolization with non-intervention during EVAR were eligible for inclusion in the general meta-analysis. Single-arm studies were also retrieved for inclusion in the network meta-analysis. We adapted the terms to meet the specific requirements of the explicit search strategy used for each database. A total of 100 citations were obtained from the databases, of which 67 were excluded after browsing the titles and abstracts, yielding 33 articles for detailed review. After reviewing the full texts of the remaining studies and their cited references to identify additional studies, 32 studies were finally selected.

Study selection

Eligibility assessment was performed independently in an unblinded standardized manner by two reviewers (Guo and Zhang).

Data extraction and assessment of study quality

Data were extracted from the primary studies and consolidated into single spreadsheets. One author collected the data from the included articles, while another author explicitly checked the presented information. The data analyzed in the present review were all published in the included studies in case of record form or as alphanumeric text. Information filtering from relevant studies was performed manually. Study quality and risk of bias were assessed using the Newcastle Ottawa Scale (NOS) (23) (selection, comparability, and outcome) and the Cochrane Handbook for Systematic Reviews of Interventions (random sequence generation, allocation concealment, blinding of participants and personnel, blinding of outcome assessment, incomplete outcome data, selective reporting, and other bias). Two reviewers (Wu and Yin) determined the eligibility and compared the quality of the included studies. A cumulative NOS of 7 or more was considered to indicate high quality.

Extracted data

1. Publication details: first author and year.
2. Study details: number of participating institutions, number of participants, controls and interventions, mean follow-up period, inclusion criteria, exclusion criteria, and country.
3. Participants: number of patients undergoing EVAR with or without prophylactic embolization.
4. Primary outcomes: incidences of T2EL and enlargement of the aneurysm sac during follow-up.
5. Secondary outcomes: late all-cause-related mortality and the rate of re-intervention during follow-up.

Statistical analysis

Statistical analysis was performed in accordance with the Cochrane Handbook for Systematic Reviews, using Stata® Version 16.0, RStudio (version 1.4.1103 for Windows, Boston, MA, United States), Stata package base, metan, mvmeta, metareg, network, R (version 4.1.2, R Foundation for Statistical Computing, Vienna, Austria) and R packages base, ggplot2, metafor, meta and gemtc (24). The gemtc package was used in connection with the Just Another Gibbs Sampler package to generate simulations. Statistical applications were set up to statistically analyze which prophylactic embolization treatment had the greatest effect on the progression of AAA after EVAR. There was no significant methodological heterogeneity between the datasets regarding the study design and risk of bias. The primary and secondary outcomes were analyzed as dichotomous variables by estimating the relative risk (RR) with a 95% confidence interval (CI). The I^2 value was calculated to assess the statistical heterogeneity between studies. The heterogeneity among studies was considered significant when I^2 was $> 50\%$, and was considered highly significant when I^2 was $> 75\%$. Publication bias was assessed through funnel plots and Egger tests. The fixed-effect model based on the Mantel-Haenszel estimator was used when there was no or only slight heterogeneity among the studies. When the heterogeneity was significant, the analysis was performed with the random-effects model based on the DerSimonian-Laird estimator. The results were summarized using forest plots.

Flow diagram of studies included in the systematic review (please refer to the Supplementary Appendix)

Description of studies

The search strategy retrieved a total of 3,345 articles, of which 3,314 were excluded after the title and abstract screening because they were not relevant or because they were comments only. After full-text review and data abstraction, 31 studies met all inclusion criteria and were included in the qualitative and quantitative syntheses (2, 17–20, 25–50).

One study was a prospective randomized controlled trial, while 30 were retrospective studies. All studies were published between 2001 and 2022. A total of 18,542 patients were involved in the included studies, of which 1,882 received prophylactic embolization treatment during EVAR and 16,660 did not. One study based on data from the Vascular Quality Initiative database included 15,060 patients (43). The study characteristics, study quality, and literature quality evaluation based on the NOS are summarized in **Table 1**. The mean NOS was 7.38 (out of a possible 9 points), suggesting that the included studies were high-quality studies. A lack of representativeness and comparability was the main reason for low NOS scores.

Results

Primary and secondary outcomes

T2EL

Overall, a total of 31 studies including 18,542 patients were analyzed (15,976 in the NS-ASSB group, 998 in the IMA-ASSB group, and 1,568 in the ASCE group). The prevalence of

TABLE 1 General characteristics of included studies.

Author (publication year)	Study period	Nation	Study design	Embolized arteries (experimental group)	Devices of embolization	Follow up period (mean, months)	Number of patients in emboliation group	Number of patients in control group	Total number of patients in endpoint	NOS	Technical success	Re-interventions	Enlargement of sac
Parry et al. (25)	09/1996 to 04/2001	United Kingdom	Single-center Retrospective	IMA and LA	Coils	E = 24.0 C = 30.0	14	22	36	7	73.7% (14/19)	E = 0 C = 6	E = 0 C = 3
Gould et al. (15)	N.S.	United Kingdom	Single-center Retrospective	IMA and LA	Coils	E = 18.4 C = 18.9	20	43	63	6	84% (21/25)	E = 0 C = 3	E = 0 C = 4
Fabre et al. (20)	01/2009 to 12/2013	France	Single-center Retrospective	IMA and LA	Coils	24.0	83	104	187	8	100% (83/83)	N.S.	N.S.
Burbelko et al. (32)	01/2008 to 04/2010	Germany	Single-center Retrospective	IMA and LA	AVP	E = 30.1 C = 30.2	33	38	71	6	100% (33/33)	E = 0 C = 4	E = 0 C = 5
Aoki et al. (44)	10/2009 to 08/2019	Japan	Single-center Retrospective	IMA and LA	Coils	E = 53.5 C = 53.0	48	34	82	6	IMA: 96.4% (54/56) and LAs: 74.5% (108/145)	N.S.	N.S.
Chikazawa et al. (29)	05/2007 to 04/2012	Japan	Single-center Retrospective	IMA and LA	Coils	6.0	10	131	141	7	IMA: 100% (N.S.) and LAs: 79.8% (N.S.)	N.S.	E = 0 C = 2
Alerci et al. (45)	03/1999 to 12/2009	Switzerland	Single-center Retrospective	IMA and LA	Coils	60.5	56	64	120	8	96% (119/124)	N.S.	N.S.
Bonvini et al. (46)	03/1999 to 12/2001	Switzerland	Single-center Retrospective	IMA and LA	Coils	17.0	22	N.S.	22		IMA: 100% (14/14) and LAs: 65% (24/37)	N.S.	1
Sheehan et al. (27)	06/2001 to 06/2005	United States	Single-center Retrospective	IMA and LA	Coils	15.0	55	N.S.	55	6	44% (14/32)	N.S.	1
Branzan et al. (39)	09/2014 to 09/2019	Canada	Single-center Retrospective	IMA and LA	Coils	23.0	139	N.S.	105		N.S.	6	7
Rokosh et al. (43)	01/2009 to 11/2020	United States	Multi-center Retrospective	IMA and LA	N.S.	E = 15.0 C = 14.6	272	14,788	15,060		N.S.	E = 17 C = 621	E = 10 C = 960

(Continued)

10.3389/fcvm.2022.947809

TABLE 1 (Continued)

Author (publication year)	Study period	Nation	Study design	Embolized arteries (experimental group)	Devices of embolization	Follow up period (mean, months)	Number of patients in emboliation group	Number of patients in control group	Total number of patients in endpoint	NOS	Technical success	Re-interventions	Enlargement of sac
Vaillant et al. (37)	11/2007 to 06/2016	France	Single-center Retrospective	IMA	Coils	E = 21.4 C = 57.2	33	45	78	9	100% (43/43)	E = 5 C = 14	E = 1 C = 15
Samura et al. (38)	04/2014 to 03/2018	Japan	Single-center Retrospective	IMA	AVP	E = 22.5 C = 22.4	46	51	97		88.7% (47/53)	E = 0 C = 0	E = 1 C = 9
Fukuda et al. (47)	07/2007 to 04/2014	Japan	Single-center Retrospective	IMA	Coils	E = 15.4 C = 37.5	143	189	332	7	N.S.	E = 1 C = 12	
Müller-Wille et al. (33)	07/2011 to 06/2013	Germany	Single-center Retrospective	IMA	AVP	E = 6.0 C = 26.0	31	43	74	6	100% (29/29)	N.S.	E = 0 C = 8
Ward et al. (31)	08/2002 to 05/2010	United States	Single-center Retrospective	IMA	Coils	E = 32.4 C = 21.2	108	158	266	6	100% (108/108)	E = 1 C = 12	E = 13 C = 21
Nevala et al. (28)	01/2000 to 10/2006	Finland	Multi-center Retrospective	IMA	Coils	E = 39.6 C = 40.8	40	39	79	7	84.8% (67/79)	E = 1 C = 11	N.S.
Axelrod et al. (26)	N.S.	United States	Single-center Retrospective	IMA	Coils	E = 6.0 C = 6.0	18	54	72	7	94% (30/32)	E = 0 C = 4	N.S.
Muthu et al. (48)	02/1999 to 04/2006	New Zealand	Single-center Retrospective	SAC	Thrombin	E = 12.0 C = 36.0	65	67	132		42% (29/69)	E = 2 C = 10	N.S.
Ronsivalle et al. (49)	01/2005 to 02/2008	Poland	Single-center Retrospective	SAC	Fibrin glue and Coils	E = 18.5 C = 20.0	18	20	38	9	100% (18/18)	E = 1 C = 2	N.S.
Pilon et al. (19)	09/1999 to 12/2008	Italy	Single-center Retrospective	SAC	Fibrin glue and Coils	E = 26.0 C = 72.0	180	224	404	9	N.S.	E = 14 C = 21	N.S.
Piazza et al. (30)	01/2008 to 12/2009	United States	Single-center Retrospective	SAC	Fibrin glue and Coils	E = 13.2 C = 37.2	79	83	162	9	100% (79/79)	E = 1 C = 5	E = 8 C = 21

(Continued)

10.3389/fcvm.2022.947809

TABLE 1 (Continued)

Author (publication year)	Study period	Nation	Study design	Embolized arteries (experimental group)	Devices of embolization	Follow up period (mean, months)	Number of patients in emboliation group	Number of patients in control group	Total number of patients in endpoint	NOS	Technical success	Re-interventions	Enlargement of sac
Piazza et al. (36)	01/2012 to 12/2014	United States	Single-center Retrospective	SAC	Fibrin glue and Coils	E = 16.4 C = 15.9	50	55	105	9	100% (55/55)	E = 1 C = 6	N.S.
Mascoli et al. (34)	2008 to 2013	Italy	Single-center Retrospective	SAC	Coils	12.0	25	44	69	9	N.S.	E = 0 C = 0	E = 0 C = 5
Natrella et al. (17)	01/2011 to 04/2014	Italy	Single-center Retrospective	SAC	Coils	12.0	36	36	72	8	100% (36/36)	N.S.	N.S.
Dosluoglu et al. (18)	09/2007 to 10/2015	United States	Single-center Retrospective	SAC	Coils	44.0	16	31	47	9	93.7% (15/16)	E = 1 C = 9	E = 1 C = 14
Fabre et al. (40)	06/2014 to 02/2017	France	Multi-center Randomized Controlled Trial	SAC	Coils	24.0	29	32	61	9	100% (29/29)	E = 1 C = 7	E = 0 C = 0
Mascoli et al. (41)	01/2012 to 03/2015	Italy	Single-center Prospectively	SAC	Coils	12.0	61	265	326	9	N.S.	N.S.	N.S.
Zanchetta et al. (50)	06/2003 to 12/2005	Italy	Single-center Retrospective	SAC	Fibrin glue	14.4	84	N.S.	84		99% (83/84)	4	1
Nakai et al. (35)	12/2013 to 04/2015	Japan	Single-center Retrospective	SAC	Coils	12.1	24	N.S.	24		N.S.	N.S.	0
Mathlouthi et al. (42)	2015 to 2019	United States	Single-center Retrospective	SAC	Thrombin, morcellated gelfoam and non-heparinized saline	14.0	44	N.S.	44		100% (44/44)	3	0

10.3389/fcvm.2022.947809

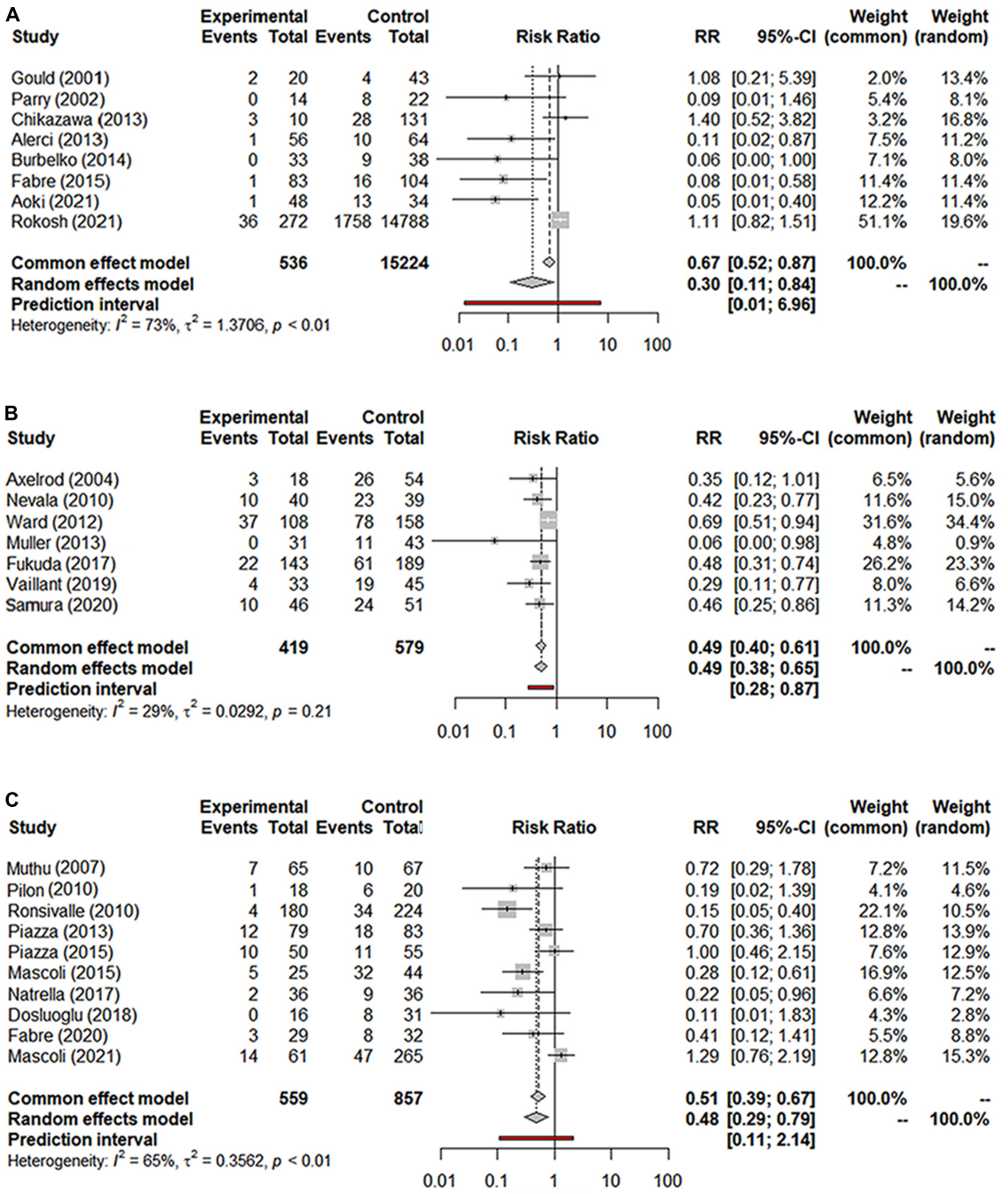

FIGURE 1
(A) Forest graph of T2EL in NS-ASSB group (RR 0.30 95% CI 0.11–0.84); **(B)** forest graph of T2EL in IMA-ASSB group (RR 0.49 95% CI 0.38–0.65); **(C)** forest graph of T2EL in ASCE group (RR 0.48 95% CI 0.29–0.79). NS-ASSB, non-selective embolization of aneurysm sac side branches; IMA-ASSB, embolization of the inferior mesenteric artery; ASCE: aneurysm sac coil embolization.

each embolization treatment was 0%–30% for NS-ASSB, 0%–34% for IMA-ASSB, and 0%–23.0% for ASCE. Patients who received prophylactic embolization had a significantly lower risk of T2EL after EVAR than those who did not receive prophylactic embolization in all studies. In the analysis of 25 controlled studies, the relative risk (RR) of T2EL was 0.30 (95% CI 0.11–0.84) for NS-ASSB, 0.49 (95% CI 0.38–0.65) for IMA-ASSB, and 0.48 (95% CI 0.29–0.79) for ASCE. Single-arm studies were not included in the routine meta-analysis because they contained smaller amounts of data. Network meta-analysis including single-arm studies using a multiple regression model demonstrated that both ASCE and IMA-ASSB were inferior

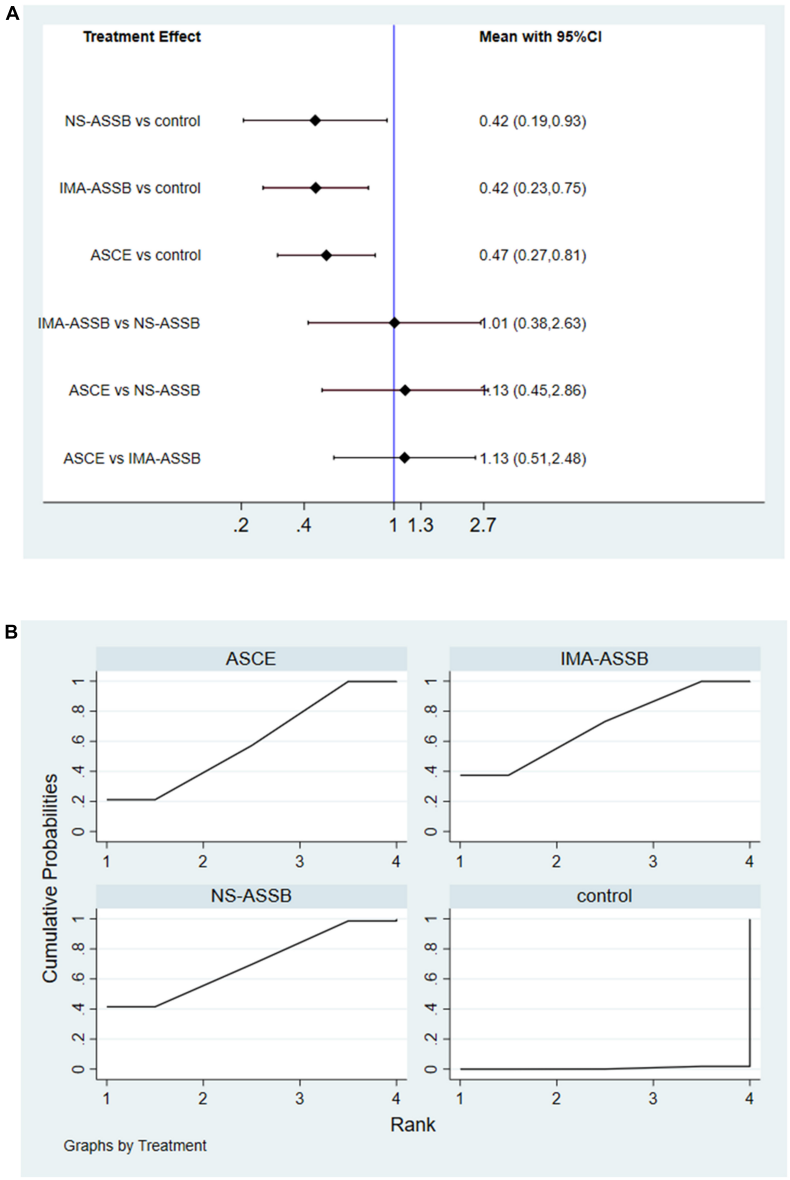

FIGURE 2
(A) Network meta-analysis forest graph of T2EL in NS-ASSB, IMA-ASSB and ASCE groups; **(B)** SUCRA curve of T2ELin NS-ASSB, IMA-ASSB and ASCE groups; NS-ASSB, non-selective embolization of aneurysm sac side branches; IMA-ASSB, embolization of the inferior mesenteric artery; ASCE, aneurysm sac coil embolization.

to NS-ASSB in preventing T2EL. The effect of IMA-ASSB in preventing T2EL was similar (RR 1.01, 95% CI 0.38–2.63) to that of NS-ASSB and ASCE (RR 0.88, 95% CI 0.40–1.96). The results suggested that the protective effects of NS-ASSB and IMA-ASSB were not significantly different. The surface under the cumulative ranking (SUCRA) curve analysis showed a similar result (**Figures 1**, **2**).

Re-intervention

Data on the rate of re-intervention during follow-up were presented in 21 studies with a total of 17,405 patients (15,335 in the NS-ASSB group, 924 in the IMA-ASSB group, and 1,146 in the ASCE group). The rate of re-intervention ranged from 0% to 15.1% (0%–13.6% for NS-ASSB, 0%–15.1% for IMA-ASSB, and 0%–7.78% for ASCE). Prophylactic embolization resulted in a reduction in the incidence of re-intervention after EVAR. The RR of re-intervention in all controlled studies was 0.49 (95% CI 0.16–1.53) for NS-ASSB, 0.26 (95% CI 0.13–0.52) for IMA-ASSB, and 0.44 (95% CI 0.25–0.77) for ASCE. The single-arm studies were not analyzed because of a shortage of data. Network meta-analysis showed that IMA-ASSB was the best in preventing re-intervention after EVAR when all studies were incorporated

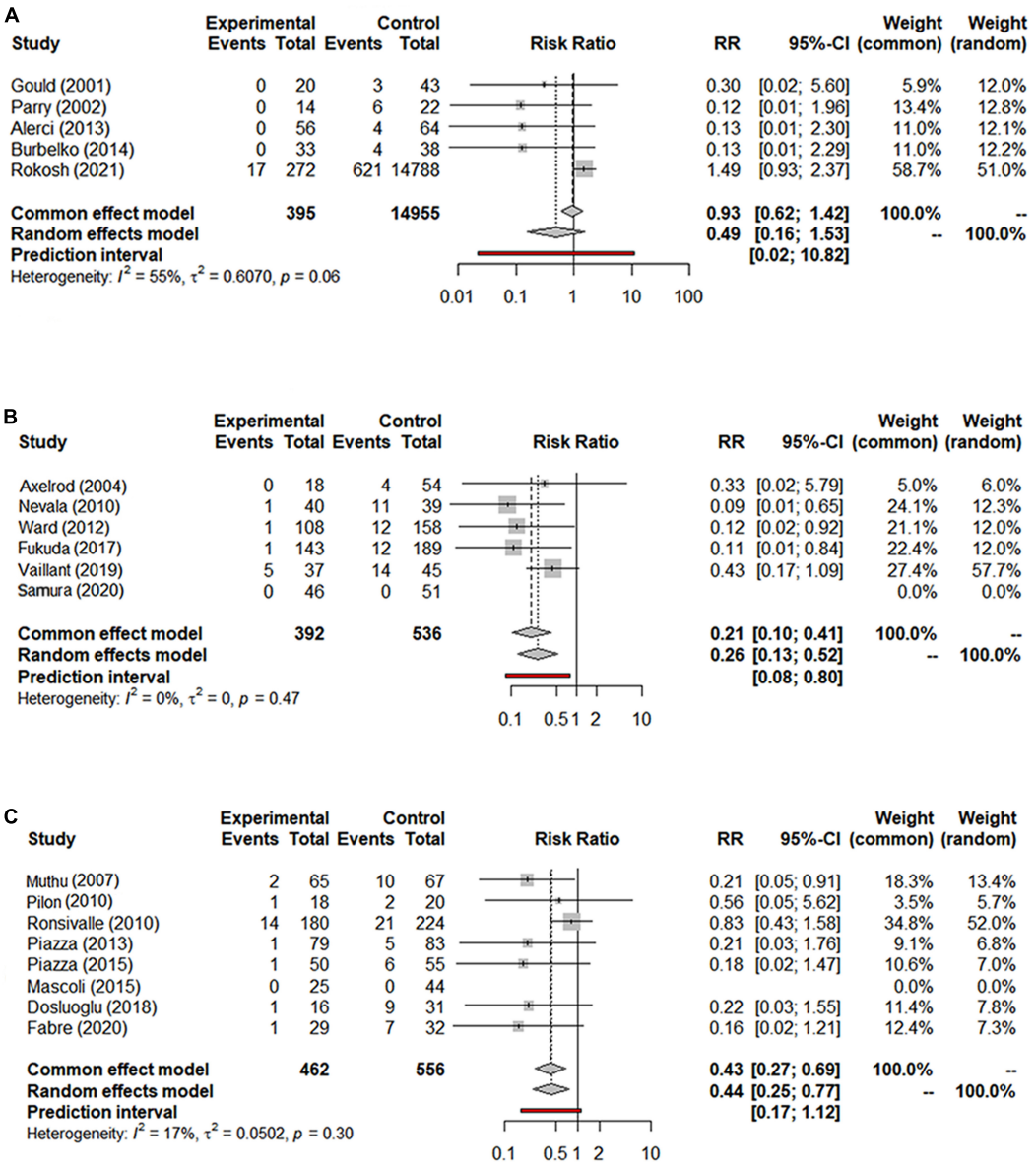

FIGURE 3
(A) Forest graph of re-intervention in NS-ASSB group (RR 0.49 95% CI 0.16–1.53); **(B)** forest graph of re-intervention in IMA-ASSB group (RR 0.26 95% CI 0.13–0.52); **(C)** forest graph of re-intervention in ASCE group (RR 0.44 95% CI 0.25–0.77). NS-ASSB, non-selective embolization of aneurysm sac side branches; IMA-ASSB, embolization of the inferior mesenteric artery; ASCE, aneurysm sac coil embolization.

in the analysis (RR 0.24, 95% CI 0.09–0.61) and was superior to NS-ASSB (RR 0.34, 95% CI 0.08–1.53) and ASCE (RR 0.66, 95% CI 0.19–2.22). The SUCRA curves were analyzed (Figures 3, 4).

Enlargement of the aneurysm sac

Data on the enlargement of the aneurysm sac were provided in 19 studies with a total of 16,559 patients (15,553 in the NS-ASSB group, 515 in the IMA-ASSB group, and 491 in the ASCE group). Aneurysm sac enlargement occurred in 0% to 12.0% of patients during follow-up (0%–3.7% for NS-ASSB, 0%–12.0% for IMA-ASSB, and 0%–10.1% for ASCE). The cumulative results showed that prophylactic embolization led to a significant decrease in the risk of aneurysm sac enlargement after EVAR. However, the results of individual studies showed the opposite conclusion. The RR of aneurysm sac enlargement in 13 controlled studies was 0.52 (95% CI 0.30–0.92) for NS-ASSB, 0.32 (95% CI 0.14–0.72) for IMA-ASSB, and 0.33 (95% CI 0.17–0.66) for ASCE. The single-arm studies were not analyzed because of a shortage of data. Network meta-analysis using a frequentist model proved that IMA-ASSB had the best performance in preventing enlargement of the aneurysm sac when all studies were incorporated in the analysis (RR 0.29,

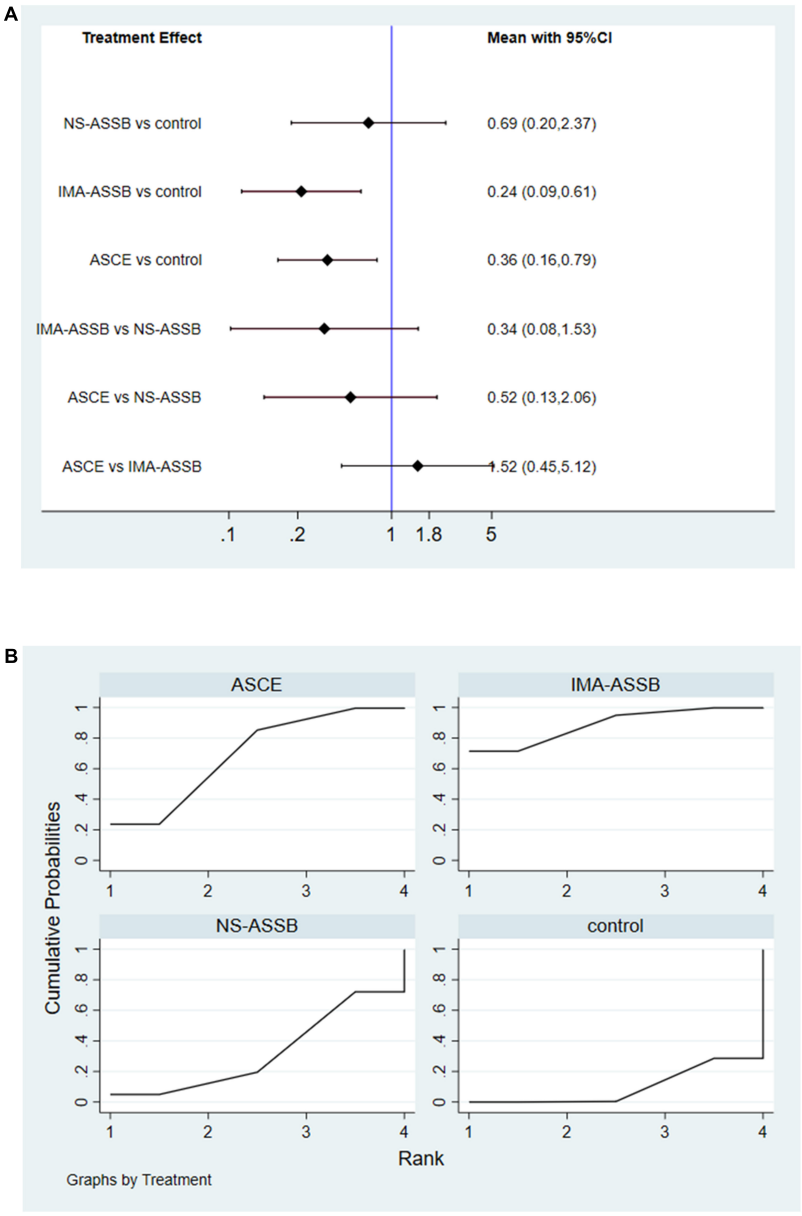

FIGURE 4
(A) Network meta-analysis forest graph of re-intervention in NS-ASSB, IMA-ASSB and ASCE groups; **(B)** SUCRA curve of re-intervention in NS-ASSB, IMA-ASSB and ASCE groups; NS-ASSB, non-selective embolization of aneurysm sac side branches; IMA-ASSB, embolization of the inferior mesenteric artery; ASCE, aneurysm sac coil embolization.

95% CI 0.09–1.00), and was superior to NS-ASSB (RR 0.67, 95% CI 0.14–3.34) and similar to ASCE (RR 0.99, 95% CI 0.19–5.26). The same result was shown in the SUCRA curve analysis (Figures 5, 6).

Discussion

The potential effects of T2EL after EVAR remain controversial. Therefore, there are still disputes regarding the management of T2EL and its influence on further outcomes. There is currently no consensus regarding the need for intensive treatment of T2EL. Evidence indicates that T2EL is not an isolated complication and is associated with the occurrence of other types of endoleaks. Despite the controversy over the past two decades around whether prophylactic embolization prevents T2EL, an increasing body of evidence suggests that such treatments may dramatically improve the outcome of EVAR. Studies have reported that prophylactic embolization has potential benefits in decreasing

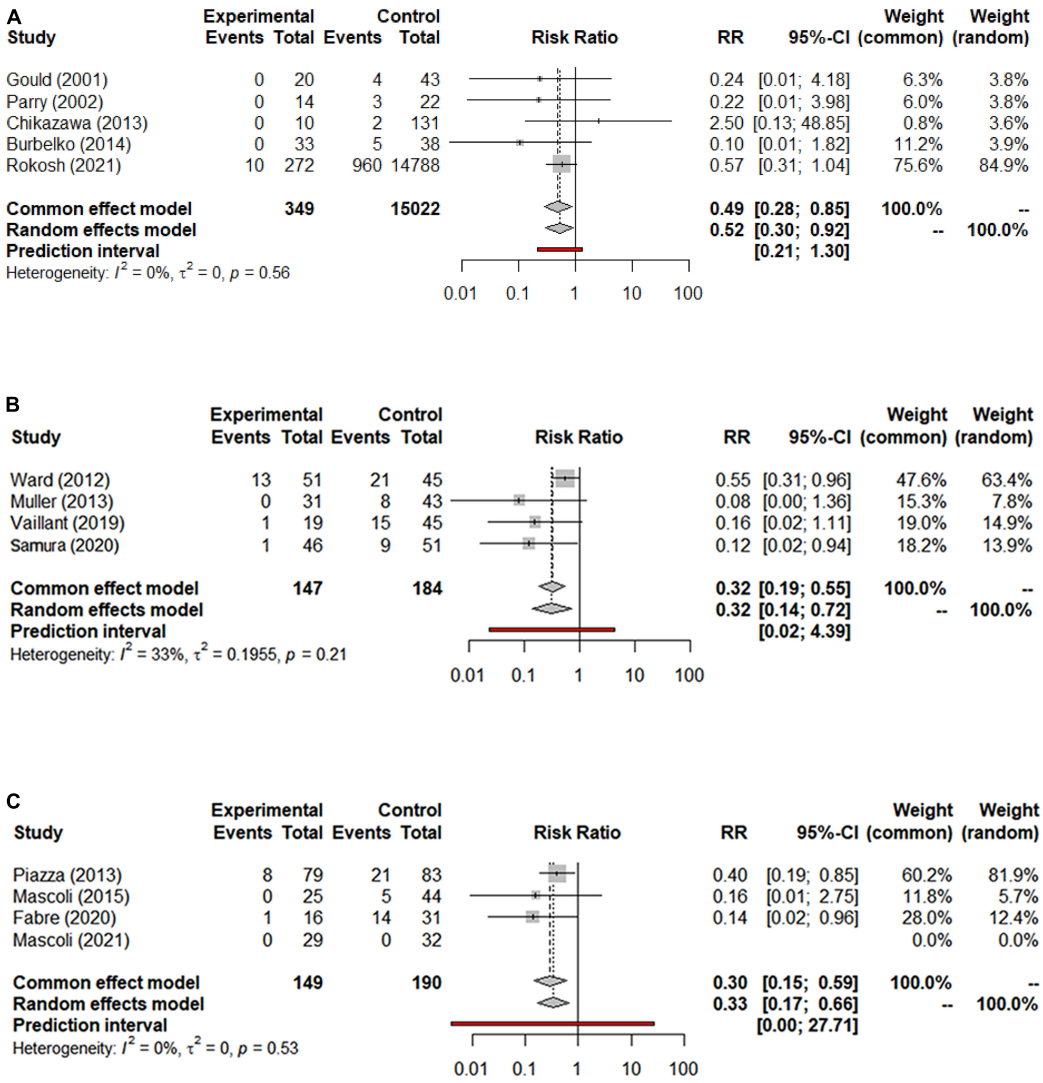

FIGURE 5
(A) Forest graph of enlargement of the aneurysm sac in NS-ASSB group (RR 0.52 95% CI 0.30–0.92); **(B)** forest graph of enlargement of the aneurysm sac in IMA-ASSB group (RR 0.32 95% CI 0.14–0.72); **(C)** forest graph of enlargement of the aneurysm sac in ASCE group (RR 0.33 95% CI 0.17–0.66). NS-ASSB, non-selective embolization of aneurysm sac side branches; IMA-ASSB, embolization of the inferior mesenteric artery; ASCE, aneurysm sac coil embolization.

the incidence of T2EL, preventing enlargement of the aneurysm sac, and decreasing the rate of re-intervention (21, 51). The major limitation of these previous studies was a lack of a comparison of different interventions. However, it is difficult to make such comparisons in clinical practice because of the wide variations in the technical difficulty and cost of the interventions.

The clinical benefit of NS-ASSB has been discussed extensively since the first study was published in 2001 (15). The previous meta-analysis has given evidence of the safety and effectiveness of ASCE in preventing T2EL (21). Another meta-analysis shows a different rate of 19.9% vs. 41.4% in patients who accept IMA embolization or not (52). But there is still little information available on the comparison of the re-intervention rate and diameter change in different embolization strategies and no network meta-analysis is available until now. The present systematic review and network meta-analysis investigated the value of prophylactic embolization in preventing adverse outcomes after EVAR and compared different therapeutic regimens. We found that prophylactic embolization had a positive effect on the outcome of EVAR. Non-selective embolization of the IMA and LAs showed the best results in preventing T2EL, but embolization of the IMA alone might provide better benefits in suppressing the expansion of the aneurysm sac and reducing the re-intervention rate. Although all three methods lead to common

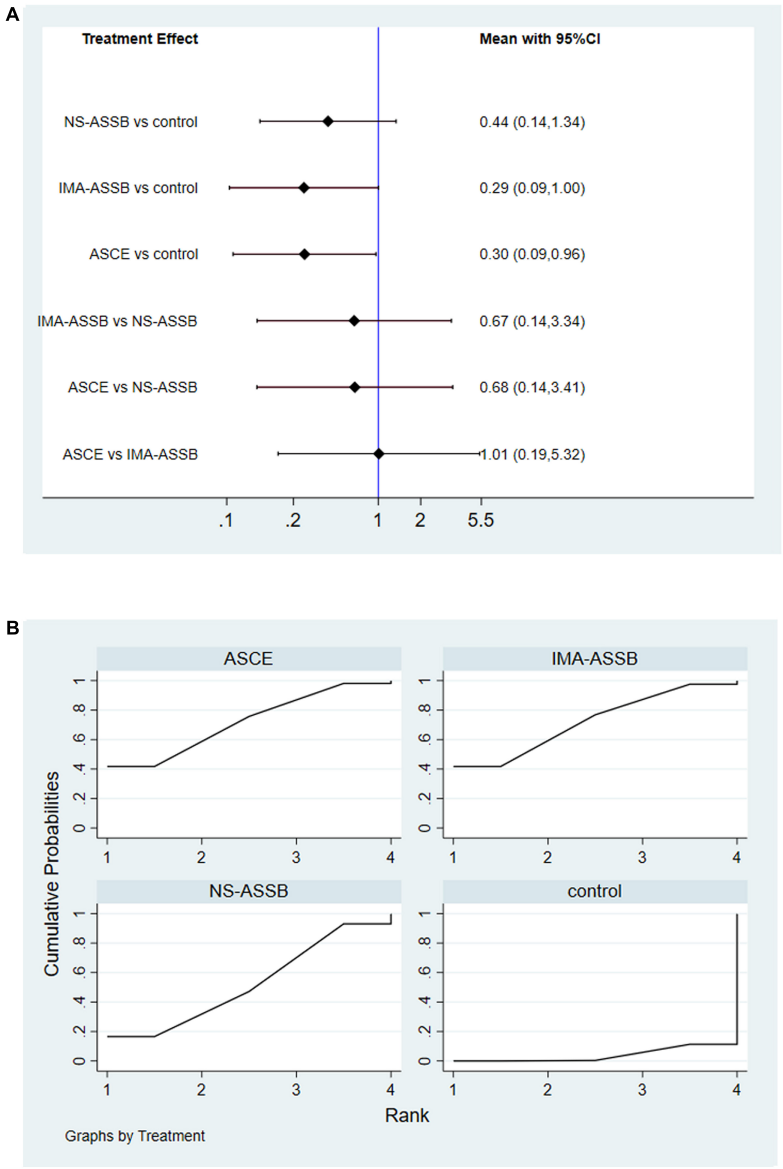

FIGURE 6
(A) Network meta-analysis forest graph of enlargement of the aneurysm sac in NS-ASSB, IMA-ASSB and ASCE groups; **(B)** SUCRA curve of enlargement of the aneurysm sac in NS-ASSB, IMA-ASSB and ASCE groups; NS-ASSB, non-selective embolization of aneurysm sac side branches; IMA-ASSB, embolization of the inferior mesenteric artery; ASCE, aneurysm sac coil embolization.

effects of sac regression and free form re-intervention. The long-term effects of the rate of diameter reduction and the second operation seem to be better when embolization of IMA was carried out in isolation. LAs may play an important role in the outflow tract in sac regression after EVAR. The embolization of LAs may reduce outflow efficiency which decreases the rate of diameter reduction. As mentioned above, the effects of T2EL after EVAR still require verification; however, T2EL may eventually lead to aneurysm sac expansion (53). Aneurysm sac expansion is a predictor of late complications after EVAR (54, 55) and increases the risk of AAA rupture (56). The guidelines of the European Society for Vascular Surgery and prior studies recommend surgical intervention when the diameter of the aneurysm sac enlarges by 10–13 mm during follow-up using the same imaging modality (11, 53, 57). The presence of a T2EL and an increasing aneurysm sac size is likely to lead to a type I endoleak (57), which has a potential correlation with the risk of AAA rupture (58) and requires immediate treatment. There seems to be no consensus on the indications for re-intervention. A previous study assessed type I or III endoleaks, aneurysm sac expansion of more than 10 mm, and the existence

of a collateralized IMA feeding vessel as indications for intervention (53). Our results indicated that prophylactic embolization of the IMA reduced the rate of aneurysm sac enlargement and improved the clinical outcomes of EVAR. These results suggest an underlying positive correlation between embolization of the LAs and expansion of the aneurysm sac diameter, which eventually increased the risk of re-intervention. Muthu et al. reported a high incidence of lumbar endoleaks after EVAR (48), which may result in the difference between the outcome of NS-ASSB and the stable optimal outcome of IMA-ASSB and ASCE demonstrated in the present study. More clinical data about the outcome of embolization of the LAs alone during EVAR is needed to confirm whether the hemodynamics are changed by this process or whether the hemodynamics are only changed by occlusion of the IMA. With regards to potential risks of ASSB and ASCE, Ward et (31) reported a 9.3% rate of complications among embolization patients, only one of them died because of multiorgan failure caused by colonic infarction after IMA embolization.

Although there were limited data available regarding the outcomes after prophylactic embolization during EVAR, even fewer data were available regarding the association of specific embolization treatments with aneurysm sac enlargement and re-intervention. Only one of the included studies was a randomized controlled trial, and most of the included studies had small sample sizes while one multicenter retrospective study had an extremely large sample size. Although the network meta-analysis was performed after the exclusion of the data from the large study by Rokosh et al. (43) showed similar results, bias may still exist. Eleven of the included studies were performed in the past 5 years, and most studies were performed over long time intervals that would bring bias caused by technological innovation. In addition, there were limited data on the incidences of aneurysm sac enlargement and re-intervention, and on complications after EVAR with versus without prophylactic embolization treatments. Furthermore, some patients did not receive embolization because they underwent emergency surgery, had unsuitable artery anatomy, or were physically unable to tolerate the procedure, which resulted in bias. Because all the calculated I^2 values were less than 75%, publication bias was proved by funnel plots and Egger's test (p = 0.0027 for the NS-ASSB group, p = 0.0252 for the IMA-ASSB group, and p = 0.0047 for the ASCE group). Besides, network meta-analysis has its advantages and drawbacks. Mvmeta package on Stata platform made based on multivariate regression analysis could obtain outcomes very close to Bayesian model. But only one dummy variable can be set in each operation. Moreover, heterogeneity and transitivity assumptions are still been challenged and stand in the way. To reduce the bias introduced by the performance of retrospective studies at single centers, more randomized controlled trials (preferably multicenter) are needed to verify the safety and efficacy of prophylactic embolization. Studies should be registered and carried out in accordance with the standard instructions for clinical trials. Blinded raters should perform CTA and assess the symptoms and disease progress at admission, every 6 or 12 months, and at discharge. Any CTA imaging data should be measured by independent reviewers using the same software tool. There should also be more precise definitions of aneurysm sac enlargement and indications for re-interventions.

Conclusion

Prophylactic embolization during EVAR effectively prevents T2EL, suppresses the aneurysm sac expansion, and reduces the rate of re-intervention. Non-selective embolization of the IMA and LAs shows the best results in preventing T2EL. IMA embolization demonstrated certain benefits in achieving long-term aneurysm sac stability and lowering the risk of secondary surgery. Embolization of the LAs increases the operation time and medical expenses, but leads to potentially negative effects on the long-term outcome. We recommend conducting prophylactic embolization, especially IMA embolization alone or ASCE, to enhance the clinical benefits. More high-quality studies are needed to confirm the present findings.

Data availability statement

The datasets presented in this study can be found in online repositories. The names of the repository/repositories and accession number(s) can be found in the article/ **Supplementary Material**.

Author contributions

YW and JY conceived the study, designed the method, contributed to the literature searches, provided statistical analysis, and wrote the manuscript. ZH investigated the literatures. GW excluded the documents. All authors interpreted the data, read the manuscript, and approved the final version.

Funding

This work was supported by Capital's Funds for Health Improvement and Research, 2020-2Z-5014.

Conflict of interest

The authors declare that the research was conducted in the absence of any commercial or financial relationships that could be construed as a potential conflict of interest.

Publisher's note

All claims expressed in this article are solely those of the authors and do not necessarily represent those of their affiliated organizations, or those of the publisher, the editors and the reviewers. Any product that may be evaluated in this article, or claim that may be made by its manufacturer, is not guaranteed or endorsed by the publisher.

Supplementary material

The Supplementary Material for this article can be found online at: https://www.frontiersin.org/articles/10.3389/fcvm.2022.947809/full#supplementary-material

References

1. Greenhalgh RM, Brown LC, Kwong GP, Powell JT, Thompson SG, EVAR trial participants. Comparison of endovascular aneurysm repair with open repair in patients with abdominal aortic aneurysm (EVAR trial 1), 30-day operative mortality results: randomised controlled trial. *Lancet.* (2004) 364:843–8.

2. Patel R, Sweeting MJ, Powell JT, Greenhalgh RM, EVAR trial investigators. Endovascular versus open repair of abdominal aortic aneurysm in 15-years' follow-up of the UK endovascular aneurysm repair trial 1 (EVAR trial 1): a randomised controlled trial. *Lancet.* (2016) 388:2366–74. doi: 10.1016/S0140-6736(16)31135-7

3. De Bruin JL, Baas AF, Buth J, Prinssen M, Verhoeven EL, Cuypers PW, et al. Long-term outcome of open or endovascular repair of abdominal aortic aneurysm. *N Engl J Med.* (2010) 362:1881–9.

4. Dijkstra ML, Zeebregts CJ, Verhagen HJM, Teijink JAW, Power AH, Bockler D, et al. Incidence, natural course, and outcome of type II endoleaks in infrarenal endovascular aneurysm repair based on the ENGAGE registry data. *J Vasc Surg.* (2020) 71:780–9. doi: 10.1016/j.jvs.2019.04.486

5. Sidloff DA, Gokani V, Stather PW, Choke E, Bown MJ, Sayers RD. Type II endoleak: conservative management is a safe strategy. *Eur J Vasc Endovasc Surg.* (2014) 48:391–9. doi: 10.1016/j.ejvs.2014.06.035

6. Rehman ZU. Endoleaks: current concepts and treatments - A narrative review. *J Pak Med Assoc.* (2021) 71:2224–9. doi: 10.47391/JPMA.03-345

7. Mulay S, Geraedts ACM, Koelemay MJW, Balm R, ODYSSEUS study group. Type 2 endoleak with or without intervention and survival after endovascular aneurysm repair. *Eur J Vasc Endovasc Surg.* (2021) 61:779–86. doi: 10.1016/j.ejvs.2021.01.017

8. Jones JE, Atkins MD, Brewster DC, Chung TK, Kwolek CJ, LaMuraglia GM, et al. Persistent type 2 endoleak after endovascular repair of abdominal aortic aneurysm is associated with adverse late outcomes. *J Vasc Surg.* (2007) 46:1–8. doi: 10.1016/j.jvs.2007.02.073

9. Rayt HS, Sandford RM, Salem M, Bown MJ, London NJ, Sayers RD. Conservative management of type 2 endoleaks is not associated with increased risk of aneurysm rupture. *Eur J Vasc Endovasc Surg.* (2009) 38:718–23. doi: 10.1016/j.ejvs.2009.08.006

10. El Batti S, Cochennec F, Roudot-Thoraval F, Becquemin JP. Type II endoleaks after endovascular repair of abdominal aortic aneurysm are not always a benign condition. *J Vasc Surg.* (2013) 57:1291–7. doi: 10.1016/j.jvs.2012.10.118

11. Wanhainen A, Verzini F, Van Herzeele I. Editor's Choice - European Society for Vascular Surgery (ESVS) 2019 clinical practice guidelines on the management of abdominal aorto-iliac artery aneurysms. *Eur J Vasc Endovasc Surg.* (2019) 57:8–93. Erratum in: Eur J Vasc Endovasc Surg. 2020;59(3):494. doi: 10.1016/j.ejvs.2018.09.020

12. Schlösser FJ, Gusberg RJ, Dardik A, Lin PH, Verhagen HJ, Moll FL, et al. Aneurysm rupture after EVAR: can the ultimate failure be predicted? *Eur J Vasc Endovasc Surg.* (2009) 37:15–22.

13. Sidloff DA, Stather PW, Choke E, Bown MJ, Sayers RD. Type II endoleak after endovascular aneurysm repair. *Br J Surg.* (2013) 100:1262–70.

14. Patel R, Powell JT, Sweeting MJ, Epstein DM, Barrett JK, Greenhalgh RM. The UK EndoVascular Aneurysm Repair (EVAR) randomised controlled trials: long-term follow-up and cost-effectiveness analysis. *Health Technol Assess.* (2018) 22:1–132.

15. Gould DA, McWilliams R, Edwards RD, Martin J, White D, Joekes E, et al. Aortic side branch embolization before endovascular aneurysm repair: incidence of type II endoleak. *J Vasc Interv Radiol.* (2001) 12:337–41.

16. Zhang H, Yang Y, Kou L, Sun H, Chen Z. Effectiveness of collateral arteries embolization before endovascular aneurysm repair to prevent type II endoleaks: a systematic review and meta-analysis. *Vascular.* (2021):17085381211032764. [Online ahead of print], doi: 10.1177/17085381211032764

17. Natrella M, Rapellino A, Navarretta F, Iob G, Cristoferi M, Castagnola M, et al. Embo-EVAR: a technique to prevent Type II endoleak? A single-center experience. *Ann Vasc Surg.* (2017) 44:119–27. doi: 10.1016/j.avsg.2017.01.028

18. Dosluoglu HH, Rivero M, Khan SZ, Cherr GS, Harris LM, Dryjski ML. Pre-emptive nonselective perigraft aortic sac embolization with coils to prevent type II endoleak after endovascular aneurysm repair. *J Vasc Surg.* (2019) 69:1736–46. doi: 10.1016/j.jvs.2018.10.054

19. Pilon F, Tosato F, Danieli D, Campanile F, Zaramella M, Milite D. Intrasac fibrin glue injection after platinum coils placement: the efficacy of a simple intraoperative procedure in preventing type II endoleak after endovascular aneurysm repair. *Interact Cardiovasc Thorac Surg.* (2010) 11:78–82. doi: 10.1510/icvts.2009.231167

20. Fabre D, Fadel E, Brenot P, Hamdi S, Gomez Caro A, Mussot S, et al. Type II endoleak prevention with coil embolization during endovascular aneurysm repair in high-risk patients. *J Vasc Surg.* (2015) 62:1–7.

21. Li Q, Hou P. Sac embolization and side branch embolization for preventing Type II endoleaks after endovascular aneurysm repair: a meta-analysis. *J Endovasc Ther.* (2020) 27:109–16.

22. Liberati A, Altman DG, Tetzlaff J, Mulrow C, Gøtzsche PC, Ioannidis JP, et al. The PRISMA statement for reporting systematic reviews and meta-analyses of studies that evaluate health care interventions: explanation and elaboration. *J Clin Epidemiol.* (2009) 62:e1–34.

23. Wells G, Shea B, O'Connell D, Peterson J, Welch V, Losos M, et al. *The Newcastle-Ottawa Scale (NOS) for Assessing The Quality Of Nonrandomised Studies In Meta-Analyses*. Ottawa: Ottawa Hospital Research Institute (2021).

24. RStudio Team. *RStudio: Integrated Development Environment for R*. Boston, MA: RStudio, PBC (2021).

25. Parry DJ, Kessel DO, Robertson I, Denton L, Patel JV, Berridge DC, et al. Type II endoleaks: predictable, preventable, and sometimes treatable? *J Vasc Surg.* (2002) 36:105–10. doi: 10.1067/mva.2002.125023

26. Axelrod DJ, Lookstein RA, Guller J, Nowakowski FS, Ellozy S, Carroccio A, et al. Inferior mesenteric artery embolization before endovascular aneurysm repair: technique and initial results. *J Vasc Interv Radiol.* (2004) 15:1263–7. doi: 10.1097/01.RVI.0000141342.42484.90

27. Sheehan MK, Hagino RT, Canby E, Wholey MH, Postoak D, Suri R, et al. Type 2 endoleaks after abdominal aortic aneurysm stent grafting with systematic mesenteric and lumbar coil embolization. *Ann Vasc Surg.* (2006) 20:458–63. doi: 10.1007/s10016-006-9103-2

28. Nevala T, Biancari F, Manninen H, Matsi P, Mäkinen K, Ylönen K, et al. Inferior mesenteric artery embolization before endovascular repair of an abdominal aortic aneurysm: effect on type II endoleak and aneurysm shrinkage. *J Vasc Interv Radiol.* (2010) 21:181–5. doi: 10.1016/j.jvir.2009.10.014

29. Chikazawa G, Yoshitaka H, Hiraoka A, Tanaka K, Mouri N, Tamura K, et al. Preoperative coil embolization to aortic branched vessels for prevention of aneurysmal sac enlargement following EVAR: early clinical result. *Ann Vasc Dis.* (2013) 6:175–9. doi: 10.3400/avd.oa.12.00079

30. Piazza M, Frigatti P, Scrivere P, Bonvini S, Noventa F, Ricotta JJ II, et al. Role of aneurysm sac embolization during endovascular aneurysm repair in the prevention of type II endoleak-related complications. *J Vasc Surg.* (2013) 57:934–41. doi: 10.1016/j.jvs.2012.10.078

31. Ward TJ, Cohen S, Fischman AM, Kim E, Nowakowski FS, Ellozy SH, et al. Preoperative inferior mesenteric artery embolization before endovascular aneurysm repair: decreased incidence of type II endoleak and aneurysm sac enlargement with 24-month follow-up. *J Vasc Interv Radiol.* (2013) 24:49–55. doi: 10.1016/j.jvir.2012.09.022

32. Burbelko M, Kalinowski M, Heverhagen JT, Piechowiak E, Kiessling A, Figiel J, et al. Prevention of type II endoleak using the AMPLATZER vascular plug before endovascular aneurysm repair. *Eur J Vasc Endovasc Surg.* (2014) 47:28–36. doi: 10.1016/j.ejvs.2013.10.003

33. Müller-Wille R, Uller W, Gössmann H, Heiss P, Wiggermann P, Dollinger M, et al. Inferior mesenteric artery embolization before endovascular aortic aneurysm repair using amplatzer vascular plug type 4. *Cardiovasc Interv Radiol.* (2014) 37:928–34. doi: 10.1007/s00270-013-0762-4

34. Mascoli C, Freyrie A, Gargiulo M, Gallitto E, Pini R, Faggioli G, et al. Selective Intra-procedural AAA sac embolization during EVAR reduces the rate of Type II endoleak. *Eur J Vasc Endovasc Surg.* (2016) 51:632–9. doi: 10.1016/j.ejvs.2015.12.009

35. Nakai M, Ikoma A, Sato M, Sato H, Nishimura Y, Okamura Y. Prophylactic intraoperative embolization of abdominal aortic aneurysm sacs using N-Butyl cyanoacrylate/lipiodol/ethanol mixture with proximal neck aortic balloon occlusion during endovascular abdominal aortic repair. *J Vasc Interv Radiol.* (2016) 27:954–60. doi: 10.1016/j.jvir.2016.03.037

36. Piazza M, Squizzato F, Zavatta M, Menegolo M, Ricotta JJ II, Lepidi S, et al. Outcomes of endovascular aneurysm repair with contemporary volume-dependent sac embolization in patients at risk for Type II endoleak. *J Vasc Surg.* (2016) 63:32–8. doi: 10.1016/j.jvs.2015.08.049

37. Vaillant M, Barral PA, Mancini J, De Masi M, Bal L, Piquet P, et al. Preoperative inferior mesenteric artery embolization is a cost-effective technique that may reduce the rate of aneurysm sac diameter enlargement and reintervention after EVAR. *Ann Vasc Surg.* (2019) 60:85–94. doi: 10.1016/j.avsg.2019.03.012

38. Samura M, Morikage N, Otsuka R, Mizoguchi T, Takeuchi Y, Nagase T, et al. Endovascular aneurysm repair with inferior mesenteric artery embolization for preventing Type II endoleak: a prospective randomized controlled trial. *Ann Surg.* (2020) 271:238–44. doi: 10.1097/SLA.0000000000003299

39. Branzan D, Geisler A, Steiner S, Doss M, Matschuck M, Scheinert D, et al. Type II endoleak and aortic aneurysm sac shrinkage after preemptive embolization of aneurysm sac side branches. *J Vasc Surg.* (2021) 73:1973–9.e1. doi: 10.1016/j.jvs.2020.11.032

40. Fabre D, Mougin J, Mitilian D, Cochennec F, Garcia Alonso C, Becquemin JP, et al. Prospective, randomised two centre trial of endovascular repair of abdominal aortic aneurysm with or without sac embolisation. *Eur J Vasc Endovasc Surg.* (2021) 61:201–9. doi: 10.1016/j.ejvs.2020.11.028

41. Mascoli C, Faggioli G, Gallitto E, Pini R, Fenelli C, Cercenelli L, et al. Tailored Sac embolization during EVAR for preventing persistent Type II endoleak. *Ann Vasc Surg.* (2021) 76:293–301. doi: 10.1016/j.avsg.2021.01.118

42. Mathlouthi A, Guajardo I, Al-Nouri O, Malas M, Barleben A. Prophylactic aneurysm embolization during EVAR is safe, improves sac regression and decreases the incidence of Type II endoleak. *Ann Vasc Surg.* (2021) 74:36–41. doi: 10.1016/j.avsg.2020.12.060

43. Rokosh RS, Chang H, Butler JR, Rockman CB, Patel VI, Milner R, et al. Prophylactic sac outflow vessel embolization is associated with improved sac regression in patients undergoing endovascular aortic aneurysm repair. *J Vasc Surg.* (2021) 76:113–21.e8. doi: 10.1016/j.jvs.2021.11.070

44. Aoki A, Maruta K, Omoto T, Masuda T. Midterm outcomes of endovascular abdominal aortic aneurysm repair with prevention of Type 2 endoleak by intraoperative aortic side branch coil embolization. *Ann Vasc Surg.* (2022) 78:180–9. doi: 10.1016/j.avsg.2021.06.037

45. Alerci M, Giamboni A, Wyttenbach R, Porretta AP, Antonucci F, Bogen M, et al. Endovascular abdominal aneurysm repair and impact of systematic preoperative embolization of collateral arteries: endoleak analysis and long-term follow-up. *J Endovasc Ther.* (2013) 20:663–71. doi: 10.1583/12-4188MR.1

46. Bonvini R, Alerci M, Antonucci F, Tutta P, Wyttenbach R, Bogen M, et al. Preoperative embolization of collateral side branches: a valid means to reduce type II endoleaks after endovascular AAA repair. *J Endovasc Ther.* (2003) 10:227–32. doi: 10.1177/152660280301000210

47. Fukuda T, Matsuda H, Tanaka H, Sanda Y, Morita Y, Seike Y. Selective Inferior mesenteric artery embolization during endovascular abdominal aortic aneurysm repair to prevent Type II endoleak. *Kobe J Med Sci.* (2018) 63:E130–5.

48. Muthu C, Maani J, Plank LD, Holden A, Hill A. Strategies to reduce the rate of type II endoleaks: routine intraoperative embolization of the inferior mesenteric artery and thrombin injection into the aneurysm sac. *J Endovasc Ther.* (2007) 14:661–8. doi: 10.1177/152660280701400509

49. Ronsivalle S, Faresin F, Franz F, Rettore C, Zanchetta M, Olivieri A. Aneurysm sac "thrombization" and stabilization in EVAR: a technique to reduce the risk of type II endoleak. *J Endovasc Ther.* (2010) 17:517–24. doi: 10.1583/09-3004.1

50. Zanchetta M, Faresin F, Pedon L, Ronsivalle S. Intraoperative intrasac thrombin injection to prevent type II endoleak after endovascular abdominal aortic aneurysm repair. *J Endovasc Ther.* (2007) 14:176–83. doi: 10.1177/152660280701400209

51. Yu HYH, Lindström D, Wanhainen A, Tegler G, Hassan B, Mani K. Systematic review and meta-analysis of prophylactic aortic side branch embolization to prevent type II endoleaks. *J Vasc Surg.* (2020) 72:1783–92.e1. doi: 10.1016/j.jvs.2020.05.020

52. Biancari F, Mäkelä J, Juvonen T, Venermo M. Is inferior mesenteric artery embolization indicated prior to endovascular repair of abdominal aortic aneurysm? *Eur J Vasc Endovascular Surg.* (2015) 50:671–4. doi: 10.1016/j.ejvs.2015.06.116

53. Ajalat M, Williams R, Wilson SE. The natural history of type 2 endoleaks after endovascular aneurysm repair justifies conservative management. *Vascular.* (2018) 26:524–30. doi: 10.1177/1708538118766103

54. Bastos Gonçalves F, Baderkhan H, Verhagen HJ, Wanhainen A, Björck M, Stolker RJ, et al. Early sac shrinkage predicts a low risk of late complications after endovascular aortic aneurysm repair. *Br J Surg.* (2014) 101:802–10. doi: 10.1002/bjs.9516

55. Schanzer A, Greenberg RK, Hevelone N, Robinson WP, Eslami MH, Goldberg RJ, et al. Predictors of abdominal aortic aneurysm sac enlargement after endovascular repair. *Circulation.* (2011) 123:2848–55. Erratum in: Circulation. 2012;125(2):e266. doi: 10.1161/CIRCULATIONAHA.110.014902

56. Chaikof E, Dalman R, Eskandari M, Jackson B, Lee W, Mansour M, et al. The society for vascular surgery practice guidelines on the care of patients with an abdominal aortic aneurysm. *J Vasc Surg.* (2018) 67:2–77. doi: 10.1016/j.jvs.2017.10.044

57. Eden CL, Long GW, Major M, Studzinski D, Brown OW. Type II endoleak with an enlarging aortic sac after endovascular aneurysm repair predisposes to the development of a type IA endoleak. *J Vasc Surg.* (2020) 72:1354–9. doi: 10.1016/j.jvs.2020.01.038

58. van Marrewijk C, Buth J, Harris PL, Norgren L, Nevelsteen A, Wyatt MG. Significance of endoleaks after endovascular repair of abdominal aortic aneurysms: the EUrosTAR experience. *J Vasc Surg.* (2002) 35:461–73. doi: 10.1067/mva.2002.118823

frontiers | Frontiers in Cardiovascular Medicine

TYPE Original Research
PUBLISHED 04 August 2022
DOI 10.3389/fcvm.2022.955838

Check for updates

OPEN ACCESS

EDITED BY
Zhenjie Liu,
The Second Affiliated Hospital of Zhejiang University School of Medicine, China

REVIEWED BY
Tao Han,
Northern Theater General Hospital, China
Mohammad Reza Asadi,
Tabriz University of Medical Sciences, Iran
Jian Zhang,
The First Affiliated Hospital of China Medical University, China
Song Yi,
First Affiliated Hospital of Zhengzhou University, China

*CORRESPONDENCE
Shuofei Yang
doctor_yangshuofei@163.com
Guanhua Xue
guanhuaxue2018@163.com

SPECIALTY SECTION
This article was submitted to General Cardiovascular Medicine, a section of the journal Frontiers in Cardiovascular Medicine

RECEIVED 29 May 2022
ACCEPTED 12 July 2022
PUBLISHED 04 August 2022

CITATION
Chen L, Wang S, Wang Z, Liu Y, Xu Y, Yang S and Xue G (2022) Construction and analysis of competing endogenous RNA network and patterns of immune infiltration in abdominal aortic aneurysm. *Front. Cardiovasc. Med.* 9:955838. doi: 10.3389/fcvm.2022.955838

COPYRIGHT
© 2022 Chen, Wang, Wang, Liu, Xu, Yang and Xue. This is an open-access article distributed under the terms of the Creative Commons Attribution License (CC BY). The use, distribution or reproduction in other forums is permitted, provided the original author(s) and the copyright owner(s) are credited and that the original publication in this journal is cited, in accordance with accepted academic practice. No use, distribution or reproduction is permitted which does not comply with these terms.

Construction and analysis of competing endogenous RNA network and patterns of immune infiltration in abdominal aortic aneurysm

Liang Chen[1], Shuangshuang Wang[2], Zheyu Wang[1], Yuting Liu[1], Yi Xu[1], Shuofei Yang[1]* and Guanhua Xue[1]*

[1]Department of Vascular Surgery, Renji Hospital, School of Medicine, Shanghai Jiaotong University, Shanghai, China, [2]Songyuan Central Hospital, Songyuan Children's Hospital, Songyuan, China

Background: Various studies have highlighted the role of circular RNAs (circRNAs) as critical molecular regulators in cardiovascular diseases, but its role in abdominal aortic aneurysm (AAA) is unclear. This study explores the potential molecular mechanisms of AAA based on the circRNA-microRNA (miRNA)-mRNA competing endogenous RNA (ceRNA) network and immune cell infiltration patterns.

Methods: The expression profiles of circRNAs (GSE144431) and mRNAs (GSE57691 and GSE47472) were obtained from the Gene Expression Omnibus (GEO). Then, the differentially expressed circRNAs (DEcircRNAs) and mRNAs (DEmRNAs) between AAA patients and healthy control samples, and the target miRNAs of these DEmRNAs and DEcircRNAs were identified. Based on the miRNA-DEmRNAs and miRNA-DEcircRNAs pairs, the ceRNA network was constructed. Furthermore, the proportion of the 22 immune cell types in AAA patients was assessed using cell type identification by estimating relative subsets of RNA transcripts (CIBERSORT) algorithm. The expressions of key genes and immune cell infiltration were validated using clinical specimens.

Results: A total of 214 DEmRNAs were identified in the GSE57691 and GSE47472 datasets, and 517 DEcircRNAs were identified in the GSE144431 dataset. The ceRNA network included 19 circRNAs, 36 mRNAs, and 68 miRNAs. Two key genes, *PPARG* and *FOXO1*, were identified among the hub genes of the established protein-protein interaction between mRNAs in the ceRNA network. Moreover, seven types of immune cells were differentially expressed between AAA patients and healthy control samples. Hub genes in ceRNA, such as *FOXO1*, *HSPA8*, and *RAB5C*, positively correlated with resting CD4 memory T cells or M1 macrophages, or both.

Conclusion: In conclusion, a ceRNA interaction axis was constructed. The composition of infiltrating immune cells was analyzed in the abdominal aorta

of AAA patients and healthy control samples. This may help identify potential therapeutic targets for AAA.

KEYWORDS

abdominal aortic aneurysm, circular RNA, competing endogenous RNA network, immune cell infiltration, bioinformatic analysis

Introduction

Abdominal aortic aneurysm (AAA) is a progressive vascular accompanies the risk of rupturing the dilated aortic segment and is potentially lethal (1). However, the mechanism of AAA progression is unclear; hence it is essential to explore the underlying molecular causes of AAA that will help improve the diagnosis and treatment of AAA patients (2). Recent studies have shown the role of circular RNAs (circRNAs) in the pathogenesis of cardiovascular diseases (3, 4). circRNAs are a unique class of RNA molecules; they form a circular closed-loop structure by a covalent bond linkage by back-splicing linear RNA (5). It has been shown that circRNAs act as competitive endogenous RNA (ceRNA) and are involved in cardiovascular disease pathogenesis (6). In the ceRNA network, circRNAs compete with microRNAs (miRNAs) through miRNA response elements (MRE), thereby negatively regulating the mRNA expression of protein-coding genes (7). A unique circRNA-miRNA-mRNA interaction could be a potential mechanism for the development and progression of AAA.

The main pathological features of AAA include smooth muscle cell (SMC) dysfunction, inflammation, immune cell infiltration, and extracellular matrix remodeling (8). Studies have shown an association between circ-FNDC3B and angiotensin II (Ang II) induced SMC dysfunction, suggesting that circ-FNDC3B/miR-143-3p/ADAM10 axis may regulate AAA pathogenesis (9). Further investigation of circ-Sirt1/miR-132/212/SIRT1 in SMC phenotypic switching provided another perspective on the pathogenesis of AAA (10). Recently, Ma et al. showed the involvement of hsa_circ_0087352 in promoting the inflammatory response of macrophages in AAA. The target miRNAs and mRNAs were identified, and a ceRNA network of hsa_circ_0087352/ hsa-miR-149-5p/ IL-6 in AAA was constructed (11). Results suggest hsa_circ_0087352 promotes IL-6 transcription and secretion of inflammatory cytokine via endogenous hsa-miR-149-5p in macrophages thereby hsa_circ_0087352 could be potentially used in AAA therapeutics. These findings suggest that circRNA may have different targets and functions in other cells and tissues, and the circRNA-miRNA-mRNA network could play a significant role in AAA pathogenesis. Studies have proven the involvement of the infiltrating immune cells, such as neutrophils, macrophages, and T cells, in the occurrence and development of AAA (12). AAA is characterized by the infiltration of immune cells, suggesting that the immune system plays a critical role in AAA progression (13, 14). However, the ceRNA network and its association with infiltrating immune cells in AAA have not been thoroughly elucidated (15, 16).

This study aims to explore a novel circRNA-miRNA-mRNA ceRNA axis in AAA by analyzing microarray datasets from publicly available databases. Various patterns of immune cell infiltration in AAA were studied using the "cell type identification by estimating relative subsets of RNA transcripts (CIBERSORT)" algorithm. The co-expression patterns of immune cells and hub genes of the ceRNA network were also identified. Moreover, the target mRNAs of DEcircRNAs and immune infiltration were validated in healthy control samples and AAA patients. This study sheds light on the potential role of ceRNA in the pathogenesis of AAA and its underlying immune infiltration signature.

Materials and methods

Data collection and differential expression analysis

The microarray data of AAA were retrieved from the National Center for Biotechnology Information Gene Expression Omnibus (NCBI_GEO) database (https://www.ncbi.nlm.nih.gov/geo/). The species type as "Homo sapiens." was set as a filter and the results obtained included three datasets GSE47472, GSE57691, and GSE144431. The data of circRNA expression (GSE144431) was ncRNA profiling by array, and the data of the microarray platform by 074301 Arraystar Human ncRNA microarray V2 (platform: GPL21825), the mRNA expression datasets (GSE47472 and GSE57691) by expression profiling by array, and the data of the microarray platform by Illumina HumanHT-12 V4.0 expression BeadChip (platform: GPL10558). Each dataset includes data from patients with AAA and normal aorta (which will be referred to as the healthy control group). Series matrix files and expressive data were retrieved from the GEO database.

The differentially expressed mRNAs (DEmRNAs) and circRNAs (DEcircRNAs) between the AAA patients and the healthy control group were analyzed and compared using

the "Linear Models for Microarray Data (limma)" R package. mRNAs and circRNAs were considered as DEmRNAs and DEcircRNAs if they met the criteria: |log2 fold change (FC)| > 1 and false discovery rate (FDR) adjusted p-value < 0.05. The differential analysis results were presented as volcano plots and heat maps, and related tabular information was derived.

Functional enrichment and pathway analysis

Kyoto Encyclopedia of Genes and Genomes (KEGG) enrichment analysis and Gene Ontology (GO) were used to explore the biological functions of DEmRNAs in AAA. The KEGG enrichment analysis and GO analysis included biological processes (BP), molecular functions (MF), and cellular components (CC), and the analysis was performed using the "clusterProfiler" package of the R software. FDR adjusted p-value < 0.05 was considered statistically significant.

Construction of the ceRNA network

The DEcircRNAs (GSE144431) and DEmRNAs (GSE57691 and GSE47472) between AAA patients and healthy control samples were identified, and the target miRNAs of the key DEmRNAs and DEcircRNAs were predicted. The DEmRNA-miRNA pairs were predicted using the target miRNA information from the databases like miRcode, miRDB, TargetScan, miRmap, and miRanda databases (17–21). The DEcircRNA-miRNA pairs were determined using the starBase database (http://starbase.sysu.edu.cn/index.php). DEcircRNA-miRNA pairs and DEmRNA-miRNA pairs were used to construct the ceRNA network and visualized using cytoHubba in Cytoscape 3.4.0 software.

Protein-protein interaction (PPI) network analysis and hub genes identification

The Search Tool for the Retrieval of Interacting Genes (STRING; version 11.0) was used to explore the protein-protein interactions between mRNAs in the ceRNA network (22). The PPI network of the DEmRNAs with combined score >0.4 in STRING was considered as a functional link. The PPI network was visualized by Cytoscape 3.4.0. The cytoHubba plugin of the Cytoscape software calculates the dense relationship through the degree, betweenness centrality, and closeness centrality algorithms. The hub genes of the PPI network were confirmed by cytoHubba.

Analysis of immune cell infiltration

The mRNA microarray dataset GSE57691 was analyzed to study the proportion of 22 infiltrating immune cells in the tissues between AAA patients and the healthy control samples using the CIBERSORT algorithm (23). The significantly different cell types (p < 0.05) between AAA patients and the healthy control samples were filtered out in the CIBERSORT analysis. Subsequently, the Wilcoxon rank-sum test was applied to assess differentially infiltrating immune cells between patients with AAA and controls, visualized by "heatmap" and "Violin plot" packages of the R software.

Human studies

The study was approved by the Institutional Review Board of the Shanghai Jiaotong University School of Medicine, Renji Hospital (No. KY2021–168). All experiments were conducted in accordance with the Declaration of Helsinki. Written informed consent was obtained from all patients or their families before the collection of the biological specimens. The presence of an aortic aneurysm was confirmed prior to the echocardiography (ECG) or computed tomography (CT)/magnetic resonance imaging (MRI). The clinical diagnosis was established before surgery by expert clinicians. Healthy control aortic samples were obtained from organ donors.

Immunofluorescence

The abdominal aortas were harvested and fixed using 4% paraformaldehyde (PFA), embedded in paraffin, and serial sections of five μm thickness were prepared on poly-l-lysine coated slides. The sections were dewaxed, rehydrated, and permeabilized using 0.1% Triton X-100. The sections were then blocked using 1% goat serum for 1 h at room temperature and further incubated with anti-rabbit CD68 antibody (1:200, ab213363, Abcam, MA, USA) and anti-rabbit CD86 antibody (1:200, ab239075, Abcam, USA) at 4°C overnight. The following day, slides containing sections were incubated with fluorescent-conjugated secondary antibodies diluted in blocking buffer for 1 h at room temperature and mounted using 4′,6-diamidino-2-phenylindole (DAPI, Vector, ZsBio, Beijing, China). Imaging was done using a confocal microscope (Leica-SP8, Wetzlar, Germany).

Quantitative reverse transcription polymerase chain reaction (qRT-PCR)

Total RNA from tissue samples was isolated using TRIzol (15596018, Invitrogen, Carlsbad, CA) per the manufacturer's

instructions. Complementary DNA was synthesized using 500 ng of total RNA using the Reverse Transcription Kit (EZBioscience, MN, USA) per the manufacturer's instructions. qRT-PCR was performed using SYBR Green qPCR Master Mix (EZBioscience, MN, USA). Relative gene expression was calculated using the $2^{-\Delta\Delta CT}$ method. PCR was performed using three biological and technical replicates and normalized using the housekeeping gene glyceraldehyde 3-phosphate dehydrogenase. Primer sequences are listed in Supplementary Table S1.

Statistical analysis

The statistical analysis was carried out using Statistical Package for Social Sciences (SPSS, Chicago, Illinois) version 22.0. The data are expressed as the mean ± standard deviation or percentage. The variables between the two groups were compared using Student's *t*-test. Spearman's rank correlation analysis was performed to study the correlation between the hub genes of the ceRNA network and differentially expressed infiltrating immune cells. $p < 0.05$ was accepted as statistically significant.

Results

Identification of the DEmRNAs and DEcircRNAs

The schematic diagram in Figure 1 illustrates the course of this study. A total of 1,135 upregulated mRNA and 2830 downregulated mRNAs were identified in the GSE47472 dataset. The GSE57691 had 2497 DEmRNAs, of which 247 mRNAs were upregulated, and 2250 mRNAs were downregulated. DEmRNAs were visualized by hierarchical clustering heatmap analysis (Figures 2A,B) and volcano plots analysis (Figures 2C,D). In the GSE14431 dataset, 225 upregulated and 292 downregulated circRNAs were visualized by hierarchical clustering heat map analysis (Figure 2E) and volcano plot analysis (Figure 2F). The most significant differentially expressed DEmRNAs and DEcircRNAs were shown in Tables 1, 2.

GO and KEGG enrichment analysis of the DEmRNAs

The Venn diagram showed 214 overlapping DEmRNAs, of which 11 mRNAs were upregulated, and 203 mRNA were downregulated between GSE47472 and GSE57691 (Figure 3A). GO analysis of these DEmRNAs indicated that BP was significantly enriched in the circulatory system development, negative regulation of cell population proliferation, and response to insulin (Figure 3B; Supplementary Figure S1). The CC ontology cellular processes that were enriched were related to the intracellular membrane-bounded organelle, cytoplasmic ribonucleoprotein granule, and ribonucleoprotein granule (Figure 3C; Supplementary Figure S2). In the MF ontology, enriched processes included snRNA binding, double-stranded RNA binding, and ligand-binding domain (LBD) domain binding (Figure 3D; Supplementary Figure S3). Additional GO analysis was shown in (Supplementary Figure S4. Furthermore, KEGG pathway analysis revealed that these DEmRNAs are mainly involved in the spliceosome, non-alcoholic fatty liver disease (NAFLD), oxidative phosphorylation, and tumor necrosis factor (TNF) signaling pathway (Figure 3E; Supplementary Figure S5). GO and KEGG enrichment analyses are presented in Supplementary Tables S2, S3.

Construction of the ceRNA network

The starBase predicted and identified 311 miRNA targets of the DEcircRNAs from the GSE144431 dataset. The interactions between 311 miRNAs and 214 DEmRNAs were analyzed using the miRcode, miRDB, TargetScan, miRmap, and miRanda. The circRNA-miRNA-mRNA ceRNA network was constructed based on DEcircRNA-miRNA and DEmRNA-miRNA pairs, including 68 miRNAs, 19 circRNAs, and 36 mRNAs (Figure 4).

PPI network construction and hub genes identification

The PPI network was constructed using the STRING database based on the mRNAs from the ceRNA network. After excluding the genes that failed to interact, PPI network consisted of 25 nodes and 27 edges (Figure 5). Subsequently, nine hub genes were identified; among the genes that were upregulated were *SOCS3* (suppressor of cytokine signaling 3) and *PTGS2* (prostaglandin-endoperoxide synthase 2). The downregulated genes were *NOTCH2* (notch receptor 2), *RAB5C* (*RAB5C*, member RAS oncogene family), *HSP90AA1* (heat shock protein 90 alpha family class A member 1), *HSPA8* [heat shock protein family A (Hsp70) member 8] and *PIK3R1* (phosphoinositide-3-kinase regulatory subunit 1), *PPARG* (peroxisome proliferator-activated receptor gamma), and *FOXO1* (forkhead box O1). Among them, two key genes were identified: *PPARG* and *FOXO1*.

Composition of the infiltrating immune cells in AAA

The proportions and composition of 22 infiltrating immune cells were compared between the aortic tissues of AAA

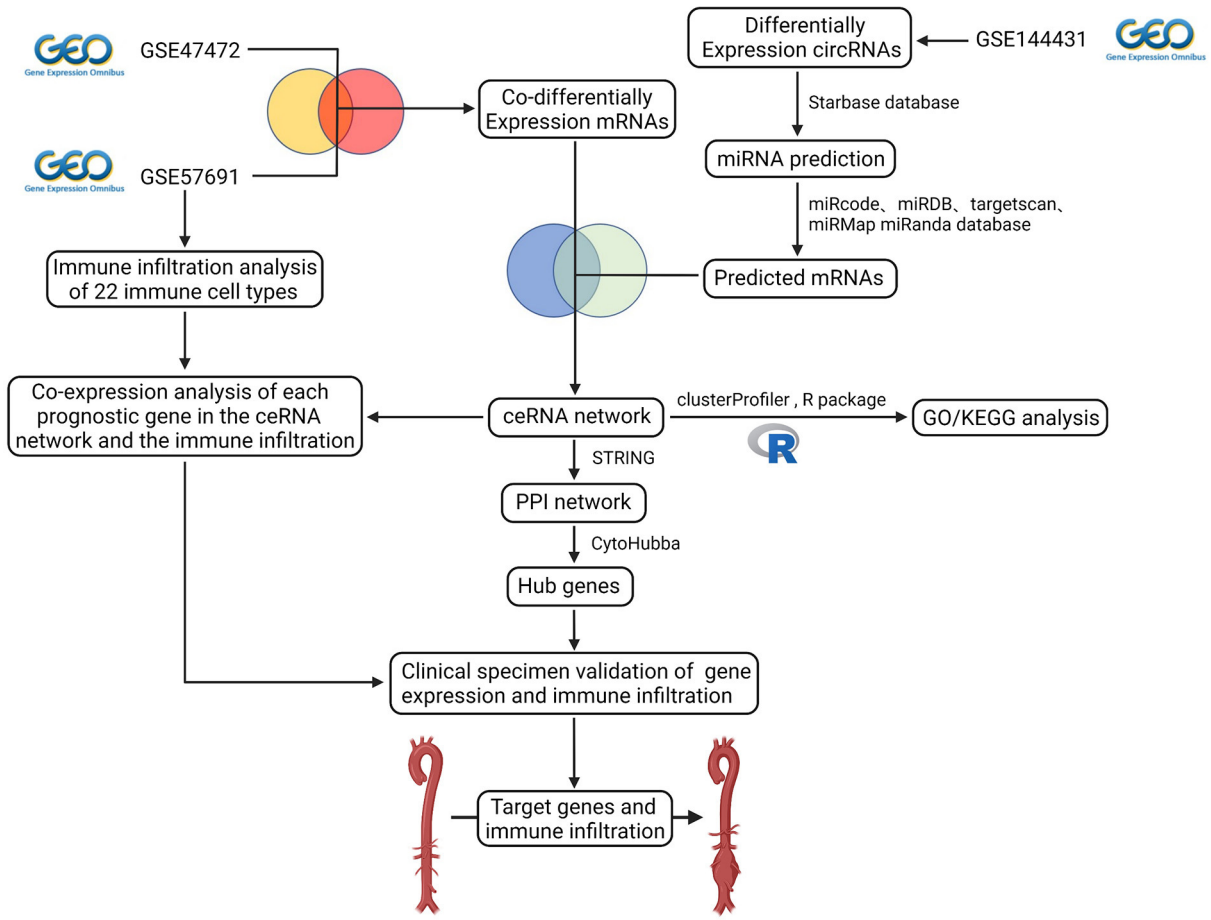

FIGURE 1
Flow diagram of the analytic process. The difference expression of three datasets (circRNA dataset and mRNA dataset) was analyzed. Construction of ceRNA network, protein-protein interaction network, functional enrichment analysis, co-expression analysis of essential genes and the immune infiltration, and validation of gene expression and immune infiltration.

patients and healthy control samples by CIBERSORT algorithm (Figures 6A,B). The relationships between the abundance of 22 immune cells cells are shown in Figure 6C. The correlation analysis revealed a positive correlation between follicular helper T cells and naive B cells ($R = 0.54$) and a negative correlation between activated mast cells and resting mast cells ($R = -0.53$). Other immune cell subpopulations were weak to moderately correlated. Other immune cell subpopulations were weak to moderately correlated.

The relative proportions of infiltrating immune cells between AAA patients and healthy control samples were analyzed by Wilcoxon rank-sum test. Compared with the controls, activated dendritic cells ($p = 0.006$), monocytes ($p = 0.016$), neutrophils ($p = 0.009$), activated CD4 memory T cells ($p = 0.043$), and regulatory T cells ($p = 0.002$) were significantly enriched in AAA patients (Figure 6D; Supplementary Figure S6). The M1 macrophages ($p = 0.04$) and resting CD4 memory T cells ($p = 0.004$) were significantly less enriched in AAA samples compared with the controls (Figure 6D; Supplementary Figure S6).

Co-expression patterns of infiltrating immune cells and key genes

The correlation between hub genes of the ceRNA network and differentially expressed infiltrating immune cells was estimated using Spearman's rank correlation analysis (Figures 7A–F). The *RAB5C* gene was positively correlated with resting CD4 memory T cells and M1 macrophages ($R = 0.55$ and $R = 0.54$, respectively). *HSPA8* gene was positively correlated with resting CD4 memory T cells ($R = 0.60$). The *FOXO1* gene was positively correlated with resting CD4 memory T cells and M1 macrophages ($R = 0.58$ and $R = 0.50$, respectively). The

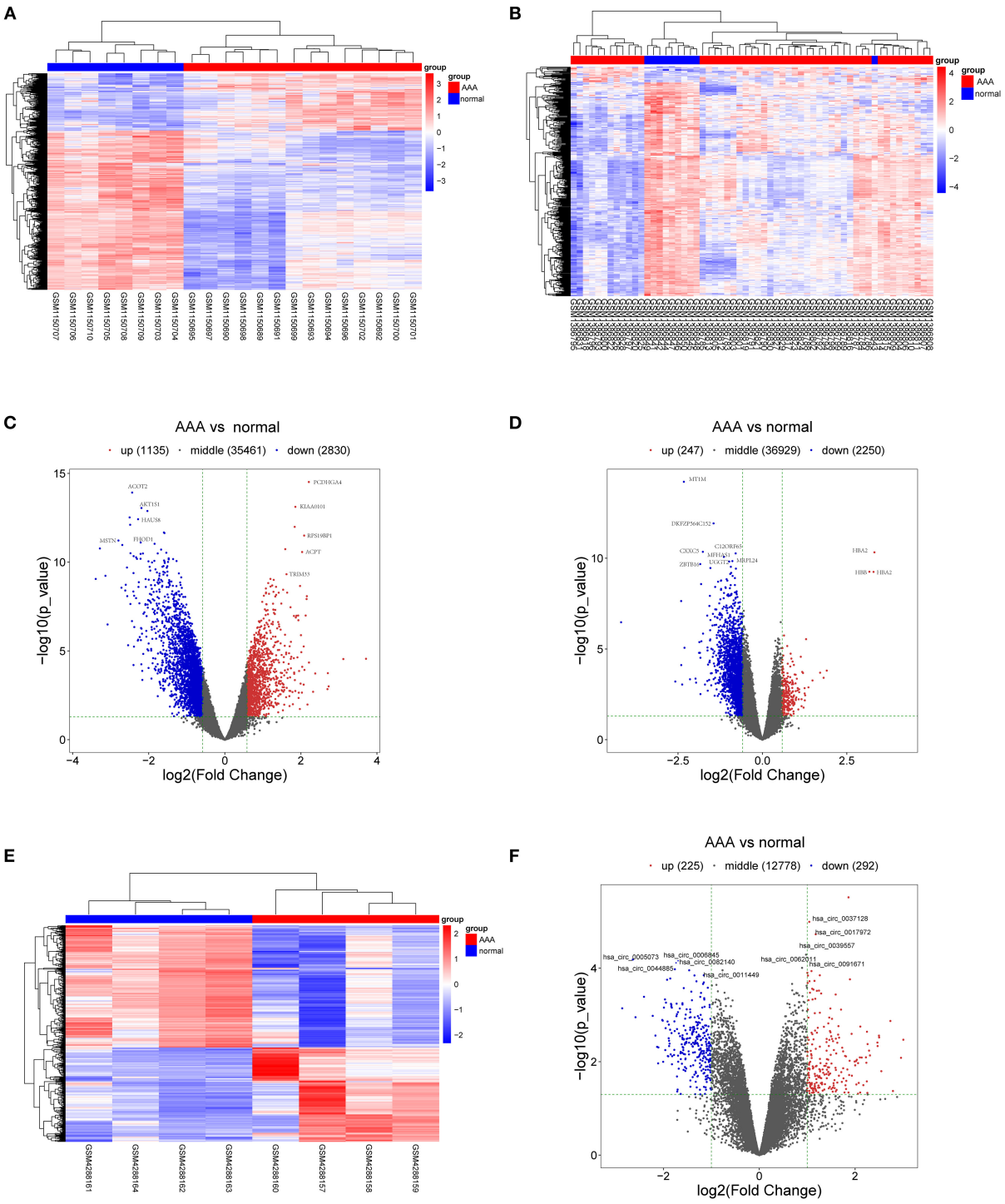

FIGURE 2
DEmRNAs and DEcircRNAs in aortic tissues between patients with AAA and normal controls. **(A)** The heat map of GSE47472, mRNAs. **(B)** The heat map of GSE57691, mRNAs. **(C)** The volcano plot of GSE47472, mRNAs. **(D)** The volcano plot of GSE57691, mRNAs. **(E)** The heat map of GSE144431, circRNAs. **(F)** The volcano plot of GSE144431, circRNAs. mRNAs, messenger RNAs; circRNAs, circular RNAs; DEmRNAs, differentially expressed messenger RNAs; DEcircRNAs, differentially expressed circular RNAs.

TABLE 1 Top20 differentially expressed mRNA between normal tissue and AAAs.

GSE47472			GSE57691		
Gene symbol	*P*-value	LogFC	Gene symbol	*P*-value	LogFC
DYNLL1	0.001007989	3.713704803	HBA2	1.60E-06	3.293491798
ANP32AP1	5.28308E-07	−3.390945819	HBB	1.60E-06	3.170975286
WDR82	3.87398E-08	−3.283955683	RNA28S5	0.012924033	−2.581261085
MSTN	1.81266E-08	−2.794857846	CTSZ	1.74E-05	−2.406532079
LEPR	1.0643E-06	−2.715442603	RPL10A	0.003290958	−2.405450673
ABI1	0.019371581	2.697968288	S100A4	0.016550251	−2.375031783
CARM1	2.61275E-08	−2.695557916	MT1M	2.45E-10	−2.325607304
BRINP3	0.000272617	−2.542055148	RPS17	0.010658672	−2.14452781
KAAG1	2.72774E-05	−2.439965976	RPL21	0.014103802	−1.963001154
ACOT2	2.33003E-10	−2.435730836	FOSB	0.005096434	1.907473194
FAM156A	0.001804728	−2.400505381	MT1X	0.001242665	−1.877340613
XPA	0.000312092	−2.387135524	PPP1R3C	0.000505801	−1.867351411
NAPSA	2.24906E-06	−2.381882488	UBB	0.001242665	−1.849839701
LSM2	4.99234E-05	−2.37779002	ZBTB16	9.16E-07	−1.84119325
ZNF575	7.6998E-08	−2.331880674	RPL26	0.037574325	−1.835326334
LARP7	0.024917017	2.31996564	SCRG1	0.00179909	−1.835280995
NR2F6	0.000175356	−2.286478187	IL6	0.009440574	1.815048907
CNGA3	4.85705E-06	−2.24473153	CXXC5	4.29E-07	−1.764643947
UBE3C	0.001423926	2.211969517	MAOA	0.000268881	−1.757136092
FHOD1	2.15387E-08	−2.211095781	SIK1	0.006202667	1.710707835

correlation between hub genes (*FOXO1*, *RAB5C*, and *HSPA8*) and M1 macrophages was estimated using Spearman's rank correlation analysis (Figure 7G). The expression levels of M1 macrophages and hub genes are illustrated using the heatmap (Figure 7H).

Clinical specimen validation

Resting CD4 memory T cells are important cell types of the immune system and play a crucial role in resistance to pathogens. They are the reservoir for human immunodeficiency virus-1, rendering unrealistic hopes of virus eradication with current antiretroviral regimens (24). Few studies show the involvement of resting CD4 memory T cells in biological processes related to AAA. M1 macrophages circulate in the peripheral blood and reside in specific tissues, thereby conferring protection by attacking foreign substances such as bacteria and engulfing them by phagocytosis. We validated the expression of the M1 macrophage marker in clinical specimens, i.e., abdominal aortas, from AAA patients and healthy control samples. The immunofluorescence staining of CD68 and CD86 showed the infiltrating M1 macrophages were downregulated in large AAA samples (abdominal aorta diameter >55 mm), upregulated in both small AAA samples (abdominal aorta diameter ≤55 mm) and ruptured AAA samples compared to the healthy aorta (Figure 8A).

The mRNA levels of *FOXO1*, *RAB5C*, *HSPA8*, and *PPARG* were significantly decreased in AAA than in healthy control samples (Figure 8B). Significantly lower levels of *HSPA8* and higher levels of *FOXO1* and *RAB5C* in ruptured AAA than in unruptured AAA samples were observed (Figure 8C). The correlation between hub genes (*FOXO1*, *RAB5C*, *HSPA8*, and *PPARG*) and M1 macrophages in the clinical specimens was estimated using Spearman's rank correlation analysis (Figure 8D). The M1 macrophages positively correlated with *FOXO1* and *RAB5C* ($R = 0.61$ and $R = 0.56$, respectively). In addition, RNA expression of *FOXO1* and *PPARG* in clinical specimens were detected using RT-qPCR, confirming that hsa_circ_0002722-miR-130a/b-3p-*PPARG* and hsa_circ_0001837/hsa_circ_0000941-miR-135a/b-5p-*FOXO1* were associated with the pathogenesis of AAA (Figures 8E,F).

Discussion

AAA is a chronic vascular disease with potentially fatal outcomes (25). Microarray-based screening methods helped identify new diagnostic and therapeutic targets. Evidence suggests the role of circRNAs in the pathogenesis of AAA

TABLE 2 Top20 differentially expressed circRNA between normal tissue and AAAs in GSE144431.

circRNA	*P*-value	LogFC
hsa_circ_0001588	3.007621	0.111332
hsa_circ_0000517	2.957863	0.133612
hsa_circ_0092291	−2.8589	0.095681
hsa_circ_0092342	2.790772	0.231818
hsa_circ_0006156	2.736588	0.103484
hsa_circ_0005073	−2.63757	0.094948
hsa_circ_0090069	−2.5822	0.103484
hsa_circ_0000518	2.547719	0.159934
hsa_circ_0000524	2.501812	0.11042
hsa_circ_0007148	2.497819	0.109058
hsa_circ_0068655	2.470108	0.116696
hsa_circ_0008285	2.465435	0.112551
hsa_circ_0057691	−2.40486	0.094948
hsa_circ_0042268	2.291068	0.125054
hsa_circ_0000512	2.25612	0.242569
hsa_circ_0008410	2.245111	0.193686
hsa_circ_0009361	2.235248	0.141517
hsa_circ_0007249	2.226477	0.133612
hsa_circ_0003249	−2.22267	0.103484
hsa_circ_0014213	2.173152	0.20738

(4). Unlike traditional linear RNA, circRNA has a unique covalent closed circular structure, which confers high stability and tolerance to exonuclease activity (26). According to the ceRNA hypothesis, circRNAs act as miRNA sponges, which affects and inhibits miRNA activity and alters the expression of miRNA target genes (27). To understand and explore the effect of circRNA on gene expression *via* miRNA, in this study, the ceRNA network was constructed, and immune infiltration in AAA was analyzed using bioinformatics tools.

We integrated mRNAs with the same regulated trend in the NCBI_GEO database (GSE47472 and GSE57691) and obtained 214 DEmRNAs. GO analysis revealed that these DEmRNAs were significantly enriched in the circulatory system development and negative regulation of cell population proliferation. These processes play a key role in the crucial lesion formation in vascular diseases like AAA. Consistent with the results from Batra et al., KEGG analysis revealed that the oxidative phosphorylation and TNF signaling pathway are closely related to AAA pathogenesis (28, 29). After screening out the DEcircRNAs in the NCBI_GEO database (GSE144431), we predicted the DEcircRNA-miRNA and miRNA-DEmRNA pairs that construct the ceRNA network. Hub genes play a central role in the biological mechanisms underlying the potential pathogenesis of AAAs. Two key genes, namely, *PPARG* and *FOXO1*, among hub genes in the PPI network were identified.

PPARG are transcription factors of the nuclear hormone receptor family that binds to peroxisome proliferators. On activation by a ligand, the nuclear receptor binds to DNA-specific PPARG response elements and regulates the transcription of its target genes (30). Studies in the Ang II-induced AAA mouse model reveal that *PPARG* upregulates the expression of anti-inflammatory cytokines such as IL-10, thereby slowing the process of AAA development and rupture (31). The activators of *PPARG*, such as rosiglitazone and pioglitazone, have been shown to alleviate the development and rupture of Ang II-induced aneurysms in mouse models (32–34). Besides, this study also found that *PPARG* may exert its impacts through hsa_circ_0002722-miR-130a/b-3p. The downregulation of *PPARG* in SMC increases pro- inflammatory factors such as MMP and OPN, thereby promoting SMC proliferation, migration, and vascular remodeling, which is associated with atherosclerosis (35, 36). Additionally, *PPARG* can also act *via* hsa_circ_0002722-miR-130a/b-3p. miR-130a promotes inflammation which accelerates disease progression in atherosclerosis by downregulating the expression of *PPARG* (37). Similarly, previous studies show upregulation of miR-130b, specifically in AAA tissue (38). Further reports suggest polymorphisms in PPARG are associated with the development and progression of AAA (39). Therefore, the changes in *PPARG* expression can alter the inflammatory response and SMC function, making it a potential therapeutic target for AAA.

FOXO1 is a transcription factor that acts as a master switch to regulate the apoptosis of multiple cell types, including cardiomyocytes, pulmonary artery SMC, and endothelial cells (40). *FOXO1*-mediated SMC apoptosis has been reported to regulate plaque instability in advanced atherosclerotic lesions, providing new ideas for AAA formation, as SMC apoptosis is a classic pathological feature of AAA (41). *FOXO1* is also involved in cell migration, invasion, proliferation, and physiological processes such as inflammation and autophagy (42, 43). It has been shown to promote the migration, invasion, and inflammatory response of human umbilical vein endothelial cells, leading to the development and progression of a cerebral aneurysm (44). Hou et al. discovered that *FOXO1* promoted the proliferation of SMC, which contributes to the progression of cerebral aneurysm and atherosclerosis (45, 46). Moreover, *FOXO1*-mediated cellular autophagy plays a vital role in a variety of diseases, such as liver steatosis, cancer, cerebral ischemia/reperfusion injury, diabetic kidney disease, and oxidative damage (47–51). Reports suggest metformin acts as an inhibitor of autophagy and reduces the Ang II-induced AAA in mouse models, suggesting that *FOXO1* may regulate AAA pathogenesis (52). Further, results from this study reveal, *FOXO1* may exert its impacts through hsa_circ_0001837/hsa_circ_0000941-miR-135a/b-5p. It has been shown that the expression of miR-135a/b was upregulated in AAAs, and the mechanism by which they function in AAA remains to be investigated (38). A recent study suggests that

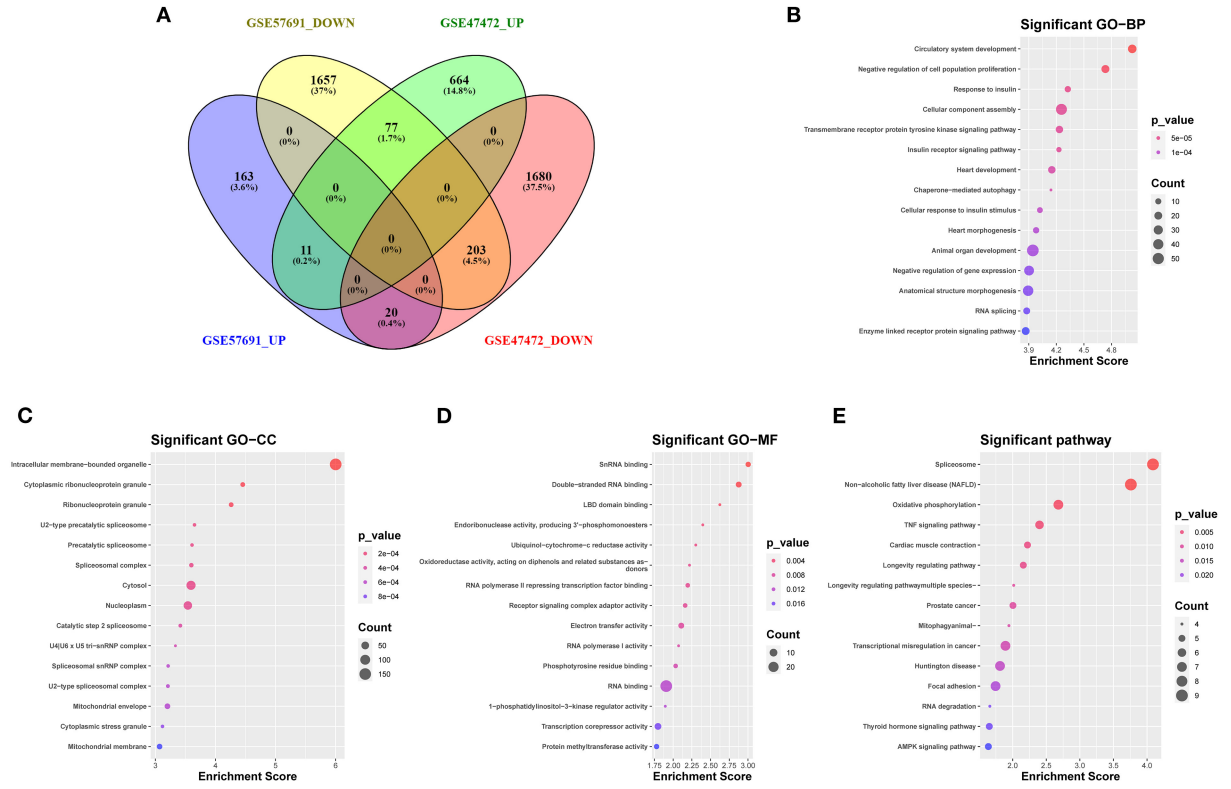

FIGURE 3
Venn diagram analysis and GO/KEGG analysis of 214 DEmRNAs coregulation modes in the two datasets **(A)** The intersection of downregulated and upregulated DEmRNAs (GSE57691 and GSE47472). **(B)** Biological process of 214 DEmRNAs by GO analysis. **(C)** Cellular component of 214 DEmRNAs by GO analysis. **(D)** Molecular function of 214 DEmRNAs by GO analysis. **(E)** KEGG enrichment analysis of DEmRNAs. GO, Gene Ontology; KEGG, Kyoto Encyclopedia of Genes and Genomes; DEmRNAs, differentially expressed messenger RNAs; BP, biological process; CC, cellular component; MF, molecular function.

miR-135a-5p inhibits SMC proliferation and migration by inactivating *FOXO1*, which is consistent with our finding (53). Although *FOXO1* has been extensively studied in cardiovascular diseases, the role of *FOXO1* in AAA requires further investigation.

AAA is caused by multiple factors, such as immune cell infiltration, inflammation, and extracellular matrix remodeling (54). This study identified the proportion of infiltrating immune cells in aortic tissues with differentially expressed immune cells, including M1 macrophages. As M1 macrophage polarization is key in promoting AAA formation, it has been widely accepted to play a part in AAA pathogenesis (4). In the Ang II-induced AAA mouse model, the Chemokine C-C motif ligand contributes to the AAA development and pathogenesis by promoting the M1 polarization of macrophages (55). Furthermore, it has been noted that miR-144-5p is a novel regulator of AAA pathology, inhibiting the M1 polarization of macrophages (56). Our results show the downregulation of M1 macrophages in AAA patients samples compared with healthy control samples. The majority of AAAs in GSE57691 were large AAAs, showing downregulation of M1 macrophages compared to controls. To validate the expression of M1 macrophages in different stages of AAA, we used clinical samples for validation. Compared to the healthy aorta, the expression of the M1 macrophages was downregulated in large-diameter AAA aorta samples. However, it was upregulated in small diameter and ruptured AAA aorta samples. This may be because AAA is a dynamic vascular disease in which M1 macrophages are initially recruited to the injured aorta early in the pathogenesis to induce inflammation. The infiltration of M1 macrophages in AAAs is associated with the long-term effects of multiple factors (4). As the AAA progresses, M1 macrophages cause chronic inflammation, which prevents the repair of the injured aorta. In large aorta AAAs, the M2 polarization of macrophages reduces inflammation, contributing to wound healing, followed by the downregulation of M1 macrophages (57, 58). Our result demonstrates that the M1 polarization of macrophages may change over time in AAA formation, and the massive infiltration of M1 macrophages may be associated with AAA rupture.

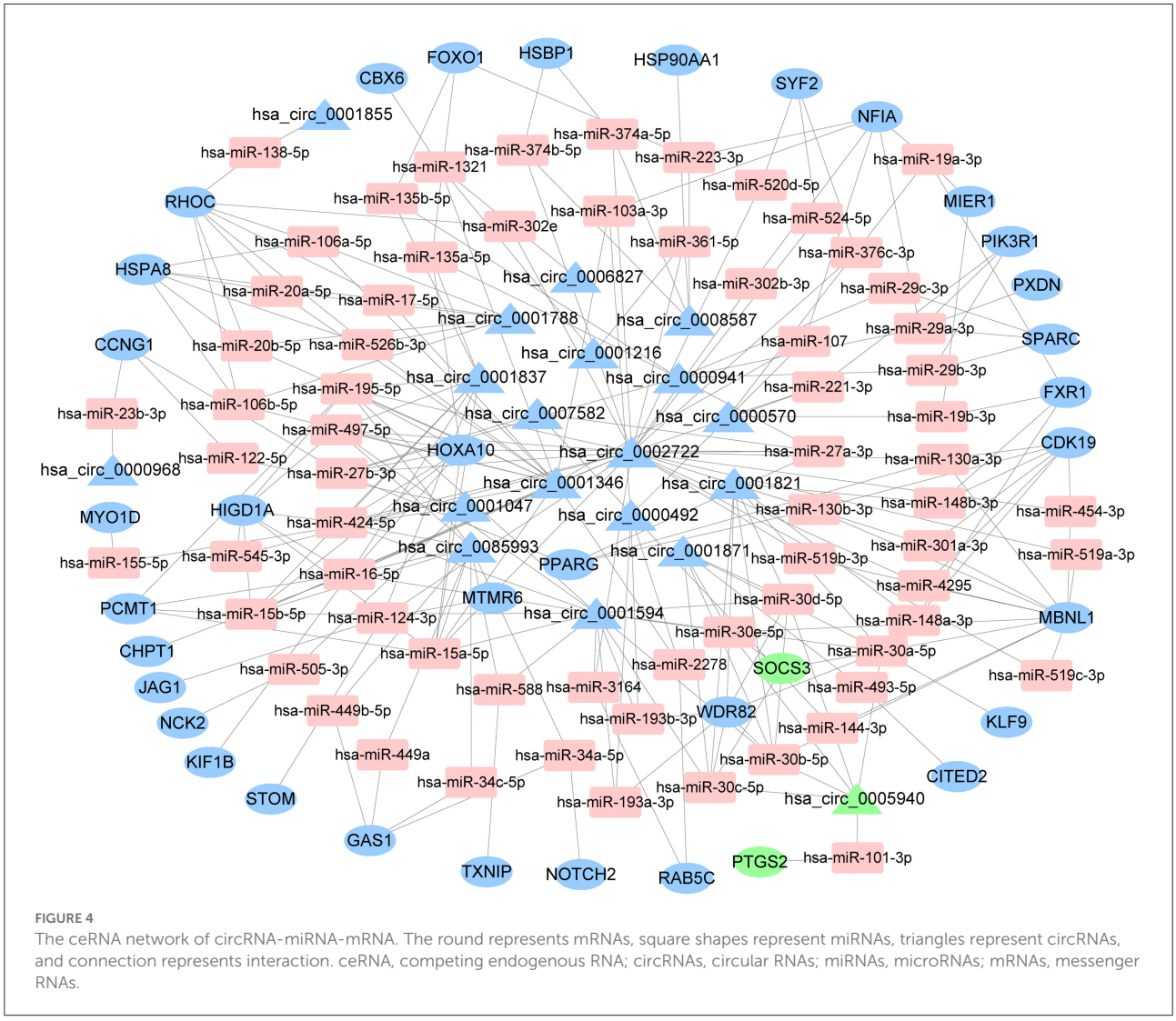

FIGURE 4
The ceRNA network of circRNA-miRNA-mRNA. The round represents mRNAs, square shapes represent miRNAs, triangles represent circRNAs, and connection represents interaction. ceRNA, competing endogenous RNA; circRNAs, circular RNAs; miRNAs, microRNAs; mRNAs, messenger RNAs.

To explore the potential regulatory mechanisms of genes in infiltration immune cells, we performed the correlation analysis between hub genes and differentially expressed immune cells in aortic tissues of patients with AAA. It has been shown that hub genes, such as *FOXO1*, *RAB5C*, and *HSPA8*, were positively correlated with M1 macrophages or resting CD4 memory T cells. The expression of *FOXO1*, *RAB5C*, and *HSPA8* in aortic samples was downregulated in AAA compared to the healthy control samples Furthermore, *HSPA8* levels were low, and FOXO1 and RAB5C were higher in ruptured AAA samples compared to unruptured AAA samples. Macrophage polarization plays an important role in various diseases, such as atherosclerosis, tissue inflammation, and abdominal aortic aneurysm. However, the role of resting CD4 memory T cells in AAA has not yet been reported. A previous study shows the involvement of *FOXO1* in macrophage polarization; hence the overexpression of *FOXO1* drives macrophages to M1 phenotypes (59). *FOXO1*-mediated M1 polarization has been demonstrated in gastric cancer, periodontal bone loss, and NAFLD and can be investigated as potential pathogenesis of AAA (60, 61). It is tempting to postulate that the correlation analysis provides new insights into the mechanisms of the immune system of AAA. Further in-depth investigation is required to establish concrete conclusions.

Some limitations include that the study was conducted on a small sample size, and the data were obtained from only three microarray datasets. However, it is important to note the challenges of obtaining AAA samples. Only 22 immune cells were included, which fails to incorporate the complexities of the immune microenvironment and requires further investigation. Finally, the underlying regulatory mechanisms of the ceRNA network and their relationship with immune cell infiltration were not elucidated, and other functional experiments are required.

In summary, *PPARG*, *FOXO1*, *RAB5C*, and *HSPA8* likely play significant roles in AAA. Besides, M1

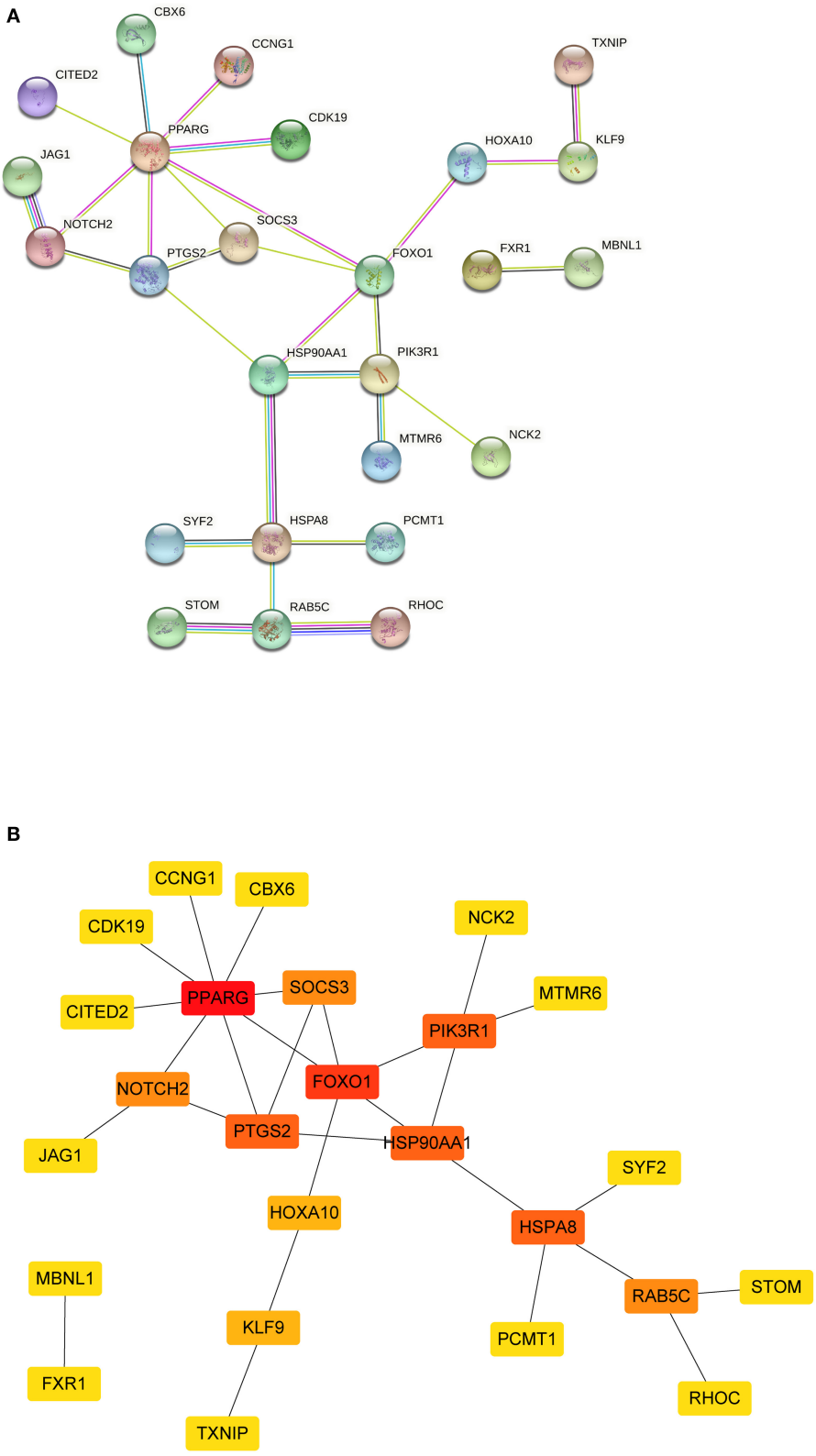

FIGURE 5
The PPI network of mRNAs from ceRNA network. **(A)** The results of the STRING database showed the protein-protein interaction network. Yellow line, interactions form textmining; blue-green line, known interactions from curated databases; dark blue, predicted interactions form gene co-occurrence; black line, interactions form co-expression; purple line, known interactions from experimentally determined; light blue, interactions form protein homology. **(B)** Square shapes represent genes, and lines represent interaction relationships. PPI, protein-protein interaction; mRNAs, messenger RNAs; ceRNA, competing endogenous RNA.

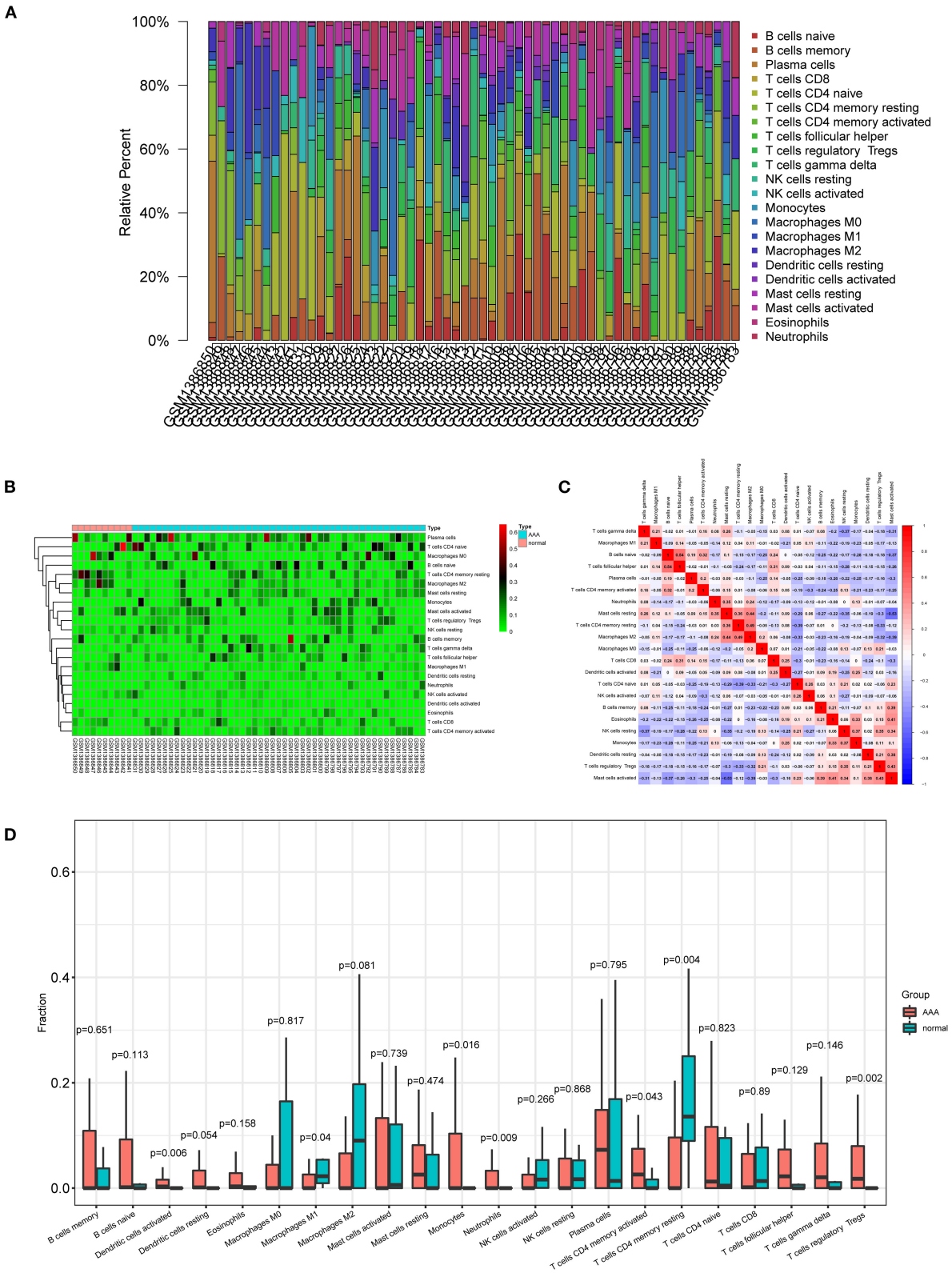

FIGURE 6
Composition of infiltrating immune cells in aortic tissues. **(A)** Distribution of immune cell types in each sample. **(B)** Heat map of infiltrating immune cells. **(C)** The correlation among infiltrating immune cells. **(D)** Violin plot of infiltrating immune cells.

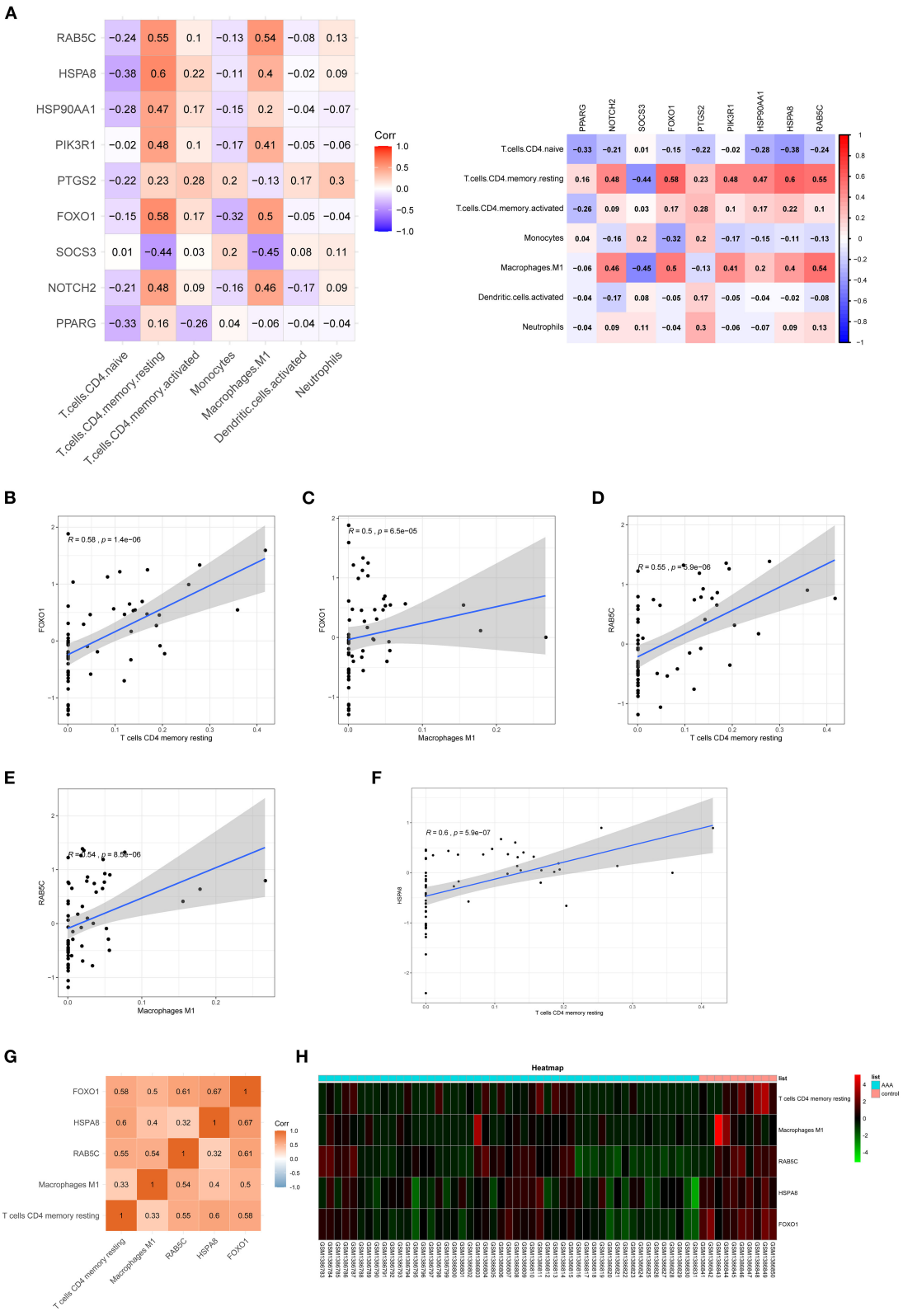

FIGURE 7
Co-expression patterns of infiltrating immune cells and key genes. **(A)** The correlation between hub genes of ceRNA network and differentially expressed infiltrating immune cells. **(B–F)** The significantly correlated pairs with correlation coefficient > 0.5 and $p < 0.001$. **(G)** The correlation between key genes (*FOXO1*, *RAB5C*, and *HSPA8*) and differentially expressed infiltrating immune cells. **(H)** Heat map of key genes (*FOXO1*, *RAB5C*, and *HSPA8*) and differentially expressed infiltrating immune cells. mRNAs, messenger RNAs; ceRNA, competing endogenous RNA.

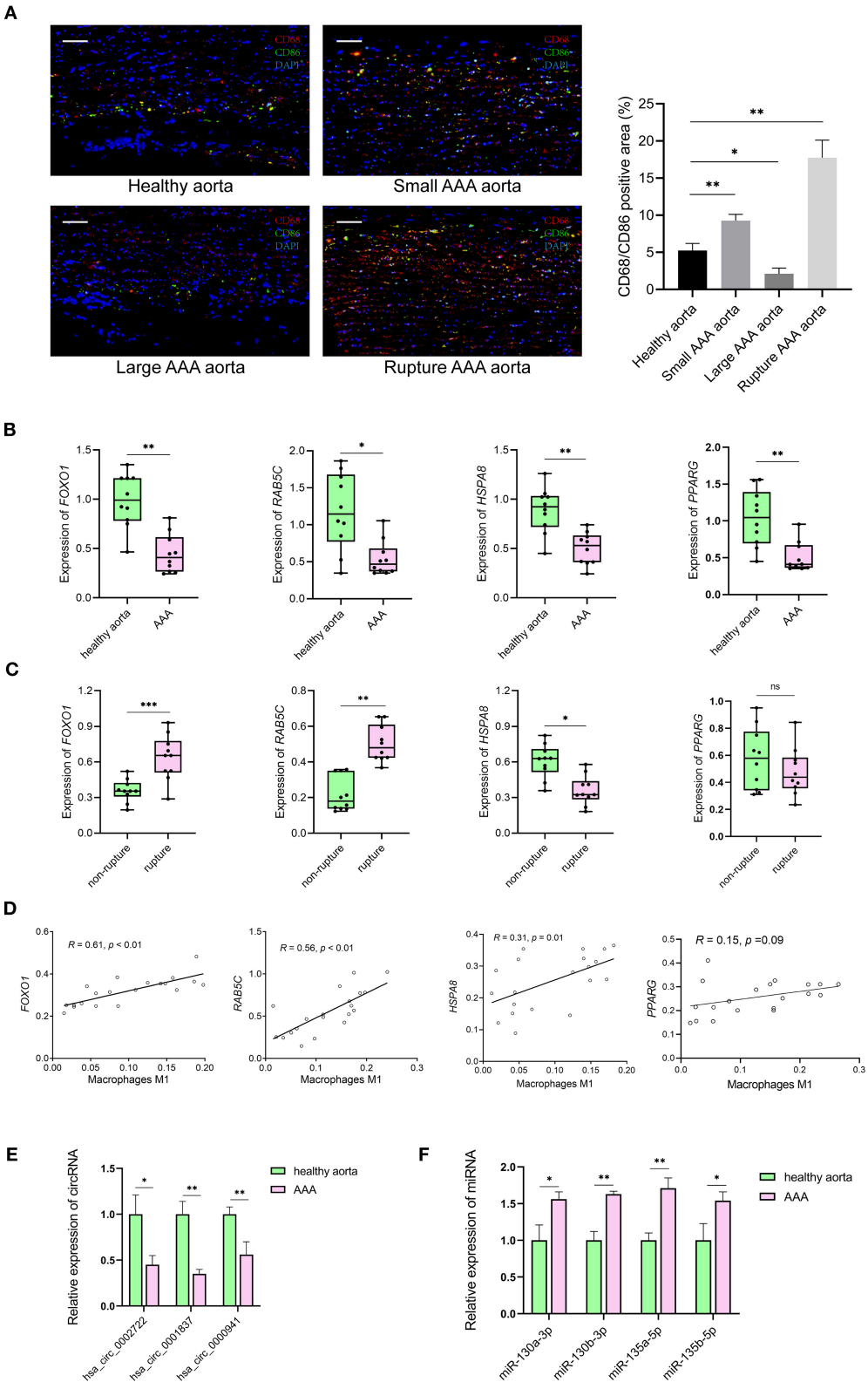

FIGURE 8
The results of preliminary clinical specimen validation. **(A)** Immunofluorescence staining of CD68 (red), CD86 (green) and DAPI (blue) in tissue samples of patients with AAA and controls. Scale bar = 100 μm. $^{*}p < 0.05$, $^{**}p < 0.01$, Student's *t*-test. **(B)** The expression levels of *RAB5C*, *HSPA8*, *FOXO1*, *PPARG* genes in tissue samples of AAA vs. controls. $n = 10$ in each group, $^{*}p < 0.05$, $^{**}p < 0.01$, Student's *t*-test. **(C)** The expression levels

(Continued)

FIGURE 8
of *RAB5C*, *HSPA8*, *FOXO1*, *PPARG* genes in tissue samples of non-rupture AAA vs. rupture AAA. $n = 10$ in each group, $^{*}p < 0.05$, Student's *t*-test. **(D)** Correlation curves between the levels of M1 macrophages and key genes in tissue samples of patients with AAA and controls. Total $n = 20$. **(E)** Quantification of the relative expression levels of hsa_circ_0002722, hsa_circ_0001837, hsa_circ_0000941 in tissue samples of AAA vs. controls. $n = 3$ in each group, $^{*}p < 0.05$, $^{**}p < 0.01$, Student's *t*-test. **(F)** Quantification of the relative expression levels of miR-130a-3p, miR-130b-3p, miR-135a-5p, miR-135b-5p in tissue samples of AAA vs. controls. $n = 3$ in each group, $^{*}p < 0.05$, $^{**}p < 0.01$, Student's *t*-test.

macrophages and resting CD4 memory T cells could be involved in AAA formation. A ceRNA network was established, hsa_circ_0002722-miR-130a/b-3p-*PPARG* and hsa_circ_0001837/hsa_circ_0000941-miR-135a/b-5p-*FOXO1*, may be associated with the pathogenesis of AAA. Although the expression of *FOXO1*, *RAB5C*, *HSPA8*, *PPARG*, and M1 macrophages were verified using clinical specimens, further studies are required to establish a correlation between DEmRNAs and differentially expressed infiltrating immune cells. This study enhances our understanding of the biological role of ceRNA and infiltrating immune cells in the pathogenesis of AAA. This may provide potential therapeutic insights for AAA, which requires further validation.

Data availability statement

The datasets presented in this study can be found in online repositories. The names of the repository/repositories and accession number(s) can be found in the article/Supplementary material.

Ethics statement

The studies involving human participants were reviewed and approved by Institutional Review Board of the Shanghai Jiaotong University School of Medicine, Renji Hospital. The patients/participants provided their written informed consent to participate in this study.

Author contributions

LC and SY draft the article and contribute to the conception, design, acquisition, and interpretation of data. LC, SW, ZW, YL, and YX contribute to acquisition and analysis of data. SY and GX revise the manuscript critically for important intellectual content and make final approval of the version to be published. All authors contributed to the article and approved the submitted version.

Funding

This work was supported by the National Natural Science Foundation of China (Grants No. 81873526).

Acknowledgments

The authors show great acknowledgments to all participants involved in the study.

Conflict of interest

The authors declare that the research was conducted in the absence of any commercial or financial relationships that could be construed as a potential conflict of interest.

Publisher's note

All claims expressed in this article are solely those of the authors and do not necessarily represent those of their affiliated organizations, or those of the publisher, the editors and the reviewers. Any product that may be evaluated in this article, or claim that may be made by its manufacturer, is not guaranteed or endorsed by the publisher.

Supplementary material

The Supplementary Material for this article can be found online at: https://www.frontiersin.org/articles/10.3389/fcvm.2022.955838/full#supplementary-material

References

1. Sakalihasan N, Limet R, Defawe OD. Abdominal aortic aneurysm. *Lancet.* (2005) 365:1577–89. doi: 10.1016/S0140-6736(05)66459-8

2. Golledge J, Muller J, Daugherty A, Norman P. Abdominal aortic aneurysm: pathogenesis and implications for management. *Arterioscler Thromb Vasc Biol.* (2006) 26:2605–13. doi: 10.1161/01.ATV.0000245819.32762.cb

3. Huang S, Li X, Zheng H, Si X, Li B, Wei G, et al. Loss of super-enhancer-regulated circrna nfix induces cardiac regeneration after myocardial infarction in adult mice. *Circulation.* (2019) 139:2857–76. doi: 10.1161/CIRCULATIONAHA.118.038361

4. Song H, Yang Y, Sun Y, Wei G, Zheng H, Chen Y, et al. Circular Rna Cdyl promotes abdominal aortic aneurysm formation by inducing M1 macrophage polarization and M1-Type inflammation. *Mol Ther.* (2022) 30:915–31. doi: 10.1016/j.ymthe.2021.09.017

5. Chen L, Wang C, Sun H, Wang J, Liang Y, Wang Y, et al. The bioinformatics toolbox for circrna discovery and analysis. *Brief Bioinform.* (2021) 22:1706–28. doi: 10.1093/bib/bbaa001

6. Gu X, Jiang YN, Wang WJ, Zhang J, Shang DS, Sun CB, et al. Comprehensive circrna expression profile and construction of circrna-related cerna network in cardiac fibrosis. *Biomed Pharmacother.* (2020) 125:109944. doi: 10.1016/j.biopha.2020.109944

7. Karreth FA, Pandolfi PP. Cerna cross-talk in cancer: when ce-bling rivalries go awry. *Cancer Discov.* (2013) 3:1113–21. doi: 10.1158/2159-8290.CD-13-0202

8. Quintana RA, Taylor WR. Cellular mechanisms of aortic aneurysm formation. *Circ Res.* (2019) 124:607–18. doi: 10.1161/CIRCRESAHA.118.313187

9. Liu Y, Zhong Z, Xiao L, Li W, Wang Z, Duan Z, et al. Identification of Circ-Fndc3b, an overexpressed circrna in abdominal aortic aneurysm, as a regulator of vascular smooth muscle cells. *Int Heart J.* (2021) 62:1387–98. doi: 10.1536/ihj.21-186

10. Kong P, Yu Y, Wang L, Dou YQ, Zhang XH, Cui Y, et al. Circ-Sirt1 controls Nf-kappab activation via sequence-specific interaction and enhancement of Sirt1 expression by binding to Mir-132/212 in vascular smooth muscle cells. *Nucleic Acids Res.* (2019) 47:3580–93. doi: 10.1093/nar/gkz141

11. Ma X, Xu J, Lu Q, Feng X, Liu J, Cui C, et al. Hsa_Circ_0087352 promotes the inflammatory response of macrophages in abdominal aortic aneurysm by adsorbing Hsa-Mir-149-5p. *Int Immunopharmacol.* (2022) 107:108691. doi: 10.1016/j.intimp.2022.108691

12. Li H, Bai S, Ao Q, Wang X, Tian X, Li X, et al. Modulation of immune-inflammatory responses in abdominal aortic aneurysm: emerging molecular targets. *J Immunol Res.* (2018) 2018:7213760. doi: 10.1155/2018/7213760

13. Horimatsu T, Blomkalns AL, Ogbi M, Moses M, Kim D, Patel S, et al. Niacin protects against abdominal aortic aneurysm formation via Gpr109a independent mechanisms: role of Nad+/Nicotinamide. *Cardiovasc Res.* (2020) 116:2226–38. doi: 10.1093/cvr/cvz303

14. Davis FM, Tsoi LC, Melvin WJ, denDekker A, Wasikowski R, Joshi AD, et al. Inhibition of macrophage histone demethylase Jmjd3 protects against abdominal aortic aneurysms. *J Exp Med.* (2021) 218:e20201839. doi: 10.1084/jem.20201839

15. Tian L, Hu X, He Y, Wu Z, Li D, Zhang H. Construction of Lncrna-Mirna-Mrna networks reveals functional lncrnas in abdominal aortic aneurysm. *Exp Ther Med.* (2018) 16:3978–86. doi: 10.3892/etm.2018.6690

16. Li T, Wang T, Yan L, Ma C. Identification of potential novel biomarkers for abdominal aortic aneurysm based on comprehensive analysis of Circrna-Mirna-Mrna networks. *Exp Ther Med.* (2021) 22:1468. doi: 10.3892/etm.2021.10903

17. Jeggari A, Marks DS, Larsson E. Mircode: A map of putative microrna target sites in the long non-coding transcriptome. *Bioinformatics.* (2012) 28:2062–3. doi: 10.1093/bioinformatics/bts344

18. Chen Y, Wang X. Mirdb: An online database for prediction of functional microrna targets. *Nucleic Acids Res.* (2020) 48:D127–D31. doi: 10.1093/nar/gkz757

19. Agarwal V, Bell GW, Nam JW, Bartel DP. Predicting effective microrna target sites in mammalian mrnas. *Elife.* (2015) 4:e05005. doi: 10.7554/eLife.05005

20. Vejnar CE, Zdobnov EM. Mirmap: comprehensive prediction of microrna target repression strength. *Nucleic Acids Res.* (2012) 40:11673–83. doi: 10.1093/nar/gks901

21. Enright AJ, John B, Gaul U, Tuschl T, Sander C, Marks DS. Microrna targets in drosophila. *Genome Biol.* (2003) 5:R1. doi: 10.1186/gb-2003-5-1-r1

22. Szklarczyk D, Gable AL, Lyon D, Junge A, Wyder S, Huerta-Cepas J, et al. String V11: Protein-protein association networks with increased coverage, supporting functional discovery in genome-wide experimental datasets. *Nucleic Acids Res.* (2019) 47:D607–D13. doi: 10.1093/nar/gky1131

23. Newman AM, Liu CL, Green MR, Gentles AJ, Feng W, Xu Y, et al. Robust enumeration of cell subsets from tissue expression profiles. *Nat Methods.* (2015) 12:453–7. doi: 10.1038/nmeth.3337

24. Pierson T, McArthur J, Siliciano RF. Reservoirs for Hiv-1: mechanisms for viral persistence in the presence of antiviral immune responses and antiretroviral therapy. *Annu Rev Immunol.* (2000) 18:665–708. doi: 10.1146/annurev.immunol.18.1.665

25. Nordon IM, Hinchliffe RJ, Loftus IM, Thompson MM. Pathophysiology and epidemiology of abdominal aortic aneurysms. *Nat Rev Cardiol.* (2011) 8:92–102. doi: 10.1038/nrcardio.2010.180

26. Cheng Z, Yu C, Cui S, Wang H, Jin H, Wang C, et al. Circtp63 functions as a cerna to promote lung squamous cell carcinoma progression by upregulating Foxm1. *Nat Commun.* (2019) 10:3200. doi: 10.1038/s41467-019-11162-4

27. Wang J, Zhao X, Wang Y, Ren F, Sun D, Yan Y, et al. Circrna-002178 act as a cerna to promote Pdl1/Pd1 expression in lung adenocarcinoma. *Cell Death Dis.* (2020) 11:32. doi: 10.1038/s41419-020-2230-9

28. Jeong SJ, Cho MJ, Ko NY, Kim S, Jung IH, Min JK, et al. Deficiency of peroxiredoxin 2 exacerbates angiotensin ii-induced abdominal aortic aneurysm. *Exp Mol Med.* (2020) 52:1587–601. doi: 10.1038/s12276-020-00498-3

29. Batra R, Suh MK, Carson JS, Dale MA, Meisinger TM, Fitzgerald M, et al. Il-1beta (Interleukin-1beta) and Tnf-Alpha (Tumor Necrosis Factor-Alpha) impact abdominal aortic aneurysm formation by differential effects on macrophage polarization. *Arterioscler Thromb Vasc Biol.* (2018) 38:457–63. doi: 10.1161/ATVBAHA.117.310333

30. Ma S, Zhou B, Yang Q, Pan Y, Yang W, Freedland SJ, et al. A transcriptional regulatory loop of master regulator transcription factors, pparg, and fatty acid synthesis promotes esophageal adenocarcinoma. *Cancer Res.* (2021) 81:1216–29. doi: 10.1158/0008-5472.CAN-20-0652

31. Wang WD, Sun R, Chen YX. Pparγ agonist rosiglitazone alters the temporal and spatial distribution of inflammation during abdominal aortic aneurysm formation. *Mol Med Rep.* (2018) 18:3421–8. doi: 10.3892/mmr.2018.9311

32. Golledge J, Cullen B, Rush C, Moran CS, Secomb E, Wood F, et al. Peroxisome proliferator-activated receptor ligands reduce aortic dilatation in a mouse model of aortic aneurysm. *Atherosclerosis.* (2010) 210:51–6. doi: 10.1016/j.atherosclerosis.2009.10.027

33. Jones A, Deb R, Torsney E, Howe F, Dunkley M, Gnaneswaran Y, et al. Rosiglitazone reduces the development and rupture of experimental aortic aneurysms. *Circulation.* (2009) 119:3125–32. doi: 10.1161/CIRCULATIONAHA.109.852467

34. Que Y, Shu X, Wang L, Wang S, Li S, Hu P, et al. Inactivation of Serca2 Cys(674) accelerates aortic aneurysms by suppressing Pparγ. *Br J Pharmacol.* (2021) 178:2305–23. doi: 10.1111/bph.15411

35. Meredith D, Panchatcharam M, Miriyala S, Tsai YS, Morris AJ, Maeda N, et al. Dominant-negative loss of ppargamma function enhances smooth muscle cell proliferation, migration, and vascular remodeling. *Arterioscler Thromb Vasc Biol.* (2009) 29:465–71. doi: 10.1161/ATVBAHA.109.184234

36. Halabi CM, Beyer AM, de Lange WJ, Keen HL, Baumbach GL, Faraci FM, et al. Interference with Ppar gamma function in smooth muscle causes vascular dysfunction and hypertension. *Cell Metab.* (2008) 7:215–26. doi: 10.1016/j.cmet.2007.12.008

37. Liu F, Liu Y, Du Y, Li Y. Mirna-130a promotes inflammation to accelerate atherosclerosis via the regulation of proliferator-activated receptor Γ (Pparγ) expression. *Anatol J Cardiol.* (2021) 25:630–7. doi: 10.5152/AnatolJCardiol.2021.56721

38. Kin K, Miyagawa S, Fukushima S, Shirakawa Y, Torikai K, Shimamura K, et al. Tissue- and plasma-specific microrna signatures for atherosclerotic abdominal aortic aneurysm. *J Am Heart Assoc.* (2012) 1:e000745. doi: 10.1161/JAHA.112.000745

39. Moran CS, Clancy P, Biros E, Blanco-Martin B, McCaskie P, Palmer LJ, et al. Association of Ppargamma allelic variation, osteoprotegerin and abdominal aortic aneurysm. *Clin Endocrinol (Oxf).* (2010) 72:128–32. doi: 10.1111/j.1365-2265.2009.03615.x

40. Alikhani M, Alikhani Z, Graves DT. Foxo1 functions as a master switch that regulates gene expression necessary for tumor necrosis factor-induced fibroblast apoptosis. *J Biol Chem.* (2005) 280:12096–102. doi: 10.1074/jbc.M412171200

41. Jia G, Aggarwal A, Tyndall SH, Agrawal DK. Tumor necrosis factor-alpha regulates p27 kip expression and apoptosis in smooth muscle cells of human carotid plaques via forkhead transcription factor O1. *Exp Mol Pathol.* (2011) 90:1–8. doi: 10.1016/j.yexmp.2010.11.001

42. Stöhr R, Kappel BA, Carnevale D, Cavalera M, Mavilio M, Arisi I, et al. Timp3 interplays with apelin to regulate cardiovascular metabolism in hypercholesterolemic mice. *Mol Metab.* (2015) 4:741–52. doi: 10.1016/j.molmet.2015.07.007

43. Malik S, Sadhu S, Elesela S, Pandey RP, Chawla AS, Sharma D, et al. Transcription factor Foxo1 Is essential for Il-9 induction in T helper cells. *Nat Commun.* (2017) 8:815. doi: 10.1038/s41467-017-00674-6

44. Wang RK, Sun YY Li GY, Yang HT, Liu XJ Li KF, et al. Microrna-124-5p delays the progression of cerebral aneurysm by regulating foxo1. *Exp Ther Med.* (2021) 22:1172. doi: 10.3892/etm.2021.10606

45. Hou WZ, Chen XL, Wu W, Hang CH. Microrna-370-3p inhibits human vascular smooth muscle cell proliferation via targeting Kdr/Akt signaling pathway in cerebral aneurysm. *Eur Rev Med Pharmacol Sci.* (2017) 21:1080–7.

46. Li X, Li L, Dong X, Ding J, Ma H, Han W. Circ_Grn promotes the proliferation, migration, and inflammation of vascular smooth muscle cells in atherosclerosis through Mir-214-3p/Foxo1 axis. *J Cardiovasc Pharmacol.* (2021) 77:470–9. doi: 10.1097/FJC.0000000000000982

47. Zhang J, Ng S, Wang J, Zhou J, Tan SH, Yang N, et al. Histone deacetylase inhibitors induce autophagy through Foxo1-dependent pathways. *Autophagy.* (2015) 11:629–42. doi: 10.1080/15548627.2015.1023981

48. Zhang L, Zhang Z, Li C, Zhu T, Gao J, Zhou H, et al. S100a11 promotes liver steatosis via foxo1-mediated autophagy and lipogenesis. *Cell Mol Gastroenterol Hepatol.* (2021) 11:697–724. doi: 10.1016/j.jcmgh.2020.10.006

49. Mei ZG, Huang YG, Feng ZT, Luo YN, Yang SB, Du LP, et al. Electroacupuncture ameliorates cerebral ischemia/reperfusion injury by suppressing autophagy via the Sirt1-Foxo1 signaling pathway. *Aging.* (2020) 12:13187–205. doi: 10.18632/aging.103420

50. Ren H, Shao Y, Wu C, Ma X, Lv C, Wang Q. Metformin alleviates oxidative stress and enhances autophagy in diabetic kidney disease via Ampk/Sirt1-Foxo1 pathway. *Mol Cell Endocrinol.* (2020) 500:110628. doi: 10.1016/j.mce.2019.110628

51. Shen M, Cao Y, Jiang Y, Wei Y, Liu H. Melatonin protects mouse granulosa cells against oxidative damage by inhibiting foxo1-mediated autophagy: implication of an antioxidation-independent mechanism. *Redox Biol.* (2018) 18:138–57. doi: 10.1016/j.redox.2018.07.004

52. Wang Z, Guo J, Han X, Xue M, Wang W, Mi L, et al. Metformin represses the pathophysiology of Aaa by suppressing the activation of Pi3k/Akt/Mtor/Autophagy pathway in Apoe(-/-) Mice. *Cell Biosci.* (2019) 9:68. doi: 10.1186/s13578-019-0332-9

53. Li D, An Y. Mir-135a-5p inhibits vascular smooth muscle cells proliferation and migration by inactivating foxo1 and Jak2 signaling pathway. *Pathol Res Pract.* (2021) 224:153091. doi: 10.1016/j.prp.2020.153091

54. Yang H, Zhou T, Stranz A, DeRoo E, Liu B. Single-cell Rna sequencing reveals heterogeneity of vascular cells in early stage murine abdominal aortic aneurysm-brief report. *Arterioscler Thromb Vasc Biol.* (2021) 41:1158–66. doi: 10.1161/ATVBAHA.120.315607

55. Xie C, Ye F, Zhang N, Huang Y, Pan Y, Xie X. Ccl7 contributes to angiotensin ii-induced abdominal aortic aneurysm by promoting macrophage infiltration and pro-inflammatory phenotype. *J Cell Mol Med.* (2021) 25:7280–93. doi: 10.1111/jcmm.16757

56. Shi X, Ma W, Li Y, Wang H, Pan S, Tian Y, et al. Mir-144-5p limits experimental abdominal aortic aneurysm formation by mitigating m1 macrophage-associated inflammation: suppression of Tlr2 and Olr1. *J Mol Cell Cardiol.* (2020) 143:1–14. doi: 10.1016/j.yjmcc.2020.04.008

57. Pope NH, Salmon M, Davis JP, Chatterjee A, Su G, Conte MS, et al. D-series resolvins inhibit murine abdominal aortic aneurysm formation and increase M2 macrophage polarization. *FASEB J.* (2016) 30:4192–201. doi: 10.1096/fj.201600144RR

58. Dale MA, Xiong W, Carson JS, Suh MK, Karpisek AD, Meisinger TM, et al. Elastin-derived peptides promote abdominal aortic aneurysm formation by modulating M1/M2 macrophage polarization. *J Immunol.* (2016) 196:4536–43. doi: 10.4049/jimmunol.1502454

59. Liu XL, Pan Q, Cao HX, Xin FZ, Zhao ZH, Yang RX, et al. Lipotoxic hepatocyte-derived exosomal microrna 192-5p activates macrophages through Rictor/Akt/Forkhead box transcription factor O1 signaling in nonalcoholic fatty liver disease. *Hepatology.* (2020) 72:454–69. doi: 10.1002/hep.31050

60. Ren J, Han X, Lohner H, Liang R, Liang S, Wang H. Serum- and glucocorticoid-inducible kinase 1 promotes alternative macrophage polarization and restrains inflammation through Foxo1 and Stat3 signaling. *J Immunol.* (2021) 207:268–80. doi: 10.4049/jimmunol.2001455

61. Xie C, Guo Y, Lou S. Lncrna ancr promotes invasion and migration of gastric cancer by regulating foxo1 expression to inhibit macrophage M1 polarization. *Dig Dis Sci.* (2020) 65:2863–72. doi: 10.1007/s10620-019-06019-1

frontiers | Frontiers in Cardiovascular Medicine

TYPE Systematic Review
PUBLISHED 09 August 2022
DOI 10.3389/fcvm.2022.949538

Check for updates

OPEN ACCESS

EDITED BY
Carlos Alves,
University of Coimbra, Portugal

REVIEWED BY
Antonino S Rubino,
University of Campania Luigi Vanvitelli, Italy
Chih-Fen Hu,
Tri-Service General Hospital, Taiwan
Xiao-Ce Dai,
First Hospital of Jiaxing, China

*CORRESPONDENCE
Xiaoyu Li
li.xiaoyu@zs-hospital.sh.cn
Weiguo Fu
fu.weiguo@zs-hospital.sh.cn
Baolei Guo
guo.baolei@zs-hospital.sh.cn

†These authors have contributed equally to this work and share first authorship

SPECIALTY SECTION
This article was submitted to General Cardiovascular Medicine, a section of the journal Frontiers in Cardiovascular Medicine

RECEIVED 21 May 2022
ACCEPTED 13 July 2022
PUBLISHED 09 August 2022

CITATION
Chen C, Patterson B, Simpson R, Li Y, Chen Z, Lv Q, Guo D, Li X, Fu W and Guo B (2022) Do fluoroquinolones increase aortic aneurysm or dissection incidence and mortality? A systematic review and meta-analysis. *Front. Cardiovasc. Med.* 9:949538. doi: 10.3389/fcvm.2022.949538

Do fluoroquinolones increase aortic aneurysm or dissection incidence and mortality? A systematic review and meta-analysis

Can Chen[1†], Benjamin Patterson[2†], Ruan Simpson[3], Yanli Li[1], Zhangzhang Chen[1], Qianzhou Lv[1], Daqiao Guo[4,5], Xiaoyu Li[1*], Weiguo Fu[4,5*] and Baolei Guo[4,5,6*]

[1]Department of Pharmacy, Zhongshan Hospital, Fudan University, Shanghai, China, [2]Department of Vascular Surgery, University Hospital Southampton, Southampton, United Kingdom, [3]Department of Pathology, Portsmouth Hospitals NHS Trust, United Kingdom, [4]Department of Vascular Surgery, Zhongshan Hospital, Institute of Vascular Surgery, Fudan University, Shanghai, China, [5]National Clinical Research Center for Interventional Medicine, Shanghai, China, [6]Qingpu Branch of Zhongshan Hospital, Fudan University, Shanghai, China

Objective: The aim of this study was to determine the association between fluoroquinolones (FQs) use, the risk of *de novo* aortic aneurysm or dissection (AAD), and the prognosis of patients with pre-existing AAD.

Materials and methods: We searched PubMed, EMBASE, CENTRAL, Scopus, and Web of Science on 31 March 2022. Observational studies that evaluated the association of FQs with AAD risk in the general population or FQs with the prognosis of patients with preexisting AAD and presented adjusted effect estimates were included. Two reviewers assessed study eligibility, extracted data, and assessed the risk of bias and certainty of evidence using GRADE.

Results: Of the 13 included studies, 11 focused on the association of FQs with *de novo* AAD incidence, and only one study investigated the association of FQs with the patient with AAD prognosis. FQ use was associated with an increased risk of *de novo* AAD within 30 days (RR: 1.42; 95% CI: 1.11–1.81; very low certainty) and 60 days (RR: 1.44; 95% CI: 1.26–1.64; low certainty). Specifically, the association was significant when compared with amoxicillin, azithromycin, doxycycline, or no antibiotic use. Furthermore, patients with preexisting AAD exposure to FQ had an increased risk of all-cause mortality (RR: 1.61; 95% CI: 1.50–1.73; moderate certainty) and aortic-specific mortality (RR: 1.80; 95% CI: 1.50–2.15; moderate certainty), compared to the non-exposed FQ group within a 60-day risk period.

Conclusion: FQs were associated with an increased incidence of AAD in the general population and a higher risk of adverse outcomes in patients with preexisting AAD. Nevertheless, the results may be affected by unmeasured confounding factors. This should be considered by physicians contemplating using FQs in patients with aortic dilation and those at high risk of AAD.

Systematic Review Registration: [https://www.crd.york.ac.uk/prospero/], identifier [CRD42021230171].

KEYWORDS

fluoroquinolones, aortic aneurysm, aortic dissection, systematic review, meta-analysis

Introduction

Fluoroquinolones (FQs) are one of the most commonly used classes of antibiotics, partly due to their wide activity spectrum, excellent bioavailability, extensive penetration of tissue, and successful microbiological outcomes (1, 2). Although FQs are well tolerated (3, 4), it has been suggested that they might exacerbate collagen-associated diseases owing to collagen loss and tissue degeneration (5–8).

Type I and type III collagen comprise the majority (80–90%) of collagen in the aorta (9), and FQs may contribute to the development of aortic disease (10, 11). Despite this plausible link, studies to characterize this relationship have yielded conflicting results. Several studies (12–17) using large administrative datasets found that recent FQs exposure was strongly associated with an increased risk of AAD, but after adjusting for the comparator antibiotics, two recent studies (18, 19) did not support this finding. Although a consensus on whether FQ causes *de novo* aortic disease has not yet been reached (20, 21), this potential association has raised several other important clinical questions, particularly regarding whether FQs can precipitate aortic complications in patients with existing aortic disease. It has been shown that FQ exposure could increase the risk of acute aortic dissection or rupture for patients with underlying aortopathy (10, 11, 22). Subsequently, Chen et al. (23) found that FQ exposure in patients with preexisting AAD was associated with a higher risk of adverse outcomes relative to non-exposure.

Although aortic events associated with FQs are thought to be rare (15), the United States alone has approximately 14 million annual FQ prescriptions (24, 25), and 20% of patients with AAD receive FQs during their hospitalization (26). Considering the serious adverse outcomes associated with aortopathy, including death, FQ-associated aortopathy constitutes a major health problem worldwide. We analyzed the association between FQs and the incidence and prognosis of AAD by systematic review and meta-analysis.

Materials and methods

This systematic review and meta-analysis followed the recommendations (27) and was reported in accordance with the Preferred Reporting Items for Systematic Reviews and Meta-Analyses (PRISMA) statement (28). The review was registered through PROSPERO with the registration number CRD42021230171.

Data sources and searches

We searched PubMed, EMBASE, the Cochrane Central Register of Controlled Trials, Scopus, and Web of Science on 31 March 2022, for studies on the association between FQs and the risk of AAD incidence, all-cause mortality, and aortic-specific mortality in patients with AAD. In addition, the reference lists of relevant publications were reviewed to identify any additional studies that met the eligibility criteria. The electronic search strategy is presented in the ESM.

Study selection and eligibility criteria

Studies were included if the following criteria were met: (1) population: participants who were initially free of AAD and did not have an AAD history when they entered a cohort that was subsequently followed to determine the risk of AAD incidence, or patients with AAD who were enrolled in a cohort that was followed to determine the risk of aortic-specific mortality or all-cause mortality; (2) definition of FQ exposure: participant received at least one prescription or a reimbursement for FQs; (3) studies reported the risk estimates of AAD incidence or mortality exposed to FQs vs. no FQs. Studies that did not report multivariable-adjusted estimates for at least one of the outcomes of interest, reported as abstracts only, presented without any data on relevant outcomes, or included data from Vigibase or

the US Food and Drug Administration Adverse Event Reporting System (FAERS) database were excluded. Two reviewers (C.C. and B.G.) independently and in duplicate screened titles and abstracts, followed by full-text screening of potentially eligible studies. Discrepancies were solved through consensus or by the involvement of a third reviewer (W.F.).

The outcomes were the risk of AAD incidence in general populations and the risk of aortic-specific mortality, or all-cause mortality, in patients with AAD, within 30-, 60-, and 90-day risk periods following FQ exposure.

Data extraction, risk of bias assessments, and certainty of evidence

We extracted the following data from eligible studies: (1) study characteristics (first author, publication year, country, data source, definition of FQs exposure, and comparators); (2) population characteristics (age, gender, and number of participants); and (3) outcomes (number of events, exposure to FQs risk period, and the variables used for adjustment).

We assessed the risk of bias in the studies using the Quality in Prognosis Studies (QUIPS) tool (29). We categorized studies as having an overall low risk of bias if they had 5 or 6 low risk of bias domains, an overall high risk of bias if they had 2 or more high risk of bias domains, and an overall moderate risk of bias if they had all other studies (30).

The certainty of the evidence was assessed as high, moderate, low, or very low using the Grading of Recommendations Assessment, Development, and Evaluation (GRADE) approach adapted to prognosis studies (31). This assessment was based on risk of bias, consistency, precision, directness, and other concerns including publication bias (32), where two reviewers (C.C. and B.G.) independently, and in duplicate, extracted data, assessed risk of bias, and assessed certainty of evidence using GRADE. Any discrepancies were resolved by consensus or through the involvement of a third reviewer (W.F.).

Data synthesis and statistical analyzes

We performed a meta-analysis by extracting and pooling adjusted relative effect estimates (27, 33). When merging data from studies that reported only an odds ratio (OR), we treated the OR as an RR (34) because the AA annual incidence is low (0.4–0.67%) (35). Studies comparing FQs to various controls, including other, or no antibiotics were included in the meta-analysis by making multiple pair-wise comparisons between all possible intervention group pairs (33). Statistical heterogeneity was addressed through the consistency of point estimates and the extent of CIs overlapped (36). We conducted subgroup analyzes according to age, sex, study type, comparators, ruptured or unruptured AA/AD, type of aortic disease, or anatomical site. In the sensitivity analyzes, we restricted analysis to AAD patients with baseline imaging to minimize potential surveillance bias and to individuals with infections to reduce selection bias. For outcomes reported by two or more studies, sensitivity analyzes were performed using a fixed effects model and individually excluded studies to explore the impact of each study on the overall results. For studies that gathered data from the same database and reported similar outcomes, recent publications were selected for primary analysis, and early publications were selected for sensitivity analysis. All meta-analyzes were conducted using Review Manager 5.4. The probability of publication bias was tested by means of Egger's test using Stata 14.0 software. Two-sided P-values < 0.05 and 95% CIs, not including 1.00, were considered as statistically significant.

Results

Study selection and characteristics

We screened 1,434 abstracts and 38 full-text papers and included 13 studies (12–19, 23, 37–40) (**Figure 1** and **Supplementary Table 1**). A total of 11 studies (12–19, 37–40) focused on the association of FQs with *de novo* AAD incidence, and only one study (23) investigated the association of FQs with all-cause mortality and aortic-specific mortality of patients with existing AAD. Six studies (12, 15, 17, 19, 23, 40) were cohort studies, three (13, 18, 39) were nest case-control studies, and four (14, 16, 37, 38) were self-controlled studies, including two case-time-control studies (14, 16), one case-crossover studies (38), and one self-controlled case series studies (37). Five studies (13, 14, 18, 23, 40) were from Taiwan, three (17, 19, 37) from the United States, and the others were from Canada (12), Sweden (15), France (16), Denmark (38), and Korea (39). Data used in all studies were obtained from various administrative healthcare databases across countries. Seven studies (13, 14, 17, 18, 23, 37, 40) limited inclusion to patients aged 18 years or older of which two (18, 23) applied an age limit of 20 years, four (15, 19, 38, 39) included 40 years or older, and one (12) included 65 years or older. The definition of FQ exposure in all studies relied on the occurrence of a FQ prescription or reimbursement. The identification of AAD in all studies was based on the ICD-9 or ICD-10 codes with, or without, advanced imaging. There was substantial variation in the analytic strategies used, including the adjusted variables.

The risk of bias was low in 4 studies and moderate in 9 studies. The bias mainly came from the outcome measurement and study of confounding domains (**Supplementary Tables 1–13** in the ESM). Additional study characteristics are shown in **Table 1** and **Supplementary Tables 1–13** in the ESM.

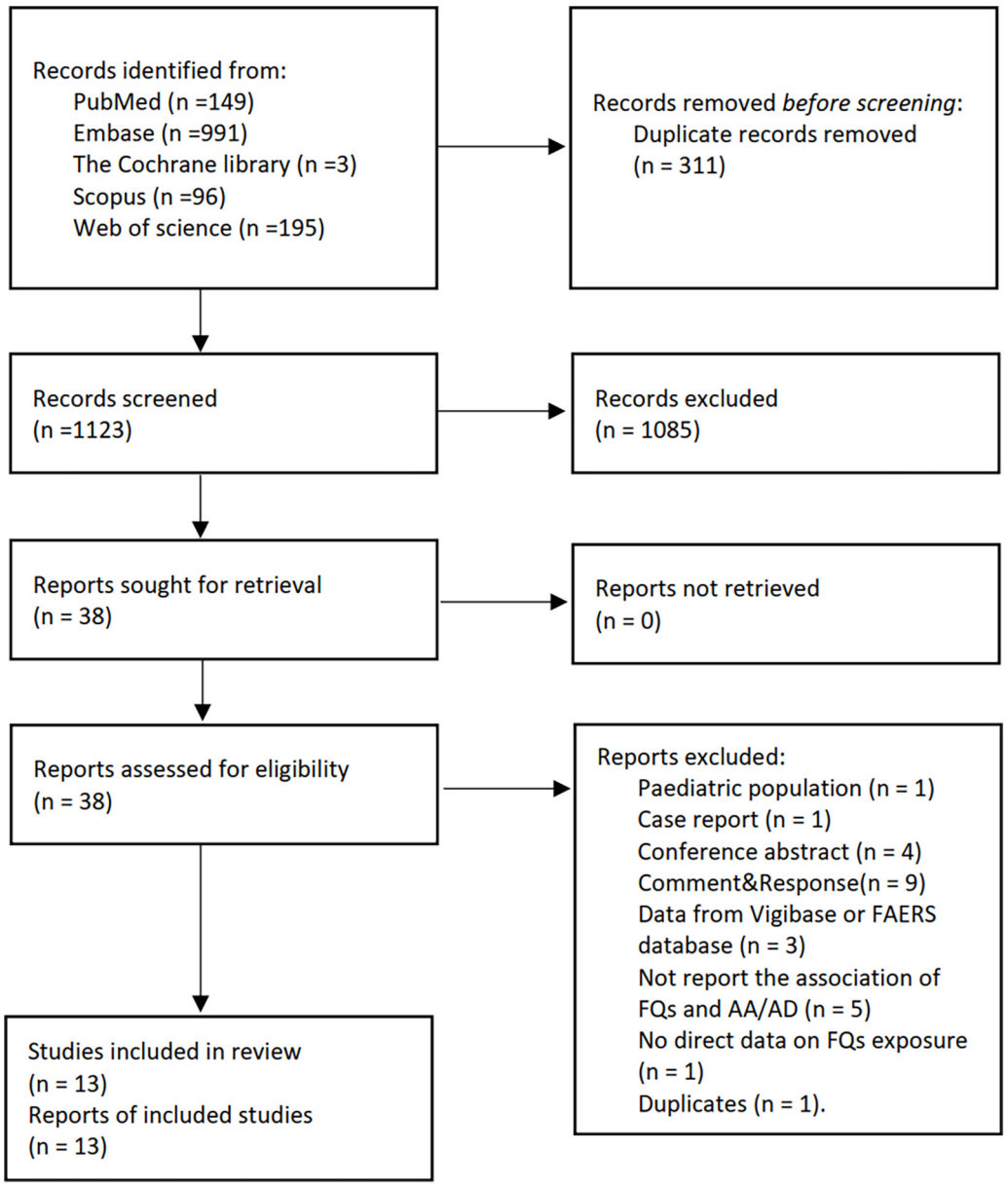

FIGURE 1
The PRISMA flow diagram for literature screening. FQs, fluoroquinolones; AA, aortic aneurysm; AD, aortic dissection.

Synthesis of results

Fluoroquinolones (FQs) and the risk of aortic aneurysm or dissection (AAD) incidence

There were four (12, 18, 37, 38), eight (13, 15, 16, 18, 19, 37–39), and four (16, 37, 38, 40) studies that linked the association of FQ use with the incidence of *de novo* AAD within 30-, 60-, and 90-day risk windows, respectively. The meta-analysis indicated that FQs were associated with an increased *de novo* AAD risk at 30-day (RR: 1.42; 95% CI: 1.11–1.81; very low certainty) and 60-day (RR: 1.44; 95% CI: 1.26–1.64; low certainty) risk window. AAD incidence showed a trend to increase after exposure to FQs within 90 days, but the difference did not reach statistical significance (RR: 1.45; 95% CI: 1.00–2.10; low certainty). When stratified by comparators, the association of FQs with AAD risk was significantly different across various comparators at 30-day (P = 0.006), 60-day (P < 0.001), and 90-day (P < 0.001) risk periods. Within any risk period, FQs were only associated with higher AAD risk when compared with amoxicillin, azithromycin, or no antibiotics and had a higher AAD rate compared with doxycycline in a 60-day risk period. The forest plots of the

meta-analyzes are displayed in **Figures 2–4**, with different comparator subgroups also shown separately. The summary estimates of the FQ association with AAD risk are presented in **Table 15**.

When analyzing the AA and AD patients separately, the effect of FQs on AD and AA risks was not significantly different (**Supplementary Figures 1A,B**). When stratified by study type, the association of FQs with the incidence of AAD varied significantly across various study designs. Specifically, within a 30-day risk period (self-control studies: RR: 1.46; 95% CI: 1.23–1.73; cohort studies: RR: 2.24; 95% CI: 2.02–2.48; nest case-control studies: RR: 1.02; 95% CI: 0.85–1.22; $P < 0.001$); within a 90-day risk period (self-control studies: RR: 1.90; 95% CI: 1.38–2.62; cohort studies: RR: 1.20; 95% CI: 1.17–1.23; $P = 0.005$). However, the association was not significantly different across various study designs within a 60-day risk period (self-control studies: RR: 1.64; 95% CI: 1.30–2.06; cohort studies: RR: 1.56; 95% CI: 0.96–2.56; nest case-control studies: RR: 1.34; 95% CI: 0.95–1.89; $P = 0.64$). Minimal differences were observed when stratified by age, sex, incidence of ruptured or unruptured AA or AD, or anatomical site (**Supplementary Tables 16–18**).

In the sensitivity analysis, we explored the comparison of FQ and controls with analysis restricted to patients with AAD with baseline imaging and found that the association was attenuated (RR: 1.05; 95% CI: 0.94–1.18). Results were similar when the analysis was restricted to individuals with infection (**Supplementary Table 19**). The sensitivity analysis performed *via* a fixed effects model did not change appreciably when compared to the primary analyzes. Furthermore, we performed sensitivity analyzes by excluding each study individually from the primary analyzes, and the outcomes remained unchanged. The two studies (13, 14) reported using the same database and had the same outcomes within 60 days, and hence the sensitivity analysis results were similar to those of the primary analysis.

Fluoroquinolones (FQs) and mortality of aortic aneurysm or dissection (AAD) patients

Only one study (23) investigated whether the use of FQs increases the 60-day risk of mortality in the AAD population. The findings suggest that exposure to FQs is associated with a higher risk of all-cause mortality (RR: 1.61; 95% CI: 1.50–1.73; moderate certainty) and aortic-specific mortality (RR: 1.80; 95% CI: 1.50–2.15; moderate certainty) compared with non-FQs (**Figure 5**, **Supplementary Table 20**). However, patients with AAD exposed to amoxicillin were not significantly associated with any risk outcomes compared with non-amoxicillin antibiotics (**Supplementary Table 21**). By comparing the risk of outcomes between the FQ and amoxicillin exposure periods for the same patient, the results demonstrated that the mortality risks were significantly higher during the FQ exposure period than during the amoxicillin exposure period (**Supplementary Table 22**). The summary estimates for the association of FQs and the AAD patient prognosis are presented in **Supplementary Table 23**.

When analyzing the AA and AD patients separately, the effect of FQs did not differ significantly between the AD and AA groups (**Supplementary Table 24**).

Publication bias

When analyzing the association of FQ use with the *de novo* AAD incidence within 30-day ($P = 0.37$), 60-day ($P = 0.68$), and 90-day ($P = 0.51$) risk windows, the Egger's test indicated that no evidence of publication bias was found.

Discussion

Early studies (12–15) suggesting a possible association between FQs use and the risk of AAD, combined with reasonable evidence of a mechanistic link with other collagen-related diseases disorders (7, 8), led to the US Food and Drug Administration (FDA) (41) issuing a warning against FQ use in patients who were at risk of aortic disease. This study adds to the evidence that FQ use is associated with an increased risk of *de novo* AAD within a 90-day risk window. Patients with preexisting AAD and exposure to FQ had an increased risk of all-cause mortality and aortic-specific mortality relative to controls within a 60-day risk period, adding further weight to the FDA warning, which was based on inferences from studies designed for the general population rather than specific high-risk groups.

Although the use of FQs appears to lead to a higher risk of AAD incidence than no use of FQs, we found that the associations between FQs and AAD risk may change with various comparator antibiotics. Specifically, the associations were only significant when compared with antibiotics with a broad antimicrobial profile. Patients who are prescribed a broad-spectrum antibiotic potentially have more severe infections than those prescribed narrow-spectrum antibiotics or no antibiotics. Since severe infection may also independently damage the aortic endothelium, the infection may itself increase the risk of AAD (18). Another reason is that patients with more severe infections or indications for FQs therapy are more likely to receive an imaging examination, leading to a higher ascertainment rate (42, 43). Consequently, if the analysis was restricted to patients with prior imaging, then the association was attenuated, probably due to decreased ascertainment of "new" disease. These biases may confound the apparent association between FQs and AAD incidence. Additionally, Newton et al. (17) considered that this inconsistency may be due to the different analytical approaches employed in the studies, such as the inclusion of different populations, different definitions of FQ exposure, different sample sizes, and different ways to adjust confounding factors.

TABLE 1 Characteristics of included studies.

Authors	Year	Region	Study type	Population	Intervention and control	Age (years)*	Sex, male (%)	Risk period
FQs and the risk of AAD incidence								
Newtonet al. (17)	2021	United States	Cohort study	Adults aged 18 to 64 years	I: Oral FQ C: amox-clav, azithromycin, cephalexin, clindamycin, and SMX-TMP	I: 47 (36–57); C: 43 (31–54)	I: 38.7%; C: 40.5%	90 days
Gopalakrishnan et al. (19)	2020	United States	Cohort study	Patients ≥ 50 years diagnosed with pneumonia or UTI	Pneumonia cohort: I: FQ; C: azithromycin; UTI cohort: I: FQ; C: SMX-TMP; Amoxicillin cohort: I: FQ; C:Amoxicillin;	Pneumonia cohort: I: 63.68 ± 10.93; C: 63.63 ± 10.92; UTI cohort: I: 62.07 ± 10.36; C: 62.04 ± 10.30; Amoxicillin cohort: I: 60.55 ± 9.34; C: 60.68 ± 9.28;	Pneumonia cohort: I: 46.4%; C: 46.3% UTI cohort: I: 13.3%; C:13.0% Amoxicillin cohort: I: 44.0%; C: 44.0%	60 days
Pasternak et al. (15)	2018	Sweden	Cohort study	Patients ≥ 50 years	I: FQ; C:Amoxicillin;	I: 47 (36-57); C: 43 (31–54)	I: 45.0%; C: 45.0%	60 days
Daneman et al. (12)	2015	Canada	Cohort study	Adults aged 65	I: FQ; C: No FQ**;	I: 65 C: 65	I: 51.4%; C: 51.1%	30 days
Dong et al. (18)	2020	Taiwan	Nested case-control study	Patients ≥ 20 years	I: FQ; C1: Amox-clav or amp-sulb C2: Extended-spectrum ceph	AAD patients: 67.41 ± 15.03; Matched controls patients: 67.41 ± 15.03	AA/AD patients: 71.4%; Matched controls: 71.4%	30, 60 days
Lee et al. (13)	2015	Taiwan	Nested case-control	Adults' patients diagnosed with AAD.	I: FQ; C: No FQ**;	AA/AD patients: 74.17 ± 11.7(AA)/ 66.2 ± 14.5(AD); Matched controls patients: 71.0 ± 13.7	AA/AD patients: 74.1%(AA)/71.5%(AD); Matched controls patients: 72.9%	60, 61–365 days
Lawaetz Kristensen et al. (38)	2021	Denmark	Case-crossover study	Patients ≥ 50 years diagnosed with ruptured AA	I: FQ; C: No FQ**;	FQ group: 77 (70–81); Control group: 77 (71–82)	FQ group, 69.0%; Control group, 66.5%	28, 60, 90 days
Aspinall et al. (37)	2020	United States	Self-controlled case series analysis study	Veterans ≥ 18 years who had the outcomes of AAD	I: FQ; C1: Amoxicillin; C2: Azithromycin; C3: Cefuroxime/cephalexin; C5: Doxycycline; C6: SMX-TMP; C7: No antibiotics	FQ group, 68.6 ± 8.8; Control group, NR.	FQ group, 98.3%; Control group, NR.	30, 60 days

(Continued)

10.3389/fcvm.2022.949538

TABLE 1 Continued

Authors	Year	Region	Study type	Population	Intervention and control	Age (years)*	Sex, male (%)	Risk period
Maumus-Robert et al. (16)	2019	France	Case-time-control study	Patients ≥ 18 years with incident aortoiliac aneurysm or dissection	I: FQ; C1: Amoxicillin	FQ group, 70 (62–80); Amoxicillin group, 67 (57–79)	FQ group, 64.0%; Amoxicillin group, 74.7%	30, 60, 90 days
Lee et al. (14)	2018	Taiwan	Case-crossover analysis/control-crossover (case-time-control analysis)	Inpatients diagnosed with AAD	I: FQ; C: No FQ**	AAD patients, 70.58 ± 13.77; Matched controls patients without AAD, 70.48 ± 13.69.	AA/AD patients, 72.46%; Matched controls patients without AA/AD, 72.46%	60, 120, 180 days
Son et al. (39)	2022	Korea	Nested case–control study	Patients ≥ 40 years diagnosed with AAD	I: FQ; C: No FQ**	NR	AAD 62.5% Matched controls 62.5%	60 days
Chen et al. (40)	2022	Taiwan	Cohort study	Patients diagnosed with urinary tract infections.	I: FQ; C: Cephalosporins	NR	I: 28.2%; C: 28.1%	90 days
FQs and mortality of patients with AAD								
Chen et al. (23)	2021	Taiwan	Cohort study	Patients who were admitted for AAD	I: FQ; C1: No FQ**; C2: Amoxicillin C2: No amoxicillin**	FQ group, 73.1 (63.4–79.9); control group (No FQ): 68.5 (55.7–77.3); Amoxicillin group, 67.2 (55.2–76.0); control group (No Amoxicillin): 68.7 (55.9–77.4).	FQ group, 69.7%; control group (No FQ):72.0%; Amoxicillin group, 74.5%; control group (No Amoxicillin): 71.9%.	60 days

*Present as mean ± standard deviation or median (interquartile range). **No antibiotics or other antibiotics. FQ, fluoroquinolone; AAD, aortic aneurysm or dissection; AA, aortic aneurysm; AD, aortic dissection; I, intervention; C, control; UTI, urinary tract infection.

10.3389/fcvm.2022.949538

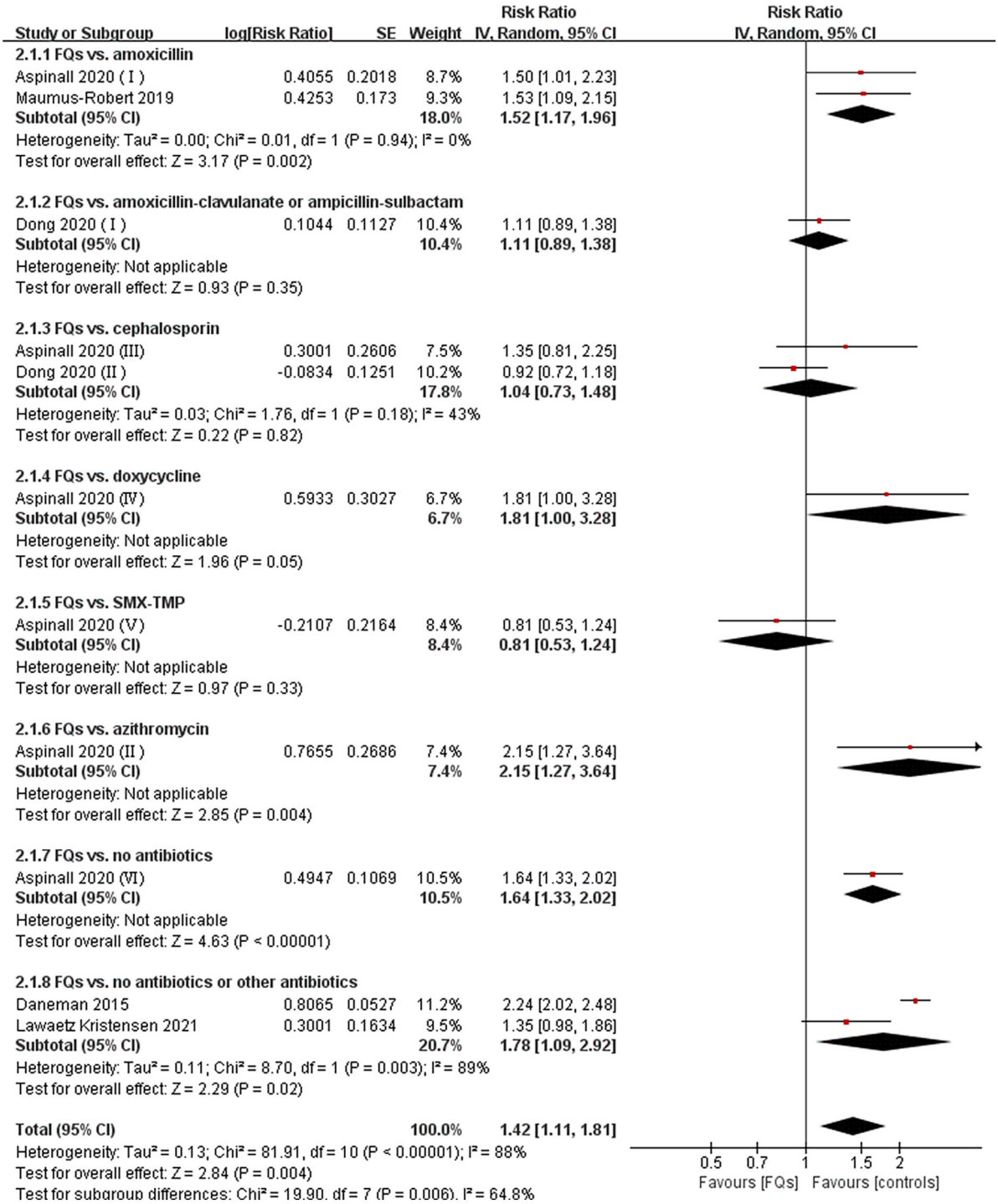

FIGURE 2
Forest plot of the risk of aortic aneurysm or dissection (AAD) in the comparison of fluoroquinolones (FQs) vs. controls within a 30-day risk period. FQs, fluoroquinolones; SMX-TMP, combined trimethoprim and sulfamethoxazole; IV, inverse variance; CI, confidence interval.

While there is limited evidence for a mechanistic link between antimicrobial use and aortic disease in humans, LeMaire et al. (22) found that wild-type mice given a high-fat diet, angiotensin II infusion, and exposure to ciprofloxacin experienced more severe aortic wall degeneration and a higher incidence of aortic aneurysm, dissection, and rupture, compared with test control mice. Another study (11) revealed that ciprofloxacin-treated mice suffered accelerated aortic

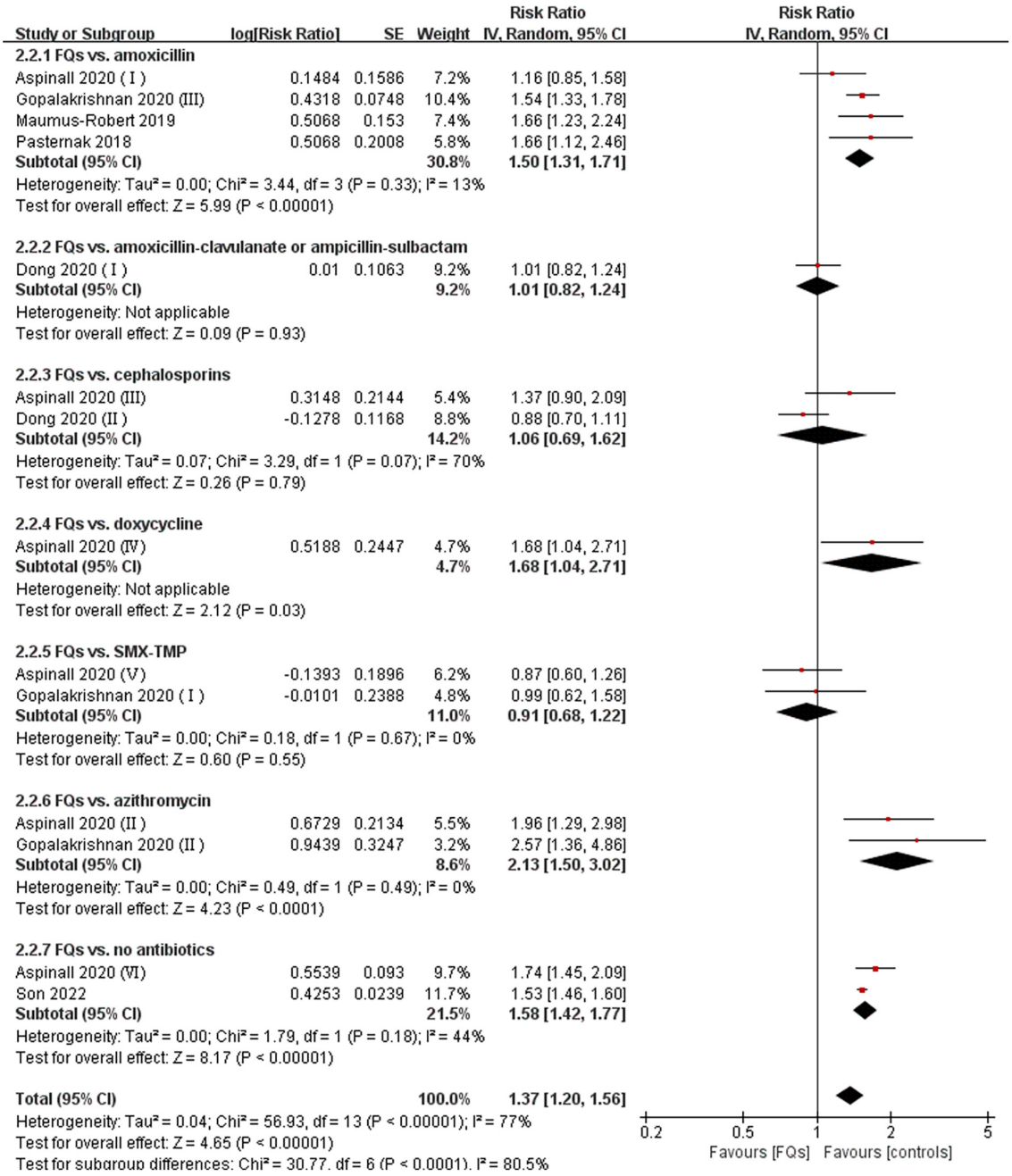

FIGURE 3
Forest plot of the risk of aortic aneurysm or dissection (AAD) in the comparison of fluoroquinolones (FQs) vs. controls within a 60-day risk period. FQs, fluoroquinolones; SMX-TMP, combined trimethoprim and sulfamethoxazole; IV, inverse variance; CI, confidence interval.

enlargement and an increased incidence of aortic dissection and rupture, compared with vehicle-treated mice. This suggests that ciprofloxacin should be avoided in patients with Marfan syndrome. Campana et al. (11, 44) reported a patient who presented fever of unknown origin, elevated systemic inflammation markers, and radiological evidence of aortitis and pneumonia, who was subsequently treated with levofloxacin. Aortic rupture then occurred after 5 days after levofloxacin therapy was commenced. It was postulated that FQs could trigger the activation of ECM remodeling and an increase in MMP activity as a potential mechanism for this effect. Guzzardi et al. (44, 45) published a report suggesting that patients with alpha-1 antitrypsin (A1AT) deficiency and longstanding FQ use (26 months) may have a higher risk of AAD, although patients

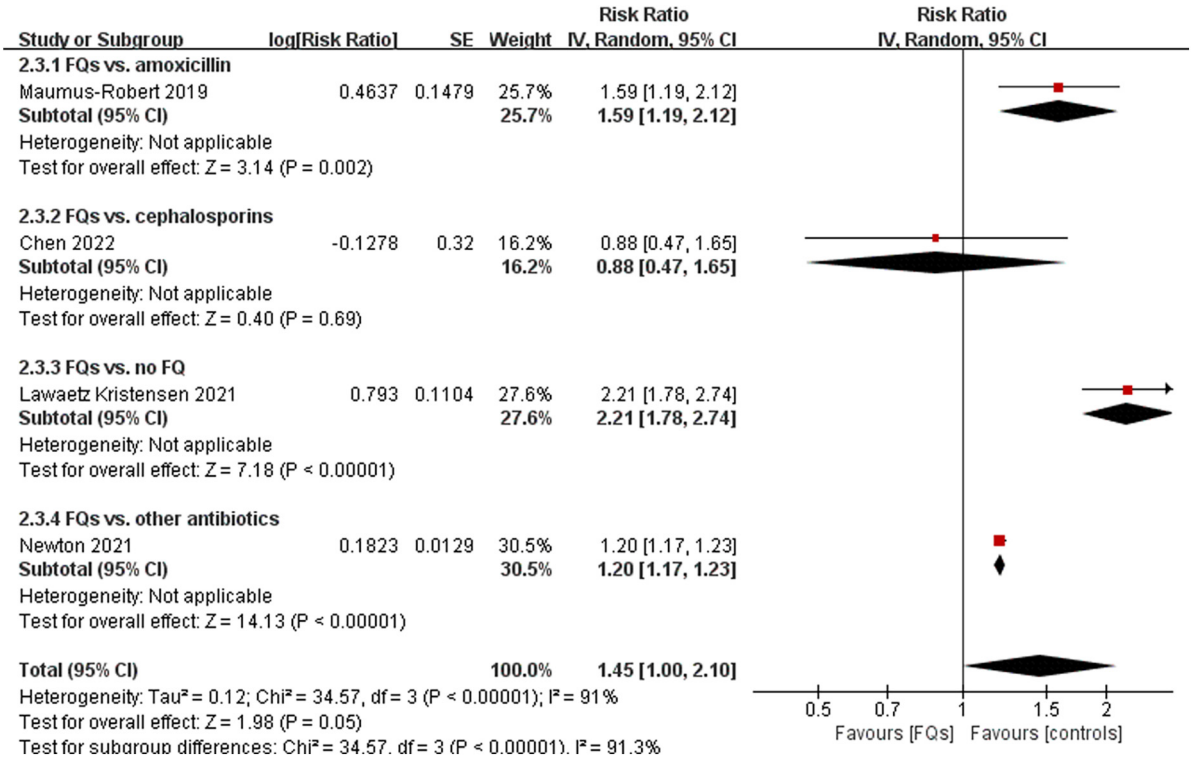

FIGURE 4
Forest plot of the risk of aortic aneurysm or dissection (AAD) in the comparison of fluoroquinolones (FQs) vs. controls within a 90-day risk period. FQs, fluoroquinolones; IV, inverse variance; CI, confidence interval.

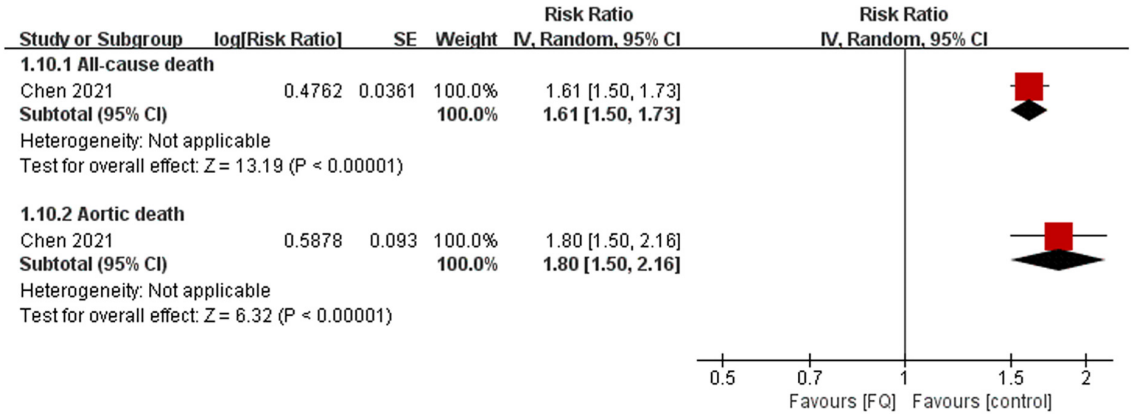

FIGURE 5
Forest plot of mortality risk of aortic aneurysm or dissection (AAD) patients in the comparison of fluoroquinolones (FQs) vs. control within a 60-day risk period. FQs, fluoroquinolones; IV, inverse variance; CI, confidence interval.

with A1AT deficiency are not typically considered at risk of aortopathy despite maladaptive connective tissue changes.

The suppression of extracellular matrix (ECM) biosynthesis and stability and the induction of ECM degradation may be key mechanisms underlying the effects of FQ on aortic destruction, dissection, and rupture (22). Consistent with that reported in the cornea (46, 47), tendon cells and tissues (48), and fibroblasts (49), ciprofloxacin exposure significantly increased MMP-2 and MMP-9 expression in the aortic wall, facilitating increased ECM destruction (11, 22). Guzzardi et al. (10) showed that FQ exposure induced a proteolytic MMP-TIMP imbalance driven by decreased TIMP expression, while

simultaneously attenuating collagen expression in human aortic myofibroblast mediated ECM dysregulation. Furthermore, ciprofloxacin decreases the expression of Lysyl oxidase (LOX) (22), which is critical in elastic fiber assembly and stabilization and plays an important role in maintaining the integrity of aortic wall. In addition, the activation of stimulator of interferon genes (STING) (50–52), a pro-inflammatory cytosolic DNA sensor that plays a critical role in aortic degeneration, dissection, and rupture (53), is involved in the ciprofloxacin-induced suppression of LOX expression and the induction of MMP expression. Ciprofloxacin may also cause aortic destruction by increasing the number of TUNEL-positive cells in the aortic wall and inducing cell death in cultured aortic SMCs. This finding, corroborated by other studies, shows that ciprofloxacin induces cytotoxicity and death in various types of cells such as tenocytes (50, 51), lens epithelial cells (54), chondrocytes (55), and osteoblasts (56).

There are several potentially important implications of this study. FQs are commonly used in the empirical treatment of infected AAs to cover *Salmonella* species and sensitive *Staphylococcus*, which are highly prevalent bacterial species in this setting (57, 58). Alternate antibiotics should be sought as this could potentially increase the risk of aortic rupture in this already high-risk group. Furthermore, a retrospective cohort study (26) revealed that a large number of AAD patients received FQs during hospital admissions in general. Stronger evidence of the association of FQs with aortic-related adverse events may help inform enhanced antimicrobial stewardship around their use, especially given that more than 20% of patients with FQs may not have an appropriate indication for their use (17). Finally, for high-risk patients who have no choice but to use FQs, appropriate surveillance will be needed to minimize the hazard of aortic adverse events.

Despite these associations, additional research is needed to prove a causal link between FQs and aortic events. An *in vitro* study (10) showed that higher doses for longer periods may increase the susceptibility to FQ-associated acute aortic events. Clinical studies investing in the dose–response relationship between FQ use and the risk of aortic-related adverse events may be warranted. Furthermore, since FQ exposure might have different effects on cells in patients with variable comorbidities, clinical phenotypes, and connective tissue defects (10), clinical studies are needed to clarify differences between these subpopulations. This review only included one study (23) on the association of FQs and the mortality of AAD patients, and from this, it was difficult to determine whether FQ exposure conferred poor prognosis to AAD patients compared with other broad-spectrum antibiotics. Third-generation FQs do not appear to be associated with an increased risk of Achilles tendon rupture compared with first- and second-generation FQs and non-FQs (59), but the potential effect on AAD needs further study.

This systematic review has several strengths. First, the datasets used in this analysis may have contained overlapping patients, and thus complete independence between the databases cannot be ascertained. By reporting the association between FQ use and aortic events grouped by different risk periods (30, 60, or 90 days), this study effectively avoided data merging from studies using the same database. Second, compared with previously published meta-analyses (60–63), this review added to the current literature in studying the relationship between FQs and AAD mortality, and conducted more detailed subgroup analyzes to explore differences in the effects of FQ across different subgroups, and indeed found that differences in the selection of comparators had a substantial effect on the results.

Limitations include that the AAD diagnosis was according to ICD-9/10 codes with or without baseline advanced imaging examination, which is less accurate than clinical adjudication. This implies that some undiagnosed aneurysms were not identified, and aneurysm size or indications for surgical intervention were unavailable. Furthermore, since abdominal imaging was not routinely performed, it is possible that aneurysms classified as incidental may have been preexisting, or FQs simply aggravated a preexisting condition rather than initiated a *de novo* aneurysm. Second, as with all administrative databases, there is no available information on adherence to prescriptions. Therefore, the possibility of exposure misclassification cannot be excluded. Some included studies suggest that such exposure misclassification was random and did not bias the results (14, 17). Third, systematic reviews and meta-analyzes of observational studies are extremely sensitive to biases resulting from confounding factors. Although adjustment for numerous covariates was conducted, unknown confounders may have caused residual confounding. For instance, several risk factors associated with aneurysm development, such as smoking, were not captured (or reliably captured) in the claims data. Zhang et al. (64) quantified the potential influence of unmeasured confounding by smoking in FQ-AA association using three published approaches, and suggested that confounding by smoking is an unlikely explanation for the apparent association between FQ use and aortic aneurysm. These findings addressed a major limitation of epidemiologic studies regarding confounding by smoking due to an absence of data and strengthened the evidence for a FQ-related AA. Fourth, due to the limited number of included studies and limited data in the reports, we could not establish a safe window for FQ dose or duration, and it seems that higher doses or longer durations of FQ treatment exhibit stronger associations with aortic pathology (10, 13, 14). Finally, due to a lack of pharmacological interaction comparisons, we cannot determine whether FQs combined with other drugs, such as systemic corticosteroids and non-steroidal anti-inflammatory agents, increase the occurrence of aortic diseases (65).

Conclusion

FQ use was associated with an increased short-term risk of developing AAD in the general population and a poor prognosis in patients who have been diagnosed with AAD. There are several important confounding factors from this study, which means that more data are required before this relationship is proven. Regardless, it can help physicians when considering prescribing FQs to patients with aortic dilatation and those at high risk of AAD. We propose considering an alternative antibiotic for patients with aortic pathology and avoiding this class of antibiotics in patients who are prone to AAD.

Data availability statement

The original contributions presented in this study are included in the article/**Supplementary material**, further inquiries can be directed to the corresponding authors.

Author contributions

WF, DG, and BG proposed the conception and supervised the implementation process. CC and BG conducted the study search and screening, data extraction, and risk of bias assessment. CC, YL, and XL were responsible for data analysis. CC wrote the manuscript. BP, RS, ZC, and QL revised the manuscript. All authors reviewed and approved the final version of the work.

Funding

This study was sponsored by the National Natural Science Foundation of China (82000436) and the Science and Technology of Shanghai (201409004800 and 21410710500).

Conflict of interest

The authors declare that the research was conducted in the absence of any commercial or financial relationships that could be construed as a potential conflict of interest.

Publisher's note

All claims expressed in this article are solely those of the authors and do not necessarily represent those of their affiliated organizations, or those of the publisher, the editors and the reviewers. Any product that may be evaluated in this article, or claim that may be made by its manufacturer, is not guaranteed or endorsed by the publisher.

Supplementary material

The Supplementary Material for this article can be found online at: https://www.frontiersin.org/articles/10.3389/fcvm.2022.949538/full#supplementary-material

References

1. Millanao AR, Mora AY, Villagra NA, Bucarey SA, Hidalgo AA. Biological effects of quinolones: A family of broad-spectrum antimicrobial agents. *Molecules.* (2021) 26:7153. doi: 10.3390/molecules26237153

2. Chan T, Bunce PE. Fluoroquinolone antimicrobial drugs. *CMAJ.* (2017) 189:E638. doi: 10.1503/cmaj.160938

3. Owens RC Jr, Ambrose PG. Antimicrobial safety: Focus on fluoroquinolones. *Clin Infect Dis.* (2005) 41(Suppl. 2):S144–57. doi: 10.1086/428055

4. Liu HH. Safety profile of the fluoroquinolones: Focus on levofloxacin. *Drug Saf.* (2010) 33:353–69. doi: 10.2165/11536360-000000000-00000

5. Yu X, Jiang DS, Wang J, Wang R, Chen T, Wang K, et al. Fluoroquinolone use and the risk of collagen-associated adverse events: A systematic review and meta-analysis. *Drug Saf.* (2019) 42:1025–33. doi: 10.1007/s40264-019-00828-z

6. Sendzik J, Shakibaei M, Schäfer-Korting M, Stahlmann R. Fluoroquinolones cause changes in extracellular matrix, signalling proteins, metalloproteinases and caspase-3 in cultured human tendon cells. *Toxicology.* (2005) 212:24–36. doi: 10.1016/j.tox.2005.04.002

7. Stephenson AL, Wu W, Cortes D, Rochon PA. Tendon injury and fluoroquinolone use: A systematic review. *Drug Saf.* (2013) 36:709–21. doi: 10.1007/s40264-013-0089-8

8. Chui CS, Wong IC, Wong LY, Chan EW. Association between oral fluoroquinolone use and the development of retinal detachment: A systematic review and meta-analysis of observational studies. *J Antimicrob Chemother.* (2015) 70:971–8. doi: 10.1093/jac/dku507

9. Berillis P. The role of collagen in the aorta's structure. *Open Circ Vasc J.* (2013) 6:1–8. doi: 10.2174/1877382601306010001

10. Guzzardi DG, Teng G, Kang S, Geeraert PJ, Pattar SS, Svystonyuk DA, et al. Induction of human aortic myofibroblast-mediated extracellular matrix dysregulation: A potential mechanism of fluoroquinolone-associated aortopathy. *J Thorac Cardiovasc Surg.* (2019) 157:109.e–19.e. doi: 10.1016/j.jtcvs.2018.08.079

11. LeMaire SA, Zhang L, Zhang NS, Luo W, Barrish JP, Zhang Q, et al. Ciprofloxacin accelerates aortic enlargement and promotes dissection and rupture in Marfan mice. *J Thorac Cardiovasc Surg.* (2020) 163:e215–26. doi: 10.1016/j.jtcvs.2020.09.069

12. Daneman N, Lu H, Redelmeier DA. Fluoroquinolones and collagen associated severe adverse events: A longitudinal cohort study. *BMJ open.* (2015) 5:e010077. doi: 10.1136/bmjopen-2015-010077

13. Lee CC, Gabriel Lee MT, Chen YS, Lee SH, Chen YS, Chen SC, et al. Risk of aortic dissection and aortic aneurysm in patients taking oral fluoroquinolone. *JAMA Internal Med.* (2015) 175:1839–47. doi: 10.1001/jamainternmed.2015.5389

14. Lee CC, Lee MTG, Hsieh R, Porta L, Lee WC, Lee SH, et al. Oral fluoroquinolone and the risk of aortic dissection. *J Am Coll Cardiol.* (2018) 72:1369–78. doi: 10.1016/j.jacc.2018.06.067

15. Pasternak B, Inghammar M, Svanström H. Fluoroquinolone use and risk of aortic aneurysm and dissection: Nationwide cohort study. *BMJ.* (2018) 360:k678. doi: 10.1136/bmj.k678

16. Maumus-Robert S, Berard X, Mansiaux Y, Tubert-Bitter P, Debette S, Pariente A. Short-term risk of aortoiliac aneurysm or dissection associated with fluoroquinolone use. *J Am Coll Cardiol.* (2019) 73:875–7. doi: 10.1016/j.jacc.2018.12.012

17. Newton ER, Akerman AW, Strassle PD, Kibbe MR. Association of fluoroquinolone use with short-term risk of development of aortic aneurysm. *JAMA Surg.* (2021) 156:264–72. doi: 10.1001/jamasurg.2020.6165

18. Dong YH, Chang CH, Wang JL, Wu LC, Lin JW, Toh S. Association of infections and use of fluoroquinolones with the risk of aortic aneurysm or aortic dissection. *JAMA Intern Med.* (2020) 180:1787–95. doi: 10.1001/jamainternmed.2020.4192

19. Gopalakrishnan C, Bykov K, Fischer MA, Connolly JG, Gagne JJ, Fralick M. Association of fluoroquinolones with the risk of aortic aneurysm or aortic dissection. *JAMA Intern Med.* (2020) 180:1596–605. doi: 10.1001/jamainternmed.2020.4199

20. DeGette RL, Grant RW, Mph MD. Observational study design challenges-the case of fluoroquinolones and aortic disease. *JAMA Intern Med.* (2020) 180:1605–6. doi: 10.1001/jamainternmed.2020.4191

21. Lai CC, Lu CT, Kao KC, Lu MC, Ko WC, Hsueh PR. Association of fluoroquinolones use with the risk of aortic aneurysm or aortic dissection: Facts and myths. *J Microbiol Immunol Infect.* (2021) 54:182–4. doi: 10.1016/j.jmii.2021.03.002

22. LeMaire SA, Zhang L, Luo W, Ren P, Azares AR, Wang Y, et al. Effect of ciprofloxacin on susceptibility to aortic dissection and rupture in mice. *JAMA Surg.* (2018) 153:e181804. doi: 10.1001/jamasurg.2018.1804

23. Chen SW, Chan YH, Chien-Chia Wu V, Cheng YT, Chen DY, Lin CP, et al. Effects of fluoroquinolones on outcomes of patients with aortic dissection or aneurysm. *J Am Coll Cardiol.* (2021) 77:1875–87. doi: 10.1016/j.jacc.2021.02.047

24. Buehrle DJ, Wagener MM, Clancy CJ. Outpatient fluoroquinolone prescription fills in the United States, 2014 to 2020: Assessing the impact of food and drug administration safety warnings. *Antimicrob Agents Chemother.* (2021) 65:e0015121. doi: 10.1128/AAC.00151-21

25. Umarje SP, Alexander CG, Cohen AJ. Ambulatory fluoroquinolone use in the United States, 2015-2019. *Open Forum Infect Dis.* (2021) 8:ofab538. doi: 10.1093/ofid/ofab538

26. Frankel WC, Trautner BW, Spiegelman A, Grigoryan L, LeMaire SA. Patients at risk for aortic rupture often exposed to fluoroquinolones during hospitalization. *Antimicrob Agents Chemother.* (2019) 63:e1712–8. doi: 10.1128/AAC.01712-18

27. Riley RD, Moons KGM, Snell KIE, Ensor J, Hooft L, Altman DG, et al. A guide to systematic review and meta-analysis of prognostic factor studies. *BMJ.* (2019) 364:k4597. doi: 10.1136/bmj.k4597

28. Page MJ, Moher D, Bossuyt PM, Boutron I, Hoffmann TC, Mulrow CD, et al. PRISMA 2020 explanation and elaboration: Updated guidance and exemplars for reporting systematic reviews. *BMJ.* (2021) 372:n160. doi: 10.1136/bmj.n160

29. Hayden JA, van der Windt DA, Cartwright JL, Côté P, Bombardier C. Assessing bias in studies of prognostic factors. *Ann Intern Med.* (2013) 158:280–6. doi: 10.7326/0003-4819-158-4-201302190-00009

30. Foroutan F, Guyatt GH, O'Brien K, Bain E, Stein M, Bhagra S, et al. Prognosis after surgical replacement with a bioprosthetic aortic valve in patients with severe symptomatic aortic stenosis: Systematic review of observational studies. *BMJ.* (2016) 354:i5065. doi: 10.1136/bmj.i5065

31. Iorio A, Spencer FA, Falavigna M, Alba C, Lang E, Burnand B, et al. Use of GRADE for assessment of evidence about prognosis: Rating confidence in estimates of event rates in broad categories of patients. *BMJ.* (2015) 350:h870. doi: 10.1136/bmj.h870

32. Lau J, Ioannidis JP, Terrin N, Schmid CH, Olkin I. The case of the misleading funnel plot. *BMJ.* (2006) 333:597–600. doi: 10.1136/bmj.333.7568.597

33. Higgins JPT, Thomas J, Chandler J, Cumpston M, Li T, Page MJ, et al. *Cochrane handbook for systematic reviews of Interventions version 6.2.* (2021). Available online at: www.training.cochrane.org/handbook (accessed March 31, 2022).

34. Zhang J, Yu KF. What's the relative risk? A method of correcting the odds ratio in cohort studies of common outcomes. *JAMA.* (1998) 280:1690–1. doi: 10.1001/jama.280.19.1690

35. Forsdahl SH, Singh K, Solberg S, Jacobsen BK. Risk factors for abdominal aortic aneurysms: A 7-year prospective study: The Tromsø study, 1994-2001. *Circulation.* (2009) 119:2202–8. doi: 10.1161/CIRCULATIONAHA.108.817619

36. Granholm A, Zeng L, Dionne JC, Perner A, Marker S, Krag M, et al. Predictors of gastrointestinal bleeding in adult ICU patients: A systematic review and meta-analysis. *Intensive Care Med.* (2019) 45:1347–59. doi: 10.1007/s00134-019-05751-6

37. Aspinall SL, Sylvain NP, Zhao X, Zhang R, Dong D, Echevarria K, et al. Serious cardiovascular adverse events with fluoroquinolones versus other antibiotics: A self-controlled case series analysis. *Pharmacol Res Perspect.* (2020) 8:e00664. doi: 10.1002/prp2.664

38. Lawaetz Kristensen K, Hallas J, Sanddal Lindholt J. Fluoroquinolones as a trigger for rupture of abdominal aortic aneurysm: A case-crossover analysis. *Basic Clin Pharmacol Toxicol.* (2021) 129:44–51. doi: 10.1111/bcpt.13591

39. Son N, Choi E, Chung SY, Han SY, Kim B. Risk of aortic aneurysm and aortic dissection with the use of fluoroquinolones in Korea: A nested case-control study. *BMC Cardiovasc Disord.* (2022) 22:44. doi: 10.1186/s12872-022-02488-x

40. Chen YY, Yang SF, Yeh HW, Yeh YT, Huang JY, Tsao SL, et al. Association between aortic aneurysm and aortic dissection with fluoroquinolones use in patients with urinary tract infections: A population-based cohort study. *J Am Heart Assoc.* (2022) 11:e023267. doi: 10.1161/JAHA.121.023267

41. United States Food and Drug Administration. *FDA warns about increased risk of ruptures or tears in the aorta blood vessel with fluoroquinolone antibiotics in certain patients*. Silver Spring, MD: United States Food and Drug Administration (2022).

42. Sterpetti AV. Concerns about study on fluoroquinolone use and risk of development of aortic aneurysm. *JAMA Surg.* (2021) 156:1068–9. doi: 10.1001/jamasurg.2021.3026

43. Chen CH, Wang CY, Lai CC. Concerns about study on fluoroquinolone use and risk of development of aortic aneurysm. *JAMA Surg.* (2021) 156:1068. doi: 10.1001/jamasurg.2021.3023

44. Campana P, Leosco D, Petraglia L, Radice L, Parisi V. Aortic rupture in patient on oral therapy with levofloxacin. *Aging Clin Exp Res.* (2020) 32:755–7. doi: 10.1007/s40520-019-01267-7

45. Guzzardi DG, Hassanabad AF, Bromley AB, Fedak PWM. Fluoroquinolone-associated type A aortic dissection in alpha-1 anti-trypsin deficiency. *Ann Thorac Surg.* (2020) 110:e489–91. doi: 10.1016/j.athoracsur.2020.04.044

46. Reviglio VE, Hakim MA, Song JK, O'Brien TP. Effect of topical fluoroquinolones on the expression of matrix metalloproteinases in the cornea. *BMC Ophthalmol.* (2003) 3:10. doi: 10.1186/1471-2415-3-10

47. Sharma C, Velpandian T, Baskar Singh S, Ranjan Biswas N, Bihari Vajpayee R, Ghose S. Effect of fluoroquinolones on the expression of matrix metalloproteinase in debrided cornea of rats. *Toxicol Mech Methods.* (2011) 21:6–12. doi: 10.3109/15376516.2010.529183

48. Shakibaei M, Stahlmann R. Ultrastructure of Achilles tendon from rats after treatment with fleroxacin. *Arch Toxicol.* (2001) 75:97–102. doi: 10.1007/s002040000203

49. Bujor AM, Haines P, Padilla C, Christmann RB, Junie ML, Sampaio-Barros PD, et al. Ciprofloxacin has antifibrotic effects in scleroderma fibroblasts via downregulation of Dnmt1 and upregulation of Fli1. *Int J Mol Med.* (2012) 30:1473–80. doi: 10.3892/ijmm.2012.1150

50. Wu J, Sun L, Chen X, Du F, Shi H, Chen C, et al. Cyclic GMP-AMP is an endogenous second messenger in innate immune signaling by cytosolic DNA. *Science.* (2013) 339:826–30. doi: 10.1126/science.1229963

51. Ablasser A, Goldeck M, Cavlar T, Deimling T, Witte G, Röhl I, et al. cGAS produces a 2′-5′-linked cyclic dinucleotide second messenger that activates STING. *Nature.* (2013) 498:380–4. doi: 10.1038/nature12306

52. Sun L, Wu J, Du F, Chen X, Chen ZJ. Cyclic GMP-AMP synthase is a cytosolic DNA sensor that activates the type I interferon pathway. *Science.* (2013) 339:786–91. doi: 10.1126/science.1232458

53. Luo W, Wang Y, Zhang L, Ren P, Zhang C, Li Y, et al. Critical role of cytosolic DNA and its sensing adaptor STING in aortic degeneration, dissection, and rupture. *Circulation.* (2020) 141:42–66. doi: 10.1161/CIRCULATIONAHA.119.041460

54. Zhao B, Chignell CF, Rammal M, Smith F, Hamilton MG, Andley UP, et al. Detection and prevention of ocular phototoxicity of ciprofloxacin and other fluoroquinolone antibiotics. *Photochem Photobiol.* (2010) 86:798–805. doi: 10.1111/j.1751-1097.2010.00755.x

55. Li P, Cheng NN, Chen BY, Wang YM. In vivo and in vitro chondrotoxicity of ciprofloxacin in juvenile rats. *Acta Pharmacol Sin.* (2004) 25:1262–6.

56. Williams RJ III, Attia E, Wickiewicz TL, Hannafin JA. The effect of ciprofloxacin on tendon, paratenon, and capsular fibroblast metabolism. *Am J Sports Med.* (2000) 28:364–9. doi: 10.1177/03635465000280031401

57. Moneta GL, Taylor LM Jr, Yeager RA, Edwards JM, Nicoloff AD, McConnell DB, et al. Surgical treatment of infected aortic aneurysm. *Am J Surg.* (1998) 175:396–9. doi: 10.1016/S0002-9610(98)00056-7

58. Wanhainen A, Verzini F, Van Herzeele I, Allaire E, Bown M, Cohnert T, et al. Editor's choice – European society for vascular surgery (ESVS) 2019 clinical practice guidelines on the management of abdominal aorto-iliac artery aneurysms. *Eur J Vasc Endovasc Surg.* (2019) 57:8–93. doi: 10.1016/j.ejvs.2020.09.004

59. Chinen T, Sasabuchi Y, Matsui H, Yasunaga H. Association between third-generation fluoroquinolones and Achilles Tendon rupture: A self-controlled case series analysis. *Ann Fam Med.* (2021) 19:212–6. doi: 10.1370/afm.2673

60. Wee I, Chin B, Syn N, Lee KS, Ng JJ, Choong A. The association between fluoroquinolones and aortic dissection and aortic aneurysms: A systematic review and meta-analysis. *Sci Rep.* (2021) 11:11073. doi: 10.1038/s41598-021-90692-8

61. Lai CC, Wang YH, Chen KH, Chen CH, Wang CY. The association between the risk of aortic aneurysm/aortic dissection and the use of fluroquinolones: A systematic review and meta-analysis. *Antibiotics (Basel).* (2021) 10:697. doi: 10.3390/antibiotics10060697

62. Dai XC, Yang XX, Ma L, Tang GM, Pan YY, Hu HL. Relationship between fluoroquinolones and the risk of aortic diseases: A meta-analysis of observational studies. *BMC Cardiovasc Disord.* (2020) 20:49. doi: 10.1186/s12872-020-01354-y

63. Singh S, Nautiyal A. Aortic dissection and aortic aneurysms associated with fluoroquinolones: A systematic review and meta-analysis. *Am J Med.* (2017) 130:1449–57.e9. doi: 10.1016/j.amjmed.2017.06.029

64. Zhang M, Falconer M, Taylor L. A quantitative bias analysis of the confounding effects due to smoking on the association between fluoroquinolones and risk of aortic aneurysm. *Pharmacoepidemiol Drug Saf.* (2020) 29:958–61. doi: 10.1002/pds.5019

65. Persson R, Jick S. Clinical implications of the association between fluoroquinolones and tendon rupture: The magnitude of the effect with and without corticosteroids. *Br J Clin Pharmacol.* (2019) 85:949–59. doi: 10.1111/bcp.13879

COPYRIGHT

© 2022 Chen, Patterson, Simpson, Li, Chen, Lv, Guo, Li, Fu and Guo. This is an open-access article distributed under the terms of the Creative Commons Attribution License (CC BY). The use, distribution or reproduction in other forums is permitted, provided the original author(s) and the copyright owner(s) are credited and that the original publication in this journal is cited, in accordance with accepted academic practice. No use, distribution or reproduction is permitted which does not comply with these terms.

frontiers | Frontiers in Cardiovascular Medicine

TYPE Mini Review
PUBLISHED 12 August 2022
DOI 10.3389/fcvm.2022.950018

Check for updates

OPEN ACCESS

EDITED BY
Zhenjie Liu,
The Second Affiliated Hospital of Zhejiang University School of Medicine, China

REVIEWED BY
Jun-ichiro Koga,
University of Occupational and Environmental Health Japan, Japan

*CORRESPONDENCE
Bowen Wang
Bw2pw@virginia.edu

SPECIALTY SECTION
This article was submitted to General Cardiovascular Medicine, a section of the journal Frontiers in Cardiovascular Medicine

RECEIVED 22 May 2022
ACCEPTED 27 July 2022
PUBLISHED 12 August 2022

CITATION
Yin L, Kent EW and Wang B (2022) Progress in murine models of ruptured abdominal aortic aneurysm. *Front. Cardiovasc. Med.* 9:950018. doi: 10.3389/fcvm.2022.950018

COPYRIGHT
© 2022 Yin, Kent and Wang. This is an open-access article distributed under the terms of the Creative Commons Attribution License (CC BY). The use, distribution or reproduction in other forums is permitted, provided the original author(s) and the copyright owner(s) are credited and that the original publication in this journal is cited, in accordance with accepted academic practice. No use, distribution or reproduction is permitted which does not comply with these terms.

Progress in murine models of ruptured abdominal aortic aneurysm

Li Yin, Eric William Kent and Bowen Wang*

Department of Surgery, School of Medicine, University of Virginia, Charlottesville, VA, United States

Abdominal aortic aneurysm (AAA) is a focal dilation of the aorta that is prevalent in aged populations. The progressive and unpredictable expansion of AAA could result in aneurysmal rupture, which is associated with ~80% mortality. Due to the expanded screening efforts and progress in diagnostic tools, an ever-increasing amount of asymptomatic AAA patients are being identified yet without a cure to stop the rampant aortic expansion. A key barrier that hinders the development of effective AAA treatment is our incomplete understanding of the cellular and molecular basis of its pathogenesis and progression into rupture. Animal models provide invaluable mechanistic insights into AAA pathophysiology. However, there is no single experimental model that completely recapitulate the complex biology behind AAA, and different AAA-inducing methodologies are associated with distinct disease course and rupture rate. In this review article, we summarize the established murine models of ruptured AAA and discuss their respective strengths and utilities.

KEYWORDS

mouse model, abdominal aortic aneurysm, rupture aneurysm, elastase, AngII

Introduction

An abdominal aortic aneurysm, also known as AAA, is defined as a localized dilation of the abdominal aorta. The expansion involves all layers of the aortic wall. The risk factors for AAA include advanced age, male, smoking, hypertension, dyslipidemia, family history, other vascular aneurysms, other vascular diseases, atherosclerosis, and hypercholesterolemia (1–3). Current guidelines recommend a surveillance strategy for patients of small, asymptomatic AAAs with interval imaging. Surgical repair, including open surgery and endovascular aneurysm repair (EVAR), remains the only treatment for AAA (4).

The main complication of AAA is aortic rupture, which is responsible for about 200,000 deaths per year worldwide (5). The mortality associated with ruptured abdominal aortic aneurysm (rAAA) is still alarmingly high. Despite the progress in emergent surgical repairs, the in-hospital all mortality for rAAA patients remains over 50% in the USA (6). In the population-based Malmö Diet and Cancer Study (MDCS), the acute mortality, defined as death before reaching a hospital or during the first admission, was 34% for rAAA (7). Inasmuch as the high lethality of rAAA, significant efforts have been devoted to the development of robust prediction tools as well as pharmacotherapies for small, asymptomatic AAAs to prevent the deadly their deadly progressions toward

rupture, yet none have demonstrated definitive clinical benefits. These pressing unmet needs testifies to the necessity for further elucidation of the cellular and molecular basis behind AAA pathogenesis as well as its uncontrolled progression into rupture.

Animal models provide invaluable insights into AAA pathophysiologies and help inform clinical studies concerning innovative therapeutics and diagnostics. Experimental models of AAA have been described in a wide range of species, including mice, rats, rabbits, swine, sheep, etc. Due to the multifactorial etiology of AAA, the aneurysm-inducing procedures vary greatly amongst different models. The majority of the existing models focus on the onset phase of AAA, featuring varying incidence rates, anatomical locations, lesion sizes, and disease courses. So far, the three most widely adopted AAA-inducing methods are angiotensin II (AngII) infusion, porcine pancreatic elastase perfusion, and calcium salt topical application. In recent years, β-aminopropionitrile (BAPN), an irreversible inhibitor of lysyl oxidase, becomes increasingly recognized as either a highly effective inducer of aortic aneurysm, dissection, and rupture in murine models—either standalone or in combination with other classic AAA-inducing procedures. These different animal models have been shown to resemble certain aspects of the cellular compositions and pathological changes of clinical AAA, as evidenced by recent transgenic and single-cell sequencing analysis. However, very few of the existing models could faithfully recapitulate the clinical features of rAAA. In fact, the majority of the aforementioned models either do not depict rupture events at all, or are predominantly associated with ruptures in the ascending or thoracic aortas. Additionally, the timing of rupture events differs significantly amongst these models, and the rupture rates have been inconsistent throughout different reports and models. The ideal rAAA model should provide consistent aneurysm formation in the appropriate anatomical location (i.e., infrarenal aortic segment) and consistent AAA rupture over a chronic course. With the emerging interest and research efforts dedicated to the propagation phase of AAA, it is of significant mechanistic and translational values to identify the appropriate experimental models that recapitulate the progressive AAA progression into rupture (8). Herein, we will review the murine models of rAAA and discuss their respective strengths and shortcomings for preclinical studies.

Murine models with systemic agent administration

From a utility perspective, systematical administration of chemical agents is arguably the easiest fashion to establish AAA lesions. Typically, these agents are judiciously chosen based on their association with AAA's clinical risk factors. The most widely utilized ones are hypertension (e.g., AngII and high salt intake) and hypercholesterolemia (e.g., high-fat diet and ApoE/LDLr/PCSK9 loss-of-functions), which we will elaborate later. However, in comparison to the more technically challenging microsurgery-induced models, mice systemically administered with such AAA-inducing agents tend to show highly variable outcomes in terms of AAA incidence, size, location, and rupture rate. It is worth noting that both AngII- and high salt-based models feature both AAA as well as aortic aneurysm and dissection (AAD) in the ascending and thoracic aortas. Herein, we will solely focus on their relevance in rAAA.

Angiotensin II (AngII)-induced rAAA in hypercholesterolemic mice

AngII infusion is one of the most popular methodology to induce AAA in rodents. This model was first reported 20 years ago by Daugherty et al. and has remained the mainstream for aneurysmal studies, particularly concerning ascending and thoracic aortic aneurysm and dissection. In this model, an Azlet osmotic pump will be implanted subcutaneously in mice that are susceptible to hypercholesterolemia (e.g., ApoE-/-), providing subcutaneous infusion of angiotensin II at a dose of 500 or 1,000 ng/kg/min for varying durations, ranging from 14 to 28 days. High-fat or regular diets will be provided during the induction period (9, 10). As aforementioned, this model is primarily focused on aortic aneurysm and dissection in the ascending and thoracic aortas, while the incidence of AAA has been highly variable and inconsistent across different studies (11). In lieu of other modifications, a hypercholesterolemic background is indispensable for the AngII infusion model. Aside from ApoE-/- mice, LDLr mutants have also been widely utilized for this model, albeit with smaller aneurysmal lesions (12). Lu et al. recently established an alternative approach to establish the hypercholesterolemic co-morbidity, in which a PCSK9 gain-of-function adeno-associated virus (AAV) was systemically administered. This new methodology has gained significant popularity as it bypasses the necessity for the ApoE or LDLr mutant alleles, which can be considerably cumbersome and time-consuming for studies that involve additional transgene alleles.

AngII+hypercholesterolemia-induced AAAs recapitulate certain key characteristics of human AAA, such as aortic vascular inflammation, macrophage recruitment, aneurysmal tissue remodeling, and most importantly, the possibility of aneurysmal rupture. Nevertheless, critical discrepancies have been noted in AngII+hypercholesterolemia-induced AAAs vs. typical clinical lesions (13). First of all, AngII-induced aneurysms in mice have been consistently observed to be located in the suprarenal aorta, while most human AAAs are located to infrarenal aorta (11, 14). These differences may be the result of the potential hemodynamic and anatomy differences, but

the exact mechanism remains unclear. Several other chemical-induced AAA models also share such anatomical features with AngII models (11). The pathological features in AngII-induced aneurysms tissue varies spatially and temporally during AngII infusion (15). In the first few days of AngII infusion, the aorta lumen expanded rapidly and an overt thrombus exists outside the external elastic lamina in the adventitia (16, 17). The lumen diameter increases from 0.9 to 1.5 mm within a week (18, 19), resulting in a high rate of death attributed to aorta rupture in the first week and the death occurs less frequently in the following (20, 21). Finally, about 15% to 30% of mice develop abdominal or thoracic aortic rupture in 4 weeks, albeit the incidence rates vary significantly amongst reports. Some studies featuring prolonged AngII infusion observed a gradual increase in aorta lumen dimension for ∼3mm after 3 months in LDLr-/- or ApoE-/- mice, which may not lead to a significant increase in rupture rate. The most important difference is that AngII models induce more aortic dissection than AAA (16). AngII-induced aneurysms walls present intramural hematomas and intima tears, both typical characteristics of aortic dissection; in contrast, human AAA lesions feature significant less dissection but more intraluminal thrombosis (11, 16, 22, 23). Therefore, it has been widely argued that AngII-infused mice are more clinically relevant for studying aortic dissections than AAA (22).

rAAA models induced by AngII+ β-aminopropionitrile (BAPN)

BAPN is an inhibitor of lysyl oxidase and has been reported to disrupt the aortic integrity of collagen and elastin structures, mimicking the aging-associated aortic stiffness. The first documentation of BAPN in AAA was by Kanematsu et al., who reported the robust induction of rAAA in wildtype c57/b6 mice without hypercholesterolemia. BAPN (150 mg/kg per day) infusion was administered *via* osmotic pumps implanted subcutaneously for the first 2 weeks with 1000ng/kg/min AngII infusion throughout 6 weeks. The mice in this study developed thoracic and abdominal aortic aneurysms (38–50% and 30–49 %, respectively) (24). About 33% (16 of 45) died from ruptured aortic aneurysms, including thoracic aneurysms, abdominal aneurysms, and dissecting aneurysms. Aside from BAPN infusion *via* the Azlet osmotic pumps (25, 26), others have reported BAPN systemic administration *via* drinking water modification or gastric lavage (27–31), at a concentration of 0.1∼0.6%. is more popular since it's convenient (28, 30, 32–34).

AngII+BAPN-induced aneurysms have a similar histological characteristics to AngII-induced aneurysms, including ECM degeneration, SMC apoptosis, and aortic dissections. Although AngII+BAPN model presents some aortic dissection aneurysms and aortic dissection, this model leads to a higher incidence of AAA than the conventional AngII models, thereby making it a more appropriate model for studying rAAA (28, 30, 32–35). As characterized by Fashandi et al., the combination of AngII and low dose BAPN constitutes a reproducible model of aortic aneurysm rupture(32). In this study, ApoE -/- mice were given AngII at 1,500–2,000ng/kg/min and 0.2% BAPN dissolved in drinking water, resulting in 93%/79%/79% mice developing AAAs/thoracic aneurysms/ruptures over the course of 4 weeks, respectively. Additional studies further demonstrated the robustness of the BAPN-supplemented models in inducing rAAAs in lieu of hypercholesterolemic backgrounds, which provides significant benefits for transgenic studies (36). It is worth noting that BAPN alone has also been utilized to induce aneurysm rupture; however, similar to the classic AngII models, high dose BAPN administration primarily affected the ascending and thoracic aortic segments instead of abdominal aortas (27, 37).

rAAA exacerbated by high salt

Despite inconsistent reports, epidemiological studies suggests a potential association between high salt consumption and AAA risk (38, 39). In murine models, however, high salt intake alone failed to induce aneurysm formation. By combining high salt with other experimental conditions, rAAA can be robustly induced with high incidence rate within 14 days. Liu et al. implanted deoxycorticosterone acetate pellets with a high salt diet and aldosterone infusion with a high salt diet in male mice at a relatively older age (e.g., 10–12 months old), inducing aneurysm lesions similar to the conventional AngII model (40). In a separate study, high-salt challenge significantly increased the rupture risks of both thoracic and abdominal aortic aneurysm in an AngII+BAPN model. Additional studies are needed to further characterize the impact of high salt in rAAA models.

Rodent models induced by localized challenges

Elastase-induced AAA models

Elastase-induced model, including intraluminal perfusion and topical application, is the second most commonly used model in AAA studies in both mice and rats (41–44). In the classic intraluminal model, the abdominal aortas are typically filled with 0.414 U/mL Type I porcine pancreatic elastase using a syringe pump calibrated to 100 mmHg (42). After 5 min perfusion, the perfused aortas typically dilate by ∼50–70%. In this model, porcine pancreatic elastase is pressure-perfused into the aorta, which causes an immediate increase in diameter due to the inflation pressure and typically results in an aneurysm by

the second week, the aorta diameter may reach 300–400% of the initial size. This procedure also works on wild-type mice (45).

One key disadvantage of the intraluminal method lies in its technical difficulty. Indeed, the microsurgical procedure involves exposure of the infrarenal aorta, temporary occlusion, arteriotomy creation, catheterization, and aorta repairing. Creation of this model requires advanced surgical skills, and there is a substantial learning curve. Because of the technical challenge in mice, elastase perfusion procedures are alternatively performed in rats; however, considering the relative paucity of transgenic rats for genes of interest, mice are still the indispensable species of choice. Alternatively, peri-aortic topical elastase application has been recently established as an alternative approach to robustly induce aneurysms resulting in AAA (43, 46, 47). As described by Bhamidipati et al., ∼10 μL 100% porcine pancreatic elastase was topically applied to abdominal aortic segments for 10 min. After 2 weeks, the aortic diameter increased by 80% with 60% incidence (47). A later study by Lu et al. reported better outcomes with technical optimizations. For example, they applied 5 μL of the active form of elastase (10.3 mg protein/mL, 5.9 U/mg protein) topically to the adventitia of the infrarenal aorta for 5 min (an anatomical recess structure described as "boat" was utilized to "bath" the aforementioned abdominal aortic segments) (43). Aneurysms developed in 87.5% of the mice after 2 weeks; and fueled by BAPN water modification (elaborated later), the aneurysmal diameter continued to progress over the course of 100 days, recapitulating key clinical sequelae of AAA such as rupture and intraluminal thrombosis. Further studies demonstrate comparable macro and microscopic disease features between the intraluminal and topic models using elastase, thereby significantly reducing the bar for wide adoption by researchers (46, 48, 49).

rAAA models enabled by the combination of elastase and systemic chemical administration

Compared to the dissection in AngII-based models, elastase-induced models feature aortic enlargements in true lumens, more marked inflammation, and accurate anatomical lesion location (i.e., infrarenal), all of which are important features in clinical AAA. A prominent problem with the conventional elastase model lies in its lack of rupture. Additionally, while elastase-induced aneurysms can reach a rather large size, they tend to reach plateau after the first 2 weeks. However, it is worth noting that the recent introduction of BAPN significantly alleviates these forgoing concerns. Several models have been reported by combining elastase topical application with BAPN to create a more desirable rupture model. In a recent study, the topical elastase+BAPN-induced AAA lesions was characterized with high-resolution ultrasound imaging, clearly demonstrating the continuous aneurysmal expansion fueled by BAPN(50). Similarly, Lu et al. combined oral BAPN administration and topical elastase application to recapitulate the chronic progression of AAA toward rupture beyond the commonly used 4-week window (43). The mice were given 0.2% BAPN water and adventitia elastase, and the AAA formation rate reached 95% by day 14. In addition to profound AAA lesions, other sequelae, such as thrombosis, irregular shape, thin areas on aneurysm and/or iliac, and renal arteries involvement, were observed, all of which are characteristics of advanced-stage AAA. Moreover, 46.2% of the mice died of AAA rupture before the end of the experiment, including 15.4% (2/13) acute rupture and 30.8% during the chronic, advanced stage (beyond 60 days post elastase challenge). In a separate study, Yue et al. combined intraluminal elastase perfusion (2.0 U/mL elastase at 100 mmHg for 15 mmin) with AngII infusion (1,000 ng/kg/min through osmotic pumps) (51). Similar to BAPN, AngII infusion increased the rupture rate of elastase-induced AAA lesions, reaching around 60% by 4 weeks post procedure.

Calcium chloride induced model

Adventitia application of calcium salts, usually calcium chloride or calcium phosphate, is another accepted way to induce AAA (52, 53). The diameter of calcium salts induced aneurysms is typically smaller than other models (54, 55). Calcium salts induced aneurysms present inflammation, angiogenesis, elastin degradation, and calcification as found in human AAA, but they do not rupture (55, 56).

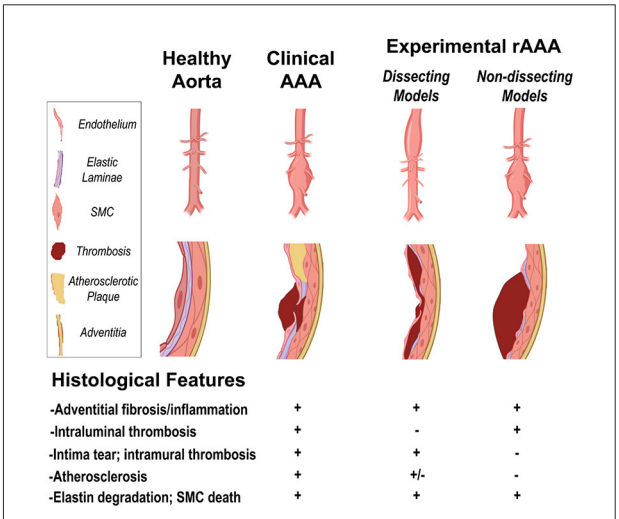

FIGURE 1
The morphological and histological features in clinical vs. experimental models of rAAA (created with BioRender.com).

TABLE 1 The distinct features of each model.

Model	Procedure	End-point	Incidence rate of aneurysm	Special genetic background	Dietary modifications	Gross morphological features	Histological features	Ruptured AAA
AngII-induced model (11)	AngII osmotic pump subcutaneous implantation	2–4 weeks	60∼100% (63)	ApoE-/-;LDLr-/-	High fat/salt diet	AD, suprarenal AAA (11, 14)	Adventitial thickening and fibrosis, leukocyte infiltration, intima tear, ECM degradation, VSMC death, atherosclerotic lesions (with hypercholesterolemia)	15–30%, most in the acute phase (20, 21)
AngII+BAPN (Cooper et al. 2020; Kanematsu et al. 2020)	AngII osmotic pump subcutaneous implantation, together with BAPN administration (osmotic pump infusion or water supplementation)	4–6 weeks	30∼49% (24)	None	Normal/high fat/high salt;	AD, AAA	Adventitial thickening and fibrosis, leukocyte infiltration, intima tear, intramural thrombosis, ECM degradation, VSMC death, atherosclerotic lesions (with hypercholesterolemia)	33–79% (24)
Intraluminal perfusion of PPE (42)	Pressure-perfusion of Type I porcine pancreatic elastase at 100mmHg	2–4 weeks	∼100%	None	None	Infrarenal AAA	Adventitial thickening and fibrosis, media degeneration, intramural thrombosis, leukocyte infiltration, luminal expansion, ECM degradation, VSMC death	Rarely
Topical application of PPE (47)	Topical, peri-adventitial application of elastase to abdominal aortic segments	2 weeks	80%∼87.5%	None	None	Small AAA	Adventitial thickening and fibrosis, leukocyte infiltration, luminal expansion, ECM degradation, VSMC death	Rarely
Combination of BAPN and topical elastase application (43)	BAPN-supplemented water modification and topical, peri-adventitial application of elastase	2–4 weeks	∼95%	None	None	AD and AAA. Irregular shape, and/or iliac, renal arteries involvement	Intraluminal thrombosis, adventitial thickening and fibrosis, leukocyte infiltration, luminal expansion, ECM degradation, VSMC death	Two peaks of rupture:15.4% at first 2 weeks; 30.8% at chronic stage
Elastase perfusion+AngII (51)	Pressure-perfusion of elastase combined with AngII pump implantation	4 weeks	∼100%	None	None		Adventitial thickening and fibrosis, leukocyte infiltration, luminal expansion, intima tear, intramural thrombosis, ECM degradation, VSMC death	60%
Calcium chloride/calcium phosphate induced model (52)	Adventitia application of calcium salts	2∼4 weeks	∼100%	None	None	Smaller AAA lesions. No thrombus. No progressive dilation of aneurysmal aortas.	Vascular calcification, adventitial thickening and fibrosis, inflammatory cell infiltration, oxidative stress, neovascularisation, elastin degradation, and VSMC death.	None

10.3389/fcvm.2022.950018

Other models of rAAA

An increasing number of modified models have been reported based on the classical AAA models, *via* introducing new chemical agents or microsurgical manipulations (57–59). Lareyre et al. conducted a topical application elastase model, and the mice were injected mouse anti-mouse TGF-β three times a week, promoting severe AAA (59). Other notable modification of classic models include retroperitoneal surgical approaches, outflow modulations, and extended elastase perfusion to the juxtarenal and aortoiliac segments (57, 58). Additionally, a hypoperfusion model of the adventitial vasa vasorum in rats was recently described, but this procedure has not been replicated in murine models and the rupture risk is suboptimal and inconsistent (60–62).

Closing remarks

An increasing number of murine models are being developed and characterized to facilitate the mechanistic and therapeutic endeavors concerning rAAA. However, there are several key barriers intrinsic to the existing models, including the inconsistent aneurysm incidence and suboptimal penetrance (particularly for systemically induced models), minimal rupture risks in abdominal aortas (e.g., unmodified elastase model and conventional AngII model), technical difficulties (e.g., intraluminal elastase perfusion model), etc. Indeed, no single experimental model described above fully recapitulate the pathophysiologies of AAA in patients. Figure 1 summarizes the morphological and histological features that are either shared or distinctive in clinical vs. experimental models. Combining different AAA-inducing approaches may offer an avenue to better recapitulate the complex pathophysiolgies of AAA. For example, the combination of intraluminal elastase perfusion and systemic AngII infusion was recently shown to effectively induce rAAA within 4 weeks; and in stark contrast to the conventional AngII-induced AAA models, the aneurysmal lesions in this modified model were primarily located in the infrarenal aortic segments. The addition of hypercholesterolemic background to the elastase model, on the other hand, failed to exacerbate the lesion progression and rupture risk. Herein, we have summarized the distinct features of each model in Table 1. Further efforts are warranted to explore the optimal combinations to establish the desirable rAAA disease course in murine models.

One key feature that is missing in all existing murine models is the gender dimorphism concerning aneurysmal rupture. For many models, e.g., AngII and elastase+BAPN models, female mice tend to develop aneurysms with smaller diameters than male, which aligns with epidemiological evidence in AAA patients. However, the rupture risk is also different between men and women. The dependence of growth and rupture rates on AAA diameter was similar in male and female patients, but the absolute rupture risk was 4-fold greater for all AAA sizes for female patients (64). Women with largest aneurysm diameter and smallest body size were at greatest rupture risks (65). Unfortunately, while most murine models could recapitulate the reduced AAA lesion size and incidence in female, the accelerated aneurysmal rupture risk has not yet been established in any of the existing models (36, 66).

Another major limitation concerning murine studies of rAAA lies in the lack of evaluation approaches. As of now, post-mortem examination remains the standard methodology to identify the presence and exact location of a bona fide rupture. Indeed, the onset of rAAA is highly unpredictable and often rapidly leads to mortality; therefore, live monitoring of rAAA is highly difficult to achieve from a utility perspective. Dissection microscopy is the most commonly used method for post-mortem examination of aortic ruptures, but the carcass quality as well as the experience level of the operators may influence the result. In recent studies, other post-mortem modalities such as nanoparticle contrast-enhanced computed tomography and high-resolution synchrotron-based x-ray have been utilized to determine aortic ruptures in murine models (59, 67). Future efforts are warranted to develop alternative strategies that could monitor or robustly predict the rupturing event in experimental models of AAA.

Feasibility is also a significant factor that should be considered in the choice of animal models. From the perspective of technical difficulties, the elastase perfusion model is undoubtedly the most challenging one. However, recent studies suggest that a topical, peri-aortic route of elastase application may provide similar outcomes in AAA disease progression and rupture, while considerably less technically demanding than the intraluminal route(49, 50). For AngII-based models, the prerequisite of a hypercholesterolemic background (e.g., ApoE-/- or LDLr-/-) dramatically increases the time and animal numbers needed, considering the breeding and expansion of double and sometimes even triple transgenic colonies. This is particularly a concern in terms of compliance with the 3Rs principle (replacement, reduction, refinement). The introduction of alternative methodologies such as viral PCSK9 gain-of-function and BAPN modification offers significant advantages in these regards, hence should be considered during the study designing phase.

In conclusion, thus far there are no single experimental models that faithfully recapitulate the disease features of rAAA. For future preclinical investigations, further modifications are still warranted to improve the clinical relevance of existing murine models.

Author contributions

LY, EK, and BW conceived the manuscript, conducted the literature search, contributed to the drafting, and editing of the

manuscript. All authors contributed to the article and approved the submitted version.

Funding

This work was supported by the National Institute of Health (NIH) grant R01HL162895 (to BW).

Conflict of interest

The authors declare that the research was conducted in the absence of any commercial or financial relationships that could be construed as a potential conflict of interest.

Publisher's note

All claims expressed in this article are solely those of the authors and do not necessarily represent those of their affiliated organizations, or those of the publisher, the editors and the reviewers. Any product that may be evaluated in this article, or claim that may be made by its manufacturer, is not guaranteed or endorsed by the publisher.

References

1. Lindholt JS, Juul S, Fasting H, Henneberg EW. Screening for abdominal aortic aneurysms: single centre randomised controlled trial. *BMJ.* (2005) 330:750. doi: 10.1136/bmj.38369.620162.82

2. Kent KC, Zwolak RM, Egorova NN, Riles TS, Manganaro A, Moskowitz AJ, et al. Analysis of risk factors for abdominal aortic aneurysm in a cohort of more than 3 million individuals. *J Vasc Surg.* (2010) 52:539k RM doi: 10.1016/j.jvs.2010.05.090

3. van Vlijmen-van Keulen CJ, Pals G, Rauwerda JA. Familial abdominal aortic aneurysm: a systematic review of a genetic background. *Eur J Vasc Endovasc Surg.* (2002) 24:105–16. doi: 10.1053/ejvs.2002.1692

4. Wanhainen A, Verzini F, Van Herzeele I, Allaire E, Bown M, Cohnert T, et al. Editor's choice - european society for vascular surgery (ESVS) 2019 clinical practice guidelines on the management of abdominal aorto-iliac artery aneurysms. *Eur J Vasc Endovasc Surg.* (2019) 57:8ndov doi: 10.1016/j.ejvs.2018.09.020

5. Sampson UK, Norman PE, Fowkes FG, Aboyans V, Song Y, Harrell FE, Jr., et al. Estimation of global and regional incidence and prevalence of abdominal aortic aneurysms 1990 to 2010. *Glob Heart.* (2014) 9:159–70. doi: 10.1016/j.gheart.2013.12.009

6. Karthikesalingam A, Holt PJ, Vidal-Diez A, Ozdemir BA, Poloniecki JD, Hinchliffe RJ, et al. Mortality from ruptured abdominal aortic aneurysms: clinical lessons from a comparison of outcomes in England and the USA. *Lancet.* (2014) 383:963m A doi: 10.1016/S0140-6736(14)60109-4

7. Landenhed M, Engstr6736(14)60109-4-Diez A, Ozdemir BA, Poloniecki JD, Hinchliffe RJ, et al. Mortality from ruptured abdominal aortic aneurysms: clinical lessons from a comparison of outcomes in E*J Am Heart Assoc.* (2015) 4:e001513. doi: 10.1161/JAHA.114.001513

8. Lu HS, Owens AP. 3rd, Liu B, Daugherty A. Illuminating the importance of studying interventions on the propagation phase of experimental mouse abdominal aortic aneurysms. *Arterioscler Thromb Vasc Biol.* (2021) 41:1518romb doi: 10.1161/ATVBAHA.121.316070

9. Daugherty A, Cassis L. Chronic angiotensin II infusion promotes atherogenesis in low density lipoprotein receptor -/- mice. *Ann N Y Acad Sci.* (1999) 892:108i.is doi: 10.1111/j.1749-6632.1999.tb07789.x

10. Cassis LA, Gupte M, Thayer S, Zhang X, Charnigo R, Howatt DA, et al. ANG II infusion promotes abdominal aortic aneurysms independent of increased blood pressure in hypercholesterolemic mice. *Am J Physiol Heart Circ Physiol.* (2009) 296:H1660t C doi: 10.1152/ajpheart.00028.2009

11. Daugherty A, Manning MW, Cassis LA. Angiotensin II promotes atherosclerotic lesions and aneurysms in apolipoprotein E-deficient mice. *J Clin Invest.* (2000) 105:1605ning doi: 10.1172/JCI7818

12. Cassis LA, Rateri DL, Lu H, Daugherty A. Bone marrow transplantation reveals that recipient AT1a receptors are required to initiate angiotensin II-induced atherosclerosis and aneurysms. *Arterioscler Thromb Vasc Biol.* (2007) 27:380hro doi: 10.1161/01.ATV.0000254680.71485.92

13. Liu J, Daugherty A, Lu H. Angiotensin II and abdominal aortic aneurysms: an update. *Curr Pharm Des.* (2015) 21:4035y A, doi: 10.2174/1381612821666150826093318

14. Bruemmer D, Collins AR, Noh G, Wang W, Territo M, Arias-Magallona S, et al. Angiotensin II-accelerated atherosclerosis and aneurysm formation is attenuated in osteopontin-deficient mice. *J Clin Invest.* (2003) 112:1318ins doi: 10.1172/JCI200318141

15. Liu S, Xie Z, Daugherty A, Cassis LA, Pearson KJ, Gong MC, et al. Mineralocorticoid receptor agonists induce mouse aortic aneurysm formation and rupture in the presence of high salt. *Arterioscler Thromb Vasc Biol.* (2013) 33:1568romb doi: 10.1161/atvb.33.suppl_1.A519

16. Saraff K, Babamusta F, Cassis LA, Daugherty A. Aortic dissection precedes formation of aneurysms and atherosclerosis in angiotensin II-infused, apolipoprotein E-deficient mice. *Arterioscler Thromb Vasc Biol.* (2003) 23:1621rom doi: 10.1161/01.ATV.0000085631.76095.64

17. Sawada H, Lu HS, Cassis LA, Daugherty A. Twenty years of studying AngII (Angiotensin II)-induced abdominal aortic pathologies in mice: continuing questions and challenges to provide insight into the human disease. *Arterioscler Thromb Vasc Biol.* (2022) 42:277hrom

18. Barisione C, Charnigo R, Howatt DA, Moorleghen JJ, Rateri DL, Daugherty A. Rapid dilation of the abdominal aorta during infusion of angiotensin II detected by noninvasive high-frequency ultrasonography. *J Vasc Surg.* (2006) 44:372har doi: 10.1016/j.jvs.2006.04.047

19. Martin-McNulty B, Vincelette J, Vergona R, Sullivan ME, Wang YX. Noninvasive measurement of abdominal aortic aneurysms in intact mice by a high-frequency ultrasound imaging system. *Ultrasound Med Biol.* (2005) 31:745 Bi doi: 10.1016/j.ultrasmedbio.2005.02.012

20. Peshkova IO, Aghayev T, Fatkhullina AR, Makhov P, Titerina EK, Eguchi S, et al. IL-27 receptor-regulated stress myelopoiesis drives abdominal aortic aneurysm development. *Nat Commun.* (2019) 10:5046. doi: 10.1038/s41467-019-13017-4

21. Ortega R, Collado A, Selles F, Gonzalez-Navarro H, Sanz MJ, Real JT, et al. SGLT-2 (Sodium-Glucose Cotransporter 2) Inhibition Reduces Ang II (Angiotensin II)-induced dissecting abdominal aortic aneurysm in apoe (apolipoprotein E) knockout mice. *Arterioscler Thromb Vasc Biol.* (2019) 39:1614romb doi: 10.1161/ATVBAHA.119.312659

22. Trachet B, Aslanidou L, Piersigilli A, Fraga-Silva RA, Sordet-Dessimoz J, Villanueva-Perez P, et al. Angiotensin II infusion into ApoE-/- mice: a model for aortic dissection rather than abdominal aortic aneurysm? *Cardiovasc Res.* (2017) 113:1230idou doi: 10.1093/cvr/cvx128

23. Golledge J, Wolanski P, Parr A, Buttner P. Measurement and determinants of infrarenal aortic thrombus volume. *Eur Radiol.* (2008) 18:1987ansk doi: 10.1007/s00330-008-0956-3

24. Kanematsu Y, Kanematsu M, Kurihara C, Tsou TL, Nuki Y, Liang EI, et al. Pharmacologically induced thoracic and abdominal aortic aneurysms in mice. *Hypertension.* (2010) 55:1267nema doi: 10.1161/HYPERTENSIONAHA.109.140558

25. Tomida S, Aizawa K, Nishida N, Aoki H, Imai Y, Nagai R, et al. Indomethacin reduces rates of aortic dissection and rupture of the abdominal aorta by inhibiting monocyte/macrophage accumulation in a murine model. *Sci Rep.* (2019) 9:10751. doi: 10.1038/s41598-019-46673-z

26. Takayanagi T, Crawford KJ, Kobayashi T, Obama T, Tsuji T, Elliott KJ, et al. Caveolin 1 is critical for abdominal aortic aneurysm formation induced by angiotensin II and inhibition of lysyl oxidase. *Clin Sci (Lond).* (2014) 126:785.awf doi: 10.1042/CS20130660

27. Ren W, Liu Y, Wang X, Jia L, Piao C, Lan F, et al. beta-Aminopropionitrile monofumarate induces thoracic aortic dissection in C57BL/6 mice. *Sci Rep.* (2016) 6:28149.

28. Aicher BO, Zhang J, Muratoglu SC, Galisteo R, Arai AL, Gray VL, et al. Moderate aerobic exercise prevents matrix degradation and death in a mouse model of aortic dissection and aneurysm. *Am J Physiol Heart Circ Physiol.* (2021) 320:H1786t Circ doi: 10.1152/ajpheart.00229.2020

29. Sawada H, Franklin MK, Moorleghen JJ, Howatt DA, Kukida M, Lu HS, et al. Ultrasound monitoring of descending aortic aneurysms and dissections in mice. *Arterioscler Thromb Vasc Biol.* (2020) 40:2557rom doi: 10.1161/ATVBAHA.120.314799

30. Aicher BO, Mukhopadhyay S, Lu X, Muratoglu SC, Strickland DK, Ucuzian AA. Quantitative micro-CT analysis of aortopathy in a mouse model of beta-aminopropionitrile-induced aortic aneurysm and dissection. *J Vis Exp.* (2018) 57589. doi: 10.3791/57589

31. Kurihara T, Shimizu-Hirota R, Shimoda M, Adachi T, Shimizu H, Weiss SJ, et al. Neutrophil-derived matrix metalloproteinase 9 triggers acute aortic dissection. *Circulation.* (2012) 126:3070izu-doi: 10.1161/CIRCULATIONAHA.112.097097

32. Fashandi AZ, Hawkins RB, Salmon MD, Spinosa MD, Montgomery WG, Cullen JM, et al. A novel reproducible model of aortic aneurysm rupture. *Surgery.* (2018) 163:397wkins doi: 10.1016/j.surg.2017.10.003

33. Ohno-Urabe S, Kukida M, Franklin MK, Katsumata Y, Su W, Gong MC, et al. Authentication of *in situ* measurements for thoracic aortic aneurysms in mice. *Arterioscler Thromb Vasc Biol.* (2021) 41:2117rom doi: 10.1161/ATVBAHA.121.315983

34. Kawai T, Takayanagi T, Forrester SJ, Preston KJ, Obama T, Tsuji T, et al. Vascular ADAM17 (a Disintegrin and Metalloproteinase Domain 17) is required for angiotensin II/beta-aminopropionitrile-induced abdominal aortic aneurysm. *Hypertension.* (2017) 70:959anag doi: 10.1161/HYPERTENSIONAHA.117.09822

35. Zhou B, Li W, Zhao G, Yu B, Ma B, Liu Z, et al. Rapamycin prevents thoracic aortic aneurysm and dissection in mice. *J Vasc Surg.* (2019) 69:921–32 e3. doi: 10.1016/j.jvs.2018.05.246

36. Qi X, Wang F, Chun C, Saldarriaga L, Jiang Z, Pruitt EY, et al. A validated mouse model capable of recapitulating the protective effects of female sex hormones on ascending aortic aneurysms and dissections (AADs). *Physiol Rep.* (2020) 8:e14631. doi: 10.14814/phy2.14631

37. Sawada H, Beckner ZA, Ito S, Daugherty A, Lu HS. beta-Aminopropionitrile-induced aortic aneurysm and dissection in mice. *JVS Vasc Sci.* (2022) 3:64.kne doi: 10.1016/j.jvssci.2021.12.002

38. Golledge J, Hankey GJ, Yeap BB, Almeida OP, Flicker L, Norman PE. Reported high salt intake is associated with increased prevalence of abdominal aortic aneurysm and larger aortic diameter in older men. *PLoS ONE.* (2014) 9:e102578. doi: 10.1371/journal.pone.0102578

39. Haring B, Selvin E, He X, Coresh J, Steffen LM, Folsom AR, et al. Adherence to the dietary approaches to stop hypertension dietary pattern and risk of abdominal aortic aneurysm: results from the ARIC study. *J Am Heart Assoc.* (2018) 7:e009340. doi: 10.1161/JAHA.118.009340

40. Liu S, Gong MC, Guo Z, A. New mouse model for introduction of aortic aneurysm by implantation of deoxycorticosterone acetate pellets or aldosterone infusion in the presence of high salt. *Methods Mol Biol.* (2017) 1614:155.uo doi: 10.1007/978-1-4939-7030-8_12

41. Anidjar S, Salzmann JL, Gentric D, Lagneau P, Camilleri JP, Michel JB. Elastase-induced experimental aneurysms in rats. *Circulation.* (1990) 82:973zman doi: 10.1161/01.CIR.82.3.973

42. Pyo R, Lee JK, Shipley JM, Curci JA, Mao D, Ziporin SJ, et al. Targeted gene disruption of matrix metalloproteinase-9 (gelatinase B) suppresses development of experimental abdominal aortic aneurysms. *J Clin Invest.* (2000) 105:1641hip doi: 10.1172/JCI8931

43. Lu G, Su G, Davis JP, Schaheen B, Downs E, Roy RJ, et al. A novel chronic advanced stage abdominal aortic aneurysm murine model. *J Vascular Surg.* (2017) 66:232–42.e4.

44. Busch A, Holm A, Wagner N, Ergun S, Rosenfeld M, Otto C, et al. Extra- and intraluminal elastase induce morphologically distinct abdominal aortic aneurysms in mice and thus represent specific subtypes of human disease. *J Vasc Res.* (2016) 53:49 A, doi: 10.1159/000447263

45. Thompson RW, Curci JA, Ennis TL, Mao D, Pagano MB, Pham CT. Pathophysiology of abdominal aortic aneurysms: insights from the elastase-induced model in mice with different genetic backgrounds. *Ann N Y Acad Sci.* (2006) 1085:59i.i doi: 10.1196/annals.1383.029

46. Xue C, Zhao G, Zhao Y, Chen YE, Zhang J. Mouse abdominal aortic aneurysm model induced by perivascular application of elastase. *J Vis Exp.* (2022) 180:e63608. doi: 10.3791/63608

47. Bhamidipati CM, Mehta GS, Lu GY, Moehle CW, Barbery C, DiMusto PD, et al. Development of a novel murine model of aortic aneurysms using peri-adventitial elastase. *Surgery.* (2012) 152:238 Meh doi: 10.1016/j.surg.2012.02.010

48. Laser A, Lu G, Ghosh A, Roelofs K, McEvoy B, DiMusto P, et al. Differential gender- and species-specific formation of aneurysms using a novel method of inducing abdominal aortic aneurysms. *J Surg Res.* (2012) 178:1038hosh doi: 10.1016/j.jss.2012.04.073

49. Berman AG, Romary DJ, Kerr KE, Gorazd NE, Wigand MM, Patnaik SS, et al. Experimental aortic aneurysm severity and growth depend on topical elastase concentration and lysyl oxidase inhibition. *Sci Rep.* (2022) 12:99. doi: 10.1038/s41598-021-04089-8

50. Romary DJ, Berman AG, Goergen CJ. High-frequency murine ultrasound provides enhanced metrics of BAPN-induced AAA growth. *Am J Physiol Heart Circ Physiol.* (2019) 317:H981rt Ci doi: 10.1152/ajpheart.00300.2019

51. Yue J, Yin L, Shen J, Liu Z. A Modified murine abdominal aortic aneurysm rupture model using elastase perfusion and angiotensin II infusion. *Ann Vasc Surg.* (2020) 67:474Shen doi: 10.1016/j.avsg.2020.03.002

52. Chiou AC, Chiu B, Pearce WH. Murine aortic aneurysm produced by periarterial application of calcium chloride. *J Surg Res.* (2001) 99:371 B, doi: 10.1006/jsre.2001.6207

53. Yamanouchi D, Morgan S, Stair C, Seedial S, Lengfeld J, Kent KC, et al. Accelerated aneurysmal dilation associated with apoptosis and inflammation in a newly developed calcium phosphate rodent abdominal aortic aneurysm model. *J Vasc Surg.* (2012) 56:455Morg doi: 10.5772/1508

54. Phillips EH, Yrineo AA, Schroeder HD, Wilson KE, Cheng JX, Goergen CJ. Morphological and biomechanical differences in the elastase and AngII apoE(-/-) rodent models of abdominal aortic aneurysms. *Biomed Res Int.* (2015) 2015:413189. doi: 10.1155/2015/413189

55. Wang Y, Krishna S, Golledge J. The calcium chloride-induced rodent model of abdominal aortic aneurysm. *Atherosclerosis.* (2013) 226:29s.S, doi: 10.1016/j.atherosclerosis.2012.09.010

56. Chen HZ, Wang F, Gao P, Pei JF, Liu Y, Xu TT, et al. Age-associated sirtuin 1 reduction in vascular smooth muscle links vascular senescence and inflammation to abdominal aortic aneurysm. *Circ Res.* (2016) 119:1076 Gao doi: 10.1161/CIRCRESAHA.116.308895

57. Zhu JX, Tang QQ, Zhou C, Shi XC Yi SY, Yang Y. Establishment of a new abdominal aortic aneurysm model in rats by a retroperitoneal approach. *Front Cardiovasc Med.* (2022) 9:808732. doi: 10.3389/fcvm.2022.808732

58. Busch A, Chernogubova E, Jin H, Meurer F, Eckstein HH, Kim M, et al. Four surgical modifications to the classic elastase perfusion aneurysm model enable haemodynamic alterations and extended elastase perfusion. *Eur J Vasc Endovasc Surg.* (2018) 56:102ova doi: 10.1016/j.ejvs.2018.03.018

59. Lareyre F, Clement M, Raffort J, Pohlod S, Patel M, Esposito B, et al. TGFbeta (Transforming Growth Factor-beta) blockade induces a human-like disease in a nondissecting mouse model of abdominal aortic aneurysm. *Arterioscler Thromb Vasc Biol.* (2017) 37:2171romb doi: 10.1161/ATVBAHA.117.309999

60. Kugo H, Sukketsiri W, Tanaka H, Fujishima R, Moriyama T, Zaima N. Time-dependent pathological changes in hypoperfusion-induced abdominal aortic aneurysm. *Biology (Basel).* (2021) 10:149. doi: 10.3390/biology10020149

61. Kugo H, Zaima N, Tanaka H, Hashimoto K, Miyamoto C, Sawaragi A, et al. Pathological analysis of the ruptured vascular wall of hypoperfusion-induced abdominal aortic aneurysm animal model. *J Oleo Sci.* (2017) 66:499N, Ta doi: 10.5650/jos.ess16219

62. Tanaka H, Zaima N, Sasaki T, Sano M, Yamamoto N, Saito T, et al. Hypoperfusion of the adventitial vasa vasorum develops an abdominal aortic aneurysm. *PLoS ONE.* (2015) 10:e0134386. doi: 10.1371/journal.pone.0134386

63. Liu J, Lu H, Howatt DA, Balakrishnan A, Moorleghen JJ, Sorci-Thomas M, et al. Associations of ApoAI and ApoB-containing lipoproteins with AngII-induced abdominal aortic aneurysms in mice. *Arterioscler Thromb Vasc Biol.* (2015) 35:1826romb doi: 10.1161/atvb.35.suppl_1.462

64. Collaborators R, Bown MJ, Sweeting MJ, Brown LC, Powell JT, Thompson SG. Surveillance intervals for small abdominal aortic aneurysms: a meta-analysis. *JAMA*. (2013) 309:806, Bo

65. Lo RC, Lu B, Fokkema MT, Conrad M, Patel VI, Fillinger M, et al. Relative importance of aneurysm diameter and body size for predicting abdominal aortic aneurysm rupture in men and women. *J Vasc Surg*. (2014) 59:1209kkem doi: 10.1016/j.jvs.2013.10.104

66. Fashandi AZ, Spinosa M, Salmon M, Su G, Montgomery W, Mast A, et al. Female mice exhibit abdominal aortic aneurysm protection in an established rupture model. *J Surg Res*. (2020) 247:387inos doi: 10.1016/j.jss.2019.10.004

67. Ghaghada KB, Ren P, Devkota L, Starosolski Z, Zhang C, Vela D, et al. Early detection of aortic degeneration in a mouse model of sporadic aortic aneurysm and dissection using nanoparticle contrast-enhanced computed tomography. *Arterioscler Thromb Vasc Biol*. (2021) 41:1534romb doi: 10.1161/ATVBAHA.120.315210

frontiers | Frontiers in Cardiovascular Medicine

TYPE Original Research
PUBLISHED 22 August 2022
DOI 10.3389/fcvm.2022.870378

Check for updates

OPEN ACCESS

EDITED BY
Xiaofeng Yang,
Temple University, United States

REVIEWED BY
Jan Brunkwall,
University of Cologne, Germany
Agneta Wikman,
Karolinska University Laboratory, Sweden

*CORRESPONDENCE
Zhihui Dong
dzh926@126.com
Weiguo Fu
fu.weiguo@zs-hospital.sh.cn

†These authors have contributed equally to this work and share first authorship

SPECIALTY SECTION
This article was submitted to General Cardiovascular Medicine, a section of the journal Frontiers in Cardiovascular Medicine

RECEIVED 06 February 2022
ACCEPTED 04 August 2022
PUBLISHED 22 August 2022

CITATION
Fang G, Yue J, Shuai T, Yuan T, Ren B, Fang Y, Pan T, Liu Z, Dong Z and Fu W (2022) Comparison between endovascular aneurysm repair-selected and endovascular aneurysm repair-only strategies for the management of ruptured abdominal aortic aneurysms: An 11-year experience at a Chinese tertiary hospital. *Front. Cardiovasc. Med.* 9:870378. doi: 10.3389/fcvm.2022.870378

COPYRIGHT
© 2022 Fang, Yue, Shuai, Yuan, Ren, Fang, Pan, Liu, Dong and Fu. This is an open-access article distributed under the terms of the Creative Commons Attribution License (CC BY). The use, distribution or reproduction in other forums is permitted, provided the original author(s) and the copyright owner(s) are credited and that the original publication in this journal is cited, in accordance with accepted academic practice. No use, distribution or reproduction is permitted which does not comply with these terms.

Comparison between endovascular aneurysm repair-selected and endovascular aneurysm repair-only strategies for the management of ruptured abdominal aortic aneurysms: An 11-year experience at a Chinese tertiary hospital

Gang Fang[1,2,3†], Jianing Yue[1,2,3†], Tao Shuai[1,2,3], Tong Yuan[1,2,3], Bichen Ren[1,2,3], Yuan Fang[1,2,3], Tianyue Pan[1,2,3], Zhenjie Liu[4], Zhihui Dong[1,2,3*] and Weiguo Fu[1,2,3*]

[1]Department of Vascular Surgery, Zhongshan Hospital, Fudan University, Shanghai, China, [2]Institute of Vascular Surgery, Fudan University, Shanghai, China, [3]National Clinical Research Center for Interventional Medicine, Shanghai, China, [4]Department of Vascular Surgery, The Second Affiliated Hospital of Zhejiang University, School of Medicine, Hangzhou, China

Objectives: The aim of this study was to review our management experience of ruptured abdominal aortic aneurysms (RAAAs) using an endovascular aneurysm repair (EVAR)-only strategy, and discuss the feasibility of this strategy.

Materials and methods: A retrospective analysis of clinical data was performed in patients with RAAAs from January 2009 to October 2020. Our strategy toward operative treatment for RAAAs evolved from an EVAR-selected (from January 2009 to April 2014) to an EVAR-only (from May 2014 to October 2020) strategy. Baseline characteristics, thirty-day mortality, perioperative complications, and long-term outcomes of patients were compared between the two periods.

Results: A total of 93 patients undergoing emergent RAAA repair were eventually included. The overall operation rate in RAAAs at our centre was 70.5% (93/132). In the EVAR-only period, all 53 patients underwent ruptured endovascular aneurysm repair (rEVAR). However, only 47.5% (19/40) of patients in the EVAR-selected period underwent rEVAR, and the remaining 21 patients underwent emergent open surgery. Thirty-day mortality in the EVAR-only group was 22.6% (12/53) compared with 25.0% (10/40) for the EVAR-selected group (P = 0.79). Systolic blood pressure ≤70 mmHg [adjusted odds ratio (OR) 4.99, 95% confidence interval (CI), 1.13–22.08, P = 0.03] and

abdominal compartment syndrome (adjusted OR 3.72, 95% CI, 1.12–12.32, P = 0.03) were identified as independent risk factors responsible for 30-day mortality. After 5 years, 47.5% (95% CI, 32.0–63.0%) of patients in the EVAR-selected group were still alive versus 49.1% (95% CI, 32.3–65.9%) of patients in the EVAR-only group (P = 0.29).

Conclusion: The EVAR-only strategy has allowed rEVAR to be used in nearly all the RAAAs with similar mortality comparing with the EVAR-selected strategy. Due to the avoidance of operative modality selection, the EVAR-only strategy was associated with a more simplified algorithm, less influence on haemodynamics, and a shorter operation and recovery time.

KEYWORDS

ruptured abdominal aortic aneurysm, ruptured endovascular aneurysm repair, abdominal compartment syndrome, emergent aneurysm repair, stent-graft

Introduction

The mortality rates of ruptured abdominal aortic aneurysms (RAAAs) following open surgical repair (OSR) remain high despite advances in surgical and anaesthetic techniques (1). The safety and effectiveness of elective endovascular repair of AAAs have been acknowledged, and ruptured endovascular aneurysm repair (rEVAR) is now considered as an alternative to operative treatment for RAAAs. Meanwhile, the discussion about the role of rEVAR has been sustained during the past two decades due to the discrepancy between randomised controlled trials (RCTs) and real-life studies (2–5). Recently, both the Society for Vascular Surgery (SVS) 2018 practice guidelines and the European Society for Vascular Surgery (ESVS) 2019 clinical practice guidelines on the management of AAAs have strongly recommended (level of recommendation: class 1) rEVAR over OSR for the treatment of RAAAs, when anatomically feasible (6, 7). However, it was reported that less than 50% of RAAA patients were candidates for EVAR based on the neck criteria of instructions for use (IFU) for abdominal aortic endografts (8). Whether the indication of rEVAR could be further extended to a larger group of RAAA patients with more challenging anatomical conditions, remains to be investigated.

Ever since the results of three RCTs (AJAX, ECAR, and IMPROVE) on OSR versus rEVAR appeared in early 2010s (3, 4, 9). A much more aggressive attitude toward rEVAR use has been adopted at our institution. In May 2014, an EVAR-only strategy that involves the complete replacement of OSR for all RAAAs with rEVAR was instituted at our centre, and this strategy is still being used currently. The aim of this study was to compare the outcomes of the "EVAR-only" strategy (from May 2014 to October 2020) with those of the "EVAR-selected" strategy (from January 2009 to April 2014) and discuss the feasibility of the "EVAR-only" strategy.

Materials and methods

Study population

A retrospective review of the database of images and electronic medical records was performed to identify patients who received a diagnosis of RAAA between January 2009 and October 2020 at our centre. Clinical data including patient demographics, coexisting medical conditions, patient status upon admission, computed tomography angiography (CTA) images, laboratory test results, surgery details, postoperative complications, and long-term follow-up results were collected. Exclusion criteria included the following: (1) suprarenal RAAAs; (2) ruptured Crawford type I–IV thoracoabdominal aortic aneurysms; (3) symptomatic AAAs without retroperitoneal haematoma or leakage of the contrast agent on preoperative CTA; (4) ruptured isolated iliac artery aneurysms; (5) abdominal aortic pseudoaneurysms without aneurysmal dilatation of the infrarenal abdominal aortic wall; and (6) RAAAs in patients who previously underwent EVAR. Patients meeting any one of these criteria were excluded from the analysis of this study. The rest of the patients receiving a diagnosis of RAAA were then included in the current study. This study was approved by the Committee for the Protection of Human Subjects at Zhongshan Hospital, Fudan University. All patients participating in the study signed an informed consent document.

Institutional setting

From January 2009 to October 2020, treatment conditions and resources for RAAAs at our centre included the following: (1) a green channel in the emergency room for priority treatment of RAAAs; (2) availability of CTA in the emergency

room within 15 min of raising a request; (3) a fully trained on-call multidisciplinary team including vascular surgeons, emergency department physicians, anaesthesiologists, operating room staff, and surgical intensive care unit (sICU) doctors; this team was capable of treating vascular emergencies throughout the day; (4) a fully equipped hybrid operating room used independently by vascular surgeons; (5) priority given for treating RAAAs in the hybrid operating room; (6) at least three brands of endografts with complete specifications stocked in the hybrid operating room; (7) all emergent RAAA repair procedures performed by senior vascular surgeons competent in open and endovascular techniques.

Treatment strategies

From January 2009 to April 2014, we implemented an "EVAR-selected" strategy. The rEVAR procedure was performed in a highly selected patient population during this period, and selection was based on patient's haemodynamic conditions, neck anatomy, and the senior vascular surgeon's preference. Haemodynamic instability was defined as a systolic blood pressure $\leq$70 mmHg for more than 10 min; patients with a systolic blood pressure $>$70 mmHg were considered haemodynamically stable in the current study. Favourable proximal aneurysm neck anatomy was defined when the well-accepted IFU criteria of endografts were met, which were as follows: (1) proximal neck length $\geq$10 mm; (2) proximal neck angulation $<$60°; and (3) proximal neck diameter $<$32 mm. A hostile proximal neck was defined if any one of the above mentioned criteria were not met. During this period, a rEVAR was performed as the first-choice treatment only in haemodynamically stable patients with a favourable proximal neck. As for haemodynamically unstable patients, the administration of rEVAR was dependent on the personal experience of the senior vascular surgeon. Notably, due to our abundant experience in elective EVAR (**Figure 1**) for treating AAAs with hostile necks, we tended to prefer rEVAR in haemodynamically stable patients with hostile aneurysm necks to achieve more rapid control of life-threatening haemorrhage.

From May 2014 to September 2020, the strategy for the management of patients with RAAAs could be summarised as "EVAR-only." Briefly, once the diagnosis of an infrarenal RAAA was established, a rEVAR would be immediately prepared for these patients, regardless of their haemodynamic status and the anatomic conditions of the proximal aneurysm neck. Therefore, rEVAR was the only technique used to repair RAAAs during this period.

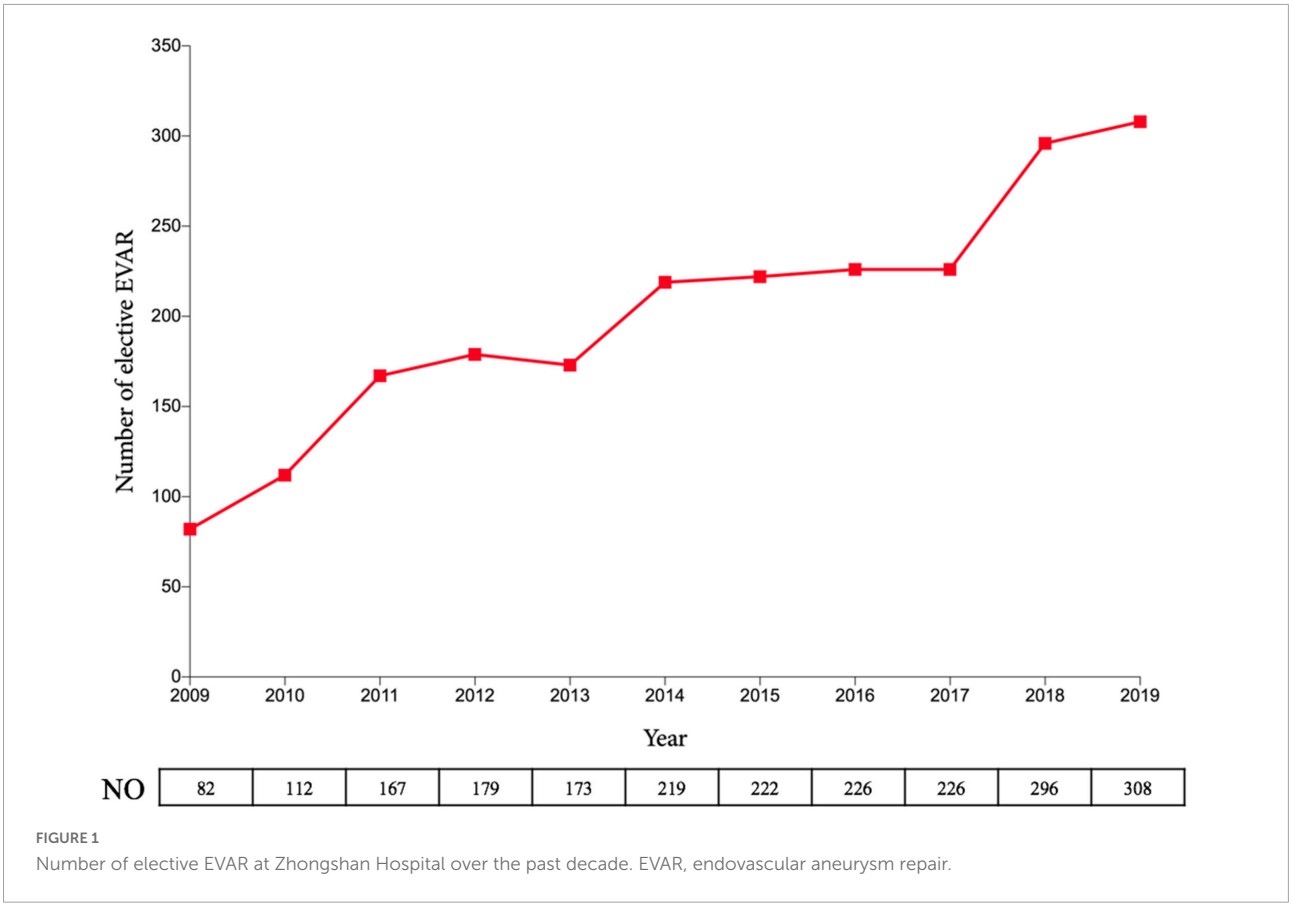

FIGURE 1
Number of elective EVAR at Zhongshan Hospital over the past decade. EVAR, endovascular aneurysm repair.

Preoperative assessment

The diagnosis of a RAAA was established when a retroperitoneal haematoma or leakage of the contrast agent was found around a true AAA on CT images. All the patients received CT imaging in the transferring hospital or at our emergency room. An expeditious CTA was mandatory for the haemodynamically stable patients. For the haemodynamically unstable patients, hypotensive haemostasis with strict limitation of fluid infusion was implemented to maintain a target systolic blood pressure of 80–100 mmHg. Surgical interventions including balloon occlusion were performed only when informed consent was obtained from the patients or their family members.

Emergent repair of ruptured abdominal aortic aneurysms

Emergent open surgery was performed under general anaesthesia. A transperitoneal RAAA repair was utilised in our centre. In haemodynamically unstable patients, transfemoral balloon occlusion of the aorta was considered before anaesthesia induction. Heparin was used selectively according to the patients' coagulation conditions. When primary abdominal closure was deemed unfeasible due to intestinal oedema, vacuum-pack temporary abdominal wound management with delayed closure was used.

A rEVAR was performed in a hybrid operation room by surgeons with extensive experience in elective EVAR. Transfemoral descending aortic balloon occlusion was performed in haemodynamically unstable patients. The anaesthesia method (local or general) for the following rEVAR procedures was determined by anaesthetists and vascular surgeons, and was mainly based on the degree of dysphoria and haemodynamic conditions in these patients. Technical success was defined as the successful deployment of the endograft into the target segment of the artery without type I and III endoleaks at complete angiogram. Additionally, decompression laparotomy was not performed at the same stage during the rEVAR procedure as during OSR.

Postoperative management

Patients undergoing rAAA repair were admitted to the sICU. Maintenance of acid-base balance, correction of coagulation function, and improvement of the haemodynamic parameters were the three main goals of our therapy; this aspect has been described in our previous study (10).

Abdominal compartment syndrome (ACS) was defined as an intraluminal bladder pressure value of $\geq$20 mmHg with a new organ dysfunction (cardiac, respiratory, or renal). For patients with ACS, vascular surgeons and sICU physicians codetermined whether a laparotomy decompression was indicated, mainly according to patients' tolerance to open surgery, coagulation functions, and willingness of their family members. Patients surviving to discharge after RAAA repair were routinely followed up by CTA at 3, 6, and 12 months, and annually thereafter.

Statistical analysis

The primary outcome was 30-day all-cause mortality. Secondary outcomes included in-hospital all-cause mortality, postoperative complications during a 30-day postoperative period, and the length of the sICU and hospital stay. Continuous variables were expressed as mean $\pm$ SD, and categorical variables were expressed as frequencies and percentages. Categorical variables were compared between groups using the χ^2 test, and the *t*-test was used to analyse continuous variables. Statistical significance was defined as a *P*-value < 0.05. Univariate and multivariate logistic analyses were used to identify potential independent risk factors of 30-day mortality after emergent repair of RAAAs and the occurrence of ACS after rEVAR. The multivariate logistic model included all variables that exhibited significant differences at the level of $P < 0.05$ in the univariate analysis. Kaplan–Meier analysis was performed to estimate the long-term survival, and the difference between the EVAR-selected and EVAR-only periods was analysed using the log-rank test. Statistical analysis was performed using the SPSS 23 software (IBM Corp., Armonk, NY, United States).

Results

Demographic and aneurysmal characteristics

A total of 132 patients with RAAAs treated at our institution between January 2009 and October 2020 were identified (**Figure 2**). Among them, 13 patients refused aneurysm repair and received palliative care, and 26 patients who agreed to surgery died in the emergency room or during transfer into the operating room. After excluding these 39 patients, a total of 93 patients undergoing emergent RAAA repair were eventually included in the current study. Hence, the overall operation rate in RAAAs at our centre was 70.5% (93/132). In the EVAR-only period, all 53 patients underwent rEVAR. However, only 47.5% (19/40) of patients in the EVAR-selected period underwent rEVAR, and the remaining 21 patients underwent emergent open surgery.

Demographic and aneurysmal characteristics were similar between patients in the EVAR-selected and EVAR-only periods. Hostile proximal necks (**Figure 3**) were found in approximately

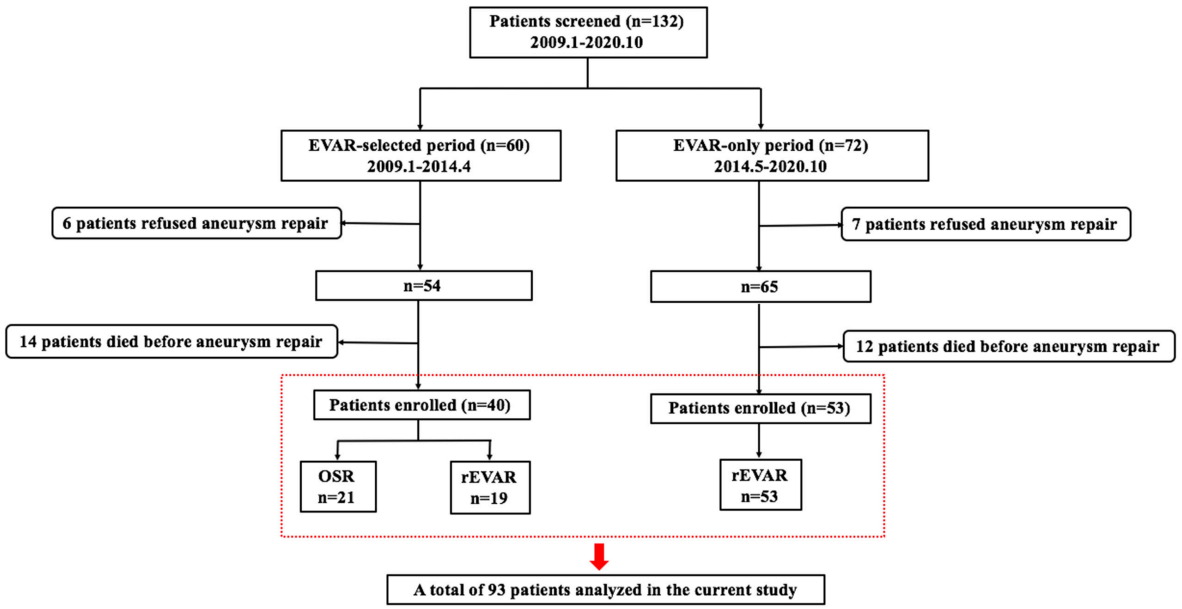

FIGURE 2
Flowchart of defined groups of patients with ruptured abdominal aortic aneurysms. OSR, open surgical repair; rEVAR, ruptured endovascular aneurysm repair.

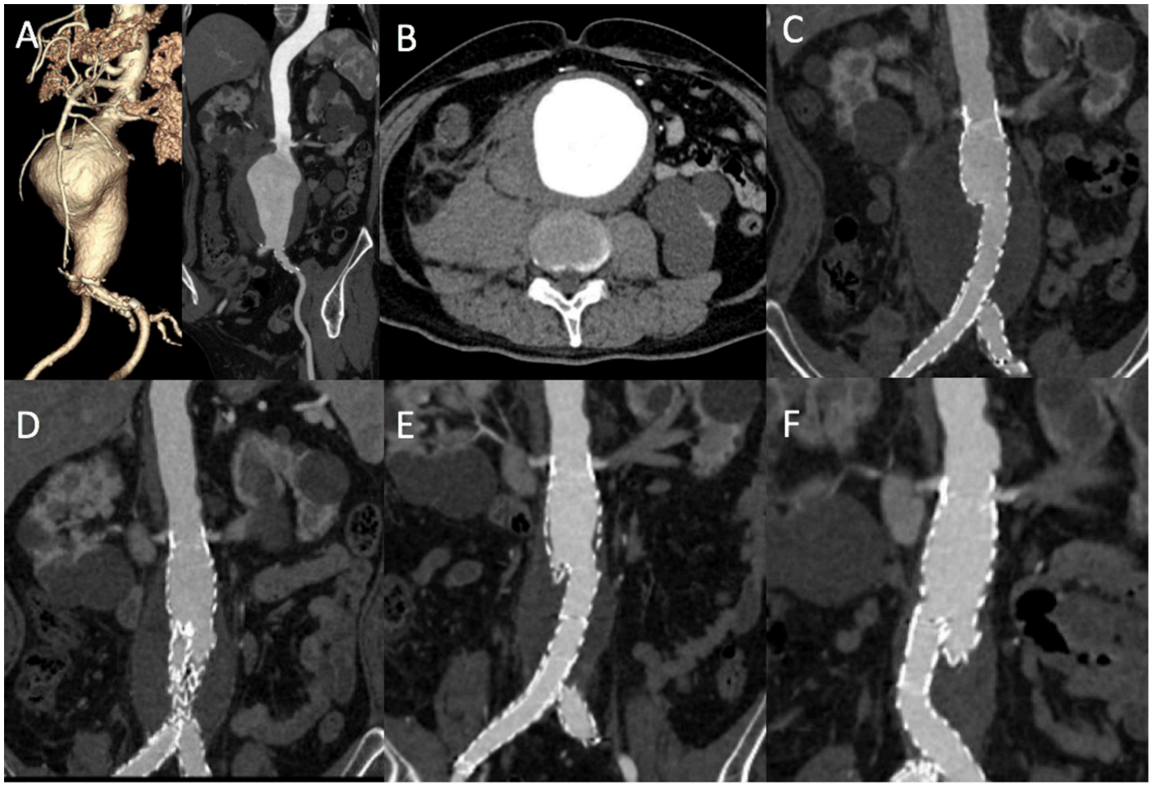

FIGURE 3
A rEVAR in a patient with a hostile proximal aneurysm neck. **(A,B)** Computed tomography angiography (CTA) showed a ruptured abdominal aneurysm with a short and angulated proximal neck. CTA demonstrated that the size of the aneurysm body with complete thrombosis gradually decreased after rEVAR at 3 months **(C)**, 1 year **(D)**, 2 years **(E)**, and 5 years **(F)**. rEVAR, ruptured endovascular aneurysm repair.

50% of the included patients, which were mostly attributed to neck angulation. The specific information pertaining to this section is displayed in Table 1.

Emergent repair

Technical success of the aneurysm repair was achieved in all patients in the EVAR-selected period. Technical failure occurred in four patients (4/53, 7.5%) in the EVAR-only period due to persistent type Ia endoleaks at completion angiogram. Open surgery conversion was not performed in these four patients considering their state of haemorrhagic shock. Patients in the EVAR-only period had significantly less operative time and lower blood transfusion needs (Table 2). When we compared the rEVAR techniques between the two periods (Table 3), a significantly higher incidence of use of local anaesthesia and percutaneous puncture of the femoral artery was observed in the EVAR-only period. Meanwhile, bifurcated endografts were more commonly used in the EVAR-only period compared to the EVAR-selected period, with a statistically significant difference ($P < 0.01$).

Early mortality

Thirty-day mortality in the EVAR-only period was 22.6% (12/53) compared with 25.0% (10/40) in the EVAR-selected period ($P = 0.79$). There was also no significant difference ($P = 0.93$) in in-hospital mortality between the EVAR-only (15/53, 28.3%) and EVAR-selected (11/40, 27.5%) periods (Table 2).

Univariate logistic regression analysis showed loss of consciousness (Glasgow Coma Scale score ≤8) at admission,

TABLE 1 Clinical and aneurysmal characteristics.

	EVAR-selected				EVAR-only ($n = 53$)	$P^{\dagger}$
	OSR ($n = 21$)	rEVAR ($n = 19$)	P^{*}	Total ($n = 40$)		
Gender						
Male	16 (76.2)	18 (94.7)	0.23	34 (85.0)	46 (86.8)	0.81
Female	5 (23.8)	1 (5.3)		6 (15.0)	7 (13.2)	
Age (years)	64.5 ± 12.0	71.9 ± 9.6	0.04	68.1 ± 11.4	70.4 ± 10.9	0.32
Comorbidities						
Hypertension	21 (100.0)	18 (94.7)	0.23	39 (97.5)	51 (96.2)	1.00
Hyperlipidaemia	13 (62.0)	8 (42.1)	0.10	21 (52.5)	32 (60.4)	0.45
DM	8 (38.1)	5 (26.3)	0.43	13 (32.5)	24 (45.3)	0.21
COPD	0 (0.0)	3 (15.8)	0.10	3 (7.5)	5 (9.4)	1.00
Haemodialysis	1 (4.8)	3 (15.8)	0.53	4 (10.0)	2 (3.8)	0.43
Coronary artery disease	3 (14.3)	2 (10.5)	1.00	5 (12.5)	8 (15.1)	0.72
History of stroke	2 (9.5)	2 (10.5)	1.00	4 (10.0)	5 (9.4)	1.00
Preoperative data						
Hospital transfer	14 (66.7)	14 (73.7)	0.63	28 (70.0)	34 (64.2)	0.55
Time to hospital (hours)	26.1 ± 34.1	27.2 ± 40.4	0.93	26.6 ± 36.7	19.7 ± 21.4	0.26
Time from admission to operation (hours)	1.5 ± 1.1	1.7 ± 1.0	0.91	1.6 ± 1.1	1.3 ± 0.9	0.79
Conscious loss	0 (0.0)	0 (0.0)	1.00	0 (0.0)	8 (15.1)	<0.01
SBP ≤70 mmHg	2 (9.5)	1 (5.3)	1.00	3 (7.5)	10 (18.9)	0.21
Hb ≤90 g/L	5 (23.8)	12 (63.2)	0.01	17 (42.5)	29 (54.7)	0.24
Creatinine >106 mmol/L	13 (61.9)	11 (57.9)	0.80	24 (60.0)	32 (60.4)	0.97
DIC	0 (0.0)	3 (15.8)	0.10	3 (7.5)	1 (1.9)	0.42
Diameter of aneurysms (cm)	7.4 ± 1.8	7.3 ± 2.1	0.81	7.36 ± 1.9	6.9 ± 1.9	0.27
Hostile proximal neck	12 (57.1)	8 (42.1)	0.34	20 (50.0)	27 (50.9)	0.93
Short	6 (28.6)	3 (15.8)	0.56	9 (22.5)	5 (9.4)	0.08
Angulated	9 (42.9)	6 (31.6)	0.46	15 (37.5)	22 (41.5)	0.70
Wide	0 (0.0)	0 (0.0)	1.00	0 (0.0)	1 (1.9)	1.00

Data are presented as n (%) or mean ± SD.

rEVAR, ruptured endovascular aneurysm repair; OSR, open surgical repair; DM, diabetes mellitus; COPD, chronic obstructive pulmonary disease; SBP, systolic blood pressure; Hb, haemoglobin; DIC, disseminated intravascular coagulation.

Chi-square or Fisher's exact test for categorical variables, and Student's t-test for continuous variables were used. $P < 0.05$ is considered statistically significant.

P^{*} for OSR versus rEVAR in the EVAR-selected period.

$P^{\dagger}$ for EVAR-selected versus EVAR-only.

TABLE 2 Operation outcomes and perioperative complications.

	EVAR-selected				EVAR-only (n = 53)	$P^{\dagger}$
	OSR (n = 21)	rEVAR (n = 19)	P^{*}	Total (n = 40)		
Technical success	21 (100.0)	19 (100.0)	1.00	40 (100.0)	49 (92.5%)	0.50
Operative time	4.9 ± 1.2	2.8 ± 1.0	< 0.01	3.9 ± 1.5	2.0 ± 0.8	< 0.01
Blood transfusion	1,976.2 ± 1521.8	736.8 ± 1,000.1	< 0.01	1,387.5 ± 1,429.0	754.7 ± 1,126.9	0.02
Perioperative complications						
ACS	0 (0.0)	7 (36.8)	< 0.01	7 (17.5)	18 (34.0)	0.08
Acute kidney injury	4 (19.0)	3 (15.8)	1.00	7 (17.5)	15 (28.3)	0.23
Myocardial infarction	1 (4.8)	0 (0.0)	1.00	1 (2.5)	1 (1.9)	1.00
Stroke	0 (0.0)	0 (0.0)	1.00	0 (0.0)	2 (3.8)	0.50
Respiratory failure	2 (9.5)	4 (21.1)	0.56	6 (15.0)	6 (11.3)	0.60
Acute lower limb ischaemia	2 (9.5)	0 (0.0)	0.49	2 (5.0)	0 (0.0)	0.18
Wound infection	3 (14.3)	0 (0.0)	0.23	3 (7.5)	0 (0.0)	0.08
Transient paraplegia	1 (4.8)	0 (0.0)	1.00	1 (2.5)	0 (0.0)	0.43
Gastrointestinal haemorrhage	2 (9.5)	1 (5.3)	1.00	3 (7.5)	2 (3.8)	0.65
Length of sICU stay	12.9 ± 20.5	4.3 ± 4.7	0.07	8.8 ± 15.7	7.3 ± 11.7	0.61
Length of hospital stay	22.1 ± 22.2	12.6 ± 9.3	0.09	17.6 ± 17.7	12.2 ± 15.5	0.13
In-hospital mortality	6 (28.6)	5 (26.3)	0.87	11 (27.5)	15 (28.3)	0.93
30-day mortality	5 (23.8)	5 (26.3)	0.86	10 (25.0)	12 (22.6)	0.79

Data are presented as n (%) or mean ± SD.
rEVAR, ruptured endovascular aneurysm repair; OSR, open surgical repair; ACS, abdominal compartment syndrome; sICU, surgical intensive care unit.
Chi-square or Fisher's exact test for categorical variables, and Student's t-test for continuous variables were used. $P < 0.05$ is considered statistically significant.
P^{*} for OSR versus rEVAR in the EVAR-selected period.
$P^{\dagger}$ for EVAR-selected versus EVAR-only.

SBP ≤90 mmHg, serum creatinine >186 mmol/L, Hb ≤60 g/L, and ACS were risk factors related to 30-day mortality (Table 4). Notably, the EVAR or the EVAR-only strategy was not identified as a risk factor of 30-day mortality after univariate analysis. Multivariate logistic regression analysis revealed that unstable haemodynamics [adjusted odds ratio (OR) 4.99, 95% confidence interval (CI), 1.13–22.08, P = 0.03] and ACS (adjusted OR 3.72, 95% CI, 1.12–12.32, P = 0.03) were independent risk factors of 30-day mortality in the current cohort of patients.

TABLE 3 Characteristics of rEVAR.

	EVAR-selected (n = 19)	EVAR-only (n = 53)	P
Anaesthesia			
Local	0 (0.0)	21 (39.6)	< 0.01
General	19 (100.0)	32 (60.4)	
Access type			
Percutaneous	3 (15.8)	46 (86.8)	< 0.01
Cut-down	16 (84.2)	7 (13.2)	
Suprarenal balloon occlusion	2 (10.5)	13 (24.5)	0.34
Stent-graft configuration			
Bifurcated	10 (52.6)	46 (86.8)	< 0.01
Tube	3 (15.8)	5 (9.4)	
Aorto-uni-iliac	6 (31.6)	2 (3.8)	
Renal artery coverage	0 (0.0)	2 (3.8)	1

Data are presented as n (%).
EVAR, endovascular aneurysm repair.
Chi-square or Fisher's exact test for categorical variables was used. $P < 0.05$ is considered statistically significant.

Perioperative complications

The specific data pertaining to complications are displayed in Table 2. In general, there was no significant difference in the rates of recorded postoperative complications between the two periods. ACS was the most common postoperative complication (25/93, 26.9%), and all instances of ACS occurred in the rEVAR group. Advanced age (>75 years), Hb level <90 g/L upon admission, massive blood transfusion (>1,500 ml), and intraoperative balloon occlusion were significantly associated with postoperative ACS. When adjusted for covariates, age >75 years (adjusted OR 4.13, 95% CI, 1.23–13.91, P = 0.02) and Hb <90 g/L (adjusted OR 6.49, 95% CI, 1.65–25.51, $P < 0.01$) were identified as independent risk predictors of ACS (Table 5).

Additionally, despite the fact that no significant difference was observed in the length of the sICU and hospital stay between the two periods, the mean length of hospital stay was about five days shorter in the EVAR-only period.

TABLE 4 Logistic regression of the 30-day mortality.

Characteristics	Unadjusted OR	95% CI	*P*	Adjusted OR	95% CI	*P*
Female	1.43	0.40–5.16	0.59			
Age (years)						
≤70	Reference					
70–80	1.68	0.57–5.00	0.35			
>80	3.14	0.84–11.72	0.09			
Coronary artery disease	2.15	0.63–7.40	0.22			
Haemodialysis	0.59	0.07–5.34	0.64			
COPD	1.02	0.19–5.42	0.99			
Stroke	2.74	0.67–11.22	0.16			
Conscious loss	6.20	1.35–28.45	0.02	2.94	0.42–20.71	0.28
SBP (mmHg)						
>90	Reference			Reference		
70–90	5.04	1.58–16.10	< 0.01	2.72	0.70–10.47	0.15
≤70	8.50	2.21–32.67	< 0.01	4.99	1.13–22.08	0.03
Creatinine (mmol/L)						
≤106	Reference			Reference		
106–186	4.00	1.10–14.49	0.04	1.53	0.31–7.61	0.60
>186	4.00	1.08–14.85	0.04	3.30	0.74–14.84	0.12
Hb (g/L)						
>90	Reference			Reference		
60–90	2.12	0.72–6.25	0.18	1.03	0.28–3.86	0.96
≤60	11.43	2.30–56.70	< 0.01	2.74	0.40–18.99	0.31
Aneurysm diameter (cm)						
≤6.5	Reference					
6.5–8.5	2.53	0.83–7.67	0.10			
>8.5	1.04	0.26–4.19	0.96			
Hostile proximal neck	1.74	0.67–4.56	0.26			
General anaesthesia	0.94	0.30–2.92	0.91			
ACS	6.28	2.24–17.64	< 0.01	3.72	1.12–12.32	0.03
EVAR	1.07	0.34–3.33	0.91			
EVAR-only strategy	0.33	0.38–2.52	0.96			

OR, odds ratio; CI, confidence interval; COPD, chronic obstructive pulmonary disease; SBP, systolic blood pressure; Hb, haemoglobin; DIC, disseminated intravascular coagulation; ACS, abdominal compartment syndrome; EVAR, endovascular aneurysm repair.
$P < 0.05$ is considered statistically significant.

Long-term survival

There were 29 and 38 patients surviving to discharge in the EVAR-selected and EVAR-only periods, respectively. The median follow-up time was 61 months (range, 7–121 months) in the EVAR-selected period and 39 months (range, 2–77 months) in the EVAR-only period. The Kaplan–Meier analysis showed no significant difference in mid-term survival between the two periods (log-rank $P = 0.88$, Figure 4). The estimated 3-year survival rates were 60% (95% CI, 44.9–75.1%) in the EVAR-selected group compared with 64.5% (95% CI, 51.2–77.8%)in the EVAR-only group ($P = 0.55$). After 5 years, 47.5% (95% CI, 32.0–63.0%) of patients in the EVAR-selected period were still alive versus 49.1% (95% CI, 32.3–65.9%) of patients in the EVAR-only period ($P = 0.29$).

Discussion

Although no early mortality benefits over OSR (Figure 5) have been demonstrated in RCTs, rEVAR has been increasingly used for the treatment of RAAAs in recent years due to its minimally invasive nature and requirement of a shorter hospital stay. In most institutions, RAAA patients with specific characteristics such as stable haemodynamics and anatomically feasible aneurysm necks have been selected for rEVAR. Hence, the strategy for the management of RAAAs has gradually evolved from the OSR-only to EVAR-selected strategies after the introduction of rEVAR. Implementation of a well-designed EVAR-selected strategy incorporating rEVAR with OSR has been reported to significantly improve perioperative morbidity and mortality. It was reported that the 30-day mortality ranged

TABLE 5 Logistic regression of ACS in the rEVAR group.

Characteristics	Unadjusted OR	95% CI	*P*	Adjusted OR	95% CI	*P*
Female	2.05	0.47–9.00	0.34			
Age >75 years	6.20	2.14–17.99	< 0.01	4.13	1.23–13.91	0.02
Conscious loss	3.67	0.80–16.86	0.10			
SBP ≤70 mmHg	2.65	0.72–9.78	0.14			
Creatinine >186 mmol/L	2.29	0.82–6.40	0.11			
Hb <90 g/L	7.09	2.10–23.90	< 0.01	6.49	1.65–25.51	<0.01
Aneurysm diameter >6.5 cm	2.56	0.87–7.56	0.09			
Hostile neck	2.62	0.96–7.14	0.06			
General anaesthesia	2.18	0.77–6.23	0.14			
AUI	0.59	0.11–3.19	0.54			
Access type	0.10	0.35–2.82	0.99			
Blood transfusion >1,500 ml	4.73	1.37–16.53	0.01	2.66	0.61–11.72	0.20
Balloon occlusion	5.60	1.65–19.06	< 0.01	2.61	0.62–11.06	0.19
EVAR-only strategy	0.88	0.30–2.63	0.82			

ACS, abdominal compartment syndrome; rEVAR, ruptured endovascular aneurysm repair; OR, odds ratio; CI, confidence interval; SBP, systolic blood pressure; Hb, haemoglobin; AUI, aorto-uni-iliac.
$P < 0.05$ is considered statistically significant.

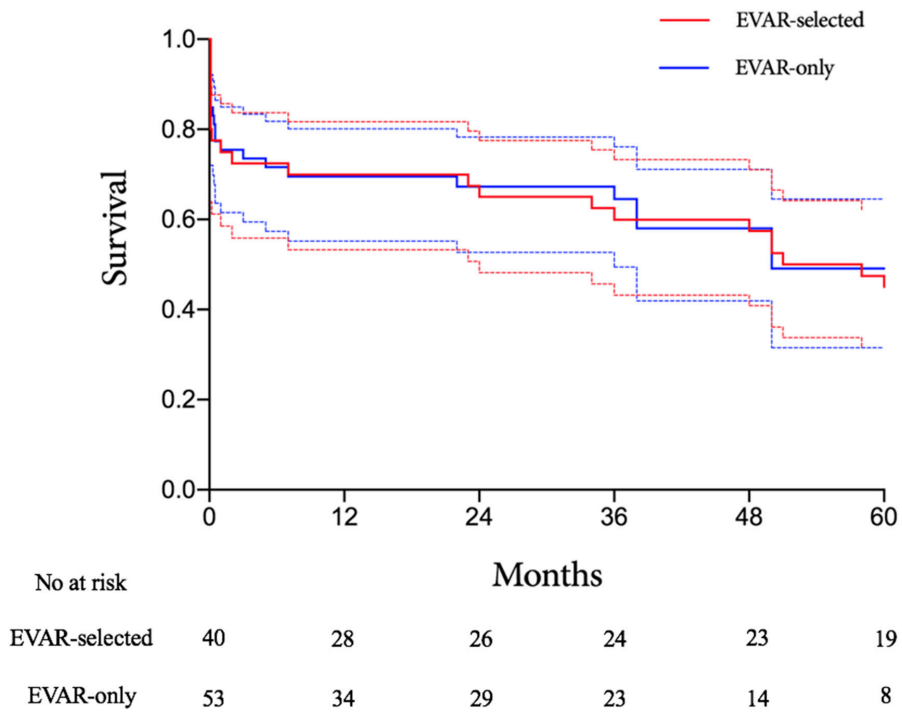

FIGURE 4
Kaplan–Meier analysis of long-term survival rates for the EVAR-selected versus EVAR-only groups. EVAR, endovascular aneurysm repair.

from 14.3 to 35.3% after implementation of a structured EVAR-selected strategy for the management of RAAAs (11–14). In the current study, the 30-day mortality in the EVAR-selected period was 25%, which was consistent with previous studies.

An EVAR-only strategy for RAAAs was first reported by Mayer et al. (12). Non-selected RAAAs were treated with rEVAR for over a period of 32 months at two centres, and favourable outcomes were achieved. The 30-day mortality in the EVAR-only period was comparable with that in the EVAR/OPEN period (24.3 versus 25.5%, $P = 0.83$), which, to some extent, implied that the superior efficacy of rEVAR for RAAAs in historical reports might be attributed to this new technique

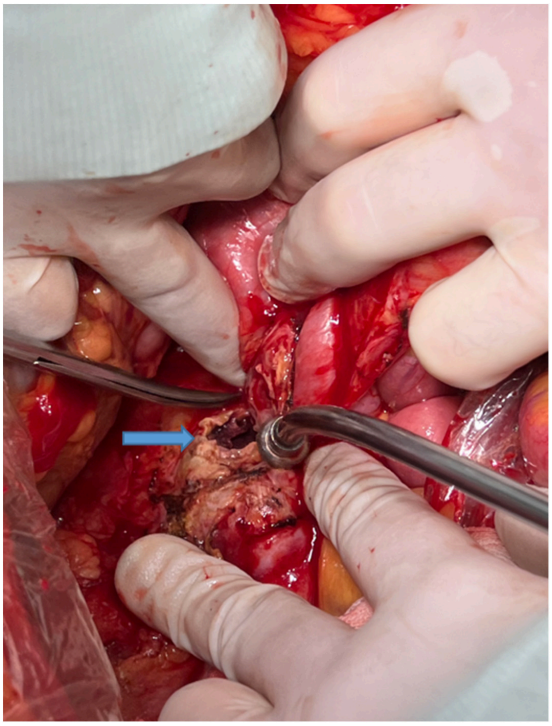

FIGURE 5
The rupture site (blue arrow) of the arterial wall in a ruptured abdominal aortic aneurysm.

rather than to patient selection. However, the implementation of this radical EVAR-only approach for RAAAs has not been reported at other centres. In the current study, the 30-day mortality in the EVAR-only period was lower than that in the EVAR-selected period, although the difference was not statistically significant. Additionally, similar long-term survival rates were observed between the two periods, which was not reported in the previous study by Meyer et al. (12).

It was estimated that more than half of the RAAAs were not candidates for EVAR with current endograft devices, due to unfavourable anatomy (15). An increasing number of RAAAs without IFU for endografts are being treated with rEVAR at other experienced vascular centres, as at our centre. Perrott et al. reported a reduction in 30-day mortality for EVAR-suitable patients following OSR compared with EVAR-unsuitable patients, although the difference was not statistically different (6.9 versus 30.4%, P = 0.07) (16). However, it was also reported that the 30-day mortality in patients with a friendly anatomy after OSR was comparable with those with a hostile anatomy (30 versus 38%, P = 0.23) (17). As for patients treated with rEVAR, Broos et al. observed similar 30-day mortality between the favourable and hostile neck groups (14 versus 12%, P = 1.00) (18). However, Baderkhan et al. did not find a significant difference in 30-day mortality between patients inside (15%) and outside (30%) the IFU (P = 0.09), and the 3-year mortality was observed to be significantly lower in EVAR-suitable patients (33.8 versus 56.0%, P = 0.02); an aneurysm neck diameter >29 mm was found to be an independent risk factor of overall mortality. In the IMPROVE trial (19), no association was found between five morphological parameters (maximum aortic diameter, aneurysm neck diameter, conicality, proximal neck angle, and maximum common iliac diameter) and mortality. Only a shorter proximal neck length was identified as an independent risk factor for overall 30-day mortality. In addition, for RAAAs treated with rEVAR, the 30-day mortality was found to be higher if the neck length decreased by less than 10 mm. The threshold was 15 mm for RAAAs treated with OSR. Based on the IMPROVE data, it seemed that a shorter neck length had an adverse impact on postoperative survival, regardless of the operative modality. In the current study, a hostile proximal neck was not identified as a risk factor of 30-day mortality. However, it was noted that all instances of technical failure occurred in patients with a hostile proximal neck, which suggested that hostile anatomy might negatively affect the technical success rates of rEVAR. Findings from our analysis demonstrated that unstable haemodynamics and postoperative ACS, but not the implementation of rEVAR or the EVAR-only strategy, were associated with significantly increased 30-day mortality. Meanwhile, the independent risk factors of ACS following rEVAR were advanced age (>75 years) and moderate or severe anaemia (Hb <90 g/L). We believe that with reference to the prognosis of RAAAs following operation, the effects of particular preoperative clinical characteristics have far outweighed those of the type of operative modality. The performance of rEVAR should not be restricted by the emergent state of patients at major centres that have abundant elective endovascular experience.

Abdominal compartment syndrome was a common complication in patients with RAAAs. rEVAR was associated with a higher incidence of postoperative ACS compared with OSR due to the untreated retroperitoneal haematoma. A meta-analysis of ACS after rEVAR by Karkos et al. estimated that the ACS rate might be higher than 20% with improved awareness and vigilant monitoring (20). In the current study, ACS was observed by routine monitoring of intraluminal bladder pressure in about 35% of patients treated with rEVAR, which was consistent with the study by Karkos et al. (20). The optimal management strategy for ACS remains debatable. Although decompression laparotomy has been recommended by some investigators for patients with sustained high bladder pressure (12, 21), this recommendation and treatment decision should be carefully evaluated considering that decompressive bleeding might be more uncontrollable in RAAA patients, and may lead to high mortality.

The current study has several limitations, including its retrospective design which could have biassed patient selection.

Second, despite the relatively large sample size of the present study, it remains too limited to generate more convincing statistical results. Third, our study extended over 11 years. There may have been learning curves for using some techniques during this period, as reflected by the fact that a significantly higher proportion of rEVAR cases in the later period were performed using local anaesthesia, percutaneous access, and bifurcated endografts. Additionally, endograft evolution during the past decade might have had a sizeable influence on the favourable outcomes in the EVAR-only period (22). However, it is difficult to further analyse the influence of these factors in this retrospective study.

Conclusion

The EVAR-only strategy has allowed rEVAR to be used in nearly all the RAAAs with similar mortality comparing with the EVAR-selected strategy. Due to the avoidance of operative modality selection, the EVAR-only strategy was associated with a more simplified algorithm, less influence on haemodynamics, and a shorter operation and recovery time. Prospective validation of the EVAR-only strategy is required at more experienced vascular centres.

Data availability statement

The original contributions presented in the study are included in the article/supplementary material, further inquiries can be directed to the corresponding authors.

Ethics statement

This study design was approved by the Ethics Committee for the Protection of Human Subjects at Zhongshan Hospital, Fudan University, Shanghai, China. All included patients were informed about the nature of the study and gave their written informed consent.

Author contributions

GF, JY, TS, TY, BR, YF, TP, and ZL collected the data. GF and JY wrote the manuscript. GF, JY, ZD, and WF critically reviewed the manuscript and contributed significantly to discussion. All authors contributed to the article and approved the submitted version.

Funding

This study was supported by the National Natural Science Foundation of China (Grant Nos. 81970395 and 81970407), Shanghai Sailing Program (Grant No. 22YF1406700), and the Program of Shanghai Academic Research Leader (Grant No. 19XD1401200).

Acknowledgments

We wish to thank all medical staff participating in the management of ruptured abdominal aortic aneurysms at Zhongshan Hospital, Fudan University.

Conflict of interest

The authors declare that the research was conducted in the absence of any commercial or financial relationships that could be construed as a potential conflict of interest.

Publisher's note

All claims expressed in this article are solely those of the authors and do not necessarily represent those of their affiliated organizations, or those of the publisher, the editors and the reviewers. Any product that may be evaluated in this article, or claim that may be made by its manufacturer, is not guaranteed or endorsed by the publisher.

References

1. Bown MJ, Sutton AJ, Bell PR, Sayers RDA. Meta-analysis of 50 years of ruptured abdominal aortic aneurysm repair. *Br J Surg.* (2002) 89:714–30. doi: 10.1046/j.1365-2168.2002.02122.x

2. Hinchliffe RJ, Bruijstens L, MacSweeney ST, Braithwaite BDA. Randomised trial of endovascular and open surgery for ruptured abdominal aortic aneurysm - results of a pilot study and lessons learned for future studies. *Eur J Vasc Endovasc.* (2006) 32:506–13. doi: 10.1016/j.ejvs.2006.05.016

3. Reimerink JJ, Hoornweg LL, Vahl AC, Wisselink W, van den Broek TA, Legemate DA, et al. Endovascular repair versus open repair of ruptured abdominal aortic aneurysms: a multicenter randomized controlled trial. *Ann Surg.* (2013) 258:248–56. doi: 10.1097/SLA.0b013e31828d4b76

4. Powell JT, Sweeting MJ, Thompson MM, Ashleigh R, Bell R, Gomes M, et al. Endovascular or open repair strategy for ruptured abdominal aortic aneurysm: 30 day outcomes from improve randomised trial. *BMJ.* (2014) 348:f7661. doi: 10.1136/bmj.f7661

5. Li Y, Li Z, Wang S, Chang G, Wu R, Hu Z, et al. Endovascular versus open surgery repair of ruptured abdominal aortic aneurysms in hemodynamically

unstable patients: literature review and meta-analysis. *Ann Vasc Surg.* (2016) 32:135–44. doi: 10.1016/j.avsg.2015.09.025

6. Wanhainen A, Verzini F, Van Herzeele I, Allaire E, Bown M, Cohnert T, et al. Editor's Choice - European society for vascular surgery (ESVS) 2019 clinical practice guidelines on the management of abdominal aorto-iliac artery aneurysms. *Eur J Vasc Endovasc Surg.* (2019) 57:8–93. doi: 10.1016/j.ejvs.2018.09.020

7. Chaikof EL, Dalman RL, Eskandari MK, Jackson BM, Lee WA, Mansour MA, et al. The society for vascular surgery practice guidelines on the care of patients with an abdominal aortic aneurysm. *J Vasc Surg.* (2018) 67:2–77.e2. doi: 10.1016/j.jvs.2017.10.044

8. Slater BJ, Harris EJ, Lee JT. Anatomic suitability of ruptured abdominal aortic aneurysms for endovascular repair. *Ann Vasc Surg.* (2008) 22:716–22. doi: 10.1016/j.avsg.2008.06.001

9. Desgranges P, Kobeiter H, Katsahian S, Bouffi M, Gouny P, Favre JP, et al. Editor's choice - ECAR (Endovasculaire ou chirurgie dans les anévrysmes aorto-iliaques rompus): a french randomized controlled trial of endovascular versus open surgical repair of ruptured aorto-iliac aneurysms. *Eur J Vasc Endovasc Surg.* (2015) 50:303–10. doi: 10.1016/j.ejvs.2015.03.028

10. Yue JN, Luo Z, Guo DQ, Xu X, Chen B, Jiang JH, et al. Evaluation of acute kidney injury as defined by the risk, injury, failure, loss, and end-stage criteria in critically ill patients undergoing abdominal aortic aneurysm repair. *Chin Med J.* (2013) 126:431–6.

11. Ullery BW, Tran K, Chandra V, Mell MW, Harris EJ, Dalman RL, et al. Association of an endovascular-first protocol for ruptured abdominal aortic aneurysms with survival and discharge disposition. *JAMA Surg.* (2015) 150:1058–65. doi: 10.1001/jamasurg.2015.1861

12. Mayer D, Aeschbacher S, Pfammatter T, Veith FJ, Norgren L, Magnuson A, et al. Complete replacement of open repair for ruptured abdominal aortic aneurysms by endovascular aneurysm repair: a two-center 14-year experience. *Ann Surg.* (2012) 256:688–95. doi: 10.1097/SLA.0b013e318271cebd

13. Starnes BW, Quiroga E, Hutter C, Tran NT, Hatsukami T, Meissner M, et al. Management of ruptured abdominal aortic aneurysm in the endovascular era. *J Vasc Surg.* (2010) 51:9–17. doi: 10.1016/j.jvs.2009.08.038

14. Moore R, Nutley M, Cina CS, Motamedi M, Faris P, Abuznadah W. Improved survival after introduction of an emergency endovascular therapy protocol for ruptured abdominal aortic aneurysms. *J Vasc Surg.* (2007) 45:443–50. doi: 10.1016/j.jvs.2006.11.047

15. Wilson WR, Fishwick G, Sir Peter RFB, Thompson MM. Suitability of ruptured AAA for endovascular repair. *J Endovasc Ther.* (2004) 11:635–40. doi: 10.1583/04-1275r.1

16. Perrott S, Puckridge PJ, Foreman RK, Russell DA, Spark JI. Anatomical suitability for endovascular aaa repair may affect outcomes following rupture. *Eur J Vasc Endovasc Surg.* (2010) 40:186–90. doi: 10.1016/j.ejvs.2010.04.002

17. van Beek SC, Reimerink JJ, Vahl AC, Wisselink W, Reekers JA, Legemate DA, et al. Outcomes after open repair for ruptured abdominal aortic aneurysms in patients with friendly versus hostile aortoiliac anatomy. *Eur J Vasc Endovasc Surg.* (2014) 47:380–7. doi: 10.1016/j.ejvs.2014.01.003

18. Broos PP, 't Mannetje YW, Cuypers PW, van Sambeek MR, Teijink JA. Endovascular treatment of ruptured abdominal aortic aneurysms with hostile aortic neck anatomy. *Eur J Vasc Endovasc Surg.* (2015) 50:313–9. doi: 10.1016/j.ejvs.2015.04.017

19. IMPROVE Trial Investigators. The effect of aortic morphology on peri-operative mortality of ruptured abdominal aortic aneurysm. *Eur Heart J.* (2015) 36:1328–34. doi: 10.1093/eurheartj/ehu521

20. Karkos CD, Menexes GC, Patelis N, Kalogirou TE, Giagtzidis IT, Harkin DWA. Systematic review and meta-analysis of abdominal compartment syndrome after endovascular repair of ruptured abdominal aortic aneurysms. *J Vasc Surg.* (2014) 59:829–42. doi: 10.1016/j.jvs.2013.11.085

21. Miranda E, Manzur M, Han S, Ham SW, Weaver FA, Rowe VL. Postoperative development of abdominal compartment syndrome among patients undergoing endovascular aortic repair for ruptured abdominal aortic aneurysms. *Ann Vasc Surg.* (2018) 49:289–94. doi: 10.1016/j.avsg.2018.02.002

22. Kansal V, Nagpal S, Jetty P. The effect of endograft device on patient outcomes in endovascular repair of ruptured abdominal aortic aneurysms. *Vascular.* (2017) 25:657–65. doi: 10.1177/1708538117711348

frontiers | Frontiers in Cardiovascular Medicine

TYPE Original Research
PUBLISHED 08 September 2022
DOI 10.3389/fcvm.2022.941185

Check for updates

OPEN ACCESS

EDITED BY
Morgan Salmon,
University of Michigan, United States

REVIEWED BY
Chunguang Guo,
First Affiliated Hospital of Zhengzhou University, China
Laura DiChiacchio,
The University of Utah, United States

*CORRESPONDENCE
Longtan Jiang
659878984@qq.com
Fanyan Luo
drlfy@csu.edu.cn

SPECIALTY SECTION
This article was submitted to General Cardiovascular Medicine, a section of the journal Frontiers in Cardiovascular Medicine

RECEIVED 11 May 2022
ACCEPTED 17 August 2022
PUBLISHED 08 September 2022

CITATION
Chen Y, Ouyang T, Fang C, Tang C-e, Lei K, Jiang L and Luo F (2022) Identification of biomarkers and analysis of infiltrated immune cells in stable and ruptured abdominal aortic aneurysms.
Front. Cardiovasc. Med. 9:941185.
doi: 10.3389/fcvm.2022.941185

COPYRIGHT
© 2022 Chen, Ouyang, Fang, Tang, Lei, Jiang and Luo. This is an open-access article distributed under the terms of the Creative Commons Attribution License (CC BY). The use, distribution or reproduction in other forums is permitted, provided the original author(s) and the copyright owner(s) are credited and that the original publication in this journal is cited, in accordance with accepted academic practice. No use, distribution or reproduction is permitted which does not comply with these terms.

Identification of biomarkers and analysis of infiltrated immune cells in stable and ruptured abdominal aortic aneurysms

Yubin Chen[1], Tianyu Ouyang[1], Cheng Fang[1], Can-e Tang[2,3], Kaibo Lei[1,4], Longtan Jiang[1]* and Fanyan Luo[1,4]*

[1]Department of Cardiac Surgery, Xiangya Hospital, Central South University, Changsha, China, [2]Department of Endocrinology, Xiangya Hospital, Central South University, Changsha, China, [3]The Institute of Medical Science Research, Xiangya Hospital, Central South University, Changsha, China, [4]National Clinical Research Center for Geriatric Disorders, Xiangya Hospital, Central South University, Changsha, China

Objectives: The mortality rate of abdominal aortic aneurysm (AAA) is extremely high in the older population. This study aimed to identify potential biomarkers of AAA and aortic rupture and analyze infiltration of immune cells in stable and ruptured AAA samples.

Methods: Raw data of GSE47472, GSE57691, and GSE98278 were downloaded. After data processing, the co-expression gene networks were constructed. Gene Ontology and pathway enrichment analysis of AAA- and aortic rupture-related gene modules were conducted using the Database for Annotation, Visualization, and Integrated Discovery. Gene set enrichment analysis (GSEA) and gene set variation analysis (GSVA) were used for further enrichment analysis. The CIBERSORT tool was used to analyze the relative abundance of immune cells in samples. Differentially expressed immune-related genes were analyzed between different samples. Predictive models were constructed *via* extreme gradient boosting, and hub genes were identified according to feature importance.

Results: Blue and yellow modules were significantly related to AAA, and genes in these modules were associated with the aortic wall and immune response, respectively. In terms of aortic rupture, the most relevant module was significantly enriched in the inflammatory response. The results of GSEA and GSVA suggested that immune cells and the inflammatory response were involved in the development of AAA and aortic rupture. There were significant differences in the infiltration of immune cells and expression levels of immune-related genes among different samples. *NFKB1* might be an important transcription factor mediating the inflammatory response of AAA and aortic rupture. After the construction of a predictive model, *CD19*, *SELL*, and *CCR7* were selected as hub genes for AAA whereas *OAS3*, *IFIT1*, and *IFI44L* were identified as hub genes for aortic rupture.

Conclusion: Weakening of the aortic wall and the immune response both contributed to the development of AAA, and the inflammatory response was closely associated with aortic rupture. The infiltration of immune cells was significantly different between different samples. *NFKB1* might be an important transcription factor in AAA and aortic rupture. *CD19*, *SELL*, and *CCR7* had potential diagnostic value for AAA. *OAS3*, *IFIT1*, and *IFI44L* might be predictive factors for aortic rupture.

KEYWORDS

abdominal aortic aneurysm, biomarker, aortic rupture, immune cells, macrophage, inflammation

Introduction

Abdominal aortic aneurysm (AAA) is characterized by the weakening and dilatation of the abdominal aorta, which affects the infrarenal part most significantly (1). The diagnostic criterion of AAA is a maximum infrarenal abdominal aortic diameter of ≥ 30 mm (1), although there are other definitions of AAA in which its meaning is based on normalizing the aortic diameter to the body surface area (1, 2). Crucial risk factors for AAA include old age; male sex; smoking; a family history of AAA; the presence of other cardiovascular diseases (e.g., ischemic heart disease or peripheral artery disease), hypertension, and dyslipidemia (3, 4). According to recent ultrasonography-based screening studies, the prevalence of AAA in men > 65 years of age was 1–2% and that in women > 70 years of age was 0.5% (5–8). Aortic rupture is an important complication of AAA, which leads to 150,000–200,000 deaths each year worldwide, thus representing a severe threat to the older population (9, 10).

The predominant pathological changes in AAA are degeneration of the aortic media and apoptosis of vascular smooth muscle cells (VSMCs) (11). The extracellular matrix (ECM) is mainly synthesized and processed by VSMCs and plays an important role in the arterial function (12). Elastin and collagen are the main components of the ECM and can prevent the dilatation of the abdominal aorta and aortic rupture, respectively (13). Degradation of the ECM occurs largely due to an imbalance between amounts of active matrix metalloproteinases (MMPs) and their inhibitors (14). The inflammatory environment, reactive oxygen species (ROS), and endoplasmic reticulum stress can lead to the loss of VSMCs in AAA, which exacerbates the degradation of the ECM (15, 16). Infiltration of immune cells, including neutrophils, dendritic cells, macrophages, mast cells, B-cells, and T-cells, also contributes to the onset and development of AAA (17). However, the exact role of these immune cells in AAA remains unknown.

Ultrasonography and computerized tomography imaging are the most commonly used methods to diagnose AAA (1), but it is hard to diagnose AAA in the early stage because many patients with AAA are asymptomatic (18). In addition, the accuracy of predicting aortic rupture only based on the AAA diameter is low (19). Thus, further exploration of the mechanism of AAA formation and aortic rupture should be conducted to identify the potential biomarkers for AAA formation and aortic rupture, which may facilitate the early diagnosis of AAA and the prediction of aortic rupture. This study aimed to construct the AAA- and aortic rupture-related gene co-expression networks, analyze the infiltration of immune cells in AAA, identify differentially expressed inflammation-related genes (IRGs), and confirm the biomarkers involved in these processes using bioinformatics.

Materials and methods

Data acquisition and processing

The analysis process of this study is shown in **Figure 1**. The non-normalized data of GSE47472 (including eight normal abdominal aorta samples and 14 AAA samples), GSE57691 (including 10 normal abdominal aorta samples and 49 AAA samples), and GSE98278 (including 31 stable AAA samples and 17 ruptured AAA samples) were downloaded from the Gene Expression Omnibus (GEO) database[1]. All of these datasets were based on the same platform, GPL10558 (Illumina HumanHT-12 V4.0 expression BeadChip). The raw data of these datasets were normalized using the "Lumi" package in R software (version 4.1.2; R Foundation for Statistical Computing, Vienna, Austria) and the normalization process, including background correction, log2 transformation, and quantile normalization.

1 https://www.ncbi.nlm.nih.gov/gds

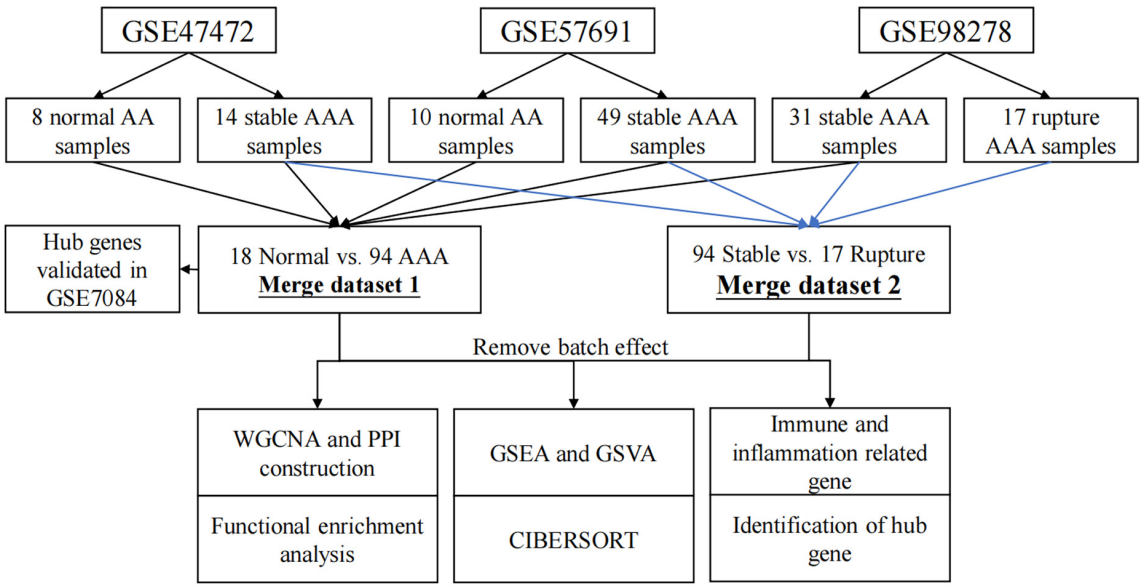

FIGURE 1
Flow chart diagram for analysis process in this study. WGCNA, weighted gene correlation network analysis; PPI, protein–protein interaction; GSEA, gene set enrichment analysis; GSVA, gene set variation analysis.

Then, the data were annotated using the "dplyr" and "limma" packages in R software (version 4.1.2). The batch effect between each dataset was removed using the "sva" package in R software (version 4.1.2) and the data were then merged for further analysis; briefly, 94 AAA samples and 18 normal abdominal aorta samples were extracted from these datasets as merged dataset 1 to explore the potential mechanisms underlying AAA formation, whereas 94 stable AAA samples and 17 AAA rupture samples were obtained from these datasets as merged dataset 2 to identify rupture-related gene modules.

Gene co-expression network construction by weighted gene correlation network analysis

Gene co-expression networks were constructed using the weighted gene correlation network analysis (WGCNA) package in R software (version 4.1.2) (20, 21). Soft-thresholding power was used to construct a weighted adjacency matrix. Relationships between a single gene and others in the analysis were incorporated, and the adjacency matrix was transformed into the topological matrix (TOM). Then, a hierarchical clustering analysis of genes was performed using 1 - TOM as the distance measure. Thereafter, modules were detected using a dynamic tree cut algorithm with a minimum module size of 50 and a minimum cut height of 0.99. The correlation between each module and the appearance of AAA or aortic rupture was calculated and shown in a heatmap. Finally, the most relevant gene modules were selected for further analysis.

Gene ontology and Kyoto encyclopedia of genes and genomes pathway enrichment analysis of genes in the relevant gene modules

In this research, the Database for Annotation, Visualization, and Integrated Discovery (DAVID, 2021 Update[2]) was used to conduct gene ontology (GO) and Kyoto encyclopedia of genes and genomes (KEGG) pathways enrichment analysis of genes in the relevant gene modules.

Construction of protein–protein interaction network and identification of candidate hub genes

Protein–protein interaction networks were constructed using the Search Tool for the Retrieval of Interacting Genes (STRING) online tool[3] and visualized using Cytoscape software (version 3.9.1; Institute for Systems Biology, Seattle, WA, United States). Then, cytoHubba, a plugin of Cytoscape

2 https://david.ncifcrf.gov/home.jsp
3 https://cn.string-db.org/

software was used to identify the top 10 genes *via* the MCC method, which were then regarded as candidate hub genes, and the corresponding protein–protein interaction (PPI) networks were constructed.

Gene set enrichment analysis and gene set variation analysis

The gene set files used in this study were downloaded from the Molecular Signatures Database version 7.5.1[4]. The enrichment scores of GO and KEGG pathways terms in each group were calculated using the gene set enrichment analysis (GSEA) software (version 4.2.3) (22), and terms enriched in the AAA or aortic rupture group were identified. A nominal p-value of < 0.05 and false-discovery rate q value of < 0.25 were considered as significantly enriched in the AAA or aortic rupture group.

Gene set variation analysis was applied to evaluate GO and KEGG pathway terms enriched in each sample by converting the gene expression matrix into a gene set expression matrix using the GSVA package in R (version 4.1.2). After that, the differentially enriched terms between two groups were identified using R (version 4.1.2) with the threshold of $p < 0.05$. The differentially enriched terms were visualized using the "pheatmap" package in R (version 4.1.2).

Analysis of infiltrated immune cells in samples

CIBERSORT[5] is an algorithm that can analyze the relative abundance of 22 types of immune cells in each sample, including T-cells, B-cells, and macrophages (21). The parameters applied in this study were as follows: (I) 100 deconvolutions (Perm) and (II) $p < 0.05$. The analysis was conducted in R (version 4.1.2).

Analysis of differentially expressed immune and inflammation-related genes and prediction of transcription factors

The IRG list was downloaded from Immport[6]. The differentially expressed IRGs (DEIRGs) between two groups were identified using R (version 4.1.2) with the threshold of $p < 0.05$. DAVID was used to identify the transcription factors (TFs) that could mediate these genes. The interaction between genes and TFs was visualized using Cytoscape (version 3.9.1).

4 http://www.gsea-msigdb.org/gsea/msigdb/index.jsp
5 https://cibersort.stanford.edu/
6 https://www.immport.org/home

Preparation of the testing set

GSE7084 was selected as the testing set for the AAA predictive model and AAA-related hub genes, which included seven normal abdominal aorta samples and six AAA samples. Raw data were normalized following download from the GEO database using the "limma" package in R (version 4.1.2). Then, the data were annotated using the "dplyr" and "limma" package in R (version 4.1.2).

Construction of a predictive model and identification of hub genes by extreme gradient boosting (XGBoost) analysis

To construct the AAA predictive model, all samples in merged dataset 1 were regarded as the training set and candidate hub genes of the AAA-related yellow module were selected as features. After the construction of a predictive model, GSE7084 was used as the testing set. To construct a rupture predictive model, samples in merged dataset 2 were divided into a training set (70%) and a testing set (30%) randomly and candidate hub genes of the rupture-related yellow module were selected as features. The rupture predictive model based on the training set was further validated in the testing set. The predictive models were constructed using the "xgboost" package in R (version 4.1.2), and hub genes were identified according to the rank of feature importance.

Statistical analysis

The difference in relative expression levels of mRNA between different groups was analyzed with Student's t-test. The proportion of each immune cell and the ratio of M1/M2 macrophages between different groups was analyzed by the Mann–Whitney U test. Pearson's correlation analysis was used to analyze the relationship between inflammation genes and the infiltration of immune cells. A value of $p < 0.05$ was considered to be statistically significant. Statistical analyses were performed using SPSS version 19 (IBM Corporation, Armonk, NY, United States).

Results

Construction of abdominal aortic aneurysm- and aortic rupture-related gene co-expression networks

Soft threshold 12 was selected for AAA-related module construction. After analysis, 12 modules were obtained

(Figure 2A); then, the relationship between different modules and AAA was analyzed and is shown in Figure 2B. The results indicated that the blue and yellow modules were significantly correlated with the appearance of AAA (blue module, $r = -0.3$, $p = 0.001$; yellow module, $r = 0.27$, $p = 0.004$). Therefore, the blue module and the yellow module were chosen for further analysis.

Soft threshold 6 was selected for aortic rupture-related module construction and 17 modules were obtained (Figure 2E). Then, the correlation between different modules and aortic rupture was calculated, and the results suggested that the yellow module was the most relevant module ($r = 0.46$, $p = 5e\text{-}07$) (Figure 2F). Thus, the yellow module was selected for further analysis.

Identification of candidate hub genes using protein–protein interaction network

The PPI networks of the AAA-related blue module, AAA-related yellow module, and aortic rupture-related yellow module were constructed *via* STRING and visualized using Cytoscape. The score of every node was calculated using the cytoHubba plugin for Cytoscape with the MCC method. Then, the top 10 nodes of each module were selected as candidate hub genes and are shown in Figures 2C,D,G.

Gene ontology and Kyoto encyclopedia of genes and genomes pathway enrichment analysis of genes in the relevant gene modules

The enrichment analysis of the AAA-related blue module showed that the top 3 terms in the GO biological process (BP) subdivision were muscle contraction, cell adhesion, and angiogenesis, whereas the top three terms among the KEGG pathways were focal adhesion, ECM–receptor interaction, and hypertrophic cardiomyopathy (Table 1). The results of AAA-related yellow module suggested that the top three terms in GO BP included the immune response, T-cell activation, and the adaptive immune response and the top three terms in KEGG pathways included hematopoietic cell lineage, primary immunodeficiency, and the T-cell receptor signaling pathway (Table 1).

The enrichment analysis of the aortic rupture-related yellow module indicated that the top 3 terms in the GO BP subdivision were inflammatory response, response to lipopolysaccharides, and angiogenesis, whereas the top three terms among the KEGG pathways were the tumor necrosis factor (TNF) signaling pathway, advanced glycation end-products receptor for advanced glycation end-products signaling pathway in diabetic complications, and interleukin (IL)-17 signaling pathway (Table 1).

Gene set enrichment analysis and gene set variation analysis

Gene set enrichment analysis was conducted to understand the pathways enriched in different groups. The enrichment results of GO BP subdivision and KEGG pathway analysis demonstrated that positive regulation of leukocyte cell–cell adhesion, positive regulation of cell–cell adhesion, the adaptive immune response, cytokine–cytokine receptor interaction, the chemokine signaling pathway, and the NOD-like receptor signaling pathway were significantly enriched in the AAA group (Figures 3A–F). In terms of aortic rupture, the enrichment analysis results indicated that the serotonin receptor signaling pathway, regulation of peptidyl serine phosphorylation of STAT protein, serine phosphorylation of STAT protein, the Hedgehog signaling pathway, the mammalian target of rapamycin (mTOR) signaling pathway, and the vascular endothelial growth factor (VEGF) signaling pathway were significantly enriched in the aortic rupture group (Figures 3G–L).

To further evaluate the pathway variations between different samples, GSVA was applied, and the results suggested that, compared to the normal abdominal aorta group, regulation of lymphocyte chemotaxis, protein poly ADP-ribosylation, regulation of T-cell chemotaxis, and graft-versus-host disease were significantly upregulated in the AAA group (Figures 4A,B). Besides, compared to the stable AAA group, sulfur metabolism, β-alanine metabolism, and valine leucine and isoleucine degradation were significantly increased in the ruptured AAA group (Figure 4C).

Changes in infiltrated immune cells in different samples

The overall relative abundances of 22 types of immune cells among the normal abdominal aorta samples and AAA samples are shown in Figure 5A. Then, the difference in the relative abundance of each type of immune cell between different groups was analyzed, and the results indicated that the proportions of activated memory CD4 T-cells and T follicular helper cells were significantly higher in the AAA group, whereas the proportion of M2 macrophages was significantly decreased in the AAA group (Figure 5B). We further compared the M1/M2 macrophage ratio and found that the ratio was significantly higher in the AAA group (Figure 5C).

The relative abundances of 22 types of immune cells among the stable AAA samples and ruptured AAA samples are displayed in Figure 5D. Compared to the stable AAA group, the proportions of naïve CD4 T-cells, resting memory CD4

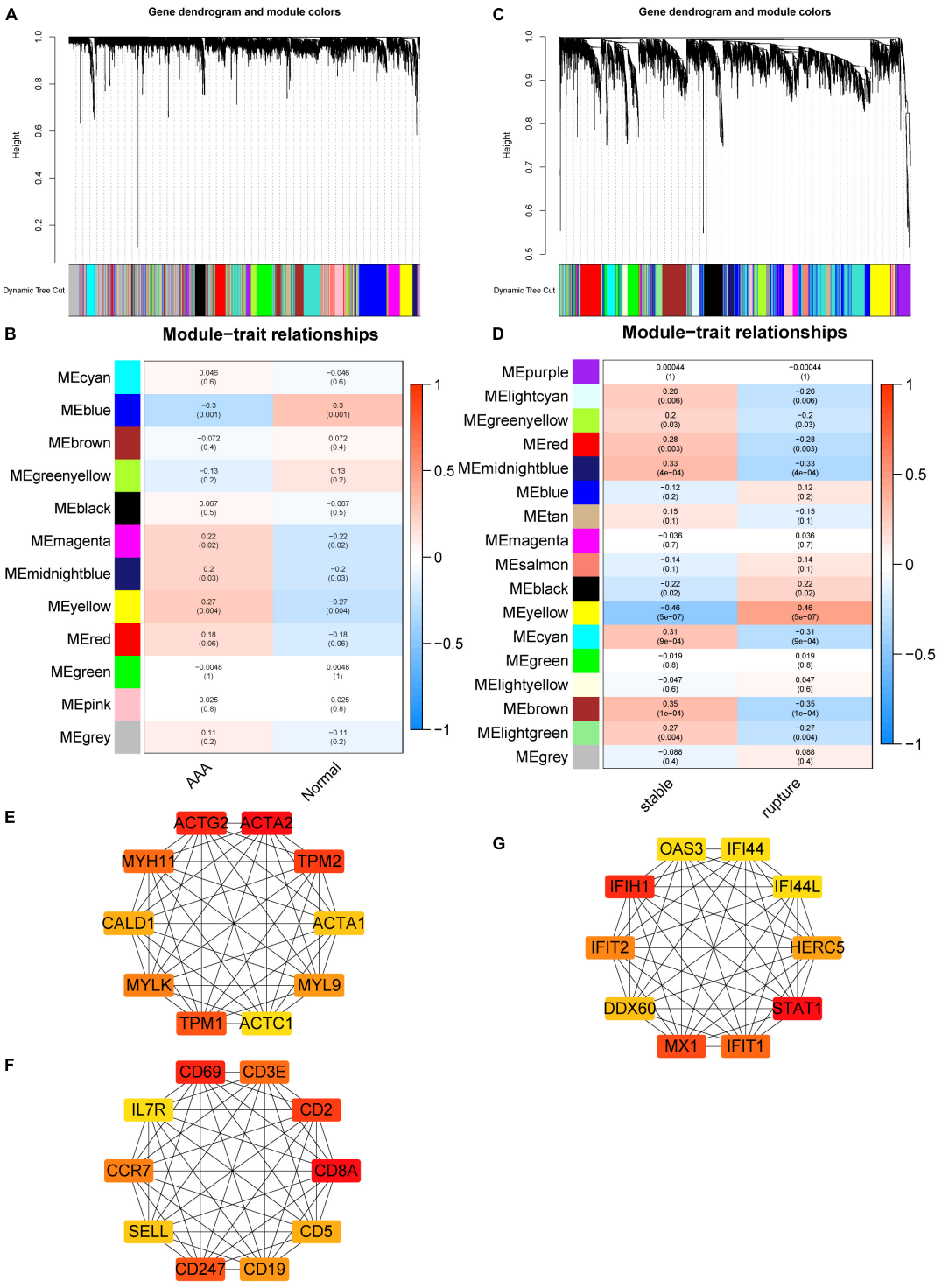

FIGURE 2
Construction of AAA- and aortic rupture-related gene co-expression networks using WGCNA and PPI networks of candidate hub genes. **(A)** Dendrogram and clustering for identification of gene co-expression modules of AAA-related merged dataset 1. **(B)** Correlation analysis of gene co-expression modules with AAA. The numbers above brackets were correlation coefficients and the numbers in brackets were *p*-values. **(C)** Dendrogram and clustering for identification of gene co-expression modules of aortic rupture-related merged dataset 2. **(D)** Correlation analysis of gene co-expression modules with aortic rupture. The numbers above brackets were correlation coefficients and the numbers in brackets were *p*-values. **(E,F)** The PPI networks of candidate hub genes of AAA-related blue module and yellow module, respectively. **(G)** The PPI networks of candidate hub genes of aortic rupture-related yellow module. AAA, abdominal aortic aneurysm; WGCNA, weighted gene correlation network analysis; PPI, protein–protein interaction.

T-cells, activated memory CD4 T-cells, and activated dendritic cells were significantly greater in the ruptured AAA group, whereas the proportions of regulatory T-cells and M0, M1, and M2 macrophages, respectively, were significantly lower in the ruptured AAA group (Figure 5E). Further analysis indicated that the M1/M2 macrophage ratio was significantly higher in the ruptured AAA group (Figure 5F).

Changes in inflammation-related genes in different groups and the relationship between inflammation-related genes and infiltration of immune cells

The DEIRGs between normal abdominal aorta samples and AAA samples were analyzed and the results revealed 453 DEIRGs, including 284 upregulated genes and 169 downregulated genes, with $p < 0.05$ (Figure 6A). Then, the TFs that could mediate these DEIRGs were predicted using DAVID. *STAT1*, *NFKB1*, *CREL*, and *P300* were the most relevant TFs considering the aforementioned DEIRGs, and the expression level of *NFKB1* was significantly upregulated in the AAA group (Figures 6B,C). The relationship among the top three upregulated DEIRGs, *NFKB1*, and significantly changed immune cells is displayed in Figure 6D. Similarly, we found 307 DEIRGs between the stable AAA group and ruptured AAA group, including 141 upregulated genes and 166 downregulated genes, with $p < 0.05$ (Figure 7A). *NFKB1*, *AP1*, *STAT1*, *BACH2*, and *STAT3* were the most relevant TFs considering these DEIRGs, and the expression level of *NFKB1* was also significantly increased in the ruptured AAA group (Figures 7B,C). In addition, the relationship among the top three upregulated DEIRGs, *NFKB1*, and significantly changed immune cells is displayed in Figure 7D.

Construction of the predictive model and identification of hub genes

The top 10 candidate hub genes in the AAA-related yellow module were selected as features to construct an AAA predictive model. The accuracy of this model was 0.7692 in testing set GSE7084 (Table 2). The identification of hub genes was performed according to the rank of feature importance, and *CD19*, *SELL*, and *CCR7* were the top three features (Figure 8A). The expression levels of *CD19*, *SELL*, and *CCR7* in the training set are shown in Figure 8B and were further validated in testing set GSE7084 (Figure 8C).

The construction of an aortic rupture predictive model was based on the top 10 candidate hub genes in the aortic rupture-related yellow module. During the construction process, four features were excluded because they did not contribute to the model (Figure 8D). The accuracy of this model was 0.9697 in the testing set (Table 3). The top three features were *OAS3*, *IFIT1*, and *IFI44L* (Figure 8D), and the expression levels of these genes are demonstrated in Figure 8E.

TABLE 1 Enrichment analysis of AAA and rupture-related gene modules.

Term	*P*-value	Benjamini
AAA-related blue module GO-BP		
Muscle contraction	5.987E-15	1.304E-11
Cell adhesion	3.207E-06	0.003
Angiogenesis	1.232E-05	0.009
Cell migration	2.111E-05	0.011
Actin filament organization	4.424E-05	0.019
AAA-related blue module KEGG pathway		
Focal adhesion	3.724E-06	0.001
ECM-receptor interaction	7.952E-05	0.001
Hypertrophic cardiomyopathy	9.489E-05	0.006
Vascular smooth muscle contraction	9.857E-05	0.006
Regulation of actin cytoskeleton	0.001	0.0232
AAA-related yellow module GO-BP		
Immune response	5.844E-12	7.778E-09
T-cell activation	4.800E-11	3.194E-08
Adaptive immune response	7.456E-08	3.308E-05
Regulation of immune response	1.687E-07	5.612E-05
T-cell costimulation	8.193E-07	<0.001
AAA-related yellow module KEGG pathway		
Hematopoietic cell lineage	1.748E-12	3.269E-10
Primary immunodeficiency	4.820E-07	4.507E-05
T-cell receptor signaling pathway	7.728E-06	<0.001
B cell receptor signaling pathway	9.066E-05	0.004
Cell adhesion molecules	<0.001	0.004
Rupture-related yellow module GO-BP		
Inflammatory response	3.032E-09	6.289E-06
Response to lipopolysaccharide	6.356E-07	<0.001
Angiogenesis	2.713E-05	0.008
Cellular response to interleukin-1	5.948E-05	0.0154
Positive regulation of p38MAPK cascade	<0.001	0.0221
Rupture-related yellow module KEGG pathway		
TNF signaling pathway	1.236E-07	3.064E-05
AGE-RAGE signaling pathway in diabetic complications	2.065E-06	<0.001
IL-17 signaling pathway	8.284E-06	0.001
HIF-1 signaling pathway	3.083E-05	0.002
Cytokine–cytokine receptor interaction	<0.001	0.005

AAA, abdominal aortic aneurysm; GO, Gene Ontology; BP, biological process; KEGG, Kyoto Encyclopedia of Genes and Genomes; ECM, extracellular matrix; MAPK, mitogen-activated protein kinase; TNF, tumor necrosis factor; AGE-RAGE, advanced glycation end-products receptor for advanced glycation end-products; IL-17, interleukin-17; HIF-1, hypoxia-induced factor-1.

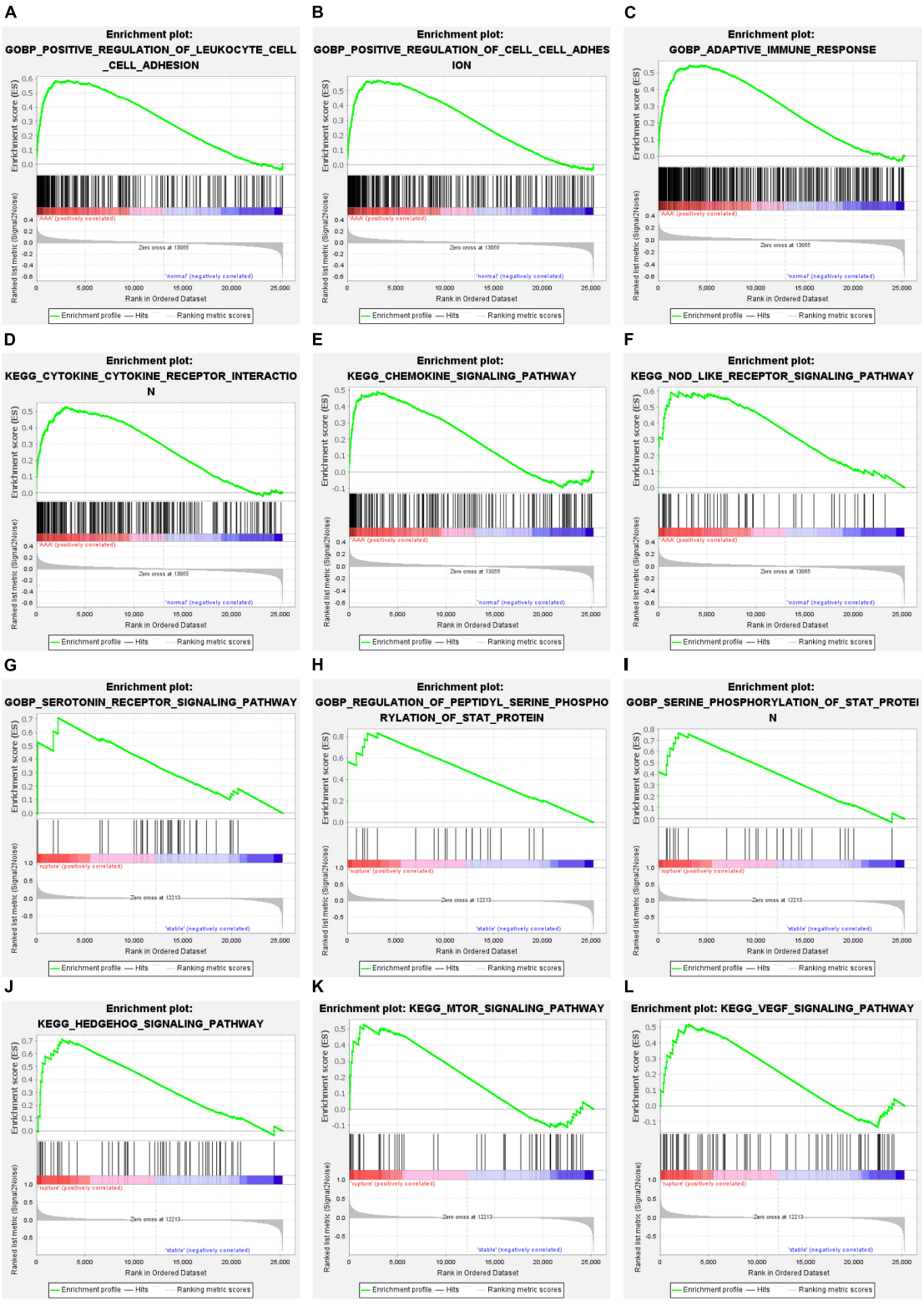

FIGURE 3
The results of GSEA. **(A–C)** The GO-BP terms significantly enriched in AAA group. **(D–F)** The KEGG pathways significantly enriched in AAA group. **(G–I)** The GO-BP terms significantly enriched in aortic rupture group. **(J–L)** The KEGG pathways significantly enriched in aortic rupture group. GSEA, gene set enrichment analysis; GO-BP, Gene Ontology-biological process; AAA, abdominal aortic aneurysm; KEGG, Kyoto Encyclopedia of Genes and Genomes.

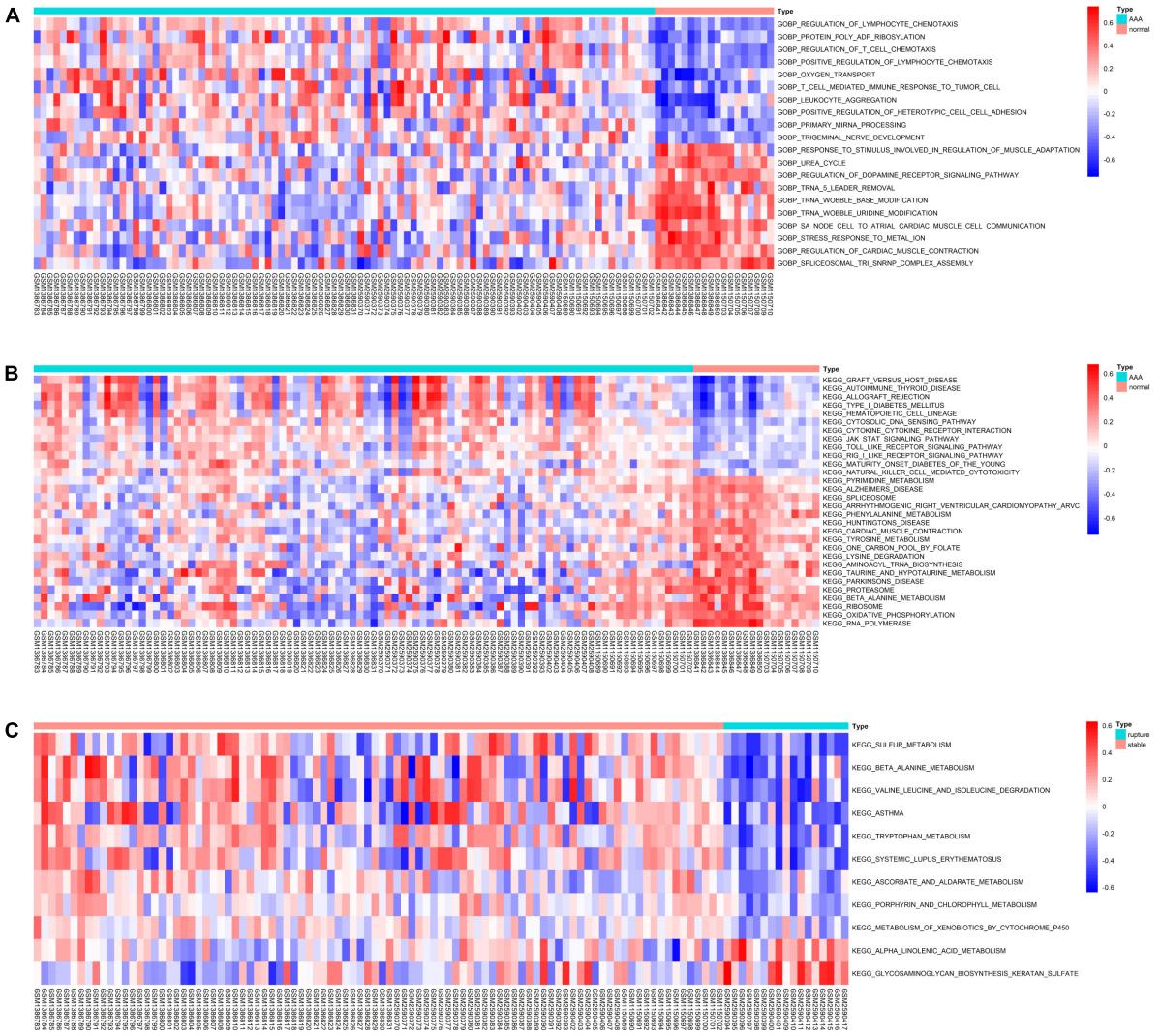

FIGURE 4
The results of GSVA. **(A)** Heatmap of top 20 significantly different GO-BP terms between normal abdominal aorta group and AAA group. **(B)** Heatmap of top 20 significantly different KEGG pathways between normal abdominal aorta group and AAA group. **(C)** Heatmap of significantly different KEGG pathways between stable AAA group and aortic rupture group. GSVA, gene set variation analysis; GO-BP, Gene Ontology-biological process; AAA, abdominal aortic aneurysm; KEGG, Kyoto Encyclopedia of Genes and Genomes.

Discussion

The prevalence of AAA is derived from ultrasonography screening programs of a few developed countries. According to these ultrasonography screening programs, the prevalence of AAA is approximately 1–2% in men > 65 years of age and 0.5% in women > 70 years of age (5–8). The exact prevalence of AAA in developing countries is unclear due to the lack of ultrasonography screening programs but has increased over the past two decades according to the literature (5, 17). Generally, smoking, older age, positive family history, male sex, hypertension, and dyslipidemia are significantly associated with the appearance of AAA (23–25). It was reported that the incidence of AAA increases by 6% per decade in men after the age of 65 years (26). In the developed countries, AAA-related death has been the 12–15th leading cause of death in those > 55 years of age, and aortic rupture is a predominant cause of AAA-related death (12, 27). The main treatment for AAA is surgical procedures such as endovascular aortic repair (EVAR) and open repair surgery (17). Currently, there is no drug-based therapy able to inhibit the AAA growth or aortic rupture (18, 28, 29). Therefore, further exploration of the mechanisms of AAA formation or aortic rupture is needed to identify new therapeutic targets or biomarkers that may allow for diagnosis and cure in early stages or the prediction of aortic rupture.

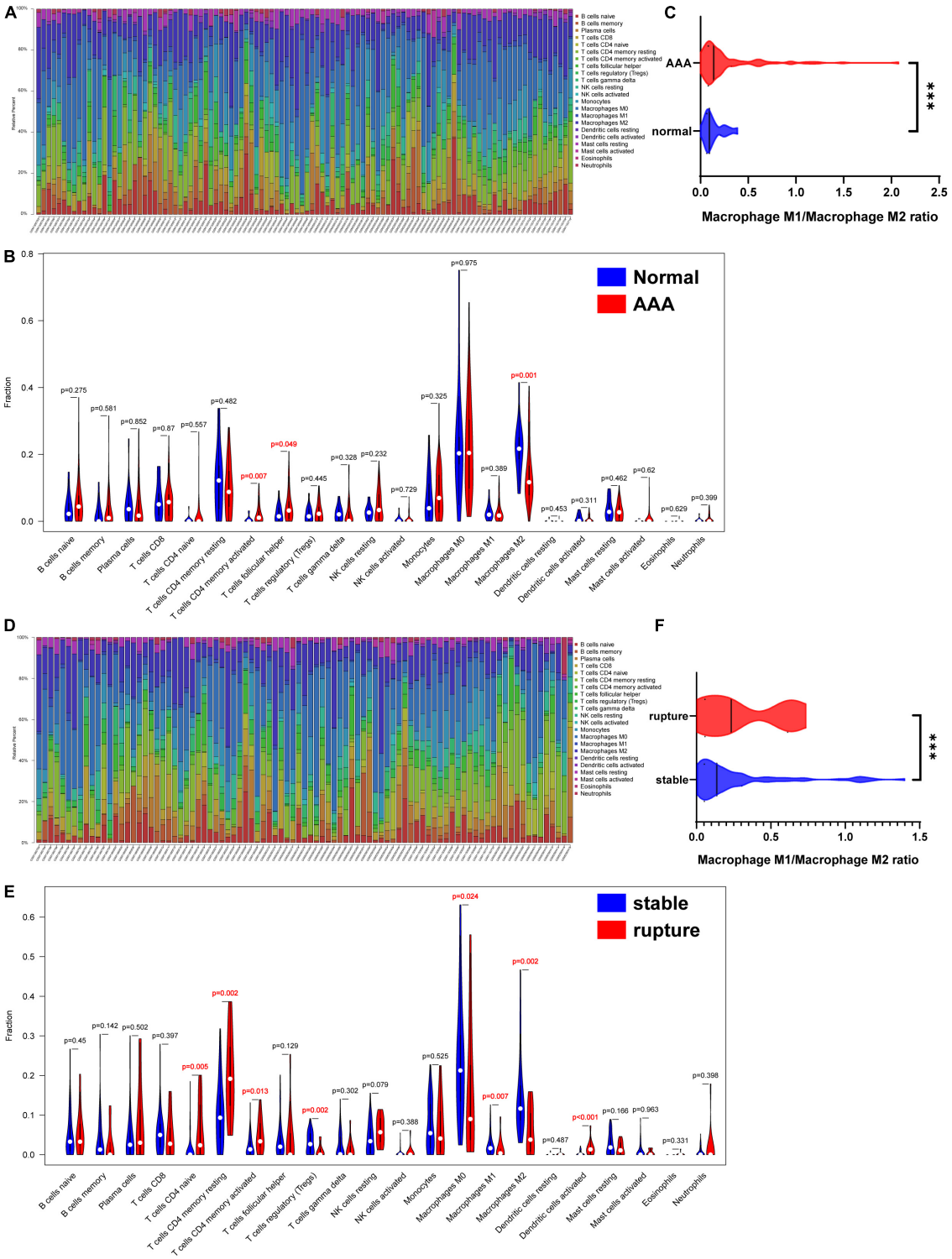

FIGURE 5
Infiltration of immune cells in different samples. **(A)** Proportion of 22 kinds of immune cells in samples of AAA-related merged dataset 1. **(B)** The difference of infiltration of immune cells between normal abdominal aorta group and AAA group. The numbers in red represented p-value < 0.05. **(C)** The macrophage M1/macrophage M2 ratio in normal abdominal aorta group and AAA group. **(D)** Proportion of 22 kinds of immune cells in samples of aortic rupture-related merged dataset 2. **(E)** The difference of infiltration of immune cells between stable AAA group and aortic rupture group. The numbers in red represented p-value < 0.05. **(F)** The macrophage M1/macrophage M2 ratio in stable AAA group and aortic rupture group. AAA, abdominal aortic aneurysm. ***$p < 0.001$.

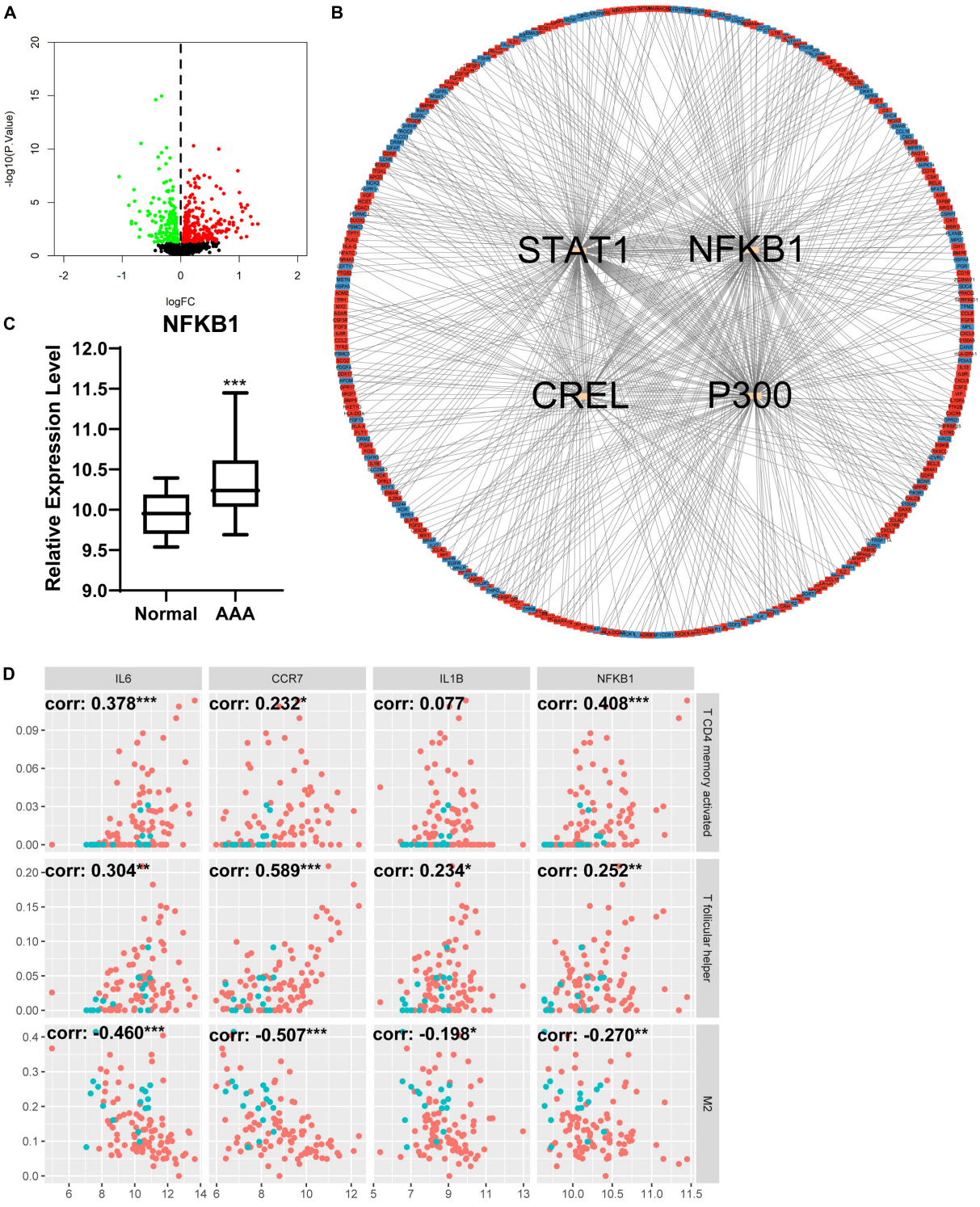

FIGURE 6
Differentially expressed immune and inflammation-related genes (DEIRGs) between normal abdominal aorta group and AAA group. **(A)** The volcano plot of DEIRGs between normal abdominal aorta group and AAA group. Dots in green: downregulated gene, dots in red: upregulated gene. **(B)** The PPI network of DEIRGs and upstream transcription factors. **(C)** The expression level of NFKB1 in normal abdominal aorta group and AAA group. **(D)** The relationship between top three upregulated DEIRGs, NFKB1, and significantly changed immune cells. Dots in blue: normal abdominal aorta samples, dots in red: AAA samples. AAA, abdominal aortic aneurysm; PPI, protein–protein interaction; NFKB1, nuclear factor kappa B 1; corr, correlation coefficient. *$p < 0.05$, **$p < 0.01$, ***$p < 0.001$.

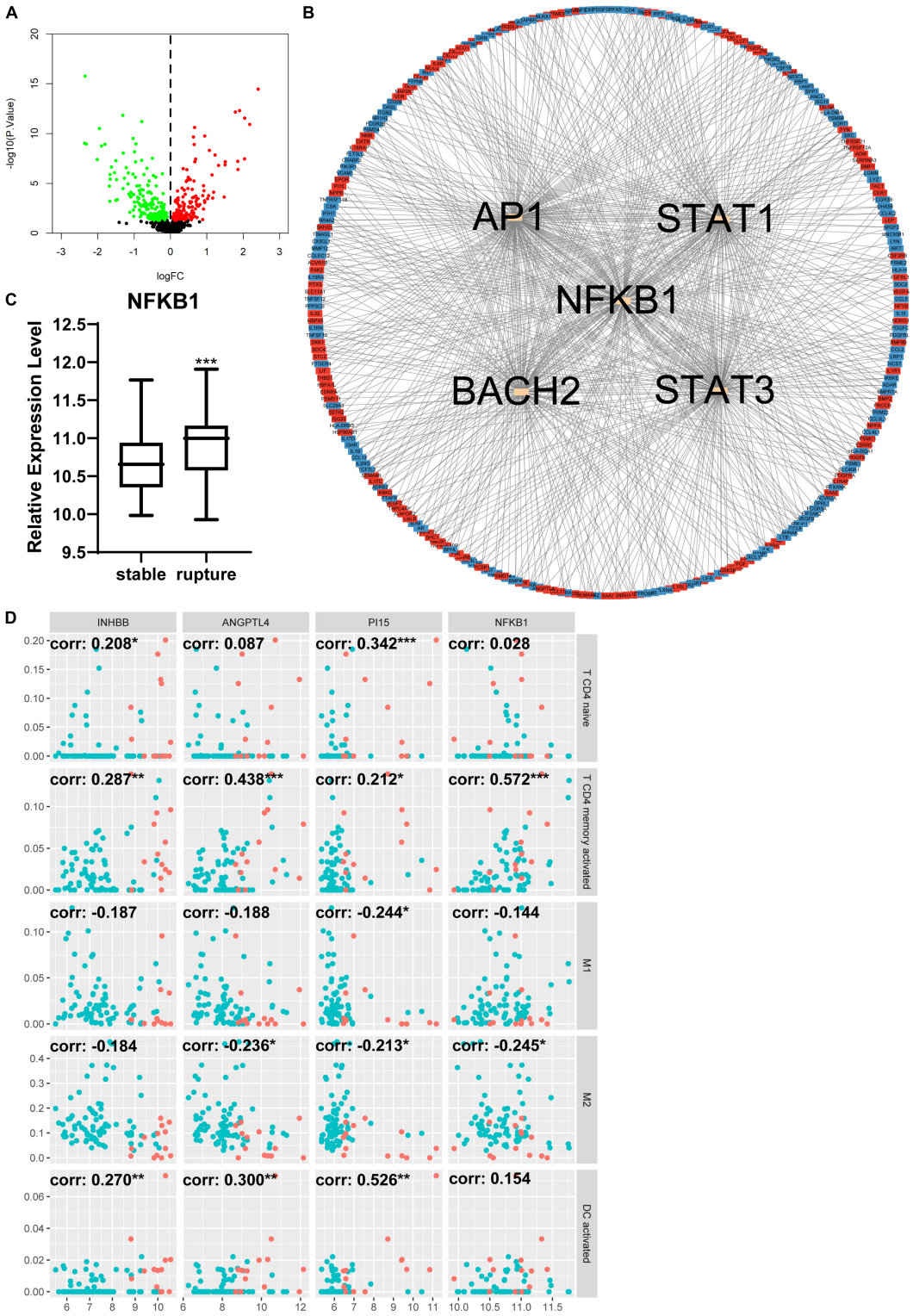

FIGURE 7
Differentially expressed immune and inflammation-related genes (DEIRGs) between stable AAA group and aortic rupture group. **(A)** The volcano plot of DEIRGs between stable AAA group and aortic rupture group. Dots in green: downregulated gene, dots in red: upregulated gene. **(B)** The PPI network of DEIRGs and upstream transcription factors. **(C)** The expression level of NFKB1 in stable AAA group and aortic rupture group. **(D)** The relationship between top three upregulated DEIRGs, NFKB1, and significantly changed immune cells. Dots in blue: stable AAA samples, dots in red: aortic rupture samples. AAA, abdominal aortic aneurysm; PPI, protein–protein interaction; NFKB1, nuclear factor kappa B 1; corr, correlation coefficient. *$p < 0.05$, **$p < 0.01$, ***$p < 0.001$.

GSE47472, GSE57691, and GSE98278 were chosen and selectively merged for further bioinformatics analysis. These three datasets were detected using the same platform, which facilitates the consistency of the detection process. Considering the bioinformatics studies of Xie et al. (30) and Yuan et al. (31), this study contained more datasets and samples than either of the former. Moreover, instead of identifying differentially expressed genes directly, AAA- and aortic rupture-related gene co-expression networks were constructed using WGCNA first in this research. After evaluating the correlation between AAA-related gene modules and the appearance of AAA, the results revealed that the absolute correlation coefficient of the blue module was the largest among these modules, with $p < 0.05$. However, we also noticed that the absolute correlation coefficient of the yellow module was close to that of the blue module, so the blue and yellow modules were both selected for further analysis. The results of enrichment analysis of the AAA-related blue module indicated that genes in this module were involved in processes, including muscle contraction, structural constituent of muscle, and vascular smooth muscle contraction, both of which are closely related to the aortic wall. This finding is consistent with current opinions about the development of AAA. One of the main causes of AAA is a progressive degenerated abdominal artery wall, which is characterized by degradation of the ECM in the adventitia and the loss of VSMCs (32). The main components of the ECM are microfibrillar (elastin and collagen) and microfibrillar (fibronectin and fibrillin) structures of crosslinked proteins, which maintain the function of the artery wall and resist its dilatation and rupture (13). Increases in serine proteases and activated MMPs lead to degradation of the ECM and eventually result in dilation and rupture of the abdominal artery wall (33, 34). VSMCs synthesize ECM components and secret enzymes such as lysyl oxidase, thus involving themselves in the maturation of fibrillar structures in the ECM (12). The proteolytic, inflammatory, and oxidative environments in the abdominal artery wall could lead to the detachment and death of VSMCs and affect the synthesis of ECM components (15, 35).

Genes in the AAA-related yellow module were significantly enriched in terms like immune response, T-cell activation, and the B-cell receptor signaling pathway. Similarly, the results of GSEA and GSVA suggested that positive regulation of leukocyte cell–cell adhesion, the chemokine signaling pathway, and regulation of lymphocyte chemotaxis were significantly enriched in the AAA group. These results indicate that the immune and inflammation response is another important mechanism of AAA. Previous studies have revealed that both innate and adaptive immunity contribute to the development of AAA (12). In healthy individuals, the media of the abdominal aorta is an immune-privileged site devoid of capillaries, while the adventitia of the abdominal aorta is fully vascularized with many capillaries, enabling immune cell diapedesis and triggering an immune response (36). Under the AAA condition, the relative hypoxia environment in the abdominal aorta would induce the expression of VEGF in macrophages and VSMCs and eventually lead to angiogenesis in the adventitia and media of the abdominal aorta (37). The innate immune activity includes diapedesis, activation, and death of polymorphonuclear leukocytes in AAA, whereas leukocytes release proteases, oxidant peptides, myeloperoxidase, and pro-inflammatory factors, both of which could accelerate the development of AAA (32). However, the proteolytic and/or oxidative environments in the abdominal artery wall of patients with AAA can trigger an adaptive immune response, which commonly takes place in the adventitia of the abdominal artery (36). The adaptive immune response in AAA is associated with the formation of an adventitial tertiary lymphoid organ (TLO), whose center is composed of B-cells and surrounded by endothelial venules, follicular dendritic cells, and T follicular helper cells. The function of the TLO includes antibody production and immunoglobulin switching (38). Our bioinformatics analysis further confirmed that the immune and inflammation response is a key process in the development of AAA.

TABLE 2 The predictive ability of XGBoost model in GSE7084.

		XGBoost model predicted		Accuracy
		Normal	AAA	
Actual	Normal	5	1	0.7692
	AAA	2	5	

XGBoost, extreme gradient boosting; AAA, abdominal aortic aneurysm.

Aortic rupture is the main cause of death in patients with AAA, so it is necessary to further explore the potential mechanisms underlying aortic rupture. The enrichment analysis of the aortic rupture-related yellow module revealed that genes in this module were associated with the cytokine-mediated signaling pathway and inflammatory response. In addition, the results of GSEA indicated that the STAT, mTOR, and VEGF signaling pathways were significantly enriched in the aortic rupture group. The traditional risk factors for aortic rupture include AAA size, wall thickness, hypertension, smoking, advanced age, and systemic inflammation (39). There is an increasing number of studies suggesting that inflammation is significantly associated with aortic rupture. Aurelian et al. reported that the neutrophil-to-lymphocyte ratio (NLR) was increased in patients with aortic rupture compared to patients with intact AAAs, and an NLR of > 5 indicated a fivefold increased risk of aortic rupture (40). Studies by Treska et al., Cheuk et al., and Wallinder et al. demonstrated that pro-inflammatory cytokines such as IL-6, IL-8, and TNF-α were upregulated in the plasma and aneurysm tissue of patients with AAA rupture (41–43). STAT signaling pathways could mediate cellular activity, including the inflammatory response, and Wang et al. reported that the STAT4 signaling pathway is

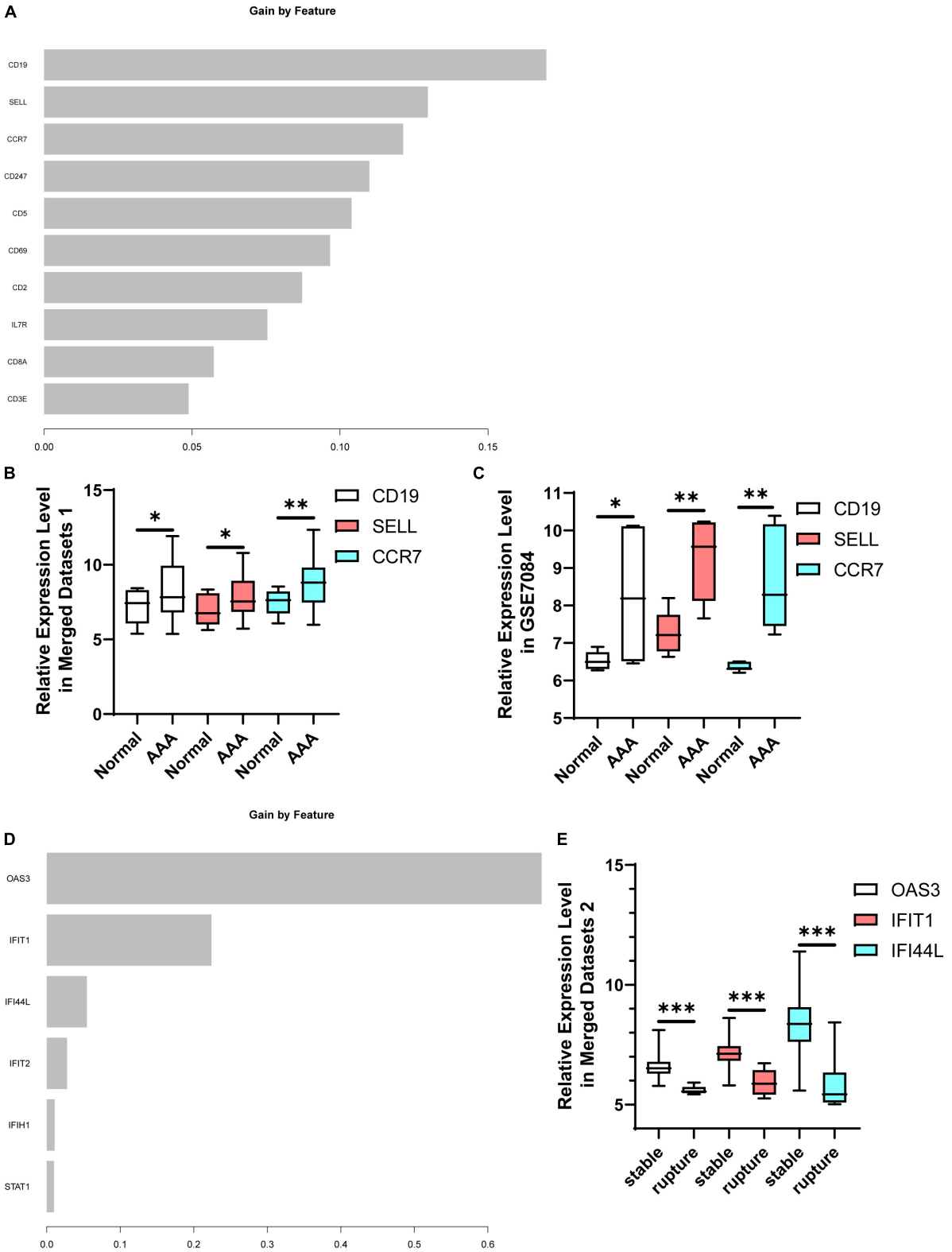

FIGURE 8
Identification of hub genes. **(A)** The rank of feature importance in AAA predictive model. **(B)** The expression levels of CD19, SELL, and CCR7 in AAA-related merged dataset 1. **(C)** The expression levels of CD19, SELL, and CCR7 in testing set GSE7084. **(D)** The rank of feature importance in aortic rupture predictive model. **(E)** The expression levels of OAS3, IFIT1, and IFI44L in aortic rupture-related merged dataset 2. AAA, abdominal aortic aneurysm. *$p < 0.05$, **$p < 0.01$, ***$p < 0.001$.

TABLE 3 The predictive ability of XGBoost model in the testing set.

		XGBoost model predicted		Accuracy
		Stable	Rupture	
Actual	Stable	26	0	0.9697
	Rupture	1	6	

XGBoost, extreme gradient boosting.

involved in the development and rupture of AAA (44). There are also studies demonstrating that the mTOR and VEGF signaling pathways play the important roles in the development of AAA (45, 46), but their roles in aortic rupture remain unclear.

According to the results of enrichment analysis, GSEA, and GSVA, immune and inflammatory responses participate in the development of AAA and aortic rupture. Thus, we further investigated the infiltration of immune cells in each sample using CIBERSORT. The results showed that the proportion of M2 macrophages was significantly decreased in AAA samples compared to normal abdominal artery samples and the M1/M2 macrophage ratio was significantly greater in AAA samples compared to normal abdominal artery samples. Studies have demonstrated that M1 is a pro-inflammatory phenotype of macrophages, whereas M2 is an anti-inflammatory phenotype of macrophages (47). Our findings further validated the idea that the aneurysmal wall is under a severe inflammatory condition. In addition, macrophages secret VEGF and MMPs, which could provoke angiogenesis in the adventitia and media of the abdominal aorta and result in weakening of the aneurysmal wall (37). The results also indicated that the proportions of activated memory CD4 T-cells and T follicular helper cells were significantly higher in AAA samples. Pathological study has confirmed the infiltration of T-cells in the aneurysmal wall (48). Galle et al. reported that CD4 + T-cells infiltrated into the aneurysmal wall exhibit a unique activated memory phenotype and could produce interferon-γ at a high level (49). Gao et al. also showed that infiltration of activated memory CD4 T-cells and T follicular helper cells was significantly increased in AAA samples using CIBERSORT (50). However, there remain few studies documenting the exact role of T-cells in AAA, which requires further investigation. Thus, we compared the infiltration of immune cells in stable AAA samples and ruptured AAA samples. Surprisingly, the proportions of M0, M1, and M2 macrophages, respectively, were all significantly lower in ruptured AAA samples than stable AAA samples, but the M1/M2 macrophage ratio was still significantly higher in the ruptured AAA samples, revealing their severe inflammatory environment. In contrast to our findings, a bioinformatics analysis performed by Lei et al. suggested that the proportions of M0, M1, and M2 macrophages were similar among stable AAA samples and ruptured AAA samples (51). This difference in results might be due to the choice of dataset selected for analysis. In this research, GSE47472, GSE57691, and GSE98278 were selected to investigate the potential mechanism of aortic rupture, whereas Lei et al. (51) only chose GSE98278 for further analysis. In addition, we found that the proportions of naïve CD4 T-cells, resting memory CD4 T-cells, and activated memory CD4 T-cells were significantly lower in stable AAA samples compared to ruptured AAA samples. These findings were consistent with those of Amin et al., whose research indicated that the reduced infiltration of CD4 + T-cells could attenuate inflammation, preserve integrity of the artery, and reduce the risk of aortic rupture (52). We also noticed that the proportion of regulatory T-cells was significantly lower in ruptured AAA samples. Similarly, Ait-Oufella et al. found that natural regulatory T-cells limit angiotensin II-induced AAA formation and rupture in mice (53).

We continued to investigate the DEIRGs between different samples. There were 453 DEIRGs between normal abdominal aorta samples and AAA samples, and *STAT1*, *NFKB1*, *CREL*, and *P300* were the most relevant TFs that could mediate these DEIRGs according to the enrichment analysis of DAVID. Among these TFs, NFKB1 was significantly increased in AAA samples. Similarly, there were 307 DEIRGs between stable and ruptured AAA samples; *NFKB1*, *AP1*, *STAT1*, *BACH2*, and *STAT3* were the most relevant TFs, and *NFKB1* was significantly upregulated in ruptured AAA samples. Studies have demonstrated the importance of the NFKB1 signaling pathway in the development of AAA (54, 55), suggesting that the NFKB1 signaling pathway might be a promising therapeutic target of AAA.

As mentioned above, most patients with AAA are asymptomatic in the early stage and it is hard to predict aortic rupture in these individuals (18). Therefore, in a subsequent study, we investigated which potential biomarkers had diagnostic value for AAA or could predict aortic rupture. First of all, we constructed an AAA predictive model using XGBoost, which could effectively avoid the overfitting problem (56). The candidate hub genes of the AAA-related yellow module were selected as features of this model. These genes were inflammation-related and their expression levels can also change in peripheral blood, which allows us to conveniently detect them with limited damage. The accuracy of the AAA

predictive model in testing set GSE7084 was 0.7692. Thereafter, genes were ranked according to feature importance, and the top three genes were *CD19*, *SELL*, and *CCR7*, which were selected as hub genes. CD19 is a marker of B-cells and the micro-array study of Biros et al. indicated that CD19 was significantly increased in AAA samples (57). Shi et al. found that CD19-positive cells were significantly infiltrated in AAA samples using immunohistochemical staining (58). Marie et al. reported that SELL was associated with the development of AAA (59). Furthermore, several bioinformatics studies revealed that *CCR7* is one of the hub genes of AAA (60, 61). Our findings and previous investigations suggest that these genes might be involved in the development of AAA and could be potential biomarkers for AAA, but their diagnostic value needs further validation.

An aortic rupture predictive model was constructed using XGBoost and the candidate hub genes of the aortic rupture-related yellow module were features in the model. The accuracy of this model in the inner testing set was 0.9697 and the top 3 hub genes were *OAS3*, *IFIT1*, and *IFI44L*. OAS3 is a member of the 2'-5'-oligoadenylate synthetase family and is involved in immune responses, which could restrict the replication of certain types of viruses (62, 63). Interferon-induced protein with tetratricopeptide repeats (IFIT) 1 is a member of the IFIT family and plays an important role in antiviral processes, and research has revealed that IFIT1 is involved in the development of systemic lupus erythematosus (SLE) (64, 65). Interferon-induced protein 44-like is an interferon-induced gene overexpressed in patients with SLE that might be a drug target of SLE (66). However, the relationships between these three genes and aortic rupture are unclear, and the predictive values of aortic rupture require further exploration.

The main limitation of these hub genes is that they are not suitable for clinical diagnosis because they were detected in AAA tissue samples. However, these genes were found to be closely related to the immune or inflammation process, and expression levels of these genes might change in peripheral blood. Further research needs to be done to investigate the changes of these genes in peripheral blood. Other genes that could interact with these hub genes should be investigated as well. On the other hand, non-coding RNAs, including microRNAs, circular RNAs, and long non-coding RNAs, could be promising biomarkers for some diseases (67). In the next step, a competing endogenous RNA network of these hub genes should be constructed and the RNAs with diagnostic value identified.

In conclusion, weakening of the artery wall and the immune response significantly contributed to the development of AAA, and the inflammatory response was one of the most important factors leading to aortic rupture. The infiltration of immune cells was significantly different between normal abdominal artery samples and AAA samples, stable AAA samples, and ruptured AAA samples. NFKB1 might be an important TF that mediates the inflammatory response of AAA and aortic rupture. CD19, SELL, and CCR7 had potential diagnostic value for AAA. OAS3, IFIT1, and IFI44L may be predictive factors for aortic rupture.

Data availability statement

Publicly available datasets were analyzed in this study. This data can be found here: https://www.ncbi.nlm.nih.gov/geo/query/acc.cgi?acc=GSE47472, https://www.ncbi.nlm.nih.gov/geo/query/acc.cgi?acc=GSE57691, https://www.ncbi.nlm.nih.gov/geo/query/acc.cgi?acc=GSE98278, and https://www.ncbi.nlm.nih.gov/geo/query/acc.cgi?acc=GSE7084.

Author contributions

YBC analyzed the data, completed the figures, and wrote the manuscript. TYOY and CF processed the raw data. C-eT, KBL, LTJ, and FYL designed the research. LTJ and FYL reviewed and edited the manuscript. All authors contributed to the article and approved the submitted version.

Funding

This study was funded by the National Natural Science Foundation of China (81873494 and 82070352) and the Hunan Key R&D Programs (2021SK2022).

Acknowledgments

We thank Zhanwei Zhu from Institute of Medical Science Research, Xiangya Hospital, Central South University for advices on data process and Yangjie Zhou from Xiangya Hospital, Central South University for the advices on writing this manuscript.

Conflict of interest

The authors declare that the research was conducted in the absence of any commercial or financial relationships that could be construed as a potential conflict of interest.

Publisher's note

All claims expressed in this article are solely those of the authors and do not necessarily represent those of their affiliated organizations, or those of the publisher, the editors and the reviewers. Any product that may be evaluated in this article, or claim that may be made by its manufacturer, is not guaranteed or endorsed by the publisher.

References

1. Golledge J, Muller J, Daugherty A, Norman P. Abdominal aortic aneurysm: pathogenesis and implications for management. *Arterioscler Thromb Vasc Biol.* (2006) 26:2605–13. doi: 10.1161/01.ATV.0000245819.32762.cb

2. Lederle FA, Johnson GR, Wilson SE, Chute EP, Littooy FN, Bandyk D, et al. Prevalence and associations of abdominal aortic aneurysm detected through screening. Aneurysm detection and management (ADAM) veterans affairs cooperative study group. *Ann Intern Med.* (1997) 126:441–9. doi: 10.7326/0003-4819-126-6-199703150-00004

3. Singh K, Bonaa KH, Jacobsen BK, Bjork L, Solberg S. Prevalence of and risk factors for abdominal aortic aneurysms in a population-based study : the Tromso study. *Am J Epidemiol.* (2001) 154:236–44. doi: 10.1093/aje/154.3.236

4. Jamrozik K, Norman PE, Spencer CA, Parsons RW, Tuohy R, Lawrence-Brown MM, et al. Screening for abdominal aortic aneurysm: lessons from a population-based study. *Med J Aust.* (2000) 173:345–50. doi: 10.5694/j.1326-5377.2000.tb125684.x

5. Sampson UK, Norman PE, Fowkes FG, Aboyans V, Song Y, Harrell FE Jr., et al. Estimation of global and regional incidence and prevalence of abdominal aortic aneurysms 1990 to 2010. *Glob Heart.* (2014) 9:159–70. doi: 10.1016/j.gheart.2013.12.009

6. Svensjo S, Bjorck M, Wanhainen A. Current prevalence of abdominal aortic aneurysm in 70-year-old women. *Br J Surg.* (2013) 100:367–72. doi: 10.1002/bjs.8984

7. Oliver-Williams C, Sweeting MJ, Turton G, Parkin D, Cooper D, Rodd C, et al. Lessons learned about prevalence and growth rates of abdominal aortic aneurysms from a 25-year ultrasound population screening programme. *Br J Surg.* (2018) 105:68–74. doi: 10.1002/bjs.10715

8. Grondal N, Sogaard R, Lindholt JS. Baseline prevalence of abdominal aortic aneurysm, peripheral arterial disease and hypertension in men aged 65-74 years from a population screening study (VIVA trial). *Br J Surg.* (2015) 102:902–6. doi: 10.1002/bjs.9825

9. GBD 2013 Mortality and Causes of Death Collaborators. Global, regional, and national age–sex specific all-cause and cause-specific mortality for 240 causes of death, 1990–2013: a systematic analysis for the global burden of disease study 2013. *The Lancet.* (2015) 385:117–71. doi: 10.1016/S0140-6736(14)61682-2

10. Sampson UK, Norman PE, Fowkes FG, Aboyans V, Yanna S, Harrell FE Jr, et al. Global and regional burden of aortic dissection and aneurysms: mortality trends in 21 world regions, 1990 to 2010. *Glob Heart.* (2014) 9:171–80.e10. doi: 10.1016/j.gheart.2013.12.010

11. López-Candales A, Holmes DR, Liao S, Scott MJ, Wickline SA, Thompson RW. Decreased vascular smooth muscle cell density in medial degeneration of human abdominal aortic aneurysms. *Am J Pathol.* (1997) 150:993–1007.

12. Sakalihasan N, Michel JB, Katsargyris A, Kuivaniemi H, Defraigne JO, Nchimi A, et al. Abdominal aortic aneurysms. *Nat Rev Dis Primers.* (2018) 4:34. doi: 10.1038/s41572-018-0030-7

13. Dobrin PB, Baker WH, Gley WC. Elastolytic and collagenolytic studies of arteries. Implications for the mechanical properties of aneurysms. *Arch Surg.* (1984) 119:405–9. doi: 10.1001/archsurg.1984.01390160041009

14. Fanjul-Fernandez M, Folgueras AR, Cabrera S, Lopez-Otin C. Matrix metalloproteinases: evolution, gene regulation and functional analysis in mouse models. *Biochim Biophys Acta.* (2010) 1803:3–19. doi: 10.1016/j.bbamcr.2009.07.004

15. Wang Q, Liu Z, Ren J, Morgan S, Assa C, Liu B. Receptor-interacting protein kinase 3 contributes to abdominal aortic aneurysms via smooth muscle cell necrosis and inflammation. *Circ Res.* (2015) 116:600–11. doi: 10.1161/CIRCRESAHA.116.304899

16. Qin Y, Wang Y, Liu O, Jia L, Fang W, Du J, et al. Tauroursodeoxycholic acid attenuates angiotensin II induced abdominal aortic aneurysm formation in apolipoprotein E-deficient mice by inhibiting endoplasmic reticulum stress. *Eur J Vasc Endovasc Surg.* (2017) 53:337–45. doi: 10.1016/j.ejvs.2016.10.026

17. Golledge J. Abdominal aortic aneurysm: update on pathogenesis and medical treatments. *Nat Rev Cardiol.* (2019) 16:225–42. doi: 10.1038/s41569-018-0114-9

18. Golledge J, Norman PE. Current status of medical management for abdominal aortic aneurysm. *Atherosclerosis.* (2011) 217:57–63. doi: 10.1016/j.atherosclerosis.2011.03.006

19. Sweeting MJ, Thompson SG, Brown LC, Powell JT, Rescan collaborators. Meta-analysis of individual patient data to examine factors affecting growth and rupture of small abdominal aortic aneurysms. *Br J Surg.* (2012) 99:655–65. doi: 10.1002/bjs.8707

20. Langfelder P, Horvath S. WGCNA: an R package for weighted correlation network analysis. *BMC Bioinformatics.* (2008) 9:559. doi: 10.1186/1471-2105-9-559

21. Guo C, Liu Z, Yu Y, Zhou Z, Ma K, Zhang L, et al. EGR1 and KLF4 as diagnostic markers for abdominal aortic aneurysm and associated with immune infiltration. *Front Cardiovasc Med.* (2022) 9:781207. doi: 10.3389/fcvm.2022.781207

22. Guo C, Liu Z, Cao C, Zheng Y, Lu T, Yu Y, et al. Development and validation of ischemic events related signature after carotid endarterectomy. *Front Cell Dev Biol.* (2022) 10:794608. doi: 10.3389/fcell.2022.794608

23. Bobadilla JL, Kent KC. Screening for abdominal aortic aneurysms. *Adv Surg.* (2012) 46:101–9. doi: 10.1016/j.yasu.2012.03.006

24. Larsson E, Granath F, Swedenborg J, Hultgren R. A population-based case-control study of the familial risk of abdominal aortic aneurysm. *J Vasc Surg.* (2009) 49:47–50; discussion 1. doi: 10.1016/j.jvs.2008.08.012

25. Sakalihasan N, Defraigne JO, Kerstenne MA, Cheramy-Bien JP, Smelser DT, Tromp G, et al. Family members of patients with abdominal aortic aneurysms are at increased risk for aneurysms: analysis of 618 probands and their families from the Liege AAA Family Study. *Ann Vasc Surg.* (2014) 28:787–97. doi: 10.1016/j.avsg.2013.11.005

26. Kent KC, Zwolak RM, Egorova NN, Riles TS, Manganaro A, Moskowitz AJ, et al. Analysis of risk factors for abdominal aortic aneurysm in a cohort of more than 3 million individuals. *J Vasc Surg.* (2010) 52:539–48. doi: 10.1016/j.jvs.2010.05.090

27. Bengtsson H, Bergqvist D. Ruptured abdominal aortic aneurysm: a population-based study. *J Vasc Surg.* (1993) 18:74–80. doi: 10.1067/mva.1993.42107

28. Kokje VB, Hamming JF, Lindeman JH. Pharmaceutical management of small abdominal aortic aneurysms: a systematic review of the clinical evidence. *Eur J Vasc Endovasc Surg.* (2015) 50:702–13. doi: 10.1016/j.ejvs.2015.08.010

29. Rughani G, Robertson L, Clarke M. Medical treatment for small abdominal aortic aneurysms. *Cochrane Database Syst Rev.* (2012) 9:CD009536. doi: 10.1002/14651858.CD009536.pub2

30. Xie X, Wang EC, Xu D, Shu X, Zhao YF, Guo D, et al. Bioinformatics analysis reveals the potential diagnostic biomarkers for abdominal aortic aneurysm. *Front Cardiovasc Med.* (2021) 8:656263. doi: 10.3389/fcvm.2021.656263

31. Yuan K, Liang W, Zhang J. A comprehensive analysis of differentially expressed genes and pathways in abdominal aortic aneurysm. *Mol Med Rep.* (2015) 12:2707–14. doi: 10.3892/mmr.2015.3709

32. Michel JB, Martin-Ventura JL, Egido J, Sakalihasan N, Treska V, Lindholt J, et al. Novel aspects of the pathogenesis of aneurysms of the abdominal aorta in humans. *Cardiovasc Res.* (2011) 90:18–27. doi: 10.1093/cvr/cvq337

33. Sakalihasan N, Delvenne P, Nusgens BV, Limet R, Lapiere CM. Activated forms of MMP2 and MMP9 in abdominal aortic aneurysms. *J Vasc Surg.* (1996) 24:127–33. doi: 10.1016/S0741-5214(96)70153-2

34. Busuttil RW, Rinderbriecht H, Flesher A, Carmack C. Elastase activity: the role of elastase in aortic aneurysm formation. *J Surg Res.* (1982) 32:214–7. doi: 10.1016/0022-4804(82)90093-2

35. Michel JB. Anoikis in the cardiovascular system: known and unknown extracellular mediators. *Arterioscler Thromb Vasc Biol.* (2003) 23:2146–54. doi: 10.1161/01.ATV.0000099882.52647.E4

36. Michel JB, Thaunat O, Houard X, Meilhac O, Caligiuri G, Nicoletti A. Topological determinants and consequences of adventitial responses to arterial wall injury. *Arterioscler Thromb Vasc Biol.* (2007) 27:1259–68. doi: 10.1161/ATVBAHA.106.137851

37. Ho-Tin-Noe B, Michel JB. Initiation of angiogenesis in atherosclerosis: smooth muscle cells as mediators of the angiogenic response to atheroma formation. *Trends Cardiovasc Med.* (2011) 21:183–7. doi: 10.1016/j.tcm.2012.05.007

38. Clement M, Guedj K, Andreata F, Morvan M, Bey L, Khallou-Laschet J, et al. Control of the T follicular helper-germinal center B-cell axis by CD8(+) regulatory T cells limits atherosclerosis and tertiary lymphoid organ development. *Circulation.* (2015) 131:560–70. doi: 10.1161/CIRCULATIONAHA.114.010988

39. Anagnostakos J, Lal BK. Abdominal aortic aneurysms. *Prog Cardiovasc Dis.* (2021) 65:34–43. doi: 10.1016/j.pcad.2021.03.009

40. Aurelian SV, Adrian M, Andercou O, Bruno S, Alexandru O, Catalin T, et al. Neutrophil-to-lymphocyte ratio: a comparative study of rupture to nonruptured infrarenal abdominal aortic aneurysm. *Ann Vasc Surg.* (2019) 58:270–5. doi: 10.1016/j.avsg.2018.11.026

41. Treska V, Kocova J, Boudova L, Neprasova P, Topolcan O, Pecen L, et al. Inflammation in the wall of abdominal aortic aneurysm and its role in the symptomatology of aneurysm. *Cytokines Cell Mol Ther.* (2002) 7:91–7. doi: 10.1080/13684730310001652

42. Cheuk BL, Cheng SW. Differential secretion of prostaglandin E(2), thromboxane A(2) and interleukin-6 in intact and ruptured abdominal aortic aneurysms. *Int J Mol Med.* (2007) 20:391–5.

43. Wallinder J, Skagius E, Bergqvist D, Henriksson AE. Early inflammatory response in patients with ruptured abdominal aortic aneurysm. *Vasc Endovascular Surg.* (2010) 44:32–5.

44. Wang L, Hu C, Dong Y, Dai F, Xu Y, Dai Y, et al. Silencing IL12p35 promotes angiotensin II-mediated abdominal aortic aneurysm through activating the STAT4 pathway. *Mediators Inflamm.* (2021) 2021:9450843. doi: 10.1155/2021/9450843

45. Xiao J, Wei Z, Chen X, Chen W, Zhang H, Yang C, et al. Experimental abdominal aortic aneurysm growth is inhibited by blocking the JAK2/STAT3 pathway. *Int J Cardiol.* (2020) 312:100–6. doi: 10.1016/j.ijcard.2020.03.072

46. Wang Z, Guo J, Han X, Xue M, Wang W, Mi L, et al. Metformin represses the pathophysiology of AAA by suppressing the activation of PI3K/AKT/mTOR/autophagy pathway in ApoE(−/−) mice. *Cell Biosci.* (2019) 9:68. doi: 10.1186/s13578-019-0332-9

47. Yang H, Sun Y, Li Q, Jin F, Dai Y. Diverse epigenetic regulations of macrophages in atherosclerosis. *Front Cardiovasc Med.* (2022) 9:868788. doi: 10.3389/fcvm.2022.868788

48. Henderson EL, Geng YJ, Sukhova GK, Whittemore AD, Knox J, Libby P. Death of smooth muscle cells and expression of mediators of apoptosis by T lymphocytes in human abdominal aortic aneurysms. *Circulation.* (1999) 99:96–104. doi: 10.1161/01.cir.99.1.96

49. Galle C, Schandene L, Stordeur P, Peignois Y, Ferreira J, Wautrecht JC, et al. Predominance of type 1 CD4+ T cells in human abdominal aortic aneurysm. *Clin Exp Immunol.* (2005) 142:519–27.

50. Gao H, Wang L, Ren J, Liu Y, Liang S, Zhang B, et al. Interleukin 2 receptor subunit beta as a novel hub gene plays a potential role in the immune microenvironment of abdominal aortic aneurysms. *Gene.* (2022) 827:146472. doi: 10.1016/j.gene.2022.146472

51. Lei C, Yang D, Chen S, Chen W, Sun X, Wu X, et al. Patterns of immune infiltration in stable and raptured abdominal aortic aneurysms: a gene-expression-based retrospective study. *Gene.* (2020) 762:145056. doi: 10.1016/j.gene.2020.145056

52. Amin HZ, Sasaki N, Yamashita T, Mizoguchi T, Hayashi T, Emoto T, et al. CTLA-4 protects against angiotensin II-induced abdominal aortic aneurysm formation in mice. *Sci Rep.* (2019) 9:8065. doi: 10.1038/s41598-019-44523-6

53. Ait-Oufella H, Wang Y, Herbin O, Bourcier S, Potteaux S, Joffre J, et al. Natural regulatory T cells limit angiotensin II-induced aneurysm formation and rupture in mice. *Arterioscler Thromb Vasc Biol.* (2013) 33:2374–9. doi: 10.1161/ATVBAHA.113.301280

54. Liu CL, Liu X, Zhang Y, Liu J, Yang C, Luo S, et al. Eosinophils protect mice from angiotensin-II perfusion-induced abdominal aortic aneurysm. *Circ Res.* (2021) 128:188–202. doi: 10.1161/CIRCRESAHA.120.318182

55. Zhai Z, Zhang X, Ding Y, Huang Z, Li Q, Zheng M, et al. Eugenol restrains abdominal aortic aneurysm progression with down-regulations on NF-kappaB and COX-2. *Phytother Res.* (2022) 36:928–37. doi: 10.1002/ptr.7358

56. Bi Y, Xiang D, Ge Z, Li F, Jia C, Song J. An interpretable prediction model for identifying N(7)-methylguanosine sites based on XGBoost and SHAP. *Mol Ther Nucleic Acids.* (2020) 22:362–72. doi: 10.1016/j.omtn.2020.08.022

57. Biros E, Moran CS, Rush CM, Gabel G, Schreurs C, Lindeman JH, et al. Differential gene expression in the proximal neck of human abdominal aortic aneurysm. *Atherosclerosis.* (2014) 233:211–8. doi: 10.1016/j.atherosclerosis.2013.12.017

58. Shi Y, Yang CQ, Wang SW, Li W, Li J, Wang SM. Characterization of Fc gamma receptor IIb expression within abdominal aortic aneurysm. *Biochem Biophys Res Commun.* (2017) 485:295–300. doi: 10.1016/j.bbrc.2017.02.088

59. Vandestienne M, Zhang Y, Santos-Zas I, Al-Rifai R, Joffre J, Giraud A, et al. TREM-1 orchestrates angiotensin II-induced monocyte trafficking and promotes experimental abdominal aortic aneurysm. *J Clin Invest.* (2021) 131:e142468. doi: 10.1172/JCI142468

60. Zhang H, Bian C, Tu S, Yin F, Guo P, Zhang J, et al. Construction of the circRNA-miRNA-mRNA regulatory network of an abdominal aortic aneurysm to explore its potential pathogenesis. *Dis Markers.* (2021) 2021:9916881. doi: 10.1155/2021/9916881

61. Bi S, Liu R, He L, Li J, Gu J. Bioinformatics analysis of common key genes and pathways of intracranial, abdominal, and thoracic aneurysms. *BMC Cardiovasc Disord.* (2021) 21:14. doi: 10.1186/s12872-020-01838-x

62. Chebath J, Benech P, Revel M, Vigneron M. Constitutive expression of (2'-5') oligo A synthetase confers resistance to picornavirus infection. *Nature.* (1987) 330:587–8. doi: 10.1038/330587a0

63. Li Y, Banerjee S, Wang Y, Goldstein SA, Dong B, Gaughan C, et al. Activation of RNase L is dependent on OAS3 expression during infection with diverse human viruses. *Proc Natl Acad Sci USA.* (2016) 113:2241–6. doi: 10.1073/pnas.1519657113

64. Pichlmair A, Lassnig C, Eberle CA, Gorna MW, Baumann CL, Burkard TR, et al. IFIT1 is an antiviral protein that recognizes 5'-triphosphate RNA. *Nat Immunol.* (2011) 12:624–30. doi: 10.1038/ni.2048

65. Mahonen K, Hau A, Bondet V, Duffy D, Eklund KK, Panelius J, et al. Activation of NLRP3 inflammasome in the skin of patients with systemic and cutaneous lupus erythematosus. *Acta Derm Venereol.* (2022) 102:adv00708. doi: 10.2340/actadv.v102.2293

66. Luo S, Wu R, Li Q, Zhang G. Epigenetic regulation of IFI44L expression in monocytes affects the functions of monocyte-derived dendritic cells in systemic lupus erythematosus. *J Immunol Res.* (2022) 2022:4053038. doi: 10.1155/2022/4053038

67. Jet T, Gines G, Rondelez Y, Taly V. Advances in multiplexed techniques for the detection and quantification of microRNAs. *Chem Soc Rev.* (2021) 50:4141–61. doi: 10.1039/D0CS00609B

frontiers | Frontiers in Cardiovascular Medicine

TYPE Original Research
PUBLISHED 13 September 2022
DOI 10.3389/fcvm.2022.950588

Check for updates

OPEN ACCESS

EDITED BY
Zhenjie Liu,
The Second Affiliated Hospital of Zhejiang University School of Medicine, China

REVIEWED BY
Ravi Kant Narayan,
Dr. B. C. Roy Multispeciality Medical Research Center (Under IIT Kharagpur), India
Li Yin,
University of Virginia, United States
Wenjie Tian,
Massachusetts General Hospital and Harvard Medical School, United States

*CORRESPONDENCE
Jingli Pan
panjl@enzemed.com
Wenjun Zhao
zhaowj@enzemed.com

†These authors have contributed equally to this work and share first authorship

‡These authors have contributed equally to this work and share last authorship

SPECIALTY SECTION
This article was submitted to General Cardiovascular Medicine, a section of the journal Frontiers in Cardiovascular Medicine

RECEIVED 23 May 2022
ACCEPTED 15 August 2022
PUBLISHED 13 September 2022

CITATION
Wang X, Jin S, Wang Q, Liu J, Li F, Chu H, Zheng D, Zhang X, Ding J, Pan J and Zhao W (2022) Reference values of normal abdominal aortic areas in Chinese population measured by contrast-enhanced computed tomography.
Front. Cardiovasc. Med. 9:950588.
doi: 10.3389/fcvm.2022.950588

COPYRIGHT
© 2022 Wang, Jin, Wang, Liu, Li, Chu, Zheng, Zhang, Ding, Pan and Zhao. This is an open-access article distributed under the terms of the Creative Commons Attribution License (CC BY). The use, distribution or reproduction in other forums is permitted, provided the original author(s) and the copyright owner(s) are credited and that the original publication in this journal is cited, in accordance with accepted academic practice. No use, distribution or reproduction is permitted which does not comply with these terms.

Reference values of normal abdominal aortic areas in Chinese population measured by contrast-enhanced computed tomography

Xiang Wang[1†], Shasha Jin[2†], Qing Wang[3†], Jiawei Liu[1], Fei Li[1], Haiwei Chu[1], Dexing Zheng[1], Xiaolong Zhang[1], Jianrong Ding[4], Jingli Pan[4*‡] and Wenjun Zhao[1*‡]

[1]Department of Vascular Surgery, Taizhou Hospital of Zhejiang Province, Wenzhou Medical University, Linhai, China, [2]Department of Information and Technology Center, Taizhou Hospital of Zhejiang Province, Wenzhou Medical University, Linhai, China, [3]Department of Central Laboratory, Taizhou Hospital of Zhejiang Province, Wenzhou Medical University, Linhai, China, [4]Department of Radiology, Taizhou Hospital of Zhejiang Province, Wenzhou Medical University, Linhai, China

Objective: To generate reference values of the normal areas of the abdominal aorta at various levels among Chinese people and to explore the factors that may promote the expansion of the abdominal aorta.

Methods: The areas of normal abdominal aortas were gauged at various levels based on inner-to-inner measurements in 1,066 Chinese adult patients (>18 years) without the abdominal aortic disease. The areas of subphrenic abdominal, suprarenal abdominal, infrarenal abdominal, and distal abdominal aortas were measured. The demographic and clinical characteristics were collected into a specifically designed electronic database. Multivariable linear regression was used to analyze the potential risk factors promoting the expansion of the abdominal aorta.

Results: In males, the median areas of the subphrenic abdominal aorta, suprarenal abdominal aorta, infrarenal abdominal aorta, and distal abdominal aorta were 412.1, 308.0, 242.2, and 202.2 mm^2, respectively. In females, the median areas of the subphrenic abdominal aorta, suprarenal abdominal aorta, infrarenal abdominal aorta, and distal abdominal aorta were 327.7, 243.4, 185.4, and 159.6 mm^2, respectively. The areas of the abdominal aorta at different levels were larger in males than in females and increased with age. Multiple linear stepwise regression analysis showed that the subphrenic abdominal aortic area was significantly related to age ($\beta = 0.544$, $p < 0.001$), sex ($\beta = 0.359$, $p < 0.001$), and hypertension ($\beta = 0.107$, $p < 0.001$). Suprarenal abdominal aortic area was related to age ($\beta = 0.398$, $p < 0.001$), sex ($\beta = 0.383$, $p < 0.001$), history of smoking ($\beta = 0.074$, $p = 0.005$), and hypertension ($\beta = 0.111$, $p < 0.001$). The infrarenal abdominal aortic area was correlated with age ($\beta = 0.420$, $p < 0.001$), sex ($\beta = 0.407$, $p < 0.001$), and history of smoking ($\beta = 0.055$, $p = 0.036$). The distal abdominal aortic area was correlated with age

(β = 0.463, $p < 0.001$), sex (β = 0.253, $p < 0.001$), and hypertension (β = 0.073, $p = 0.013$).

Conclusion: The abdominal aortic areas at different levels were larger in males than in females. Aging, hypertension, and smoking prompt the expansion of abdominal aorta.

KEYWORDS

abdominal aortic area, reference value, contrast-enhanced computed tomography, abdominal aortic aneurysm, diameter

Introduction

Abdominal aortic aneurysm (AAA) is generally defined as an enlargement of the abdominal aorta with a maximum diameter ≥ 3.0 cm or as a focal dilation ≥ 1.5 times the diameter of the normal aorta. Surgical repair is recommended for patients with AAA with a maximum diameter > 5.5 cm in males and 5.0 cm in females (1). Larger diameter aneurysms have a higher risk of rupture (2). Hence, at present, the maximum diameter plays an important role in the management of an AAA.

However, some scholars have also raised questions about the use of maximum diameter in AAA management. They demonstrated that AAA-related complications, neck-related events, and secondary interventions were not associated with the largest AAA diameter in patients with AAA (3). Therefore, they considered that the maximum abdominal aortic diameter may not be the best indicator for AAA management. Moreover, these studies have suggested other indicators that are more sensitive in predicting AAA progression, such as c-reactive protein (CRP), insulin-like growth factor 1 (IGF-1), antiphospholipid (APL) antibodies, and matrix metalloproteinase-9 (MMP-9) (4). One of the most discussed surrogates was the flow lumen area of an AAA. The shapes of cross-sections of an AAA perpendicular to its center lumen line are not always circular. Hence, the maximum diameter cannot fully represent the morphology of the AAA. Current studies have shown that the flow lumen area is more robust in predicting the rupture risk of AAAs (5). Therefore, the normal area of the abdominal aorta needs to be defined to provide a detailed reference for diagnosing an AAA and help make proper clinical decisions.

Given that few studies have reported normal abdominal aortic areas at different levels, this study gauged the areas of the abdominal aorta in Chinese adults without AAA at various levels and explored the factors that may promote the expansion of the abdominal aorta.

Materials and methods

Study sample

A retrospective study was performed to determine the normal abdominal aortic areas at different levels in hospitalized adult patients (>18 years) without AAA who had undergone abdominal contrast-enhanced computed tomography (CT) scans from July 2021 to December 2021. The exclusion criteria were a history of aortic diseases (aneurysm, dissection, and intramural hematoma).

Imaging technology and information collection

A 256-row CT or a 64-row CT (Revolution Apex CT or Discovery CT 750 HD CT, GE Healthcare) was used for examination. Scanning parameters were as follows: the tube voltage,100–120 kv; tube current, 200–250 mA; thickness,5 mm; gantry rotation time, 0.5 s; and the scanning range was from diaphragm top to pubic symphysis.

In total, two experienced radiologists independently investigated the CT images captured from 1,066 patients independently using the Vessel IQ software on an offline workstation (Advantage Workstation 4.7, GE Healthcare). The areas of aortic cross-sections perpendicular to the aorta's center lumen line were gauged based on inner-to-inner measurements at four levels: the subphrenic abdominal aorta (**Figure 1A**), suprarenal abdominal aorta (**Figure 1B**), infrarenal abdominal aorta (**Figure 1C**), and distal abdominal aorta (**Figure 1D**). For each level of every aorta, the average area was calculated and subjected to subsequent analysis.

The demographic and clinical characteristics were collected into a specifically designed electronic database.

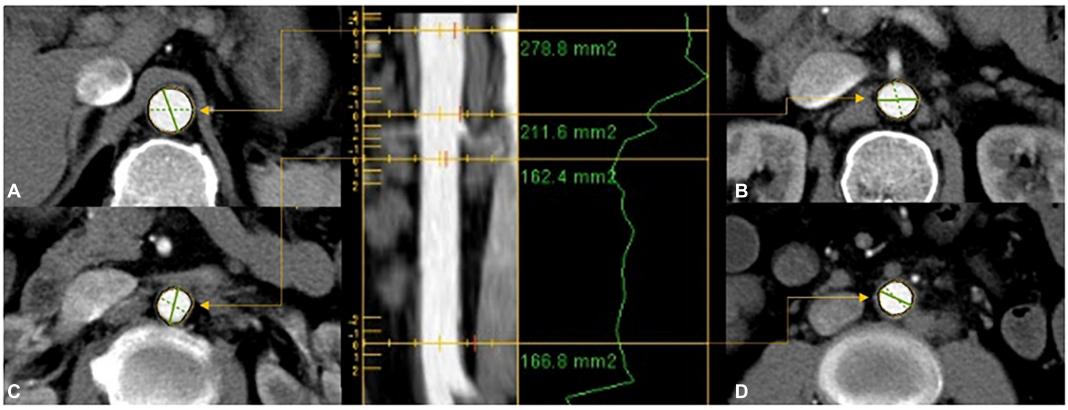

FIGURE 1
The areas of aortic cross-sections were gauged based on inner-to-inner measurements at four levels: **(A)** proximal abdominal aorta; **(B)** suprarenal abdominal aorta; **(C)** infrarenal abdominal aorta; **(D)** distal abdominal aorta.

The body mass index (BMI) and body surface area (BSA) was calculated by the following formula.

$$\text{BMI} = \frac{\text{Weight(kg)}}{\text{Height}^2(\text{m}^2)}$$

$$\text{BSA} = 0.007184 \times \text{W(kg)}0.425 \times \text{H(cm)}\ 0.725$$

Statistical analysis

Statistical analysis was performed using statistical package for social sciences (SPSS 26.0). Continuous variables data are reported as the mean ± standard deviation. The patients were grouped by age with an interval of 10 years. For each group, different percentiles (5th, 25th, 50th, 75th, and 95th) of abdominal aortic areas were calculated. Gender-based subgroup analysis was performed. Categorical and ordinal data are reported as frequencies and percentages. Linear regression was used to determine potential risk factors promoting the expansion of the abdominal aorta. Comparisons between groups were performed by Student's *t*-tests for normally distributed data with homogeneous variances or by non-parametric Mann–Whitney Wilcoxon test. Kruskal-Wallis test followed by Dunn's multiple comparisons test were used to compare data among groups of ≥ 3 with non-normal distributions. A two-sided, p-value < 0.05 was considered statistically significant.

Results

Patient characteristics

From July 2021 to December 2021, 1,087 adult patients have undergone abdominal contrast-enhanced CT scans. According to the exclusion criteria, 21 patients were excluded (15 patients had AAA, 4 patients had abdominal aortic intramural hematoma, and 2 patients had abdominal aortic dissection). At last, 1,066 patients were included in our study.

The average age of all 1,066 patients was 61.32 ± 14.61 years (range from 18 to 95 years). 608 patients (57.0%) were male, with an average age of 62.08 ± 14.50 years (range from 18 to 95 years), and 458 patients (43.0%) were female, with an average age of 60.31 ± 14.71 years (range from 18 to 93 years). The characteristics of the patients are presented in Table 1.

TABLE 1 Clinical characteristic of 1,066 subjects.

Variables	Male	Female	Overall
N	608 (57.0)	458 (43.0)	1,066
Age	62.08 ± 14.50	60.31 ± 14.71	61.32 ± 14.61
Weight (kg)	66.10 ± 11.07	57.04 ± 9.45	62.28 ± 11.37
Height (cm)	167.56 ± 6.47	156.79 ± 6.33	162.92 ± 8.36
BMI	23.51 ± 3.73	23.21 ± 3.59	23.43 ± 3.58
BSA	24.56 ± 4.71	19.83 ± 3.64	22.58 ± 4.86
History of smoking (%)	182 (29.9)	2 (0.4)	184 (17.3)
History of drinking (%)	103 (16.9)	1 (0.2)	104 (9.8)
Hypertension (%)	182 (29.9)	133 (29.0)	315 (29.5)
Diabetes (%)	65 (10.7)	61 (13.3)	126 (11.8)
Cardiovascular disease (%)[a]	55 (9.0)	37 (8.1)	92 (8.6)
Digestive system disease (%)[b]	512 (84.2)	355 (77.5)	867 (81.3)
Respiratory system disease (%)[c]	139 (22.9)	75 (16.4)	214 (20.1)
Urinary system disease (%)[d]	90 (14.8)	42 (9.2)	132 (12.4)
Cerebrovascular disease (%)[e]	54 (8.9)	40 (8.7)	94 (8.8)

Continuous variables data are given as mean ± standard deviation.
BMI, body mass index; BSA, body surface area.
[a]Mainly ischemic heart disease.
[b]Mainly digestive cancer.
[c]Mainly chronic obstructive pulmonary disease.
[d]Including renal impairment and urinary cancer.
[e]Including transient ischemic attack, reversible ischemic neurologic deficit, and stroke.

Reference values for abdominal aortic areas

In males, the median areas of the subphrenic abdominal aorta, suprarenal abdominal aorta, infrarenal abdominal aorta, and distal abdominal aorta were 412.1, 308.0, 242.2 and 202.2 mm^2, respectively. In females, the median areas of the subphrenic abdominal aorta, suprarenal abdominal aorta, infrarenal abdominal aorta, and distal abdominal aorta were 327.7, 243.4, 185.4 and 159.6 mm^2, respectively. The areas of abdominal aorta at different levels were larger in males than in females and increased with age ($p < 0.05$ for all levels). The values for 5th, 25th, 50th, 75th, and 95th percentiles of the abdominal aortic areas at different levels are shown in **Table 2**. The distributions of abdominal aortic areas at different levels grouped by age and sex are shown in **Figure 2**.

Abdominal aortic areas were reduced from the subphrenic abdominal aorta to the distal abdominal aorta. The reduction was 50.9% in males and 51.3% in females.

Expansion rate of abdominal aortic areas

The areas of abdominal aorta increased with age in both males and females ($p < 0.001$ for all aortic levels). Comparing the oldest group to the youngest group, the increase rate of the subphrenic abdominal aortic areas was the fastest (108.7% in males, 106.0% in females), followed by those of the suprarenal abdominal aortic areas were the second (75.3% in males, 72.7% in females), the infrarenal abdominal aortic areas were the third (71.1% in males, 65.7% in females), and distal abdominal aortic areas were the slowest (68.3% in males, 61.7% in females).

Related influencing factors

Multiple linear stepwise regression analysis showed that the subphrenic abdominal aortic areas were significantly related to age (β = 0.544, $p < 0.001$), sex (β = 0.359, $p < 0.001$), and hypertension (β = 0.107, $p < 0.001$). The suprarenal abdominal aortic areas were related to age (β = 0.398, $p < 0.001$), sex (β = 0.383, $p < 0.001$), history of smoking (β = 0.074, $p = 0.005$), and hypertension (β = 0.111, p < 0.001). The infrarenal abdominal aortic areas were correlated with age (β = 0.420, $p < 0.001$), sex (β = 0.407, $p < 0.001$), and history of smoking (β = 0.055, $p = 0.036$). The distal abdominal aortic area was correlated with age (β = 0.463, $p < 0.001$), sex (β = 0.253, $p < 0.001$), and hypertension (β = 0.073, $p = 0.013$). The multiple linear regression Equation is as follows:

$$\text{Area}_{\text{subphrenic}} = 111.088 + 3.631X_1 + 70.728X_2 + 22.952X_3 (R^2 = 0.491)$$

$$\text{Area}_{\text{suprarenal}} = 121.582 + 1.981X_1 + 56.354X_2 + 17.752X_3 + 14.297X_4 (R^2 = 0.385)$$

$$\text{Area}_{\text{infrarenal}} = 84.400 + 1.743X_1 + 49.805X_2 + 8.791X_4 (R^2 = 0.382)$$

$$\text{Area}_{\text{distal}} = 87.150 + 1.221X_1 + 37.733X_2 + 11.404X_3 (R^2 = 0.324)$$

X_1 is age (year), X_2 is sex (male is 1 and female is 0), X_3 is hypertension, and X_4 is the history of smoking.

Discussion

This study is the first to present the reference areas for the abdominal aorta in the normal Chinese adult population.

In our study, the respective median areas of the subphrenic abdominal aorta, suprarenal abdominal aorta, infrarenal abdominal aorta, and distal abdominal aorta were 412.1, 308.0, 242.2, and 202.2 mm^2 in males. In females, the median areas of the subphrenic abdominal aorta, suprarenal abdominal aorta, infrarenal abdominal aorta, and distal abdominal aorta were 327.7, 243.4, 185.4, and 159.6 mm^2, respectively. The area of the abdominal aorta decreased from proximal to distal. The different levels of abdominal aortic areas were lower in females than in males, which is consistent with published studies on abdominal aortic diameters (6–10).

The areas of the abdominal aorta were significantly increased with age. The most obvious is the subphrenic abdominal aorta. Comparing the subphrenic abdominal aortic areas between the 80+ years group and the 18–29 years group, the increase rate reached 108.7% in males and 106.0% in females. The distal abdominal aortic areas dilated the slowest, but also reached 68.3% in males and 61.7% in females. The abdominal aortic diameters also increased with age (7, 10–13). Our previous study showed a growth rate of 26.54% in the infrarenal abdominal aortic diameters compared between the 18–29 years old group and the 80–99 years old group (10). In this study, the infrarenal abdominal aortic area increased 71.1% in males and 65.7% in females. The increase rate of abdominal aortic areas was more obvious than the increase in abdominal aortic diameter. In a hemodynamic study of ruptured AAAs, an increase in the cross-sectional area of the flow lumen preceded an increase in AAA diameter (14). For the management of AAA, abdominal aortic areas may be a more sensitive indicator.

Our study found that abdominal aortic areas at different levels were positively correlated with age, sex, and hypertension. A history of smoking was also a positive factor of partial abdominal aortic area. This is similar to the factors associated with abdominal aortic diameter (15). Female sex was associated

TABLE 2 Age- and sex-specific percentiles of abdominal aortic areas (mm^2) in the study sample.

Abdominal aorta	Age (years)	Male						Female					
		Percentiles						Percentiles					
		n	5th	25th	50th	75th	95th	*n*	5th	25th	50th	75th	95th
Subphrenic	18–29	21	132.2	173.2	241.2	273.8	344.5	20	133.6	166.3	205.1	231.3	260.8
	30–39	24	242.6	256.7	282.2	322.1	444.2	22	166.1	189.5	240.2	294.1	366.5
	40–49	51	223.6	293.7	350.8	386.6	531	55	190.5	240.1	267.4	299.1	350.4
	50–59	154	283.2	343.8	386.8	442.5	551.3	108	232.3	274.0	307.5	345.4	425.1
	60–69	162	324.9	388.3	421.8	457.7	547.8	115	262.3	311.1	343.9	403.6	457.2
	70–79	132	348.0	395.5	450.0	505.7	603.2	103	282.0	342.1	383.7	440.5	510.0
	80+	64	327.5	428.9	503.5	542.1	620.3	35	241.2	342.2	422.4	483.3	578.9
Suprarenal	18–29	21	111.5	128.5	191.8	239.9	325.9	20	121.0	145.7	160.9	179.7	205.8
	30–39	24	173.9	210.3	249.6	273.9	417.2	22	121.6	164.7	194.8	234.1	296.0
	40–49	51	176.7	233.8	283.3	317.8	421.5	55	148.7	181.4	210.6	227.9	282.2
	50–59	154	208.9	258.8	295.5	339.4	403.5	108	157.3	200.1	232.9	259.1	311.9
	60–69	162	226.7	280.7	313.0	359.4	405.7	115	187.4	218.2	255.1	285.2	373.0
	70–79	132	241.0	295.3	328.3	362.3	434.9	103	185.3	236.8	273.3	298.1	373.2
	80+	64	244.5	306.3	336.3	390.3	465.5	35	174.8	232.2	277.8	346.2	395.3
Infrarenal	18–29	21	91.9	126.4	165.2	199.7	243.3	20	92.9	113.8	129.9	150.3	170.8
	30–39	24	127.4	164.3	185.1	207.4	315.1	22	90.5	130.2	149.3	168.4	219.0
	40–49	51	150.2	187.3	215.1	249.7	306.5	55	118.7	138.2	152.3	173.9	210.9
	50–59	154	149.1	197.8	230.2	265.3	341.5	108	114.2	149.8	171.7	202.7	236.4
	60–69	162	171.6	217.2	247.1	288.1	344.6	115	135.4	171.1	199.8	229.6	278.3
	70–79	132	172.6	224.9	261.1	288.6	360.3	103	144.9	184.4	205.5	242.4	292.2
	80+	64	208.0	243.8	282.7	312.7	397.1	35	129.0	189.7	215.2	246.3	342.0
Distal	18–29	21	100.4	119.1	134.4	170.6	272.3	20	76.3	106.9	113.3	129.3	159.5
	30–39	24	119.7	154.4	163.3	176.4	285.1	22	76.9	109.1	128.3	150.3	165.7
	40–49	51	121.5	159.8	180.0	199.9	246.7	55	96.5	120.3	135.7	153.9	177
	50–59	154	136.9	172.3	197.2	219.3	273.8	108	109.1	136.2	151.9	169.4	217.2
	60–69	162	139.6	174.2	210.3	233.8	264.4	115	111.7	145.3	170.1	192.4	246.7
	70–79	132	151.8	183.2	213.4	238.3	302.9	103	116.9	158.6	182.5	209.1	253.4
	80+	64	157.3	198.1	226.2	255.5	362.6	35	122.5	152.8	183.2	213.4	293.5

with 70.728, 56.354, 45.354, 37.733 mm^2 reductions in the subphrenic abdominal aorta, suprarenal abdominal aorta, infrarenal abdominal aorta, and distal abdominal aorta, respectively. Hypertension was associated with 22.952, 17.752, and 11.404 mm^2 increases in the subphrenic abdominal aorta, suprarenal abdominal aorta, and distal abdominal aorta, respectively. A history of smoking was associated with 14.297 and 8.791 mm^2 increases in suprarenal abdominal aorta and infrarenal abdominal aorta, respectively. The subphrenic abdominal aorta, suprarenal abdominal aorta, infrarenal abdominal aorta, and distal abdominal aorta will expand 36.31, 19.81, 17.43, and 12.21 mm^2, respectively, for 10 years.

The abdominal aortic diameter is currently a standard for the diagnosis and treatment of AAA, and it is an accessible and valid indicator. However, small diameter AAA can also rupture (16, 17). Therefore, finding other predictors of aneurysm expansion could identify high-risk patients, indicate early intervention, prevent disease progression, and reduce morbidity and mortality. In the past, limitations in medical technology precluded obtaining more image information, but the development and popularization of technology have provided increasingly abundant information from images. This information warrants exploration to improve the management of AAA.

At present, endovascular aneurysm repair (EVAR) is a mainstream method for the treatment of AAA. Compared with open surgery, EVAR is advantageous because it is less invasive and associated with fewer perioperative complications (18, 19). The size of the stent in the EVAR evaluation by the surgeon is mainly calculated based on the diameter of the abdominal aorta at the anchoring sites. After being released, the shape of a stent's proximal end will be adjusted according to the

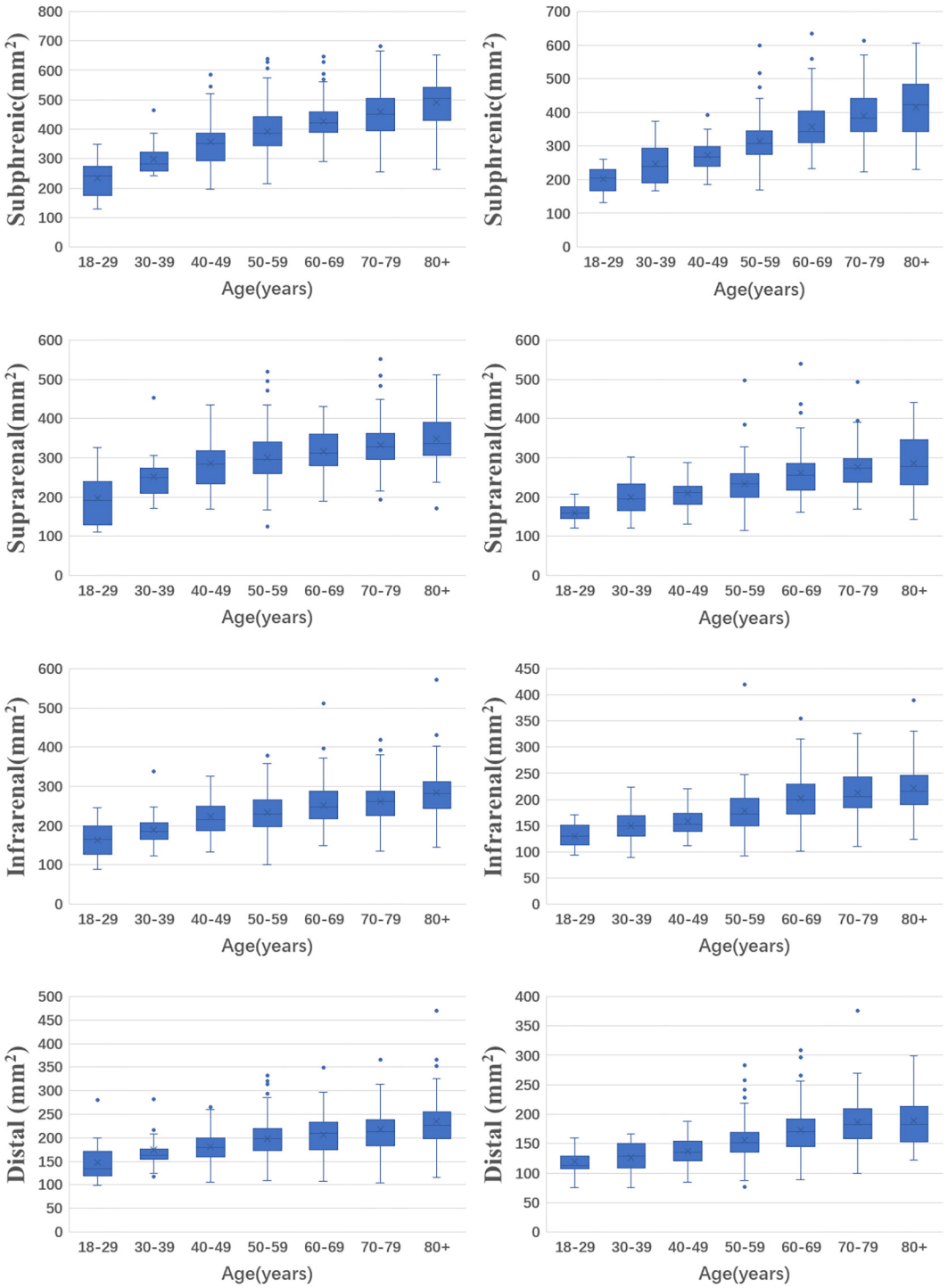

FIGURE 2
The distributions of abdominal aortic areas with age and sex in different levels. (The left column is for men and the right column is for women).

shape of the anchoring site of the abdominal aorta. Poor-fitting between stents and the anchoring sites may lead to endoleak. In clinical practice, oversized stents are usually chosen to solve this problem (20). However, the choice of oversize remains controversial, and selecting the stent according to the area of the anchoring sites may be preferable. Further research is needed. This study was limited by the sample size of patients aged 18–39 years. This study is a single-center study, and it may not fully

represent the Chinese population. A larger population-based study is needed.

Conclusion

The abdominal aortic areas at different levels were larger in males than in females. Aging, hypertension, and smoking prompt the expansion of the abdominal aorta.

Data availability statement

The raw data supporting the conclusions of this article will be made available by the authors, without undue reservation.

Ethics statement

The studies involving human participants were reviewed and approved by the Taizhou Hospital of Zhejiang Province Ethic Committee. Written informed consent for participation was not required for this study in accordance with the national legislation and the institutional requirements.

Author contributions

XW, SJ, JP, and WZ contributed to the conception and design. JP and JD performed the measurement of the abdominal aortic area. XW, SJ, QW, JL, FL, HC, DZ, and XZ performed the clinical data collection and interpretation. XW and SJ analyzed the datasets and wrote the manuscript. All authors read and approved the final manuscript.

Conflict of interest

The authors declare that the research was conducted in the absence of any commercial or financial relationships that could be construed as a potential conflict of interest.

Publisher's note

All claims expressed in this article are solely those of the authors and do not necessarily represent those of their affiliated organizations, or those of the publisher, the editors and the reviewers. Any product that may be evaluated in this article, or claim that may be made by its manufacturer, is not guaranteed or endorsed by the publisher.

References

1. Chaikof EL, Dalman RL, Eskandari MK, Jackson BM, Lee WA, Mansour MA, et al. The Society for Vascular Surgery practice guidelines on the care of patients with an abdominal aortic aneurysm. *J Vasc Surg.* (2018) 67:2–77.e2. doi: 10.1016/j.jvs.2017.10.044

2. Parkinson F, Ferguson S, Lewis P, Williams IM, Twine CP, South East Wales Vascular Network [SEWVN]. Rupture rates of untreated large abdominal aortic aneurysms in patients unfit for elective repair. *J Vasc Surg.* (2015) 61:1606–12. doi: 10.1016/j.jvs.2014.10.023

3. Soares Ferreira R, Verhagen HJM, Bastos Gonçalves F. Space matters! Maximum abdominal aortic aneurysm diameter is a rough surrogate for luminal volume. *J Vasc Surg.* (2021) 74:1769–70. doi: 10.1016/j.jvs.2021.04.061

4. Li Y, Yang D, Zheng Y. Challenges of applying circulating biomarkers for abdominal aortic aneurysm progression. *Exp Biol Med (Maywood).* (2021) 246:1054–9. doi: 10.1177/1535370221992530

5. Siika A, Lindquist Liljeqvist M, Hultgren R, Gasser TC, Roy J. Aortic lumen area is increased in ruptured abdominal aortic aneurysms and correlates to biomechanical rupture risk. *J Endovasc Ther.* (2018) 25:750–6. doi: 10.1177/1526602818808292

6. Zhu F, Arshi B, Ikram MA, De Knegt RJ, Kavousi M. Sex-specific normal values and determinants of infrarenal abdominal aortic diameter among non-aneurysmal elderly population. *Sci Rep.* (2021) 11:17762. doi: 10.1038/s41598-021-97209-3

7. Rogers IS, Massaro JM, Truong QA, Mahabadi AA, Kriegel MF, Fox CS, et al. Distribution, determinants, and normal reference values of thoracic and abdominal aortic diameters by computed tomography (from the Framingham Heart Study). *Am J Cardiol.* (2013) 111:1510–6. doi: 10.1016/j.amjcard.2013.01.306

8. Norman PE, Muller J, Golledge J. The cardiovascular and prognostic significance of the infrarenal aortic diameter. *J Vasc Surg.* (2011) 54:1817–20. doi: 10.1016/j.jvs.2011.07.048

9. Mensel B, Heßelbarth L, Wenzel M, Kühn JP, Dörr M, Völzke H, et al. Thoracic and abdominal aortic diameters in a general population: MRI-based reference values and association with age and cardiovascular risk factors. *Eur Radiol.* (2016) 26:969–78. doi: 10.1007/s00330-015-3926-6

10. Wang X, Zhao WJ, Shen Y, Zhang RL. Normal diameter and growth rate of infrarenal aorta and common iliac artery in chinese population measured by contrast-enhanced computed tomography. *Ann Vasc Surg.* (2020) 62:238–47. doi: 10.1016/j.avsg.2019.05.030

11. Yao GH, Deng Y, Liu Y, Xu MJ, Zhang C, Deng YB, et al. Echocardiographic measurements in normal chinese adults focusing on cardiac chambers and great arteries: A prospective, nationwide, and multicenter study. *J Am Soc Echocardiogr.* (2015) 28:570–9. doi: 10.1016/j.echo.2015.01.022

12. Lederle FA, Johnson GR, Wilson SE, Gordon IL, Chute EP, Littooy FN, et al. Relationship of age, gender, race, and body size to infrarenal aortic diameter. The aneurysm detection and management (ADAM) veterans affairs cooperative study investigators. *J Vasc Surg.* (1997) 26:595–601. doi: 10.1016/s0741-5214(97)70057-0

13. Allison MA, Kwan K, DiTomasso D, Wright CM, Criqui MH. The epidemiology of abdominal aortic diameter. *J Vasc Surg.* (2008) 48:121–7. doi: 10.1016/j.jvs.2008.02.031

14. McClarty DB, Kuhn DCS, Boyd AJ. Hemodynamic changes in an actively rupturing abdominal aortic aneurysm. *J Vasc Res.* (2021) 58:172–9. doi: 10.1159/000514237

15. Chen T, Yang X, Fang X, Tang L, Zhang Y, Weng Y, et al. Potential influencing factors of aortic diameter at specific segments in population with cardiovascular risk. *BMC Cardiovasc Disord.* (2022) 22:32. doi: 10.1186/s12872-022-02479-y

16. Lo RC, Lu B, Fokkema MT, Conrad M, Patel VI, Fillinger M, et al. Relative importance of aneurysm diameter and body size for predicting abdominal aortic

aneurysm rupture in men and women. *J Vasc Surg.* (2014) 59:1209–16. doi: 10.1016/j.jvs.2013.10.104

17. Bellamkonda KS, Nassiri N, Sadeghi MM, Zhang Y, Guzman RJ, Ochoa Chaar CI. Characteristics and outcomes of small abdominal aortic aneurysm rupture in the American College of Surgeons National Surgical Quality Improvement Program database. *J Vasc Surg.* (2021) 74:729–37. doi: 10.1016/j.jvs.2021.01.063

18. Antoniou GA, Antoniou SA, Torella F. Editor's choice - endovascular vs. open repair for abdominal aortic aneurysm: Systematic review and meta-analysis of updated peri-operative and long term data of randomised controlled trials. *Eur J Vasc Endovasc Surg.* (2020) 59:385–97. doi: 10.1016/j.ejvs.2019.11.030

19. Scallan O, Novick T, Power AH, DeRose G, Duncan A, Dubois L. Long-term outcomes comparing endovascular and open abdominal aortic aneurysm repair in octogenarians. *J Vasc Surg.* (2020) 71:1162–8. doi: 10.1016/j.jvs.2019.06.207

20. Charlton-Ouw KM, Ikeno Y, Bokamper M, Zakhary E, Smeds MR, GREAT participants. Aortic endograft sizing and endoleak, reintervention, and mortality following endovascular aneurysm repair. *J Vasc Surg.* (2021) 74:1519–26.e2. doi: 10.1016/j.jvs.2021.04.045

frontiers | Frontiers in Cardiovascular Medicine

TYPE Original Research
PUBLISHED 14 September 2022
DOI 10.3389/fcvm.2022.913661

Check for updates

OPEN ACCESS

EDITED BY
Wei Wang,
Xiangya Hospital, Central South University, China

REVIEWED BY
Dayun Sui,
Department of Pharmacology, Jilin University, China
Hao Yue,
Changchun University of Chinese Medicine, China

*CORRESPONDENCE
Hong-song Wang
wanghongsong@ahtcm.edu.cn
Xiao-yu Cheng
Cxy478@163.com

†These authors have contributed equally to this work

SPECIALTY SECTION
This article was submitted to General Cardiovascular Medicine, a section of the journal Frontiers in Cardiovascular Medicine

RECEIVED 06 April 2022
ACCEPTED 21 July 2022
PUBLISHED 14 September 2022

CITATION
Hong L-l, Zhao Y, Chen W-d, Yang C-y, Li G-z, Wang H-s and Cheng X-y (2022) Tentative exploration of pharmacodynamic substances: Pharmacological effects, chemical compositions, and multi-components pharmacokinetic characteristics of ESZWD in CHF-HKYd rats. *Front. Cardiovasc. Med.* 9:913661. doi: 10.3389/fcvm.2022.913661

COPYRIGHT
© 2022 Hong, Zhao, Chen, Yang, Li, Wang and Cheng. This is an open-access article distributed under the terms of the Creative Commons Attribution License (CC BY). The use, distribution or reproduction in other forums is permitted, provided the original author(s) and the copyright owner(s) are credited and that the original publication in this journal is cited, in accordance with accepted academic practice. No use, distribution or reproduction is permitted which does not comply with these terms.

Tentative exploration of pharmacodynamic substances: Pharmacological effects, chemical compositions, and multi-components pharmacokinetic characteristics of ESZWD in CHF-HKYd rats

Li-li Hong[1,2,3,4†], Yan Zhao[1,2,3,4†], Wei-dong Chen[1,2,3,4], Chen-yu Yang[1,2,3,4], Guo-zhuan Li[1,2,3,4], Hong-song Wang[1,2,3,4*] and Xiao-yu Cheng[5*]

[1]School of Pharmacy, Anhui University of Chinese Medicine, Hefei, China, [2]Anhui Province Key Laboratory of Chinese Medicinal Formula, School of Pharmacy, Anhui University of Chinese Medicine, Hefei, China, [3]Synergetic Innovation Center of Anhui Authentic Chinese Medicine Quality Improvement, School of Pharmacy, Anhui University of Chinese Medicine, Hefei, China, [4]MOE-Anhui Joint Collaborative Innovation Center for Quality Improvement of Anhui Genuine Chinese Medicinal Materials, School of Pharmacy, Anhui University of Chinese Medicine, Hefei, China, [5]Department of Geriatric Cardiology, First Affiliated Hospital of Anhui University of Chinese Medicine, Anhui University of Traditional Chinese Medicine, Hefei, China

The chemical components of Xin'an famous prescription Ershen Zhenwu Decoction (ESZWD) are still unclear. The results showed that ESZWD could significantly reduce left ventricular end diastolic diameter, decrease N-terminal pro-brain natriuretic peptide (NT-proBNP), angiotensinII, aldosterone, reactive oxygen species, and malondialdehyde, increase serum superoxide dismutase, while had no significant effect on inflammatory factors. Ultra-performance liquid chromatography/quadrupole-time-of-flight mass spectrometry (UPLC/Q-TOF-MS) analysis detected 30 prototype components in model rats' serum, mainly including alkaloids, saponins, terpenoids, tanshinones, phenols. UPLC-MS/MS successfully detected the pharmacokinetic parameters of four components, and correlation analysis shows that there are negative correlations between four compounds and serum NT-proBNP. Thirty components of ESZWD may play a therapeutic role in chronic heart failure with heart-kidney Yang deficiency (CHF-HKYd) by improving myocardial injury, reducing oxidative stress levels, and inhibiting activation of the RAAS system in rats. Salsolinol, aconitine, paeoniflorin, and miltrione are equipped with potential characteristics as pharmacodynamic substances for ESZWD in treating CHF-HKYd. Additionally, the constituents of ESZWD in CHF-HKYd rats are different from normal rats, which provided a reference for the selection of subjects for further study.

KEYWORDS

Ershen Zhenwu Decoction, chronic heart failure with heart-kidney Yang deficiency, UPLC/Q-TOF-MS, pharmacokinetic, pharmacodynamic substances

Introduction

Chronic heart failure (CHF) is a complex clinical syndrome of ventricular ejection and/or filling caused by a variety of cardiac structural or functional diseases, it is the end-stage manifestation of cardiovascular diseases and the main cause of death. According to the epidemiological data in recent years, there are about 4.5 million patients with heart failure (HF) in China, accompanied by gender and regional differences (1, 2). In modern times, as a dual inhibitor of angiotensin receptor and enkephalin enzyme, shakubactrivalsartan has been listed in the international guidelines for HF, and its efficacy is remarkable. Regrettably, there are still some adverse reactions to shakubactrivalsartan, such as angioedema, hypotension, renal function impairment, hyperkalemia, and so on. Therefore, looking for a more appropriate therapeutic paradigm is currently a concern to be solved in CHF treatment. Under this situation, people gradually turn their attention to Traditional Chinese Medicine (TCM), which can greatly ameliorate the life quality and the medication compliance of patients as well as decrease the side effects compared with western medicine, they therefore have a good application prospect.

Ershen Zhenwu Decoction (ESZWD) is a classical prescription of Xin'an Cheng's internal medicine in treating CHF, which is composed of *Aconiti* Lateralis Radix Praeparata, *Poria*, *Atractylodis Macrocephalae* Rhizoma, *Paeoniae* Radix Alba, *Zingiberis Rhizoma* Recens, *Ginseng* Radix et Rhizoma Rubra and *Salviae Miltiorrhizae* Radix et Rhizoma, clinical records show that it has significant effects in the treatment of chronic heart failure with heart-kidney Yang deficiency (CHF-HKYd) (3–14). Despite the definite effects of ESZWD on CHF-HKYd, these findings still leave open the question that what are the effective material substances of this prescription. Due to the complex composition of TCM compounds, their efficacy has always been explained by TCM theories, in order to cope with this issue, the focus of modern TCM research is to explore the pharmacodynamic substances and mechanisms (15). Here, we refer to the idea of serum spectroscopic study, first, the chromatographic technique is used to characterize the chemical information of the serum components of TCM, and then the pharmacological experiments are combined to obtain the efficacy information of TCM, finally, the "spectrum-effect relationship" of TCM is constructed through relevant analysis methods. This research model remedy for the drawbacks of traditional spectrum effect research that the filtration and metabolism of TCM in the body are not taken into consideration (16), promotes the research of effective substances of TCM.

In the previous research of our group, the ultra-performance liquid chromatography/quadrupole time-of-flight mass spectrometry (UPLC/Q-TOF-MS) technology has been used to analyze the chemical components of ESZWD and its serum components in normal rats (17). In this present study, we set up to create the CHF-HKYd rat model by bilateral thyroidectomy combined with doxorubicin injection and explore the effects of ESZWD on model rats. Then, the chemical constituents profiling of ESZWD in CHF-HKYd rats serum was carried out by utilizing UPLC/Q-TOF-MS technology and screened out for representative chemical components. Finally, the pharmacokinetic parameters of the four chemical components in the model rats and the changes of serum N-terminal pro-brain natriuretic peptide (NT-proBNP) levels at different time points were determined by UPLC-MS/MS and ELISA kit, respectively, and the correlation analysis method was used to investigate the relationship between four components and NT-proBNP level. This study is in order to provide references for pharmacodynamic substances exploration of ESZWD.

Abbreviations: ALD, aldosterone; Ang II, angiotensin II; ATR1, angiotensin receptor 1; AUC, area under the curve; CE, collision energy; CHF-HKYd, chronic heart failure of heart and kidney yang deficiency; CL, clearance; CYP450, cytochrome P450; DP, declustering potential; E/A, ratio of peak flow velocity between early and late mitral valve diastole; ESI, electrospray ionization; ESZWD, er shen zhenwu Decoction; FS, left ventricular short axis systolic fraction; HOQ, high of qualification; IL-6, interleukin 6; IVSD, diastolic interventricular septum; IVSS, systolic interventricular septum; LLOQ, low limit of qualification; LOQ, low of qualification; LVEF, left ventricular ejection fraction; LVIDd, left ventricular internal diastolic diameter; LVIDs, left ventricular internal systolic diameter; LVPWd, left ventricular posterior wall diastolic diameter; LVPWs, left ventricular posterior wall systolic diameter; MDA, malondialdehyde; MOQ, medium of qualification; MRM, multiple reaction monitoring; NT-proBNP, N-terminal pro brain natriuretic peptide; RAAS, renin-angiotensin-aldosterone; ROS, reactive oxygen species; RT, retention time; SOD, superoxide dismutase; SV, stroke volume; T1/2, half-life time; TCM, traditional Chinese medicine; TIC, total ion chromatogram; TNF-α, tumor necrosis factor α; UHPLC/Q-TOF-MS, ultra-high-performance liquid chromatography/quadrupole time-of-flight mass spectrometry; V, volume.

Instruments and material

Doppler electrocardiograph (CHISON Medical Technologies Co., Ltd, China), Multiskan Spectrum Full Wavelength Microplate (Thermo Fisher Scientific, USA), Waters ACQUITY-CSH-C_{18} column, Waters ACQUITY^{TM} ultra performance liquid chromatography, Waters XEVO G2 Q-TOF high resolution time-of-flight mass spectrometer (Waters, USA), IKA RV10 digital rotary evaporator (IKA, Germany), LC-4016 low speed centrifuge (CZJ Scientific Instrument Co., Ltd.), Milli-Q Gradient A10 Ultra-Pure Water System [Milliple (Shanghai) Trading Co., Ltd.], Micropipette gun (Eppendorf, Germany).

Paeoniflorin (LOT: 110736201539) was purchased from the State Food and Drug Administration; Aconitine (LOT:

15121111), ginsenoside Rb1 (LOT: Z20S9X70603), miltrione (LOT: W29A10Z96532), Salsolinol (LOT: A22GB146211) were purchased from Shanghai Yuanye Biotechnology Co., Ltd., TanshinoneIIA (LOT: DST191017-011) was purchased from Chengdu Deste Biotechnology Co., Ltd. Paeoniflorin (No. ZLSW201128-1) was purchased from Xi'an Chengxiang Biotechnology Co., Ltd.

Aconiti Lateralis Radix Praeparata (Aconiti) was purchased from Jiangsu Huahong Pharmaceutical Technology Co., Ltd., No. 181027; *Poria* (Poria) was purchased from Anhui Linlan Co., Ltd., No. 1901001; *Atractylodis Macrocephalae* Rhizoma (Atractylodes, Atractylodis Macrocephalae) was purchased from Anhui Hua Tianbao Traditional Chinese Medicine Decoction Pieces Co., Ltd., No. 1901001; *Paeoniae* Radix Alba (Paeonia L., Paeoniae) was purchased from Bozhou Chengyuan Traditional Chinese Medicine Pieces Co., Ltd. No. 20181101; *Salviae Miltiorrhizae* Radix et Rhizoma (Salvia Linn., Salviae Miltiorrhizae) was collected from Taihe County, Anhui Province. *Ginseng* Radix et Rhizoma Rubra (Panax L., Ginseng) was purchased from Zhejiang Zhenyuantang TCM Decoction Pieces Co., Ltd., No. 20191001; *Zingiberis* Rhizoma Recens (Zingiber, Zingiberis) is homemade. All the medicinal materials were identified by Professor Yu Nianjun of Anhui University of Traditional Chinese Medicine and met the standards of the Chinese Pharmacopoeia (2020 edition).

Experimental animals

All male rats were kept at a room temperature of 20 ± 2°C with a 12-h light/dark cycle and 50 ± 5% relative humidity for 1 week. Animals reported here have been approved by the Institutional Animal Care and Use Committee of Anhui Medical University [Certification of fitness number: scxk (Anhui) 2017-001], and the experimental procedures were conducted in accordance with the Guidelines for Proper Conduct of Animal Experiments. Animal experiments have been approved by the Ethics Committee of Anhui University of Chinese Medicine (Ethics Number: AHUCM-rats-2021032).

Methods

Replication and evaluation of CHF-HKYd rat model

SPF SD male rats were anesthetized by intraperitoneal injection of 25% urethane (1,000 mg/kg). Cut off the skin tissue for about 1 cm, blunt away from bilateral neck muscles, separate and excise the bilateral thyroid glands, and the parathyroid glands were retained. The mixture of noradrenaline and normal saline (1:4,000) was used to stop intraoperative bleeding during the operation, the muscle and skin were sutured and 0.1% calcium gluconate solution was given postoperatively. On the 10th day after thyroidectomy, the rats were intraperitoneally injected with 0.02% doxorubicin hydrochloride (1 mL/100 g), twice a week for 3 weeks.

The general state of rats was observed: the basic criteria for the symptoms of HKYd were dark purple coating on the tongue, asthma, edema, fear of cold, emaciation, loose stools, sleepiness, hypotrichosis, etc. The urine volume of rats was measured: 1 week after the last injection, 24 h urine volume of rats in the normal and model group were collected in the metabolic cage, and the urine samples were frozen at −80°C. Evaluation of cardiac function in rats by Doppler echocardiography: After urine collection, the rats were anesthetized and fixed in the supine position. The precardiac area of the rats was depilated and the coupling agent was applied, a frequency of 12 MHz. M-mode ultrasound and pulsed Doppler ultrasound were used to detect diastolic interventricular septum (IVSD), left ventricular internal diastolic diameter (LVIDd), left ventricular posterior wall diastolic diameter (LVPWd), systolic interventricular septum (IVSs) and left ventricular internal systolic diameter (LVIDs), left ventricular posterior wall systolic diameter (LVPWs), stroke volume (SV), left ventricular ejection fraction (LVEF), left ventricular short-axis systolic fraction (FS), and the ratio of peak flow velocity between early and late mitral valve diastole (E/A) through the left ventricular macropinacoid of left sternal bone and four-chamber view. Neuroendocrine factor detection: After the echocardiography, 1 mL of blood was taken from the canthus of rats in each group, blood was placed in the water at 37°C for 1.5 h, centrifuged to obtain serum (3,000 rpm, 10 min), frozen at −80°C. The contents of serum NT-proBNP, T_3, and T_4 were detected by ELISA.

Preparation of ESZWD solution

Aconiti Lateralis Radix Praeparata soaked (3.0 g) in 10 times distilled water decocted for 0.5 and 1 h with high and low temperature, respectively. Afterward, they were decocted with other six herbs including *Ginseng* Radix et Rhizoma Rubra (6.0 g), *Poria* (10.0 g), *Atractylodis Macrocephalae* Rhizoma (10.0 g), *Paeoniae* Radix Alba (10.0 g), *Salviae Miltiorrhizae* Radix et Rhizoma (30.0 g), *Zingiberis* Rhizoma Recens (6.0 g) for 0.5 h (18), filtered, and the residue decocted with eight times water for 0.5 h again. Finally, the two filtrates were combined and concentrated under reduced pressure in the rotary evaporator for centrifugation, the supernatant was vacuum dried and stored at −20°C after vacuum drying. The accurately weighed 10.0 g freeze-dried powder was dispersed in 1 mL initial proportion of mobile phase, then centrifuged at high speed (12,000 rpm·min^{-1}, 10 min), filtered through 0.22 μm membrane, and analyzed.

Animal treatment and index detection

All rats were randomly divided into control group, model group, ESZWD low-dose (3.96 g/kg), medium-dose (7.92 g/kg), high-dose (15.84 g/kg) groups, and positive control group (benazepril, 0.5 mg/kg), with six rats in each group. The CHF-HKYd was established after 1 week of feeding. ESZWD and benazepril were administered by gavage separately for 4 weeks after successful modeling, except for the control group. Blood was collected for 5, 10, 20, 30, 45 min, 1, 2, 4, 6, 8, 12, and 24 h, standing for 2 h and centrifuged at 4°C, 3,500 rpm for 10 min, the supernatant was retained. The state of rats was observed and the urine volume at 24 h was measured. The structure and function of rat heart were evaluated by doppler ultrasonography. Serum biomarkers including myocardial injury indicators NT-proBNP, angiotensinII (AngII), aldosterone (ALD), reactive oxygen species (ROS), superoxide dismutase (SOD), malondialdehyde (MDA), and tumor necrosis factor α (TNF-α) and interleukin 6 (IL-6) were detected by ELISA.

Test conditions of ESZWD in serum

Chromatographic conditions

Chromatographic analysis was performed using ACQUITY UPLC BEH C_{18} column (2.1 × 50 mm, 1.7 m), the mobile phase was acetonitrile (A) 0.1% formic acid water (B), the flow rate was set as 0.2 mL·min^{-1}, the column temperature was 35°C, the injection volume was 2 μL, and the gradient conditions were as follows: 0–8 min: 6–11%A, 8–23 min: 11–19%A, 23–45 min: 19–38%A, 45–55 min: 38–47%A, 55–55.1 min: 47–52%A, 55.1–65 min: 52–90%A, 65–66 min: 90–6%A of UPLC-Q-TOF/MS analysis and 0–3 min: 8–10%A, 3–3.5 min: 10–70% A, 3.5–5: 70–80%A, 5–5.1 min: 80–8% A, 5.1–6 min: 8% A of UPLC-MS/MS.

Mass spectrometry conditions

Mass spectrometric detection of UPLC-Q-TOF/MS was carried out on electrospray ionization (ESI) ion source, the scanning range of *m/z* 50–1,200 Da, scan time is 0.5 S, capillary voltage is 3.0 kV in positive mode and 2.5 kV in negative mode, cone voltage is 40 V, source temperature is 120°C (ESI$^+$) and 110°C (ESI$^-$), desolvation gas temperature of 350°C, desolvation gas (N_2) flow of 600 L·h^{-1}, collision energy is 35 V in positive mode and −10 V in negative mode, vertebral hole gas velocity: 50 L·h^{-1}, the quality of the correction fluid for Leu-enkephalin, nucleo ratio of *m/z* 556.2766 in positive mode and *m/z* 554.2620 in negative mode.

Mass spectrometric detection of UPLC-MS/MS analysis was carried out on electrospray ionization (ESI) ion source, multiple reaction monitoring (MRM) mode, ion spray voltage of 5,500 V, the curtain gas and collision gas were 40 and 9 kPa, respectively, declustering potential (DP) and collision voltage (CE) are shown in Table 1.

TABLE 1 Mass spectral parameters of five compounds.

Compound	m/z (Da)	DP (V)	CE (V)
Salsolinol	179.4/145.0	69.04	26.90
Aconitine	645.5/586.4	111.98	50.88
Miltrione	284.2/88.0	107.29	31.83
Paeoniflorin	480.3/121.9	10.99	30.94
TanshinoneIIA	302.2/88.1	118.93	47.06

Data processing and analysis

For cytokine testing: Results were expressed as mean ± standard deviation ($\bar{x} \pm$ SD), SPSS 25.0 software was used for statistical analyses. The Kruskal–Wallis test, one-way analysis of variance (ANOVA), and the least-significant difference (LSD) test were used for statistical parameter analysis. $P < 0.05$ was regarded as statistically significant.

For chemical composition analysis: By searching online databases (CNKI, PubMed and WebScience, and PubChem, ChemBook, and ChemSpider), the ESZWD chemical composition database was constructed and imported into UNIFI software. Using the UNIFI^{TM} data analysis platform to identify the chromatographic peaks of ESZWD whole formula and disassembled formula; A binary sample model was used for comparative analysis, that is, between the blank solvent sample and the sample solution. Besides, in the positive ion mode, $[M+H]^+$ or $[M+Na]^+$ were selected as the main additive ion mode, and in the negative ion mode, $[M-H]^-$ or $[M+HCOO]^-$ were selected as the main additive ion mode, and the upper and lower limits of molecular weight deviation of ESZWD and its disassembled formula were set as 10 ppm.

Results

Evaluation of CHF-HKYd rat model

Doppler echocardiography

To verify the success of the model, we examined the cardiac function of the rats. The cardiac function of each rat was analyzed by echocardiography after modeling. As can be seen from Figure 1 and Table 2, compared with the normal group, the IVSD (mm) and LVEDD (mm) in the model group were significantly increased, the E/A < 1. This indicated that the diastolic function of the model rats was impaired.

Serum NT-ProBNP, T_3, T_4 level in normal and model rats

In order to observe the level of neuroendocrine factors changes in the model rats, we detected NT-proBNP, T_3, and T_4. In Figure 2, compared with the normal group, the serum levels of NT-proBNP, T_3, and T_4 in the model group were significantly decreased ($P < 0.05$). NT-proBNP is one of the specific markers of CHF, increased levels of this factor indicate the occurrence of CHF, while decreased levels of T_3 and T_4 indicate thyroid insufficiency.

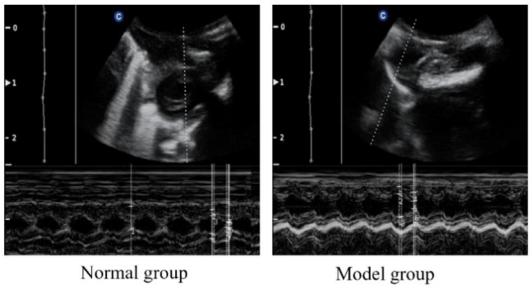

FIGURE 1
Doppler echocardiography of normal and CHF-HKYd rats.

Effects of ESZWD on CHF-HKYd rats

Effects of ESZWD on cardiac function in CHF-HKYd rats

In Table 3, IVSD, LVED, and LVIDS of model rats were significantly increased in comparison with normal rats, while LVEF, FS, and E/A were significantly decreased, indicating decreased diastolic function and ejection ability in response to CHF-HKYd rats. Low and medium doses of ESZWD could significantly reduce LVIDd, while LVIDs was reduced only in the medium-dose group, all doses could significantly improve the E/A ratio.

Effects of ESZWD on serum levels of NT-proBNP, ALD, and AngII in CHF-HKYd rats

As can be seen from Figure 3, compared with the normal group, serum NT-proBNP, ALD and AngII were significantly increased in the model group. Compared with the model group, medium and high doses of ESZWD could significantly reduce the level of NT-proBNP, and medium and high doses of ESZWD could significantly reduce the levels of ALD and AngII in

TABLE 2 Doppler cardiac function parameters of normal and CHF-HKYd rats.

	IVSd/mm	LVIDd/mm	LVPWd/mm	IVSs/mm	LVIDs/mm
Normal group	1.180 ± 0.11	4.480 ± 0.50	1.260 ± 0.23	2.140 ± 0.79	1.140 ± 0.40
Model group	1.460 ± 0.19#	5.820 ± 0.86#	1.420 ± 0.40	2.380 ± 0.66	1.760 ± 0.72
	SV/mL	**LVEF%**	**FS%**	**LVPWs/mm**	**E/A**
Normal group	0.454 ± 0.47	97.55 ± 2.62	74.25 ± 8.38	3.220 ± 0.80	2.399 ± 0.24
Model group	0.456 ± 0.21	95.35 ± 5.70	69.41 ± 12.52	2.500 ± 1.08	0.756 ± 0.08#

Compared with normal group, #P < 0.05, difference has significance.

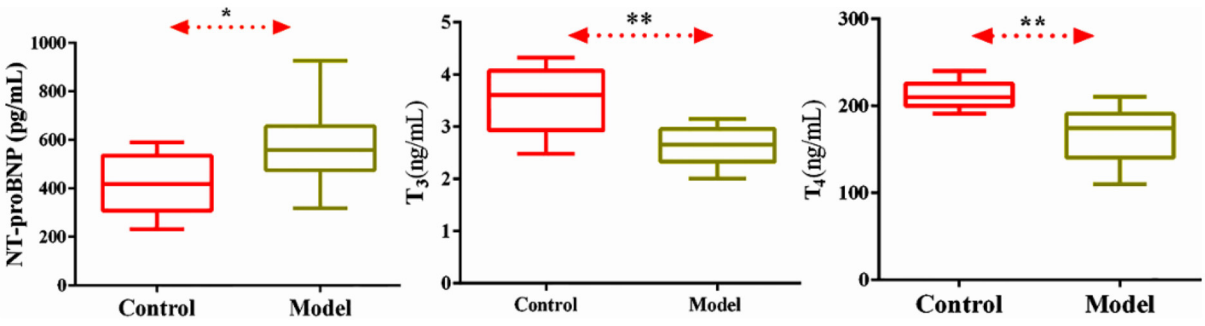

FIGURE 2
Level of serum NT-proBNP, T_3, T_4 in normal and CHF-HKYd rats. Compared with control group, *$P < 0.05$. **$P < 0.01$.

TABLE 3 Effects of ESZWD on cardiac function of CHF-HKYd rats.

	IVSd/mm	LVIDd/mm	LVPWd/mm	IVSs/mm	LVIDs/mm	SV/mL	LVEF%	FS%	LVPWs/mm	E/A
Normal	1.213 ± 0.29	5.288 ± 0.52	1.650 ± 0.37	2.538 ± 0.86	2.363 ± 0.81	0.3138 ± 0.09	88.64 ± 9.03	57.53 ± 15.98	1.685 ± 0.25	1.542 ± 0.15
Model	1.643 ± 0.27$^{\#}$	6.129 ± 0.33$^{\#}$	1.671 ± 0.22	2.243 ± 0.38	3.757 ± 0.70$^{\#\#}$	0.3929 ± 0.07	73.55 ± 12.7$^{\#\#}$	38.73 ± 9.89$^{\#\#}$	1.891 ± 0.10	0.729 ± 0.12$^{\#}$
ESZWD-L	2.033 ± 0.58	5.633 ± 0.25*	2.000 ± 0.36	3.067 ± 0.25	3.433 ± 0.67	0.3100 ± 0.09*	76.99 ± 16.0	38.65 ± 13.4	2.667 ± 0.45	1.863 ± 0.43*
ESZWD-M	1.817 ± 0.57	5.450 ± 0.63*	2.017 ± 0.38	2.767 ± 0.30	2.900 ± 0.87*	0.3183 ± 0.08	82.41 ± 9.61	47.66 ± 12.2	3.033 ± 0.66**	2.013 ± 0.42*
ESZWD-H	1.433 ± 0.12	6.133 ± 0.80	1.733 ± 0.35	2.367 ± 0.23	3.60 ± 0.56	0.4767 ± 0.22	84.37 ± 8.85	49.65 ± 12.4	2.933 ± 0.68*	1.976 ± 0.36*
Benazepril	1.800 ± 0.62	5.950 ± 1.28	1.900 ± 0.67	3.425 ± 0.88	2.350 ± 0.72**	0.4950 ± 0.25	92.30 ± 4.09**	60.31 ± 8.10**	3.525 ± 0.79**	1.794 ± 0.28*

Compared with control group, $^{\#}P < 0.05$, $^{\#\#}P < 0.01$, difference has significance; Compared with model group, $^{*}P < 0.05$, $^{**}P < 0.01$, difference has significance.

serum. Benazepril significantly reduced the contents of these three cytokines.

Effects of ESZWD on serum levels of ROS, MDA, and SOD in CHF-HKYd rats

As illustrated in Figure 4, compared with the normal group, serum ROS and MDA in the model group were significantly increased, while SOD was significantly decreased. Obviously, medium and high doses of ESZWD could significantly reduce ROS and MDA levels, while SOD was increased only in ESZWD medium-dose group. Additionally, benazepril can significantly reduce ROS and MDA levels.

Effects of ESZWD on serum levels of TNF-α and IL-6 in CHF-HKYd rats

As shown in Figure 5, compared with the normal group, serum TNF-α and IL-6 in the model group were significantly increased, indicating that inflammation occurred in the model group. Compared with the model group, ESZWD had no significant effects on TNF-α and IL-6, indicating that these two cytokines may not be the therapeutic targets of ESZWD, but it is not excluded that ESZWD may inhibit inflammation. Benazepril significantly reduced levels of both inflammatory factors.

Chemical compositions of ESZWD in CHF-HKYd rats

Analysis of main components of ESZWD in CHF-HKYd rats

As shown in Table 4, there were 30 compounds of ESZWD identified in CHF-HKYd rats, including alkaloids, saponins, 3 terpenoids, tanshinone, phenols, individual fat, fatty acids, flavonoids, and sulfonate, nucleic acid compounds. There were 12 compounds from monarch medicine, 12 compounds from minister medicine, and 10 kinds of assistant medicine.

Establishment of UPLC-MS/MS for simultaneous determination of four chemical components in ESZWD

Validation of method

Specificity and linear ranges

The specificity results (Supplementary Figure 1) indicated that endogenous substances did not substantially interfere with the retention time of probe drugs and internal standard (IS) in blank serum. The linear ranges of the four compounds were

TABLE 4 Serum components of ESZWD in CHF-HKYd rats.

Peak	Component name	Formula	Observed RT (min)	Observed m/z	Fragment ions (m/z) (±)	Mass error (ppm)	Origin
1	Salsolinol	$C_{10}H_{13}NO_2$	7.22	$[M+H]^+$:180.1026	146.06105	3.6	A
2	Paeoniflorin*	$C_{23}H_{28}O_{11}$	8.39	$[M+HCOO]^-$:525.1578	/	−6.8	BC
3	Dimethyl D-malate	$C_6H_{10}O_5$	11.41	$[M+H]^+$:163.0597	133.01354	−2.4	B
4	letestuianin B	$C_{21}H_{22}O_6$	13.86	$[M+H]^+$:371.1515	217.08122	6.9	C
5	1-(4-Hydroxy-3-methoxyphenyl)-3-oxo-5-decanesulfonic acid	$C_{17}H_{26}O_6S$	14.86	$[M+H]^+$:359.1542	203.10301,217.08327	5.4	C
6	(1a,3a,6a,14a,15a,16b)-20-Ethyl-1,6,16-trimethoxy-4-(methoxymethyl)aconitane-3,8,13,14,15-pentol 8-Acetate 14-(4-Methoxybenzoate)	$C_{35}H_{49N}O_{12}$	17.65	$[M+Na]^+$:698.3217	375.14910,458.18640, 517.27153,588.30833	10	A
7	24-methylenecycloartanol	$C_{31}H_{52}O$	17.71	$[M+H]^+$:441.4101	175.11843	2.3	C
8	Aconitine	$C_{34}H_{47}NO_{11}$	19.69	$[M+Na]^+$:341.1	173.12716,201.12205,479.21224	0.1	A
9	Acetylaconitine	$C_{36}H_{49}NO_{12}$	21.32	$[M+Na]^+$:710.3082	175.1174,301.11698, 517.30894,588.30894	−9.2	A
10	(6S)-6,7,8,9-Tetrahydro-6-hydroxy-6-hydroxymethyl-1-methylphenanthro[1,2-b]furan-10,11-dione	$C_{18}H_{16}O_5$	24.11	$[M+HCOO]^-$:357.0952	225.12635	−7.7	B
11	Adenosine	$C_{10}H_{13}N_5O_4$	33.04	$[M+H]^+$:268.1039	165.06844	−0.6	B
12	20-Ethyl-8-hydroxy-1,16-dimethoxy-4-(methoxymethyl)aconitan-14-yl acetate	$C_{26}H_{41}NO_6$	33.73	$[M+H]^+$:464.2993	209.1264,335.23656,353.25368	−2.9	A
13	Ginsenoside Rb1*	$C_{54}H_{92}O_{23}$	37.63	$[M+HCOO]^-$:1153.5997	/	−1.2	BC
14	Ginsenoside Rb3	$C_{54}H_{92}O_{23}$	37.66	$[M+HCOO]^-$:1153.5997	783.48919,945.54043	−0.2	B
15	TanshinoneIIB	$C_{19}H_{18}O_4$	41.28	$[M+H]^+$:311.1251	199.07924,213.09088	−8.6	B
16	3-Hydroxy-2-isopropyl-8-methyl-1,4-phenanthrenedione	$C_{18}H_{16}O_3$	44.65	$[M+HCOO]^-$:325.1068	265.08506	−4.3	A

(Continued)

10.3389/fcvm.2022.913661

TABLE 4 (Continued)

Peak	Component name	Formula	Observed RT (min)	Observed m/z	Fragment ions (m/z) (±)	Mass error (ppm)	Origin
17	(1α,5ξ,6β,9ξ,10ξ,13ξ,14α,16β,17ξ)-20-Ethyl-14,16-dimethoxy-4-(methoxymethyl)aconitane-1,6,7,8-tetrol	$C_{24}H_9NO_7$	48.58	$[M+Na]^+$:476.2603	119.08554	−3.3	A
18	(1R,4aR,7R,8aR)-7-(2-Hydroxy-2-propanyl)-1,4a-dimethyldecahydro-1-naphthalenol	$C_{15}H_{28}O_2$	51.63	$[M+Na]^+$:263.1989	95.08448	3	C
19	Poricoic acid E	$C_{30}H_{44}O_6$	55.11	$[M-H]^-$:499.3033	301.21485	−6.5	B
20	(16β,17ξ)-20-Ethyl-8,13-dihydroxy-1,16-dimethoxyaconitan-14-yl benzoate	$C_{29}H_{39}NO_6$	56.71	$[M+Na]^+$:520.2662	184.07261,319.19338	−1.5	A
21	Ginsenoside Rs1	$C_{55}H_{92}O_{23}$	57.27	$[M+Na]^+$:1143.591	184.06991,520.33039,544.32997	−1	A
22	Miltrione	$C_{19}H_{22}O_2$	57.96	$[M+Na]^+$:305.1516	155.00831	1.4	B
23	Ginsenoside Rk2	$C_{36}H_{60}O_7$	58.55	$[M+H]^+$:605.4366	105.06872,337.26457,426.35458	−7.5	A
24	(16β)-3,13,15-Trihydroxy-1,6,8,16-tetramethoxy-4-(methoxymethyl)-20-methylaconitan-14-yl benzoate	$C_{31}H_{57}NO_{10}$	60.97	$[M+Na]^+$:626.2949	104.10528,184.06999	2.1	A
25	3-Phenanthrenol, 4b,5,6,7,8,8a,9,10-octahydro-4b,8,8-trimethyl-2-(1-methylethyl)-, (4bS,8aS)-	$C_{20}H_{30}O$	63.12	$[M+H]^+$:287.2375	95.08582,121.10144	1.9	B
26	Lecithin	$C_{42}H_{81}NO_8P^+$	64.78	$[M+H]^+$:758.5661	104.10657,187.01850,362.18849	−4.3	C
27	Ginsenoside Rk3	$C_{36}H_{60}O_8$	65.12	$[M+HCOO]^-$:665.4253	281.24682	−2.6	ABC
28	2-Methyl-5-[(2R)-6-methyl-5-hepten-2-yl]phenol	$C_{15}H_{22}O$	65.28	$[M+Na]^+$:241.1546	95.08448	−6.8	C
29	kaempferol 3,7-di-O-β-D-glucoside	$C_{27}H_{29}O_{16}$	66.17	$[M+HCOO]^-$:655.1566	223.02565	−6.3	B
30	1,2,3,4,6-Pentagalloyl glucose	$C_{41}H_{32}O_{26}$	66.3	$[M+Na]^+$:963.1134	355.0616	6.2	C

*Contrast with reference solution.
A, Monarch medicine; B, Minister medicine; C, Assist medicine.

10.3389/fcvm.2022.913661

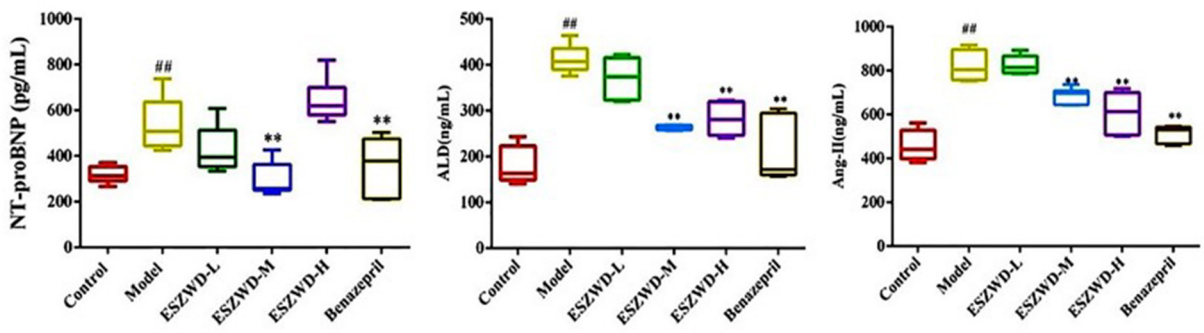

FIGURE 3
Effects of ESZWD on serum NT-proBNP, ALD, and AngII level of CHF-HKYd rats. Compared with control group, $^{\#\#}P < 0.05$; compared with model group, $^{**}P < 0.01$.

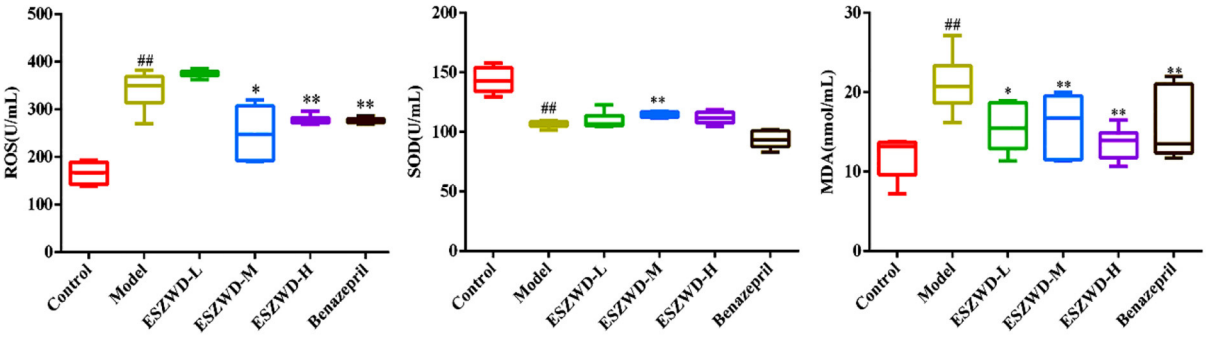

FIGURE 4
Effects of ESZWD on serum ROS, SOD, and MDA level of CHF-HKYd rats. Compared with control group, $^{\#\#}P < 0.05$; compared with model group, $^{*}P < 0.05$, $^{**}P < 0.01$.

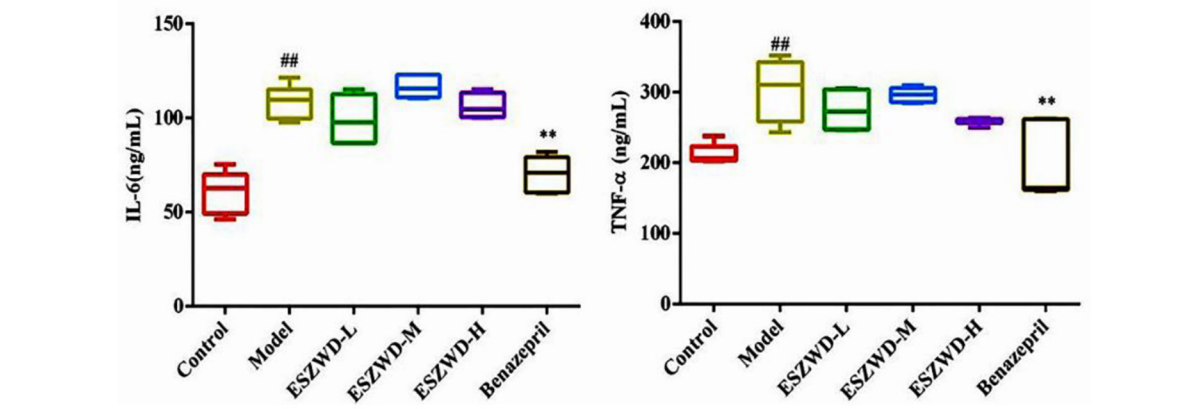

FIGURE 5
Effects of ESZWD on serum TNF-α and IL-6 level of CHF-HKYd rats. Compared with control group, $^{\#\#}P < 0.05$; compared with model group, $^{**}P < 0.01$.

TABLE 5 Main pharmacokinetic parameters of salsolinol, aconitine, paeoniflorin, and miltrione in CHF-HKYd rat serum ($\bar{x} \pm SD$, $n = 6$).

	Salsolinol	Aconitine	Paeoniflorin	Miltrione
$AUC_{(0-t)}$ (ng/mL·h)	2,327 ± 261.0	48.94 ± 16.43	2239 ± 177.8	1,098 ± 69.72
$AUC_{(0-\infty)}$ (ng/mL·h)	2,344 ± 265.7	50.11 ± 16.01	2258 ± 178.8	1,125 ± 84.73
$T_{1/2}$ (h)	3.271 ± 0.58	4.24 ± 1.83	3.223 ± 0.34	4.25 ± 0.82
T_{max} (h)	1.25 ± 0.59	0.75 ± 0.00	6.00 ± 2.54	1.00 ± 0.00
CL/F (L/h/kg)	8.625 ± 0.96	424.7 ± 97.65	8.86 ± 5.55	17.87 ± 1.38
V/F (L/kg)	40.68 ± 9.03	2679 ± 1574	41.20 ± 0.83	108.7 ± 15.80
C_{max} (ng/mL)	314.2 ± 36.84	8.96 ± 2.22	197.6 ± 27.66	178.9 ± 16.24

10.00–1000.00, 0.40–200.00, 0.40–200.00, 0.50–200.00 ng/mL and the correction coefficients (r) were 0.9984, 0,9981, 0.9993, 0.9993, respectively.

Precision and accuracy

Interday precision and intraday precision of the method were assessed by detecting the low limit of qualification (LLOQ) and the low-, medium-, and high-quantification concentrations (LQC, MQC, and HQC) of plasma samples. Relative standard deviation (RSD) values of the precision do not exceed ±15% (Supplementary Tables 1, 2).

Matrix effect

By comparing the different results of analytes added into the blank sample and ultrapure water, the matrix effect was determined at LQC, MQC, and HQC concentrations. The RSD values (Supplementary Table 3) were <4%, indicating that the matrix effect of plasma is negligible for quantitative analysis of all samples.

Stability

The stability of all probe drugs was evaluated by LQC and HQC samples under different experimental conditions, including short-term stability [4 h at room temperature (25°C), 8 h in the automatic sampler, and three freeze and thaw cycles, respectively] and long-term stability (7 d at −80°C). Results showed that the probe substrates tested were within the recommended limits, RSD < 10% (Supplementary Table 4).

Pharmacodynamic substances of ESZWD in treating CHF-HKYd

Pharmacokinetic parameters of four chemical components in ESZWD in CHF-HKYd rats

Results are presented in Table 5 and Figure 6, and the area under the curve (AUC) indicates the amount of drug exposure in the body, volume (V) is positively correlated with clearance (CL) and negatively correlated with C_{max}. The content of salsolinol in the body is large, half-life time ($T_{1/2}$) is about 3 h, CL is low, V is small, T_{max} is 1.25 h, indicating it is a compound with fast absorption and elimination. With the bimodal phenomenon, paeoniflorin is higher in the serum, $T_{1/2}$ is about 3 h, CL is low, V is small, and T_{max} is 6 h. Aconitine has the lowest AUC, supporting that it is present at very low levels in the body, which may be the reason that the compound is effective but not toxic, given its highly toxic nature. In addition, the T_{max} of this compound is only 0.75 h, and the $T_{1/2}$ is about 4 h, which is a compound with fast absorption and slow elimination. The V is far more than the body fluid, it is speculated that aconitine is a fat-soluble compound and is mainly distributed in the tissues and organs rich in fat. The pharmacokinetic characteristic of miltrione is similar to salsolinol, but the AUC is much less than salsolinol while the V is higher, so miltrione enters into tissues more easily.

Relationship between four compounds and serum NT-ProBNP level

Serum NT-proBNP levels at different time points are shown in Supplementary Table 4, correlation analysis results showed that salsolinol, aconitine, paeoniflorin, and miltrione were negatively correlated with serum NT-proBNP level, with correlation coefficients of −0.576 ($P < 0.05$), −0.753 ($P < 0.05$), −0.705 ($P < 0.05$), −0.477, respectively.

Discussion

In this study, the CHF-HKYd rat model was replicated by bilateral thyroidectomy combined with adriamycin injection, and the therapeutic effects of ESZWD on the model rats were explored from the perspectives of cardiac function, myocardial injury, oxidative stress, and inflammatory response. The results showed that ESZWD could significantly reduce LVIDd and increase E/A value in model rats, medium and high doses of ESZWD could significantly reduce the levels of Ang II and ALD in serum, and NT-proBNP level was reduced only in the medium-dose group. The serum ROS and MDA levels were significantly reduced while the SOD level was increased only in the medium-dose group. However, the formula had no significant effects on the contents of TNF-α and IL-6 in serum. Echocardiography is commonly performed to evaluate cardiac diastolic function in clinical practice as a convenient and non-invasive means, and both the LVIDd and E/A values are ordinarily used indicators. NT-proBNP (19) is produced by myocardial cells vascular peptide hormones, the value of this cytokine will be significantly increased during HF and ejection fraction decreased process, leading to ventricular wall expansion and myocardial remodeling, accelerating the progression of

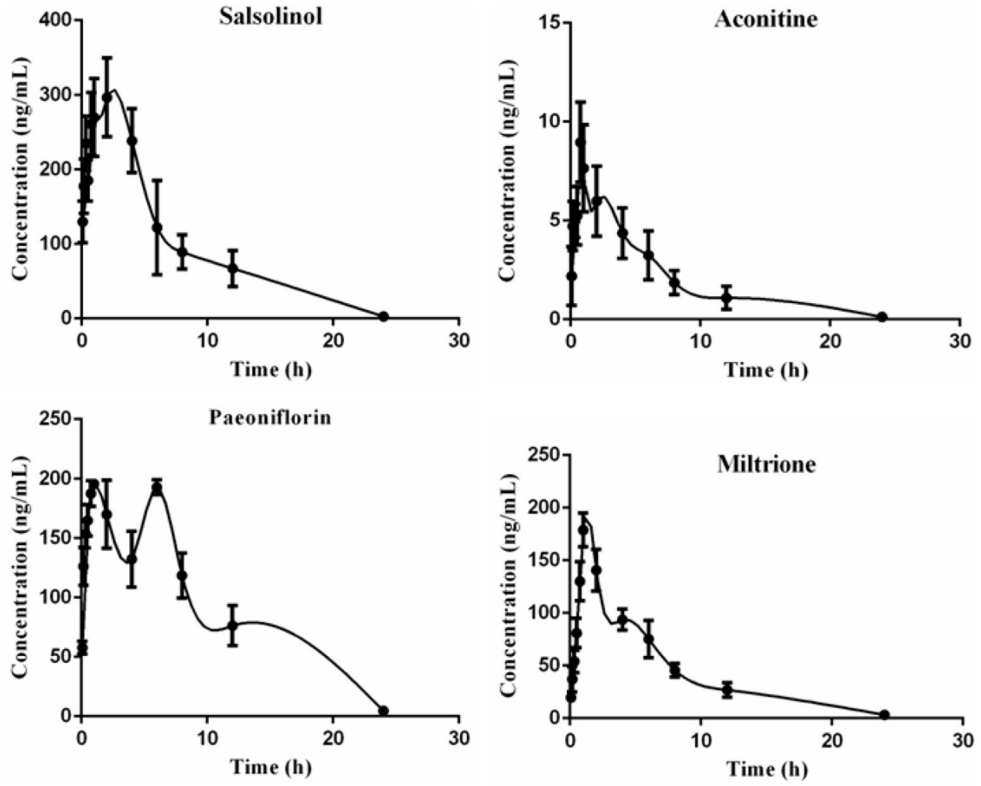

FIGURE 6
Time-concentration curves of salsolinol, aconitine, paeoniflorin and miltrione in CHF-HKYd rat serum ($\bar{x} \pm$ SD, $n = 6$).

the disease. Ang II and ALD are polypeptide substances and steroid hormones produced by RAAS system activation, one of the important indicators in ventricular remodeling. Ang II (20) has the ability to promote the ALD release by combining with ATR1 and triggering an inflammatory response, thus, inhibiting RAAS system activation has been recommended by the European Heart Pathology Association in the therapeutic strategy of CHF (21). Oxidative stress participates in the mechanisms of cardiovascular disease, and it is defined as the excessive production of live free radicals. ROS (22) is a single-electron reduction product of a class of oxygen in the body, mainly including O2●, ●OH, H2O2, etc, excessive ROS in the heart is involved in the processes of reduced systole function, hypertrophy signal transduction, myocardial growth, matrix remodeling, fibroblast proliferation, etc. However, the dangerous effects of ROS can be prevented by scavenging enzymes such as SOD and glutathione peroxidase (GSHPx). SOD (23) is a vital antioxidant enzyme that is able to catalyze the disproportionation of superoxide anion radicals to produce O and H2O2, it is often measured together with MDA, a final product of lipid peroxidation with the content often reflects the degree of lipid peroxidation and cell damage in the body. Studies have shown that elevated serum MDA in CHF patients increases the risk of death by 103.0% and is associated with poor prognosis (24, 25). The activation of the RAAS system is becoming more pronounced in CHF patients, and there is a positive correlation between oxidative stress and RAAS system biomarkers, for instance, Ang II is able to induce an oxidative stress response. That means to say, combined application of RAAS blockers or (and) antioxidants could be more conducive to the improvement of the disease. The experiment yielded that ESZWD has sound effects of protecting cardiac dysfunction, ameliorating oxidative stress responses including ROS and MDA levels reduction, it may be attributed to RAAS system inhibition like diminishing the production of Ang II and ALD so as to play a therapeutic role in CHF-HKYd. In the later research, the mechanism can be systematically explored in depth.

Serum components of ESZWD in normal and CHF-HKYd rats were mainly saponins, terpenoids, and alkaloids, interestingly, there were significant differences in compounds. Ginsenoside Rc, ginsenoside Rg5, ginsenoside R1, ginsenoside Rb1, ginsenoside Rg1 and ginsenoside Re were the main ginsenoside compounds in normal rats (17), while ginsenosides Rb3, ginsenosides Rs1, ginsenosides Rb1, ginsenosides Rk2 and ginsenosides Rk3 account for the main proportion in CHF-HKYd rats. Ginsenoside Rs1 can be obtained by the decarboxylation reaction of ginsenoside Rb2 (26) which is considered a new marker for distinguishing ginseng from

American ginseng (27). Our previous study (28) appeared that the activities of CYP1A2, CYP2B1, CYP2C6, CYP2C11, and CYP3A1 in CHF rats were significantly reduced, as we know, CYP450 mediated 90% of drug metabolism (29), the change of metabolic enzyme activity caused by CHF-HKYd may be one of the reasons for the chemical compounds inconsistencies. The results of this study illustrated that the differences between normal and disease animals should be taken into consideration in further research on the pharmacodynamic substances of ESZWD, the animal subjects therefore should be selected reasonably.

Salsolinol (30) and aconitine are components of *Aconiti* Lateralis Radix Praeparata with strong cardiac effect, in addition, studies have reported that aconitine can significantly down-regulate cardiomyocyte hyperplasia induced by Ang II, and its toxicity can be reduced when used in combination with paeoniflorin (31–33). Paeoniflorin can protect myocardial ischemia reperfusion injury rats by increasing SOD activity, decreasing MDA level, and alleviating oxidative stress as well as apoptosis (34). Miltrione is derived from the diterpenoid quinone active ingredient in Salvia miltiorrhiza, which has the effects of inducing apoptosis of cancer cells, anti-platelet aggregation, anti-oxidation, and anti-inflammation, but its role in cardiovascular diseases protection has not been reported (35–37). Nevertheless, there is evidence that miltrione can inhibit the oxidative stress response of endothelial cells induced by LDL (38), which may be the main factor in cardiovascular disease protection and deserve further exploration. Based on UPLC-MS/MS, the pharmacokinetic behavior of these four compounds in CHF-HKYd rats was investigated. AUC indicated the compounds' exposure, it could be concluded that the absorption degree of salsolinol was the largest. According to CL results, aconitine is the most easily cleared compound in model rats. The V of aconitine, paeoniflorin, and salsolinol were larger than the total liquid content, which means the wide distribution in the body, and the tissue distribution of these ingredients are therefore should be investigated in the latter study, which may be the key critical elements affecting the efficacy of these compounds. However, Cmax lets us know that the blood concentration of aconitine was very low, as a kind of herb with strong toxicity, which may be a major cause that why aconitine exerts its efficacy but does not generate toxicity. In addition, the double peaks of paeoniflorin indicated that it was re-enriched, hepatoenteric circulation, gastric motility, uneven distribution of P-glycoprotein in the intestinal tract, and transformation of TCM components may be the causes of this phenomenon (39), while other three ingredients consistent with normal pharmacokinetic behavior. At last, correlation analysis demonstrated that these four chemicals are associated with the reduction of serum NT-proBNP, and their suitable pharmacokinetic characteristics make them have the potential to be the pharmacodynamic substances in the treatment of CHF-HKYd.

Conclusion

In this research, we found that ESZWD process the ability to treat CHF-HKYd by reducing the levels of NT-proBNP, Ang II, ALD, ROS, and MDA in serum, and increasing the content of SOD, while having no effects on TNF-α and IL-6. The constituents of ESZWD in CHF-HKYd rats mainly include alkaloids, saponins, terpenoids, and tanshinones, among which salsolinol, aconitine, paeoniflorin, and miltrione have suitable pharmacokinetic profiles and are negatively correlated with NT-proBNP, they are equipped with potential characteristics as pharmacodynamic substances for ESZWD in treatment of CHF-HKYd. Additionally, the constituents of ESZWD in CHF-HKYd rats are different from normal rats, which provided a reference for the selection of subjects for further study.

Data availability statement

The original contributions presented in the study are included in the article/Supplementary material, further inquiries can be directed to the corresponding author/s.

Ethics statement

The animal study was reviewed and approved by Institutional Animal Care and Use Committee of Anhui Medical University [Certification of fitness number: scxk (Anhui) 2017-001].

Author contributions

YZ for assisting with the sample detection and data processing of this experiment. W-dC for providing the platform for this experiment. C-yY and G-zL for their efforts in animal experiments. H-sW and X-yC for their guidance in the project design of this research. All authors contributed to the article and approved the submitted version.

Funding

This research was supported by the Natural Science Foundation of Anhui Universities (grant number KJ2020A0380), Chinese Medicine Leading Personnel Training Object Special Project of Anhui Provincial Health, and Family Planning Commission [Chinese Medicine Development Secret (2018) grant number 23].

Conflict of interest

The authors declare that the research was conducted in the absence of any commercial or financial relationships that could be construed as a potential conflict of interest.

Publisher's note

All claims expressed in this article are solely those of the authors and do not necessarily represent those of their affiliated organizations, or those of the publisher, the editors and the reviewers. Any product that may be evaluated in this article, or claim that may be made by its manufacturer, is not guaranteed or endorsed by the publisher.

Supplementary material

The Supplementary Material for this article can be found online at: https://www.frontiersin.org/articles/10.3389/fcvm.2022.913661/full#supplementary-material

References

1. Xuejuan J, Jingmin Z, Junbo G. Progress in heart failure epidemiology. *Clin Med J China*. (2013) 20:852–5.

2. Jun H. Epidemiological characteristics and prevention strategies of heart failure in China. *Chin J Heart Heart Rhythm*. (2015) 3:2–3. doi: 10.3877/cma.j.issn.2095-6568.2015.2.002

3. Xiaoyu C, Wandong Z, Chonghui L, Liwei Q, Ruixue Z, Yebin H. Effect of compound Zhenwu granules on neuroendocrine of chronic congestive heart failure patients. *Chin J Inter Trad West Med Inten Criti Care*. (2002) 6:317–9. doi: 10.3321/j.issn:1008-9691.2002.06.004

4. Yexiang Z, Yebin H, Huaifang Y, Xiaoyu C, Jian W. Controlled study measuring the effects of Wenshenyixin pill on BNP in patients with congestive heart failure. *J Emerg Tradit Chin Med*. (2008) 2:137–9. doi: 10.3969/j.issn.1004-745X.2008.02.001

5. Xiaoyu C, Jing Z, Lan G, Gaowen H. Effect of compound Zhenwu granule on HS-CRP and BNP in patients with heart failure. *Chin J Integ Med Cardio-Cerebrovascu Dis*. (2009) 7:1018–9. doi: 10.13194/j.issn.1673-842x.2017.08.016

6. Xiaoyu C, Lan G, Jing Z, Gaowen H. Effects of Fufangzhenwu electuary on traditional chinese medicine syndrome, plasma high sensitivity C-reactive protein and atrial natriuretic patients with chronic congestive heart failure. *J Emerg Tradit Chin Med*. (2010) 19:365–8. doi: 10.3969/j.issn.1004-745X.2010.03.001

7. Hong L, Xiaoyu C, Lan G. Effect of Wenshen Yixin decoction on 32 cases of chronic congestive heart failure. *J Shandong Univ Trad Chin Med*. (2012) 36:124–5. doi: 10.16294/j.cnki.1007-659x.2012.02.013

8. Huaifang Y, Yebin H, Xiaoyu C, Jian W, Wandong Z, Yexiang Z. Clinical observation on the effects of Wenshenyixin pill in treating congestive heart failure. *J Anhui Tradit Chin Med*. (2005) 4:4–7. doi: 10.3969/j.issn.1000-2219.2005.04.002

9. WeiPu D, Yebin H, Yexiang Z, Xiaoyu C, Jia H. Effects of Wenshenyixin pellet on myocardial cell apoptosis in old patients with chronic heart failure. *J Emerg Tradit Chin Med*. (2012) 21:1053–4. doi: 10.3969/j.issn.1004-745X.2012.07.012

10. Koichi S, Yoshihiko S, Takeshi O, Toshiaki O, Kohji S, Teruo T. Ongoing myocardial damage in chronic heart failure is related to activated tumor necrosis factor and Fas/Fas ligand system. *Circ J*. (2004) 68:747–50. doi: 10.1253/circj.68.747

11. Xiaoyu C, Lan G, Xiuhuan Z, Huadan L, Hong L. Effects of compound fufangzhenwu granule on clinical efficacy and plasma interleukin-6 and tumor necrosis factor -α in patients with chronic heart failure. *Chin J Clin Healthc*. (2012) 15:530–2. doi: 10.3969/J.issn.1672-6790.2012.05.031

12. Xiaoyu C, Shuangyan Z, Dan C. Effects of compound Zhenwu granule on NT-probNP and MMP-3 in patients with chronic congestive heart failure. In: *Proceedings of the 2015 Annual Conference on Geriatric Medicine. Geriatric Branch of Zhejiang Medical Association*. Zhejiang: Zhejiang Science and Technology Association (2015).

13. Lan G, Xiaoyu C. Effects of Zhenwu granule on TCM syndromes, McP-1 and BNP in patients with chronic heart failure. *J Liaoning Unive Trad Chin Med*. (2017) 19:60–3.

14. Huaifang Y, Yebin H, Xiaoyu C, Jian W, Wandong Z, Yexiang Z. Effects of Wenshen Yixin pellet on levels of inflammatory cytokines in patients with congestive heart failure. *Chin J Inter Trad West Med Inten Criti Care*. (2005) 3:149–52. doi: 10.3321/j.issn:1008-9691.2005.03.006

15. Wang M, Chen DQ, Chen L, Liu D, Zhao H, Zhang ZH, et al. Novel RAS inhibitors poricoic acid ZG and poricoic acid ZH attenuate renal fibrosis via a Wnt/β-catenin pathway and targeted phosphorylation of smad3 signaling. *J Agric Food Chem*. (2018) 66:1828–42. doi: 10.1021/acs.jafc.8b00099

16. Chunsheng Z, Zhuoxi J, Jiajing L, Bing Z. Overview research status in serum spectrum-effect of Chinese materia medica. *Chin Tradit Herbal Drugs*. (2020) 51:3569–74. doi: 10.7501/j.issn.0253-2670.2020.13.027

17. Hong LL, Zhao Y, Yang CY, Li GZ, Wang HS, Chen WD, et al. Identification of chemical constituents *in vitro* and *in vivo* of Er Shen Zhenwu Decoction by utilizing ultra-high-performance liquid chromatography with quadrupole time-of-flight mass spectrometry. *J Separ Sci*. (2021) 44:4327–42. doi: 10.1002/jssc.202100624

18. Fu Weina, Cheng X. Clinical efficacy of compound Zhenwu granule in the treatment of elderly patients with chronic heart failure. *Clin J Trad Chinese Med*. (2021) 33:2385–9. doi: 10.16448/j.cjtcm.2021.1230

19. Rørth R, Jhund PS, Yilmaz MB, Kristensen SL, Welsh P, Desai AS, et al. Comparison of BNP and NT-proBNP in patients with heart failure and reduced ejection fraction. *Circ Heart Fail*. (2020) 13:e006541. doi: 10.1161/CIRCHEARTFAILURE.119.006541

20. Špinarová M, Špinar J, Parenica J, Špinarová L, Málek F, Lábr K, et al. Prescription and dosage of RAAS inhibitors in patients with chronic heart failure in the FAR NHL registry. *Vnitr Lek*. (2019) 65:13–4. doi: 10.36290/vnl.2019.004

21. McMurray JJ, Adamopoulos S, Anker SD, Auricchio A, Böhm M, Dickstein K, et al. ESC Guidelines for the diagnosis and treatment of acute and chronic heart failure 2012: The Task Force for the Diagnosis and Treatment of Acute and Chronic Heart Failure 2012 of the European Society of Cardiology. Developed in collaboration with the Heart Failure Association (HFA) of the ESC. *Eur Heart J*. (2012) 33:1787–847. doi: 10.1093/eurheartj.ehs104

22. Mancini A, Vergani E, Bruno C, Olivieri G, Segni C, Silvestrini D, et al. Oxidative stress as a possible mechanism underlying multi-hormonal deficiency in chronic heart failure. *Eur Rev Med Pharmacol Sci*. (2018) 22:3936–61. doi: 10.26355/eurrev_201806_15279

23. Ma D, Xu T, Cai G, Wu X, Lei Z, Liu X, et al. Effects of ivabradine hydrochloride combined with trimetazidine on myocardial fibrosis in rats with chronic heart failure. *Exp Ther Med*. (2019) 18:1639–44. doi: 10.3892/etm.2019.7730

24. Romuk E, Wojciechowska C, Jacheć W, Zemła-Woszek A, Momot A, Buczkowska M, et al. Malondialdehyde and uric acid as predictors of adverse outcome in patients with chronic heart failure. *Oxid Med Cell Longev*. (2019) 2019:9246138. doi: 10.1155/2019/9246138

25. Reina-Couto M, Afonso J, Carvalho J, Morgado L, Ronchi FA, de Oliveira Leite A, et al. Interrelationship between renin-angiotensin-aldosterone system and oxidative stress in chronic heart failure patients with or without renal impairment. *Biomed Pharmacother*. (2021) 133:110938. doi: 10.1016/j.biopha.2020.110938

26. Xuanxuan P, Xianggao L. Study on decarboxylation degradation of saponins and its products in red ginseng processing. *J Jilin Agric Univ*. (2000) 4:64–70. doi: 10.13327/j.jjlau.2000.04.017

27. Yang W, Qiao X, Li K, Fan J, Bo T, Guo DA, et al. Identification and differentiation of *Panax ginseng*, *Panax quinquefolium*, and *Panax notoginseng* by monitoring multiple diagnostic chemical markers. *Acta Pharm Sin B*. (2016) 6:568–75. doi: 10.1016/j.apsb.2016.05.005

28. Hong LL, Wang HS, Cheng XY, Zhang S, Zhao Y, Wang Q, et al. Evaluation and clinical implication of Zhenwu decoction on seven cytochrome P450 enzyme in chronic heart failure rats. *Curr Drug Metab*. (2021) 22:746–55. doi: 10.2174/1389200222666210701171047

29. Chen JJ, Zhang JX, Zhang XQ, Qi MJ, Shi MZ, Yang J, et al. Effects of diosmetin on nine cytochrome P450 isoforms, UGTs and three drug transporters *in vitro*. *Toxicol Appl Pharmacol*. (2017) 334:1–7. doi: 10.1016/j.taap.2017.08.020

30. Anonymous. Pharmacology of Aconite. *Chin Med Mod Dis Edu CN*. (2012) 10:139.

31. Ningning W, Jia W, Hongling T, Yuguang W, Yue G, Zengchun M. Aconitine ameliorates cardiomyocyte hypertrophy induced by angiotensin II. *Chin J Chin Mater Med*. (2019) 44:1642–7. doi: 10.19540/j.cnki.cjcmm.20190117.002

32. Li J, Zhang SH, He D, Wang JF, Li JQ. Paeoniflorin reduced the cardiotoxicity of aconitine in h9c2 cells. *J Biol Regul Homeost Agents*. (2019) 33:1425–36. doi: 10.23812/19-257A

33. Xue Z, Bingxiang Z, Yuqin S, Yuting Y, Yanhong D, Xiaofang X, et al. Compatibility effect of aconitine and ginsenosides Rb1 on energy metabolism of primary cultured myocardial cells. *Mod Tradit Chin Med Mat Med-Worl Sci Tech*. (2015)17:1785–9. doi: 10.11842/wst.2015.09.006

34. Wu F, Ye B, Wu X, Lin X, Li Y, Wu Y, et al. Paeoniflorin on rat myocardial ischemia reperfusion injury of protection and mechanism research. *Pharmacology*. (2020) 105:281–8. doi: 10.1159/000503583

35. Zhang X, Zhang P, An L, Sun N, Peng L, Tang W, et al. Miltirone induces cell death in hepatocellular carcinoma cell through GSDME-dependent pyroptosis. *Acta Pharm Sin B*. (2020) 10:1397–413. doi: 10.1016/j.apsb.2020.06.015

36. Song W, Ma YY, Miao S, Yang RP, Zhu Y, Shu D, et al. Ming, pharmacological actions of miltirone in the modulation of platelet function. *Acta Pharmacol Sin*. (2019) 40:199–207. doi: 10.1038/s41401-018-0010-1

37. Wang H, Gu J, Hou X, Chen J, Yang N, Liu Y, et al. Anti-inflammatory effect of miltirone on inflammatory bowel disease via TLR4/NF-κB/IQGAP2 signaling pathway. *Biomed Pharmacother*. (2017) 85:531–40. doi: 10.1016/j.biopha.2016.11.061

38. Zhang L, Zhang H, Li X, Jia B, Yang Y, Zhou P, et al. Miltirone protects human EA.hy926 endothelial cells from oxidized low-density lipoprotein-derived oxidative stress via a heme oxygenase-1 and MAPK/Nrf2 dependent pathway. *Phytomedicine*. (2016) 23:1806–13. doi: 10.1016/j.phymed.2016.11.003

39. Yan W, Guoping Y, Chengxian G, Qi P, Ranran Z, Lu H. Plasma double-peak phenomenon following oral administration. *Chin J Clin Pharma Ther*. (2014) 19:341–5.

frontiers | Frontiers in Cardiovascular Medicine

TYPE Original Research
PUBLISHED 16 September 2022
DOI 10.3389/fcvm.2022.942342

Check for updates

OPEN ACCESS

EDITED BY
Morgan Salmon,
University of Michigan, United States

REVIEWED BY
Bhupesh Singla,
University of Tennessee Health Science Center (UTHSC), United States
Stephen Lee Rego,
University of North Carolina at Chapel Hill, United States

*CORRESPONDENCE
Jane Stubbe
jstubbe@health.sdu.dk

†These authors have contributed equally to this work

SPECIALTY SECTION
This article was submitted to General Cardiovascular Medicine, a section of the journal Frontiers in Cardiovascular Medicine

RECEIVED 12 May 2022
ACCEPTED 08 August 2022
PUBLISHED 16 September 2022

CITATION
Griepke S, Grupe E, Lindholt JS, Fuglsang EH, Steffensen LB, Beck HC, Larsen MD, Bang-Møller SK, Overgaard M, Rasmussen LM, Lambertsen KL and Stubbe J (2022) Selective inhibition of soluble tumor necrosis factor signaling reduces abdominal aortic aneurysm progression.
Front. Cardiovasc. Med. 9:942342.
doi: 10.3389/fcvm.2022.942342

COPYRIGHT
© 2022 Griepke, Grupe, Lindholt, Fuglsang, Steffensen, Beck, Larsen, Bang-Møller, Overgaard, Rasmussen, Lambertsen and Stubbe. This is an open-access article distributed under the terms of the Creative Commons Attribution License (CC BY). The use, distribution or reproduction in other forums is permitted, provided the original author(s) and the copyright owner(s) are credited and that the original publication in this journal is cited, in accordance with accepted academic practice. No use, distribution or reproduction is permitted which does not comply with these terms.

Selective inhibition of soluble tumor necrosis factor signaling reduces abdominal aortic aneurysm progression

Silke Griepke[1†], Emilie Grupe[1†], Jes Sanddal Lindholt[2,3], Elizabeth Hvitfeldt Fuglsang[1], Lasse Bach Steffensen[1], Hans Christian Beck[2,4], Mia Dupont Larsen[1], Sissel Karoline Bang-Møller[1], Martin Overgaard[2,4], Lars Melholt Rasmussen[2,4], Kate Lykke Lambertsen[5,6,7] and Jane Stubbe[1,2*]

[1]Department of Cardiovascular and Renal Research, Institute of Molecular Medicine, University of Southern Denmark, Odense, Denmark, [2]Elite Research Centre for Individualized Medicine in Arterial Diseases (CIMA), Odense University Hospital, Odense, Denmark, [3]Department of Cardiothoracic and Vascular Surgery, Odense University Hospital, Odense, Denmark, [4]Department of Clinical Biochemistry and Pharmacology, Odense University Hospital, Odense, Denmark, [5]Department of Neurobiology, Institute of Molecular Medicine, University of Southern Denmark, Odense, Denmark, [6]Department of Neurology, Odense University Hospital, Odense, Denmark, [7]BRIDGE—Brain Research—Inter-Disciplinary Guided Excellence, Department of Clinical Research, University of Southern Denmark, Odense, Denmark

Background: Tumor necrosis factor (TNF) is pathologically elevated in human abdominal aortic aneurysms (AAA). Non-selective TNF inhibition-based therapeutics are approved for human use but have been linked to several side effects. Compounds that target the proinflammatory soluble form of TNF (solTNF) but preserve the immunomodulatory capabilities of the transmembrane form of TNF (tmTNF) may prevent these side effects. We hypothesize that inhibition of solTNF signaling prevents AAA expansion.

Methods: The effect of the selective solTNF inhibitor, XPro1595, and the non-selective TNF inhibitor, Etanercept (ETN) was examined in porcine pancreatic elastase (PPE) induced AAA mice, and findings with XPro1595 was confirmed in angiotensin II (ANGII) induced AAA in hyperlipidemic apolipoprotein E (*Apoe*)$^{-/-}$ mice.

Results: XPro1595 treatment significantly reduced AAA expansion in both models, and a similar trend (p = 0.06) was observed in PPE-induced AAA in ETN-treated mice. In the PPE aneurysm wall, XPro1595 improved elastin integrity scores. In aneurysms, mean TNFR1 levels reduced non-significantly (p = 0.07) by 50% after TNF inhibition, but the histological location in murine AAAs was unaffected and similar to that in human AAAs. Semi-quantification of infiltrating leucocytes, macrophages, T-cells, and neutrophils in the aneurysm wall were unaffected by TNF inhibition. XPro1595 increased systemic TNF levels, while ETN increased systemic IL-10 levels. In ANGII-induced AAA mice, XPro1595 increased systemic TNF and IL-5 levels. In early AAA development, proteomic analyses revealed that XPro1595 significantly

upregulated ontology terms including "platelet aggregation" and "coagulation" related to the fibrinogen complex, from which several proteins were among the top regulated proteins. Downregulated ontology terms were associated with metabolic processes.

Conclusion: In conclusion, selective inhibition of solTNF signaling reduced aneurysm expansion in mice, supporting its potential as an attractive treatment option for AAA patients.

KEYWORDS

cardiovascular disease, abdominal aortic aneurysm, tumor necrosis factor inhibitor, inflammation, translational research, vascular inflammation

Introduction

Abdominal aortic aneurysm (AAA) is an irreversible dilatation of the abdominal aorta that occurs in approximately 5% of elderly males (1). AAA progresses asymptomatically, but aneurysm rupture leads to acute intra-abdominal hemorrhage that is associated with up to 90% mortality (2). Current treatment options for AAA are limited to surgical intervention when AAA expansion reaches 55 mm in diameter in males (3), and no effective pharmacological alternative to slow AAA growth or prevent rupture is available (4). AAA pathophysiology is not fully understood, but local destruction of elastin and collagen in the aortic wall is considered an early event leading to the reorganization of extracellular matrix (ECM) composition (5). Disruption of the aortic wall structure releases elastokines which initiates an acute immunoreaction and infiltration of immune cells primarily dominated by macrophages, neutrophils, and T lymphocytes, releasing several pro-inflammatory cytokines, including tumor necrosis factor (TNF) (6–8). These cytokines stimulate macrophages and vascular smooth muscle cells (VSMCs) to release matrix metalloproteinases (MMPs), with MMP-2 and MMP-9 being the most critical ones in AAA progression (9, 10). MMP-9 derives primarily from infiltrating monocytes and macrophages, whereas MMP-2 derives primarily from activated vascular smooth muscle cells (11). Continued degradation of the ECM will eventually weaken the aortic wall, causing vascular smooth muscle cells to undergo apoptosis and thereby lead to thinning of the media (12), which ultimately results in AAA rupture.

Elevated TNF levels have been observed in both plasma and aneurysm wall samples from patients with AAA, suggesting that TNF plays a significant role in the pathogenesis of the disease (13–15). In support of this, a lack of functional TNF in mice has been shown to attenuate $CaCl_2$–induced aneurysm development (16). TNF exists in two bioactive forms (17), but it is unclear whether both forms contribute to AAA development. TNF is synthesized as a transmembrane protein (tmTNF) (18) that is cleaved from the cell membrane by metalloproteinase TNF-converting enzyme (TACE/ADAM17) and released to the circulation and surrounding tissue as a soluble trimer complex (solTNF) (19). The effect of TNF is mediated by TNF receptor (TNFR) 1 and TNFR2, resulting in both overlapping and distinct biological outcomes (17). SolTNF has a higher affinity for TNFR1, and thus primarily drives a proinflammatory response through TNFR1 activation (20), whereas tmTNF acts in a paracrine fashion and mainly signal through TNFR2, resulting in tissue repair and regeneration as well as immune-regulating functions (21–24). Although the specific contributions of solTNF and tmTNF in AAA development remain uncertain, temporal systemic deletion of TACE prevents AAA formation in mice by attenuating inflammation and ECM disruption, indicating a crucial role of solTNF-TNFR1 signaling in AAA development (25). Thus, blocking solTNF is a promising therapeutic target for preventing AAA expansion.

Non-selective pharmacological inhibition of TNF using etanercept (ETN; a fusion protein consisting of TNFR2 attached to Fc of IgG that target both forms of TNF) has been effective in treating inflammatory diseases such as rheumatoid arthritis and inflammatory bowel disease (26). ETN is now recognized as an effective strategy in the management of chronic inflammation. Xiong et al. reported that Infliximab (another non-selective anti-TNF therapy) could inhibit aneurysm growth, attenuate elastic fiber disruption, and reduce macrophage infiltration in a $CaCl_2$-induced AAA murine model (16), indicating that this strategy of TNF-antagonism may also apply to the treatment of AAA. It is uncertain, however, whether infliximab is effective in mice or whether the observed effects were mediated through off-target effects (27). Unfortunately, the use of non-selective TNF inhibition has been linked to rare but severe side effects, including increased susceptibility to serious

infections (28, 29), potential risk of congestive heart failure (30), and demyelinating events (31, 32). Therefore, a new class of drugs called dominant-negative TNF (DN-TNF) inhibitors, which only inhibit solTNF signaling, has been developed to counteract the side effects of non-selective TNF therapy (33). The use of DN-TNF allows selective inhibition of the suggested proinflammatory solTNF-TNFR1 signaling pathway while preserving the suggested immunoregulatory and tissue-repairing functions of tmTNF-TNFR2 signaling, thereby hopefully diminishing the adverse effects of non-selective TNF treatment. Among the leading DN-TNFs today is the experimental drug XPro1595, which is a mutein of TNF that forms complexes with naïve solTNF. These complexes are incapable of binding to TNFRs, particularly TNFR1 (33, 34). XPro1595 treatment has successfully dampened several TNF-driven experimental diseases such as arthritis, Huntington's disease, multiple sclerosis, spinal cord injury, and stroke (33, 35–38). We therefore hypothesize that selective inhibition of solTNF using XPro1595 will prevent AAA expansion by inhibiting the proinflammatory solTNF-TNFR1 signaling. This hypothesis was tested in two experimental murine AAA-models: 1) intraluminal porcine pancreatic elastase (PPE) infusion of the infrarenal aorta to test the effects of selective inhibition of solTNF by XPro1595 and non-selective inhibition of TNF by ETN on AAA expansion; and 2) chronic angiotensin II (ANGII) infusion in hyperlipidemic apolipoprotein E (*Apoe*)$^{-/-}$ mice to test only the effect of XPro1595 on AAA expansion.

Materials and methods

Animals and human tissue

Experiments were performed according to an approved protocol by the Danish Animal Experiments Inspectorate (2015-15-0201-00474). Male C57BL/6J mice were purchased from Janvier Laboratories, Le Genest-Saint-Isle, France, and were allowed to acclimatize for 1 week prior to experiments. *Apoe*$^{-/-}$ mice originated from Jackson Laboratory, United States, and were bred in house at the Biomedical Laboratory, University of Southern Denmark. Genotyping of the *Apoe*$^{-/-}$ was done using primers (Sigma-Aldrich, Søborg, Denmark), with sequences provided by Jackson Laboratory. The experiments were performed at our facility where the mice were housed in a 12 h light/dark cycle, room temperature of 20°C, and air humidity of 55%. During the entire experiment, the animals had free access to food and tap water. Human aneurysm tissue and human ascending aortic punch specimens were collected after written consent and with approval from the Regional Committee on Health Research Ethics for Southern Denmark (S20140202 and M20080028).

Induction of abdominal aortic aneurysm by perfusion of porcine pancreatic elastase (PPE)

Male C57BL/6J mice (9–10 weeks old) were anesthetized using a ketamine (Ketalar, Pfizer, Sandwich, Kent, United kingdom), and xylazine (Bayer Healthcare, Shawnee Mission, KS, United States) mixture and underwent laparotomy, followed by isolation of the abdominal aorta from the left renal vein to the iliac artery bifurcation. The baseline outer abdominal aortic diameter (OAD) during systole was measured using video recordings captured by a Nikon D3400 camera. The infrarenal aorta was then occluded using a silk suture (6.0, Amann, FST, Heidelberg, Germany) and a polyethylene catheter (4.0 Ethilon suture, Ethicon) was placed in the infrarenal aorta, allowing infusion of PPE (1.5 units/mL, Sigma-Aldrich, Søborg, Denmark) to expand the aorta to twice its size for 5 min. After removal of the catheter, the aortotomy was sutured with an 11.0 Ethilon suture (Ethicon), blood flow was reestablished, and the laparotomy was closed. Mice were given rimadyl (Zoetis, Farum, Denmark) for pain management. The health status and body weight of the mice were monitored daily for the following 14 days. On the day of surgery, mice were divided into three groups and treated by intraperitoneal injections (IP) of either XPro1595 [20 mg/kg, INmune Bio Inc, La Jolla, CA, United States, $n = 14$, (34)], etanercept (ETN, 20 mg/kg, Enbrel, Sandoz, Kundl, Austria, $n = 14$) or vehicle (physiological saline, Fresenius Kabi, Copenhagen, Denmark, $n = 14$) every third day during the next 14 days. At the end of the experiment, mice were re-anesthetized, the infrarenal aorta was isolated, and the final OAD was recorded. The percentage of increase in OAD (ΔOAD) was determined by an observer blinded to the treatment using the difference between baseline and final OAD of the infrarenal aorta. Collected organs were snap frozen in liquid nitrogen and stored together with EDTA-plasma at –80℃. Mice were terminated by perfusion with 10% normal formalin (Hounisen Laboratorieudstyr A/S, Skanderborg, Denmark) through the heart for 4 min at 120 mmHg pressure. For determination of abundant proteins in the aortic wall in the early phase of AAA expansion, a series of mice (vehicle $n = 6$; XPro1595 $n = 7$) were terminated 7 days post-surgery.

Induction of abdominal aortic aneurysm by subcutaneous angiotensin II infusions in hyperlipidemic *Apoe* $^{-/-}$ mice

AAAs were induced in 8–12 weeks old male *Apoe*$^{-/-}$ mice by chronic ANGII infusion *via* subcutaneous minipumps (Alzet model 2004, DURECT TM Corporation, Cupertino, CA, United States) releasing 60 μg/kg/hour ANGII (Calbiochem,

Merck, Søborg, Denmark) for 28 days as previously described (39). In brief, pumps were implanted subcutaneously in the dorsal region of the mice through a neck incision under 3% isoflurane (IsoFlo® vet, Orion Pharma, Nivå, Denmark) anesthesia. Mice were given *ad libitum* high-fat diet (RD Western diet D12079B, Research Diets Inc., Brogården, Hørsholm, Denmark) from 1 week before pump insertion and throughout the experiment. The mice were monitored daily and treated with XPro1595 (2 mg/kg, INmune Bio Inc., La Jolla, CA, United States n = 20 total, n = 14 completed) or vehicle (physiological saline, Fresenius Kabi, Copenhagen, Denmark, n = 19 total, n = 13 completed) by IP injections every third day for 28 days, starting on the day of surgery (day 0). Mice found dead during the experiment were analyzed for aortic rupture (12 died of aortic rupture, one died of unidentified reasons). Changes in inner aortic diameter were followed in anesthetized mice (3% isoflurane) by ultrasound using LOGIQ e portable ultrasound imaging system (GE Healthcare, Brøndby, Denmark) with a 22 MHz central frequency probe (L10-22-RS, GE healthcare, Brøndby, Denmark), starting on day 0 before surgery and then once a week for the following 4 weeks. Ultrasound measurements were determined by an observer blinded to the treatment.

Mice were terminated on day 28, and the aortas were fixed in 10% normal formalin (Hounisen Laboratorieudstyr A/S, Skanderborg, Denmark) for 24 h. The aortas were then placed on black wax Petri dishes and imaged with a Leica M80 dissecting microscope and a Leica IC80 HD digital microscope camera. The maximal outer abdominal aortic diameter and AAA surface area as a measure of aneurysm volume (surface area defined at a longitudinal piece of 7.7 mm to contain the full dilation of all aortas) were measured using Image J software (1.53a Wayne Rasband, National Institutes of Health, Bethesda, MA, United States). All measurements were performed by an observer blinded to treatment. The suprarenal abdominal aortas were embedded in paraffin for later histological analysis.

Immunohistochemical staining

For immunohistochemical staining, human full wall AAA samples were collected during open surgical repair of growing AAAs, and ascending aortic wall punches were collected during coronary artery bypass surgeries. All human and murine tissues for histological analyses were fixed in 10% normal formalin (Hounisen Laboratorieudstyr A/S, Skanderborg, Denmark) and embedded in paraffin. Then, 5 μm sections were deparaffinized and hydrated in ethanol (99–75%) followed by demasking in either citrate buffer pH 6 (10 mM, Merck Søborg, Denmark) or TEG buffer pH 9 (10 mM, Tris Base, VWR, Søborg, Denmark). The sections were blocked for endogenous peroxidase activity in 3% H_2O_2 (Merck, Søborg, Denmark) in TBS and then blocked in 5% skimmed milk (Merck, Søborg, Denmark) or 3% bovine serum albumin (BSA, Sigma-Aldrich, Søborg, Denmark) in TBS containing 0.05% Tween20 (TBST, Sigma-Aldrich, Søborg, Denmark). Sections were then incubated overnight at 4°C with primary antibody directed against; CD45 (1:100, #550539, BD Pharmingen, Albertslund, Denmark), CD3 (1:200 Abcam, ab16669, Cambridge, United Kingdom), CD206 (1:1,000, Abcam, ab64693, Cambridge, United Kingdom), Ly6G (1:500, ab238132, Abcam, Cambridge, United Kingdom), fibronectin (1:300, ab268020, Abcam, Cambridge, United Kingdom), MMP-9 (1:200, ab38898, Abcam, Cambridge, United Kingdom), TNFR1 (1:500, ab19139, Abcam, Cambridge, United Kingdom), or TNFR2 (1:100, LS-B5301, LSBio, Copenhagen, Denmark). The following day, sections were incubated with appropriate horseradish-peroxidase (HRP)-conjugated secondary antibodies (1:1,000, DAKO, Agilent, Glostrup, Denmark) or with anti-rabbit EnVision+ System (DAKO, Agilent, Glostrup, Denmark), then washed in TBST. Positive staining was detected by applying diaminobenzidine (DAB, K3468, DAKO, Agilent, Glostrup, Denmark). Nuclei were counterstained using Mayer's hematoxylin (Sigma-Aldrich). As negative controls, staining was tested on parallel sections of aortic aneurysmal samples by omitting the primary antibody or with the appropriate isotype IgG control (DAKO, Agilent, Glostrup, Denmark). All immunohistochemically stained tissue sections were analyzed by Olympus BX51 microscope, and images were captured by Olympus DP26 camera and analyzed in Image J. Cell counts of DAB positive cells (MMP-9, CD45, Ly6G and CD3) and % area of positive staining (TNFR1 and TNFR2) were measured based on means of duplicate AAA tissue sections for each mouse and expressed as the number of cells pr. mm^2 AAA tissue or % positive staining, respectively. All analyses were done blinded. To assess elastin integrity, sections of aortic aneurysms were stained in 1% acidified Miller's Elastin stain (Atom Scientific, Hyde, United Kingdom) according to the manufacturer's instructions. The structural composition of elastin in the aneurysmal wall was semi-quantified by a scoring system described in Sun et al. (40).

Measurement of cytokines, chemokines, and tumor necrosis factor receptor levels in aneurysm and plasma samples

Aneurysm tissues sampled 14 days after induction by the PPE model were lysed in Complete Mesoscale Lysis Buffer [10 mL 1x TRIS lysis buffer containing; 100 μL phosphate inhibitor cocktail #2 (Sigma-Aldrich, Søborg, Denmark), 100 μL phosphate inhibitor cocktail #3 (Sigma-Aldrich,

Søborg, Denmark), and 1 tablet complete Mini, EDTA-free (Roche, Hvidovre, Denmark)] and homogenized by beads in a Tissue Lyzer II (Qiagen, Aarhus, Denmark) (Qiagen, Germany) for 3 min with maximum speed of 300 rpm and centrifuged for 20 min at +4°C at 12.000 × g. The supernatants were collected and stored at −80°C. Protein concentrations were determined using the Pierce BSA Protein Assay kit (Thermo Fischer, Roskilde, Denmark) (Bio-Rad, Copenhagen, Denmark). Cytokines and chemokines were then measured in aneurysmal protein samples and plasma samples using two different Mesoscale Discovery™ (MSD, Rockville, MA, United States) mouse pro-inflammatory V-Plex plus kits while TNFR1 and TNFR2 levels were determined using Ultra-Sensitive Kit (MSD, Rockville, MA, United States). Protocols were performed according to the manufacturer's instructions. All samples were run in duplicate. Data were analyzed using MSD Workbench software. The cut-off threshold for inclusion of results was set at CV < 20%.

Explorative mass spectrometry proteome analyses of XPro1595 and vehicle-treated abdominal aortic aneurysms at early development

Murine abdominal aorta aneurysms sampled 7 days after AAA induction by the PPE model were homogenized using a TissueLyser system (Qiagen, Aarhus, Denmark) with stainless steel beads (Qiagen, Aarhus, Denmark) in a lysis buffer [100 mM DTT, 5% sodium deoxycholate, 1% β-octylglucoside, 20 mM Tris, pH 8.8, supplemented with complete, Mini, EDTA-free Protease Inhibitor Cocktail Tablets and PhosSTOP (Roche, Hvidovre, Denmark)]. Protein samples were acetone-precipitated, re-dissolved in 0.2 M tetraethylammonium bicarbonate, and trypsinized overnight. Samples (4 µg tryptic peptides per sample) were randomly labeled with 11-plex tandem mass tags (TMT, Thermo Fisher Scientific, San Jose, CA, United States); mass tag 131°C was a pool of all AAA samples and served as internal control. Proteome data are protein abundances relative to the internal control. Mixed peptide samples were high pH fractionated as previously described (41). Nano-LC-MSMS of fractionated samples was performed on an Orbitrap Eclipse tribrid mass spectrometer (Thermo Fisher Scientific, San Jose, CA, United States) equipped with a nanoHPLC interface (Dionex UltiMate 3000 nano HPLC). The samples (5 µL) were loaded onto a custom-made fused capillary pre-column [2 cm length, 360 µm OD, 75 µm ID packed with ReproSil Pur C18 3 µm resin (Dr. Maish, GmbH)] with a flow of 5 µL/min for 7 min. Trapped peptides were separated on a custom-made fused capillary column (25 cm length, 360 µm OD, 75 µm ID, packed with ReporSil Pur C13 1.9 µm resin) using linear gradient ranging from 88 to 86% solution A (0.1% formic acid) to 27–32% B (80% acetonitrile in 0.1% formic acid) over 119 min. Mass spectra were acquired with an Orbitrap Eclipse Tribrid mass spectrometer with FAIMS Pro interface (Thermo Fisher Scientific, San Jose, CA, United States), switching between CVs of −50 and −70 V with 2 s cycle time. MS1 spectra were acquired at 60,000 resolutions with a scan range from 400 to 1,200 m/z, normalized AGC target of 100%, and maximum injection time of 50 ms. Precursors were filtered using monoisotopic peak determination set to peptide, charge state 2–4, dynamic exclusion of 60 s with ± 10 ppm tolerance excluding isotopes and different charge states, and a precursor fit of 70% in a window of 0.4 m/z for MS2 (50.000 resolution, normalized AGC target of 100 %, maximum fill time 86 of ms). All Eclipse raw data files were processed and quantified using Proteome Discoverer version 2.4 (Thermo Scientific, Waltham, MA, United States) as previously described (41).

Enrichment analysis was performed using R clusterProfiler 4.0 (arguments: ont = BP; nPerm = 10,000; minGSsize = 3; maxGSSize = 800; pvalueCutoff = 0.05; pAdjustMethod = "BH") (42).

Statistics

The primary endpoint of the study is the aneurysmal progression rate. In previous experiments, we observed a mean relative maximal aortic diameter increase of 127.3% ± 36.8 SD for the PPE-model (unpublished data). An aortic diameter difference of 30–33% is considered clinically significant. For a *t*-test with 5% significance and 80% power, each group needs 13 animals, when the ratio between intervened and control mice is 1:1. Therefore, we used 13–14 mice per group for the two experiments.

Statistical analyses and graphical representation of data were performed using GraphPad Prism version 6.0 (GraphPad Software, San Diego, CA, United States). All normally distributed data passing the D'Agostino and omnibus tests were analyzed by Student's *t*-test for two-group comparisons, and significance of change between more than two groups was calculated using one-way analysis of variance (ANOVA) followed by Bonferroni's *post-hoc* test for comparing means between groups or using two-way ANOVA with repeated measurements followed by Bonferroni's *post hoc* testing. Data are represented as mean ± standard error of mean (SEM). Differences between non-Gaussian data not passing the normality test were analyzed by Mann-Whitney *U*-test and presented as median with interquartile range.

For normally distributed data, Grubb's outlier test was used to identify outliers. Here, one sample in the XPro1595-treated-group in the ANGII model was identified as an outlier after

analysis of both aortic diameters and surface area of AAAs and was excluded from the statistical analysis and all further downstream analyses. The sample is shown as a red square (■) in the corresponding figures. A Fisher exact probability test with Freeman-Halton extension was used for a test of statistical significance for contingency table data of elastin degradation grade distributions. Explorative proteomic data were analyzed by unpaired *t*-test for each protein followed by *fdr* correction for multiple testing.

Comparisons with $P < 0.05$ were considered statistically significant and were denoted by asterisk(s).

Results

Selective inhibition of soluble form of tumor necrosis factor reduces expansion of elastase-induced abdominal aortic aneurysms

To determine whether TNF inhibition dampens elastase-induced AAA, mice were treated with the selective solTNF inhibitor, XPro1595, or with the non-selective TNF inhibitor ETN for 14 days. XPro1595 significantly reduced AAA expansion by 40% when compared to vehicle-treated control mice assessed by external outer abdominal aortic diameter (OAD) *in vivo* (**Figures 1A,B**). A similar, but non-significant, trend was seen with ETN treatment ($p = 0.06$, **Figures 1A,B**). TNF inhibition did not affect body weight or the relative mass of heart, liver, and kidneys to body weight (**Supplementary Figures 1A,B**).

Selective inhibition of soluble form of tumor necrosis factor protects against elastic fiber degradation in the aneurysm wall

To address the disintegration of elastin in the aneurysm wall, elastin was stained using Miller's elastin stain. In both the vehicle- and the ETN-treated group, the aneurysmal elastic lamellae were disorganized, stretched with areas containing multiple ruptured elastic fibers (**Figure 1**, arrows), while the elastin lamellae in the XPro1595-treated group were more organized with only few ruptured elastin lamellae (**Figure 1C**). Using a scoring system of elastin integrity described in Sun et al. (40), a significantly lower score was found in the XPro1595-treated mice than the vehicle-treated mice (**Figure 1D**). In contrast, elastin preservation was not observed after ETN treatment ($p = 0.69$, **Figure 1D**). The preserved elastin in the XPro1595-treated group was not caused by fewer MMP-9 positive cells/mm^2 located within the aneurysm wall (**Figure 1E**), where MMP-9-positive cells were mainly associated with macrophage like cells in the adventitia (**Figure 1F**) that were evenly distributed between treatment groups (**Figures 1E,F**).

Tumor necrosis factor receptor localization in the murine aneurysmal wall is comparable to that of humans

XPro1595 and ETN treatment resulted in a trend toward a 50% reduction in TNFR1 protein levels in the aneurysm wall when compared to vehicle-treated mice ($p = 0.07$, **Figure 2A**, left graph), while TNFR2 protein levels were unaffected by TNF inhibition (**Figure 2A**, right graph). This reduction in TNFR1 did not appear to be confined to a specific cell type in the aneurysm wall, as TNFR1 was localized in some VSMCs, infiltrating leukocyte-like cells, and endothelial cells with no apparent differences (**Figure 2B**, upper panel). TNFR2 was associated with leukocyte-like cells in the adventitia and some VSMCs and was unaffected by treatment (**Figure 2B**, lower panel). In thoracic mouse unchallenged aorta, TNFR1 immunolabeling was identified in most cells in media and adventitia, while in endothelial cells only a discrete labeling was observed (**Figure 2C**, arrow). The localization of TNFR1 in human AAA specimens and ascending aorta punches resembled that of murine aneurysms and thoracic aorta (**Figure 2D**). In the aneurysm wall, mainly leukocytes-like cells were found to be TNFR1-positive, while TNFR1 immunolabeling in human ascending aorta was associated with discrete staining in VSMCs, with more pronounced labeling in endothelial cells.

Protection of abdominal aortic aneurysm expansion by soluble form of tumor necrosis factor inhibition is not associated with reduced leukocyte infiltration in the aneurysm wall

We observed no difference in the number of infiltrating CD45-positive leukocytes/mm^2 in the aneurysm wall after TNF inhibition (**Figure 3A**). All groups displayed CD45-positive cells primarily in tunica adventitia and to lesser extent tunica media (**Figure 3A**, arrows). Also, the numbers of anti-inflammatory M2-like CD206-positive macrophages/mm^2 (**Figure 3B**, arrows), of CD3-positive T-cells/mm^2 (**Figure 3C**, arrows), and of Ly6G-positive neutrophil cells/mm^2 (**Figure 3D**, arrows) were similar between treatment groups, and all positive staining was restricted to tunica adventitia (**Figures 3B–D**, arrows).

10.3389/fcvm.2022.942342

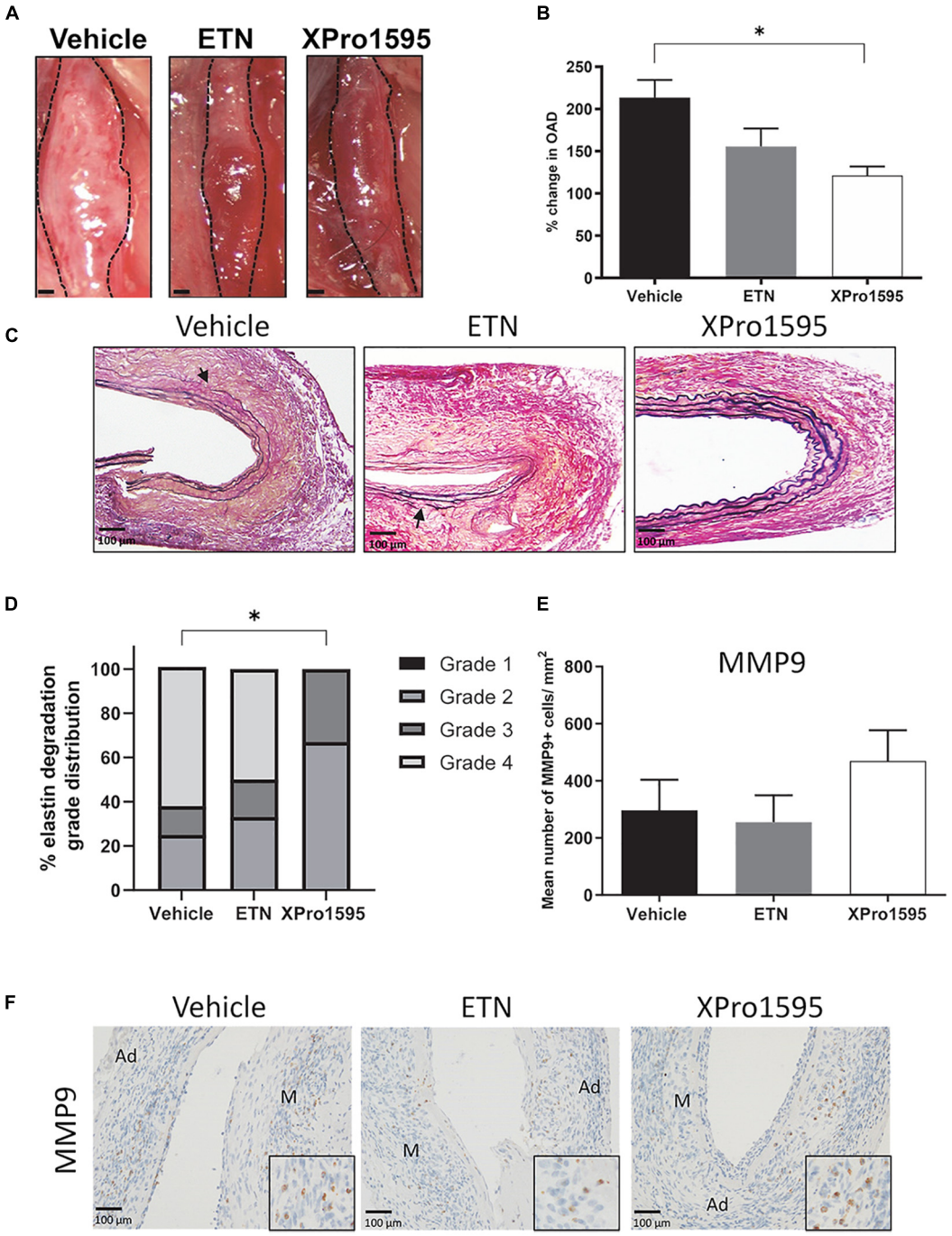

FIGURE 1
Selective inhibition of solTNF prevents expansion in PPE-induced AAA. **(A)** Representative macroscopic images displaying PPE-induced AAAs after 14 days of treatment with vehicle (saline), ETN (20 mg/kg), or XPro1595 (20 mg/kg). **(B)** *In vivo* AAA expansion measured as percentage change in the maximal outer diameter of the abdominal aorta (OAD) from day 0 to day 14 (n = 15–16). **(C)** AAA cross-sections stained with Miller's elastic stain (black) after TNF inhibition (n = 3–5). Breaks in elastic fibers are marked with arrows. **(D)** Percentage distribution of elastic fiber integrity (grades 1–4) according to treatment groups (n = 3–5). **(E,F)** The number of MMP-9-positive cells/mm^2 cross-sectional aneurysmal area from mice treated with vehicle-, ETN-, or XPro1595 (n = 3–5). Data are shown as mean SEM. * Indicates $p < 0.05$ analyzed by one-way ANOVA using Bonferroni test for multiple comparisons. Contingency table data in E was analyzed by Fisher exact probability test with Freeman-Halton extension. M, media; Ad, adventitia.

10.3389/fcvm.2022.942342

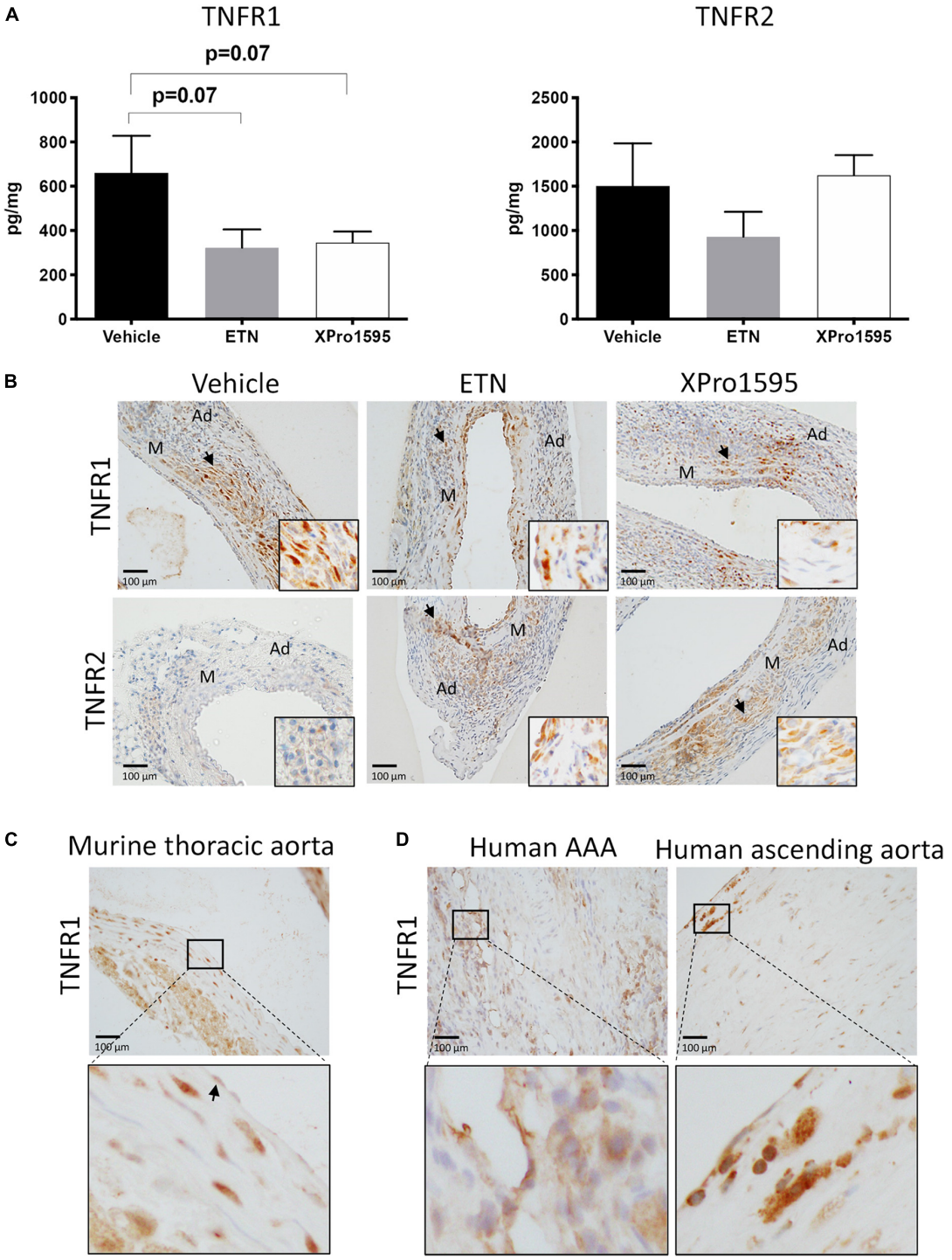

FIGURE 2

TNF receptor protein levels and receptor localization in murine and human abdominal aortic tissue. **(A)** Aneurysmal protein levels of TNFR1 and TNFR2 from PPE- induced aneurysm in mice treated with vehicle (saline), ETN (20 mg/kg), or XPro1595 (20 mg/kg) (n = 3–5). Data are shown as mean SEM. A non-significant trend was detected in TNFR1 levels by one-way ANOVA using Bonferroni test for multiple comparisons. **(B)** Representative distribution of TNFR1 and TNFR2 in the PPE-induced AAA wall after treatment with saline, ETN, or XPro1595 for 14 days (n = 3–5). **(C)** TNFR1 distribution in unchallenged thoracic murine aorta. **(D)** Distribution of TNFR1 in human AAA specimens (n = 2) and human ascending aortas (n = 2). Black arrowheads indicate positive stained cells. M, media; Ad, adventitia.

10.3389/fcvm.2022.942342

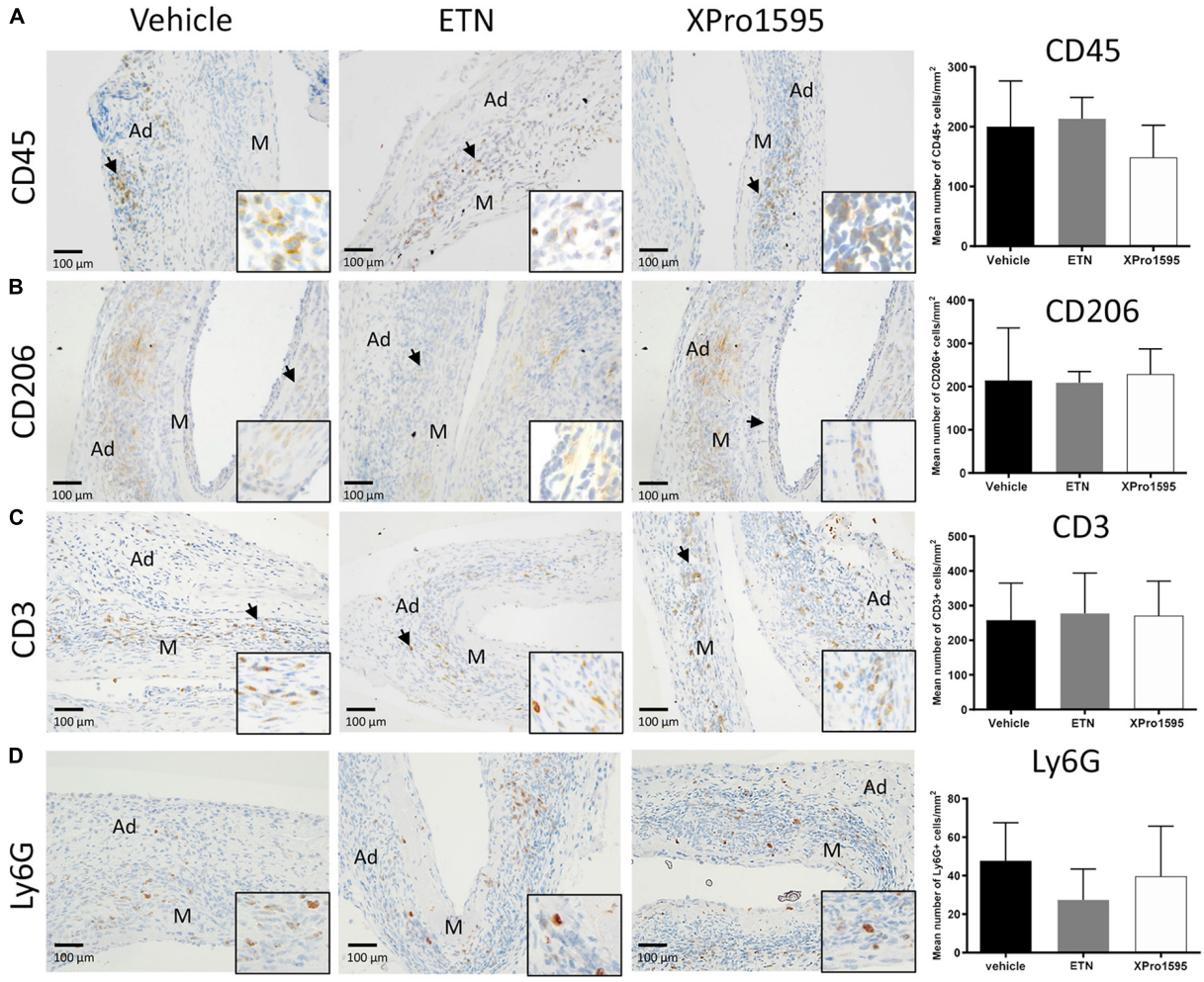

FIGURE 3
Effect of TNF inhibition on infiltrating immune cells 14 days after PPE-induced AAA formation. Representative micrographs after TNF inhibition showing the distribution of infiltrating immune cells (left) and semi-quantification (right, number of positive cells/mm^2) of CD45-positive leukocytes **(A)**, CD206-positive M2-like macrophages **(B)**, CD3-positive T-cells **(C)**, and Ly6G-positive neutrophils **(D)** in the aneurysm wall after TNF inhibition (n = 3–5). Black arrowheads indicate positive stained cells. Data are shown as mean SEM. None of the semi-quantifications reached significance on one-way ANOVA using Bonferroni test for multiple comparisons. M, media; Ad, adventitia.

Selective soluble tumor necrosis factor inhibition and non-selective tumor necrosis factor inhibition differentially regulate cytokine levels locally and systemically in porcine pancreatic elastase-induced abdominal aortic aneurysms mice

We next examined whether TNF inhibition affected local and/or systemic production of cytokines. Locally in the aneurysmal wall, there was a non-significant 50% increase in TNF protein levels in the ETN-treated AAAs when compared to vehicle-treated (p = 0.11), whereas TNF levels were significantly reduced in XPro1595-treated AAAs compared to ETN treatment (**Figure 4A**). A similar trend was seen with the pro-inflammatory cytokine interferon-gamma (IFNγ, **Figure 4B**) and the anti-inflammatory cytokine interleukin (IL)-10 (**Figure 4C**). No differences were observed in levels of IL-1β, IL-2, IL-4, IL-5, IL-6, IL-12p70, or KC/GRO in aneurysm tissue (**Supplementary Table 1**). In contrast to the aneurysm wall, there was a 10-times increase in plasma solTNF levels after XPro1595 treatment, whereas ETN treatment did not affect circulating solTNF levels (**Figure 4D**). Plasma levels of IL-1β (**Figure 4E**) and IL-10 (**Figure 4F**) were increased in ETN-treated mice, whereas the IL-10 levels in XPro1595-treated mice were similar to the levels in vehicle-treated mice. The levels

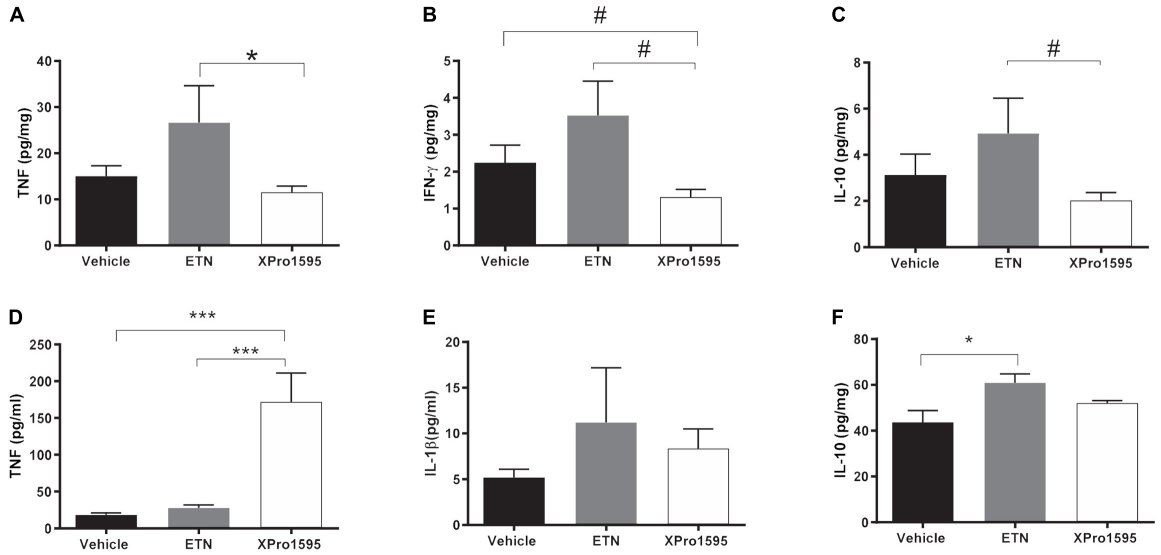

FIGURE 4
Pro- and anti-inflammatory cytokine profile systemically or locally produced in PPE-induced aneurysms after TNF inhibition. Changes in aneurysmal cytokine levels of TNF (n = 5–8) **(A)**, IFN-γ (n = 6–8) **(B)**, and IL-10 (n = 6–8) **(C)** 14 days after PPE-induced AAA mice treated with vehicle (saline), ETN (20 mg/kg), or XPro1595 (20 mg/kg). Changes in plasma levels of TNF (n = 7–8) **(D)**, IL-1β (n = 8) **(E)**, and IL-10 (n = 7–8) **(F)**. Data are shown as mean SEM. No significance was observed by one-way ANOVA using Bonferroni test for multiple comparisons. P-values are denoted *$p < 0.05$, ***$p < 0.001$, and $^{\#}$ denotes $p < 0.05$ for unpaired Student's t-test for two-group comparisons.

of other measured circulating cytokines (IL-2, IL-4, IL-5, IL-6, KC/GRO) were not affected by TNF inhibition (**Supplementary Table 2**).

Selective inhibition of soluble tumor necrosis factor increases fibrinogens and fibronectin in early abdominal aortic aneurysms

To explore the effect of TNF inhibition in initial stages of AAA development, aneurysms were examined by mass spectrometry 7 days after disease onset. None of the 5,469 identified proteins were significantly regulated by XPro1595 treatment after adjustment for multiple testing (see **Supplementary Table 3** for a complete list of identified proteins). However, enrichment analysis revealed ontologies including "hemostasis," "platelet aggregation," and "coagulation" to be significantly upregulated by XPro1595 treatment (**Figure 5A**). In addition, significantly upregulated ontologies included "leukocyte migration," "zymogen activation," and "leukocyte-mediated immunity," while downregulated ontologies covered a variety of metabolic processes (**Figure 5A**). In particular, three fibrinogen chains (FGA, FGB, and FGG) and fibronectin (FN1), which are key players in platelet aggregation and coagulation biological processes, were among the top regulated proteins shown in the volcano plot (green colored dots in **Figure 5B**) while prostaglandin E2 synthase (MPGES2) was among the most downregulated proteins after XPro1595 treatment (**Figure 5B**, red colored dot). Immunohistochemistry showed fibronectin in intima draining into media (**Figure 5C**, arrows) in the aneurysm wall in both vehicle- and XPro1595-treated mice.

Selective inhibition of soluble tumor necrosis factor inhibits abdominal aortic aneurysm expansion in angiotensin II-treated *Apoe* $^{-/-}$ mice

As seen with the PPE-induced aneurysms, XPro1595 significantly attenuated AAA progression in ANGII-induced AAA according to different parameters of aneurysmal size (**Figure 6**). Inner luminal aortic circumference measured by ultrasound revealed a significant reduction in the relative luminal size at day 28 when measured as circumference of the inner aorta (**Figures 6A–C**). Also, the percentage increase from days 0 to 28 in the aortic luminal circumference was smaller in the XPro1595-treated group (**Figure 6D**). The abdominal aorta distal to the renal artery branch was used as a control reference point for aortic expansion, and no difference in percentage circumference increase (day 0 to post-surgery day 28) was observed between groups (vehicle: 1.17 ± 5.8% vs. XPro1595: 4.43 ± 6.16%, n = 13–14, p = 0.70). Similarly, external AAA *ex vivo*

10.3389/fcvm.2022.942342

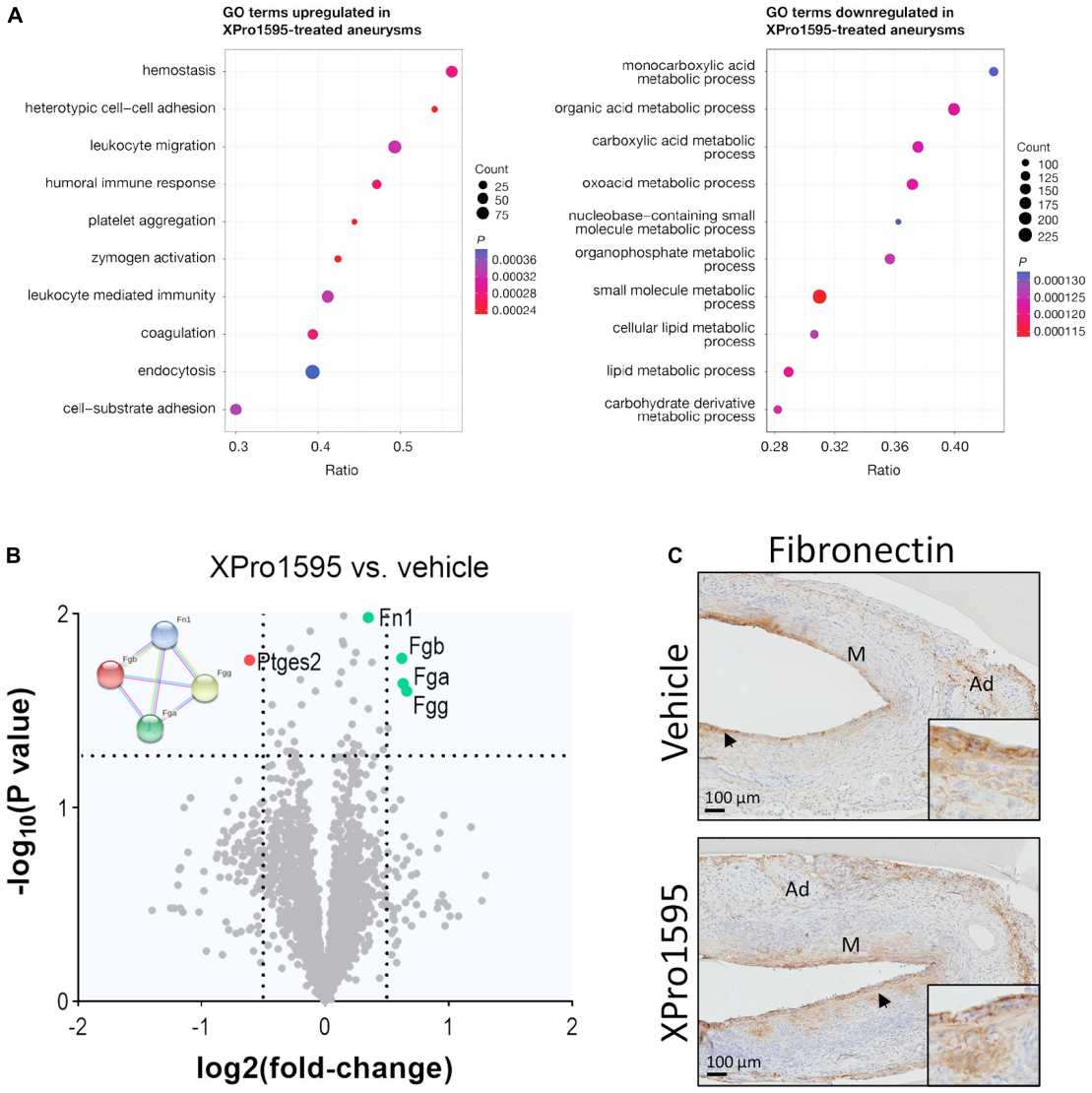

FIGURE 5

The fibronectin/fibrinogen complex is upregulated in aneurysms after inhibition of solTNF by XPro1595. **(A)** Dot plots show the top 10 enriched biological function terms from proteins up- (left) or down-regulated (right) in PPE-induced aneurysms from XPro1595-treated mice (n = 7) vs. vehicle (n = 6) at day 7. Dot size indicates number of proteins found to be regulated by XPro1595 for a given term. The ratio shows the proportion of a functional term covered by proteins regulated by XPro1595, and the dot color indicates the level of significance. **(B)** Volcano plot of aneurysmal proteins and their differential expression in aneurysms from XPro1595-treated mice vs. vehicle. Horizontal dashed line denotes a 0.05 cut-off p-value, and vertical dashed lines denote a log2(fold-change) of 0.5 in either direction. Fibronectin (FN1), fibrinogen chains FGA, FGB, and FGG and their protein-protein interactions are illustrated by use of the STRING resource (74), showing interactions determined experimentally (pink lines), from curated databases (blue lines), and/or from text-mining (yellow lines) (left upper corner of volcano plot). **(C)** Fibronectin contents in representative abdominal aortic aneurysmal tissue sections from mice infused with elastase and treated with XPro1595 (20 mg/kg) or vehicle (n = 3–5). Black arrowheads indicate positive stained cells. Proteomics data were analyzed by unpaired t-test for each protein followed by fdr correction for multiple testing. M, media; Ad, adventitia.

measurements of maximum outer abdominal aortic diameter and surface area of AAAs were significantly decreased in mice receiving XPro1595 (Figures 6E,F). The decrease in AAA size after selective inhibition of solTNF by XPro1595 was not associated with changes in body weight and organ-to-body weight ratios of heart, spleen, liver, and kidneys were unaffected by treatment (Supplementary Figures 1C,D). Despite a decrease in aneurysm expansion, the survival rate of mice treated with XPro1595 (70.0%) was similar to that of vehicle-treated mice (68.4%). Six mice in each group died between experimental days 2 and 26; all died from either AAA rupture or rupture of the

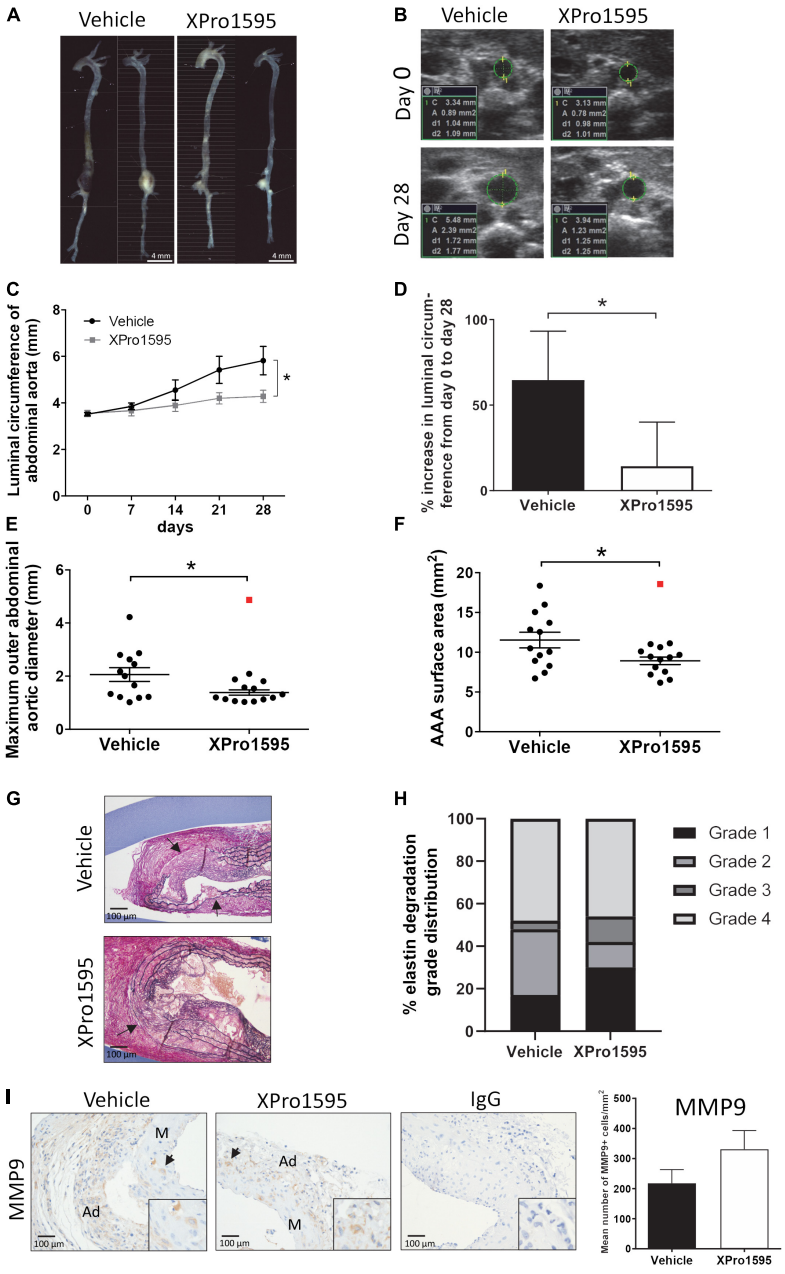

FIGURE 6
Inhibition of solTNF prevents ANGII-induced AAA expansion. **(A)** Representative macroscopic images showing AAA expansion in vehicle (saline) or XPro1595 (2 mg/kg) ANGII-infused *Apoe*$^{-/-}$ mice. **(B)** Representative ultrasound images of the abdominal aorta at its maximal inner circumference at day 0 and day 28 of the ANGII-induced AAA from vehicle-treated and XPro1595-treated mice. **(C)** ANGII-induced AAA expansion assessed by inner abdominal aortic circumference. **(D)** The percentage change in the maximal inner abdominal aortic circumference from day 0 to day 28 in vehicle- and XPro1595-treated mice assessed by ultrasound€ **(E)** *Ex vivo*-measured maximal outer aortic diameter in the two groups. **(F)** *Ex vivo*-measured surface area of the AAA treated with vehicle and XPro1595. **(G)** Representative micrographs of AAA cross-sections stained with Miller's elastin stain (black) in vehicle- and XPro1595-treated AAAs. Arrows point to rupture of elastic fibers. **(H)** Medial elastin degradation semi-quantified by a 4-grade system in aneurysms from XPro1595- and vehicle-treated mice. **(I)** MMP-9 immunoreactivity in cross-sections of vehicle- and XPro1595-treated aneurysms and the representative semi-quantification (number of positive cells/mm^2). Black arrowheads indicate positive stained cells. IgG isoform was used as negative control. Results are shown as mean SEM if data passed the D'Agostino and Pearson omnibus normality tests. Mann–Whitney test was applied in D and presented as median with interquartile range as data were non-normally distributed. *Denotes $p < 0.05$ analyzed by unpaired student *t*-test for two-group comparison or two-way ANOVA with Bonferroni test for multiple comparisons. Contingency table data in H was analyzed by Fisher exact probability test with Freeman-Halton extension. Outliers were identified by Grubb's outlier test for normally distributed data and indicated by red squares (■) and excluded from the statistical analyses. M, media; Ad, adventitia.

ascending aorta, except one in the vehicle group that died from unknown causes.

Inhibition of soluble tumor necrosis factor in angiotensin II-induced abdominal aortic aneurysms did not affect elastic fiber degradation nor immune cell infiltration

In the ANGII model, inhibition of solTNF did not have any apparent effect on elastin integrity (**Figures 6G,H**). Around 50% of the aneurysms in both groups were associated with severe destruction of elastic fibers (indicated by arrows in **Figure 6G**) and thereby reached an elastin degradation score of grade 4. As in the elastase induced aneurysms (**Figures 1E,F**), the mean number of MMP-9-positive cells/mm^2 in aneurysmal tissue was unaltered after XPro1595 treatment compared to vehicle-controls (**Figure 1I**). The MMP-9-positive cells were abundant in tunica adventitia of the aneurysm, supposedly associated with inflammatory cells of this layer, but MMP-9-positive cells were also present in the tunica media and assumed to be in VSMCs (**Figure 6I**, arrows). In line with above results, the CD45-positive infiltrating leukocytes (**Figure 7A**, arrows), Ly6G-positive infiltrating neutrophils (**Figure 7B**, arrows), and CD3-positive T-cells (**Figure 7C**) were primarily localized to tunica adventitia and to a smaller extent in tunica media, and their numbers/mm^2 were not affected by XPro1595. TNFR1-positive cells were primarily limited to fibroblast-like cells in tunica adventitia of the aneurysmal wall (**Figure 7D**, arrows) and TNFR1 aneurysmal contents showed a trend toward a 60% reduction after selective TNF inhibition with XPro1595 (**Figure 7D**, graph), as also seen in the elastase induced aneurysms immunolabeling of TNFR2-positive cells was detected in leukocyte-like cells in tunica adventitia (**Figure 7E**, arrows), but no difference in the levels of TNFR2 were detected after selective TNF inhibition (**Figure 7E**, graph). In this AAA model TNF plasma levels were also significantly increased (24 times) in XPro1595-treated ANGII infused mice (**Figure 7F**). Circulating plasma levels of the T-cell associated cytokine IL-5 were also significantly elevated (**Figure 7G**), while plasma levels of IL-1β, IL-2, IL-4, IL-6, IL-10, and KC/GRO did not differ between treatment groups (**Supplementary Table 1**).

Discussion

The present study aimed at elucidating whether treatment with the selective solTNF inhibitor XPro1595 could prevent AAA expansion by dampening the inflammatory response mediated *via* TNFR1 signaling. We found that selective inhibition of solTNF by XPro1595 reduced AAA development in both the PPE aneurysm model and ANGII-induced aneurysms in hyperlipidemic *Apoe* $^{-/-}$ mice. This inhibitory effect on aneurysm growth was more pronounced than non-selective inhibition of TNF by ETN treatment, where we observed a similar but non-significant 40% reduction of maximal outer aortic diameter. Others have previously shown that inhibition of TNF by gene deletion reduces $CaCl_2$-induced aneurysm growth (16). The underlying mechanism was ascribed to decreased inflammatory response and diminished MMP-2 and MMP-9 activity, thereby resulting in the preservation of the elastin lamellae structure. It is widely accepted that dysregulation of TNF adversely affects elastin by directly suppressing elastin mRNA levels in aortic smooth muscle cells (43) and increases expression of elastin-degrading enzymes MMP-2 and MMP-9 in aneurysmal tissue (16). In the present study, the underlying mechanism of solTNF inhibition also resulted in more intact and organized elastic lamellae when compared to both ETN-treatment and controls. This indicates that the degrading effects on elastin are mediated by solTNF. However, we did not detect differences in the distribution of MMP-9 in the aneurysm wall. This does not rule out a potential reduction in MMP-9 activity by XPro1595 treatment as reported by others using non-selective TNF inhibitors (16, 44, 45). Future studies are needed to address this point.

As mentioned earlier, solTNF is released from cells by cleavage of tmTNF by the metalloprotease-disintegrin TACE (46). As TACE is elevated in human AAAs, local high levels of solTNF are assumed to be present in growing AAAs and to drive inflammatory processes in the aneurysm wall (25). These findings are supported by *ex vivo* experiments where the release of solTNF, TNFR1 and TNFR2 correlated with the levels of TACE in aortic lesions of *Apoe*$^{-/-}$ mice (47). SolTNF, not tmTNF, is thought to be the main factor in the growth of AAA. This is based on the discovery of genetic variants in the promoter region of TACE that raise the risk of AAA development (47, 48). Therefore, the net effect of TACE inhibition is expected to be like XPro1595 inhibition, as both interventions prevent solTNF binding to TNFRs. In line with our results, Kaneko et al. (25), showed that global knockdown of TACE inhibited AAA expansion by reducing the inflammatory response and thereby preserving elastin lamellae integrity in the aneurysm wall.

In the present study, local cytokines in the aneurysms were differentially affected by selective solTNF inhibition. We observed that TNF levels locally in the aneurysm wall tended to be increased after ETN treatment, but this increase was significantly lower in the XPro1595-treated mice. A similar pattern was seen for IFNγ and IL10, indicating that solTNF inhibition reduced the inflammatory response in the aneurysm wall. It is well established that TNF and IFNγ synergistically promote leukocyte entry into the aortic wall by activating endothelial cells to express the intercellular adhesion molecule 1 (ICAM1) (49). This may explain why the protective effect of ETN on AAA development is less pronounced compared to XPro1595 treatment. Although we did not observe any apparent

10.3389/fcvm.2022.942342

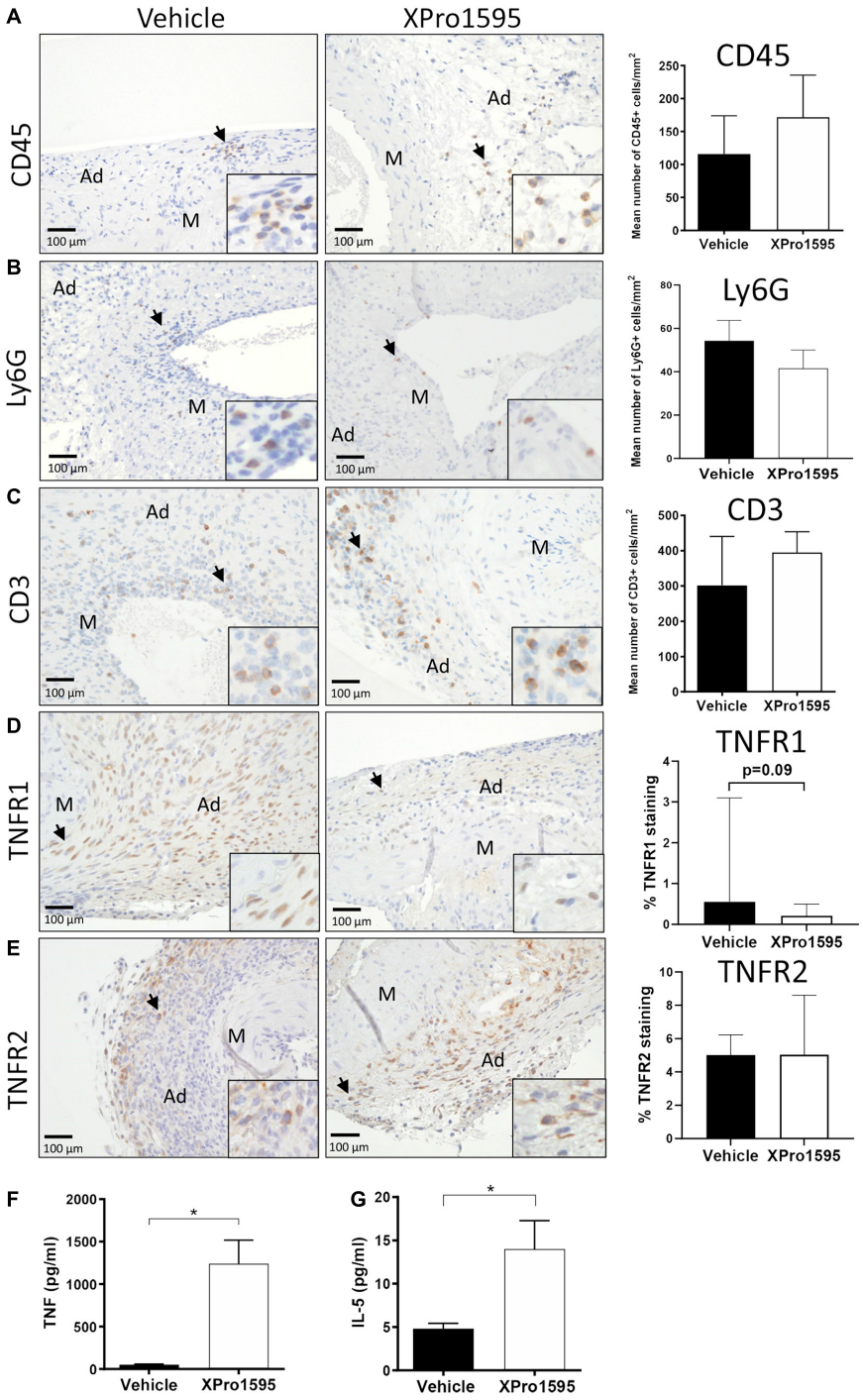

FIGURE 7
Characterization of aneurysm wall composition after inhibition of solTNF in ANGII-induced abdominal aortic aneurysms. Representative micrographs of CD45-positive leukocytes **(A)**, Ly6G-positive neutrophils **(B)**, CD3-positive T cells **(C)** (n = 13), TNFR1 localization **(D)**, TNFR2 localization **(E)** (n = 6) and their respective semi-quantification (number of positive cells/mm^2 or % positive staining) in cross-sections of ANGII-induced AAA treated with vehicle or XPro1595 (2 mg/kg). Black arrows point to examples of positive stained cells. Circulating TNF plasma levels (n = 4–5) **(F)** and IL-5 (n = 6–7) **(G)** in ANGII-induced AAA treated with vehicle or XPro1595. Data are shown as mean SEM if data passed the D'Agostino and Pearson omnibus normality tests **(B,C,E–G)**. *Denotes $p < 0.05$ analyzed by unpaired Student's t-test for normally distributed data, otherwise by Mann-Whitney test represented as median with interquartile range **(A,D)**. M, media; Ad, adventitia.

difference in infiltrating macrophages, M2-like macrophages, T-cells, or neutrophils in the aneurysm wall at the end of the experiments, it remains to be seen whether delayed entry of infiltrating leukocytes in XPro1595-treated mice can explain part of XPro1595's protective role against AAA expansion. The local changes in cytokine levels were not reflected in circulating levels. In both AAA models, there was a 10–24-times increase in circulating TNF after XPro1595 treatment. However, since XPro1595 is a TNF mutein that forms trimer complexes with native TNF, it is expected that plasma solTNF levels will increase as our ELISA assay detects both active and inactive TNF-XPro1595 trimer complexes. This might also partly explain our previous findings of elevated circulating TNF in unchallenged mice treated with XPro1595 (50). Furthermore, loss of solTNF signaling due to XPro1595 treatment increases *Tnf* mRNA levels in brain tissue 1 and 3 days after permanent middle cerebral artery occlusion (51), which indicates that loss of solTNF signaling promotes TNF expression. Elevated levels of IL-10 were detected systemically only after ETN inhibition, which is in line with previous studies showing that not only the expression of IL-10 in macrophages and T-cells is increased after ETN treatment, but also their secretion (52, 53). Thus, inhibition of both forms of TNF has systemic anti-inflammatory effects mediated *via* IL-10. Surprisingly, circulating levels of IL-5, which is primarily produced by mast cells and T-helper 2 cells (54, 55), increased in the ANGII AAA model after XPro1595 treatment. Others have reported that IL-5 potentiates AAA expansion by directly or indirectly upregulating MMP-2 and MMP-9 expression (56); this does not correspond with our findings, although perhaps some of the expected beneficial effects of XPro1595 were masked by elevated circulating IL-5 levels.

TNF signaling in the vascular wall involves most cell types with TNFR1 expressed in endothelial cells, VSMCs, immune cells, and fibroblasts, as shown here and by others (57). As solTNF has a higher binding affinity for TNFR1, and tmTNF has a higher binding affinity for TNFR2, the effect of solTNF will mainly be mediated *via* TNFR1 activation (20, 58), while tmTNF-TNFR2 signaling may be more pronounced when solTNF is inhibited. TNFR1 signaling contributes significantly to the formation of intracranial aneurysms and to coronary aneurysm formation in association with Kawasaki Disease (59, 60). In the present study, selective TNF inhibition reduced aneurysmal TNFR1 levels non-significantly by 50–60% depending on the AAA mouse model. A general reduction of TNFR1 in the aneurysm wall could be explained by increasing TACE activity (25). In $Tnf^{-/-}$ mice, dendritic cells display a higher TACE expression (61). Also, circulating levels of TNFRs has been shown to be elevated in patients with thoracic aortic aneurysm and in patients with ruptured AAA compared to patients undergoing elective surgery (62), which correlates well with elevated TACE activity. The apparent reduction of TNFR1 compared to controls could be explained by the loss of solTNF signaling that dampens TNFR1 expression (63). The distribution of TNFR1 in the aneurysm wall did not appear to be associated with a reduction in any specific cell type in the aneurysm wall. TNFR2 levels and distribution in the aneurysm wall were unaffected by TNF inhibition, which raises the question of whether the trend toward reduced TNFR1 aneurysm levels was caused solely by changes in TACE activity.

The balance between M1- and M2-like macrophages plays an important role in AAA progression (64). In our experiments, there was no obvious difference in the number of CD206-positive M2 cells infiltrating the wall of the aneurysms. To our surprise, leukocyte infiltration was indifferent after TNF inhibition even though TNF signaling increases ICAM1 expression in endothelial cells, allowing leukocyte entry into the aortic wall (63, 65). Inhibition of solTNF signaling potentially reduced ICAM1 expression in endothelial cells and thereby leukocyte entry to the damaged aortic wall at the initiation of AAA expansion (days 3–7), which could partly explain the reduced AAA formation in the XPro1595-treated mice. Another likely possibility for the protective effects of XPro1595 could be a blood pressure-lowering effect. TNF inhibition by ETN has been reported to have no or a slightly lowering effect on blood pressure (66). It has further been reported that chronic infusion of XPro1595 does not alter mean arterial blood pressure or heart rate 2–4 weeks after spinal cord injury in mice (67). We did not detect any between-group differences in heart-to-body ratio in either model, which suggests that no pronounced differences in arterial blood pressure were present.

Because fibrinogen complex, fibronectin, and fibrinogens are elevated in XPro1595 in the early stages of aneurysm formation, it is possible that they initially support the fibro-protective effects of the damaged aortic wall. Fibrinogen deposition in the aortic wall may trigger an autoimmune response that could lead to activation of the complement alternative pathway and AAA progression (68). In human AAAs, increased deposition of pro-thrombosis fibrin/fibrinogen complexes within the AAA wall has been identified, along with an association of circulating fibrin/fibrinogen degradation products (D-dimers) and AAA growth or perhaps more likely, luminal thrombus formation (69–71), all believed to augment AAA progression. Thus, it is not clear from the present study whether the elevated fibrin-fibrinogen complex in AAA development after solTNF inhibition is associated with profibrotic stabilization of the AAA wall or simply indicates delayed AAA development in comparison to vehicle treatment.

In our study we did not detect any signs of toxicity by using XPro1595. XPro1595 treatment in both AAA models, did not affect changes in body weights or organ to body weight ratios of heart, kidney, and liver. Furthermore, XPro1595 is a mutated form of the human protein of

TNF which makes the trimer complex unable to bind to TNFRs (33) and is therefore a natural pharmaceutical substance. We did not examine whether liver steatosis is present in XPro1595-treated mice with ANGII induced AAA. However, others have shown that XPro1595 can improve diet induced obesity (high-fat high-carbohydrate diet) and central-peripheral insulin impairment, in wild type mice partly through dampening of hepatic lipocalin-2, which is associated with and elevated in liver steatosis. These alterations suggest reduced risk of diet induced late onset of Alzheimer's disease (72). Furthermore, we have previously shown in healthy, adult WT mice that long term XPro1595 treatment (2 months) in contrast to ETN treatment did not alter neurogenic zones and impair spatial learning and memory (50). These findings suggest that selective inhibition of SolTNF with XPro1595 is non-toxic in the tested doses. Furthermore, human clinical trials using XPro1595 in patients with mild Alzheimer's disease (ClinicalTrials.gov Identifier: NCT05318976) and in patients with mild cognitive impairments (ClinicalTrials.gov Identifier: NCT05321498) have been successful and is currently in phase 2, thus has also passed toxicity testing in humans. Like in AAA patients, both of these diseases meet the criteria of high peripheral inflammation based on elevated blood levels of the inflammatory biomarker high-sensitivity c-reactive protein (hs-CRP) (73).

In conclusion, inhibition of solTNF prevents AAA expansion by a mechanism involving the preservation of elastin lamellae. These findings support that targeting the solTNF-TNFR1 signaling pathway would be an attractive treatment strategy and potentially even better than non-selective TNF therapy for patients with growing AAA, which is highly desired.

Data availability statement

The mass spectrometry proteomics dataset presented in this study is publicly available. The data can be found below: http://www.proteomexchange.org/, PXD035178.

Ethics statement

The studies involving human participants were reviewed and approved by the Regional Committee on Health Research Ethics for Southern Denmark (S20140202 and M20080028). The patients/participants provided their written informed consent to participate in this study. The animal study was reviewed and approved by The Danish Animal Experiments Inspectorate (2015-15-0201-00474).

Author contributions

JS, JL, and KL designed the study. SG, EG, EF, ML, SB-M, HB, MO, and LS performed the experiments, data analyses, and interpret the results. LR and JL provided the human samples. SG, EG, and JS drafted the manuscript. All authors critically reviewed, edited, and approved the final version of the manuscript.

Funding

This study was partly funded from a grant to CIMA from OUH's Research Fund, the Danish Heart Association (18-R124-A8475-22094 and 18-R125-A8506-22109), Augustinus fund, Svend Petersens Mindefond, King Christian the 10th fund, and A. P. Moellers Fund.

Acknowledgments

We thank our skillful technicians Lene Bundgaard Andersen, Amalie Kamstrup Mogensen, Kenneth Kjærsgaard, Ann Sofie Madsen, Inger Nissen, Anette Rasmussen, Ulla Damgaard Munk, and Pia Klingenberg Mortensen for their excellent technical assistance. We thank David E. Szymkowski from Xencor Inc., and CJ Barnum and RT Tesi from Inmune Bio Inc., for kindly providing us with XPro1595. We also thank Claire Gudex for language editing.

Conflict of interest

The authors declare that the research was conducted in the absence of any commercial or financial relationships that could be construed as a potential conflict of interest.

Publisher's note

All claims expressed in this article are solely those of the authors and do not necessarily represent those of their affiliated organizations, or those of the publisher, the editors and the reviewers. Any product that may be evaluated in this article, or claim that may be made by its manufacturer, is not guaranteed or endorsed by the publisher.

Supplementary material

The Supplementary Material for this article can be found online at: https://www.frontiersin.org/articles/10.3389/fcvm.2022.942342/full#supplementary-material

SUPPLEMENTARY FIGURE 1
Increase in body weight and organ-to-body weight ratio at the endpoint of either PPE (0–14 days)- or ANGII treatment (0–28 days), showing the body weight difference **(A,C)** and the organ-to-body weight ratios **(B,D)**. (PPE: vehicle n = 14; ETN n = 14; XPro1595 n = 14); (ANGII: vehicle n = 13; XPro1595 n = 14). The data are shown as mean ± SEM. No significance was observed by one-way ANOVA using Bonferroni test for multiple comparisons or unpaired Student's t-test for normally distributed data.

SUPPLEMENTARY TABLE 1
Table of cytokine levels measured in AAA homogenate but not affected by TNF inhibition treatment in PPE animals (n = 4–8). The data are shown as mean ± SEM. No significance was observed by one-way ANOVA using Bonferroni test for multiple comparisons.

SUPPLEMENTARY TABLE 2
Table of cytokine levels measured in plasma but not affected by TNF inhibition treatment in PPE (n = 6–8) and ANGII-treated animals (n = 13–14). The data are shown as mean ± SEM. * Indicates $p < 0.05$ analyzed by one-way ANOVA using Bonferroni test for multiple comparisons or unpaired Student's t-test for normally distributed data. § Denotes data already represented in **Figures 5E,F**. ¤ Denotes data already represented in **Figure 7G**.

SUPPLEMENTARY TABLE 3
Complete list of identified proteins in the abdominal aortic wall by mass spectrometry 7 days after PPE-induced AAA in mice. Mice were treated with XPro1595 (20 mg/kg) (n = 7) or vehicle (n = 6).

References

1. Kuivaniemi H, Elmore JR. Opportunities in abdominal aortic aneurysm research: epidemiology, genetics, and pathophysiology. *Ann Vasc Surg.* (2012) 26:862–70. doi: 10.1016/j.avsg.2012.02.005

2. Roger VL, Go AS, Lloyd-Jones DM, Benjamin EJ, Berry JD, Borden WB, et al. Heart disease and stroke statistics–2012 update: a report from the American Heart Association. *Circulation.* (2012) 125:e2–220.

3. Brewster DC, Cronenwett JL, Hallett JW Jr., Johnston KW, Krupski WC, Matsumura JS. Guidelines for the treatment of abdominal aortic aneurysms. Report of a subcommittee of the joint council of the American association for vascular surgery and society for vascular surgery. *J Vasc Surg.* (2003) 37:1106–17. doi: 10.1067/mva.2003.363

4. Baxter BT, Terrin MC, Dalman RL. Medical management of small abdominal aortic aneurysms. *Circulation.* (2008) 117:1883–9. doi: 10.1161/CIRCULATIONAHA.107.735274

5. Sakalihasan N, Heyeres A, Nusgens BV, Limet R, Lapiére CM. Modifications of the extracellular matrix of aneurysmal abdominal aortas as a function of their size. *Eur J Vasc Surg.* (1993) 7:633–7. doi: 10.1016/S0950-821X(05)80708-X

6. Ocana E, Bohórquez JC, Pérez-Requena J, Brieva JA, Rodríguez C. Characterisation of T and B lymphocytes infiltrating abdominal aortic aneurysms. *Atherosclerosis.* (2003) 170:39–48. doi: 10.1016/S0021-9150(03)00282-X

7. Galle C, Schandene L, Stordeur P, Peignois Y, Ferreira J, Wautrecht JC, et al. Predominance of type 1 CD4+ T cells in human abdominal aortic aneurysm. *Clin Exp Immunol.* (2005) 142:519–27. doi: 10.1111/j.1365-2249.2005.02938.x

8. Curci JA, Liao S, Huffman MD, Shapiro SD, Thompson RW. Expression and localization of macrophage elastase (matrix metalloproteinase-12) in abdominal aortic aneurysms. *J Clin Invest.* (1998) 102:1900–10. doi: 10.1172/JCI2182

9. Davis V, Persidskaia R, Baca-Regen L, Itoh Y, Nagase H, Persidsky Y, et al. Matrix metalloproteinase-2 production and its binding to the matrix are increased in abdominal aortic aneurysms. *Arterioscler Thromb Vasc Biol.* (1998) 18:1625–33. doi: 10.1161/01.ATV.18.10.1625

10. Tamarina NA, McMillan WD, Shively VP, Pearce WH. Expression of matrix metalloproteinases and their inhibitors in aneurysms and normal aorta. *Surgery.* (1997) 122:264–71;discussion271–2. doi: 10.1016/S0039-6060(97)90017-9

11. Thompson RW, Holmes DR, Mertens RA, Liao S, Botney MD, Mecham RP, et al. Production and localization of 92-kilodalton gelatinase in abdominal aortic aneurysms. An elastolytic metalloproteinase expressed by aneurysm-infiltrating macrophages. *J Clin Invest.* (1995) 96:318–26. doi: 10.1172/JCI118037

12. Bennett MR, Evan GI, Schwartz SM. Apoptosis of human vascular smooth muscle cells derived from normal vessels and coronary atherosclerotic plaques. *J Clin Invest.* (1995) 95:2266–74. doi: 10.1172/JCI117917

13. Satoh H, Nakamura M, Satoh M, Nakajima T, Izumoto H, Maesawa C, et al. Expression and localization of tumour necrosis factor-alpha and its converting enzyme in human abdominal aortic aneurysm. *Clin Sci (Lond).* (2004) 106:301–6. doi: 10.1042/CS20030189

14. Treska V, Topolcan O, Pecen L. Cytokines as plasma markers of abdominal aortic aneurysm. *Clin Chem Lab Med.* (2000) 38:1161–4. doi: 10.1515/CCLM.2000.178

15. Juvonen J, Surcel HM, Satta J, Teppo AM, Bloigu A, Syrjala H, et al. Elevated circulating levels of inflammatory cytokines in patients with abdominal aortic aneurysm. *Arterioscler Thromb Vasc Biol.* (1997) 17:2843–7. doi: 10.1161/01.ATV.17.11.2843

16. Xiong W, MacTaggart J, Knispel R, Worth J, Persidsky Y, Baxter BT. Blocking TNF-alpha attenuates aneurysm formation in a murine model. *J Immunol.* (2009) 183:2741–6. doi: 10.4049/jimmunol.0803164

17. Tartaglia LA, Weber RF, Figari IS, Reynolds C, Palladino MA Jr., Goeddel DV. The two different receptors for tumor necrosis factor mediate distinct cellular responses. *Proc Natl Acad Sci USA.* (1991) 88:9292–6. doi: 10.1073/pnas.88.20.9292

18. Moss ML, Jin SL, Milla ME, Bickett DM, Burkhart W, Carter HL, et al. Cloning of a disintegrin metalloproteinase that processes precursor tumour-necrosis factor-alpha. *Nature.* (1997) 385:733–6. doi: 10.1038/385733a0

19. Black RA, Rauch CT, Kozlosky CJ, Peschon JJ, Slack JL, Wolfson MF, et al. A metalloproteinase disintegrin that releases tumour-necrosis factor-alpha from cells. *Nature.* (1997) 385:729–33. doi: 10.1038/385729a0

20. Holtmann MH, Neurath MF. Differential TNF-signaling in chronic inflammatory disorders. *Curr Mol Med.* (2004) 4:439–44. doi: 10.2174/1566524043360636

21. Fontaine V, Mohand-Said S, Hanoteau N, Fuchs C, Pfizenmaier K, Eisel U. Neurodegenerative and neuroprotective effects of tumor Necrosis factor (TNF) in retinal ischemia: opposite roles of TNF receptor 1 and TNF receptor 2. *J Neurosci.* (2002) 22:RC216. doi: 10.1523/JNEUROSCI.22-07-j0001.2002

22. Horiuchi T, Mitoma H, Harashima S, Tsukamoto H, Shimoda T. Transmembrane TNF-alpha: structure, function and interaction with anti-TNF agents. *Rheumatology (Oxford).* (2010) 49:1215–28. doi: 10.1093/rheumatology/keq031

23. Alexopoulou L, Kranidioti K, Xanthoulea S, Denis M, Kotanidou A, Douni E, et al. Transmembrane TNF protects mutant mice against intracellular bacterial infections, chronic inflammation and autoimmunity. *Eur J Immunol.* (2006) 36:2768–80. doi: 10.1002/eji.200635921

24. Olleros ML, Guler R, Vesin D, Parapanov R, Marchal G, Martinez-Soria E, et al. Contribution of transmembrane tumor necrosis factor to host defense against *Mycobacterium bovis* bacillus Calmette-guerin and *Mycobacterium tuberculosis* infections. *Am J Pathol.* (2005) 166:1109–20. doi: 10.1016/S0002-9440(10)62331-0

25. Kaneko H, Anzai T, Horiuchi K, Kohno T, Nagai T, Anzai A, et al. Tumor necrosis factor-α converting enzyme is a key mediator of abdominal aortic aneurysm development. *Atherosclerosis.* (2011) 218:470–8. doi: 10.1016/j.atherosclerosis.2011.06.008

26. Kollias G, Douni E, Kassiotis G, Kontoyiannis D. The function of tumour necrosis factor and receptors in models of multi-organ inflammation, rheumatoid arthritis, multiple sclerosis and inflammatory bowel disease. *Ann Rheum Dis.* (1999) 58(Suppl. 1):I32–9. doi: 10.1136/ard.58.2008.i32

27. Assas MB, Levison SE, Little M, England H, Battrick L, Bagnall J, et al. Anti-inflammatory effects of infliximab in mice are independent of tumour necrosis factor α neutralization. *Clin Exp Immunol.* (2017) 187:225–33. doi: 10.1111/cei.12872

28. Singh JA, Wells GA, Christensen R, Ghogomu E. Tanjong, Maxwell L, Macdonald JK, et al. Adverse effects of biologics: a network meta-analysis and Cochrane overview. *Cochrane Database Syst Rev.* (2011) 2011:Cd008794. doi: 10.1002/14651858.CD008794.pub2

29. Bellini G, Benziger J, Bick D, Bonetti S, Bonfini G, Buizza Avanzini M, et al. Precision measurement of the (7)Be solar neutrino interaction rate in Borexino. *Phys Rev Lett.* (2011) 107:141302.

30. Setoguchi S, Schneeweiss S, Avorn J, Katz JN, Weinblatt ME, Levin R, et al. Tumor necrosis factor-alpha antagonist use and heart failure in elderly patients with rheumatoid arthritis. *Am Heart J.* (2008) 156:336–41. doi: 10.1016/j.ahj.2008.02.025

31. Weimer LH, Sachdev N. Update on medication-induced peripheral neuropathy. *Curr Neurol Neurosci Rep.* (2009) 9:69–75. doi: 10.1007/s11910-009-0011-z

32. Kristensen LB, Lambertsen KL, Nguyen N, Byg KE, Nielsen HH. The role of non-selective TNF inhibitors in demyelinating events. *Brain Sci.* (2021) 11:38. doi: 10.3390/brainsci11010038

33. Zalevsky J, Secher T, Ezhevsky SA, Janot L, Steed PM, O'Brien C, et al. Dominant-negative inhibitors of soluble TNF attenuate experimental arthritis without suppressing innate immunity to infection. *J Immunol.* (2007) 179:1872–83. doi: 10.4049/jimmunol.179.3.1872

34. Steed PM, Tansey MG, Zalevsky J, Zhukovsky EA, Desjarlais JR, Szymkowski DE, et al. Inactivation of TNF signaling by rationally designed dominant-negative TNF variants. *Science.* (2003) 301:1895–8. doi: 10.1126/science.1081297

35. Hsiao HY, Chiu FL, Chen CM, Wu YR, Chen HM, Chen YC, et al. Inhibition of soluble tumor necrosis factor is therapeutic in Huntington's disease. *Hum Mol Genet.* (2014) 23:4328–44. doi: 10.1093/hmg/ddu151

36. Brambilla R, Ashbaugh JJ, Magliozzi R, Dellarole A, Karmally S, Szymkowski DE, et al. Inhibition of soluble tumour necrosis factor is therapeutic in experimental autoimmune encephalomyelitis and promotes axon preservation and remyelination. *Brain.* (2011) 134(Pt 9):2736–54. doi: 10.1093/brain/awr199

37. Clausen BH, Degn M, Martin NA, Couch Y, Karimi L, Ormhoj M, et al. Systemically administered anti-TNF therapy ameliorates functional outcomes after focal cerebral ischemia. *J Neuroinflammation.* (2014) 11:203. doi: 10.1186/s12974-014-0203-6

38. Novrup HG, Bracchi-Ricard V, Ellman DG, Ricard J, Jain A, Runko E, et al. Central but not systemic administration of XPro1595 is therapeutic following moderate spinal cord injury in mice. *J Neuroinflammation.* (2014) 11:159. doi: 10.1186/s12974-014-0159-6

39. Wintmo P, Johansen SH, Hansen PBL, Lindholt JS, Urbonavicius S, Rasmussen LM, et al. The water channel AQP1 is expressed in human atherosclerotic vascular lesions and AQP1 deficiency augments angiotensin II-induced atherosclerosis in mice. *Acta Physiol (Oxf).* (2017) 220:446–60. doi: 10.1111/apha.12853

40. Sun J, Sukhova GK, Yang M, Wolters PJ, Macfarlane LA, Libby P, et al. Mast cells modulate the pathogenesis of elastase-induced abdominal aortic aneurysms in mice. *J Clin Invest.* (2007) 117:3359–68. doi: 10.1172/JCI31311

41. Mulorz J, Spin JM, Beck HC, Thi M.L. Tha, Wagenhäuser MU, Rasmussen LM, et al. Hyperlipidemia does not affect development of elastase-induced abdominal aortic aneurysm in mice. *Atherosclerosis.* (2020) 311:73–83. doi: 10.1016/j.atherosclerosis.2020.08.012

42. Wu T, Hu E, Xu S, Chen M, Guo P, Dai Z, et al. clusterProfiler 4.0: a universal enrichment tool for interpreting omics data. *Innovation (N Y).* (2021) 2:100141. doi: 10.1016/j.xinn.2021.100141

43. Kahari VM, Chen YQ, Bashir MM, Rosenbloom J, Uitto J. Tumor necrosis factor-alpha down-regulates human elastin gene expression. Evidence for the role of AP-1 in the suppression of promoter activity. *J Biol Chem.* (1992) 267:26134–41. doi: 10.1016/S0021-9258(18)35727-2

44. Lee PP, Hwang JJ, Murphy G, Ip MM. Functional significance of MMP-9 in tumor necrosis factor-induced proliferation and branching morphogenesis of mammary epithelial cells. *Endocrinology.* (2000) 141:3764–73. doi: 10.1210/endo.141.10.7697

45. Tsai CL, Chen WC, Hsieh HL, Chi PL, Hsiao LD, Yang CM. TNF-alpha induces matrix metalloproteinase-9-dependent soluble intercellular adhesion molecule-1 release *via* TRAF2-mediated MAPKs and NF-kappaB activation in osteoblast-like MC3T3-E1 cells. *J Biomed Sci.* (2014) 21:12. doi: 10.1186/1423-0127-21-12

46. Mohan MJ, Seaton T, Mitchell J, Howe A, Blackburn K, Burkhart W, et al. The tumor necrosis factor-alpha converting enzyme (TACE): a unique metalloproteinase with highly defined substrate selectivity. *Biochemistry.* (2002) 41:9462–9. doi: 10.1021/bi0260132

47. Canault M, Peiretti F, Kopp F, Bonardo B, Bonzi MF, Coudeyre JC, et al. The TNF alpha converting enzyme (TACE/ADAM17) is expressed in the atherosclerotic lesions of apolipoprotein E-deficient mice: possible contribution to elevated plasma levels of soluble TNF alpha receptors. *Atherosclerosis.* (2006) 187:82–91. doi: 10.1016/j.atherosclerosis.2005.08.031

48. Li Y, Yang C, Ma G, Cui L, Gu X, Chen Y, et al. Analysis of ADAM17 polymorphisms and susceptibility to sporadic abdominal aortic aneurysm. *Cell Physiol Biochem.* (2014) 33:1426–38. doi: 10.1159/000358708

49. Borish LC, Steinke JW. 2. Cytokines and chemokines. *J Allergy Clin Immunol.* (2003) 111(Suppl. 2):S460–75. doi: 10.1067/mai.2003.108

50. Yli-Karjanmaa M, Larsen KS, Fenger CD, Kristensen LK, Martin NA, Jensen PT, et al. TNF deficiency causes alterations in the spatial organization of neurogenic zones and alters the number of microglia and neurons in the cerebral cortex. *Brain Behav Immunity.* (2019) 82:279–97. doi: 10.1016/j.bbi.2019.08.195

51. Yli-Karjanmaa M, Clausen BH, Degn M, Novrup HG, Ellman DG, Toft-Jensen P, et al. Topical administration of a soluble TNF inhibitor reduces infarct volume after focal cerebral ischemia in mice. *Front Neurosci.* (2019) 13:781. doi: 10.3389/fnins.2019.00781

52. Evans HG, Roostalu U, Walter GJ, Gullick NJ, Frederiksen KS, Roberts CA, et al. TNF-α blockade induces IL-10 expression in human CD4+ T cells. *Nat Commun.* (2014) 5:3199. doi: 10.1038/ncomms4199

53. Degboé Y, Rauwel B, Baron M, Boyer JF, Ruyssen-Witrand A, Constantin A, et al. Polarization of rheumatoid macrophages by TNF targeting through an IL-10/STAT3 mechanism. *Front Immunol.* (2019) 10:3. doi: 10.3389/fimmu.2019.00003

54. Bradding P, Roberts JA, Britten KM, Montefort S, Djukanovic R, Mueller R, et al. Interleukin-4, -5, and -6 and tumor necrosis factor-alpha in normal and asthmatic airways: evidence for the human mast cell as a source of these cytokines. *Am J Respir Cell Mol Biol.* (1994) 10:471–80. doi: 10.1165/ajrcmb.10.5.8179909

55. Mosmann TR, Cherwinski H, Bond MW, Giedlin MA, Coffman RL. Two types of murine helper T cell clone. I. Definition according to profiles of lymphokine activities and secreted proteins. *J Immunol.* (1986) 136:2348–57.

56. Xu J, Ehrman B, Graham LM, Eagleton MJ. Interleukin-5 is a potential mediator of angiotensin II-induced aneurysm formation in apolipoprotein E knockout mice. *J Surg Res.* (2012) 178:512–8. doi: 10.1016/j.jss.2011.12.016

57. Al-Lamki RS, Sadler TJ, Wang J, Reid MJ, Warren AY, Movassagh M, et al. Tumor necrosis factor receptor expression and signaling in renal cell carcinoma. *Am J Pathol.* (2010) 177:943–54. doi: 10.2353/ajpath.2010.091218

58. Ruuls SR, Hoek RM, Ngo VN, McNeil T, Lucian LA, Janatpour MJ, et al. Membrane-bound TNF supports secondary lymphoid organ structure but is subservient to secreted TNF in driving autoimmune inflammation. *Immunity.* (2001) 15:533–43. doi: 10.1016/S1074-7613(01)00215-1

59. Hui-Yuen JS, Duong TT, Yeung RS. TNF-alpha is necessary for induction of coronary artery inflammation and aneurysm formation in an animal model of Kawasaki disease. *J Immunol.* (2006) 176:6294–301. doi: 10.4049/jimmunol.176.10.6294

60. Aoki T, Fukuda M, Nishimura M, Nozaki K, Narumiya S. Critical role of TNF-alpha-TNFR1 signaling in intracranial aneurysm formation. *Acta Neuropathol Commun.* (2014) 2:34. doi: 10.1186/2051-5960-2-34

61. Ge L, Vujanovic NL. Soluble TNF regulates TACE *via* AP-2alpha transcription factor in mouse dendritic cells. *J Immunol.* (2017) 198:417–27. doi: 10.4049/jimmunol.1600524

62. Rabajdova M, Urban P, Spakova I, Panagiotis A, Ferencakova M, Rybar D, et al. Detection of pathological changes in the aorta during thoracic aortic aneurysm progression on molecular level. *Dis Markers.* (2017) 2017:9185934. doi: 10.1155/2017/9185934

63. Schäfers M, Schmidt C, Vogel C, Toyka KV, Sommer C. Tumor necrosis factor-alpha (TNF) regulates the expression of ICAM-1 predominantly through TNF receptor 1 after chronic constriction injury of mouse sciatic nerve. *Acta Neuropathol.* (2002) 104:197–205. doi: 10.1007/s00401-002-0541-9

64. Dale MA, Xiong W, Carson JS, Suh MK, Karpisek AD, Meisinger TM, et al. Elastin-derived peptides promote abdominal aortic aneurysm formation by modulating M1/M2 macrophage polarization. *J Immunol.* (2016) 196:4536–43. doi: 10.4049/jimmunol.1502454

65. Pyo R, Lee JK, Shipley JM, Curci JA, Mao D, Ziporin SJ, et al. Targeted gene disruption of matrix metalloproteinase-9 (gelatinase B) suppresses development of experimental abdominal aortic aneurysms. *J Clin Invest.* (2000) 105:1641–9. doi: 10.1172/JCI8931

66. Kroetsch JT, Levy AS, Zhang H, Aschar-Sobbi R, Lidington D, Offermanns S, et al. Constitutive smooth muscle tumour necrosis factor regulates microvascular myogenic responsiveness and systemic blood pressure. *Nat Commun.* (2017) 8:14805. doi: 10.1038/ncomms14805

67. Mironets E, Osei-Owusu P, Bracchi-Ricard V, Fischer R, Owens EA, Ricard J, et al. Soluble TNFα Signaling within the spinal cord contributes to the development

of autonomic dysreflexia and ensuing vascular and immune dysfunction after spinal cord injury. *J Neurosci.* (2018) 38:4146–62. doi: 10.1523/JNEUROSCI.2376-17.2018

68. Zhou H-F, Yan H, Bertram P, Hu Y, Springer LE, Thompson RW, et al. Fibrinogen-specific antibody induces abdominal aortic aneurysm in mice through complement lectin pathway activation. *Proc Natl Acad Sci USA.* (2013) 110:E4335–44. doi: 10.1073/pnas.1315512110

69. Molacek J, Mares J, Treska V, Houdek K, Baxa J. Proteomic analysis of the abdominal aortic aneurysm wall. *Surg Today.* (2014) 44:142–51. doi: 10.1007/s00595-012-0480-6

70. Lee AJ, Fowkes FG, Lowe GD, Rumley A. Haemostatic factors, atherosclerosis and risk of abdominal aortic aneurysm. *Blood Coagul Fibrinolysis.* (1996) 7:695–701. doi: 10.1097/00001721-199610000-00006

71. Takagi H, Manabe H, Kawai N, Goto S, Umemoto T. Plasma fibrinogen and D-dimer concentrations are associated with the presence of abdominal aortic aneurysm: a systematic review and meta-analysis. *Eur J Vasc Endovasc Surg.* (2009) 38:273–7. doi: 10.1016/j.ejvs.2009.05.013

72. Rodrigues MED, Houser MC, Walker DI, Jones DP, Chang JJ, Barnum CJ, et al. Targeting soluble tumor necrosis factor as a potential intervention to lower risk for late-onset Alzheimer's disease associated with obesity, metabolic syndrome, and type 2 diabetes. *Alzheimers Res Ther.* (2019) 12:1. doi: 10.1186/s13195-019-0546-4

73. MacPherson KP, Sompol P, Kannarkat GT, Chang J, Sniffen L, Wildner ME, et al. Peripheral administration of the soluble TNF inhibitor XPro1595 modifies brain immune cell profiles, decreases beta-amyloid plaque load, and rescues impaired long-term potentiation in 5xFAD mice. *Neurobiol Dis.* (2017) 102:81–95. doi: 10.1016/j.nbd.2017.02.010

74. Szklarczyk D, Gable AL, Lyon D, Junge A, Wyder S, Huerta-Cepas J, et al. STRING v11: protein–protein association networks with increased coverage, supporting functional discovery in genome-wide experimental datasets. *Nucleic Acids Res.* (2018) 47:D607–13. doi: 10.1093/nar/gky1131

frontiers | Frontiers in Cardiovascular Medicine

TYPE Mini Review
PUBLISHED 21 September 2022
DOI 10.3389/fcvm.2022.949262

Check for updates

OPEN ACCESS

EDITED BY
Zhenjie Liu,
The Second Affiliated Hospital of Zhejiang University School of Medicine, China

REVIEWED BY
Lei Ji,
Zhejiang University, China

*CORRESPONDENCE
Bowen Wang
bw2pw@virginia.edu

SPECIALTY SECTION
This article was submitted to General Cardiovascular Medicine, a section of the journal Frontiers in Cardiovascular Medicine

RECEIVED 20 May 2022
ACCEPTED 29 August 2022
PUBLISHED 21 September 2022

CITATION
Yin L, Gregg AC, Riccio AM, Hoyt N, Islam ZH, Ahn J, Le Q, Patel P, Zhang M, He X, McKinney M, Kent E and Wang B (2022) Dietary therapy in abdominal aortic aneurysm — Insights from clinical and experimental studies. *Front. Cardiovasc. Med.* 9:949262. doi: 10.3389/fcvm.2022.949262

COPYRIGHT
© 2022 Yin, Gregg, Riccio, Hoyt, Islam, Ahn, Le, Patel, Zhang, He, McKinney, Kent and Wang. This is an open-access article distributed under the terms of the Creative Commons Attribution License (CC BY). The use, distribution or reproduction in other forums is permitted, provided the original author(s) and the copyright owner(s) are credited and that the original publication in this journal is cited, in accordance with accepted academic practice. No use, distribution or reproduction is permitted which does not comply with these terms.

Dietary therapy in abdominal aortic aneurysm — Insights from clinical and experimental studies

Li Yin[1], Alexander Christopher Gregg[1], Alessandra Marie Riccio[1], Nicholas Hoyt[1,2], Zain Hussain Islam[1], Jungeun Ahn[1], Quang Le[1], Paranjay Patel[1], Mengxue Zhang[1], Xinran He[1], Matthew McKinney[1], Eric Kent[1] and Bowen Wang[1]*

[1]Department of Surgery, School of Medicine, University of Virginia, Charlottesville, VA, United States, [2]School of Medicine and Health Sciences, George Washington University, Washington, DC, United States

Abdominal aortic aneurysm (AAA) is a prevalent vascular disease with high mortality rates upon rupture. Despite its prevalence in elderly populations, there remain limited treatment options; invasive surgical repair, while risky, is the only therapeutic intervention with proven clinical benefits. Dietary factors have long been suggested to be closely associated with AAA risks, and dietary therapies recently emerged as promising avenues to achieve non-invasive management of a wide spectrum of diseases. However, the role of dietary therapies in AAA remains elusive. In this article, we will summarize the recent clinical and pre-clinical efforts in understanding the therapeutic and mechanistic implications of various dietary patterns and therapeutic approaches in AAA.

KEYWORDS

diet, abdominal aortic aneurysm, dietary therapy, dietary restriction (DR), nutrient-sensing pathway, gut microbiome

Introduction

Abdominal aortic aneurysm (AAA) is a localized, progressive weakening and dilation of the aortic wall, primarily in the infrarenal segment. It is a common vascular disease in elderly populations (i.e., >65-year old), and up to 8% of males and 6% of females are estimated to develop AAA over a lifetime (1). While most cases are asymptomatic, AAA features a highly unpredictable disease course, which could culminate in the highly deadly rupture of the aneurysmal aorta (2). Ruptured AAAs have up to an 85% mortality rate, and thus far no single parameter or tool can robustly predict the risk of rupture (3). Owing to the expanded AAA screening in at-risk populations, an increasing number of diagnosed yet asymptomatic patients have been identified, albeit the majority of which are small-diameter AAAs. Unfortunately, these patients do not meet the criteria for open or endovascular repairs, which remain the standard of care (4). In these scenarios, a "watchful waiting" strategy is often employed to monitor the AAA growth rate overtime to triage patients that are considered stable; but due to the lack of effective

pharmacotherapies to block AAA expansion, these patients are left unprotected from the risk of unpredictable and lethal rupture (5). The absence of therapeutic modalities alternative and complementary to surgical repairs has greatly hindered the success brought about by the AAA surveillance initiative, causing unnecessary anxiety to the patients as well as burdens to the healthcare system (6).

Strategies to counter AAA's modifiable risk factors have long been recommended as secondary preventative measures to reduce overall cardiovascular mortality risks (5). Aside from the non-modifiable risk factors such as advanced age, male gender, Caucasian race, and family history, modifiable risk factors offer potential avenues for risk reduction strategies (7–9). Tobacco smoking is arguable the strongest modifiable risk factor associated with AAA expansion and rupture, and smoking cessation has been widely and strongly recommended for all patients with AAA (10, 11). Other modifiable factors, including hypertension and atherosclerosis, have also been subjected to extensive studies. However, at present, none of the anti-hypertensive (e.g., beta blockers) or atherosclerosis medications (e.g., statins) have demonstrated clear therapeutic efficacies against AAA expansion and rupture (12).

The lack of definitive clinical benefits in the foregoing risk reduction strategies necessitates further efforts toward the first non-surgical treatment of AAA. Over the past two decades, numerous FDA-approved drugs have been repurposed for treating AAAs, yet none have yielded any clinical success (12). The most prominent example is doxycycline, a previously approved tetracycline antibiotic for anti-bacterial infections that was hypothesized to possess potent anti-AAA efficacy due to its additional benefits in inhibiting proteolytic enzyme activities and inflammasome activation. Unfortunately, after almost twenty years of active investigations, the two randomized clinical trials — the N-TA3CT trial in the US and the PHAST trial in Netherland — led to the conclusion that doxycycline had no benefits against, if not further exacerbating the expansion of small-diameter AAAs (13, 14). Other promising candidate drugs, such as metformin and sirolimus, are still far from the clinical utility at the current stage (15, 16). As such, other alternative strategies are urgently needed to address the unmet clinical need, that is a safe and effective non-invasive management of AAA.

In light of the aforementioned challenges and obstacles, recent years have witnessed a surging interest in pursuing lifestyle changes for AAA management. While smoking cessation and physical exercise both have shown promising benefits in reducing AAA risks, there is a scarcity of studies concerning the role of healthy dietary patterns, at both clinical and preclinical levels (10, 17, 18). Especially with the ever-increasing benefits of various dietary regimens against cardiovascular diseases as recently reported (19, 20), understanding the therapeutic and mechanistic implications of certain dietary patterns would hold significant value in informing the future guideline of AAA management. Herein, we will summarize the recent progress in dietary therapies for AAA based on epidemiological and experimental evidence, (see Figure 1). Additionally, we will discuss the perspectives of emerging dietary regimens and potential molecular basis.

Clinical evidence supporting dietary regimens in AAA

In contrast to surgical repairs and drug treatments, dietary therapies are uniquely advantageous in multiple aspects, ranging from accessibility to the lack of invasiveness. For the management of cardiovascular diseases and metabolic syndromes, healthy dietary patterns have long been recommended to patients with proven benefits (19–22). However, in the case of AAA, the number of clinical studies examining the role of dietary patterns is sparse, with the epidemiological data almost exclusively derived from the following cohort studies: the Life Line Screening study, Atherosclerosis Risk in Communities (ARIC) study, the Malmö Diet and Cancer Study (MDCS), the Cohort of Swedish Men and the Swedish Mammography Cohort, and the Health In Men Study (HIMS), and most recently, the Brazilian Cardioprotective Nutritional Program Trial (23).

The first epidemiological evidence concerning dietary elements came from the Life Line Screening study in the US. In this retrospective cohort of 3.1 million patients, Kent et al. reported that consumption of nuts, vegetables, and fruits at a frequency of >three times per week were associated with reduced risk of AAA, as was the case for exercise (≥1 time per week) and smoking cessation (7). However, in this questionnaire study, fruits and vegetables were combined, thus their respective link to AAA risk was not discerned.

Built upon the seminal work from Kent et al., Stackelberg et al. continued to investigate dietary factors, particularly fruit and vegetable consumption, using the prospective Cohort of Swedish Men and Mammography Cohort (24). Surprisingly, while consumption of fruit was found to be negatively associated with the risk of AAA (particularly the ruptured ones), no link was established for vegetable consumption. In a follow-up study, the same team reported their finding that moderate alcohol consumption was inversely associated with AAA (25).

The role of dietary fiber and vegetable intake in AAA was not established until the reports from Harring et al. in 2018 and Bergwall et al. in 2019. In the former study, the ARIC study cohort was investigated regarding the association between AAA risk and their adherence to the Dietary Approaches To Stop Hypertension (DASH) dietary patterns (26). In addition to fruits, nuts, and legumes, high consumption of vegetables, whole grains, and low-fat dairy were revealed to be associated with decreased AAA burden, respectively. The latter study, conducted in the MDCS cohort, showed that linear protective associations between high intakes of fruits, berries, vegetables with AAA. Surprisingly, potato consumption was

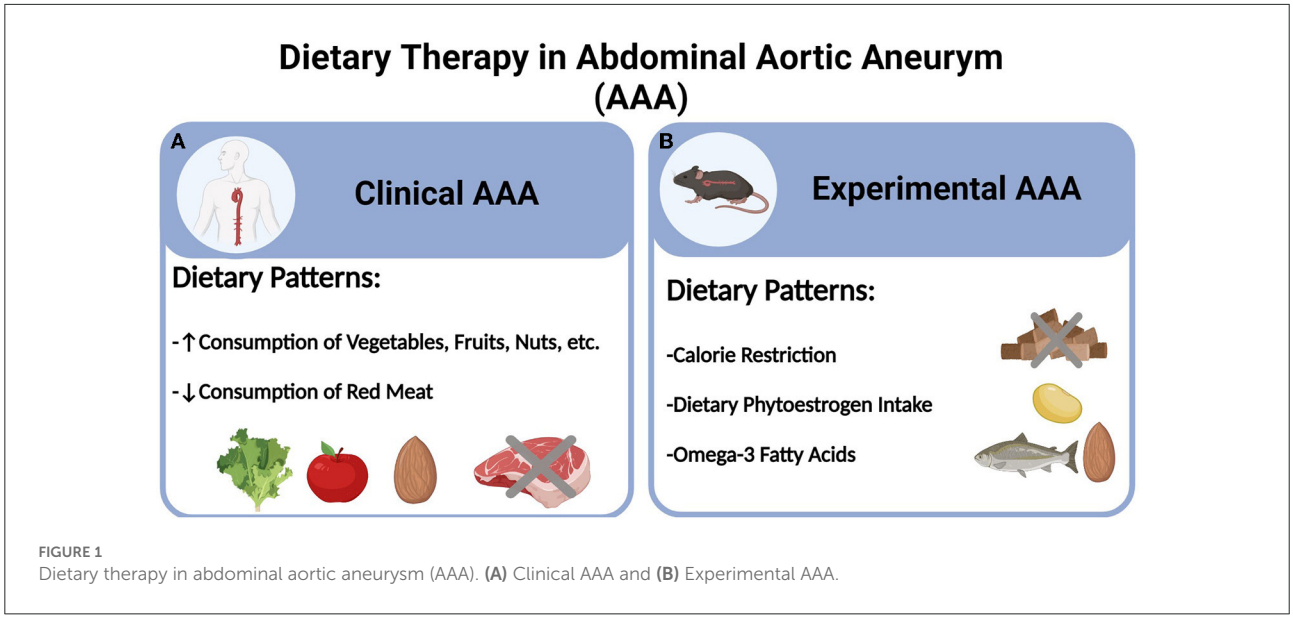

FIGURE 1
Dietary therapy in abdominal aortic aneurysm (AAA). **(A)** Clinical AAA and **(B)** Experimental AAA.

positively associated with AAA risk (27). Of particular note in both studies is the lack of statistically significant correlation between AAA risk and salt consumption, contradicting a prior population screening study in 11,742 elderly Australian males (28). Considering the uncertain clinical benefits of anti-hypertensive medications and the increasing popularity of the DASH dietary style, further experimental and clinical investigations are warranted to clarify the interventional value of such dietary patterns with restricted salt intake.

Similar to the DASH diet studied in the ARIC cohort, other similar dietary patterns have also been studied, including the anti-inflammatory diet and Mediterranean diet (29, 30). Similarly, diets high in antioxidant contents have also been recently reported to be associated with reduced AAA risks (23, 31). All these dietary patterns feature similar compositions, such as high consumption of fruit, vegetables, nuts, legumes, wholegrains, fish, and low consumption of red and processed meat. From a utility perspective, studying dietary patterns and eating styles may hold more translational value than focusing on individual food item consumption, as the former can encompass a variety of healthy dietary elements as aforementioned.

Preclinical studies concerning dietary patterns in AAA

Dietary therapies in experimental models

Notwithstanding the growing interest and epidemiological evidence, experimental studies concerning dietary therapies are very limited. Based on our literature search, three types of dietary regimens have been identified with preclinical therapeutic efficacies in murine models of AAA, i.e., calorie restriction, dietary phytoestrogen intake, and consumption of long-chain Omega-3 polyunsaturated fatty acids (PUFAs).

Calorie restriction

Calorie restriction is a dietary regimen that consists of decreased calorie intake without causing malnutrition and is often prescribed to achieve weight loss. Experimental data derived from rodent and non-human primate models support a pleiotropic role of calorie-restricted diets in mediating a myriad of health benefits, most notably in prolonging lifespan (32, 33). Data from the calorie restriction and cardiometabolic risk (CALERIE) study revealed a clear benefit of calorie restriction in reducing cardiometabolic risk factors (34). To date, only two experimental reports concerning the impact of such dietary patterns are available. Liu et al. observed profound mitigation of AAA formation using a calorie-restricted diet in angiotensin II (AngII)-infused, Apoe-/- mice (35). Additionally, they further found that sirtuin 1 (SIRT1), but not other metabolic/energy sensors such as SIRT3, mechanistic target of rapamycin (mTOR), and AMP-activated protein kinase α (AMPKα), was the main mediator of the aortic benefits exerted by calorie restriction. Such AAA-protective effect was later recapitulated using the same murine model and dietary regimen, and an alternative mediator, p53, was discovered to contribute to the aforementioned phenotype, possibly through maintaining mitochondrial bioenergetics (36).

Phytoestrogen diet

Phytoestrogens are a group of plant-derived chemicals with structural and functional similarities to 17-β-estradiol,

an estrogen with a presumed protective role against AAA. The primary sources of phytoestrogen intake are through consumption of soy and many other legumes, which have been previously linked to reduced AAA risk. Using a murine model with topical elastase application, Lu et al. showed that a phytoestrogen-rich diet could effectively ameliorate AAA development in male but not in female mice (37). In line with this observation, supplementation with the phytoestrogen Daidzein attenuated AngII-induced AAA in murine models (38). However, a follow-up study by Fashandi et al. using a modified AngII model failed to demonstrate any impact of a high-phytoestrogen Western diet on AAA rupture rates or survival (39). The inconsistency amongst these studies could be potentially attributed to the different experimental models, dietary regimens, and the phytoestrogen level/compositions in different chows, as demonstrated in the work from Lu et al. Considering the striking gender dimorphism in AAA, future experimental efforts are poised to address the question concerning the link among dietary phytoestrogen, endogenous estrogen, and AAA risk (40).

Omega-3 PUFA-rich diet

Increased consumption of the PUFAs (e.g., Omega-3) — often deemed as the healthy fats — is a key component of the aforementioned diets (e.g., Mediterranean diet) featuring high consumption of fish and nuts. Indeed, numerous Omega-3 PUFAs have been studied in murine models, in which dietary supplementation could reduce AAA development (41–43). While small-scale clinical studies suggest a potential correlation between Omega-3 PUFAs and reduced AAA risk as well as early benefits in improving pre-AAA pathologies (i.e., aortic stiff), further studies are warranted to fully elucidate the role of such dietary component(s) in the clinical management of AAA (44, 45).

AAA-promoting diets in experimental models

In stark contrast to the paucity of experimental studies concerning dietary therapies, a plethora of literature are available, detailing the pathophysiological/phenotypic impacts upon experimental AAA pathogenesis. Most notable examples include dietary patterns that recapitulate AAA's established risk factors, such as high-fat diets (atherosclerosis/hypercholesterolemia) (46, 47), high-salt consumption (hypertension), excessive supplementation with homocysteine, or methionine (red meat consumption and hyperhomocysteinemia), etc (48–50).

Perspectives

Emerging dietary regimens to be explored in preclinical AAA models

Protein restriction

Similar to calorie restriction, protein restriction has also been shown to help prolong lifespan in fruit flies and mice (51, 52). In epidemiological studies, reduced intake of proteins, especially red meat consumption, has been related to reduced risk of all-cause mortality in populations aged 50–65 years. However, in elderly populations aged above 65 years that are also at risk of AAA, low protein intake rather increased, whereas high protein consumption reduced all-cause mortality (53). These observations highlight the duality behind dietary restrictions on general nutrient intake: on the one hand, such strategies have yielded pleiotropic benefits; but on the flip side, concerns of malnutrition and frailty have been persistently plaguing their widespread adoption and long-term adherence, particularly for the AAA-prone aged populations that are more susceptible to side effects like sarcopenia. Interestingly, recent studies suggest that short-term dietary restrictions, such as pre-operative protein restriction under inpatient settings, may present an alternative, viable path as dietary preconditioning to safely capitalize on the benefits of such dietary therapies. Indeed, mounting preclinical evidence has pointed to the role of pre-operative protein restriction in reducing surgical stress as well as vascular (re)stenosis. Inspired by the safety data from an exploratory trial in elective carotid endarterectomy patients (54), another trial is currently underway to chart the baseline information from healthy subjects, with the ultimate goal of comparing with patients undergoing AAA surgical repair in a future study (NCT03995979). However, sufficient protein intake has also been suggested to be critical in post-operative recovery, and hence cautions should be noted concerning the frailties caused by protein restriction (55, 56).

Amino acid restriction

Unlike calorie or protein restriction, limiting the intake of amino acid(s) has been shown to produce similar health benefits in preclinical studies without significant risks of malnutrition. Clinical studies further established the safety profile as well as the early efficacy of a methionine-restricted diet in healthy and cancer patients, with additional randomized clinical trials currently ongoing (57, 58). While restrictions of single (e.g., methionine) or multiple (e.g., branch-chained amino acids) amino acids have been studied in experimental models and even human subjects of other cardiometabolic diseases, their implications in AAA have not been reported (59–63). Considering the clinical association between certain

amino acids/metabolites (e.g., homocysteine, methionine) and AAA risk, it is of significant translational value to pursue the preclinical impacts of such dietary restriction patterns in future studies.

Intermittent fasting

Intermittent fasting is a dietary pattern that features time-restricted eating with or without reducing calorie intake. Due to its reduced risk of malnutrition and ease of adherence, intermittent fasting has garnered significant popularity during the past decade as an alternative regimen. Clinical studies have suggested beneficial associations of intermittent fasting with cardiometabolic risks, albeit long-term outcomes are still pending (64, 65). In light of the aortic protection exerted by calorie restriction in murine AAA models, it is reasonable to postulate whether a similar effect could be observed with intermittent fasting. However, it is worth noting that current intermittent fasting protocols are highly variable, thus making comparisons amongst different studies difficult. A recent murine study further demonstrated that the circadian schedules of the time-restricted eating could critically determine the outcomes of different fasting protocols, which informs the challenges and critical parameters to be considered when designing future preclinical studies in AAA (66).

Emerging diet-mediated mechanisms potentially implicated in AAA

There is no pathway or molecular basis that could completely account for the health benefits of a given diet. Past studies have unveiled various mechanisms implicated in the aforementioned dietary regimens, such as overall energy expenditure reduction, antioxidant supplementation, increased production of hepatokines (e.g., FGF21) (67–71), etc. Due to the scarcity of relevant literature on AAA, we will focus on two emerging dietary mechanisms that are recently implicated in AAA pathophysiologies while more in-depth investigations are still needed.

Metabolism/nutrient sensors

Studies from other disciplines have uncovered a series of sensor proteins and pathways for cellular metabolism, energy expenditure, and certain nutrient cues. Amongst the sensors known thus far, the NAD+-dependent protein deacetylase sirtuin family member SIRT1 is the most notable example. Not only has SIRT1 been established to negatively modulate AAA pathogenesis (35, 72), experimental evidence further revealed its critical role in mediating the benefits of calorie restriction in mitigating AAA risk. Similarly, deletion of SIRT3, another sirtuin member, exacerbated, whereas its overexpression mitigated aneurysmal formation and progression (73). Another kinase commonly associated with dietary restriction is AMPKα, the activation of which has been the presumed mode of action behind established therapeutic regimens such as calorie restriction and metformin. Indeed, although no definitive link has been made between AMPKα and any diet-mediated AAA mitigation, data in murine models did suggest a protective role of AMPKα against AAA formation (74, 75); and while metformin, a calorie restriction mimetic therapy recapitulated the therapeutic benefits, AMPK blockade effectively abolished the protection against AAA (15, 74, 76).

mTOR and general control non-derepressible 2 (GCN2) constitute the only two identified sensors for amino acids (77). While mTOR is activated by recognizing the presence and intracellular level of amino acids, GCN2, on the other hand, senses amino acid starvation (78, 79). Both mTOR (inactivation) and GCN2 (activation) have been implicated in the cardiometabolic benefits of dietary restrictions (60, 80, 81). While chronic activation of mTOR was recently reported to drive aortic degeneration and hence aneurysmal formation, the specific role of GCN2 remains unknown in AAA (82). Further studies concerning GCN2 and amino acid restriction are poised to determine the clinical utility of such innovative dietary therapies.

Gut microbiome

You are what you eat. This is particularly true for the gut microbiome, as all the aforementioned diets have been shown to modulate gut microbiota (83–88). Although largely neglected as "bystanders" for a long time, the gut microbiome has been increasingly recognized to contribute to a wide range of biological and pathological processes (89). Only very recently were alterations of gut microbiota reported in experimental and clinical subjects with AAA, suggesting a microbial dysbiosis that is yet to be elucidated in aneurysm (90, 91). Although no studies thus far have investigated the exact role of diet-induced microbiota in AAA, it is highly plausible that certain dietary regimens could impact AAA pathogenesis *via* cultivating distinct microbiome compositions and hence driving a shift toward beneficial microbiota-derived metabolic compositions. In fact, some microbiota-derived metabolites that are profoundly inhibited upon dietary restrictions (57, 92, 93), such as trimethylamine N-oxide (TMAO), were recently revealed to contribute to AAA development (94).

Closing remarks

The past decade has witnessed tremendous progress in dietary therapies for the management of cardiometabolic

diseases and cancer, yet their therapeutic and mechanistic implications in AAA are still elusive. The current study provides the first comprehensive review of preclinical and clinical evidence supporting the potential adoption of certain dietary patterns in preventing and managing AAA. Also discussed are selected emerging dietary regimens as well as diet-mediated mechanisms, in which further investigations are still pending. We envision that future research efforts will be increasingly dedicated to a better understanding of as well as translational development of the first non-surgical management of AAA in the form of dietary therapies.

Author contributions

LY and BW conceived the manuscript. AG, AR, NH, ZI, JA, QL, PP, MZ, XH, MM, and EK conducted the literature search and contributed to the drafting and editing of the manuscript. ZI, PP, and MM created the graphical abstract using BioRender.com. All authors contributed to the article and approved the submitted version.

Funding

This work was supported by the National Institute of Health (NIH) grant R01HL162895 (to BW).

Conflict of interest

Author BW is the corresponding author, the coordinator for this research topic, and has recused from the peer-review and editorial processes.

The remaining authors declare that the research was conducted in the absence of any commercial or financial relationships that could be construed as a potential conflict of interest.

Publisher's note

All claims expressed in this article are solely those of the authors and do not necessarily represent those of their affiliated organizations, or those of the publisher, the editors and the reviewers. Any product that may be evaluated in this article, or claim that may be made by its manufacturer, is not guaranteed or endorsed by the publisher.

References

1. Tang W, Yao L, Roetker NS, Alonso A, Lutsey PL, Steenson CC, et al. lifetime risk and risk factors for abdominal aortic aneurysm in a 24-year prospective study: the aric study (atherosclerosis risk in communities). *Arterioscler Thromb Vasc Biol.* (2016) 36:2468–77. doi: 10.1161/ATVBAHA.116.308147

2. Karthikesalingam A, Holt PJ, Vidal-Diez A, Ozdemir BA, Poloniecki JD, Hinchliffe RJ, et al. Mortality from ruptured abdominal aortic aneurysms: clinical lessons from a comparison of outcomes in England and the USA. *Lancet.* (2014) 383:963–9. doi: 10.1016/S0140-6736(14)60109-4

3. Force USPST, Owens DK, Davidson KW, Krist AH, Barry MJ, Cabana M, et al. Screening for abdominal aortic aneurysm: us preventive services task force recommendation statement. *JAMA.* (2019) 322:2211–8. doi: 10.1001/jama.2019.18928

4. Wanhainen A, Verzini F, Van Herzeele I, Allaire E, Bown M, Cohnert T, et al. Editor's choice - European Society for Vascular Surgery (ESVS) 2019 clinical practice guidelines on the management of abdominal aorto-iliac artery aneurysms. *Eur J Vasc Endovasc Surg.* (2019) 57:8–93. doi: 10.1016/j.ejvs.2018.09.020

5. Chaikof EL, Dalman RL, Eskandari MK, Jackson BM, Lee WA, Mansour MA, et al. The Society for Vascular Surgery practice guidelines on the care of patients with an abdominal aortic aneurysm. *J Vasc Surg.* (2018) 67:2–77 e2. doi: 10.1016/j.jvs.2017.10.044

6. Arnaoutakis DJ, Upchurch GRJr. Abdominal aortic aneurysm screening is safe yet lacks effectiveness. *Circulation.* (2019) 139:1381–3. doi: 10.1161/CIRCULATIONAHA.118.038809

7. Kent KC, Zwolak RM, Egorova NN, Riles TS, Manganaro A, Moskowitz AJ, et al. Analysis of risk factors for abdominal aortic aneurysm in a cohort of more than 3 million individuals. *J Vasc Surg.* (2010) 52:539–48. doi: 10.1016/j.jvs.2010.05.090

8. Lindholt JS, Juul S, Fasting H, Henneberg EW. Screening for abdominal aortic aneurysms: single centre randomized controlled trial. *BMJ.* (2005) 330:750. doi: 10.1136/bmj.38369.620162.82

9. van Vlijmen-van Keulen CJ, Pals G, Rauwerda JA. Familial abdominal aortic aneurysm: a systematic review of a genetic background. *Eur J Vasc Endovasc Surg.* (2002) 24:105–16. doi: 10.1053/ejvs.2002.1692

10. Aune D, Schlesinger S, Norat T, Riboli E. Tobacco smoking and the risk of abdominal aortic aneurysm: a systematic review and meta-analysis of prospective studies. *Sci Rep.* (2018) 8:14786. doi: 10.1038/s41598-018-32100-2

11. Wilmink TB, Quick CR, Day NE. The association between cigarette smoking and abdominal aortic aneurysms. *J Vasc Surg.* (1999) 30:1099–105. doi: 10.1016/S0741-5214(99)70049-2

12. Lindeman JH, Matsumura JS. Pharmacologic management of aneurysms. *Circ Res.* (2019) 124:631–46. doi: 10.1161/CIRCRESAHA.118.312439

13. Baxter BT, Matsumura J, Curci JA, McBride R, Larson L, Blackwelder W, et al. Effect of doxycycline on aneurysm growth among patients with small infrarenal abdominal aortic aneurysms: a randomized clinical trial. *JAMA.* (2020) 323:2029–38. doi: 10.1001/jama.2020.5230

14. Meijer CA, Stijnen T, Wasser MN, Hamming JF, van Bockel JH, Lindeman JH, et al. Doxycycline for stabilization of abdominal aortic aneurysms: a randomized trial. *Ann Intern Med.* (2013) 159:815–23. doi: 10.7326/0003-4819-159-12-201312170-00007

15. Yuan Z, Heng Z, Lu Y, Wei J, Cai Z. The protective effect of metformin on abdominal aortic aneurysm: a systematic review and meta-analysis. *Front Endocrinol.* (2021) 12:721213. doi: 10.3389/fendo.2021.721213

16. Rouer M, Xu BH, Xuan HJ, Tanaka H, Fujimura N, Glover KJ, et al. Rapamycin limits the growth of established experimental abdominal aortic aneurysms. *Eur J Vasc Endovasc Surg.* (2014) 47:493–500. doi: 10.1016/j.ejvs.2014.02.006

17. Aune D, Sen A, Kobeissi E, Hamer M, Norat T, Riboli E. Physical activity and the risk of abdominal aortic aneurysm: a systematic review and meta-analysis of prospective studies. *Sci Rep.* (2020) 10:22287. doi: 10.1038/s41598-020-76306-9

18. Weston M, Batterham AM, Tew GA, Kothmann E, Kerr K, Nawaz S, et al. Patients awaiting surgical repair for large abdominal aortic aneurysms can exercise at moderate to hard intensities with a low risk of adverse events. *Front Physiol.* (2016) 7:684. doi: 10.3389/fphys.2016.00684

19. Brandhorst S, Longo VD. Dietary restrictions and nutrition in the prevention and treatment of cardiovascular disease. *Circ Res.* (2019) 124:952–65. doi: 10.1161/CIRCRESAHA.118.313352

20. Fontana L, Meyer TE, Klein S, Holloszy JO. Long-term calorie restriction is highly effective in reducing the risk for atherosclerosis in humans. *Proc Natl Acad Sci U S A.* (2004) 101:6659–63. doi: 10.1073/pnas.0308291101

21. Oh M, Kim S, An KY, Min J, Yang HI, Lee J, et al. Effects of alternate day calorie restriction and exercise on cardio-metabolic risk factors in overweight and obese adults: an exploratory randomized controlled study. *BMC Public Health.* (2018) 18:1124. doi: 10.1186/s12889-018-6009-1

22. Huffman KM, Parker DC, Bhapkar M, Racette SB, Martin CK, Redman LM, et al. Calorie restriction improves lipid-related emerging cardiometabolic risk factors in healthy adults without obesity: distinct influences of BMI and sex from CALERIE a multicentre, phase 2, randomised controlled trial. *EClin Med.* (2022) 43:101261. doi: 10.1016/j.eclinm.2021.101261

23. da Silva A, Caldas APS, Pinto SL, Hermsdorff HHM, Marcadenti A, Bersch-Ferreira AC, et al. Dietary total antioxidant capacity is inversely associated with cardiovascular events and cardiometabolic risk factors: a cross-sectional study. *Nutrition.* (2021) 89:111140. doi: 10.1016/j.nut.2021.111140

24. Stackelberg O, Bjorck M, Larsson SC, Orsini N, Wolk A. Fruit and vegetable consumption with risk of abdominal aortic aneurysm. *Circulation.* (2013) 128:795–802. doi: 10.1161/CIRCULATIONAHA.112.000728

25. Stackelberg O, Bjorck M, Larsson SC, Orsini N, Wolk A. Alcohol consumption, specific alcoholic beverages, and abdominal aortic aneurysm. *Circulation.* (2014) 130:646–52. doi: 10.1161/CIRCULATIONAHA.113.008279

26. Haring B, Selvin E, He X, Coresh J, Steffen LM, Folsom AR, et al. Adherence to the dietary approaches to stop hypertension dietary pattern and risk of abdominal aortic aneurysm: results from the ARIC study. *J Am Heart Assoc.* (2018) 7:e009340. doi: 10.1161/JAHA.118.009340

27. Bergwall S, Acosta S, Sonestedt E. Intake of fibre and plant foods and the risk of abdominal aortic aneurysm in a large prospective cohort study in Sweden. *Eur J Nutr.* (2020) 59:2047–56. doi: 10.1007/s00394-019-02054-w

28. Golledge J, Hankey GJ, Yeap BB, Almeida OP, Flicker L, Norman PE. Reported high salt intake is associated with increased prevalence of abdominal aortic aneurysm and larger aortic diameter in older men. *PLoS ONE.* (2014) 9:e102578. doi: 10.1371/journal.pone.0102578

29. Kaluza J, Stackelberg O, Harris HR, Bjorck M, Wolk A. Anti-inflammatory diet and risk of abdominal aortic aneurysm in two Swedish cohorts. *Heart.* (2019) 105:1876–83. doi: 10.1136/heartjnl-2019-315031

30. Kaluza J, Stackelberg O, Harris HR, Akesson A, Bjorck M, Wolk A. Mediterranean diet is associated with reduced risk of abdominal aortic aneurysm in smokers: results of two prospective cohort studies. *Eur J Vasc Endovasc Surg.* (2021) 62:284–93. doi: 10.1016/j.ejvs.2021.04.017

31. Nordkvist S, Sonestedt E, Acosta S. Adherence to diet recommendations and risk of abdominal aortic aneurysm in the Malmo Diet and Cancer Study. *Sci Rep.* (2018) 8:2017. doi: 10.1038/s41598-018-20415-z

32. Weindruch R, Walford RL, Fligiel S, Guthrie D. The retardation of aging in mice by dietary restriction: longevity, cancer, immunity and lifetime energy intake. *J Nutr.* (1986) 116:641–54. doi: 10.1093/jn/116.4.641

33. Mattison JA, Colman RJ, Beasley TM, Allison DB, Kemnitz JW, Roth GS, et al. Caloric restriction improves health and survival of rhesus monkeys. *Nat Commun.* (2017) 8:14063. doi: 10.1038/ncomms14063

34. Kraus WE, Bhapkar M, Huffman KM, Pieper CF, Krupa Das S, Redman LM, et al. 2 years of calorie restriction and cardiometabolic risk (CALERIE): exploratory outcomes of a multicentre, phase 2, randomized controlled trial. *Lancet Diabetes Endocrinol.* (2019) 7:673–83. doi: 10.1016/S2213-8587(19)30151-2

35. Liu Y, Wang TT, Zhang R, Fu WY, Wang X, Wang F, et al. Calorie restriction protects against experimental abdominal aortic aneurysms in mice. *J Exp Med.* (2016) 213:2473–88. doi: 10.1084/jem.20151794

36. Gao P, Zhang H, Zhang Q, Fang X, Wu H, Wang M, et al. Caloric restriction exacerbates angiotensin II-induced abdominal aortic aneurysm in the absence of p53. *Hypertension.* (2019) 73:547–60. doi: 10.1161/HYPERTENSIONAHA.118.12086

37. Lu G, Su G, Zhao Y, Johnston WF, Sherman NE, Rissman EF, et al. Dietary phytoestrogens inhibit experimental aneurysm formation in male mice. *J Surg Res.* (2014) 188:326–38. doi: 10.1016/j.jss.2013.11.1108

38. Liu YF, Bai YQ Qi M. Daidzein attenuates abdominal aortic aneurysm through NF-kappaB, p38MAPK and TGF-beta1 pathways. *Mol Med Rep.* (2016) 14:955–62. doi: 10.3892/mmr.2016.5304

39. Fashandi AZ, Spinosa M, Salmon M, Su G, Montgomery W, Mast A, et al. Female mice exhibit abdominal aortic aneurysm protection in an established rupture model. *J Surg Res.* (2020) 247:387–96. doi: 10.1016/j.jss.2019.10.004

40. Lo RC, Bensley RP, Hamdan AD, Wyers M, Adams JE, Schermerhorn ML, et al. Gender differences in abdominal aortic aneurysm presentation, repair, and mortality in the Vascular Study Group of New England. *J Vasc Surg.* (2013) 57:1261–8. doi: 10.1016/j.jvs.2012.11.039

41. Wang JH, Eguchi K, Matsumoto S, Fujiu K, Komuro I, Nagai R, et al. The omega-3 polyunsaturated fatty acid, eicosapentaenoic acid, attenuates abdominal aortic aneurysm development *via* suppression of tissue remodeling. *PLoS ONE.* (2014) 9:e96286. doi: 10.1371/journal.pone.0096286

42. Yoshihara T, Shimada K, Fukao K, Sai E, Sato-Okabayashi Y, Matsumori R, et al. Omega 3 polyunsaturated fatty acids suppress the development of aortic aneurysms through the inhibition of macrophage-mediated inflammation. *Circ J.* (2015) 79:1470–8. doi: 10.1253/circj.CJ-14-0471

43. Kavazos K, Nataatmadja M, Wales KM, Hartland E, Williams C, Russell FD. Dietary supplementation with omega-3 polyunsaturated fatty acids modulate matrix metalloproteinase immunoreactivity in a mouse model of pre-abdominal aortic aneurysm. *Heart Lung Circ.* (2015) 24:377–85. doi: 10.1016/j.hlc.2014.11.005

44. Meital LT, Schulze K, Magee R, O'Donnell J, Jha P, Meital CY, et al. Long chain omega-3 polyunsaturated fatty acids improve vascular stiffness in abdominal aortic aneurysm: a randomized controlled trial. Nutrients. (2020) 13. doi: 10.3390/nu13010138

45. Aikawa T, Miyazaki T, Shimada K, Sugita Y, Shimizu M, Ouchi S, et al. Low serum levels of EPA are associated with the size and growth rate of abdominal aortic aneurysm. *J Atheroscler Thromb.* (2017) 24:912–20. doi: 10.5551/jat.38315

46. Saburi M, Yamada H, Wada N, Motoyama S, Sugimoto T, Kubota H, et al. Maternal high-fat diet promotes abdominal aortic aneurysm expansion in adult offspring by epigenetic regulation of irf8-mediated osteoclast-like macrophage differentiation. *Cells.* (2021) 10:2224. doi: 10.3390/cells10092224

47. Lu H, Howatt DA, Balakrishnan A, Graham MJ, Mullick AE, Daugherty A. Hypercholesterolemia induced by a PCSK9 gain-of-function mutation augments angiotensin II-induced abdominal aortic aneurysms in C57BL/6 mice-brief report. *Arterioscler Thromb Vasc Biol.* (2016) 36:1753–7. doi: 10.1161/ATVBAHA.116.307613

48. Nishida N, Aoki H, Ohno-Urabe S, Nishihara M, Furusho A, Hirakata S, et al. High salt intake worsens aortic dissection in mice: involvement of IL (Interleukin)-17A-dependent ECM (extracellular matrix) metabolism. *Arterioscler Thromb Vasc Biol.* (2020) 40:189–205. doi: 10.1161/ATVBAHA.119.313336

49. Liu Z, Luo H, Zhang L, Huang Y, Liu B, Ma K, et al. Hyperhomocysteinemia exaggerates adventitial inflammation and angiotensin II-induced abdominal aortic aneurysm in mice. *Circ Res.* (2012) 111:1261–73. doi: 10.1161/CIRCRESAHA.112.270520

50. Fan Y, Li N, Liu C, Dong H, Hu X. Excessive methionine supplementation exacerbates the development of abdominal aortic aneurysm in rats. *J Vasc Res.* (2019) 56:230–40. doi: 10.1159/000501313

51. Richardson NE, Konon EN, Schuster HS, Mitchell AT, Boyle C, Rodgers AC, et al. Lifelong restriction of dietary branched-chain amino acids has sex-specific benefits for frailty and lifespan in mice. *Nat Aging.* (2021) 1:73–86. doi: 10.1038/s43587-020-00006-2

52. Babygirija R, Lamming DW. The regulation of healthspan and lifespan by dietary amino acids. *Transl Med Aging.* (2021) 5:17–30. doi: 10.1016/j.tma.2021.05.001

53. Kitada M, Ogura Y, Monno I, Koya D. The impact of dietary protein intake on longevity and metabolic health. *EBioMed.* (2019) 43:632–40. doi: 10.1016/j.ebiom.2019.04.005

54. Kip P, Trocha KM, Tao M, O'Leary J J, Ruske J, Giulietti JM, et al. Insights from a short-term protein-calorie restriction exploratory trial in elective carotid endarterectomy patients. *Vasc Endovascular Surg.* (2019) 53:470–6. doi: 10.1177/1538574419856453

55. Yeung SE, Hilkewich L, Gillis C, Heine JA, Fenton TR. Protein intakes are associated with reduced length of stay: a comparison between Enhanced Recovery After Surgery (ERAS) and conventional care after elective colorectal surgery. *Am J Clin Nutr.* (2017) 106:44–51.

56. Weimann A, Braga M, Carli F, Higashiguchi T, Hubner M, Klek S, et al. ESPEN guideline: clinical nutrition in surgery. *Clin Nutr.* (2017) 36:623–50. doi: 10.1016/j.clnu.2017.02.013

57. Gao X, Sanderson SM Dai Z, Reid MA, Cooper DE, Lu M, et al. Dietary methionine influences therapy in mouse cancer models and alters human metabolism. *Nature.* (2019) 572:397–401. doi: 10.1038/s41586-019-1437-3

58. Hoffman RM. Clinical studies of methionine-restricted diets for cancer patients. *Methods Mol Biol.* (2019) 1866:95–105. doi: 10.1007/978-1-4939-8796-2_9

59. Han L, Wu G, Feng C, Yang Y, Li B, Ge Y, et al. Dietary methionine restriction improves the impairment of cardiac function in middle-aged obese mice. *Food Funct.* (2020) 11:1764–78. doi: 10.1039/C9FO02819F

60. Longchamp A, Mirabella T, Arduini A, MacArthur MR, Das A, Trevino-Villarreal JH, et al. Amino acid restriction triggers angiogenesis via GCN2/ATF4 regulation of VEGF and H2S production. Cell. 2018;173:117–29 e14. doi: 10.1016/j.cell.2018.03.001

61. Ables GP, Ouattara A, Hampton TG, Cooke D, Perodin F, Augie I, et al. Dietary methionine restriction in mice elicits an adaptive cardiovascular response to hyperhomocysteinemia. *Sci Rep.* (2015) 5:8886. doi: 10.1038/srep08886

62. Ramzan I, Taylor M, Phillips B, Wilkinson D, Smith K, Hession K, et al. A novel dietary intervention reduces circulatory branched-chain amino acids by 50%: a pilot study of relevance for obesity and diabetes. *Nutrients.* (2020) 13:95. doi: 10.3390/nu13010095

63. McGarrah RW, Zhang GF, Christopher BA, Deleye Y, Walejko JM, Page S, et al. Dietary branched-chain amino acid restriction alters fuel selection and reduces triglyceride stores in hearts of Zucker fatty rats. *Am J Physiol Endocrinol Metab.* (2020) 318:E216–E23. doi: 10.1152/ajpendo.00334.2019

64. Patikorn C, Roubal K, Veettil SK, Chandran V, Pham T, Lee YY, et al. Intermittent fasting and obesity-related health outcomes: an umbrella review of meta-analyses of randomized clinical trials. *JAMA Netw Open.* (2021) 4:e2139558. doi: 10.1001/jamanetworkopen.2021.39558

65. Maroofi M, Nasrollahzadeh J. Effect of intermittent vs. continuous calorie restriction on body weight and cardiometabolic risk markers in subjects with overweight or obesity and mild-to-moderate hypertriglyceridemia: a randomized trial. *Lipids Health Dis.* (2020) 19:216. doi: 10.1186/s12944-020-01399-0

66. Acosta-Rodriguez V, Rijo-Ferreira F, Izumo M, Xu P, Wight-Carter M, Green CB, et al. Circadian alignment of early onset caloric restriction promotes longevity in male C57BL/6J mice. *Science.* (2022) 376:1192–202. doi: 10.1126/science.abk0297

67. Capo X, Martorell M, Ferrer MD, Sureda A, Pons V, Domingo JC, et al. Calorie restriction improves physical performance and modulates the antioxidant and inflammatory responses to acute exercise. *Nutrients.* (2020) 12:930. doi: 10.3390/nu12040930

68. Most J, Redman LM. Impact of calorie restriction on energy metabolism in humans. *Exp Gerontol.* (2020) 133:110875. doi: 10.1016/j.exger.2020.110875

69. Hill CM, Berthoud HR, Munzberg H, Morrison CD. Homeostatic sensing of dietary protein restriction: a case for FGF21. *Front Neuroendocrinol.* (2018) 51:125–31. doi: 10.1016/j.yfrne.2018.06.002

70. Laeger T, Henagan TM, Albarado DC, Redman LM, Bray GA, Noland RC, et al. FGF21 is an endocrine signal of protein restriction. *J Clin Invest.* (2014) 124:3913–22. doi: 10.1172/JCI74915

71. Ungvari Z, Parrado-Fernandez C, Csiszar A, de Cabo R. Mechanisms underlying caloric restriction and lifespan regulation: implications for vascular aging. *Circ Res.* (2008) 102:519–28. doi: 10.1161/CIRCRESAHA.107.168369

72. Budbazar E, Rodriguez F, Sanchez JM, Seta F. The role of Sirtuin-1 in the vasculature: focus on aortic aneurysm. *Front Physiol.* (2020) 11:1047. doi: 10.3389/fphys.2020.01047

73. Qiu L, Yi S, Yu T, Hao Y. Sirt3 protects against thoracic aortic dissection formation by reducing reactive oxygen species, vascular inflammation, and apoptosis of smooth muscle cells. *Front Cardiovasc Med.* (2021) 8:675647. doi: 10.3389/fcvm.2021.675647

74. He J, Li N, Fan Y, Zhao X, Liu C, Hu X. metformin inhibits abdominal aortic aneurysm formation through the activation of the AMPK/mTOR signaling pathway. *J Vasc Res.* (2021) 58:148–58. doi: 10.1159/000513465

75. Yang L, Shen L, Gao P, Li G, He Y, Wang M, et al. Effect of AMPK signal pathway on pathogenesis of abdominal aortic aneurysms. *Oncotarget.* (2017) 8:92827–40. doi: 10.18632/oncotarget.21608

76. Fujimura N, Xiong J, Kettler EB, Xuan H, Glover KJ, Mell MW, et al. Metformin treatment status and abdominal aortic aneurysm disease progression. *J Vasc Surg.* (2016) 64:46–54 e8. doi: 10.1016/j.jvs.2016.02.020

77. Eleftheriadis T, Pissas G, Antoniadi G, Liakopoulos V, Tsogka K, Sounidaki M, et al. Differential effects of the two amino acid sensing systems, the GCN2 kinase and the mTOR complex 1, on primary human alloreactive CD4(+) T-cells. *Int J Mol Med.* (2016) 37:1412–20. doi: 10.3892/ijmm.2016.2547

78. Goberdhan DC, Wilson C, Harris AL. Amino acid sensing by mTORC1: intracellular transporters mark the spot. *Cell Metab.* (2016) 23:580–9. doi: 10.1016/j.cmet.2016.03.013

79. Battu S, Minhas G, Mishra A, Khan N. amino acid sensing via general control nonderepressible-2 kinase and immunological programming. *Front Immunol.* (2017) 8:1719. doi: 10.3389/fimmu.2017.01719

80. Sciarretta S, Forte M, Frati G, Sadoshima J. New insights into the role of mTOR signaling in the cardiovascular system. *Circ Res.* (2018) 122:489–505. doi: 10.1161/CIRCRESAHA.117.311147

81. Qin P, Arabacilar P, Bernard RE, Bao W, Olzinski AR, Guo Y, et al. Activation of the amino acid response pathway blunts the effects of cardiac stress. *J Am Heart Assoc.* (2017) 6:e004453. doi: 10.1161/JAHA.116.004453

82. Li G, Wang M, Caulk AW, Cilfone NA, Gujja S, Qin L, et al. Chronic mTOR activation induces a degradative smooth muscle cell phenotype. *J Clin Invest.* (2020) 130:1233–51. doi: 10.1172/JCI131048

83. von Schwartzenberg RJ, Bisanz JE, Lyalina S, Spanogiannopoulos P, Ang QY, Cai J, et al. Caloric restriction disrupts the microbiota and colonization resistance. *Nature.* (2021) 595:272–7. doi: 10.1038/s41586-021-03663-4

84. Karakan T. Intermittent fasting and gut microbiota. *Turk J Gastroenterol.* (2019) 30:1008. doi: 10.5152/tjg.2019.101219

85. Fan P, Liu P, Song P, Chen X, Ma X. Moderate dietary protein restriction alters the composition of gut microbiota and improves ileal barrier function in adult pig model. *Sci Rep.* (2017) 7:43412. doi: 10.1038/srep43412

86. Seyed Hameed AS, Rawat PS, Meng X, Liu W. Biotransformation of dietary phytoestrogens by gut microbes: a review on bidirectional interaction between phytoestrogen metabolism and gut microbiota. *Biotechnol Adv.* (2020) 43:107576. doi: 10.1016/j.biotechadv.2020.107576

87. Wallis KF, Melnyk SB, Miousse IR. Sex-specific effects of dietary methionine restriction on the intestinal microbiome. *Nutrients.* (2020) 12:781. doi: 10.3390/nu12030781

88. De Filippis F, Pellegrini N, Vannini L, Jeffery IB, La Storia A, Laghi L, et al. High-level adherence to a Mediterranean diet beneficially impacts the gut microbiota and associated metabolome. *Gut.* (2016) 65:1812–21. doi: 10.1136/gutjnl-2015-309957

89. Keshavarzian A, Engen P, Bonvegna S, Cilia R. The gut microbiome in Parkinson's disease: a culprit or a bystander? *Prog Brain Res.* (2020) 252:357–450. doi: 10.1016/bs.pbr.2020.01.004

90. Xie J, Lu W, Zhong L, Hu Y, Li Q, Ding R, et al. Alterations in gut microbiota of abdominal aortic aneurysm mice. *BMC Cardiovasc Disord.* (2020) 20:32. doi: 10.1186/s12872-020-01334-2

91. Zhang K, Yang S, Huang Y, Qin X, Qu K, Chen Y, et al. Alterations in gut microbiota and physiological factors associated with abdominal aortic aneurysm. *Med Device Techno.* (2022) 14:100122. doi: 10.1016/j.medntd.2022.100122

92. Videja M, Sevostjanovs E, Upmale-Engela S, Liepinsh E, Konrade I, Dambrova M. Fasting-mimicking diet reduces trimethylamine N-oxide levels and improves serum biochemical parameters in healthy volunteers. *Nutrients.* (2022) 14:1093. doi: 10.3390/nu14051093

93. Erickson ML, Malin SK, Wang Z, Brown JM, Hazen SL, Kirwan JP. Effects of lifestyle intervention on plasma trimethylamine N-oxide in obese adults. *Nutrients.* (2019) 11:179. doi: 10.3390/nu11010179

94. Hu J, Xu J, Shen S, Zhang W, Chen H, Sun X, et al. Trimethylamine N-oxide promotes abdominal aortic aneurysm formation by aggravating aortic smooth muscle cell senescence in mice. *J Cardiovasc Transl Res.* (2022) 1. doi: 10.1007/s12265-022-10211-6

frontiers | Frontiers in Cardiovascular Medicine

TYPE Original Research
PUBLISHED 21 September 2022
DOI 10.3389/fcvm.2022.944287

Check for updates

OPEN ACCESS

EDITED BY
Morgan Salmon,
University of Michigan, United States

REVIEWED BY
Mevlut Celik,
Erasmus Medical Center, Netherlands
Jia Hu,
Sichuan University, China
Mark G. Davies,
The University of Texas Health Science Center at San Antonio, United States

*CORRESPONDENCE
Chengliang Zhang
zhangchengliang@csu.edu.cn

SPECIALTY SECTION
This article was submitted to General Cardiovascular Medicine, a section of the journal Frontiers in Cardiovascular Medicine

RECEIVED 15 May 2022
ACCEPTED 23 August 2022
PUBLISHED 21 September 2022

CITATION
Huang L, Chen X, Hu Q, Luo F, Hu J, Duan L, Wang E, Ye Z and Zhang C (2022) The application of modular multifunctional left heart bypass circuit system integrated with ultrafiltration in thoracoabdominal aortic aneurysm repair.
Front. Cardiovasc. Med. 9:944287.
doi: 10.3389/fcvm.2022.944287

COPYRIGHT
© 2022 Huang, Chen, Hu, Luo, Hu, Duan, Wang, Ye and Zhang. This is an open-access article distributed under the terms of the Creative Commons Attribution License (CC BY). The use, distribution or reproduction in other forums is permitted, provided the original author(s) and the copyright owner(s) are credited and that the original publication in this journal is cited, in accordance with accepted academic practice. No use, distribution or reproduction is permitted which does not comply with these terms.

The application of modular multifunctional left heart bypass circuit system integrated with ultrafiltration in thoracoabdominal aortic aneurysm repair

Lingjin Huang[1,2], Xuliang Chen[1,2], Qinghua Hu[1,2], Fanyan Luo[1,2], Jiajia Hu[2,3], Lian Duan[1,2], E. Wang[2,3], Zhi Ye[2,3] and Chengliang Zhang[1,2]*

[1]Department of Cardiovascular Surgery, Xiangya Hospital, Central South University, Changsha, China, [2]National Clinical Research Center for Geriatric Disorders, Xiangya Hospital, Central South University, Changsha, China, [3]Department of Anesthesiology, Xiangya Hospital, Central South University, Changsha, China

Open thoracoabdominal aortic aneurysm (TAAA) repair is a complex and challenging operation with a high incidence of serious complications, and high perioperative mortality and morbidity. Left heart bypass (LHB) is a circulatory support system used to perfuse the distal aorta during TAAA operation, and the advantages of LHB include guaranteeing distal perfusion, reducing the use of heparin, and diminishing the risk of bleeding and postoperative neurological deficits. In China, the circuit for TAAA repair is deficient, and far from the perfusion requirements. We designed a modular multifunctional LHB circuit for TAAA repair. The modular circuit consisted of cannulation pipelines, functional consumables connection pipelines, and accessory pipelines. The accessory pipelines make up lines for selective visceral perfusion and kidney perfusion, suckers and rapid infusion. The circuit can be assembled according to surgical requirements. The ultrafilter and heat exchanger are integrated into the circuit to fulfill the basic demands of LHB. The LHB circuit also has pipelines for selective visceral perfusion to the celiac artery and superior mesenteric artery and renal perfusion pipelines. Meanwhile, the reserved pipelines facilitate the quick switch from LHB to conventional cardiopulmonary bypass (CPB). The reserved pipelines reduce the time of reassembling the CPB circuit. Moreover, the rapid infusion was integrated into the LHB circuit, which can rapid infusion when massive hemorrhage during the open procedures such as exposure and reconstruction of the aorta. The ultrafiltration can diminish the consequent hemodilution of hemorrhage and rapid infusion. A hemoperfusion cartridge also can be added to reduce the systemic inflammatory during operation. The circuit can meet the needs of LHB and

quickly switch to conventional CPB. No oxygenator was required during LHB, which reduce the use of heparin and reduce the risk of bleeding. The heat exchanger contributes to temperature regulation; ultrafiltration, arterial filter, and rapid-infusion facilitated the blood volume management and are useful to maintain hemodynamic stability. This circuit made the assembly of the LHB circuit more easily, and more efficient, which may contribute to the TAAA repair operation performed in lower volume centers easily. 26 patients who received TAAA repair under the modular multifunctional LHB from January 2018-March 2022 were analyzed, and we achieved acceptable clinical outcomes. The in-hospital mortality and 30-day postoperative mortality were 15.4%, and the postoperative incidences of paraparesis (4%), stroke (4%), and AKI need hemodialysis (12%) were not particularly high, based on the limited patients sample size in short research period duration.

KEYWORDS

thoracoabdominal aortic aneurysm repair, left heart bypass, cardiopulmonary bypass, hospital volume, spinal cord protection, selective visceral perfusion, kidney protection

Introduction

Open thoracoabdominal aortic aneurysm (TAAA) repair is a complex and challenging operation including extensive exposure and reconstruction of the thoracoabdominal aorta and vital aortic branches (1). Open TAAA repair has life-altering complications, and high perioperative mortality (2, 3), and the reported in-hospital mortality after TAAA repair was 15–25% (4, 5). It has been associated with an increased risk of late death and serious complications at specialized aortic centers (6, 7). The clinical outcomes were especially poor for patients undergoing urgent or emergent procedures at low-volume centers (4), and open TAAA repair remains a monumental undertaking limited to experienced surgeons and high-volume centers (6).

Left heart bypass (LHB) and cardiopulmonary bypass (CPB) with or without hypothermic circulatory arrest are important perfusion-assisted techniques strategy for organ protection in TAAA repair. LHB is a widespread circulatory support system used to perfuse the distal aorta during TAAA operation, and the advantages of LHB include guaranteeing distal perfusion, reducing the use of heparin and diminishing the risk of bleeding and postoperative neurological deficits (8, 9). The use of LHB was limited while the open TAAA repair developed rapidly in China, mainly due to the shortage of equipment and consumables, and the hospital volume. The circuit for TAAA repair is deficient, and far from the perfusion requirements.

We designed a modular multifunctional LHB circuit that can be assembled according to surgical requirements for TAAA repair.

Indication

The LHB circuitry is modified to accommodate surgical needs specific to the surgical procedure. The LHB circuit is used for patients undergoing Crawford extent II TAAA repair to extend from the left subclavian artery down to the aortic bifurcation organ perfusion. LHB can provide isothermic self-oxygenated blood while the proximal anastomosis is being completed, so the cardiac function and pulmonary function should meet systemic oxygenation and perfusion.

Selection of equipment

The circuit consists of reusable equipment and disposable. The pipelines of the LHB circuit mainly consist of three supplied sterile and individually wrapped bags as shown in **Figures 1–5**. Other disposable equipment includes a heat exchanger, two hard-shell reservoirs, a centrifugal pump, an ultrafilter, and arterial filter, a hemoperfusion cartridge, an oxygen saturation monitor, suction tips, and three pressure monitors, connectors, and other subsidiary tubes. Reusable equipment such as a CPB console, cooler-heater, and rapid-infusion system.

The structure of the left heart bypass circuit

The LHB circuit mainly includes three parts: cannulation pipelines, functional consumables connection pipelines, and

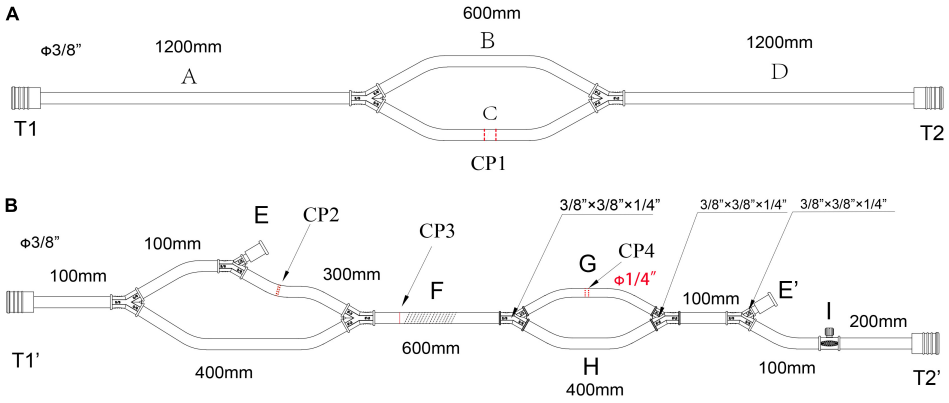

FIGURE 1
The main pipelines for cannulation and functional consumables connection in the LHB circuit. **(A)** The pipelines for cannulation, all diameters of the circuits are 3/8 inch, CP1 is the cut-point for connection of the cannulation of the inferior left pulmonary vein and the aortic cannulation. **(B)** The functional consumables connection pipelines of the LHB circuit. CP2 is the cut-point for the connection of a hard-shell reservoir, CP3 is the cut-point for a centrifugal pump, and CP4 for the heat exchanger. Line F can be occluded by a roller pump rather than a centrifugal pump in CP3. The port E and port E' are a pair for an ultrafilter. Port I with a side hole is connected with a T-type adapter, which can be connected to a pressure monitor, and an arterial sampling connector. Both the port T1 in panel **(A)** and the port T1' in panel **(B)** are connected with an oxygen saturation monitor or a connector. The port T2 in panel **(A)** and the port T2' in panel **(B)** were connected with a Y-type connector (φ3/8" x3/8" x1/4"), and the 1/4-inch port of the connector is linked to the line for the selective visceral perfusion.

accessory pipelines. The accessory pipelines make up lines for selective visceral perfusion, kidney perfusion, suckers and rapid infusion.

The cannulation pipelines are shown in **Figure 1A**. The diameter is 3/8 inch, and the length is marked as the captions. Parallel lines B and C are the cannulation sites and the reserved cannulation sites. Line C can be separated into two parts in the cut-point CP1, one port is connected to the cannulation of the inferior left pulmonary vein to establish a drainage line, and another port is connected to the aortic cannulation as a perfusion line in the distal descending thoracic aorta or the proximal abdominal aorta. Line B is reserved for CPB. When LHB was performed, line B is clamped without blood flow. When LHB needs to switch to CPB, line C is separated into two ports, one connects to venous cannulation or cavoatrial cannulation as venous drainage, and the other port connects to another arterial cannulation as a perfusion line. The ports T1 and T2 in the terminal can be connected with the corresponded ports T1' and T2' in **Figure 2**.

Figure 1B displays the functional consumables connection pipelines of the LHB circuit. The diameter is 3/8 inch, except for the line marked with the red caption that the diameter is 1/4, and the length is also marked as the captions. The site of CP2 separates into two ports, one port is connected to the inlet port of the hard-shell reservoir for the solution or blood drainage, and the other port is connected to the outlet port of the hard-shell reservoir, which is a source of fluid for rapid transfusion. The site of CP4 can be separated into two ports to connect to the heat exchanger. The line can be cut into two ports in site CP3 for the connection of a centrifugal pump. Meanwhile, line F also can be occluded by a roller pump rather than a centrifugal pump in CP3 as the force of perfusion when a centrifugal pump is hard to get. Connector I with a side hole is connected with a T-type **adapter, which can be connected to a** pressure monitor, and an arterial sampling connector. The sealed port E and port E' were a pair of ports for an ultrafilter. Both the port T1 in **Figure 1A** and the port T1' in **Figure 1B** are connected with an oxygen saturation monitor or a connector. The port T2 in **Figure 1A** and the port T2' in **Figure 1B** were connected with a Y-type connector (φ3/8" *3/8" *1/4"), and the 1/4-inch port of the connector is linked to the T1 side of the line (**Figure 2A**) for the selective visceral perfusion to the celiac artery and superior mesenteric artery.

The lines are shown in **Figures 2A,B** are used for the selective visceral perfusion. The port T1 was connected to the 1/4-inch port of the T-type adapter connected to T2 in **Figure 1A** and T2' in **Figure 1B**, and the T-type adapter on the side T2 is connected to the port of T1 in the Y-type line (**Figure 2C**) for the selective visceral perfusion, and also connected to a pressure monitor. The tubes in **Figure 3** with 1/4-inch are occluded by roller pumps, **t**he T-type adapter on the right side is connected to a pressure monitor, and also connect to the port T1 (**Figure 2C**) of the Y-type line for kidney perfusion.

As shown in **Figures 3A,B**, two lines for the sucker are connected to sucker tips to collect the shed blood to another hard-shell reservoir, which is used for autologous blood transfusion and rapid infusion. **Figure 3C** displays the reserved pipelines for rapid fusion, which are connected with an arterial filter and an ultrafilter, and collected the blood to the rapid-fusion system by a roller pump. The joint points S1 and S2 are connected with ultrafiltration and arterial filter, respectively. The terminal site marked T2 is connected to the rapid-infusion

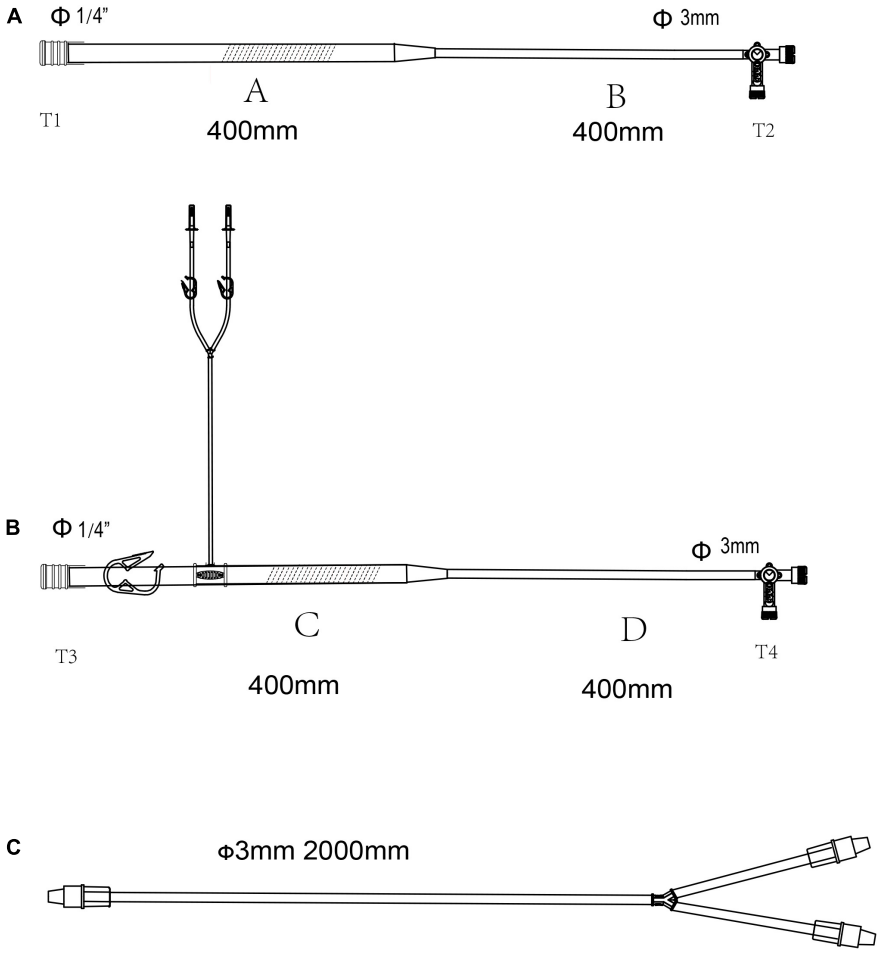

FIGURE 2
The pipelines for selective organ perfusion in the LHB circuit. **(A)** Line for selective visceral perfusion. **(B)** Line for selective kidney perfusion. **(C)** Y-type line connected to the T2 celiac axis for SMA and celiac axis perfusion or T4 to renal arteries for the selective perfusion. The line marked oblique dotted line is used for roller pumps.

system. Figure 3D is used for blood sampling, which is the link between site I in Figure 1B and the inlet port of the hard-shell reservoir for perfusion.

Assemble the circuit

The whole circuit can be assembled as previously described above. Briefly, the ports T1 and T1' are a pair that can be connected by an adapter, T2 and T2' in Figure 1 are connected by a Y-type three-way connector as well. A hard-shell reservoir inset to CP2 and a centrifugal pump add to CP3 when a centrifugal pump is used in the bypass. Line F marked with oblique dotted lines is occluded by a roller pump when the centrifugal pump cannot get. The heat exchanger is connected to CP4. Port I is connected by a pressure monitor and the sampling line in Figure 3D. The sealed port E and port E' in Figure 1 are connected by an ultrafilter with a 1/4 inch tube for inflow and outflow. Each of the ports of T2 and T4 in Figure 2 is connected to one of the perfusion lines in Figure 2C. Each of the sucker lines is linked with a sucker tip and another hard-shell reservoir for autologous blood transfusion. T1 port in the rapid-fusion line (Figure 3C) connects to the outlet port of the hard-shell reservoir for autologous blood transfusion, while T2 connects to the rapid-fusion system. Meanwhile, an ultrafilter and an arterial filter are inserted into the sites of CP1 and CP2. The lines marked by the oblique dotted lines in Figure 3 are occluded by roller pumps for sucker or perfusion. The assembled circuit is shown in Figures 4, 5. The flow diagram was shown in Supplementary Video 1.

Priming the circuit

1,500 ml multiple electrolytes injection (plasma-lyte A) with 30 mg heparin was added to the hard-shell reservoir (A in

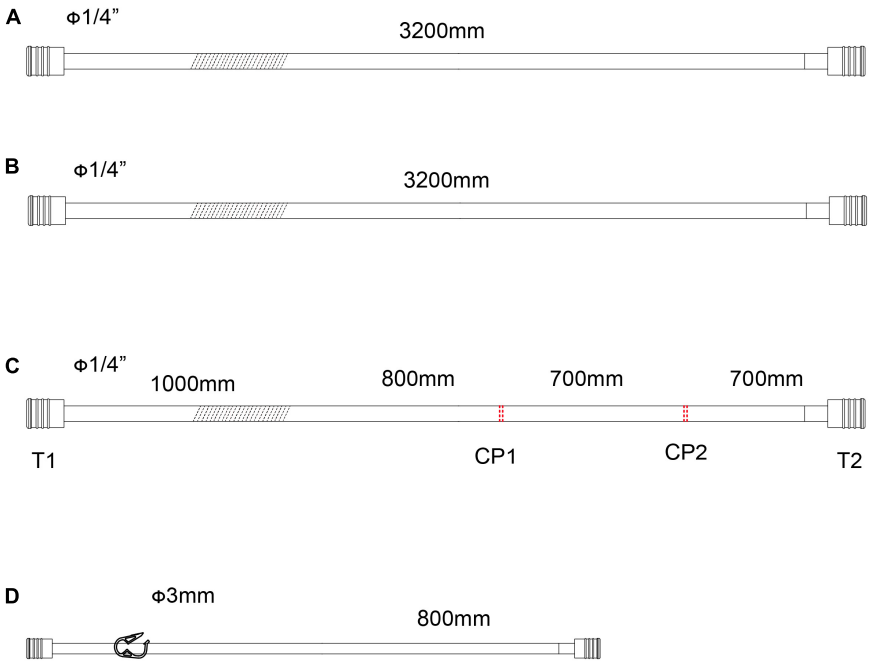

FIGURE 3
The accessory pipelines for shed blood collection, rapid infusion and blood sampling. **(A,B)** Pipeline for the sucker. The line marked oblique dotted line is used for roller pumps. **(C)** Accessory pipelines for rapid infusion, S1 is the cut-point for connection of ultrafilter, and S2 is the cut-point for an arterial filter. The line marked oblique dotted line is used for roller pumps. **(D)** The accessory pipelines for blood sampling.

Figure 4) as a priming solution. Once the connected devices are mounted on the CPB console, the water source to the heat exchanger (C in Figure 6) should be turned on. Start the pump to empty the circuit, loosen all the tube clumps (C1-C5 in Figure 4) and stop-flow clips (C1-C3 in Figure 4). The C2 is clamped when the line is full with solution, then start the centrifugal pump. Empty all the tubes and adjust the occlusion of the tube by the roller pumps for selective visceral perfusion. The microemboli gas in the ultrafilter, heater exchanger, and hemoperfusion cartridge should be eliminated. Warming the prime solution in the circuit by a water tank is an effective means to minimize the risk of releasing microbubbles of gas from the solution. Calibrate the zero values for pressure monitors and test the accuracy of the perfusion flow. Clamp all the tube clamps and stop-flow clips before bypassing initiating.

Anesthesia management

All patients are intubated with a double-lumen endobronchial tube for later single right-lung ventilation. The blood pressures of the right radial or brachial for the upper limb monitoring, and the dorsal pedis artery for the lower limb in the opposite of the fusion cannulation in the iliac artery or femoral artery. A large-bore triple lumen central venous line is placed in the right internal jugular vein for central venous pressure monitoring, fluid infusion, anesthetics and vasoactive medications infusion, followed by the insertion of an 8.5F catheter sheath for fluid and blood rapid infusion. Transesophageal echocardiography (TEE) is also monitored to assess the hemodynamics and cardiac function changes. Cerebral oximetry is measured with near-infrared spectroscopy (NIRS), and the depth of anesthesia is also evaluated using the bispectral index (BIS). A temperature probe is positioned in the patient's nasopharynx for temperature monitoring. Moreover, a urethral catheter integrated with a temperature probe is placed for urine output and temperature management. Self-adhesive defibrillation electrodes were located on the chest wall, and an external defibrillator is a standby. Cell-saving and rapid-infusion devices are set up so that shed blood can be salvaged and volume can be rapidly replaced, respectively. The baseline of activated *coagulation* time (ACT) and mixed venous oxygen saturation (SvO2) are examined when the central venous line is placed successfully.

Left heart bypass management

Cannulation

The inferior left pulmonary vein is the routine site of atrial cannulation for the outflow line, and the proximal abdominal aorta, the iliac artery, or the femoral artery is selected to establish an inflow line. Heparin is administered

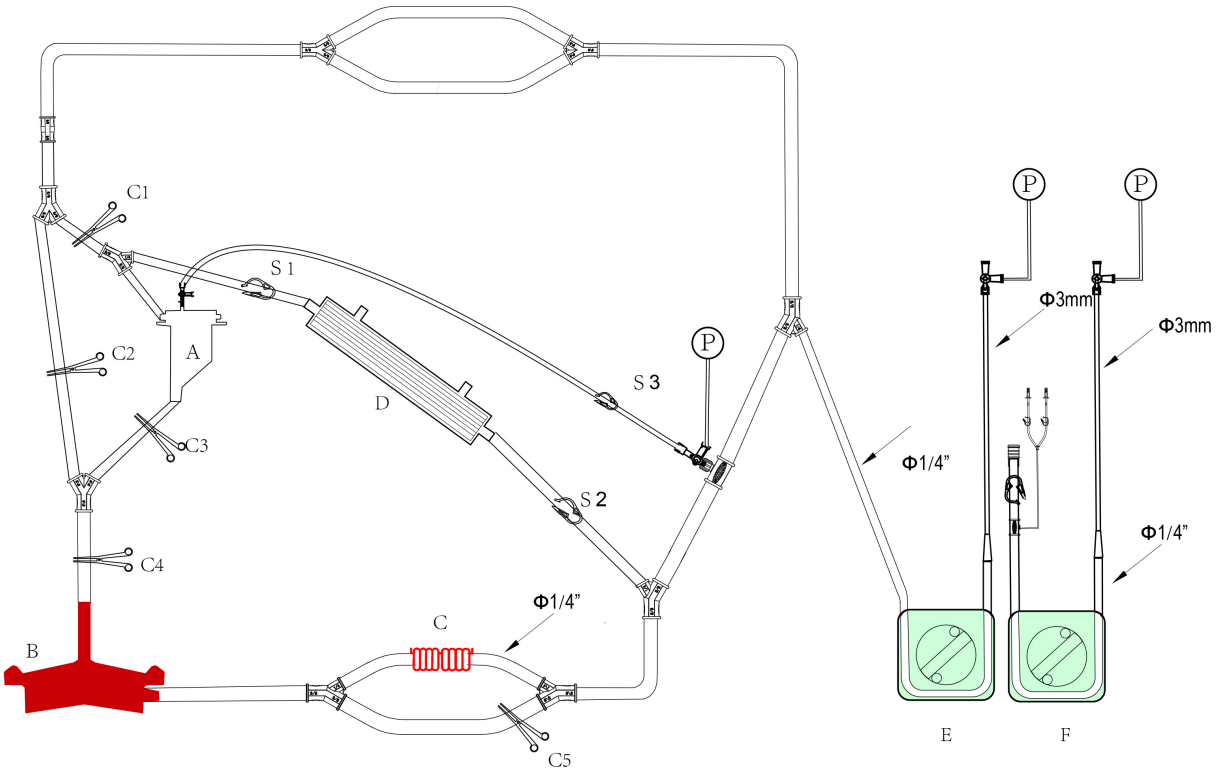

FIGURE 4
The assembled LHB circuit for perfusion. **A**, Hard-shell reservoir for priming and CPB reservation. **B**, centrifugal pump; **C**, heat exchanger; **D**, ultrafilter, **E,F**, roller pumps. **C1-C5**, Tube clumps; **S1-S3**, stop-flow clips.

intravenously at a dose of 1.5 mg/kg cannulation performs until the patient's ACT is verified to be more than 280 s. A 22- or 24-Fr angled-tip venous cannula is connected to the outflow line of the LHB circuit, which is named C1 in Figure 1. Meanwhile, a 20- or 22-Fr straight tip arterial cannula is connected to port C2 in Figure 1 as a return line for LHB. Meanwhile, a Y-connector is attached to the return line that splits pump return between the line going to the distal aortic cannula and another line leading to the perfusion catheters for later delivery of selective visceral perfusion to the celiac artery and superior mesenteric artery (SMA).

Conduct of left heart bypass

The LHB is initiated at a flow rate of 0.5 L/min after the ACT > 280 s, and the cannulation is performed and connected to the circuit correctly. Pay more attention to the drainage and perfusion pressure, the drainage is evaluated by the movement of cannulation in the pulmonary vein caused by the vacuum, and the perfusion pressure is read from the pressure monitor. The cannulation of pulmonary vein and artery are adjusted to maintain sufficient blood can be drained from the left heart to perfuse the lower body. The distal aortic perfusion mainly relays on the LHB flow rate when an aortic cross-clamp is applied. The flow rate is 2.5–3.5 L/min to keep the patient's mean arterial pressure (MAP), both the upper limb and lower limb, maintain in the range of 70–90 mm Hg. The reserved pipeline marked B in Figure 2, which is paralleled with the line connected to the heat exchanger, can release to enhance the flow rate. Two suckers are used to collect the shed blood to the hard-shell reservoir, and then remove it to the rapid infuser system after ultrafiltration and filtering, which can rapidly infuse to main the volume. Meanwhile, volume and pharmacologic agents are adjusted to maintain an adequate MAP. Nasopharyngeal temperature and bladder temperature are monitored and adjust the water temperature in the heat exchangers regulates the body temperature according to the surgical processes. Ultrafiltration can be applied (Release the stop-flow clips C1 and C1 in Figure 6) when the volume is overloaded and excessive hemodilution.

Overall, the rapid infusion system the 8.5F catheter sheath can afford high to 1,000 ml/min warming fluid delivery to fulfillment of the volume demands of patients. Whereas the reserved rapid infusion modular will be applied, when the fusion flow is hard to successfully maintain the target MAP due to

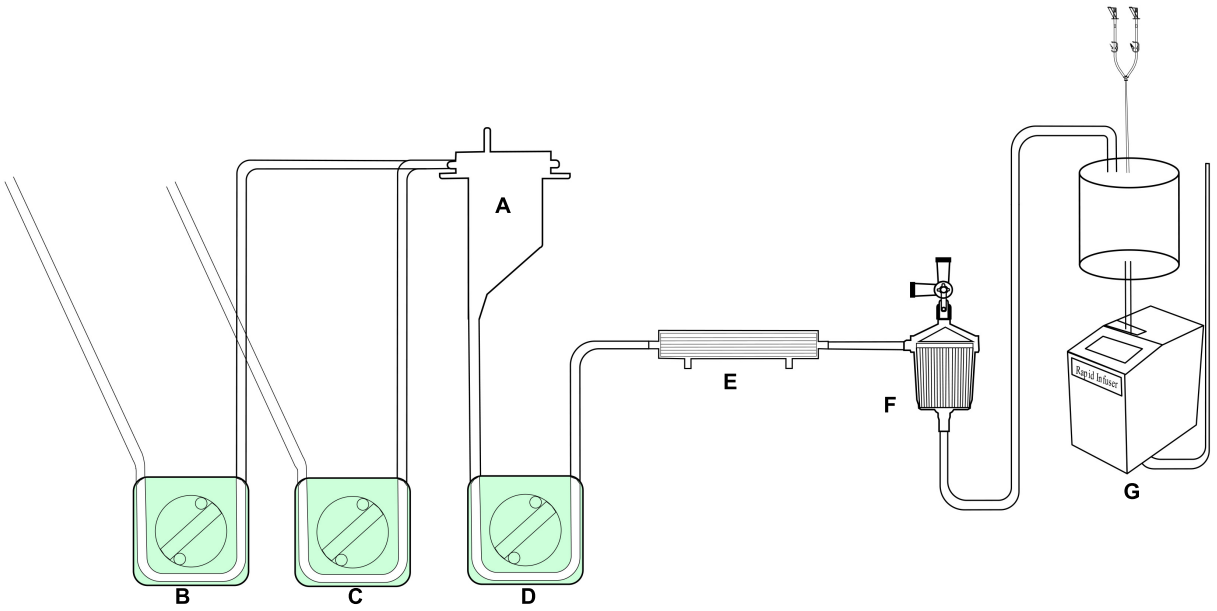

FIGURE 5
The assembled reserved LHB circuit for the sucker and rapid-infusion perfusion. **A**, Hard-shell reservoir for shed filed blood collection by the pump suckers. **B,C**, roller pumps for suckers; **D**, roller pump for shifting blood to the rapid-infusion system; **E**, ultrafilter, **F**, arterial filter, **G**, rapid-infusion system.

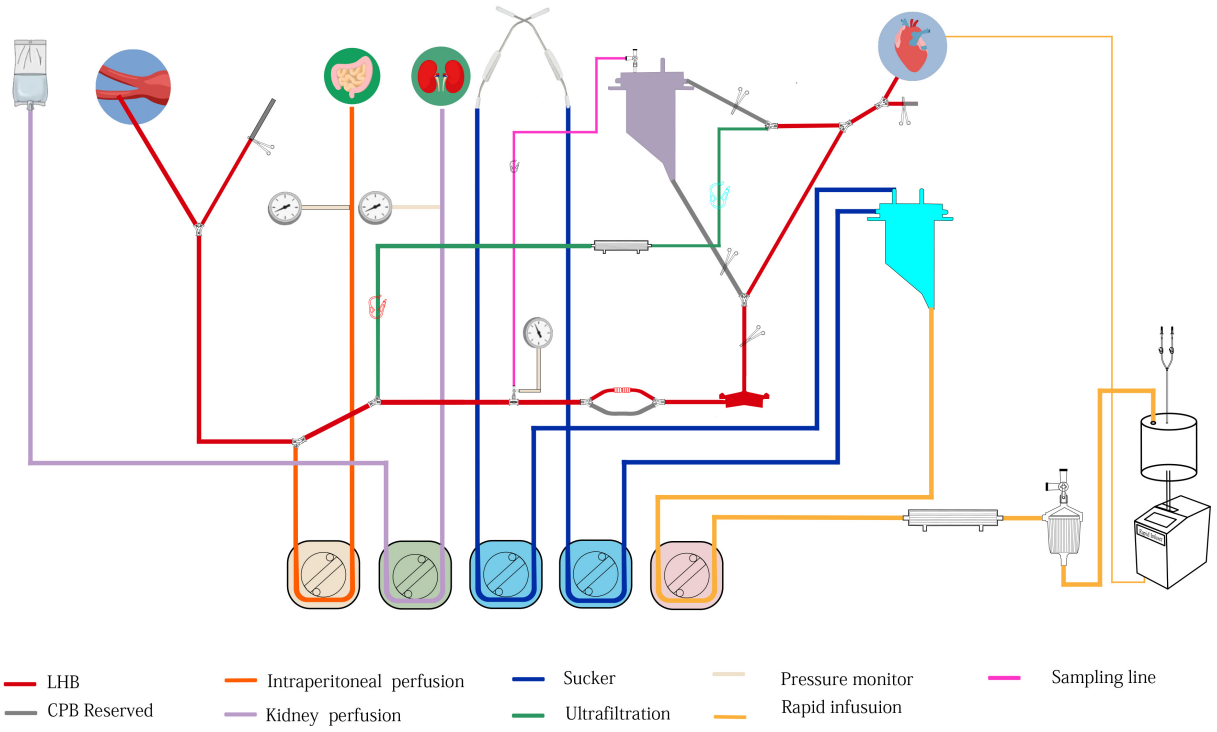

FIGURE 6
The structure of modular multifunctional LHB circuit integrated with ultrafiltration and reserved pipelines for TAAA repair. The functions were indicted by different colors at the bottom of the figure.

massive blood volume lost in the condition of catastrophic bleeding or aneurysm rupture. Our reserved hard-shell reservoir and pipelines can afford a more rapid infusion rate. Like the structure in **Figure 6**, partially or completely clamp the tube clump C2, and releasee the tube clump C3, which allows the blood or solution in the hard-shell reservoir (A in **Figure 6**) can be rapidly infused into the closed-loop pipeline of LHB circulation to enhance the blood volume. Blood gas and electrolyte analysis should be performed to evaluate the homeostasis during the LHB. The ACT should keep in a range of 250–400 s. 8% sodium citrate anticoagulant is used for the anticoagulation of the rapid fusion system, so serum sodium and serum calcium should be adjusted to the normal physiological ranges.

Spinal cord protection

The intercostal and/or lumbar arteries, which are the main feeding artery of the spinal cord, should be revascularized with one branch of the aortic graft. During the reimplantation period, the MAP is kept relatively high (usually with a target MAP of 80–100 mm Hg) as part of a spinal protection strategy. Meanwhile, the temperature sustains at a relatively lower level near 34℃, which is another spinal cord protection strategy. It is better to enhance the hematocrit by ultrafiltration, and blood transfusion. Rewarming the patient to keep the Nasopharyngeal temperature near 36℃ when the intercostal and/or lumbar arteries anastomosis is completed.

Selective visceral perfusion and renal perfusion

Selective visceral perfusion and kidney perfusion are essential principles for TAAA repair during the abdominal aorta reconstruction, which aims to minimize the duration of abdominal-organ ischemia and reduce the incidence of renal and hepatic insufficiency, coagulopathy, and bowel ischemia. Selective visceral artery perfusion is performed with the oxygenated isothermic blood continuously delivered from the LHB circuit through a Y-type three-way connector of the perfusion line (E in **Figure 6**). A Y-branch off the line for selective is connected to the 10-Fr balloon catheters inserted into the celiac axis and the SMA. The oxygenated isothermic blood perfuses the celiac axis and the SMA at a flow rate of 500 mL/min, which is delivered continuously by a roller pump. Moreover, it is important to maintain the pressure of visceral perfusion to less than 200 mmHg. The flow halves when perfusion is applied only to the celiac axis or the SMA.

A renal perfusion system is used to maintain selective renal hypothermia for the preservation of renal function. The renal perfusion is conducted with the renal perfusion system, which is set up with a separated tube connected with a solution inlet, a Y-branch off the line connected with two10-Fr balloon catheters, which is placed in the renal arteries to accept the cold crystalloid perfusion. Cold crystalloid (lactated Ringer's solution with mannitol and methylprednisolone or HTK solution in 4°C) is delivered with boluses of 200–400 mL intermittent by another roller pump, The cold crystalloid is administered every 6 min with a flow rate of 300 ml/min for 1–2 min, and the perfusion pressure should be less than 200 mmHg. Ultrafiltration and rewarm can be performed to alleviate the hemodilution and hypothermia due to the massive cold crystalloid solution perfusion. The urine volumes of renal in the periods of renal perfusion and post reimplantation should be evaluated, and diuretics can be administrated.

Switch to cardiopulmonary bypass from left heart bypass

The switch is implemented in the condition that the pulmonary function and cardiac function are far from covering the need for LHB. Our LHB circuit is integrated with reserved pipelines that can be switched to conventional CPB easily. Stop the LHB circulation, cut line C into two two-port C1 and C2, and C1 connects to venous cannulation or cavoatrial cannulation as venous drainage while port C2 connects to another arterial cannulation as perfusion line after cannulate is completed. move down the hard-shell reservoir (A in **Figure 6**), which is beneficial to the blood gravity drainage. The site of D can be separated into two ports to connect to the oxygenator integrated with an arterial filter (Terumo, Japan), and empty the gas through the recycle line. Additional heparin is administrated to take the ACT more than 480 s. Run the centrifugal pump, release the tube clump C1 and C4, release the tube clump C3, and the CPB can conduct again.

The application of the left heart bypass circuit in thoracoabdominal aortic aneurysm repair

We retrospectively analyzed the clinical data of patients undergoing TAAA repair under LHB from 2017 to 2022. This retrospective study was approved by the Committee on the Medical Ethics of Xiangya Hospital, Central South University (No. 202101022), and the requirement for informed consent was waived because of the retrospective design. Trial registration was performed in the Chinese Clinical Trial Registry[1] (No. ChiCTR2200058222).

1 http://www.chictr.org.cn

We analyzed 26 patients that received TAAA repair under the modular multifunctional LHB from January 2018-March 2022 in Xiangya Hospital, Central South University. The demographic characteristics and extent type of TAAA were shown in Table 1. All patients were managed by the same team of anesthesiologists, surgeons, and perfusionists during the operation. LHB was performed for all patients, while selective visceral perfusion and renal perfusion were applied for the patient Extent II and III TAAA patients. The operative characteristics were shown in Table 2. The average LHB time was206.7 ± 78.60 min, and the operation time was587.8 ± 213.0 min. The renal perfusion performed for Extent II and III patients were 1,810 ± 742 ml with 5.8 ± 1.6 times. The lowest temperature during bypass was 33.0 ± 1.0 ℃, which was mainly presented at the initiation of LHB, then the temperature would be enhanced by the heat exchanger, and reached 36.56 ± 0.4 at the termination of LHB. Meanwhile, the lactate concentration (Lac) was 6.9 ± 4.1 mmol/L at the termination of LHB, and 6.9 ± 4.9 mmol/L at the termination of the operation. The volume of ultrafiltration was high to 7,071.1 ± 5,315.0 ml while the urine volume was 1,242.3 ± 1,421.4 ml.

The results of blood product transfusion were listed in Table 3. The blood transfusion was performed for all erythrocytes was 12.3 ± 9.7 Units, apheresis platelets were 0.9 ± 1.1 Units, cryoprecipitate was 1.2 ± 1.0 Units, plasma was 965.0 ± 859.2 ml and autologous blood was 1,546.5 ± 1,100.0 ml.

Finally, 22 patients were cured and discharged from the hospital, one of the 26 patients died in the operation due to bleeding, and three died in the hospital after the repair. No more patients died during the 30-day postoperative. Two patients required re-exploration for bleeding. The permanent spinal cord deficit appeared in two patients, and one was paraparesis while another one recovered. One patient had a stroke after surgery. Three patients who got acute renal injury (AKI) need hemodialysis. Pneumothorax was the most frequent adverse event after repair with nine patients. The causes of death were postoperative rupture, multiple organ dysfunction syndromes, and severe infection, and all of them were Extent II with a long length of surgery and LHB duration. The postoperative mechanical ventilation time was 20.6 ± 16.1 h, the length of ICU stay was 72.5 ± 46.5 h, and hospital stay time was 13.8 ± 7.1 days for the patients cured and discharged (Table 4). Meanwhile, the laboratory test results including blood routine test, liver and kidney function, electrolyte, myocardial enzyme, and N-terminal pro-B type natriuretic peptide (NT-proBNP) were collected and analyzed with paired *t*-tests for the preoperative and the first day of postoperative data. The results showed that Hb and Platelets were significantly decreased after surgery, and NT-proBNP, Urea, creatinine (Cre), direct bilirubin (DBil), Total bile acid (TBA), lactate dehydrogenase (LHD), creatine kinase (CK), Myoglobin (Mb), prothrombin time (PT), international normalized ratio (INR), activated partial thromboplastin time (APTT), thrombin time (TT), and fibrinogen (FIB), D-Dimer (D2) were rapidly increased. No significant difference was found in the comparison of the levels of Troponin I, Uric acid, alanine aminotransferase (ALT), and aspartate aminotransferase (AST), and creatine kinase-*MB* isoenzyme (*CK-MB*). The details were listed in Table 5.

TABLE 1 Preoperative patient characteristics.

Variables (n = 26)	n/Medium (IQR)	(%)/Mean±SD
Age (years)	50.0 (38.0-61.0)	49.5±15.1
Male	22	84.62
High (cm)	168.0 (160.5-171.0)	168.3±7.9
weight (kg)	63.5 (55.0-72.0)	63.4±10.0
BMI	22.2 (20.2-25.5)	22.4±3.4
Extent		0
TAAA II	18	69.23
TAAA III	1	3.85
TAAA IV	0	0
TAAA V	7	26.92

Discussion

As a non-high-volume center, we achieved acceptable clinical outcomes for patients who received open TAAA repair under LHB. The in-hospital mortality and 30-day postoperative mortality were 15.4%, and the postoperative incidences of paraparesis (4%), stroke (4%), and AKI need hemodialysis (12%) were not particularly high, based on the limited patient' sample

TABLE 2 Operative characteristics of patients.

Variables (n = 26)	Medium (IQR)	Mean±SD
LHB time (min)	211.5 (159.8-251.0)	206.7±78.6
Operation time (min)	650.0 (472.0-740.0)	587.8±213.0
Renal perfusion times	5.5 (5.0-7.0)	5.8±1.6
Solution volume of renal perfusion(ml)	2000.0 (1462.5-2400.0)	1810.0±742.0
Temperature (°C)		
Lowest in LHB	34.0 (33.1-34.5)	33.0±1.0
Termination of LHB	36.7 (36.4-36.8)	36.6±0.4
HB (g/L)		
Termination of LHB	83.5 (68.3-93.0)	82.0±18.8
Termination of operation	93.0 (80.5-99.0)	88.0±23.8
Lac (mmol/L)		
Termination of LHB	6.2 (3.3-10.8)	6.9±4.1
Termination of operation	5.1 (2.9-10.5)	6.9±4.9
Ultrafiltration volume (ml)	5250.0 (2525.0-11000.0)	7071.1±5315.0
Urine volume (ml)	800.0 (412.5-1200.0)	1242.3±1421.4

HB: Hemoglobin; Lac: Lactate.

TABLE 3 The transfusions of blood products in operation.

Variables	Medium (IQR)	Mean±SD
Erythrocyte (Unit)	9.5 (4.0-19.5)	12.3±9.7
Apheresisplatelets (Unit)	1.0 (0.0-1.0)	0.9±1.1
Cryoprecipitate (Unit)	1.0 (1.0-1.0)	1.2±1.0
Plasma (ml)	700.0 (300.0-1500.0)	965.0±859.2
Autologous blood(ml)	1400.0 (1000.0-1625.0)	1546.5±1100.0

TABLE 4 The postoperative outcomes.

Variables (n = 26)	n/Medium (IQR)	(%)/Mean±SD
Mechanical ventilation time (h)	13.0 (8.4-34.8)	20.6 ± 16.1
ICU stay(h)	74.0 (40.9-89.5)	72.47 ± 46.5
Hospital stay (day)	13.0 (10.0-17.0)	13.8 ± 7.10
Intraoperative mortality	1	3.85
In-hospital mortality	4	15.4
30-day in-hospital mortality	4	15.4
Permanent spinal cord deficit	2	7.69
Paraparesis	1	3.85
Stroke	1	3.85
AMI	0	0
AKI necessitating hemodialysis	2	7.69
Re-exploration	1	3.85
MODS	2	7.69
Pneumothorax	9	34.6

AMI: Acute myocardial infarction; AKI: Acute renal injury; MODS: multiple organ dysfunction syndromes.

size in short research period duration. The mortality was 15.4%, which may blame the following factors. The characteristics of patients indicated that high to 69% of patients suffering from type II TAAA, which involves the reconstruction of descending thoracic aorta and abdominal aortic aorta with long-lasting anastomoses and a massive trauma for the patient. Moreover, more patients failed endovascular repair and re-intervention after endovascular repair cases, which made the surgical procedure more complicated. The integrated management of LHB including spinal cord protection and selective visceral perfusion and renal perfusion may contribute to the favorable results of our research.

The morbidity and mortality of the open TAAA repair continue to remain considerable, despite the advances in open surgical techniques. In-hospital mortality ranges between 2.3% (10) and 32.7% (11). Meta-analysis indicated that the total pooled in-hospital mortality rate was 11.26% among all studies including all Crawford types, and was 10.32% for Crawford types II (12). The overall in-hospital mortality of TAAA repair was reported to be more than 19% in

TABLE 5 The preoperative and postoperative laboratory tests outcomes.

Variables		Medium(IQR)	Mean±SD
Hb (g/L)	Preoperative	122.5 (99.8-127.3)	115.0±23.1
	Postoperative	103.0 (84.0-110.5)	96.6±17.6
Platelets (10^{12}/L)	Preoperative	192.5 (159.8-215.0)	202.0±73.8
	Postoperative	69.0 (54.5-104.5)	94.3±69.1
Troponin I (ng/ml)	Preoperative	0.006 (0.001-0.010)	0.010±0.010
	Postoperative	0.186 (0.065-0.300)	0.250±0.250
NT-proBNP (ng/L)	Preoperative	138.0 (59.7-300.0)	482.0±769.8
	Postoperative	337.0 (187.0-758.2)	602.3±724.4
Urea (mmol/L)	Preoperative	5.47 (4.74-7.36)	6.68±3.73
	Postoperative	8.00 (6.77-11.13)	10.29±5.46
Cre (μmol/L)	Preoperative	94.9 (74.5-117.3)	138.2±195.2
	Postoperative	159.8 (118.1-175.0)	187.7±192.3
Uric acid (μmol/L)	Preoperative	372.1 (278.2-451.6)	371.7±144.1
	Postoperative	359.4 (255.5-411.6)	339.2±117.4
ALT (U/L)	Preoperative	14.05 (10.8-17.5)	16.7±11.9
	Postoperative	28.7 (18.6-47.0)	144.2±373.6
AST (U/L)	Preoperative	17.0 (15.1-22.2)	23.2±18.8
	Postoperative	93.4 (58.6-132.8)	256.9±591.7
DBil (μmol/L)	Preoperative	4.6 (2.5-6.2)	5.7±6.2
	Postoperative	16.2 (10.0-22.3)	20.5±20.2
TBA (μmol/L)	Preoperative	9.6 (5.6-12.8)	12.2±11.8
	Postoperative	32.2 (23.6-63.3)	45.2±35.5
LHD (μmol/L)	Preoperative	186.0 (156.0-210.0)	186.9±45.7
	Postoperative	622.0 (464.2-789.5)	886.6±968.6
CK (μmol/L)	Preoperative	60.1 (51.3-81.2)	84.6±82.5
	Postoperative	2779.0 (1853.7-5011.5)	3577.1±2674.4
CK-MB (μmol/L)	Preoperative	8.9 (7.5-11.9)	12.1±11.8
	Postoperative	56.8 (36.0-82.9)	157.9±453.8
Mb (μmol/L)	Preoperative	26.9 (19.8-35.6)	38.7±50.1
	Postoperative	873.7 (444.3-3145.2)	3603.4±6110.5
PT (S)	Preoperative	13.2 (12.0-13.8)	13.1±1.3
	Postoperative	14.1 (13.3-17.6)	15.4±3.2
INR	Preoperative	1.07 (1.00-1.11)	1.06±0.10
	Postoperative	1.19 (1.09-1.50)	1.32±0.31
APTT (S)	Preoperative	33.4 (30.0-37.5)	33.3±5.2
	Postoperative	38.5 (34.2-55.9)	51.7±29.9
TT (S)	Preoperative	16.3 (15.5-17.1)	16.3±1.4
	Postoperative	20.1 (17.5-28.0)	28.2±19.6
FIB (g/L)	Preoperative	3.6 (2.9-4.7)	4.2±2.0
	Postoperative	2.3 (1.9-2.7)	2.7±1.6
D2 (mg/L)	Preoperative	1.3 (0.5-2.2)	1.7±1.7
	Postoperative	2.2 (1.1-7.2)	6.9±10.3

HB: Hemoglobin; NT-proBNP: N-terminal pro-B type natriuretic peptide;Cre: *cre*atinine, DBil: Direct bilirubin; TBA: Total bile acid; ALT: alanine aminotransferase, AST: aspartate aminotransferase; LHD: lactate dehydrogenase; CK: creatine kinase; Mb: Myoglobin; CK-MB: creatine kinase-MB isoenzyme; PT: Prothrombin time; INR: international normalized ratio; APTT: Activated partial thromboplastin time; TT: Thrombin time; FIB: fibrinogen; D2: D-Dimer.

the United States (13–15). The high incidence of severe adverse events including spinal cord ischemia, respiratory complications, permanent postoperative renal dialysis, stroke rate, and cardiac events also affect the clinical outcome. Meta-regression evidenced that the mortality had a statistically significant inverse association with the volume of the TAAA center (12). The patients who accepted TAAA repair in high-volume centers have reported excellent results: lower rate of in-hospital mortality and postoperative complications (6, 8, 15). Moreover, the rate of cardiac complications and gastrointestinal complications, as well as blood transfusion rates were also lower for patients operated on at high-volume centers (15). A volume-outcome analysis revealed that high hospital volume is associated with decreased mortality after AAA repair (16). The mortality was significantly inverse correlated with the annual open TAAA repair volume (15). The reported significant predictors of mortality in this study were age older than 65 years (OR 2.78) and emergent presentation (OR 2.41). Other significant predictors of mortality were urgent presentation (OR 1.58), use of extracorporeal circulation (OR 1.38), and annual TAAA volume (15). As a low-volume TAAA center, the morbidity and mortality in our hospital still have potential improvement.

Both open surgical and endovascular repair of TAAA achieved excellent midterm results regarding mortality and the overall survival of patients (17). TAAA has increased markedly, the endovascular repair was increased frequently, while the number of open repairs has declined in the endovascular era (18). The surgeon and hospital volume of open TAAA repairs has decreased considerably over the last two decades, subsequently leading to increased numbers of centers offering endovascular repair (18). However, the endovascular TAAA repair is associated with higher rates of re-intervention (19, 20), and increased early expenses (21). Open repair was performed in limited centers, and always performed in these conditions: complex aortic pathology, unsuitable for endovascular repair, and most reported open repairs were performed in high volume centers with an experienced surgical team (15, 18). It is undisputed that open TAAA repair is a valuable choice for aortic infection, a bailout treatment for complex anatomy, failed endovascular repair and re-intervention after endovascular repair (22). Meanwhile, it is strongly recommended for patients suffering from connective tissue disease according to the current guidelines of the European Society of Vascular Surgery (23).

LHB and CPB with or without hypothermic circulatory arrest, which is a highly invasive procedure may contribute to morbidity and mortality (9). A meta-analysis including three trials indicated that both LHB and CPB with hypothermic circulatory arrest provided adequate organ protection and equivalent clinical outcomes for open TAAA repair (24). CPB with a hypothermic circulatory arrest can afford a clean surgical field for repair (24). However, serious consequences of hypothermic circulatory arrest include coagulopathy, and ischemia/reperfusion-related injury (25, 26). Hypothermic causes coagulopathy, which is due to both CPB and hypothermia, may result in life-threatening bleeding (26, 27). Moreover, hypothermic circulatory arrest increased the risk of low cardiac output syndrome and prolonged ventilator support duration (28).

Overall, LHB is achieved using a temporary bypass from the left atrium to either the distal descending thoracic aorta or the femoral artery with a closed-circuit in-line centrifugal pump (29). LHB can provide distal aortic perfusion while the aorta is cross-clamped, thereby decreasing the ischemic times of distal organs, particularly the spinal cord. Meanwhile, selective visceral perfusion and renal perfusion can enhance the perfusion of gastrointestinal organs and kidneys.

LHB, which requires limited anticoagulation, and mild passive hypothermia, could significantly diminish the influence on physiological functions. LHB appears to provide the greatest benefit to patients undergoing the more extensive repairs and reduced the incidence of spinal cord deficits in patients undergoing extent II repairs (30). The combination of LHB and cerebrospinal fluid drainage may enhance spinal cord protection beyond that provided by either adjunct alone (9, 31). New research found that aorto-iliac bypass could offer sufficient distal aortic perfusion without complex perfusion skills, and was regarded as a substitute for CPB and LHB in spinal cord protection (32). However, the difference between aorto-iliac bypass and LHB on TAAA repair is still unclear due to the limitation of direct comparison data. TAAA repair under aorto-iliac bypass needs systemic heparinisation with heparin 3 mg/kg to acquire the ACT > 480 S, rather than 1.5 mg/kg for LHB. Meanwhile, the maintenance of body temperature and hemodynamic stability is more difficult in aorto-iliac bypass and has a higher technical requirement of the vascular anastomosis to reduce the proximal aortic cross-clamp time within the safe limit (33), because aorto-iliac bypass cannot offer distal aortic perfusion during the period of proximal aortic anastomosis (32).

The traditional LHB circuit for the TAAA repair typically involves a simple circuit consisting of inflow and outflow lines, and a centrifugal head. The blood volume fluctuation is significant, and massive fluid and blood replacement are required rapidly, as a consequence of severe bleeding during extensive exposure and reconstruction of the thoracoabdominal aorta and its aortic branches. So excessive hemodilution, hypotension, and hypothermia may occur, even resulting in overwhelming hemodynamics changes. These conditions are a common phenomenon in the early stage of a low-volume center. Ultrafilter, heater exchanger, arterial filter, and rapid-infusion circuit were added to the classical LHB circuit to diminish to hazard the of profuse bleeding due to operation. The heater exchanger contributes to the temperature regulation; The ultrafilter, arterial filter, and rapid-infusion system facilitated the blood volume management and are useful to maintain hemodynamic stability.

Our modular multifunctional LHB circuit can offer effective distal aortic perfusion during the period of proximal aortic anastomosis, which can afford sufficient time for anastomosis. The integrated rapid infusion system can maintain the systemic blood volume when hemorrhaging to reduce hemodynamic fluctuations. Meanwhile, ultrafiltration is effective to achieve hemoconcentration and hemodilution after hemorrhage and rapid infusion. The collection of shed blood from the surgical field and rapid fusion system. The combination of a rapid infusion system and ultrafiltration can take over the function of an additional cell salvage device, and retain the other components than erythrocytes to a maximum extent. Moreover, the accessibility of modified LHB circuit switching to CPB reduces the incidence of operation errors and time-saving, which may be significantly meaningful in the condition that the cardiopulmonary function can not be competent for LHB. Our circuit needs more consumables including ultrafilter, and arterial filter, which may increase the cost. However, the cost of modified LHB is lower than traditional CPB, which has the essential cost of an *oxygenator*. The cost difference between the new circuit versus the traditional circuit is unclear due to the limited data. The closed-circuit system of LHB cannot respond to sudden hemodynamic fluctuations during aortic clamping or catastrophic bleeding, so the rapid-infuser system and another infusion system should be implemented. Recent research found the reservoir-added centrifugal pump circuit system was an effective perfusion system for blood infusion to reduce hemodynamic fluctuations (34). This research also modified the centrifugal system to facilitate hemodynamic management, and the temperature may be difficult to maintain in the normal range. Our LHB system provides means to achieve rapid infusion, which includes the rapid infuser system and reservoir-added centrifugal pump. Meanwhile, temperature management is easier under the use of a heat exchanger. Moreover, ultrafiltration can be performed in our system to improve blood concentration effectively. The comparison of classical LHB circuit, modified LHB circuit, and classical CPB circuit for TAAA was listed in **Supplementary Table 1**.

The maximum infusion flow rate of the rapid infuser system is 1,000 ml/min, the actual speed is reduced due to the tube diameter and fusion pressure. The is hard to afford the complete transfusion demand when severe bleeding occurred in actual practice. The volume in the hard-shell reservoir A in **Figure 6** can be rapidly infused into the LHB circuit to achieve the blood volume supplement. The shed blood also can be collected to another hard-shell reservoir timely through the sucker lines, and pumped into the rapid infuser system after ultrafiltration by ultrafilter and remove microemboli by an arterial filter. A hemoperfusion cartridge also can be paralleled to the ultrafiltration line in the LHB circuit to reduce the systemic inflammatory responses (35).

As we know and mentioned above, cardiac and pulmonary functions are essential for the performance of LHB. The CPB with hypothermic circulatory arrest is the ultimate option for TAAA repair and should be switched from LHB if the cardiac and pulmonary functions are hard to meet the needs of LHB. The reserved cannulation lines for venous drainage and arterial perfusion, and reserved tube for oxygenator connection, make the switch easily achieved.

Spinal cord ischaemia is another life-threatening event related to increased mortality after complex aortic surgery. Research reported the total incidence of spinal cord ischaemia was 8.6% (12). The incidence of paraparesis own to spinal cord deficit was favorably low in our center. Cerebrospinal fluid drainage and intercostal artery re-implantation are important spinal cord protection strategies (6, 36). The spinal cord perfusion is enhanced when augmented distal aortic perfusion is below the level of proximal aortic cross-clamp, maintaining spinal cord perfusion pressure provides acceptable outcomes. which is another method of protecting the spinal cord against ischemia (10). In our center, cerebrospinal fluid drainage, intercostal artery re-implantation, and enhanced MAP were performed.

The circuit for selective visceral perfusion and kidney perfusion is important for the patients' need to reconstruct the renal arteries, celiac axis, and the SMA. Selective visceral perfusion and kidney perfusion are essential principles for extent II, III, or IV TAAA patients during the abdominal aorta reconstruction, which aims to minimize the duration of abdominal-organ ischemia and reduce the incidence of renal and hepatic insufficiency, coagulopathy, and bowel ischemia. Postoperative acute kidney injury (AKI) is a common complication and is a significant risk factor for mid-term survival in patients undergoing TAAA repair. Preventing AKI can modify the mid-term survival after TAAA repair (37). Research confirmed that cold crystalloid perfusion during the period of *arterial* occlusion and reconstruction is critical for kidney protection (38). The visceral perfusion is selected to avoid the splanchnic hypoperfusion and to reduce gastrointestinal complications. Gastrointestinal complications are a greater risk factor for mortality and require secondary interventions, longer intensive care unit (ICU) stay, and hospital stays (39). The mid and long-term survival was markedly poorer for patients who developed gastrointestinal complications (36).

The advantages of LHB include augmentation of distal perfusion and reduction of left ventricular strain by decreasing preload and afterload (40). Moreover, the heparin dose is significantly reduced to 1.5 mg/kg with ACT $>$ 250 s under LHB without an oxygenator, which may contribute to less surgical bleeding (40). LHB generally lacks an oxygenator, so maintenance of oxygenation is important during single-lung ventilation. LHB remains controversial when it is used as extracorporeal circulatory support in patients with preoperative pulmonary risks (40–42). Some studies have suggested the use of a CPB or an oxygenator during LHB to achieve better oxygenation in patients with impaired pulmonary function

(41, 42). The research found that LHB improved arterial oxygenation during single-lung ventilation in open TAAA repair (40, 43). The marked improvement in oxygenation was due to improvements in ventilation/perfusion mismatch and the pulmonary shunt elicited by the inserting an inflow cannula via the left pulmonary vein (44). However, there are some limitations to our present study. First, no comparative quantitative data to clarify the accessibility, effectiveness, and cost-benefit differences of our modular multifunctional LHB circuit from the traditional LHB circuit. Secondly, our experience is based on retrospectively collected data from a limited number of patients. Thus, more cases are also needed to evaluate the clinical outcomes. Finally, the circuit looks rather complicated, with too many details including cut points and connections. So, a visual guide for the assembly and use of this circuit is provided as the supplementary material (**Supplementary Video 1**).

In conclusion, the modular LHB circuit system is an effective, practical, and multifunctional perfusion system. The circuit can meet the needs of LHB and quickly switch to conventional CPB. This circuit also made the assembly of the LHB circuit more easily, and more efficient, which may contribute to the TAAA repair operation performed in lower volume centers easily.

Data availability statement

The original contributions presented in this study are included in the article/**Supplementary material**, further inquiries can be directed to the corresponding author.

Ethics statement

The studies involving human participants were reviewed and approved by Committee on the Medical Ethics of Xiangya Hospital, Central South University. Written informed consent for participation was not required for this study in accordance with the national legislation and the institutional requirements.

Author contributions

CZ and LH: conceptualization. XC, QH, and FL: methodology. XC and CZ: software. CZ, QH, and EW: validation. ZY and CZ: formal analysis, writing—review and editing. QH, EW, and LD: investigation. CZ: resources, data curation, project administration, funding acquisition, and visualization. LH and JH: writing—original draft preparation. LH: supervision. All authors have read and agreed to the published version of the manuscript.

Funding

This research was funded by the grants from the Youth Science Foundation of Xiangya Hospital (2019Q14 to CZ).

Conflict of interest

The authors declare that the research was conducted in the absence of any commercial or financial relationships that could be construed as a potential conflict of interest.

Publisher's note

All claims expressed in this article are solely those of the authors and do not necessarily represent those of their affiliated organizations, or those of the publisher, the editors and the reviewers. Any product that may be evaluated in this article, or claim that may be made by its manufacturer, is not guaranteed or endorsed by the publisher.

Supplementary material

The Supplementary Material for this article can be found online at: https://www.frontiersin.org/articles/10.3389/fcvm.2022.944287/full#supplementary-material

References

1. Green SY, Safi HJ, Coselli JS. A history of open thoracoabdominal aortic aneurysm repair: Perspective from Houston. *J Cardiovasc Surg (Torino).* (2021) 62:191–202. doi: 10.23736/S0021-9509.21.11776-8

2. Gombert A, Frankort J, Keszei A, Müller O, Benning J, Kotelis D, et al. Outcome of elective and emergency open thoraco-abdominal aortic aneurysm repair in 255 cases: A retrospective single centre study. *Eur J Vasc Endovasc Surg.* (2022) 63:578–86. doi: 10.1016/j.ejvs.2022.02.003

3. Rocha RV, Lindsay TF, Nasir D, Lee DS, Austin PC, Chan J, et al. Risk factors associated with long-term mortality and complications after thoracoabdominal aortic aneurysm repair. *J Vasc Surg.* (2022) 75:1135–41. doi: 10.1016/j.jvs.2021.09.021

4. Rocha RV, Lindsay TF, Austin PC, Al-Omran M, Forbes TL, Lee DS, et al. Outcomes after endovascular versus open thoracoabdominal aortic aneurysm repair: A population-based study. *J Thorac Cardiovasc Surg.* (2021) 161:516–27. doi: 10.1016/j.jtcvs.2019.09.148

5. Rocha RV, Lindsay TF, Friedrich JO, Shan S, Sinha S, Yanagawa B, et al. Systematic review of contemporary outcomes of endovascular and open

thoracoabdominal aortic aneurysm repair. *J Vasc Surg.* (2020) 71:1396–412. doi: 10.1016/j.jvs.2019.06.216

6. Coselli JS, LeMaire SA, Preventza O, de la Cruz KI, Cooley DA, Price MD, et al. Outcomes of 3309 thoracoabdominal aortic aneurysm repairs. *J Thorac Cardiovasc Surg.* (2016) 151:1323–37. doi: 10.1016/j.jtcvs.2015.12.050

7. Fujikawa T, Yamamoto S, Oshima S, Ozaki K, Shimamura J, Asada H, et al. Open surgery for descending thoracic aorta in an endovascular era. *J Thorac Cardiovasc Surg.* (2019) 157:2168–74. doi: 10.1016/j.jtcvs.2018.08.094

8. Murana G, Castrovinci S, Kloppenburg G, Yousif A, Kelder H, Schepens M, et al. Open thoracoabdominal aortic aneurysm repair in the modern era: Results from a 20-year single-centre experience. *Eur J Cardiothorac Surg.* (2016) 49:1374–81. doi: 10.1093/ejcts/ezv415

9. Tanaka A, Estrera AL, Safi HJ. Open thoracoabdominal aortic aneurysm surgery technique: How we do it. *J Cardiovasc Surg (Torino).* (2021) 62:295–301. doi: 10.23736/S0021-9509.21.11825-7

10. Uchino G, Yunoki K, Sakoda N, Hattori S, Kawabata T, Saiki M, et al. Spinal cord protection during thoracoabdominal aortic replacement: Spinal cord perfusion maintenance. *Interact Cardiovasc Thorac Surg.* (2017) 24:708–13.

11. Gilling-Smith GL, Worswick L, Knight PF, Wolfe JH, Mansfield AO. Surgical repair of thoracoabdominal aortic aneurysm: 10 years' experience. *Br J Surg.* (1995) 82:624–9. doi: 10.1002/bjs.1800820517

12. Moulakakis KG, Karaolanis G, Antonopoulos CN, Kakisis J, Klonaris C, Preventza O, et al. Open repair of thoracoabdominal aortic aneurysms in experienced centers. *J Vasc Surg.* (2018) 68:634–45. doi: 10.1016/j.jvs.2018.03.410

13. Anna C, Anderson JA, Green A, Chang DC, Kansal N. Hospital volume of thoracoabdominal aneurysm repair does not affect mortality in California. *J Vasc Surg.* (2011) 2:595. doi: 10.1016/j.jvs.2011.05.086

14. Rigberg DA, McGory ML, Zingmond DS, Maggard MA, Agustin M, Lawrence PF, et al. Thirty-day mortality statistics underestimate the risk of repair of thoracoabdominal aortic aneurysms: A statewide experience. *J Vasc Surg.* (2006) 43:217–22; 223. doi: 10.1016/j.jvs.2005.10.070

15. Polanco AR, D'Angelo AM, Shea NJ, Allen P, Takayama H, Patel VI. Increased hospital volume is associated with reduced mortality after thoracoabdominal aortic aneurysm repair. *J Vasc Surg.* (2021) 73:451–8. doi: 10.1016/j.jvs.2020.05.027

16. Riambau V, Böckler D, Brunkwall J, Cao P, Chiesa R, Coppi G, et al. Editor's choice - management of descending thoracic aorta diseases: Clinical practice guidelines of the European society for vascular surgery (ESVS). *Eur J Vasc Endovasc Surg.* (2017) 53:4–52. doi: 10.1016/j.ejvs.2016.06.005

17. Oderich GS, Tenorio ER, Mendes BC, Lima G, Marcondes GB, Saqib N, et al. Midterm outcomes of a prospective, nonrandomized study to evaluate endovascular repair of complex aortic aneurysms using fenestrated-branched endografts. *Ann Surg.* (2021) 274:491–9. doi: 10.1097/SLA.0000000000004982

18. Geisbüsch S, Kuehnl A, Salvermoser M, Reutersberg B, Trenner M, Eckstein HH. Editor's choice - hospital incidence, treatment, and in hospital mortality following open and endovascular surgery for thoraco-abdominal aortic aneurysms in Germany from 2005 to 2014: Secondary data analysis of the nationwide German DRG microdata. *Eur J Vasc Endovasc Surg.* (2019) 57:488–98. doi: 10.1016/j.ejvs.2018.10.030

19. Rahim AA, Ibrahim R, Yao L, Shen Cheok W, Ismail M. Re-intervention rate in endovascular vs open surgical repair for abdominal aortic aneurysms. *Ann Med Surg.* (2021) 69:102703. doi: 10.1016/j.amsu.2021.102703

20. Muncan B, Sangari A, Liu SH, Price LZ. Midterm outcomes of endovascular versus open surgical repair of intact descending thoracic aneurysms in patients with connective tissue disorders. *Ann Vasc Surg.* (2022):doi: 10.1016/j.avsg.2022.04.002 [Epub ahead of print].

21. Rocha RV, De Mestral C, Tam DY, Lee DS, Al-Omran M, Austin PC, et al. Health care costs of endovascular compared with open thoracoabdominal aortic aneurysm repair. *J Vasc Surg.* (2021) 73:1934–41. doi: 10.1016/j.jvs.2020.09.034

22. Chakfé N, Diener H, Lejay A, Assadian O, Berard X, Caillon J, et al. Editor's choice - European society for vascular surgery (ESVS) 2020 clinical practice guidelines on the management of vascular graft and endograft infections. *Eur J Vasc Endovasc Surg.* (2020) 59:339–84. doi: 10.1016/j.ejvs.2019.10.016

23. Keschenau PR, Kotelis D, Bisschop J, Barbati ME, Grommes J, Mees B, et al. Editor's choice - open thoracic and thoracoabdominal aortic repair in patients with connective tissue disease. *Eur J Vasc Endovasc Surg.* (2017) 54:588–96. doi: 10.1016/j.ejvs.2017.07.026

24. Papadimas E, Tan YK, Qi Q, Ng JJ, Kofidis T, Teoh K, et al. Left heart bypass versus circulatory arrest for open repair of thoracoabdominal aortic pathologies. *Anz J Surg.* (2020) 90:2434–40. doi: 10.1111/ans.16287

25. Kong M, Wei D, Li X, Zhu X, Hong Z, Ni M, et al. The dynamic changes in autophagy activity and its role in lung injury after deep hypothermic circulatory arrest. *J Cell Mol Med.* (2022) 26:1113–27. doi: 10.1111/jcmm.17165

26. Ise H, Kitahara H, Oyama K, Takahashi K, Kanda H, Fujii S, et al. Hypothermic circulatory arrest induced coagulopathy: Rotational thromboelastometry analysis. *Gen Thorac Cardiovasc Surg.* (2020) 68:754–61. doi: 10.1007/s11748-020-01399-y

27. Karrar S, Reniers T, Filius A, Bunge J, Bekkers JA, Hoeks SE, et al. Rotational thromboelastometry-guided transfusion protocol to reduce allogeneic blood transfusion in proximal aortic surgery with deep hypothermic circulatory arrest. *J Cardiothorac Vasc Anesth.* (2022) 36:1029–39. doi: 10.1053/j.jvca.2021.08.020

28. Yoo JS, Kim JB, Joo Y, Lee W, Jung S, Choo SJ, et al. Deep hypothermic circulatory arrest versus non-deep hypothermic beating heart strategy in descending thoracic or thoracoabdominal aortic surgery. *Eur J Cardio Thorac.* (2014) 46:678–84. doi: 10.1093/ejcts/ezu053

29. Matte GS, Regan WL, Connor KR, Daaboul DG, Hoganson DM, Quinonez LG. Hybrid left heart bypass circuit for repair of the descending aorta in an 8-kg williams syndrome patient. *J Extra Corpor Technol.* (2021) 53:186–92. doi: 10.1182/ject-2100022

30. Coselli JS. The use of left heart bypass in the repair of thoracoabdominal aortic aneurysms: Current techniques and results. *Semin Thorac Cardiovasc Surg.* (2003) 15:326–32. doi: 10.1053/S1043-0679(03)00090-X

31. Safi HJ, Estrera AL, Miller CC, Huynh TT, Porat EE, Azizzadeh A, et al. Evolution of risk for neurologic deficit after descending and thoracoabdominal aortic repair. *Ann Thorac Surg.* (2005) 80:2173–9. doi: 10.1016/j.athoracsur.2005.05.060

32. Dong XH, Ge YP, Wang R, Pan XD, Lu JK, Cheng WP. Spinal cord protection of aorto-iliac bypass in open repair of extent ii and III thoracoabdominal aortic aneurysm. *Heart Lung Circ.* (2022) 31:255–62. doi: 10.1016/j.hlc.2021.05.092

33. Cooley DA, Golino A, Frazier OH. Single-clamp technique for aneurysms of the descending thoracic aorta: report of 132 consecutive cases. *Eur J Cardiothorac Surg.* (2000) 18:162–7. doi: 10.1016/s1010-7940(00)00499-1

34. Ertugay S, Apaydin AZ, Karaca S, Ergi DG, Posacioglu H. Distal perfusion with modified centrifugal pump circuit in thoracic and thoracoabdominal aortic aneurysm repair. *Vasc Endovascular Surg.* (2022) 1159235759. doi: 10.1177/15385744221108049 [Epub ahead of print].

35. He Z, Lu H, Jian X, Li G, Xiao D, Meng Q, et al. The efficacy of resin hemoperfusion cartridge on inflammatory responses during adult cardiopulmonary bypass. *Blood Purif.* (2022) 51:31–7. doi: 10.1159/000514149

36. Coselli JS, Green SY, Price MD, Zhang Q, Preventza O, de la Cruz KI, et al. Spinal cord deficit after 1114 extent II open thoracoabdominal aortic aneurysm repairs. *J Thorac Cardiovasc Surg.* (2019):doi: 10.1016/j.jtcvs.2019.01.120 [Epub ahead of print].

37. Henmi S, Okita Y, Koda Y, Yamanaka K, Omura A, Inoue T, et al. Acute kidney injury affects mid-term outcomes of thoracoabdominal aortic aneurysms repair. *Semin Thorac Cardiovasc Surg.* (2021) 34:430–8. doi: 10.1053/j.semtcvs.2021.04.050

38. Kahlberg A, Tshomba Y, Baccellieri D, Bertoglio L, Rinaldi E, Ardita V, et al. Renal perfusion with histidine-tryptophan-ketoglutarate compared with ringer's solution in patients undergoing thoracoabdominal aortic open repair. *J Thorac Cardiovasc Surg.* (2021):doi: 10.1016/j.jtcvs.2021.02.090 [Epub ahead of print].

39. Frankel WC, Green SY, Amarasekara HS, Zhang Q, Preventza O, LeMaire SA, et al. Early gastrointestinal complications after open thoracoabdominal aortic aneurysm repair. *Ann Thorac Surg.* (2021) 112:717–24. doi: 10.1016/j.athoracsur.2020.09.032

40. Yuki K, Sakuramoto C, Matsumoto C, Hoshino M, Niimi Y. The effect of left heart bypass on pulmonary blood flow and arterial oxygenation during one-lung ventilation in patients undergoing descending thoracic aortic surgery. *J Clin Anesth.* (2009) 21:562–6. doi: 10.1016/j.jclinane.2008.12.028

41. Vaughn SB, LeMaire SA, Collard CD. Case scenario: Anesthetic considerations for thoracoabdominal aortic aneurysm repair. *Anesthesiology.* (2011) 115:1093–102. doi: 10.1097/ALN.0b013e3182303a7f

42. Leach WR, Sundt TR, Moon MR. Oxygenator support for partial left-heart bypass. *Ann Thorac Surg.* (2001) 72:1770–1. doi: 10.1016/s0003-4975(01)03058-2

43. Yuki KM, Chilson KM, DiNardo JAM. Improvement of pao2 during one-lung ventilation with partial left-heart bypass in pediatric patients is caused by increased blood flow to the dependent lung. *J Cardiothorac Vasc Anesth.* (2013) 27:542–5. doi: 10.1053/j.jvca.2011.12.011

44. Suga K, Kobayashi Y, Ochiai R. Impact of left heart bypass on arterial oxygenation during one-lung ventilation for thoracic aortic surgery. *J Cardiothorac Vasc Anesth.* (2017) 31:1197–202. doi: 10.1053/j.jvca.2016.09.026

frontiers | Frontiers in Cardiovascular Medicine

TYPE Original Research
PUBLISHED 30 September 2022
DOI 10.3389/fcvm.2022.951264

Check for updates

OPEN ACCESS

EDITED BY
Weiguo Fu,
Fudan University, China

REVIEWED BY
Fu-Zong Wu,
Kaohsiung Veterans General Hospital, Taiwan
Wolf-Hans Eilenberg,
Medical University of Vienna, Austria

*CORRESPONDENCE
Jing Cai
542078068@qq.com
Tong Qiao
qiaotongmail@aliyun.com

†These authors have contributed equally to this work

SPECIALTY SECTION
This article was submitted to General Cardiovascular Medicine, a section of the journal Frontiers in Cardiovascular Medicine

RECEIVED 23 May 2022
ACCEPTED 29 August 2022
PUBLISHED 30 September 2022

CITATION
Liu H, Chen Z, Tang C, Fan H, Mai X, Cai J and Qiao T (2022) High-density thrombus and maximum transverse diameter on multi-spiral computed tomography angiography combine to predict abdominal aortic aneurysm rupture.
Front. Cardiovasc. Med. 9:951264.
doi: 10.3389/fcvm.2022.951264

COPYRIGHT
© 2022 Liu, Chen, Tang, Fan, Mai, Cai and Qiao. This is an open-access article distributed under the terms of the Creative Commons Attribution License (CC BY). The use, distribution or reproduction in other forums is permitted, provided the original author(s) and the copyright owner(s) are credited and that the original publication in this journal is cited, in accordance with accepted academic practice. No use, distribution or reproduction is permitted which does not comply with these terms.

High-density thrombus and maximum transverse diameter on multi-spiral computed tomography angiography combine to predict abdominal aortic aneurysm rupture

Heqian Liu[1†], Zhipeng Chen[2†], Chen Tang[2], Haijian Fan[3], Xiaoli Mai[3], Jing Cai[2*] and Tong Qiao[1*]

[1]Department of Vascular Surgery, Nanjing Drum Tower Hospital Clinical College of Xuzhou Medical University, Nanjing, China, [2]Department of Vascular Surgery, Nanjing Drum Tower Hospital, The Affiliated Hospital of Nanjing University Medical School, Nanjing, China, [3]Department of Radiology, Nanjing Drum Tower Hospital, The Affiliated Hospital of Nanjing University Medical School, Nanjing, China

Objective: We attempted to measure maximum transverse diameter (MTD) of and CT values of ILT by using multi-spiral computed tomography angiography (MSCTA) to investigate the predictive value of MTD with different CT values of thrombus on the risk of AAA rupture.

Methods: Forty-five intact abdominal aortic aneurysms (IAAA) and 17 ruptured abdominal aortic aneurysms (RAAA) were included in this study. MTD and CT values in their planes were measured from MSCTA images and aneurysm lumen and thrombus volumes were calculated for the range of different CT values.

Results: The median of maximum CT value of thrombus at the plane of MTD was higher in RAAA (107.0 HU) than the median in IAAA (84.5 HU) ($P < 0.001$). Univariate logistic regression analysis showed that the maximum CT value was a risk factor for RAAA ($P < 0.001$). It was further found that the area under the ROC curve for thrombus maximum CT value in the MTD plane to predict RAAA was 0.848 ($P < 0.001$), with a cut-off value of 97.5 HU, a sensitivity of 82.35%, and a specificity of 84.44%. And the MTD of the abnormal lumen combined with the maximum CT value at its plane predicted RAAA with an area under the ROC curve of 0.901, a sensitivity of 76.47%, and a specificity of 97.78%. The further analysis of thrombus volume in the range of different CT value showed that median thrombus volume in RAAA in the range of 30 HU~150 HU was 124.2 cm^3 which was higher than the median of 81.4 cm^3 in IAAA ($P = 0.005$). To exclude confounding factors (aneurysm volume), we calculated the standardized thrombus (ILT volume/total aneurysm volume), and the thrombus volume in the range of 30 HU~150 HU in RAAA was positively correlated with the standardized thrombus volume ($\rho = 0.885$, $P < 0.001$), while the thrombus volume in the range of −100 HU~30 HU was not correlated with it ($\rho = 0.309$, $P = 0.228$).

Conclusions: High-density ILT shown on MSCTA in AAAs is associated with aneurysm rupture, and its maximum transverse diameter combined with the maximum CT value in its plane is a better predictor of RAAA.

KEYWORDS

ruptured abdominal aortic aneurysm, intraluminal thrombus, high-density, MSCTA, maximum transverse diameter

Introduction

Rupture is one of the most serious complications of abdominal aortic aneurysm (AAA), and its morbidity and mortality rates are extremely high. It has been reported in the literature that 59–83% of patients with ruptured abdominal aortic aneurysm (RAAA) die before reaching the hospital, and even after timely arrival and medical intervention, the morbidity and mortality rate are as high as 30–80% (1). Therefore, the factors that cause abdominal aortic rupture should be taken into account. There are several factors that can cause AAA rupture in previous studies, such as increased diameter or volume (2), bacterial or fungal infection (3), etc. In the present day, national and international research institutions basically agree that the risk of AAA rupture is assessed mainly by the maximum transverse diameter (MTD) of the abdominal aorta (4, 5). Although the MTD has been shown to predict rupture in population studies such as the UK Small Aneurysm Trial (6) and the Aneurysm Detection and Management Trial (7), it provides a poor assessment of individual risk while some large-diameter AAAs have been found to remain stable over a lifetime (8). There are some controversies as to whether the aneurysm diameter alone can be a reason for intervention (9). Therefore, investigating specific rupture factors will probably help to reduce the risk of aneurysm rupture.

Intraluminal thrombus (ILT) is one of the common substances in AAA. ILT has been suggested in previous studies to reduce mural stress in AAA and thus may prevent rupture of AAA (10–12). In contrast, some other studies has found that ILT can act as an inflammatory lesion of protein hydrolysis and aortic wall degeneration, thus increasing the risk of AAA rupture (13–15). While the above studies only address the effect of ILT in AAA as a whole, some studies in recent years have already started to focus on the relationship between different Hounsfield Units (HU) within the tissue and disease under computed tomography angiography (CTA). For example, some studies has reported correlation between the density of coronary arteries (16) and carotid plaques (17) on computed tomography and the stability of the atherosclerotic lesions. Banno et al. (18) analyzed the correlation between thrombus and spinal cord ischemia based on thrombus CTA density in the range of different CT value in a thoracic aortic aneurysm study. However, it has not been reported whether there is a differential effect of thrombus on RAAA in the range of different CT value. Our study rely primarily on aortic MSCTA to assess the potential association of MTD and different CT values of thrombus with RAAA.

Data and methods

Research subjects

Patients with intact abdominal aortic aneurysm (IAAA) and RAAA who attended Hospital from January 2016 to January 2022 were included and divided into two groups on this basis. Inclusion criteria: (1) patients with IAAA or RAAA clearly diagnosed through CTA (diameter $\geq$60 mm); (2) complete imaging data. Exclusion criteria: (1) no images of CTA of the abdominal aorta; (2) no ILT in the abdominal aorta; (3) Aortitis; (4) infected abdominal aortic aneurysm; (5) stable syndrome and other genetic diseases. Therefore, the clinical data of a total of 62 patients were finally analyzed in this study. Signing informed consent was exempted because the patients' identities were anonymous, and this retrospective study was approved by the Ethics Committee of Nanjing Drum Tower Hospital (Figure 1).

Research methods

Data collection

This study was a cross-sectional study and patients were screened according to inclusion and exclusion criteria. Their previous underlying medical history, clinical base data, and imaging data were collected from the electronic medical record system. The history of previous underlying diseases included hypertension, diabetes mellitus, cerebral infarction and coronary heart disease; clinical base information included gender, age, BMI, history of smoking and alcohol consumption; and imaging data mainly consisted of abdominal aortic MSCTA (Figure 2).

CTA analysis of enrolled patients

All MSCTA analyses were performed by two professional imaging physicians, and the patient's clinical symptoms and

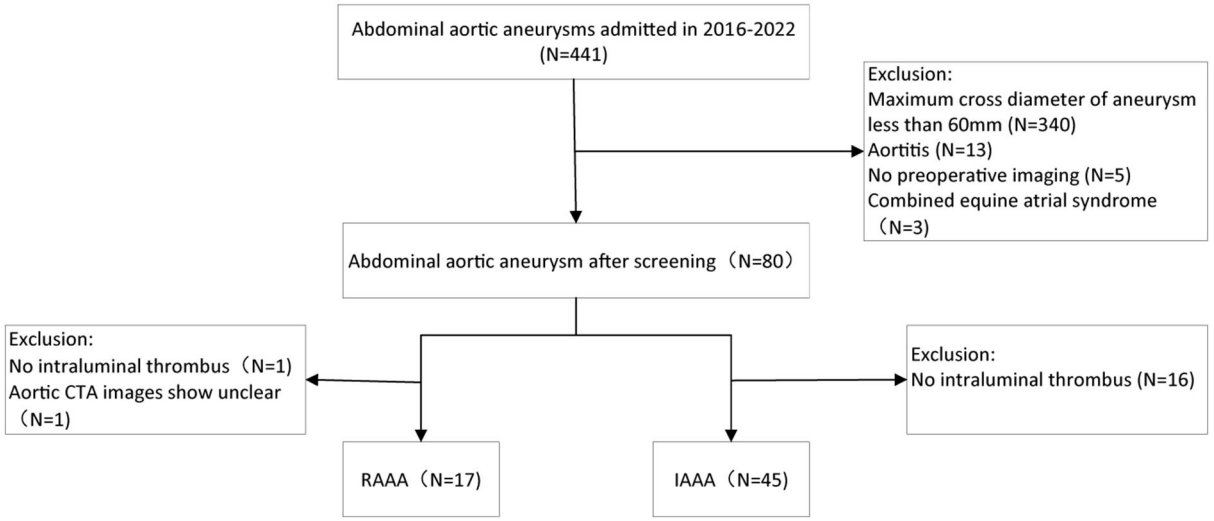

FIGURE 1
Flow chart of the patient selection.

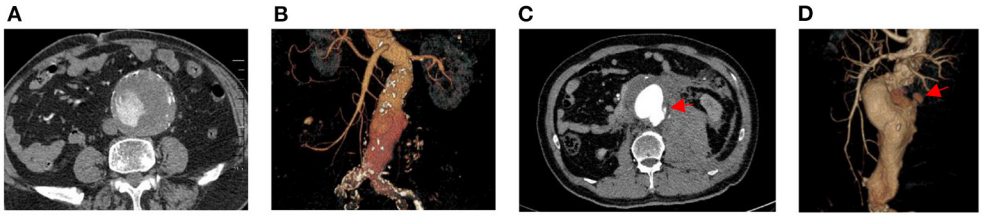

FIGURE 2
MSCTA images of intact and ruptured abdominal aortic aneurysms. **(A)** shows the cross-section image of the intact abdominal aortic aneurysm. **(B)** shows the three-dimensional image of the intact abdominal aortic aneurysm. **(C)** shows the cross-section image of the ruptured abdominal aortic aneurysm and **(D)** shows the three-dimensional image of the ruptured abdominal aortic aneurysm. The red arrow indicates the location of the ruptured wall of the abdominal aortic aneurysm.

characteristics were not reviewed. The MSCTA analysis was performed in four different phases, the first of which was to assess the quality of the images included in the patient and to exclude any abdominal aorta that showed artifacts or degrading motion artifacts in the image quality; The second phase was to find the largest transverse cross-sectional image and two imaging physicians measured the minimum CT, average CT and maximum CT of ILT in this plane by using AW443 workstation, and checked the consistency of repeated measurements. We judged the intra-group correlation coefficient of the reproducibility evaluation of the measurements based on the estimation of Single Measures, i.e., ICC = 0.811 ($P < 0.001$). Therefore, the reproducibility of CT values tested by two imaging physicians in this study was good. The final results were obtained by averaging the values measured by the two imaging physicians. The third stage is to reconstruct the AAA in 3D using the AW443 imaging workstation to outline the region of interest (ROI) of the abdominal aorta in thin layer CT images (the precise scope of the AAA is from the infrarenal abdominal aorta to above the common iliac artery bifurcation). The thrombus was reconstructed again using the same outline and its volume was calculated; In the four stage, the corresponding volumes were obtained by entering different ranges of CT values in the AW443 workstation. The classification in this study concerning the different CT values in the range is based on the most commonly used classification in the field of coronary arteries (19): (−100 HU∼30 HU), (30 HU∼150 HU) 和(>150 HU) (Figure 3).

Thrombus thickness and percentage

The thrombus thickness is measured in the plane of the largest transverse diameter of the aneurysm, starting at the edge of the aneurysm wall and ending at the thickest point of

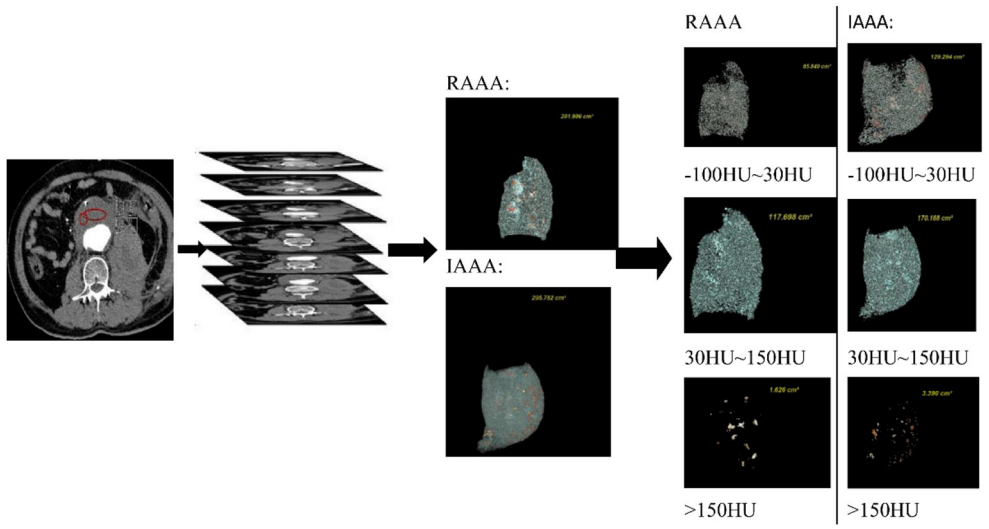

FIGURE 3
The procedure of measuring CT values at the maximum transverse diameter and calculating thrombus volumes in the range of different CT in IAAA and RAAA.

the thrombus. Percentage of thrombus thickness = thrombus thickness/maximum aneurysm diameter.

Standardized thrombus volume

ILT and intraluminal volumes were calculated using CTA through the AW443 workstation, and the percentage of total aneurysm volume accounted for the ILT was calculated for each patient: Standardized thrombus volume = ILT volume/ total AAA intraluminal volume.

Statistical analysis

Data were analyzed using the statistical software R (http://www.R-project.org, The R Foundation) and SPSS 28.0. Measured data conforming the normal distribution were expressed as $\bar{X} \pm s$, and the *t*-test was used for comparison of means between groups. Bias distributed variables were expressed as M (Q1, Q3), and the Mann-Whitney *U* test was used for comparison between groups. Qualitative data were expressed as rates or composition ratios, and comparisons between groups were made using the χ^2 test. The Receiver Operating Characteristic (ROC) curve was used to assess the sensitivity and specificity of clinical variables in predicting RAAA and to calculate cutoff values. Univariate logistic regression analysis was used to examine the association between RAAA and clinical variables. Quantitative skewed distribution variable correlation analysis was performed by using spearman, and the correlation coefficient was ρ. $P < 0.05$ was considered to be statistically significant.

The sample size was calculated by using PASS software for *post-hoc* efficacy analysis, and the maximum CT value had sufficient efficacy to detect differences between the two groups at an a error of 0.05 (efficacy = 0.99947).

Results

Baseline information of the study populations

A total of 441 patients with abdominal aortic aneurysm were admitted to our hospital. Among the collected patients with RAAAs, only one had a MTD of <60 mm in the abdominal aorta and one had no intraluminal thrombus, thus two patients were excluded. And one more was excluded because of unclear CTA images, thus causing a large difference in CT number measured by the two imagers, and was excluded after final discussion. To prevent errors due to large differences in the MTD, we analogized the lowest diameter of the collected RAAA and selected intact AAA larger than 60 mm. And we excluded non-ILT patients as there was only one case of non-ILT in the RAAA from our data. Therefore, in order to control for confounding factors, patients without ILT in the IAAA were also excluded. Finally, A total of 62 patients with AAA were included in this study, of which 45 were in the IAAA group and 17 in the RAAA group. There were 41 (91.1%) males and 4 (8.9%) females among the 45 IAAA patients, and their age was 75.1 ± 7.1 years. This compares to the age of 69.7 ± 6.9 years in the 17 RAAA patients, 13 (76.5%) of whom were male subjects. Baseline characteristics of all study populations are summarized in Table 1. Overall, RAAA patients were younger than IAAA (*P*

TABLE 1 Baseline information of intact and ruptured abdominal aortic aneurysms.

Variables	Total ($n = 62$)	IAAA group ($n = 45$)	RAAA group (n = 17)	*P*-value
Sex, *n* (%)				0.198
Female	8 (12.9)	4 (8.9)	4 (23.5)	
Male	54 (87.1)	41 (91.1)	13 (76.5)	
Age (years)	72.0 (69.0, 77.8)	74.0 (70.0, 81.0)	69.0 (65.0, 72.0)	0.008
BMI (Kg/m^2)	24.0 ± 2.8	23.9 ± 2.9	24.2 ± 2.5	0.796
Hypertension, *n* (%)				0.164
No	14 (23.0)	8 (17.8)	6 (37.5)	
Yes	47 (77.0)	37 (82.2)	10 (62.5)	
Diabetes, *n* (%)				1.000
No	49 (80.3)	36 (80)	13 (81.2)	
Yes	12 (19.7)	9 (20)	3 (18.8)	
CI, *n* (%)				0.259
No	50 (82.0)	35 (77.8)	15 (93.8)	
Yes	11 (18.0)	10 (22.2)	1 (6.2)	
CHD, *n* (%)				0.174
No	54 (88.5)	38 (84.4)	16 (100)	
Yes	7 (11.5)	7 (15.6)	0 (0)	
SBP (mm/Hg)	124.8 ± 23.7	131.0 ± 17.5	101.3 ± 29.5	<0.001
DBP (mm/Hg)	73.8 ± 14.4	77.0 ± 11.4	61.7 ± 18.1	0.001

IAAA, Intact abdominal aortic aneurysm; RAAA, Ruptured abdominal aortic aneurysm; SBP, Systolic blood pressure; DBP, Diastolic blood pressure; CI, Cerebral infarction; CHD, Coronary heart disease.

TABLE 2 Aneurysm lumen and thrombus in intact and ruptured abdominal aortic aneurysms.

Variables	Total ($n = 62$)	IAAA ($n = 45$)	RAAA ($n = 17$)	*P*-value
Maximum transverse diameter (mm)	69.5 (65.8, 78.2)	68.0 (65.1, 74.0)	78.0 (71.9, 85.0)	0.003
Thrombus thickness	32.9 ± 11.2	32.0 ± 10.5	35.2 ± 13.0	0.33
Percentage of thrombus	46.4 ± 12.4	46.3 ± 12.5	46.7 ± 12.4	0.897
Minimum CT value (HU)	−11.5 ± 16.1	−10.5 ± 14.9	−15.8 ± 16.5	0.231
Average CT value (HU)	39.4 ± 7.3	37.6 ± 5.7	42.9 ± 7.6	0.004
Maximum CT value (HU)	85.8 (78.8, 104.5)	84.5 (78.5, 89.0)	107.0 (99.0, 115.5)	<0.001
Abdominal aortic aneurysm volume	307.1 (278.3, 392.0)	293.6 (256.2, 355.2)	392.2 (307.1, 518.3)	0.002
Total volume of thrombus in lumen	148.2 (106.1, 191.6)	128.4 (97.0, 172.2)	176.4 (153.4, 261.3)	0.004
The volume of (−100 HU∼30 HU)	47.3 (27.5, 63.7)	42.2 (25.2, 60.2)	62.3 (47.2, 72.8)	0.076
The volume of (30 HU∼150 HU)	96.5 (72.1, 134.8)	81.4 (71.2, 115.2)	124.2 (99.2, 197.3)	0.005
The volume of (>150 HU)	2.0 (1.0, 3.3)	2.1 (1.0, 3.4)	2.0 (0.6, 2.7)	0.825

IAAA, Intact abdominal aortic aneurysm; RAAA, Ruptured abdominal aortic aneurysm.

= 0.008), while the weight of 23.9 ± 2.9 Kg/m^2 in the IAAA group was not significantly different from 24.2 ± 2.5 Kg/m^2 in the IAAA group, and the discrepancy between the two groups was not statistically significant ($P = 0.796$). There was also no significant difference in the history of male, hypertension, diabetes mellitus, cerebral infarction and coronary artery disease between the two groups (all $P > 0.05$). In blood pressure testing at admission, we found higher systolic ($P < 0.001$) and diastolic blood pressure ($P = 0.001$) in the IAAA group compared to the RAAA group.

ILT in the study populations

Table 2 indicates the ILT in the RAAA group vs. the IAAA group. The results showed that the median 78 cm of the RAAA group had a larger MTD in the lumen compared to the median 78 cm of the IAAA group ($P = 0.003$). Further measurement of thrombus CT values at the plane of MTD showed that the difference between the minimum CT value of thrombus in the RAAA group (−15.8 ± 16.5) HU and the minimum CT value in the IAAA group (−10.5 ± 14.9) HU was not

significant, and the difference between the two groups was not statistically significant ($P = 0.231$); however, the average CT value of thrombus at the plane of MTD in the RAAA group (42.9 ± 7.6) HU was higher than the average CT value of thrombus at the plane of MTD in the IAAA group (37.6 ± 5.7) HU, and the difference between the two groups was statistically significant ($P = 0.004$), and the median of the maximum CT value for thrombus at the plane of MTD in the RAAA group was 107 HU higher than the median of the maximum CT value for thrombus at the plane of the MTD in the IAAA group 84.5 HU ($P < 0.001$). We further observed the CT values in both groups in different diameters which showed that the maximum CT values measured at the plane of MTD of the abdominal aortic aneurysm were higher in the RAAA group than in the IAAA group in the diameter ranges of 60∼69 mm, 70∼79 mm and 80∼102 mm. This suggests that the high-density thrombus shown by MSCTA in different diameter ranges has an important effect on abdominal aortic rupture (Table 3).

The imaging physicians outlined the target range with the AW443 workstation. In terms of the total volume within the AAA lumen, the median of 392.2 cm^3 was higher in the RAAA group than the median of 293.6 cm^3 in the IAAA group, and the discrepancy between the two groups was statistically significant ($P = 0.002$). The thrombus was then isolated from the lumen of the AAA, and the results showed that the median of the total thrombus volume was 176.4 cm^3 in the RAAA group than the median of 128.4 cm^3 in the IAAA group, and the difference between the two groups was statistically significant ($P = 0.004$). Further analysis of the thrombus volume in the range of different CT values showed that in the range of −100 HU∼30 HU the thrombus volume in the RAAA group the median of thrombus volume was 62.3 cm^3 which was not significantly correlated with the median of thrombus volume in the IAAA group that was 42.2 cm^3, and there was no statistical difference between the two groups ($P = 0.076$); however, in the range of 30 HU∼150 HU, the median thrombus volume of 124.2 cm^3 in the RAAA group was significantly higher than the median thrombus volume of 81.4 cm^3 in the IAAA group, and there was a statistical difference between the two groups ($P = 0.005$); The median thrombus/plaque volume of 2.0 cm^3 in the RAAA group was not significantly different from the median thrombus/plaque volume of 2.1 cm^3 in the IAAA group in the range of >150 HU, and there was no statistical difference between the two groups ($P = 0.825$).

TABLE 3 The differences of maximum CT values at different transverse diameter ranges in the RAAA and IAAA groups.

Variable	Event(n)	Z	*P*-value
Maximum transverse diameter			
60∼69 mm	IAAA (27)	−2.95	0.003
	RAAA (4)		
70∼79 mm	IAAA (12)	−2.35	0.019
	RAAA (6)		
80∼102 mm	IAAA (5)	−2.03	0.042
	RAAA (7)		

IAAA, Intact abdominal aortic aneurysm; RAAA, Ruptured abdominal aortic aneurysm.

Risk factor analysis for RAAA

Table 4 shows that univariate logistic regression analysis of RAAA in relation to clinical variables. The results showed age (OR = 0.89, 95% CI = 0.81∼0.98, $P = 0.015$), maximum transverse diameter (OR = 1.08, 95%CI = (1.02∼1.15), $P = 0.008$), average CT value (HU) (OR = 1.14, 95%CI = 1.03∼1.25), $P = 0.009$), maximum CT value (HU) (OR = 1.13, 95%CI = (1.06∼1.20), $P < 0.001$) and the volume of (30 HU∼150 HU) (OR = 1.01, 95% CI = (1.00∼1.02), $P = 0.023$) may be strongly associated with RAAA in the univariate model.

Maximum transverse diameter and high-density thrombus shown by MSCTA can jointly predict RAAA

Figure 4 shows that the Maximum CT value measured at the plane of the MTD of the AAA lumen predicts the area under the ROC curve (AUC) for RAAA to be 0.848, with an optimal cut-off value of 97.75 HU, a sensitivity of 82.35% and a specificity of 84.44%; the average CT value measured at the plane of the MTD of the AAA lumen predicts the area under the ROC curve (AUC) for RAAA of 0.703, with the best critical value of 39.25 HU, a sensitivity of 70.59%, and a specificity of 66.67%; the MTD of the AAA lumen predicted the area under the ROC curve (AUC) for RAAA of 0.746, with the best critical value of 71.68 mm, a sensitivity of 76.47%, and a specificity of 66.67%; and the combination of AAA lumen MTD and Maximum CT value for predicting RAAA was found to have an area under the ROC curve of 0.901, a sensitivity of 76.47%, and a specificity of 97.78%. These results suggest that high-density thrombus shown by MSCTA is a good predictor for RAAA ($P < 0.001$). If MTD and Maximum CT value measured at the plane of the MTD of the AAA lumen were combined to predict RAAA, the results were better than MTD or Maximum CT value alone ($P < 0.001$) (Table 5).

Changes in the range of different CT value after standardized thrombosis

In order to see the trend of thrombus in the RAAA and IAAA groups in the range of different CT value, the authors

TABLE 4 Univariate logistic regression analysis of clinical variables and RAAA.

Variable	B	SE	OR (95CI%)	*P*-value
Sex (male)	−1.15	0.78	0.32 (0.69∼1.45)	0.139
Age (years)	−0.12	0.05	0.89 (0.81∼0.98)	0.015
BMI (Kg/m^2)	0.04	0.13	1.04 (0.80∼1.35)	0.792
Hypertension	−1.02	0.65	0.35 (0.10∼1.28)	0.115
diabetes	−0.08	0.74	0.92 (0.22∼3.95)	0.914
Cerebral infarction	−1.46	1.09	0.23 (0.03∼1.99)	0.183
Systolic blood pressure	−0.06	0.02	0.94 (0.90∼0.98)	0.002
Diastolic blood pressure	−0.08	0.03	0.92 (0.87∼0.98)	0.005
Maximum transverse diameter	0.08	0.03	1.08 (1.02∼1.15)	0.008
Thrombus thickness	0.03	0.03	1.03 (0.98∼1.08)	0.326
Percentage of thrombus	0.003	0.03	1.00 (0.96∼1.06)	0.895
CT value at the plane of maximum transverse diameter				
Minimum CT value (HU)	−0.02	0.02	0.98 (0.94∼1.02)	0.230
Average CT value (HU)	0.13	0.05	1.14 (1.03∼1.25)	0.009
Maximum CT value (HU)	0.12	0.03	1.13 (1.06∼1.20)	<0.001
Abdominal aortic aneurysm volume	0.003	0.002	1.00 (1.00∼1.01)	0.080
Total volume of thrombus in lumen	0.01	0.003	1.01 (1.00∼1.02)	0.023
The volume of (−100 HU∼30 HU)	0.02	0.01	1.02 (1.00∼1.04)	0.071
The volume of (30 HU∼150 HU)	0.01	0.01	1.01 (1.00∼1.02)	0.023
The volume of (>150HU)	−0.04	0.12	0.96 (0.76∼1.22)	0.753

RAAA, Ruptured abdominal aortic aneurysm.

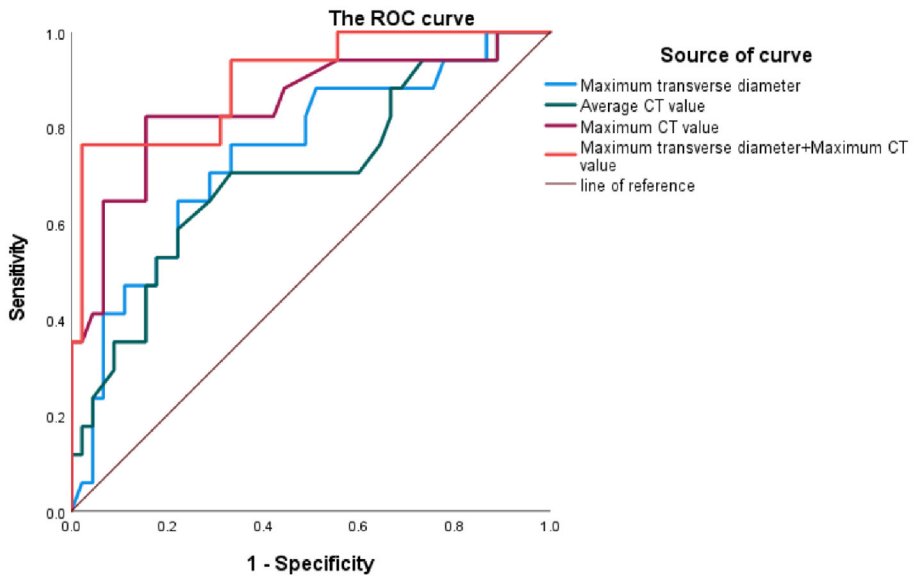

FIGURE 4
ROC curves of clinical variables and ruptured abdominal aortic aneurysm.

converted the ILT volume in both groups to the standardized thrombus volume (ILT volume / total AAA intraluminal volume). To understand the correlation, the authors made spearman correlation analysis between thrombus volumes in the range of different CT value and standardized thrombus, and Table 6 shows that in the IAAA group CT values of thrombus

TABLE 5 Clinical variables predict the area under the ROC curve for RAAA.

Variable	AUC	Cut-off	Sensitivity	Specificity	*P*-value
Maximum CT value (HU)	0.848	97.75	82.35%	84.44%	<0.001
Average CT value (HU)	0.703	39.25	70.59%	66.67%	0.011
Maximum transverse diameter	0.746	71.68	76.47%	66.67%	0.003
Maximum transverse diameter+ Maximum CT value (HU)	0.901	-	76.47%	97.78%	<0.001

RAAA, Ruptured abdominal aortic aneurysm.

TABLE 6 Correlation between thrombus volume in different CT value ranges and standardized thrombus.

Thrombus volume in different CT value ranges	IAAA group		RAAA group	
	ρ	*P*	ρ	*P*
−100 HU∼30 HU	0.652	<0.001	0.309	0.228
30 HU∼150 HU	0.667	<0.001	0.885	<0.001

Standardized thrombus, ILT volume/total aneurysm volume.

in the range of 30 HU∼150 HU and −100 HU∼30 HU volumes were positively correlated with standardized thrombus volumes, with correlation coefficients (ρ) of 0.667 and 0.652, respectively (both $P < 0.001$). In the RAAA group CT values of thrombus in the range of 30 HU∼150 HU were positively correlated with standardized thrombus volume ($\rho = 0.885$, $P < 0.001$), whereas CT values of thrombus in the range of −100 HU∼30 HU were not correlated with standardized thrombus volume ($\rho = 0.3091$, $P = 0.228$).

Discussion

Our study collected patients with AAA (MTD ≥60 mm) from January 2016 to January 2022 in the Department of Vascular Surgery. The aim of this study was to investigate the association of high-density thrombus shown by MSCTA with RAAA. The results showed that high-density thrombus shown on MSCTA may be associated with RAAA. The main findings of the study were as follows: (1) the average CT value and the highest CT value of thrombus at the plane of MTD were higher in RAAA than in IAAA; (2) the thrombus volume in the range of 30 HU∼150 HU was higher in RAAA than in IAAA, whereas the thrombus volume in the range of (−100 HU∼30 HU) was not significantly different from that in IAAA; (3) The standardized thrombus volume in RAAA was positively correlated with thrombus in the range of 30 HU∼150 HU, but not with thrombus volume in the range of −100∼30 HU.

AAA is a disease caused by chronic inflammatory degenerative lesions arising in the aortic wall, characterized by progressive aneurysmal dilatation of the infrarenal aorta (20). The AAA with large diameters are often associated with thrombus (21), which can eliminate the endothelium and intima, progressive degeneration of the middle layer and inflammation or fibrosis of the outer layer (22). But the effect of ILT on the risk of AAA rupture is still controversial. Some studies suggest that ILT reduces aortic wall shear stress, thus acting as a mechanical cushion (10, 23, 24), being negatively correlated with the rate of AAA growth (25). Nevertheless, ILT may also create an inflammatory environment in which neutrophils, cytokines, proteases and reactive oxygen species are sequestered (26), which may cause a decrease in wall strength. Some clinical studies have even found that ILT correlates with the rate of swelling and rupture of AAA (27–29). Therefore, the weakening effect of ILT on the aneurysmal wall of AAA may be greater. However, although some studies have shown a possible correlation between ILT and RAAA, it has not been reported whether thrombus in different CT value ranges has a different effect on larger diameter in RAAA.

CT values of various plaque components in previous studies have been defined as low HU for vulnerable plaques, intermediate HU for fibrofatty plaques and high HU for fibrous or calcified plaques (30). Banno et al. (18) measured intraluminal thrombus density by using preoperative CTA in patients in a thoracic aortic aneurysm study and showed that low density thrombus/plaque may be one of the mechanisms causing the development of spinal ischemia after thoracic aortic stenting. It has also been shown in clinical computed tomography studies that the higher the calcium score, the higher the likelihood of future acute coronary events in patients (31). This shows that different densities may cause different diseases. Recent studies have also found that inflammation can contribute to thrombus formation (32), which in turn contains high levels of inflammatory factors (26), and that the thrombus is thus progressively thicker and denser, such that the high-density thrombus may reflect the degree of inflammatory weakening of

the aneurysmal wall in patients. We observed the wall of the resected AAA in detail in the clinic and found that the wall of RAAA had a distinctive three-layer color, and the color of the wall of the aneurysm gradually deepened, which may be the result of different pathological responses to different densities of thrombus. Therefore, we speculate that the different densities of thrombus shown on MSCTA within the AAA may also have different effects on the RAAA as well.

In our study, firstly, we measured the CT values of thrombus at the plane of MTD in AAA and found that the average CT values and maximum CT values of thrombus in the RAAA group were significantly higher than those in the IAAA group ($P < 0.05$), and the maximum CT values in the RAAA group were still higher than those in the IAAA group in different diameter ranges of the tumor ($P < 0.05$). This can be seen that the high-density thrombus shown by MSCTA in RAAA may be an important factor causing rupture. Our findings are similar to some studies. For example, some studies have found that local bleeding from ILT predicts AAA rupture (33, 34), which may be due to the imaging findings of contrast leakage after intra-thrombotic hemorrhage, or intra-thrombotic hemorrhage has a high level of attenuation (34). To verify its diagnostic performance, we further did the ROC curve of RAAA and found that the AUC of the maximum CT value at the plane of MTD was 0.848, while the AUC value of the combined MTD with the maximum CT value at its plane predicted RAAA up to 0.901, which was a good prediction. Most of the AAA rupture risk assessments in previous studies were based on the maximum diameter of the abdominal aorta (4, 5), ignoring the effect of intraluminal thrombus on it. Although in recent years studies have begun to show that thrombus negatively affects AAA rupture (29), our study found that its influence is mainly caused by high-density thrombus rather than low-density thrombus.

As AAA is a specific larger volume of sac lumen, this study also innovatively calculated the respective volumes of ILT in AAA according to different ranges of CT values for the first time, and compared their similarities and differences in IAAA and RAAA. Overall, the MTD and total volume in the lumen of the abdominal aorta were higher in the RAAA group than in the IAAA, suggesting that larger diameter aortic aneurysms were still a risk factor for rupture in our clinic, in agreement with previous findings (35).

To more precisely understand the effect of ILT on RAAA, our study also calculated the thrombus volume within the lumen of the AAA (subrenal to bilateral common iliac artery bifurcation) at the range of different CT values and found that the total thrombus volume in the RAAA group was higher than that in the IAAA group. And the thrombus volume in the range of 30 HU∼150 HU shown on MSCTA was higher in the RAAA group than in the IAAA group, while the thrombus volume in the range of −100 HU∼30 HU was not significantly different between the two groups, which may indicate that the main growth in RAAA is still dominated by high-density thrombus and interacts with the transverse diameter in the aneurysm. Although we did note that there was no statistical difference between the two groups in the thrombus/plaque in the >150 HU range shown by MSCTA, the comparison between the two groups was not significant because the volume was so small and may have been outlined to encompass the plaque or AAA wall and not only the ILT. In previous studies, low-density thrombus shown on MSCTA in patients with thoracic aortic aneurysms may have been responsible for distal intercostal artery embolism (18). This may be due to the fact that low-density thrombus is finer and more likely to dislodge into the distal artery, whereas our study suggests that high-density thrombus shown on MSCTA may be thicker and more conductive, which in turn contributes to AAA rupture. In this study, we calculated the standardized thrombus as to rule out the confounding factors brought by the total volume in the AAA lumen. The results showed that the thrombus volumes in the range of 30 HU∼150 HU and −100 HU∼30 HU were both positively correlated with the standardized thrombus volume in IAAA, whereas only the thrombus in the range of 30 HU∼150 HU was positively correlated with the standardized thrombus in RAAA. This suggests that the growth of thrombus in RAAA is dominated by high-density thrombus rather than low-density thrombus. In summary, the MTD combined with the maximum CT value at its plane predicts the occurrence of RAAA, and such a high-density thrombus may have a weakening effect on the aneurysm wall of AAA. Several mechanisms may explain this phenomenon here: (1) In contrast to low-density thrombus, whose sparseness is easily dislodged, MSCTA shows thicker high-density thrombus with higher shear rate (36) and stronger physiological force transduction (36–38); (2) High-density thrombus shown on MSCTA may be more isolated from neutrophils, cytokines, proteases, and reactive oxygen species than low-density thrombus (26); and (3) Increased high-density thrombus shown on MSCTA may accelerate apoptosis of active smooth muscle cells in the aortic wall and enhance local tissue hypoxia (39).

To our knowledge, this is the first report to address the association between thrombus in the range of different CT value and RAAA. Although the association between thrombus and RAAA has been clearly established (35, 40), our study further found that the MTD combined with the maximum CT value of thrombus at its plane predicted the occurrence of RAAA and high-density thrombus shown on MSCTA was closely associated with RAAA rather than low-density thrombus shown on MSCTA, which may provide a clinical rationale for delaying the progression of AAA or predicting precursor rupture of AAA in the future. In addition, compared with the previous reliance on CTA for imaging observation alone, this study provides an idea to study the potential association with RAAA by quantifying the combined MTD with thrombus CT values through MSCTA, which has the advantages of being objective, economic and reliable. Finally, there is a controversy

in the scientific community regarding anti-thrombus therapy for AAA (41), and in the study it was shown that high-density thrombus shown on MSCTA may be associated with RAAA. Anti-thrombus therapy will probably prevent the appearance of high-density thrombus or its further growth in volume and thus reduce the risk of rupture of AAA, which needs to be confirmed in future prospective studies with large samples.

There are several shortcomings that need to be carefully considered. Firstly, this is a retrospective single-center cross-sectional study without a sufficiently large sample, and prospective studies are needed to justify this; Secondly, a majority of patients with RAAA die before arriving at the hospital, so there is a possibility of selection bias; Thirdly, as almost all of the RAAA admitted to our center had aneurysm diameters >60 mm, there is a need for further research as to whether the different thrombus densities of small aneurysms (<55 mm) likewise negatively affect AAA rupture; Fourthly, as there was only 1 case of non-ILT in the RAAA at our hospital, we excluded all cases of non-ILT to prevent bias. Because of this, our study was only applied to AAA patients with ILT. Finally, although we believe that the high-density ILT shown on MSCTA is a factor associated with weakening of the aortic wall, we have no tissue studies in this study to demonstrate this.

Conclusion

High-density ILT shown on MSCTA in larger diameter AAA is associated with aneurysm rupture, and its MTD combined with the maximum CT value in its plane are a better predictor of RAAA. High-density ILT may be a major factor causing aortic wall degeneration and a characteristic of high-risk aneurysms, and anti-thrombus treatment of AAA associated with ILT may reduce the formation of high-density thrombosis, especially to provide a clinical basis for the current controversy in the scientific community regarding anti-thrombus treatment of AAAs.

Data availability statement

The original contributions presented in the study are included in the article/supplementary material, further inquiries can be directed to the corresponding authors.

Ethics statement

The study involving human participants was reviewed and approved by the Ethics Committee of Drum Tower Hospital (2022-556-01). Written informed consent from patients was not required for this retrospective study because the identifying information of patients was confidential.

Author contributions

HL and ZC were involved in data preparation, drafting of the original manuscript, and designed the study. HL performed the statistical analysis. CT is responsible for the data supplementation. JC was responsible for the clinical evaluation. HF and XM were responsible for the MSCTA in which the regions of interest were outlined. TQ revised and confirmed the final article. All authors contributed to the article and approved the submitted version.

Funding

This work was supported in part by the National Nature Science Foundation of China Grant (81870348).

Conflict of interest

The authors declare that the research was conducted in the absence of any commercial or financial relationships that could be construed as a potential conflict of interest.

Publisher's note

All claims expressed in this article are solely those of the authors and do not necessarily represent those of their affiliated organizations, or those of the publisher, the editors and the reviewers. Any product that may be evaluated in this article, or claim that may be made by its manufacturer, is not guaranteed or endorsed by the publisher.

References

1. Lesperance K, Andersen C, Singh N, Starnes B, Martin MJ. Expanding use of emergency endovascular repair for ruptured abdominal aortic aneurysms: disparities in outcomes from a nationwide perspective. *J Vasc Surg.* (2008) 47:1165–70; discussion 1170-1. doi: 10.1016/j.jvs.2008.01.055

2. NICE Evidence Reviews Collection [M]. Risk factors associated with abdominal aortic aneurysm growth or rupture. In: *Abdominal Aortic Aneurysm: Diagnosis and Management*. London: National Institute for Health and Care Excellence (NICE) (2020). Available online at: https://www.ncbi.nlm.nih.gov/books/NBK556914/

3. Yen Y, Wu FZ. Ruptured emphysematous infectious aortitis after endoprothesis placement. *QJM.* (2014) 107:943–4. doi: 10.1093/qjmed/hcu086

4. Moll FL, Powell JT, Fraedrich G, Verzini F, Haulon S, Waltham M, et al. Management of abdominal aortic aneurysms clinical practice guidelines of the European society for vascular surgery. *Eur J Vasc Endovasc Surg.* (2011) 41 (Suppl 1):S1–s58. doi: 10.1016/j.ejvs.2010.09.011

5. Thompson AR, Cooper JA, Ashton HA, Hafez H. Growth rates of small abdominal aortic aneurysms correlate with clinical events. *Br J Surg.* (2010) 97:37–44. doi: 10.1002/bjs.6779

6. Powell JT, Brady AR, Brown LC, Fowkes FG, Greenhalgh RM, Ruckley CV, et al. Long-term outcomes of immediate repair compared with surveillance of small abdominal aortic aneurysms. *N Engl J Med.* (2002) 346:1445–52. doi: 10.1056/NEJMoa013527

7. Lederle FA, Wilson SE, Johnson GR, Reinke DB, Littooy FN, Acher CW, et al. Immediate repair compared with surveillance of small abdominal aortic aneurysms. *N Engl J Med.* (2002) 346:1437–44. doi: 10.1056/NEJMoa012573

8. Phan L, Courchaine K, Azarbal A, Vorp D, Grimm C, Rugonyi S, et al. Geodesics-based surface parameterization to assess aneurysm progression. *J Biomech Eng.* (2016) 138:054503. doi: 10.1115/1.4033082

9. Buijs RV, Willems TP, Tio RA, Boersma HH, Tielliu IF, Slart RH, et al. Current state of experimental imaging modalities for risk assessment of abdominal aortic aneurysm. *J Vasc Surg.* (2013) 57:851–9. doi: 10.1016/j.jvs.2012.10.097

10. Thubrikar MJ, Robicsek F, Labrosse M, Chervenkoff V, Fowler BL. Effect of thrombus on abdominal aortic aneurysm wall dilation and stress. *J Cardiovasc Surg (Torino).* (2003) 44:67–77.

11. Wang DH, Makaroun MS, Webster MW, Vorp DA. Effect of intraluminal thrombus on wall stress in patient-specific models of abdominal aortic aneurysm. *J Vasc Surg.* (2002) 36:598–604. doi: 10.1067/mva.2002.126087

12. Vande Geest JP, Schmidt DE, Sacks MS, Vorp DA. The effects of anisotropy on the stress analyses of patient-specific abdominal aortic aneurysms. *Ann Biomed Eng.* (2008) 36:921–32. doi: 10.1007/s10439-008-9490-3

13. Khan JA, Abdul Rahman MN, Mazari FA, Shahin Y, Smith G, Madden L, et al. Intraluminal thrombus has a selective influence on matrix metalloproteinases and their inhibitors (tissue inhibitors of matrix metalloproteinases) in the wall of abdominal aortic aneurysms. *Ann Vasc Surg.* (2012) 26:322–9. doi: 10.1016/j.avsg.2011.08.015

14. Carrell TW, Burnand KG, Booth NA, Humphries J, Smith A. Intraluminal thrombus enhances proteolysis in abdominal aortic aneurysms. *Vascular.* (2006) 14:9–16. doi: 10.2310/6670.2006.00008

15. Kazi M, Thyberg J, Religa P, Roy J, Eriksson P, Hedin U, et al. Influence of intraluminal thrombus on structural and cellular composition of abdominal aortic aneurysm wall. *J Vasc Surg.* (2003) 38:1283–92. doi: 10.1016/S0741-5214(03)00791-2

16. Lee SE, Sung JM, Rizvi A, Lin FY, Kumar A, Hadamitzky M, et al. Quantification of coronary atherosclerosis in the assessment of coronary artery disease. *Circ Cardiovasc Imaging.* (2018) 11:e007562. doi: 10.1161/CIRCIMAGING.117.007562

17. Porcu M, Anzidei M, Suri JS, A Wasserman B, Anzalone N, Lucatelli P, et al. Carotid artery imaging: The study of intra-plaque vascularization and hemorrhage in the era of the "vulnerable" plaque. *J Neuroradiol.* (2020) 47:464–72. doi: 10.1016/j.neurad.2019.03.009

18. Banno H, Kawai Y, Sato T, Tsuruoka T, Sugimoto M, Kodama A, et al. Low-density vulnerable thrombus/plaque volume on preoperative computed tomography predicts for spinal cord ischemia after endovascular repair for thoracic aortic aneurysm. *J Vasc Surg.* (2021) 73:1557–65.e1. doi: 10.1016/j.jvs.2020.09.026

19. Motoyama S, Sarai M, Harigaya H, Anno H, Inoue K, Hara T, et al. Computed tomographic angiography characteristics of atherosclerotic plaques subsequently resulting in acute coronary syndrome. *J Am Coll Cardiol.* (2009) 54:49–57. doi: 10.1016/j.jacc.2009.02.068

20. Maier A, Gee MW, Reeps C, Eckstein HH, Wall WA. Impact of calcifications on patient-specific wall stress analysis of abdominal aortic aneurysms. *Biomech Model Mechanobiol.* (2010) 9:511–21. doi: 10.1007/s10237-010-0191-0

21. O'Leary SA, Kavanagh EG, Grace PA, McGloughlin TM, Doyle BJ. The biaxial mechanical behaviour of abdominal aortic aneurysm intraluminal thrombus: classification of morphology and the determination of layer and region specific properties. *J Biomech.* (2014) 47:1430–7. doi: 10.1016/j.jbiomech.2014.01.041

22. Sakalihasan N, Limet R, Defawe O D. Abdominal aortic aneurysm. *Lancet.* (2005) 365:1577–89. doi: 10.1016/S0140-6736(05)66459-8

23. Rahmani S, Alagheband M, Karimi A, Alizadeh M, Navidbakhsh M. Wall stress in media layer of stented three-layered aortic aneurysm at different intraluminal thrombus locations with pulsatile heart cycle. *J Med Eng Technol.* (2015) 39:239–45. doi: 10.3109/03091902.2015.1040173

24. Riveros F, Martufi G, Gasser TC, Rodriguez-Matas JF. On the impact of intraluminal thrombus mechanical behavior in AAA passive mechanics. *Ann Biomed Eng.* (2015) 43:2253–64. doi: 10.1007/s10439-015-1267-x

25. Domonkos A, Staffa R, Kubíček L. Effect of intraluminal thrombus on growth rate of abdominal aortic aneurysms. *Int Angiol.* (2019) 38:39–45. doi: 10.23736/S0392-9590.18.04006-3

26. Koole D, Zandvoort HJ, Schoneveld A, Vink A, Vos JA, van den Hoogen LL, et al. Intraluminal abdominal aortic aneurysm thrombus is associated with disruption of wall integrity. *J Vasc Surg.* (2013) 57:77–83. doi: 10.1016/j.jvs.2012.07.003

27. Wills A, Thompson MM, Crowther M, Sayers RD, Bell PR. Pathogenesis of abdominal aortic aneurysms–cellular and biochemical mechanisms. *Eur J Vasc Endovasc Surg.* (1996) 12:391–400. doi: 10.1016/S1078-5884(96)80002-5

28. Stenbaek J, Kalin B, Swedenborg J. Growth of thrombus may be a better predictor of rupture than diameter in patients with abdominal aortic aneurysms. *Eur J Vasc Endovasc Surg.* (2000) 20:466–9. doi: 10.1053/ejvs.2000.1217

29. Haller SJ, Crawford JD, Courchaine KM, Bohannan CJ, Landry GJ, Moneta GL, et al. Intraluminal thrombus is associated with early rupture of abdominal aortic aneurysm. *J Vasc Surg.* (2018) 67:1051–8.e1. doi: 10.1016/j.jvs.2017.08.069

30. Chang HJ, Lin FY, Lee SE, Andreini D, Bax J, Cademartiri F, et al. Coronary atherosclerotic precursors of acute coronary syndromes. *J Am Coll Cardiol.* (2018) 71:2511–22. doi: 10.1016/j.jacc.2018.02.079

31. Jinnouchi H, Sato Y, Sakamoto A, Cornelissen A, Mori M, Kawakami R, et al. Calcium deposition within coronary atherosclerotic lesion: Implications for plaque stability. *Atherosclerosis.* (2020) 306:85–95. doi: 10.1016/j.atherosclerosis.2020.05.017

32. Stark K, Massberg S. Interplay between inflammation and thrombosis in cardiovascular pathology. *Nat Rev Cardiol.* (2021) 18:666–82. doi: 10.1038/s41569-021-00552-1

33. Roy J, Labruto F, Beckman MO, Danielson J, Johansson G, Swedenborg J. Bleeding into the intraluminal thrombus in abdominal aortic aneurysms is associated with rupture. *J Vasc Surg.* (2008) 48:1108–13. doi: 10.1016/j.jvs.2008.06.063

34. Hans SS, Jareunpoon O, Balasubramaniam M, Zelenock GB. Size and location of thrombus in intact and ruptured abdominal aortic aneurysms. *J Vasc Surg.* (2005) 41:584–8. doi: 10.1016/j.jvs.2005.01.004

35. Talvitie M, Lindquist Liljeqvist M, Siika A, Hultgren R, Roy J. Localized hyperattenuations in the intraluminal thrombus may predict rupture of abdominal aortic aneurysms. *J Vasc Interv Radiol.* (2018) 29:144–5. doi: 10.1016/j.jvir.2017.07.028

36. Shi X, Yang J, Huang J, Long Z, Ruan Z, Xiao B, et al. Effects of different shear rates on the attachment and detachment of platelet thrombi. *Mol Med Rep.* (2016) 13:2447–56. doi: 10.3892/mmr.2016.4825

37. Qiu Y, Brown AC, Myers DR, Sakurai Y, Mannino RG, Tran R, et al. Platelet mechanosensing of substrate stiffness during clot formation mediates adhesion, spreading, and activation. *Proc Natl Acad Sci U S A.* (2014) 111:14430–5. doi: 10.1073/pnas.1322917111

38. Ciciliano JC, Tran R, Sakurai Y, Lam WA. The platelet and the biophysical microenvironment: lessons from cellular mechanics. *Thromb Res.* (2014) 133:532–7. doi: 10.1016/j.thromres.2013.12.037

39. Vorp DA, Lee PC, Wang DH, Makaroun MS, Nemoto EM, Ogawa S, et al. Association of intraluminal thrombus in abdominal aortic aneurysm with local hypoxia and wall weakening. *J Vasc Surg.* (2001) 34:291–9. doi: 10.1067/mva.2001.114813

40. Singh TP, Wong SA, Moxon JV, Gasser TC, Golledge J. Systematic review and meta-analysis of the association between intraluminal thrombus volume and abdominal aortic aneurysm rupture. *J Vasc Surg.* (2019) 70:2065–73.e10. doi: 10.1016/j.jvs.2019.03.057

41. Cameron SJ, Russell HM, Owens AP 3rd. Antithrombotic therapy in abdominal aortic aneurysm: beneficial or detrimental? *Blood.* (2018) 132:2619–28. doi: 10.1182/blood-2017-08-743237

frontiers | Frontiers in Cardiovascular Medicine

TYPE Case Report
PUBLISHED 08 November 2022
DOI 10.3389/fcvm.2022.976616

Check for updates

OPEN ACCESS

EDITED BY
Zhenjie Liu,
The Second Affiliated Hospital of Zhejiang University School of Medicine, China

REVIEWED BY
Yohei Kawatani,
Kumagaya General Hospital, Japan
Li Yin,
University of Virginia, United States

*CORRESPONDENCE
Fubo Song
yhdxgwk@126.com
Mu Yang
ymvascular@163.com

†These authors have contributed equally to this work and share first authorship

SPECIALTY SECTION
This article was submitted to General Cardiovascular Medicine, a section of the journal Frontiers in Cardiovascular Medicine

RECEIVED 23 June 2022
ACCEPTED 27 October 2022
PUBLISHED 08 November 2022

CITATION
Li L, Liu G, Yu B, Niu W, Pei Z, Zhang J, Che H, Song F and Yang M (2022) *In situ* repair or reconstruction of the abdominal aorta-iliac artery by autologous fascia-peritoneum with posterior rectus sheath for the treatment of the infected abdominal aortic and iliac artery aneurysms: A case series and literature review. *Front. Cardiovasc. Med.* 9:976616. doi: 10.3389/fcvm.2022.976616

COPYRIGHT
© 2022 Li, Liu, Yu, Niu, Pei, Zhang, Che, Song and Yang. This is an open-access article distributed under the terms of the Creative Commons Attribution License (CC BY). The use, distribution or reproduction in other forums is permitted, provided the original author(s) and the copyright owner(s) are credited and that the original publication in this journal is cited, in accordance with accepted academic practice. No use, distribution or reproduction is permitted which does not comply with these terms.

In situ repair or reconstruction of the abdominal aorta-iliac artery by autologous fascia-peritoneum with posterior rectus sheath for the treatment of the infected abdominal aortic and iliac artery aneurysms: A case series and literature review

Lubin Li†, Guolong Liu†, Benxiang Yu†, Wenqiang Niu, Zhigang Pei, Juwen Zhang, Haijie Che, Fubo Song* and Mu Yang*

Department of Vascular Surgery, Yantai Yuhuangding Hospital, Yantai, China

Background: Infected abdominal aortic and iliac artery aneurysms are considered acute and severe diseases with insidious onset, rapid development, and high mortality in vascular surgery. Currently, there is no better treatment, either anatomic or extra-anatomical repair.

Case presentation: From February 2018 to April 2022, 7 patients with infected abdominal aortic and iliac artery aneurysms did not have sufficient autologous venous material for repair. With the consent of the Ethics Committee of the hospital, it uses the autologous peritoneal fascial tissue with rectus sheath to repair or reconstruct the infected vessels *in situ*. There were 5 cases of infected abdominal aortic aneurysm, 1 case of an infected common iliac aneurysm, and 1 case of the infected internal iliac aneurysm. Aortoduodenal fistula was found in 3 cases, all of them were given duodenal fistula repair and gastrojejunostomy and cholecystostomy. Three cases of infected abdominal aortic aneurysms were repaired with the autologous peritoneal fascial tissue patch, and 2 cases of infected abdominal aortic aneurysms were reconstructed by the autologous peritoneal fascial tissue suture to bifurcate graft *in situ*, the autologous peritoneal fascial tissue suture reconstructed the rest 2 cases of infected iliac aneurysm to tubular graft *in situ*. It was essential that Careful debridement of all infected tissue and adequate postoperative irrigation and drainage. Antibiotics were administered perioperatively, and all patients were subsequently treated with long-term antibiotics based on bacterial culture and susceptibility results of infected tissues and blood. All 7 patients had underwent surgery successfully. But there were 2 cases died of anastomotic infection or massive hemorrhage after the operation, the other 5 cases survived. The

follow-up time was 2–19 months. The enhanced CT of postoperation showed that the reconstructed arteries were smooth without obvious stenosis or expansion, and no abdominal wall hernia occurred.

Conclusion: *In situ* repair or reconstruction with autologous peritoneal fascial tissue with rectus sheath is a feasible treatment for the infected aneurysm patients without adequate autologous venous substitute, but it still needs long-term follow-up and a large sample to be further confirmed.

KEYWORDS

infected aneurysm, autologous fascia-peritoneum with posterior rectus sheath, *in situ*, repair, reconstruction

Introduction

Infected aneurysm is an uncommon but fatal disease in the general population, with an incidence of 0.8–2% reported in the literature (1). Its most common site is the abdominal aorta, especially in the lower renal segment, followed by the thoracic aorta and iliac arteries. Some literatures have also reported infectious aneurysms of the coronary arteries, carotid arteries, and popliteal arteries (2–4). The classic triad of symptoms of infectious aneurysms is fever, local pain, and pulsatile mass. However, most patients often present with non-specific symptoms. Some patients with infectious aneurysms of the abdominal aorta and iliac arteries may present with abdominal pain, back pain, and infection, while others are not diagnosed until severe sepsis or aneurysm rupture occurs. Infected aneurysms, regardless of the location, are usually irreversible and have a high chance of rupture and mortality. Complete removal of the infected tissue along with *in situ* or extra-anatomic revascularization is recommended by current guidelines. Some papers have also reported effective cases using *in situ* reconstruction or endovascular aneurysm exclusion. Autologous veins, such as great saphenous vein and superficial femoral vein, are preferred as revascularization materials. However, some patients have insufficient autologous veins, such as those with varicose veins and venous insufficiency of the lower extremities.

We herein report 7 patients with infective abdominal aortic and iliac aneurysms who were treated in the past 4 years. All 7 patients were diagnosed with infected aneurysms based on blood culture and intraoperative infected tissue culture. After consulting the relevant literature, we employed autologous fascia-peritoneum with a posterior rectus sheath to repair or reconstruct blood supply *in situ* to treat infectious aneurysms.

Case presentation

From February 2018 to April 2022, 7 patients (5 men and 2 women, age: 60–74 years, mean age: 67.3 years) with infectious abdominal aortic and iliac aneurysms were treated with autologous fascia-peritoneum with a posterior rectus sheath. The chief complaint was fever with lower back and abdominal pain. The onset time varied from 1 day to 1 year (mean: 62.0 days). The sites of infection were abdominal aorta in 5 cases and iliac artery in the other 2 cases. In addition, diabetes mellitus was present in 4 cases, while hepatobiliary infectious disease was present in 3 cases (Table 1). The operation and prognosis are listed in Table 2.

Elective surgery was performed in 4 cases. In two cases (Cases 1 and 2), the site of the disease was the lower abdominal aorta. Among them, in case 1, a localized protrusion about 2 cm above the level of the rectus abdominis bifurcation was observed during surgery, severe adhesion between the duodenum and the inferior vena cava, necrotic infected tissue around the abdominal aorta was removed, a break was found after trimming the abdominal aortic wall, and the anterior wall of the abdominal aorta was repaired *in situ* using autologous peritoneal-fascial tissue with the posterior rectus sheath as a patch; in case 2, due to the wide range of abdominal aortic infection and severe adhesion of the surrounding tissue, infectious abdominal aortic aneurysm resection was decided during surgery. A bifurcated tubular *in situ* reconstruction of the abdominal aorta-bilateral iliac arteries were made using autologous peritoneal-fascial tissue suture with the posterior rectus sheath (Figure 1). The other 2 cases (Cases 3 and 4) were found to have abdominal aorta-duodenal fistulas, one of which (Case 3) had previously undergone EVAR at another hospital, during which significant stent exposure was observed after removing the necrotic tissue around the abdominal aorta. In contrast, a fistula was observed at the horizontal duodenum; after freeing the abdominal aortic fistula, the abdominal aortic stent graft was removed to remove the local arterial wall adhered to the abscess and edematous and to avoid stenosis and tear after the abdominal aortic suture, the infected abdominal aorta was reconstructed *in situ* using autologous peritoneal-fascial tissue with the posterior rectus sheath of the rectus abdominis muscle, duodenal fistula repair, gastrojejunostomy, and cholecystostomy. In the other case (Case 4), after local debridement of the abdominal aorta at the site

TABLE 1 General information of patients.

Case#	Age	Gender	Clinical manifestations	Onset time	Concomitant disease	Past medical/surgical history	Diagnosis	Infected site and aneurysm size
#1	60	M	Low back and abdominal pain	1 d	HP	Livestock history (sheep)	Infected abdominal aortic pseudoaneurysm	The maximum section of the lower abdominal aorta was about 3.4*2.6 cm
#2	69	M	Low back pain	1 m	HP	N	Infected abdominal aortic pseudoaneurysm	The maximum section of the lower abdominal aorta was about 4.3*4.7 cm
#3	67	F	Abdominal pain with fever	1 y	HP, DM, CAD, SS	History of EVAR (2 years ago), pneumonia (*Klebsiella pneumoniae*)	AAA stent infection	The maximum section of the lower abdominal aorta was about 4.6*5.3 cm
#4	62	M	Low back pain	22 d	HP, DM	History of liver abscess (prior to 1 month)	Infected abdominal aortic pseudoaneurysm	The maximum section of the lower abdominal aorta was about 7.0 * 6.5 cm
#5	74	F	Periumbilical pain with fever	7 d	HP, DM, CAD	N	Infected abdominal aortic pseudoaneurysm	The maximum section of the lower abdominal aorta was about 6.2*7.8 cm
#6	77	M	Fever with severe left flank pain	2 d	Cholelithiasis	Laparoscopic cholecystectomy, left hepatic lobectomy + choledochotomy + choledochojejunostomy	Infected left iliac aneurysm rupture	The maximum section of LCIA was about 5.8 * 5.4 cm
#7	62	M	Abdominal pain	7 d	DM	Gallstone	Infected left iliac pseudoaneurysm	The maximum section of LCIA was 5.6 * 6.0

M, Male; F, Female; d, day; m, month; y, year; HP, hypertension; DM, Diabetes mellitus; CAD, coronary atherosclerotic heart disease; SS, Sjogren Syndrome; AAA, abdominal aortic aneurysm; LCIA, Left common iliac arte.

10.3389/fcvm.2022.976616

TABLE 2 Perioperative and prognosis of patients.

Case#	Preoperative culture results	Timing of surgery	Surgical method	Autograft shape	Autograft size (length * width/diameter * length)	Aorto-gastrointestinal fistula	Infected tissue culture	Postoperative complications	ICU time	Hospital stay	Follow-up time	Prognosis	Cause of death
#1	*Brucella*	Limited procedure	Autologous fascia-peritoneum with posterior rectus sheath repair	Patch	1.0*3.0 cm	N	*Brucella*	No	1 d	39 d	29 m	Discharge	
#2	*Salmonella*	Limited procedure	Reconstruction of abdominal aorta and iliac artery with autologous fascia-peritoneum with posterior rectus sheath repair	Bifurcated tubular	1.5*12.0 cm, 1.0*5.0 cm	N	*Salmonella*	Renal dysfunction (recovered 6 days after CVVH)	10 d	40 d	23 m	Discharge	
#3	Multidrug-resistant *Escherichia coli*	Limited procedure	Stent graft removal, autologous fascia-peritoneum with posterior rectus sheath repair + duodenal fistula repair, gastrojejunostomy, cholecystostomy	Patch	2.0*2.0 cm	Y	Large intestine	No	2 d	58 d	15 m	Discharge	
#4	*Klebsiella pneumoniae*	Limited procedure	Autologous fascia-peritoneum with posterior rectus sheath repair + enterostomy	Patch	2.0*4.0 cm	Y	*Klebsiella pneumoniae*	Aortic repair site infection major bleeding	2 d	83 d	N	Death	Major bleeding at the aortic repair site 12 days after surgery
#5	*Salmonella*	Emergency surgery	Emergency EVAR for rupture; 12 days later, open stent removal, Reconstruction of abdominal aorto-iliac autologous fascia-peritoneum with posterior rectus sheath repair + duodenal fistula repair, gastrojejunostomy, and cholecystostomy	Bifurcated tubular	2.0*8.0 cm, 1.3*3.0 cm	Y	*Salmonella*, Large intestine	Gastrointestinal fistula, aortic anastomotic leakage	14 d	66 d	N	Death	Aortic anastomotic infection and massive hemorrhage 7 d after operation

(Continued)

10.3389/fcvm.2022.976616

TABLE 2 (Continued)

Case#	Preoperative culture results	Timing of surgery	Surgical method	Autograft shape	Autograft size (length * width/diameter * length)	Aorto-gastrointestinal fistula	Infected tissue culture	Postoperative complications	ICU time	Hospital stay	Follow-up time	Prognosis	Cause of death
#6	N	Emergency surgery	Reconstruction of left common iliac-external iliac artery autologous fascia-peritoneum with posterior rectus sheath repair	Tubular	1.0*5.0 cm	N	*Enterococcus faecium*	Gastroparesis, dysbacteriosis	3 d	24 d	19 m	Discharge	
#7	*Staphylococcus aureus*	Emergency surgery	Reconstruction of left common iliac-external iliac artery autologous fascia-peritoneum with posterior rectus sheath	Tubular	0.8*10.0 cm	N	*Staphylococcus aureus*	N	1 d	17 d	3 m	Discharge	

d, day; m, month; CVVH, continuous veno-venous hemofiltration.

FIGURE 1
Autologous fascia-peritoneum with a posterior rectus sheath was sutured for bifurcated tubular.

of infection, the horizontal part of the duodenum was invaded and ulcerated by the aneurysm. The pseudoaneurysm tumor was filled with a large amount of thrombus, necrotic material, and pus, which was completely removed and sent for bacterial culture. Exploration showed large damage of about 2 × 4 cm in the left wall of the middle abdominal aorta, and an autologous peritoneal-fascial tissue patch with a posterior rectus sheath was used to repair the defective abdominal aorta, followed by duodenal fistula repair and enterostomy.

In one case (case 6), EVAR was performed in the emergency department for rupture during hospitalization for anti-infection (day 39 after hospitalization). In this case, postoperative infection control was difficult (persistent fever, abdominal pain). Laparotomy was performed 12 days after surgery; during the operation, it was found that the posterior wall of the horizontal duodenum ruptured and communicated with the abdominal aortic aneurysm. The aneurysm cavity was filled with pus and necrotic material, and covered stents were observed. Hence, stent graft removal, abdominal aorto-bilateral iliac artery resection, and *in situ* reconstruction of the abdominal aorto-bilateral iliac artery + duodenal fistula repair using autologous fascia-peritoneum with a posterior rectus sheath to suture into a bifurcated tube, gastrojejunostomy, and cholecystostomy were performed.

An ultrasound evaluation of the deep and superficial veins of the lower extremities was carried out for all the above 5 patients underwent during their hospitalization. Of these, 2 patients had varicose veins of the lower extremities and 1 had a deep venous valve insufficiency, considering that the patient had venous insufficiency of the lower extremities and did not have sufficient autologous veins to achieve vascular reconstruction, peritoneal-fascial tissue with the posterior rectus sheath was selected for vascular reconstruction. During our

postoperative follow-up, it was found that the application of tissue to reconstruct the vascular morphology was good, so after communicating with the patient and his family in Case 3, we still selected the peritoneal-fascial tissue with the posterior rectus sheath for vascular reconstruction. In Case 2, due to the wide range of abdominal aortic infections more walls of the infected abdominal aorta were removed, the length of the vein required to reconstruct the arterial vessels was long, the damage to the lower limbs was large, and adequate caliber could not be ensured for vascular reconstruction. After communicating with the family, we selected the peritoneal-fascial tissue suture "Y" tubular structure with the posterior rectus sheath for vascular reconstruction.

There were 2 cases (cases 6 and 7) of emergency surgery for ruptured infectious aneurysms. Both patients had infected left iliac aneurysms and underwent aneurysm resection, removal of necrotic tissue, tubular reconstruction of the common iliac-external iliac artery *in situ* using autologous fascia-peritoneum with a posterior rectus sheath, suture of the distal internal iliac artery, and irrigation and drainage of the infected lesion. Because the procedure was urgent, the patient's leg veins could not be assessed to ensure smooth operation, and we did not use autologous vein vessels.

In all operations, the necrotic and infected tissue in the infected lesion was completely removed and 2–4 drainage tubes were placed to facilitate postoperative irrigation and drainage.

Five cases were found to be positive for bacterial culture. Therefore, sensitive antibiotics were selected for treatment based on the drug sensitivity test results. The infected tissue was used for bacterial culture, and sensitive antibiotics were used for treatment according to the culture susceptibility results. Bacterial culture results are detailed in Table 2.

The success rate of operation was 100%. The length of hospital stay was 17–83 days. The length of ICU stay was 1–14 days. One case showed postoperative renal insufficiency, which gradually improved after 6 days of paraclinoid hemofiltration. One case had dysbacteriosis, which was improved after adjusting antibiotics and probiotics. Two patients died during hospitalization owing to postoperative massive hemorrhage of the abdominal aortic repair site, which occurred on the 7 and 12th day after operation, respectively. The remaining 5 cases were successfully discharged, and anti-inflammatory drugs were continued after the discharge. The postoperative follow-up period was 3–29 months. The re-examination of CTA suggested that the patency of *in situ* repair or reconstruction vessels was good, no rumen dilatation and severe stenosis were observed, and no abdominal hernia occurred.

In case 4, the patient had sudden abdominal pain 12 days after surgery and underwent emergency surgical treatment, during which bleeding from the abdominal aortic anastomosis was found, and emergency endovascular graft exclusion of the abdominal aorta was performed. Postoperatively, the patient developed chills and hyperpyrexia, and blood cultures showed gram-positive cocci and gram-negative bacilli. He developed massive hematemesis 16 days after the second operation and subsequently died of respiratory arrest, and the cause of death was considered to be the re-rupture of the aneurysm due to bacterial infection. In case 5, the duodenal fistula was damaged after the operation, a large amount of digestive juice was drained, and the patient died of abdominal aortic rupture and bleeding 1 week after the operation. The cause of death was considered to be that the reconstructed abdominal aorta was corroded by digestive juice resulting in a recurrence of rupture.

Discussion and conclusions

Infected aneurysms are caused by bacteria or fungi entering vascular lesions or those growing on the intima of blood vessels through hematogenous spread, lymphatic transmission, infection of adjacent tissues around blood vessels, and so on **(author?)** (5). The chief predisposing factors are acquired or innate immunodeficiency, intravascular drug use, and pre-existing defects in the arterial wall. The most common pathogens causing infectious aneurysms are *Staphylococcus aureus*, *Salmonella*, *Streptococcus*, and *Escherichia coli*, and in some specific cases, *Staphylococcus epidermidis*, *Klebsiella*, *Haemophilus influenzae*. *Mycobacterium tuberculosis* can also cause infectious aneurysms (6). However, 14–40% of patients diagnosed with an infective aneurysm still do not have an identified causative organism (7). Contrast-enhanced CT is the most commonly used imaging method for early detection of infectious aneurysms, characterized by irregularly shaped aneurysms, which may be polycystic, with gas shadows or low-density shadows in the soft tissues around the aorta and irregular peripheral enhancement of the arterial wall.

Surgical treatment of infective aneurysms often involves open surgical repair of the infected segmental artery, extensive removal of the surrounding tissue, arterial revascularization by using an orthotopic graft replacement or extra-anatomic bypass (EAB), followed by an aggressive antibiotic therapy. Although surgical open surgery has long been considered an effective treatment for infected aneurysms, there is no consensus on *in situ* graft replacement or EAB for arterial revascularization. In addition, the use of foreign grafts in infected areas violates the basic principles of surgery and is a controversial strategy (8–10).

Commonly used grafts in surgery are Dacron or polytetrafluoroethylene vascular prostheses soaked in antibiotics, bovine pericardium, cryopreserved allografts, and autologous superficial femoral and jugular veins (11–14). Batt et al. (15) conducted a meta-analysis of patient age and reported the presence of prosthetic duodenal fistula (PDF). They also showed that the presence of virulent or non-virulent microbial factors indicated that combined *in situ* reconstruction of each factor was superior to extra-anatomic bypass reconstruction of the arterial blood supply. In a

comparative analysis of cryopreserved allografts, autologous veins, and vascular grafts (silver polyester; rifampin) for infected aneurysms treated through *in situ* reconstruction surgery, the latter showed the most severe reinfection rate. Autologous veins had the lowest reinfection rate, while allografts had a higher postoperative anti-infective ability than that of the vascular grafts (16). It has been reported that the use of biological grafts is a reliable option for open repair of infected aneurysms because of its anti-infective ability and high survival rate (17). Heinola et al. (18) reported 1- and 5-year postoperative survival rates of 83 and 71%, respectively, for patients with infected aneurysms treated by using biological grafts. For larger vessels, the autologous vein does not have a sufficient caliber and resistance to perform revascularization. It is also difficult to operate when the autologous vein is sampled. Moreover, the operation time is too long for elderly patients to tolerate (19, 20). The use of allografts shortens the operation time and reduces surgical trauma. However, availability, cost, and graft-related complications (aneurysmal degeneration, dilatation, rupture, and reinfection) caused by graft degradation have limited the widespread use of allografts.

Sarac et al. (21) successfully repaired the aortic stump using autologous fascia-peritoneum tissue with abdominal aortic graft infection. They were also able to avoid postoperative rupture of the aortic stump. Embryologically, the peritoneum and fascia are derived from the cells similar to the endothelial and adventitial layers of blood vessels, respectively. The peritoneum develops from the mesoderm comprising mesothelial cells and connective tissue and contains blood vessels, lymphatic vessels, and nerves (22). Its adipose tissue contains a large number of mesenchymal stem cells and can differentiate into other cell types. Peritoneal mesothelial cells also have a certain degree of plasticity. These characteristics allow the use of the peritoneum for regenerative therapy (23, 24). The rectus fascial layer is composed of collagen. It is a tough connective tissue with good resistance to stress (21). The autologous fascia-peritoneum tissue is a highly viable and easily accessible tissue. Hence, it is an ideal vascular substitute. Pacholewicz et al. (25) successfully used the autologous fascia-peritoneum tissue as a patch on the pericardium of mongrel dogs and achieved satisfactory results as a pericardial substitute. They also demonstrated the antithrombotic properties of the peritoneum. Sarac et al. (26) demonstrated the ability of the fascia-peritoneum tissue to withstand continuous arterial pressure, good compliance, and resistance to intimal hyperplasia. García-Graz et al. (27) conducted animal experiments and showed that the fascia-peritoneum with posterior rectus sheath has good permeability and antithrombotic properties as a vascular graft.

The Chin et al. (28) study published the first autogenous peritoneo-fascial for repair after partial resection of the inferior vena cava in six patients; in 2013, the same team republished a study of 22 patients who underwent autogenous peritoneo-fascial transplantation to reconstruct the inferior vena cava (29). In the late follow-up of both studies, the conclusions were similar and the ideal surgical results were obtained. Dokmak et al. (30) showed that autogenous peritoneo-fascial tissue was also used to repair other abdominal veins, such as the hepatic and portal veins. Emmiler et al. (31) showed repair of vascular injuries following abdominal trauma with autogenous peritoneo-fascial tissue and since then provided a new treatment modality for vascular injury repair. In the study by Chin et al. (28) the authors highlight the advantages of the autogenous peritoneo-fascial patch in the repair of partial inferior vena cava resection, which has better flexibility, usability, reduces the risk of infection and thrombosis, is available in a short time and costs less, and can also be used immediately in emergencies compared to traditional repair techniques.

Antibiotics play a crucial role in the treatment of patients with infectious aneurysms, although the duration of antibiotic application is a matter of debate (32). An appropriate preoperative antibiotic therapy can not only control the inflammation, but can also effectively reduce periaortic adhesions, more easily debride perivascular infected tissue, and increase the success rate of orthotopic vascular graft replacement (1, 33). Kritpracha et al. (34) reported on 21 patients with infective aneurysms who were treated preoperatively with antibiotics for an average period of 10 days and reported a 30-day patient mortality rate of 19%. Sedivy et al. (35) preoperatively treated 32 patients with infective aneurysms using antibiotics for an average period of 16 days, and reported a 30-day patient mortality rate of 18%. Clough et al. (36) treated 11 patients with infective aneurysms using preoperative antibiotics for an average period of 42 days; the 30-day mortality rate was 11.1%. Di et al. (37) showed that the duration of preoperative antibiotic therapy was strongly associated with the 30-day mortality. For the duration of post-operative antibiotic therapy, most studies recommend at least 6 weeks of post-operative intravenous or oral antibiotic therapy (36, 38); for patients with abnormal inflammatory markers, a longer antibiotic therapy or even a lifelong oral antibiotic therapy is recommended (39, 40).

Among our 7 patients with infected aneurysms, 5 had infected abdominal aortic aneurysm, 1 had infected common iliac artery aneurysm, and the remaining 1 had infected internal iliac artery aneurysm. Because there was no suitable autologous vein for repair, we used autologous fascia-peritoneum with a posterior rectus sheath to repair or reconstruct the infected vessels *in situ*. The infected abdominal aortic aneurysms in 3 patients were repaired with an autologous fascia-peritoneum tissue patch, while the remaining 2 cases were treated with the autologous fascia-peritoneum tissue suture component forked *in situ* to reconstruct the abdominal aorta-bilateral iliac arteries. Two patients with infected iliac aneurysms were treated with autologous fascia-peritoneum tissue suture to reconstruct *in situ* tubular iliac arteries. All of them were covered with the greater omentum after reconstruction and were adequately irrigated and drained after surgery. Perioperatively, all patients underwent

long-term antibiotic therapy based on the bacterial culture and susceptibility results of the infected tissue and blood. All 7 patients had a successful operation. Two patients died of anastomotic infection and massive hemorrhage after surgery; the remaining 5 patients survived. The patients were followed up for 2–19 months. The postoperative enhanced CT scan showed that the reconstructed artery was smooth, without any obvious stenosis or dilatation, and no abdominal hernia occurred.

Autologous fascia-peritoneum with a posterior rectus sheath can fight infections, in contrast to foreign grafts. In our study, 5 patients survived with a good survival rate. When autologous veins or foreign grafts cannot meet the surgical needs, they become a viable arterial substitute, which also provides a feasible treatment for refractory infectious aneurysms. However, long-term follow-up and large-scale clinical data are still needed to further confirm the feasibility of the treatment.

Data availability statement

The original contributions presented in the study are included in the article/supplementary material, further inquiries can be directed to the corresponding authors.

Ethics statement

The studies involving human participants were reviewed and approved by the Ethics committee of the Yantai Yuhuangding Hospital. The patients/participants provided their written informed consent to participate in this study. Written informed consent was obtained from the individual(s) for the publication of any potentially identifiable images or data included in this article.

Author contributions

FS and MY: conception and design and revision of manuscript. WN, ZP, JZ, and HC: collection and assembly of data. LL, GL, and BY: data analysis and interpretation and manuscript writing. All authors contributed to the article and approved the submitted version.

Conflict of interest

The authors declare that the research was conducted in the absence of any commercial or financial relationships that could be construed as a potential conflict of interest.

Publisher's note

All claims expressed in this article are solely those of the authors and do not necessarily represent those of their affiliated organizations, or those of the publisher, the editors and the reviewers. Any product that may be evaluated in this article, or claim that may be made by its manufacturer, is not guaranteed or endorsed by the publisher.

References

1. Müller BT, Wegener OR, Grabitz K, Pillny M, Thomas L, Sandmann W. Mycotic aneurysms of the thoracic and abdominal aorta and iliac arteries: experience with anatomic and extra-anatomic repair in 33 cases. *J Vasc Surg.* (2001) 33:106–13. doi: 10.1067/mva.2001.110356

2. Fernández Guerrero ML, Aguado JM, Arribas A, Lumbreras C, de Gorgolas M. The spectrum of cardiovascular infections due to Salmonella enterica: a review of clinical features and factors determining outcome. *Medicine (Baltimore).* (2004) 83:123–38. doi: 10.1097/01.md.0000125652.75260.cf

3. Nader R, Mohr G, Sheiner NM, Tampieri D, Mendelson J, Albrecht S. Mycotic aneurysm of the carotid bifurcation in the neck: case report and review of the literature. *Neurosurgery.* (2001) 48:1152–6. doi: 10.1097/00006123-200105000-00041

4. Alonso-Bartolomé P, Alonso Valle H, Aurrecoechea E, Acha O, Blanco R, Martínez-Taboada VM, et al. Mycotic (infected) aneurysm of the popliteal artery and arthritis following Salmonella bacteriemia. *Clin Exp Rheumatol.* (2001) 19:325–8.

5. Behzadnia N, Ahmadi ZH, Mandegar MH, Salehi F, Sharif-Kashani B, Pourabdollah M, et al. Asymptomatic mycotic aneurysm of ascending aorta after heart transplantation: a case report. *Transplant Proc.* (2015) 47:213–6. doi: 10.1016/j.transproceed.2014.10.036

6. Hsu RB, Lin FY. Infected aneurysm of the thoracic aorta. *J Vasc Surg.* (2008) 47:270–6. doi: 10.1016/j.jvs.2007.10.017

7. Kakuta R, Yano H, Kanamori H, Shimizu T, Gu Y, Hatta M, et al. Helicobacter cinaedi infection of abdominal aortic aneurysm, Japan. *Emerg Infect Dis.* (2014) 20:1942–5. doi: 10.3201/eid2011.140440

8. Lee CH, Hsieh HC, Ko PJ, Li HJ, Kao TC, Yu SY. In situ versus extra-anatomic reconstruction for primary infected infrarenal abdominal aortic aneurysms. *J Vasc Surg.* (2011) 54:64–70. doi: 10.1016/j.jvs.2010.12.032

9. Sugimoto M, Banno H, Idetsu A, Matsushita M, Ikezawa T, Komori K. Surgical experience of 13 infected infrarenal aortoiliac aneurysms: preoperative control of septic condition determines early outcome. *Surgery.* (2011) 149:699–704. doi: 10.1016/j.surg.2010.12.015

10. Youn JK, Kim SM, Han A, Choi C, Min SI, Ha J, et al. Surgical treatment of infected aortoiliac aneurysm. *Vasc Specialist Int.* (2015) 31:41–6. doi: 10.5758/vsi.2015.31.2.41

11. Chiesa R, Astore D, Piccolo G, Melissano G, Jannello A, Frigerio D, et al. Fresh and cryopreserved arterial homografts in the treatment of prosthetic graft infections: experience of the Italian collaborative vascular homograft group. *Ann Vasc Surg.* (1998) 12:457–62. doi: 10.1007/s100169900184

12. Verma H, Mohan S, Tripathi RK. Pantaloon femoral vein graft as "neoaorta" in infected aortic disease. *J Vasc Surg.* (2015) 62:1083–8. doi: 10.1016/j.jvs.2015.05.010

13. Ahle SL, Cardella JA, Cleary MA, Stitelman DH, Sarac TP, Caty MG. Repair of a mycotic abdominal aortic aneurysm in a neonate using an everted jugular vein patch. *J Vasc Surg Cases Innov Tech.* (2017) 3:218–20. doi: 10.1016/j.jvscit.2017.08.003

14. Sang G, Guo X, Liu G, Che H. In situ reconstruction of ruptured mycotic iliac artery aneurysm with autologous fascial-peritoneal tissue: a case report and literature review. *BMC Surg.* (2022) 22:70. doi: 10.1186/s12893-022-01523-0

15. Batt M, Feugier P, Camou F, Coffy A, Senneville E, Caillon J, et al. A meta-analysis of outcomes after *in situ* reconstructions for aortic graft infection. *Angiology.* (2018) 69:370–9. doi: 10.1177/0003319717710114

16. Chakfé N, Diener H, Lejay A, et al. Editor's choice - European society for vascular surgery (ESVS) 2020 clinical practice guidelines on the management of vascular graft and endograft infections. *Eur J Vasc Endovasc Surg.* (2020) 59:339–84. doi: 10.1016/j.ejvs.2019.10.016

17. Jones KG, Bell RE, Sabharwal T, Aukett M, Reidy JF, Taylor PR. Treatment of mycotic aortic aneurysms with endoluminal grafts. *Eur J Vasc Endovasc Surg.* (2005) 29:139–44. doi: 10.1016/j.ejvs.2004.11.008

18. Heinola I, Sörelius K, Wyss TR, Eldrup N, Settembre N, Setacci C, et al. Open repair of mycotic abdominal aortic aneurysms with biological grafts: an international multicenter study. *J Am Heart Assoc.* (2018) 7:e008104. doi: 10.1161/JAHA.117.008104

19. Dorweiler B, Neufang A, Chaban R, Reinstadler J, Duenschede F, Vahl CF. Use and durability of femoral vein for autologous reconstruction with infection of the aortoiliofemoral axis. *J Vasc Surg.* (2014) 59:675–83. doi: 10.1016/j.jvs.2013.09.029

20. Heinola I, Kantonen I, Jaroma M, Albäck A, Vikatmaa P, Aho P, et al. Editor's choice - treatment of aortic prosthesis infections by graft removal and *in situ* replacement with autologous femoral veins and fascial strengthening. *Eur J Vasc Endovasc Surg.* (2016) 51:232–9. doi: 10.1016/j.ejvs.2015.09.015

21. Sarac TP, Augustinos P, Lyden S, Ouriel K. Use of fascia-peritoneum patch as a pledget for an infected aortic stump. *J Vasc Surg.* (2003) 38:1404–6. doi: 10.1016/s0741-5214(03)01039-5

22. Yung S, Li FK, Chan TM. Peritoneal mesothelial cell culture and biology. *Perit Dial Int.* (2006) 26:162–73.

23. Gotloib L, Gotloib LC, Khrizman V. The use of peritoneal mesothelium as a potential source of adult stem cells. *Int J Artif Organs.* (2007) 30:501–12. doi: 10.1177/039139880703000608

24. Rosellini A, Michelini M, Tanda G, Mandys V, Revoltella RP. Expansion of human mesothelial progenitor cells in a longterm three-dimensional organotypic culture of processus vaginalis peritonei. *Folia Biol.* (2007) 53:50–7.

25. Pacholewicz JK, Daloisio C, Shawarby OA, Dharan SM, Gu J, McGrath LB. Efficacy of autologous peritoneum as a biological membrane in cardiac surgery. *Eur J Cardiothorac Surg.* (1994) 8:563–5. doi: 10.1016/1010-7940(94)90077-9

26. Sarac TP, Carnevale K, Smedira N, Tanquilut E, Augustinos P, Patel A, et al. *In vivo* and mechanical properties of peritoneum/fascia as a novel arterial substitute. *J Vasc Surg.* (2005) 41:490–7. doi: 10.1016/j.jvs.2004.11.033

27. García-Graz NJ, Galindo-Ibarra JL, García-Soto G, Mejía-Arreguín H, Trejo-Suárez J, Ramírez-Salas MA. Injerto vascular de aponeurosis con peritoneo en perros. *Cir Cir.* (2008) 76:235–9.

28. Chin PT, Gallagher PJ, Stephen MS. Inferior vena caval resection with autogenous peritoneo-fascial patch graft caval repair: a new technique. *Aust N Z J Surg.* (1999) 69:391–2. doi: 10.1046/j.1440-1622.1999.01579.x

29. Pulitanó C, Crawford M, Ho P, Gallagher J, Joseph D, Stephen M, et al. The use of biological grafts for reconstruction of the inferior vena cava is a safe and valid alternative: results in 32 patients in a single institution. *HPB (Oxford).* (2013) 15:628–32. doi: 10.1111/hpb.12029

30. Dokmak S, Aussilhou B, Sauvanet A, Nagarajan G, Farges O, Belghiti J. Parietal peritoneum as an autologous substitute for venous reconstruction in hepatopancreatobiliary surgery. *Ann Surg.* (2015) 262:366–71. doi: 10.1097/SLA.0000000000000959

31. Emmiler M, Kocogullari CU, Yilmaz S, Cekirdekci A. Repair of the inferior vena cava with autogenous peritoneo-fascial patch graft following abdominal trauma: a case report. *Vasc Endovascular Surg.* (2008) 42:272–5. doi: 10.1177/1538574407311604

32. Kim YW. Infected aneurysm: current management. *Ann Vasc Dis.* (2010) 3:7–15. doi: 10.3400/avd.AVDctiia09003

33. Aoki C, Fukuda W, Kondo N, Minakawa M, Taniguchi S, Daitoku K, et al. Surgical management of mycotic aortic aneurysms. *Ann Vasc Dis.* (2017) 10:29–35. doi: 10.3400/avd.oa.16-00117

34. Kritpracha B, Premprabha D, Sungsiri J, Tantarattanapong W, Rookkapan S, Juntarapatin P. Endovascular therapy for infected aortic aneurysms. *J Vasc Surg.* (2011) 54:1259–65. doi: 10.1016/j.jvs.2011.03.301

35. Sedivy P, Spacek M, El Samman K, Belohlavek O, Mach T, Jindrak V, et al. Endovascular treatment of infected aortic aneurysms. *Eur J Vasc Endovasc Surg.* (2012) 44:385–94. doi: 10.1016/j.ejvs.2012.07.011

36. Clough RE, Black SA, Lyons OT, Zayed HA, Bell RE, Carrell T, et al. Is endovascular repair of mycotic aortic aneurysms a durable treatment option? *Eur J Vasc Endovasc Surg.* (2009) 37:407–12. doi: 10.1016/j.ejvs.2008.11.025

37. Di X, Liu C, Zeng R, Ni L. Endovascular aortic repair is a viable strategy for treatment of primary infected abdominal aortic aneurysm. *Ann Vasc Surg.* (2020) 63:117–28. doi: 10.1016/j.avsg.2018.12.080

38. Laohapensang K, Aworn S, Orrapi S, Rutherford RB. Management of the infected aortoiliac aneurysms. *Ann Vasc Dis.* (2012) 5:334–41. doi: 10.3400/avd.oa.12.00014

39. Hsu PJ, Lee CH, Lee FY, Liu JW. Clinical and microbiological characteristics of mycotic aneurysms in a medical center in southern Taiwan. *J Microbiol Immunol Infect.* (2008) 41:318–24.

40. Laohapensang K, Rutherford RB, Arworn S. Infected aneurysm. *Ann Vasc Dis.* (2010) 3:16–23. doi: 10.3400/avd.AVDctiia09002

frontiers | Frontiers in Cardiovascular Medicine

TYPE Original Research
PUBLISHED 10 November 2022
DOI 10.3389/fcvm.2022.967614

Check for updates

OPEN ACCESS

EDITED BY
Zhenjie Liu,
The Second Affiliated Hospital of Zhejiang University School of Medicine, China

REVIEWED BY
Wenjie Tian,
Massachusetts General Hospital and Harvard Medical School, United States
Amirhesam Babajani,
Iran University of Medical Sciences, Iran

*CORRESPONDENCE
Jiang Xu
xujiang81@163.com

SPECIALTY SECTION
This article was submitted to General Cardiovascular Medicine, a section of the journal Frontiers in Cardiovascular Medicine

RECEIVED 13 June 2022
ACCEPTED 27 October 2022
PUBLISHED 10 November 2022

CITATION
Luo H, Yang X, Chen K, Lan S, Liao G and Xu J (2022) Blood creatinine and urea nitrogen at ICU admission and the risk of in-hospital death and 1-year mortality in patients with intracranial hemorrhage.
Front. Cardiovasc. Med. 9:967614.
doi: 10.3389/fcvm.2022.967614

COPYRIGHT
© 2022 Luo, Yang, Chen, Lan, Liao and Xu. This is an open-access article distributed under the terms of the Creative Commons Attribution License (CC BY). The use, distribution or reproduction in other forums is permitted, provided the original author(s) and the copyright owner(s) are credited and that the original publication in this journal is cited, in accordance with accepted academic practice. No use, distribution or reproduction is permitted which does not comply with these terms.

Blood creatinine and urea nitrogen at ICU admission and the risk of in-hospital death and 1-year mortality in patients with intracranial hemorrhage

Hai Luo[1], Xuanyong Yang[1], Kang Chen[1], Shihai Lan[1], Gang Liao[2] and Jiang Xu[1]*

[1]Department of Neurosurgery, The First Affiliated Hospital, Nanchang University, Nanchang, China, [2]Institute of Medicine, Nanchang University, Nanchang, China

Background: The relationship between renal function and clinical outcomes in patients with intracranial hemorrhage is controversial.

Aims: We investigated the associations of blood creatinine and urea nitrogen levels with hospital death and 1-year mortality in patients with intracranial hemorrhage treated in the intensive care unit (ICU).

Methods: A total of 2,682 patients with intracranial hemorrhage were included from the Medical Information Mart for Intensive Care III (MIMIC-III) database. Clinical variables, including admission creatinine, urea nitrogen, type of intracranial hemorrhage, underlying diseases and other blood biochemistry parameters, were collected. Multivariable correction analysis was conducted of the relationships between blood creatinine and urea nitrogen levels on admission with hospital death and 1-year mortality in the included patients with intracranial hemorrhage. Smooth curve and subgroup analyses were also performed for these associations.

Results: A total of 2,682 patients had their blood creatinine and urea nitrogen levels measured within the first 24 h after ICU admission, with median values of 0.80 and 15.00 mg/dL, respectively. We observed steeply linear relationships between creatinine and urea nitrogen levels and the risk of in-hospital death and 1-year mortality, but the risk of in-hospital mortality and 1-year mortality increased little or only slowly above creatinine levels $>$ 1.9 mg/dL or urea nitrogen $>$ 29 mg/d (the inflection points). Consistently, conditional logistic regression analysis suggested that these inflection points had significant modification effects on the associations between blood creatinine levels, as well as blood urea nitrogen, and the risk of in-hospital death (interaction value $<$ 0.001) and 1-year mortality (interaction value $<$ 0.001).

Conclusion: Our results supported the hypothesis that elevated blood creatinine and urea nitrogen levels on admission are associated with an increased risk of in-hospital death and 1-year mortality in patients with

intracranial hemorrhage. Interestingly, these independent relationships existed only for lower levels of serum creatinine (<1.9 mg/dL) and uric acid (<29 mg/dL).

KEYWORDS

intracerebral hemorrhage, creatinine, urea nitrogen, hospital death, 1-year mortality

Introduction

Some known chronic diseases, such as hypertension, cardiac disease and diabetes, and unhealthy lifestyles, including smoking, drinking and a high-fat diet, have been found to contribute to a high stroke risk (1). Renal dysfunction has been considered a critical indicator of adverse clinical outcomes, including stroke (2, 3).

Blood creatinine and urea nitrogen, as the key indices used to evaluate renal function, play an important role in assessing the severity of the status of intensive care unit (ICU) patients, especially after cardiovascular events (4). For instance, chronic kidney disease (CKD) was found to be associated with a higher rate of adverse clinical outcomes and mortality risk, and elevated blood creatinine levels had good value in predicting short-term and long-term mortality in patients with hemorrhagic and ischemic stroke (5, 6). Previous studies also reported that admission dehydration status was independently related to an increased risk of 30-day mortality (7). Conversely, one previous study unexpectedly found that the admission estimated glomerular filtration rate (eGFR) in patients with intracranial hemorrhage, calculated using serum creatinine according to the Modification of Diet in Renal Disease (MDRD) equation, was not associated with in-hospital mortality (8). Other clinical studies have reported that admission dehydration and a blood urea-to-creatinine ratio > 80 significantly contribute to a reduced risk of in-hospital mortality in older patients with acute intracranial hemorrhage (9). The inconsistent findings among studies might be caused by populations with various age groups, different sample sizes, different stroke types, different concomitant diseases, different measurement times of serum parameters and other confounding variables. For example, malignant tumors may increase short-term mortality in patients with cardiovascular events (10). Stoke patients with intracranial hemorrhage in different parts of the brain have obviously different prognoses (11). More importantly, follow-up studies with large samples on the association between renal function and mortality risk in patients with intracranial hemorrhage are scarce.

Given the current research evidence, we collected data from a total of 2,682 ICU patients from the Medical Information Mart for Intensive Care III (MIMIC-III) database. The MIMIC-III database included enough patients with intracranial hemorrhage, and data for clinical variables, including comorbidities and blood biochemical parameters, were collected. The present study investigated and further verified the associations of blood creatinine and urea nitrogen levels on admission with intracranial hemorrhage-associated in-hospital death and 1-year mortality in ICU patients with intracranial hemorrhage.

Materials and methods

Study population

The MIMIC III (v1.4) database was used for the present study. As a single-center critical care database, the MIMIC-III is publicly available and was approved for use by the Institutional Review Boards of the Massachusetts Institute of Technology (MIT, Cambridge, MA, USA) and Beth Israel Deaconess Insurance Center (BIDMC, Boston, MA, USA). Written informed consent was obtained from each patient based on the Declaration of Helsinki guidelines.

The database contains detailed clinical information, including clinical variables such as demographic characteristics, vital signs, vital status and laboratory tests, on 46,520 patients admitted to various ICUs of the BIDMC from 2001 to 2012 in Boston, Massachusetts (12). ICU nurses recorded the physiological data obtained from bedside monitors hourly. International Classification of Diseases and Ninth Revision (ICD-9) codes were used for disease diagnosis in the present study. The use of data from this database is not considered as human subject research, and there is no requirement for patient consent due to the anonymized health information. However, users (scientific researchers) need to pass an examination to register for use of the database and must be approved by the administration staff of the MIMIC-III database. The users are allowed to use the database to extract data for study analysis only after passing the "Protecting Human Research Participants" course available on the National Institutes of Health (NIH) website.

Subject selection

ICU patients included in the MIMIC-III database who experienced intracranial hemorrhage were enrolled in our study. Intracranial hemorrhage was caused by various etiologies, including head trauma, spontaneous intracranial hemorrhage and unknown causes, according to ICD-9 codes. First, to ensure the accuracy of the review, we excluded all patients aged < 18 years and >90 years or those who had important missing variables due to common missing data in the MIMIC-III database. Then, all patients for whom initial creatinine and urea nitrogen measurements were completed within the first 24 h after ICU admission were included. In addition, we only analyzed the first ICU stay for patients who were admitted to the ICU more than once. We used the first recorded value of clinical characteristics in the ICU.

Variable extraction

The initial exposure variables were whether these ICU patients experienced "intracranial hemorrhage". Structured query language (SQL) was used. The first recorded value of clinical characteristics at baseline during the ICU stay were obtained, including age, sex, length of ICU stay, insurance status, ICU type, type of intracranial hemorrhage, head trauma, comorbidities, blood test parameters and medications.

Blood test parameters, including creatinine, urea nitrogen, sodium, potassium, phosphate, magnesium, total calcium, chloride, glucose, partial thromboplastin time (PTT), prothrombin time (PT), international normalized ratio (INR), red blood cell count, platelet count, white blood cell count and bicarbonate, were tested within the first 24 h after ICU admission. If these blood variables were recorded more than once in the first 24 h, we used the first recorded value.

The type of intracranial hemorrhage mainly included "intracerebral," "extradural," "subdural," "unspecified intracranial," "subarachnoid," and "multiple." Head trauma was defined as "yes" or "no". ICU types included cardiology care unit (CCU), cardiovascular surgery rehabilitation unit (CSRU), insurance intensive care unit (MICU), surgical intensive care unit (SICU) and trauma/surgical intensive care unit (TSICU). Medications mainly included vasopressin, nitrate esters, β receptor blockers, benzodiazepines, statins and potassium. Additionally, data on comorbidities were obtained, including heart failure, hypertension, myocardial infarction, cerebral infarction, diabetes, chronic kidney disease and malignant tumor, according to the ICD-9 codes recorded in the MIMIC-III database.

Clinical outcomes

For the purpose of this study, the clinical endpoints were classified as in-hospital death and 1-year morality. In-hospital death was defined as "the patient died during hospitalization". The definition of 1-year mortality was "the patient died within 1 year of ICU admission".

Statistical analysis

The normality of the data was examined for continuous variables by the Kolmogorov–Smirnov (KS) test. Values are expressed as medians [interquartile ranges (IQRs)] due to non-normal distributions of all continuous variables in our study. All categorical variables are expressed as total numbers and percentages. Comparisons between two groups (patients with in-hospital death vs. those without in-hospital death; patients with 1-year mortality vs. those without 1-year mortality) were made using the Mann–Whitney U test for continuous variables and the chi-square test for categorical variables.

First, multivariate logistic regression models were used to characterize the associations between blood creatinine and urea nitrogen levels at baseline and the clinical outcomes (risk of in-hospital death and 1-year mortality). Other confounding factors (baseline variables) that were clinically relevant to the clinical outcomes, including age, sex, hypertension, heart failure, myocardial infarction, diabetes and cerebral infarction, were entered into a multivariate model as covariates. Then subgroup analysis using "type of intracranial hemorrhage" and "head trauma" as grouping variables was performed for these associations. Because malignancy and insurance status are important causes of all-cause death in elderly individuals, we also used "malignant tumors" and "insurance" as covariates in the sensitivity analysis.

Additionally, we performed a smooth curve analysis for relationships between blood creatinine and urea nitrogen levels and the risk of in-hospital death and 1-year mortality. A smoothed curve can fully demonstrate the non-linear associations of two variables. Stratified analysis was further performed on the associations of blood creatinine and urea nitrogen levels with the risk of in-hospital death and 1-year mortality through the inflection points (blood creatinine = 1.9 mg/dL and blood urea nitrogen = 29 mg/dL) of the smooth curves. In the stratification analysis, conditional logistic regression analysis was used, and the modification effect of the inflection points on the associations between blood creatinine and urea nitrogen levels with the risk of in-hospital death and 1-year mortality was assessed. All statistical analyses were performed by using Stata 13.0 and EmpowerStats 3.0. A P-value < 0.05 was defined as statistically significant.

Results

Clinical characteristics at baseline

After reviewing the data of 46,520 patients, a total of 2,682 ICU patients with intracranial hemorrhage were enrolled in the present study, as shown in the flow chart of the included study subjects (Figure 1). Among our study cohort, the median age of all patients was 66.5 years, and 1,057 (51.2%) of them were female. Blood creatinine and urea nitrogen levels were measured for all 2,682 patients within the first 24 h after ICU admission, with median values of 0.80 and 15.00 mg/dL, respectively. The median ICU stay was 2.92 (1.54–7.12) days. All patients were classified into two groups according to survival state (alive or dead). Importantly, patients in the non-surviving group were significantly older, had a longer ICU stay, had higher blood creatinine and urea nitrogen levels and had a higher rate of comorbidities (heart failure, myocardial infarction, cerebral infarction and malignant tumor) than those in the surviving group. Their other clinical characteristics at baseline are described in detail in Table 1.

Elevated blood creatinine and urea nitrogen levels were related to an increased risk of in-hospital death and 1-year mortality

The multivariate logistic regression analysis demonstrated significantly adverse associations of elevated blood creatinine levels with an increased risk of in-hospital death [unadjusted odds ratio (OR) = 1.14, 95% CI 1.05–1.22, $P = 0.001$] and 1-year mortality (unadjusted OR = 1.28, 95% CI 1.17–1.40, $P < 0.001$), as shown in Table 2. Similar associations existed for urea nitrogen, with a higher risk of in-hospital death (unadjusted OR = 1.02, 95% CI 1.02–1.03, $P < 0.001$) and 1-year mortality (unadjusted OR = 1.03, 95% CI 1.03–1.04, $P < 0.001$). These results remained consistent after adjusting for confounding factors, including age, sex, hypertension, heart failure, myocardial infarction, diabetes and cerebral infarction. Furthermore, we used "malignant tumor" and "insurance" as covariates in the sensitivity analysis. We observed that this independent relationship changed only slightly (Table 3).

We also used subgroup analysis to evaluate patients with different types of intracranial hemorrhage and head trauma for these associations. Our results showed that only in patients with subarachnoid hemorrhage increased blood creatinine levels were associated with an elevated risk of in-hospital death [adjusted odds ratio (OR) = 1.68, 95% CI 1.14–2.47, $P = 0.009$] and 1-year mortality (adjusted OR = 1.65, 95% CI 1.10–2.47, $P = 0.015$), as shown in Table 4. However, a significant association did not exist among patients with intracerebral, subdural and unspecified intracranial hemorrhage. This indicates that different types of intracranial hemorrhage have different risks of death. Additionally, we also observed that elevated blood creatinine and urea nitrogen levels contributed to a higher risk of in-hospital death and 1-year mortality among patients without head trauma but not among those with head trauma (Table 5). However, head trauma did not have a significant modifying effect on the relationship.

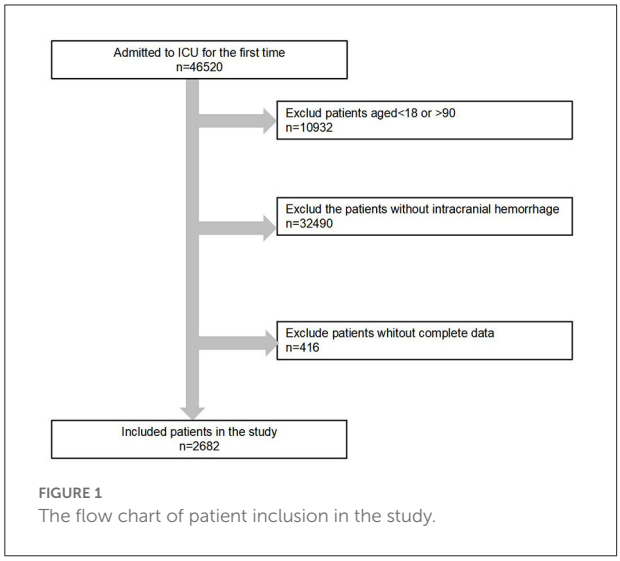

FIGURE 1
The flow chart of patient inclusion in the study.

Stratified analysis using the "inflection point" of the smooth curve for associations between blood creatinine and urea nitrogen levels and the risk of in-hospital death and 1-year mortality

To further analyze the relationships between blood creatinine and urea nitrogen and clinical outcomes, we used a smooth curve to find potential "inflection points" of the relationships. Surprisingly, the smooth curve revealed a gradual upward trend in the association between blood creatinine and the risk of in-hospital death and 1-year mortality (Figures 2A,C; inflection point of creatinine = 1.9 mg/dL). Similar results existed for urea nitrogen (Figures 2B,D; inflection point of urea nitrogen = 29 mg/dL). When the blood creatinine value was <1.9 mg/dL, we observed a steeply linear relationship between the creatinine level and the risk of in-hospital death and 1-year mortality, while the risk of in-hospital death and 1-year mortality increased only slightly or very slowly when the creatinine level exceeded 1.9 mg/dL. These results suggested that increased creatinine levels mainly strongly contributed

10.3389/fcvm.2022.967614

TABLE 1 Clinical characteristics of ICU patients with intracranial hemorrhage at baseline.

Variable	All = 2,682	In-hospital death			1-year mortality		
		Alive = 2,157	Dead = 525	*p*	Alive = 1,831	Dead = 851	*p*
Age (year)	66.5 (52.5–78.8)	64.8 (51.4–78.1)	73.4 (59.1–80.8)	<0.001	62.8 (50.0–75.8)	75.1 (61.4–82.3)	<0.001
Gender (male), *n* (%)	1,507 (56.19)	1,221 (56.61)	286 (54.48)	0.378	1,037 (56.64)	470 (55.23)	0.494
Days of ICU stay	2.92 (1.54–7.12)	2.83 (1.50–7.33)	3.67 (1.75–6.88)	0.092	2.75 (1.42–7.12)	3.38 (1.75–7.10)	0.002
Insurance							
Government, *n* (%)	87 (3.24)	82 (3.80)	5 (0.95)	<0.001	81 (4.42)	6 (0.71)	<0.001
Medicaid, *n* (%)	221 (8.24)	186 (8.62)	35 (6.67)		170 (9.28)	51 (5.99)	
Medicare, *n* (%)	1,341 (50.00)	1,012 (46.92)	329 (62.67)		768 (41.94)	573 (67.33)	
Private, *n* (%)	969 (36.13)	834 (38.66)	135 (25.71)		771 (42.11)	198 (23.27)	
Self pay, *n* (%)	64 (2.39)	43 (1.99)	21 (4.00)		41 (2.24)	23 (2.70)	
First care unit							
CCU, *n* (%)	74 (2.76)	48 (2.23)	18 (3.43)	0.041	43 (2.35)	23 (2.70)	<0.001
CSRU, *n* (%)	64 (2.39)	66 (3.06)	19 (3.62)		55 (3.00)	30 (3.53)	
MICU, *n* (%)	375 (13.98)	273 (12.66)	88 (16.76)		213 (11.63)	148 (17.39)	
SICU, *n* (%)	1,381 (51.49)	1,074 (49.79)	244 (46.48)		913 (49.86)	405 (47.59)	
TSICU, *n* (%)	788 (29.38)	696 (32.27)	156 (29.71)		607 (33.15)	245 (28.79)	
Comorbidities							
Heart failure, *n* (%)	285 (10.63)	209 (9.69)	76 (14.48)	0.001	156 (8.52)	129 (15.16)	<0.001
Hypertension, *n* (%)	1,358 (50.63)	1,086 (50.35)	272 (51.81)	0.548	915 (49.97)	443 (52.06)	0.315
Miocardial infarction, *n* (%)	28 (1.04)	17 (0.79)	11 (2.10)	0.008	13 (0.71)	15 (1.76)	0.013
Cerebral infarction, *n* (%)	185 (6.90)	138 (6.40)	47 (8.95)	0.038	107 (5.84)	78 (9.17)	0.002
Diabetes, *n* (%)	31 (1.16)	26 (1.21)	5 (0.95)	0.627	23 (1.26)	8 (0.94)	0.476
Malignant tumor, *n* (%)	128 (4.77)	104 (4.82)	24 (4.57)	0.810	53 (2.89)	75 (8.81)	<0.001
Chronic kidney disease, *n* (%)	107 (3.99)	79 (3.66)	28 (5.33)	0.079	56 (3.06)	51 (5.99)	<0.001
Blood test parameters							
Sodium (mEq/L)	139.00 (137.00–141.00)	139.00 (137.00–141.00)	139.00 (137.00–142.00)	0.154	139.00 (137.00–141.00)	139.00 (137.00–142.00)	0.898
Potassium (mEq/L)	3.90 (3.50–4.20)	3.90 (3.50–4.20)	3.80 (3.50–4.30)	0.728	3.90 (3.50–4.20)	3.90 (3.50–4.30)	0.837
Phosphate (mg/dL)	3.20 (2.70–3.70)	3.20 (2.80–3.70)	3.00 (2.50–3.80)	0.001	3.20 (2.80–3.70)	3.10 (2.50–3.75)	0.004
Magnesium (mg/dL)	1.90 (1.70–2.00)	1.90 (1.70–2.00)	1.80 (1.60–2.00)	0.514	1.90 (1.70–2.00)	1.80 (1.60–2.00)	0.556
Total calcium (mg/dL)	8.60 (8.10–9.00)	8.60 (8.20–9.00)	8.50 (8.00–9.00)	0.014	8.60 (8.20–9.00)	8.50 (8.00–9.00)	0.045
Chloride (mEq/L)	105.00 (102.00–108.00)	105.00 (102.00–108.00)	105.00 (101.00–109.00)	0.969	105.00 (102.00–108.00)	104.00 (101.00–108.00)	0.278
Glucose (mg/dL)	134.00 (112.00–166.00)	130.00 (110.00–160.00)	154.00 (127.00–198.00)	<0.001	129.00 (109.00–157.00)	147.00 (123.00–189.50)	<0.001
PTT (sec)	26.60 (24.20–29.70)	26.50 (24.40–29.40)	26.70 (23.90–31.30)	0.118	26.30 (24.20–29.20)	27.00 (24.20–31.20)	<0.001
PT (sec)	13.30 (12.60–14.30)	13.20 (12.60–14.10)	13.60 (12.70–15.30)	<0.001	13.20 (12.50–14.00)	13.60 (12.70–15.10)	<0.001
INR PT	1.20 (1.10–1.30)	1.10 (1.10–1.30)	1.20 (1.10–1.40)	<0.001	1.10 (1.10–1.20)	1.20 (1.10–1.40)	<0.001
Red blood cell count (m/uL)	3.88 (3.42–4.32)	3.91 (3.45–4.32)	3.78 (3.31–4.33)	0.028	3.95 (3.49–4.34)	3.75 (3.27–4.25)	<0.001
Platelet count (K/uL)	214.00 (166.00–268.00)	215.00 (168.00–268.00)	211.00 (151.00–271.00)	0.073	218.00 (171.50–269.50)	204.00 (149.50–264.50)	<0.001
White blood cell count (K/uL)	10.55 (7.90–13.70)	10.20 (7.70–13.00)	12.50 (9.20–16.00)	<0.001	10.10 (7.70–12.90)	11.90 (8.50–15.10)	<0.001
Bicarbonate (mEq/L)	24.00 (22.00–26.00)	24.00 (22.00–26.00)	23.00 (21.00–26.00)	<0.001	24.00 (22.00–26.00)	24.00 (21.00–26.00)	<0.001

(Continued)

10.3389/fcvm.2022.967614

TABLE 1 (Continued)

Variable	All = 2,682	In-hospital death			1-year mortality		
		Alive = 2,157	Dead = 525	*p*	Alive = 1,831	Dead = 851	*p*
Creatinine (mg/dL)	0.80 (0.70–1.10)	0.80 (0.70–1.00)	0.90 (0.70–1.30)	<0.001	0.80 (0.70–1.00)	0.90 (0.70–1.20)	<0.001
Urea nitrogen (mg/dL)	15.00 (11.00–20.00)	15.00 (11.00–20.00)	17.00 (13.00–26.00)	<0.001	14.00 (10.00–19.00)	17.00 (13.00–25.00)	<0.001
Medications							
Vasopressin, *n* (%)	105 (3.91)	44 (2.04)	61 (11.62)	<0.001	31 (1.69)	74 (8.70)	<0.001
Nitrate esters, *n* (%)	112 (4.18)	96 (4.45)	16 (3.05)	0.150	73 (3.99)	39 (4.58)	0.473
β Receptor blocker, *n* (%)	1,369 (51.04)	1,116 (51.74)	253 (48.19)	0.145	928 (50.68)	441 (51.82)	0.583
Benzodiazepine, *n* (%)	186 (6.94)	140 (6.49)	46 (8.76)	0.066	117 (6.39)	69 (8.11)	0.103
Statins, *n* (%)	277 (10.33)	242 (11.22)	35 (6.67)	0.002	189 (10.32)	88 (10.34)	0.988
Potassium, *n* (%)	357 (13.31)	288 (13.35)	69 (13.14)	0.899	241 (13.16)	116 (13.63)	0.739
Type of intracranial hemorrhage							
Intracerebral, *n* (%)	971 (36.20)	727 (33.70)	244 (46.48)	<0.001	573 (31.29)	398 (46.77)	<0.001
Extradural, *n* (%)	15 (0.56)	11 (0.51)	4 (0.76)		10 (0.55)	5 (0.59)	
Subdural, *n* (%)	625 (23.30)	546 (25.31)	79 (15.05)		453 (24.74)	172 (20.21)	
Unspecified intracranial, *n* (%)	212 (7.90)	170 (7.88)	42 (8.00)		153 (8.36)	59 (6.93)	
Subarachnoid, *n* (%)	756 (28.19)	618 (28.65)	138 (26.29)		566 (30.91)	190 (22.33)	
Multiple, *n* (%)	103 (3.84)	85 (3.94)	18 (3.43)		76 (4.15)	27 (3.17)	
Head trauma, *n* (%)	1,005 (37.47)	862 (39.96)	143 (27.24)	<0.001	754 (41.18)	251 (29.49)	<0.001

ICU, intensive care unit; CCU, cardiology care unit; CSRU, cardiovascular surgery rehabilitation unit; MICU, medical intensive care unit; SICU, surgical intensive care unit; TSICU, trauma/surgical intensive care unit; PTT, partial thromboplastin time; PT, prothrombin time; INR, international normalized ratio.

to a higher risk of in-hospital death and that 1-year mortality increased only when the creatinine values were below 1.9 mg/dL. Similarly, we found that blood urea nitrogen levels were significantly related to the risk of in-hospital death and 1-year mortality when the blood urea nitrogen value was <29 mg/dL, whereas the risk of in-hospital death and 1-year mortality increased very little or only very slowly after the creatinine level exceeded 29 mg/d.

According to the inflection point (blood creatinine = 1.9 mg/dL and blood urea nitrogen = 29 mg/dL) of the smooth curve, stratified analysis was further used to analyze the associations of blood creatinine and urea nitrogen levels with the risk of clinical outcomes, as shown in Table 6. Consistently, conditional logistic regression analysis suggested that the inflection points had significant modification effects on the associations between blood creatinine levels, as well as blood urea nitrogen, and the risk of in-hospital death (interaction value < 0.001) and 1-year mortality (interaction value < 0.001).

Discussion

Globally, stroke is an important cause of disability and death, and acute cerebral hemorrhage accounts for ∼26% of all strokes (13, 14). The Kidney Early Evaluation Program (KEEP) showed that CKD patients are at a higher risk of both myocardial infarction and stroke when their eGFR is <60 mL/min/1.73 m^2 (15). There is also a study reporting a graded association between a reduced eGFR and the risk of adverse cardiovascular outcomes, including stroke (16). However, the relationship between renal function and mortality risk in ICU patients with intracranial hemorrhage has not been studied.

We analyzed 2,682 patients with intracranial hemorrhage from the MIMIC-III database. Consistently, we observed adverse associations between blood creatinine and urea nitrogen levels and the risk of in-hospital death and 1-year mortality in these ICU patients after adjusting for all identified confounding factors. Importantly, we identified new inflection points in which elevated blood creatinine and urea nitrogen levels were associated with an increased risk of in-hospital death and 1-year mortality: a blood creatinine value < 1.9 mg/dL and a blood urea nitrogen value < 29 mg/dL. Beyond these levels, the mortality risk in these patients with intracranial hemorrhage did not increase significantly.

Renal dysfunction has been found to be an independent factor for mortality risk in various populations, including patients with heart failure, patients with myocardial infarction and the general population (17–19). However, previous evidence

TABLE 2 Corrected logistic regression analysis for associations of blood creatinine and urea nitrogen with hospital mortality and 1-year mortality in ICU patients with intracranial hemorrhage.

Variable	In-hospital death		1-year mortality	
	OR (95% CI)	*P*-value	OR (95% CI)	*P*-value
Unadjusted				
Creatinine (mg/dL)	1.14 (1.05, 1.22)	0.001	1.28 (1.17, 1.40)	<0.001
Urea Nitrogen (mg/dL)	1.02 (1.02, 1.03)	<0.001	1.03 (1.03, 1.04)	<0.001
Plus age				
Creatinine (mg/dL)	1.13 (1.04, 1.21)	0.002	1.24 (1.14, 1.35)	<0.001
Urea nitrogen (mg/dL)	1.02 (1.01, 1.02)	<0.001	1.02 (1.02, 1.03)	<0.001
Plus gender				
Creatinine (mg/dL)	1.13 (1.05, 1.22)	0.002	1.24 (1.14, 1.35)	<0.001
Urea nitrogen (mg/dL)	1.02 (1.01, 1.02)	<0.001	1.02 (1.02, 1.03)	<0.001
Plus hypertension				
Creatinine (mg/dL)	1.12 (1.04, 1.21)	0.003	1.22 (1.12, 1.33)	<0.001
Urea nitrogen (mg/dL)	1.02 (1.01, 1.02)	<0.001	1.02 (1.02, 1.03)	<0.001
Plus heart failure				
Creatinine (mg/dL)	1.11 (1.03, 1.20)	0.005	1.21 (1.11, 1.31)	<0.001
Urea nitrogen (mg/dL)	1.02 (1.01, 1.02)	<0.001	1.02 (1.01, 1.03)	<0.001
Plus miocardial infarction				
Creatinine (mg/dL)	1.11 (1.03, 1.20)	0.005	1.21 (1.11, 1.31)	<0.001
Urea nitrogen (mg/dL)	1.02 (1.01, 1.02)	<0.001	1.02 (1.01, 1.03)	<0.001
Plus diabetes				
Creatinine (mg/dL)	1.12 (1.03, 1.20)	0.004	1.21 (1.11, 1.32)	<0.001
Urea nitrogen (mg/dL)	1.02 (1.01, 1.02)	<0.001	1.02 (1.01, 1.03)	<0.001
Plus cerebral infarction				
Creatinine (mg/dL)	1.12 (1.03, 1.20)	0.005	1.22 (1.12, 1.33)	<0.001
Urea nitrogen (mg/dL)	1.02 (1.01, 1.02)	<0.001	1.02 (1.02, 1.03)	<0.001

ICU, intensive care unit.

TABLE 3 Sensitivity analysis for associations of blood creatinine and urea nitrogen with hospital mortality and 1-year mortality in ICU patients with intracranial hemorrhage.

Variable	In-hospital death		1-year mortality	
	OR (95% CI)	*P*-value	OR (95% CI)	*P*-value
Model 1 (Plus malignant)				
Creatinine (mg/dL)	1.12 (1.03, 1.20)	0.005	1.22 (1.12, 1.33)	<0.001
Urea nitrogen (mg/dL)	1.02 (1.01, 1.02)	<0.001	1.02 (1.01, 1.03)	<0.001
Model 2 (Plus insurance)				
Creatinine (mg/dL)	1.10 (1.02, 1.19)	0.016	1.20 (1.10, 1.31)	<0.001
Urea nitrogen (mg/dL)	1.02 (1.01, 1.02)	<0.001	1.02 (1.01, 1.03)	<0.001

Model 1: Adjusted for age, gender, hypertension, heart failure, miocardial infarction, diabetes, cerebral infarction and malignan.
Model 2: Adjusted for age, gender, hypertension, heart failure, miocardial infarction, diabetes, cerebral infarction, malignant and insurance.
ICU, intensive care unit.

on the association between renal dysfunction and mortality risk in acute stroke has some heterogeneity. MacWalter et al. observed that patients with increased serum creatinine (1.35 mg/dL) levels at admission had a higher risk of mortality in a cohort of 2,042 patients with stroke followed up for 7 years in Scotland (20). Yeh et al. observed that a reduced eGFR (<60 mL/min/1.73 m^2) was related to a poor prognosis within 6 months among patients with atherosclerosis stroke

TABLE 4 Subgroup analysis by "type of intracranial hemorrhage" for associations of blood creatinine and urea nitrogen with hospital mortality and 1-year mortality in ICU patients in cerebral hemorrhage.

Type of cerebral hemorrhage	Variable	In-hospital death		1-year mortality	
		OR (95% CI)	*P*-value	OR (95% CI)	*P*-value
Intracerebral	Creatinine (mg/dL)	1.09 (0.99, 1.21)	0.093	1.27 (1.09, 1.48)	0.002
	Urea nitrogen (mg/dL)	1.01 (1.00, 1.02)	0.003	1.02 (1.01, 1.03)	<0.001
Extradural	Creatinine (mg/dL)	–	–	–	–
	Urea nitrogen (mg/dL)	–	–	–	–
Subdural	Creatinine (mg/dL)	1.00 (0.85, 1.18)	0.994	1.10 (0.97, 1.24)	0.148
	Urea nitrogen (mg/dL)	1.02 (1.01, 1.03)	0.003	1.02 (1.01, 1.03)	<0.001
Unspecified intracrania	Creatinine (mg/dL)	1.13 (0.69, 1.86)	0.629	0.92 (0.55, 1.54)	0.755
	Urea nitrogen (mg/dL)	1.01 (0.98, 1.04)	0.431	1.00 (0.97, 1.03)	0.844
Subarachnoid	Creatinine (mg/dL)	1.68 (1.14, 2.47)	0.009	1.65 (1.10, 2.47)	0.015
	Urea nitrogen (mg/dL)	1.04 (1.02, 1.06)	<0.001	1.03 (1.01, 1.06)	0.002
Multiple	Creatinine (mg/dL)	3.79 (0.57, 25.31)	0.169	3.92 (0.58, 26.73)	0.163
	Urea nitrogen (mg/dL)	1.02 (0.96, 1.08)	0.521	1.04 (0.97, 1.12)	0.283

Adjusted for age, gender, hypertension, heart failure, miocardial infarction, diabetes, cerebral infarction, malignant and insurance.
ICU, intensive care unit.

TABLE 5 Subgroup analysis by "head trauma" for associations of blood creatinine and urea nitrogen with hospital mortality and 1-year mortality in ICU patients with intracranial hemorrhage.

Variable	Head trauma	In-hospital death			1-year mortality		
		OR (95% CI)	*P*-value	**P*	OR (95% CI)	*P*-value	**P*
Creatinine (mg/dL)	No	1.11 (1.01, 1.22)	0.027	0.317	1.18 (1.07, 1.31)	0.002	0.927
	Yes	1.00 (0.83, 1.21)	0.987		1.17 (1.00, 1.37)	0.053	
Urea nitrogen (mg/dL)	No	1.02 (1.01, 1.03)	<0.001	0.504	1.02 (1.01, 1.03)	<0.001	0.266
	Yes	1.01 (1.00, 1.03)	0.063		1.01 (1.00, 1.03)	0.035	

Adjusted for age, gender, hypertension, heart failure, miocardial infarction, diabetes, cerebral infarction, malignant and insurance.
* *P* for interaction value.

(21). Furthermore, Hao et al. found that a low eGFR on admission was a valuable indicator for predicting 1-year mortality in patients with acute intracranial hemorrhage but not in patients with ischemic stroke (22). In contrast, Kumia et al. found that proteinuria, but not a reduced eGFR, as evaluated by the MDRD equation, was significantly associated with an increased risk of poor functional outcomes and mortality after acute ischemic stroke (23). Another study suggested that a low eGFR level on admission, calculated by the MDRD equation, did not contribute to an increased risk of in-hospital mortality in intracranial hemorrhage patients (7). The heterogeneity of these conclusions may derive from the different study populations selected, the different stroke types included, the different methods used to evaluate renal function and the various confounding factors taken into account.

Consistent with some previous studies (20–22), the results of our study suggested that reduced blood creatinine and urea nitrogen levels were associated with a significantly higher risk of either in-hospital death or 1-year mortality in ICU patients with intracranial hemorrhage only when their blood creatinine value was <1.9 mg/dL or their blood urea nitrogen value was <29 mg/dL. The mortality risk in these patients with intracranial hemorrhage did not increase significantly as these measures increased. This confirmed the results of previous smaller studies and provided new and important information that an acute increase in blood creatinine and urea nitrogen levels within the normal range of the general population contributes to a significantly increased risk of hospitalization and long-term mortality.

Cancer and insurance status are important factors for long-term mortality in elderly patients (24–26). In our study, all included individuals were elderly patients, and 128 (4.77%) patients had malignant tumors. In addition to controlling for traditional risk factors such as age, sex

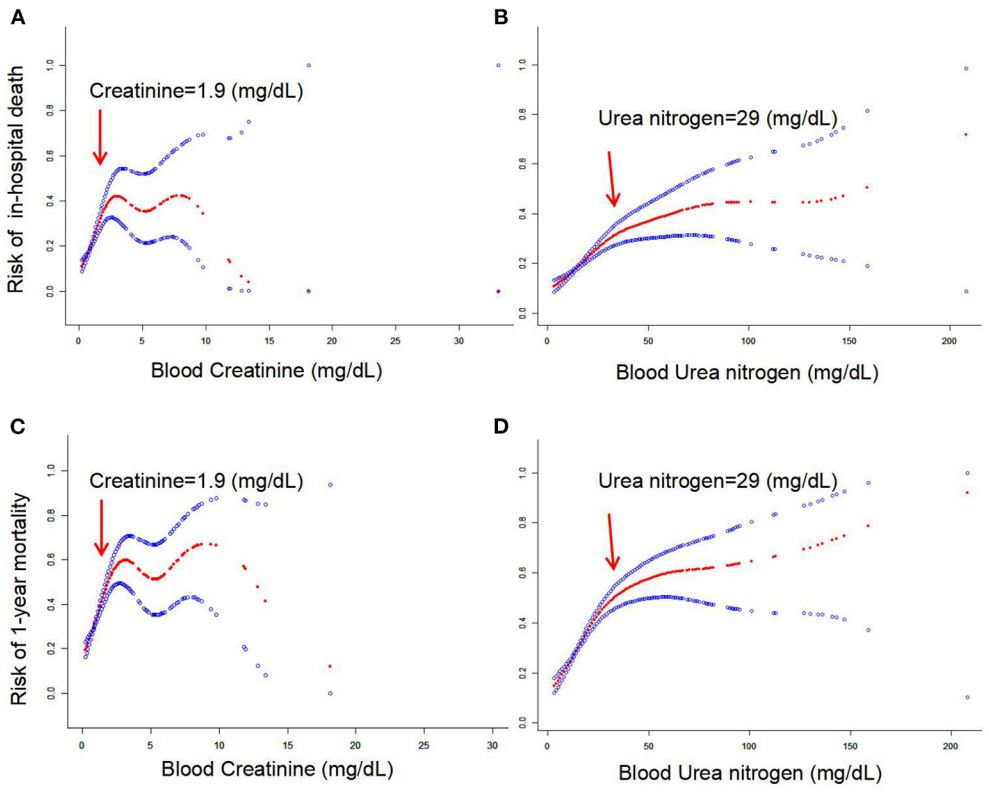

FIGURE 2
(A–D) Smoothed curves of the associations between blood creatinine and urea nitrogen and mortality risk in patients with intracranial hemorrhage.

and cardiovascular diseases that can affect the long-term survival rate of elderly individuals, our sensitivity analysis demonstrated that malignant tumor and insurance status did not significantly affect the independent association of creatinine and urea nitrogen with mortality risk among patients with intracranial hemorrhage, which was inconsistent with previous studies. Moreover, the findings of this study suggested that increased blood creatinine levels were associated with an elevated risk of in-hospital death and 1-year mortality only in patients with subarachnoid hemorrhage. A significant association did not exist for patients with intracerebral, subdural or unspecified intracranial hemorrhage. This is consistent with the clinicopathological condition that different types of intracranial hemorrhage have different mortality risks.

This study has several notable strengths. (1) Our study used intracranial hemorrhage data from the MIMIC-III database, which contains information from a large number of ICU patients with intracranial hemorrhage. This retrospective cohort study design could estimate the real-world prognosis of intracranial hemorrhage patients. (2) We observed a positive association between blood creatinine and urea nitrogen levels within 24 h of admission and a higher risk of in-hospital death and 1-year mortality in patients with intracranial hemorrhage only when their blood creatinine value was <1.9 mg/dL or their blood urea nitrogen value was <29 mg/dL. (3) Demographic characteristics, concomitant cardiovascular disease and malignant tumors were controlled in multivariate analysis, which eliminated the influence of relevant confounding factors. The present study also has several limitations. First, we did not use any information on accurate eGFR levels, which can reflect renal function well. Second, we only used the first value of the blood creatinine level measured on admission. We could not distinguish chronic renal dysfunction from acute renal dysfunction, potentially skewing the results. Third, 416 patients with intracranial hemorrhage were excluded due to missing information (Figure 1). Whether their data might affect the results is uncertain.

In conclusion, our results suggested that elevated blood creatinine and urea nitrogen levels contributed to an increased risk of in-hospital death and 1-year mortality in ICU patients with intracranial hemorrhage only when the blood creatinine value was <1.9 mg/dL or the blood urea nitrogen value was <29 mg/dL.

10.3389/fcvm.2022.967614

TABLE 6 Interaction analysis by "inflection point" for associations of blood creatinine and urea nitrogen with hospital mortality and 1-year mortality in ICU patients with intracranial hemorrhage.

Variable	In-hospital death			1-year mortality		
	OR (95% CI)	*P*-value	**P*	OR (95% CI)	*P*-value	**P*
Crude						
Creatinine < 1.9 (mg/dL)	2.50 (1.80, 3.45)	<0.001	<0.001	2.48 (1.86, 3.30)	<0.001	<0.001
Creatinine ≥ 1.9 (mg/dL)	0.90 (0.79, 1.03)	0.116		1.01 (0.92, 1.11)	0.814	
Urea nitrogen < 29 (mg/dL)	1.06 (1.03, 1.08)	<0.001	<0.001	1.07 (1.05, 1.09)	<0.001	<0.001
Urea nitrogen ≥ 29 (mg/dL)	1.01 (1.00, 1.02)	0.187		1.01 (1.00, 1.02)	0.077	
Plus age						
Creatinine < 1.9 (mg/dL)	2.00 (1.43, 2.79)	<0.001	<0.001	1.71 (1.27, 2.30)	<0.001	0.001
Creatinine ≥ 1.9 (mg/dL)	0.89 (0.78, 1.02)	0.087		1.01 (0.92, 1.11)	0.804	
Urea nitrogen < 29 (mg/dL)	1.03 (1.01, 1.05)	0.004	0.022	1.03 (1.01, 1.05)	0.001	0.042
Urea nitrogen ≥ 29 (mg/dL)	1.00 (1.00, 1.01)	0.344		1.01 (1.00, 1.02)	0.068	
Plus gender						
Creatinine < 1.9 (mg/dL)	2.27 (1.60, 3.22)	<0.001	<0.001	1.78 (1.30, 2.44)	<0.001	0.001
Creatinine ≥ 1.9 (mg/dL)	0.90 (0.79, 1.02)	0.108		1.02 (0.92, 1.12)	0.756	
Urea nitrogen < 29 (mg/dL)	1.03 (1.01, 1.06)	0.002	0.018	1.03 (1.01, 1.05)	0.001	0.045
Urea nitrogen ≥ 29 (mg/dL)	1.00 (1.00, 1.01)	0.350		1.01 (1.00, 1.02)	0.070	
Plus hypertension						
Creatinine < 1.9 (mg/dL)	2.24 (1.57, 3.17)	<0.001	<0.001	1.75 (1.27, 2.40)	<0.001	0.002
Creatinine ≥ 1.9 (mg/dL)	0.92 (0.81, 1.04)	0.168		1.02 (0.92, 1.13)	0.699	
Urea nitrogen < 29 (mg/dL)	1.04 (1.01, 1.06)	0.002	0.015	1.03 (1.01, 1.05)	<0.001	0.029
Urea nitrogen ≥ 29 (mg/dL)	1.00 (0.99, 1.01)	0.400		1.01 (1.00, 1.02)	0.104	
Plus heart failure						
Creatinine < 1.9 (mg/dL)	2.20 (1.54, 3.13)	<0.001	<0.001	1.70 (1.24, 2.34)	0.001	0.003
Creatinine ≥ 1.9 (mg/dL)	0.92 (0.81, 1.04)	0.170		1.02 (0.92, 1.12)	0.703	
Urea nitrogen < 29 (mg/dL)	1.04 (1.01, 1.06)	0.002	0.017	1.03 (1.01, 1.05)	0.001	0.035
Urea nitrogen ≥ 29 (mg/dL)	1.00 (0.99, 1.01)	0.434		1.01 (1.00, 1.02)	0.111	
Plus miocardial infarction						
Creatinine < 1.9 (mg/dL)	2.20 (1.55, 3.14)	<0.001	<0.001	1.70 (1.24, 2.34)	0.001	0.003
Creatinine ≥ 1.9 (mg/dL)	0.92 (0.82, 1.04)	0.204		1.02 (0.93, 1.13)	0.635	
Urea nitrogen < 29 (mg/dL)	1.04 (1.01, 1.06)	0.002	0.015	1.03 (1.01, 1.05)	0.001	0.031
Urea nitrogen ≥ 29 (mg/dL)	1.00 (0.99, 1.01)	0.433		1.01 (1.00, 1.02)	0.111	
Plus diabetes						
Creatinine < 1.9 (mg/dL)	2.22 (1.56, 3.16)	<0.001	<0.001	1.72 (1.25, 2.36)	0.001	0.002
Creatinine ≥ 1.9 (mg/dL)	0.92 (0.81, 1.04)	0.190		1.03 (0.93, 1.13)	0.624	
Urea nitrogen < 29 (mg/dL)	1.04 (1.01, 1.06)	0.001	0.013	1.03 (1.01, 1.05)	0.001	0.027
Urea nitrogen ≥ 29 (mg/dL)	1.00 (0.99, 1.01)	0.438		1.01 (1.00, 1.02)	0.118	
Plus cerebral infarction						
Creatinine < 1.9 (mg/dL)	2.20 (1.54, 3.14)	<0.001	<0.001	1.70 (1.23, 2.34)	0.001	0.003
Creatinine ≥ 1.9 (mg/dL)	0.91 (0.81, 1.02)	0.110		1.02 (0.91, 1.13)	0.740	
Urea nitrogen < 29 (mg/dL)	1.04 (1.01, 1.06)	0.002	0.016	1.03 (1.01, 1.05)	0.001	0.034
Urea nitrogen ≥ 29 (mg/dL)	1.00 (0.99, 1.01)	0.439		1.01 (1.00, 1.02)	0.125	
Plus malignant						
Creatinine < 1.9 (mg/dL)	2.20 (1.54, 3.14)	<0.001	<0.001	1.71 (1.24, 2.35)	0.001	0.003
Creatinine ≥ 1.9 (mg/dL)	0.90 (0.80, 1.02)	0.089		1.01 (0.89, 1.13)	0.916	
Urea nitrogen < 29 (mg/dL)	1.04 (1.01, 1.06)	0.002	0.014	1.03 (1.01, 1.05)	0.001	0.036
Urea nitrogen ≥ 29 (mg/dL)	1.00 (0.99, 1.01)	0.434		1.01 (1.00, 1.02)	0.104	

(Continued)

TABLE 6 (Continued)

Variable	In-hospital death			1-year mortality		
	OR (95% CI)	*P*-value	**P*	OR (95% CI)	*P*-value	**P*
Plus insurance						
Creatinine < 1.9 (mg/dL)	2.16 (1.51, 3.09)	<0.001	<0.001	1.68 (1.21, 2.32)	0.002	0.003
Creatinine ≥ 1.9 (mg/dL)	0.89 (0.78, 1.01)	0.067		0.99 (0.87, 1.14)	0.930	
Urea nitrogen < 29 (mg/dL)	1.04 (1.01, 1.06)	0.001	0.026	1.03 (1.01, 1.06)	<0.001	0.061
Urea nitrogen ≥ 29 (mg/dL)	1.01 (1.00, 1.02)	0.204		1.01 (1.00, 1.02)	0.032	

Inflection point for creatinine < 1.9 mg/dL ($n = 2,538$) and creatinined ≥ 1.9 mg/dL ($n = 144$); Inflection point for urea nitrogen < 29 mg/dL ($n = 2,362$) and Urea nitrogen ≥ 29 mg/dL ($n = 320$).

**P*: interaction value.

ICU, intensive care unit.

Data availability statement

The raw data supporting the conclusions of this article will be made available by the authors, without undue reservation.

Ethics statement

The studies involving human participants were reviewed and approved by Review Boards of the Massachusetts Institute of Technology (MIT, Cambridge, MA, USA) and Beth Israel Deaconess Insurance Center (BIDMC, Boston, MA, USA), and written informed consent was obtained from each patient based on the Declaration of Helsinki guidelines.

Author contributions

HL and JX completed the data analysis and first draft. XY, KC, SL, and GL completed surveillance and data duplication. All authors contributed to the article and approved the submitted version.

Conflict of interest

The authors declare that the research was conducted in the absence of any commercial or financial relationships that could be construed as a potential conflict of interest.

Publisher's note

All claims expressed in this article are solely those of the authors and do not necessarily represent those of their affiliated organizations, or those of the publisher, the editors and the reviewers. Any product that may be evaluated in this article, or claim that may be made by its manufacturer, is not guaranteed or endorsed by the publisher.

References

1. Donnell MJ, Chin SL, Rangarajan S, Xavier D, Liu L, Zhang H, et al. Global and regional effects of potentially modifiable risk factors associated with acute stroke in 32 countries (INTERSTROKE): a case-control study. *Lancet.* (2016) 388:761–75. doi: 10.1016/S0140-6736(16)30506-2

2. Ninomiya T, Kiyohara Y, Tokuda Y, Doi Y, Arima H, Harada A, et al. Impact of kidney disease and blood pressure on the development of cardiovascular disease: an overview from the Japan Arteriosclerosis Longitudinal Study. *Circulation.* (2008) 118:2694–701. doi: 10.1161/CIRCULATIONAHA.108.792903

3. Drechsler C, Delgado G, Wanner C, Blouin K, Pilz S, Tomaschitz A, et al. Galectin-3, renal function, and clinical outcomes: results from the LURIC and 4D studies. *J Am Soc Nephrol.* (2015) 26:2213–21. doi: 10.1681/ASN.2014010093

4. Joannidis M, Druml W, Forni LG, Groeneveld ABJ, Honore PM, Hoste E, et al. Prevention of acute kidney injury and protection of renal function in the intensive care unit: update 2017: expert opinion of the Working Group on Prevention, AKI section, European Society of Intensive Care Medicine. *Intensive Care Med.* (2017) 43:730–49. doi: 10.1007/s00134-017-4832-y

5. Yahalom G, Schwartz R, Schwammenthal Y, Merzeliak O, Toashi M, Orion D, et al. Chronic kidney disease and clinical outcome in patients with acute stroke. *Stroke.* (2009) 40:1296–303. doi: 10.1161/STROKEAHA.108.520882

6. Friedman PJ. Serum creatinine: an independent predictor of survival after stroke. *J Intern Med.* (1991) 229:175–9. doi: 10.1111/j.1365-2796.1991.tb00327.x

7. Lehmann F, Schenk LM, Bernstock JD, Bode C, Borger V, Gessler F, et al. Admission dehydration status portends adverse short-term mortality in patients with spontaneous intracerebral hemorrhage. *J Clin Med.* (2021) 10:5939. doi: 10.3390/jcm10245939

8. Cutting S, Castro C, Lee VH, Prabhakaran S. Impaired renal function is not associated with increased volume of intracerebral hemorrhage. *J Stroke Cerebrovasc Dis.* (2014) 23:86–90. doi: 10.1016/j.jstrokecerebrovasdis.2012.09.010

9. Gao B, Gu H, Yu W, Liu S, Zhou Q, Kang K, et al. Admission dehydration is associated with significantly lower in-hospital mortality after intracerebral hemorrhage. *Front Neurol.* (2021) 12:637001. doi: 10.3389/fneur.2021.637001

10. Totzeck M, Schuler M, Stuschke M, Heusch G, Rassaf T. Cardio-oncology - strategies for management of cancer-therapy related cardiovascular disease. *Int J Cardiol.* (2019) 280:163–75. doi: 10.1016/j.ijcard.2019.01.038

11. Eslami V, Tahsili-Fahadan P, Rivera-Lara L, Gandhi D, Ali H, Parry-Jones A, et al. Influence of intracerebral hemorrhage location on outcomes in patients with severe intraventricular hemorrhage. *Stroke.* (2019) 50:1688–95. doi: 10.1161/STROKEAHA.118.024187

12. Johnson AE, Pollard TJ, Shen L, Lehman LW, Feng M, Ghassemi M, et al. MIMIC-III, a freely accessible critical care database. *Sci Data.* (2016) 3:160035. doi: 10.1038/sdata.2016.35

13. GBD 2019 Stroke Collaborators. Global, regional, and national burden of stroke and its risk factors, 1990-2019: a systematic analysis for the Global Burden of Disease Study 2019. *Lancet Neurol.* (2021) 20:795–820. doi: 10.1016/S1474-4422(21)00252-0

14. Global, regional and country-specific burden of ischaemic stroke, intracerebral haemorrhage and subarachnoid haemorrhage: a systematic analysis of the global burden of disease study 2017. *Neuroepidemiology.* (2020) 54:171–9. doi: 10.1159/000506396

15. McCullough PA, Li S, Jurkovitz CT, Stevens LA, Wang C, Collins AJ, et al. CKD and cardiovascular disease in screened high-risk volunteer and general populations: the Kidney Early Evaluation Program (KEEP) and National Health and Nutrition Examination Survey (NHANES) 1999-2004. *Am J Kidney Dis.* (2008) 51:S38–45. doi: 10.1053/j.ajkd.2007.12.017

16. Go AS, Chertow GM, Fan D, McCulloch CE, Hsu CY. Chronic kidney disease and the risks of death, cardiovascular events, and hospitalization. *N Engl J Med.* (2004) 351:1296–305. doi: 10.1056/NEJMoa041031

17. Hillege HL, Nitsch D, Pfeffer MA, Swedberg K, McMurray JJ, Yusuf S, et al. Renal function as a predictor of outcome in a broad spectrum of patients with heart failure. *Circulation.* (2006) 113:671–8. doi: 10.1161/CIRCULATIONAHA.105.580506

18. Chronic Kidney Disease Prognosis Consortium, Matsushita K, van der Velde M, Astor BC, Woodward M, Levey AS, et al. Association of estimated glomerular filtration rate and albuminuria with all-cause and cardiovascular mortality in general population cohorts: a collaborative meta-analysis. *Lancet.* (2010) 375:2073–81. doi: 10.1016/S0140-6736(10)60674-5

19. Anavekar NS, McMurray JJ, Velazquez EJ, Solomon SD, Kober L, Rouleau JL, et al. Relation between renal dysfunction and cardiovascular outcomes after myocardial infarction. *N Engl J Med.* (2004) 351:1285–95. doi: 10.1056/NEJMoa041365

20. MacWalter RS, Wong SY, Wong KY, Stewart G, Fraser CG, Fraser HW, et al. Does renal dysfunction predict mortality after acute stroke? A 7-year follow-up study. *Stroke.* (2002) 33:1630–5. doi: 10.1161/01.STR.0000016344.49819.F7

21. Yeh SJ, Jeng JS, Tang SC, Liu CH, Hsu SP, Chen CH, et al. Low estimated glomerular filtration rate is associated with poor outcomes in patients who suffered a large artery atherosclerosis stroke. *Atherosclerosis.* (2015) 239:328–34. doi: 10.1016/j.atherosclerosis.2015.01.038

22. Hao Z, Wu B, Lin S, Kong FY, Tao WD, Wang DR, et al. Association between renal function and clinical outcome in patients with acute stroke. *Eur Neurol.* (2010) 63:237–42. doi: 10.1159/000285165

23. Kumai Y, Kamouchi M, Hata J, Ago T, Kitayama J, Nakane H, et al. Proteinuria and clinical outcomes after ischemic stroke. *Neurology.* (2012) 78:1909–15. doi: 10.1212/WNL.0b013e318259e110

24. Lortet-Tieulent J, Georges D, Bray F, Vaccarella S. Profiling global cancer incidence and mortality by socioeconomic development. *Int J Cancer.* (2020) 147:3029–36. doi: 10.1002/ijc.33114

25. Carioli G, Malvezzi M, Bertuccio P, Hashim D, Waxman S, Negri E, et al. Cancer mortality in the elderly in 11 countries worldwide, 1970-2015. *Ann Oncol.* (2019) 30:1344–55. doi: 10.1093/annonc/mdz178

26. Woolhandler S, Himmelstein DU. The relationship of health insurance and mortality: is lack of insurance deadly? *Ann Intern Med.* (2017) 167:424–31. doi: 10.7326/M17-1403

frontiers | Frontiers in Cardiovascular Medicine

TYPE Review
PUBLISHED 09 January 2023
DOI 10.3389/fcvm.2022.1021934

Check for updates

OPEN ACCESS

EDITED BY
Morgan Salmon,
Michigan Medicine, University of Michigan, United States

REVIEWED BY
Matthew Bersi,
Washington University in St. Louis, United States
Stéphanie Gayral,
INSERM U1048 Institut des Maladies Métaboliques et Cardiovasculaires, France

*CORRESPONDENCE
Bhama Ramkhelawon
✉ bhama.ramkhelawon@nyulangone.org
Muhammad Yogi Pratama
✉ muhammadyogi.pratama@nyulangone.org

†These authors have contributed equally to this work and share first authorship

‡These authors have contributed equally to this work and share last authorship

SPECIALTY SECTION
This article was submitted to General Cardiovascular Medicine, a section of the journal Frontiers in Cardiovascular Medicine

RECEIVED 17 August 2022
ACCEPTED 29 November 2022
PUBLISHED 09 January 2023

CITATION
Lowis C, Ramara Winaya A, Kumari P, Rivera CF, Vlahos J, Hermantara R, Pratama MY and Ramkhelawon B (2023) Mechanosignals in abdominal aortic aneurysms.
Front. Cardiovasc. Med. 9:1021934.
doi: 10.3389/fcvm.2022.1021934

COPYRIGHT
© 2023 Lowis, Ramara Winaya, Kumari, Rivera, Vlahos, Hermantara, Pratama and Ramkhelawon. This is an open-access article distributed under the terms of the Creative Commons Attribution License (CC BY). The use, distribution or reproduction in other forums is permitted, provided the original author(s) and the copyright owner(s) are credited and that the original publication in this journal is cited, in accordance with accepted academic practice. No use, distribution or reproduction is permitted which does not comply with these terms.

Mechanosignals in abdominal aortic aneurysms

Christiana Lowis[1,2†], Aurellia Ramara Winaya[1,2†], Puja Kumari[1,3], Cristobal F. Rivera[1,3], John Vlahos[1,3], Rio Hermantara[2], Muhammad Yogi Pratama[1,3*‡] and Bhama Ramkhelawon[1,3*‡]

[1]Division of Vascular and Endovascular Surgery, Department of Surgery, New York University Langone Medical Center, New York, NY, United States, [2]Department of Biomedicine, Indonesia International Institute for Life-Sciences, Jakarta, Indonesia, [3]Department of Cell Biology, New York University Langone Medical Center, New York, NY, United States

Cumulative evidence has shown that mechanical and frictional forces exert distinct effects in the multi-cellular aortic layers and play a significant role in the development of abdominal aortic aneurysms (AAA). These mechanical cues collectively trigger signaling cascades relying on mechanosensory cellular hubs that regulate vascular remodeling programs leading to the exaggerated degradation of the extracellular matrix (ECM), culminating in lethal aortic rupture. In this review, we provide an update and summarize the current understanding of the mechanotransduction networks in different cell types during AAA development. We focus on different mechanosensors and stressors that accumulate in the AAA sac and the mechanotransduction cascades that contribute to inflammation, oxidative stress, remodeling, and ECM degradation. We provide perspectives on manipulating this mechano-machinery as a new direction for future research in AAA.

KEYWORDS

abdominal aortic aneurysm, mechanosignals, shear stress, mechanotransduction, mechanical stress, vascular pathology

1. Divergent mechanosignals during AAA development

Although the advancement of surgical approaches as curative management of abdominal aortic aneurysm (AAA) has become more sophisticated in recent years, there is still a shortage of non-interventional treatments available to curb the growth of aneurysm sacs, thereby reducing the risk of life-threatening aortic rupture (1). This limitation is mainly due to the gap in knowledge regarding complex pathological signaling networks that are present during different phases of AAA. Clinical studies have established that the aorta is hemodynamically altered during the early and progressing phases of AAA, which is associated with sac expansion and rupture (2–4). However, the exact mechanobiology during each specific stage of the disease

remains uncertain. Understanding how the aortic cells can sense these hemodynamic changes and the mechanisms they employ to convert the mechanical stimuli into biochemical signals that modulate AAA initiation, progression and rupture are essential to design targetable therapy, consolidating prediction markers and, most importantly, improving our understanding of the complex pathobiology of AAA.

Within the vascular wall, the cells and composite extracellular matrix (ECM) are constantly exposed to the toned physical forces and mechanical stimuli from the luminal and adventitial microenvironment (5). Endothelial cells (ECs), vascular smooth muscle cells (SMCs), inflammatory cells residing in the aortic tissue, and critical elements of the ECM (collagen, elastin, and proteoglycans) are subjected to cyclic stretch, circumferential stress, and shear stress due to changes in flow and pressure in the vasculature (6–8). These applied forces could be extended beyond the endothelium layer and result in circumferential stress and stretch in the tunica media and adventitia, which likely contribute to the initial steps that promote AAA onset (9). ECs, SMCs, fibroblasts, and immune cell infiltrates likely sense these tensions, thereby triggering several signaling pathways that dictate their function, a mechanism known as mechanotransduction (10, 11). From the mechanical point of view, the critical state of AAA is formed when the mechanical stresses (internal forces per unit area) within the aneurysmal wall exceed the ability of the wall to withstand these stresses (**Figure 1**). The circumferential stress imposed by blood pressure, along with increased perivascular constraints and microstructural changes, are strongly associated with the decline of the overall wall strength and likely lead to rupture (12). To date, the current literature demonstrates that these signals could mediate vascular remodeling, immune cell activation, reactive oxygen species (ROS) generation, and apoptosis in AAA.

2. Endothelial and smooth muscle cell mechanosensors in AAA

The vascular ECs, which line the inner surface of blood vessels in direct contact with blood flow, are strategically positioned to sense and respond to these hemodynamic and biochemical changes, thereby tuning the vascular tone (13–16). In physiological states, the endothelial layer of linear segments of the aorta is subjected to high shear stress (HSS), a frictional laminar force (15–20 dynes/cm^2) generated by blood flow, which regulates local oxidative stress, reinforces the inflammatory barrier capacity and protects the overall segment against pathological remodeling (17, 18). In curved areas of the aortic tree, pulsatile blood flow with turbulent patterns produce a range of low shear stress (LSS) magnitudes (0–2 dynes/cm^2), which over-activate the ECs, thereby reprogramming their function to create oxidative stress and attract immune cells circulating in the blood (19, 20). HSS and LSS are inherent to the nature of the architecture of the aorta comprised of linear segments, curvatures, and bifurcations. The abdominal portion of the aorta is an intriguing hemodynamic carrefour comprised of several projections of the renal, mesenteric, and gonadal arteries that generate a spectrum of microflow LSS patterns at the inner curvatures of the bifurcations. ECs are equipped with multiple sophisticated mechanosensory machineries present at their membrane, including ion channels (21–24), tyrosine kinase receptors (25, 26), G protein-coupled receptors (GPCR) (27), integrins (28, 29), and the cytoskeleton (30, 31). Boyd et al. (2) demonstrated the presence of altered shear stress in patients with AAA, which was significantly upregulated at sites of AAA rupture. The cytoprotective ECs phenotype was shown to be generated under HSS during physiological conditions (8, 17). *In vivo* studies by Xie et al. (32) showed that ECs subjected to LSS and disturbed flow undergo increased apoptosis through increased monocyte adhesion and inflammatory responses. While HSS is physiologically observed in the normal abdominal aorta, the laminar flow pattern is switched to LSS patterns exerting additional stress on the endothelium once the aortic tissue is deformed into a bulged structure, introducing new curvatures within the AAA sac (33). Observations in patients with aneurysms have demonstrated that LSS magnitude is co-incident with rupture sites (2–4, 12, 34), further emphasizing the association between LSS and the severity of AAA. While these studies suggest that LSS could be an important triggering factor that elicits rupture, it might also reflect a consequence of altered aortic microarchitecture at the rupture site. Notably, other mechanical parameters were not assessed in these studies, likely due to the complexity of capturing timed rupture events, which would have provided a comprehensive pattern of hemodynamic forces that manifest during rupture. Furthermore, it is also likely that LSS leads to the activation of the endothelium at the initial phases of AAA formation, coinciding with the deformation of the aortic tissue from a luminal tube into a bulged structure. However, these studies are difficult to perform in human studies as they require close monitoring of patients at risk to capture the hemodynamics at these germinal stages of AAA formation.

The altered aortic biomechanics at critical stages during the onset, progression, and rupture of AAA likely incite downstream multifactorial mechanotransduction signaling patterns that intersect with pathological vascular remodeling programs in ECs. Notably, whole-genome sequencing performed by Erhart et al. (35) showed the association between ECM genes with different shear stress profiles in human aneurysmal tissue. In patients with LSS, their genetic profile significantly correlated with the upregulation of Laminin subunit alpha-4 (LAMA4) and Sushi-repeat containing protein x-linked-2 (SRPX2) gene that provoked ECM degradation and the downregulation of several pro-inflammatory chemokines that suppress inflammation, suggesting that shear stress dynamics are capable of directly modulating ECM degradation

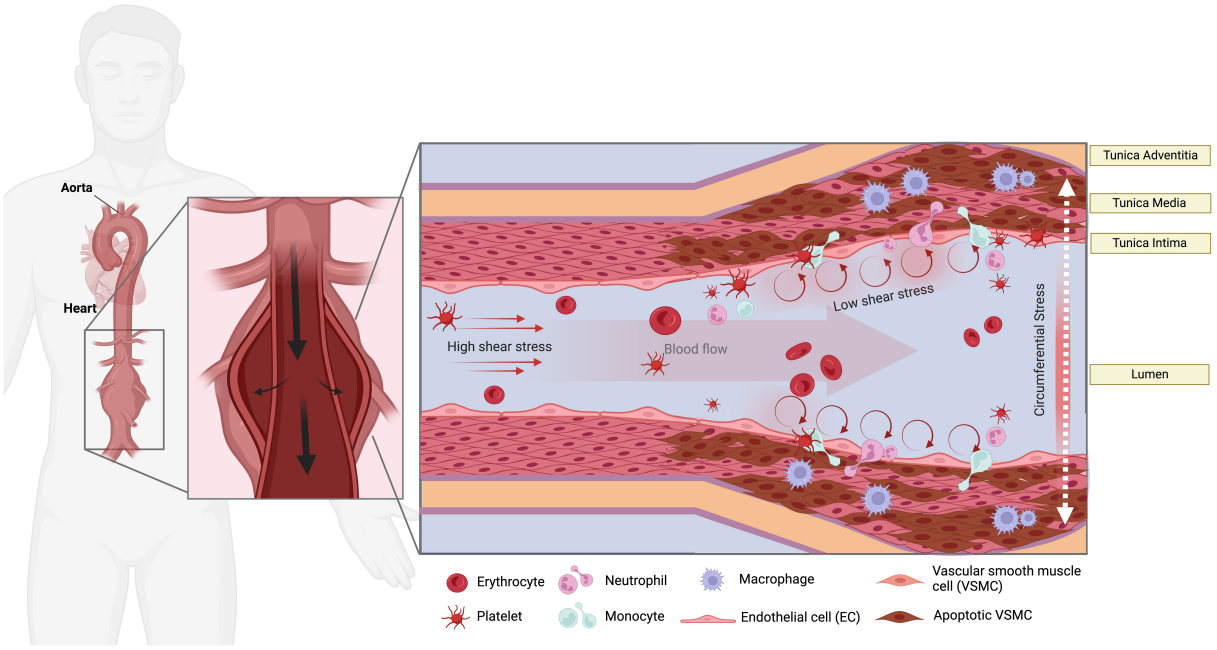

FIGURE 1
Mechanical stressors in AAA. The endothelial layer of the aorta is subjected to high shear stress (HSS) in linear segments of the aorta. Turbulent low shear stress (LSS), along with the increase of circumferential stress imposed by blood pressure and aortic stiffness, are sensed at curved areas. LSS can over-activate the ECs to attract immune cells and contribute to the pathological remodeling and SMCs apoptosis *via* mechanosensory machinery in the ECs. Platelet activation and accumulation in the AAA sac likely occur during the progression of AAA.

programs through distinct transduction pathways during the progression of AAA. Moreover, several elastin-derived peptides and enzymes generated by the degradation of elastin fibers have been linked to elicit a pro-inflammatory environment and further drive elastin degradation during AAA progression (6, 36), even though their precise role in the mechanosignaling pathways are yet to be elucidated.

2.1. Ion channel mechanotransduction pathways in AAA

It has been widely recognized that ion channels can function as essential mechanotransducers that maintain the dynamic balance in the pulsatile vascular wall. The transient receptor potential isoform-4 (TRPV4) is a calcium-permeable channel commonly expressed by ECs and SMCs, which can regulate calcium influx *via* shear stress sensing and subsequently induce vasodilation (NO and PGI2) in AAA when shear stress increases (37–41). Calcium-induced membrane depolarization is considered a major event that occurs following the activation of the ion channel, which potentially contributes to the early development of AAA. Shannon et al. (42) demonstrated that a specific TRPV4 antagonist, GSK2193874, was able to attenuate aortic growth and decrease pro-inflammatory cytokines in both angiotensin II (AngII)-induced AAA in ApoE$^{-/-}$ mice and in ECs in culture, thereby reducing the activation of SMCs and trans-endothelial migration during AAA formation (**Table 1** and **Figure 2**).

Several *in vivo* studies have been conducted in rodents with AAA modeled by calcium chloride ($CaCl_2$) or calcium phosphate ($CaPO_4$) treatment. These models are based on vasodilation, calcification, oxidative stress, and SMCs apoptosis (43, 44) that culminate in ECM degradation and AAA onset. This suggests the critical role of calcium-induced mechanisms as central regulatory hubs in the pathogenesis of AAA. Indeed, Ca^{2+} is a vital cofactor that fuels the activation of matrix metalloproteinases (MMPs), widely regarded as the pathological culprits that exaggeratedly degrade the ECM during AAA. Hence, strategies to manipulate Ca^{2+} levels are desirable to curb AAA. However, it is worth noting that the use of broad-spectrum Ca^{2+} blockers did not show beneficial effects in treating thoracic aneurysm progression associated with Marfan syndrome (45). Future studies are needed to delineate the triggers and downstream signaling pathways that interconnect with Ca^{2+} signaling in distinct vascular cell types during AAA to optimally devise strategies to specifically modulate pathological Ca^{2+} programs such as those mediated by Piezo1, as discussed later.

Li et al. (46) showed that the activation of calpain, calcium-dependent cysteine proteases, through shear stress-coupling

TABLE 1 Summary of mechanosensors, actions, and their phenotypic effects in AAA.

Cells	Mechanosensors	Actions	Phenotypic effects	References
SMCs	Piezo1	Increase in cytoskeleton cross-linking of α-actinin2 regulated by Netrin-1, elevated MMP3	Matrix stiffness alters SMCs function, ECM degradation	(52)
ECs and SMCs	TRPV4	Release of vasodilators mediators (NO, PGI2) through Ca^{2+} influx. Increased migration of myeloid cells, elevated MMP2, and MMP9	Vasodilation and migration of SMCs, aortic inflammation, vascular remodeling	(42)
ECs	Integrin α5β1	FAK activation leading to NO production	Vasodilation and migration of SMCs	(65)
SMCs	AT1R	Activate ERK1/2 signaling	ECM degradation, SMCs migration, release of proinflammatory cytokines	(69)

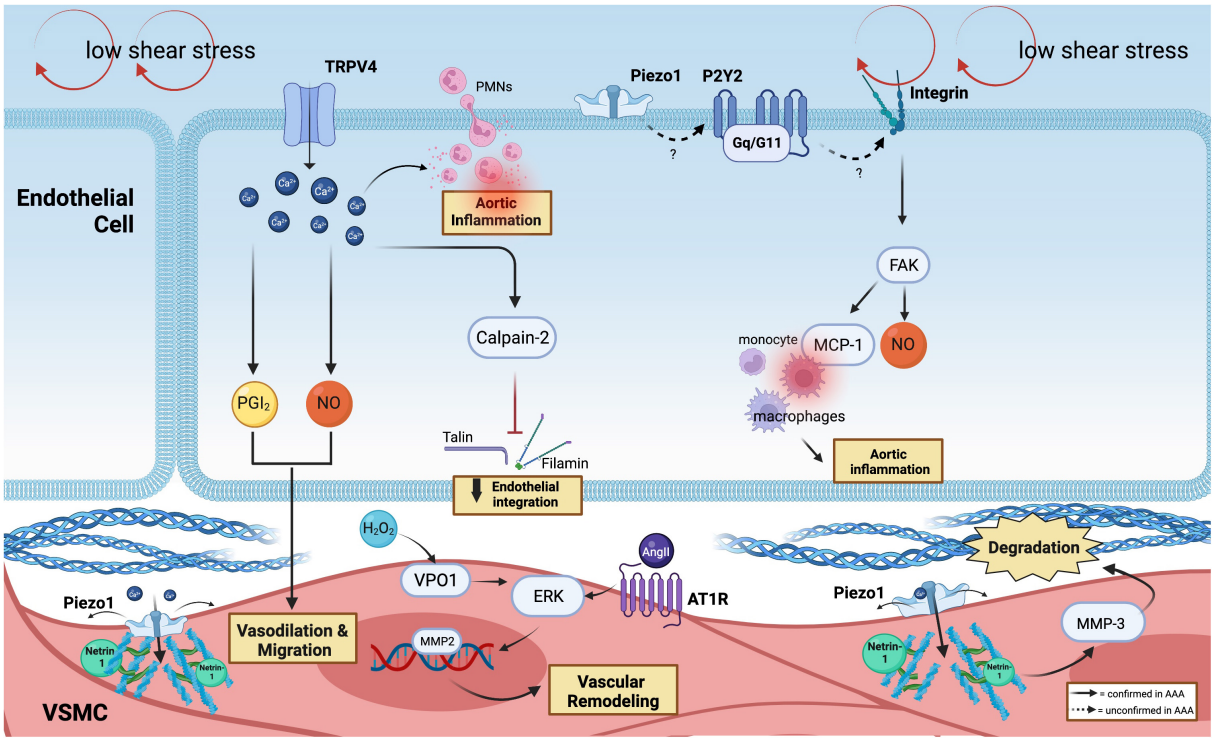

FIGURE 2
Mechanoreceptors involved in AAA. In the ECs, low shear stress is sensed by the ion channel (TRPV4 and Piezo1) and purinergic-coupled receptors (P2Y2-Gq11). Through Ca^{2+}-responses, which produce PGI_2 and NO, SMCs vasodilate and migrate, followed by the release of calpain-2 that induce the loss of endothelial integration. Ca^{2+} flux facilitates PMNs infiltration and inflammation. P2Y2-Gq11 is predicted to activate integrin, which can drive FAK activation. FAK plays a vital role in mediating and recruitment of macrophages *via* MCP-1 and participating in the production of NO. Netrin-1 promotes Piezo1 opening in SMCs, which activates MMP3 and causes collagen degradation. PECAM-1, VE-cadherin, and VEGFR2 can further activate FAK and MCP-1 secretion that recruits macrophages. The phenotypic switching of SMCs is induced by the H_2O_2/VPO1/ERK pathway in AAA and *via* AT1R activation.

could target the ECM cytoskeleton. Specifically, calpain-2 could fragment talin and filamin, disrupting endothelial organization and alignment that facilitates ECs and SMCs migration in AngII-induced AAA in $LDLR^{-/-}$ mice (47). Subramanian et al. (48) later conducted *in vivo* pharmacological inhibition of a novel calpain inhibitor, BDA-410, which successfully reduced the incidence and development of AAA by attenuating the activation of MMP12, pro-inflammatory cytokines, and macrophage infiltration into the aorta using similar AAA mice models.

The recently discovered ion channel mechanosensor, Piezo1, has gained much interest in the cardiovascular field. Piezo1 channel exhibits a three-bladed, propeller-shaped homotrimer structure with a dome mechanism, which sustains a potential energy source for its mechanosensitive gating (49). Accordingly, Piezo1 is known to be activated with a

half-maximal shear stress intensity of 57 ± 3 dynes/cm^2 that leads to a cascade of downstream signaling pathways in ECs and SMCs (14). Indeed, Kang et al. (24) have shown the alteration of both physiological and functional properties of ECs following shear-induced activation of Piezo1. In atherosclerosis, Albarrán-Juárez et al. (50) demonstrated the role of Piezo1 as a shear stress sensor, thereby causing the polarization of ECs under disturbed flow, triggering the release of ATP that activates the P2Y2-Gq/G11 coupled-receptor in promoting integrin activation. This could be a relevant pathway to be examined in AAA, given the similar shear perturbations in the aneurysmal sac. Further investigations are warranted using the inducible conditional loss of Piezo1 in ECs since Piezo1 disruption during early embryogenesis has led to lethal vascular impairment in mice (46, 51).

The discovery made by Qian et al. (52) remains the only study that directly addressed the role of Piezo1 in AAA. Unlike ECs, SMCs are predominantly activated *via* mechanical stretch that influences the structural organization and signaling in SMCs (53, 54). Arterial stiffness and increased cytoskeleton cross-linking of α-actinin2 by Netrin-1 in SMCs were observed in AAA walls, powering the opening of Piezo1 (52) and leading to downstream activation of MMP3. Thus, we showed the detailed signaling trajectory that lead to the activation of Piezo1 in AAA, which was further supported by atomic force microscopy (AFM) analysis, which demonstrated elevated stiffness within the SMCs. In addition, single-cell RNA sequencing of mice AAA specimens revealed the increase of Piezo1 expression in SMCs in AAA groups, suggesting the transcriptional regulation of Piezo1.

Currently, the GsMTx4 peptide is the only Piezo1 inhibitor tested in AAA, which has been shown to repress matrix degradation *via* MMP3 and reduce aortic dilatation in the AngII and elastase-induced AAA mice models (52). However, GsMTx4 was reported to exert off-target effects, such as the inhibition of voltage-gated sodium channels (55), warranting further studies to design more specific inhibitors. Hadi et al. (56) described that the deficiency of MMP3 in mice protects against AAA, suggesting that this ECM degrading program could be at the intersection of mechanosensory signals during AAA development.

2.2. Integrin-mediated pathways in AAA

In static conditions, the mechanosensitive integrins are inactively assembled as dormant unphosphorylated complexes (57). Shear stress patterns can activate signaling *via* several integrins such as PECAM-1, vascular endothelial cadherin (VE-cadherin), and vascular endothelial growth factor-2 (VEGFR2), through conformational changes and specific interactions of the α and β subunits which can drive focal adhesion kinase (FAK) activation (58–60). FAK plays an essential role in macrophage-mediated chronic progression of AAA as FAK inhibitor attenuates macrophage inflammatory responses during AAA development (61). According to prior reports, FAK can stimulate fibroblasts to secrete monocyte chemoattractant protein (MCP-1), which then causes macrophage recruitment. MCP-1 is essential for the onset of AAA and vascular inflammation (62).

It was previously reported that the integrin subset, α5β1, selectively binds collagen and fibronectin (63). Cheuk and Cheng showed that the distinct reduction in integrin α5β1 expression was seen in human aneurysmal aortic tissues and was associated with a reduction in the density of SMCs (64). Therefore, the lack of this integrin subset may impede matrix protein attachment and alter the geometry of the aortic media, potentially forming aneurysms. This discovery is in line with other studies which postulated that the absence of β1 may influence vascular mechano-adaptivity and alter its phenotype (12, 65). The activation of β1 integrin by shear stress using the fibronectin–integrin–cytoskeleton connection in primary human umbilical vein ECs (HUVEC) subjected to different levels of shear stress confirmed these studies. It was found that β1 integrin serves as a signaling mediator of three different levels of shear stress (0.04, 2.0, and 3.7 Pa), suggesting the critical role of this protein in scaling the mechanosensory potential of ECs (66).

2.3. G-protein coupled receptors (GPCRs) signaling pathway in AAA

G-Protein coupled receptors are characterized by the presence of seven transmembrane alpha-helics and are considered the largest protein superfamily observed in a higher organism (67). Several GPCRs, such as β_2ARs (β_2-adrenergic receptor) and AT1R (angiotensin II type I receptor), are present in ECs and SMCs, regulating an array of functions including vascular tone, angiogenesis, and cell proliferation. AT1R has also been demonstrated to act as a mechanosensor in ECs and can be activated under excess mechanical stretch (68). It was observed that the mechanical activation of AT1R in hypertensive mice amplifies AAA growth and significantly elevates the activity of ERK1/2 in hypertensive (BPH/2) and normotensive (BPH/3) mice (69). The hyperactivation of AT1R may increase macrophage infiltration, which leads to the production of inflammatory cytokines, ECM degradation, and sac expansion, with a propensity to rupture (70, 71). Despite the need for mechanistic validation study in larger animal models, AT1R blockers, such as Losartan and Telmisartan (69, 72), were shown to slow AAA growth and rupture in elastase-treated brown rats and hypertensive BPH/2 mice even though conflicting result was observed from a randomized clinical trial in patients with AAA (73).

3. Mechanical stress, inflammation, and redox stress circuits in AAA

AAA is established as an inflammatory and redox condition of the aortic tissue. Various immune cells interact with each other and mediate crosstalk with vascular cells within the AAA sac. To this end, persistent LSS that fuel the release of inflammatory cytokines may encourage matrix remodeling and severe inflammation influencing aneurysmal growth (74). It is established that LSS is the prime origin of elevated levels of reactive oxygen species (ROS) and inflammatory genes that sustain ECM degradation in AAA through nuclear factor kappa B (NF-κB), MAP protein kinase (MAPK), and transforming growth factor beta (TGF-β) pathways (75–77).

Oxidative stress plays a significant role in mechanotransduction (78, 79). ROS persists at high levels in response to low and turbulent SS. Flow-mediated ROS such as O_2^- may transform into H_2O_2, and through the Fenton reaction, H_2O_2 can spontaneously transform into hydroxyl radical (OH), all of which have been detected in increased amounts in AAA samples and positively associated with aneurysm size and mortality risk of patients (80). There are multiple sources of ROS production such as uncoupled eNOS, xanthine oxidase (XO), cyclooxygenase, mitochondria, and NADPH oxidase (81). Shear stress may increase endothelial XO expression and activity by utilizing molecular oxygen as an electron acceptor together with H_2O, O_2^-, and xanthine/hypoxanthine, XO produces O_2^- and H_2O_2 (82). Mitochondrial ROS produced from aortic macrophages was also described to induce matrix degradation *via* receptor-interacting serine/threonine-protein kinase-3 (RIPK3) in AAA induced by injured lungs, suggesting the pathological role of RIPK3 to trigger ROS production (83). Moreover, it was observed that ROS produced from these pro-inflammatory macrophages can activate MMP12, subsequently leading to matrix degradation in the aorta and fueling AAA expansion (83). It is interesting to further explore whether this macrophage-derived ROS circuit is also induced by mechanical stresses with or without underlying inflammation. However, a clinical study performed in patients with AAA undergoing surgical repair showed that oxidase systems such as XO and mitochondria were not altered by their corresponding inhibitors in AAA (84). Mice with a deficiency in eNOS pre-uncoupled HPH-1 gene treated with angiotensin II spontaneously developed AAA and died from ruptured AAA. Oral administration of folic acid prevented AAA formation in these mice by restoring vascular remodeling through MMP2 and MMP9 reduced activity and alleviated macrophage accumulation in the wall (85).

NADPH oxidase is an important source of O_2^- in AAA. Mechanical stimuli can trigger NADPH oxidase to utilize NADH/NADPH as an electron donor to reduce the molecular oxygen (86). In iNOS$^{-/-}$ deficient mice, specific inhibition of NADPH oxidases successfully prevented aneurysm formation (87), suggesting a circuit between NADPH, iNOS, and NO levels in stimulating AAA progression (**Figure 3**).

4. Intraluminal thrombus and mechanosensing in AAA

In recent years, many studies have tried establishing the role of activated platelets in the development and progression of AAA. Aside from their crucial role in thrombosis and hemostasis, a non-occlusive intraluminal thrombus (ILT) formation is known to contribute to the pro-inflammatory and prothrombotic backdrop of AAA (88–90). It was initially hypothesized that ILT could act as a protective mechanism to reduce mechanical stress induced on the vascular wall (91). The formation of ILT occurs following platelet activation, aggregation, and adhesion in regions of LSS, subsequently decreasing the mechanical stress on the aortic wall and maintaining AAA stability (92). However, evidence shows that the presence of ILT is associated with the production of hypoxia, elastolysis, and pro-inflammatory microenvironment surrounding the aneurysmal wall (93). It was demonstrated that different shear stress patterns that might occur during thrombotic events within the aortic walls could contribute to the progression of ILT and consequently exacerbate AAA (94, 95). Based on these studies, it has been concluded that while there may be early beneficial effects of ILT, it is likely that the presence of ILT might have deleterious effects as the disease progresses.

Surprisingly, thrombus formation is also observed in regions exposed to low (13, 96) and oscillatory SS (97). High shear rates can further activate the von Willebrand factor (vwf), a key player in platelet adhesion (98). Whereas at LSS, fibrinogen binding to GPIIb/IIa is mainly responsible for aggregation (99). Previous clinical studies have shown the positive effect of anticoagulant therapy on lowering ILT thickness and volume (100). The exact mechanism of the role of platelet in the mechanotransduction is still unknown, whether the mechanical changes associated with AAA development subsequently modulate the phenotype of activated platelets, whether platelets contribute to the shear sensing of ECs and interfere with its mechanoreceptors within the AAA sac still warrants further investigation.

5. Mechanotransduction in AAA: A translational perspective

It is clear that mechanical disturbance in the aortic environment and the changes in mechanotransduction within aortic tissue are progressive events during AAA development; hence, monitoring these events in a clinical setting could be beneficial for improved surveillance and therapeutic purpose.

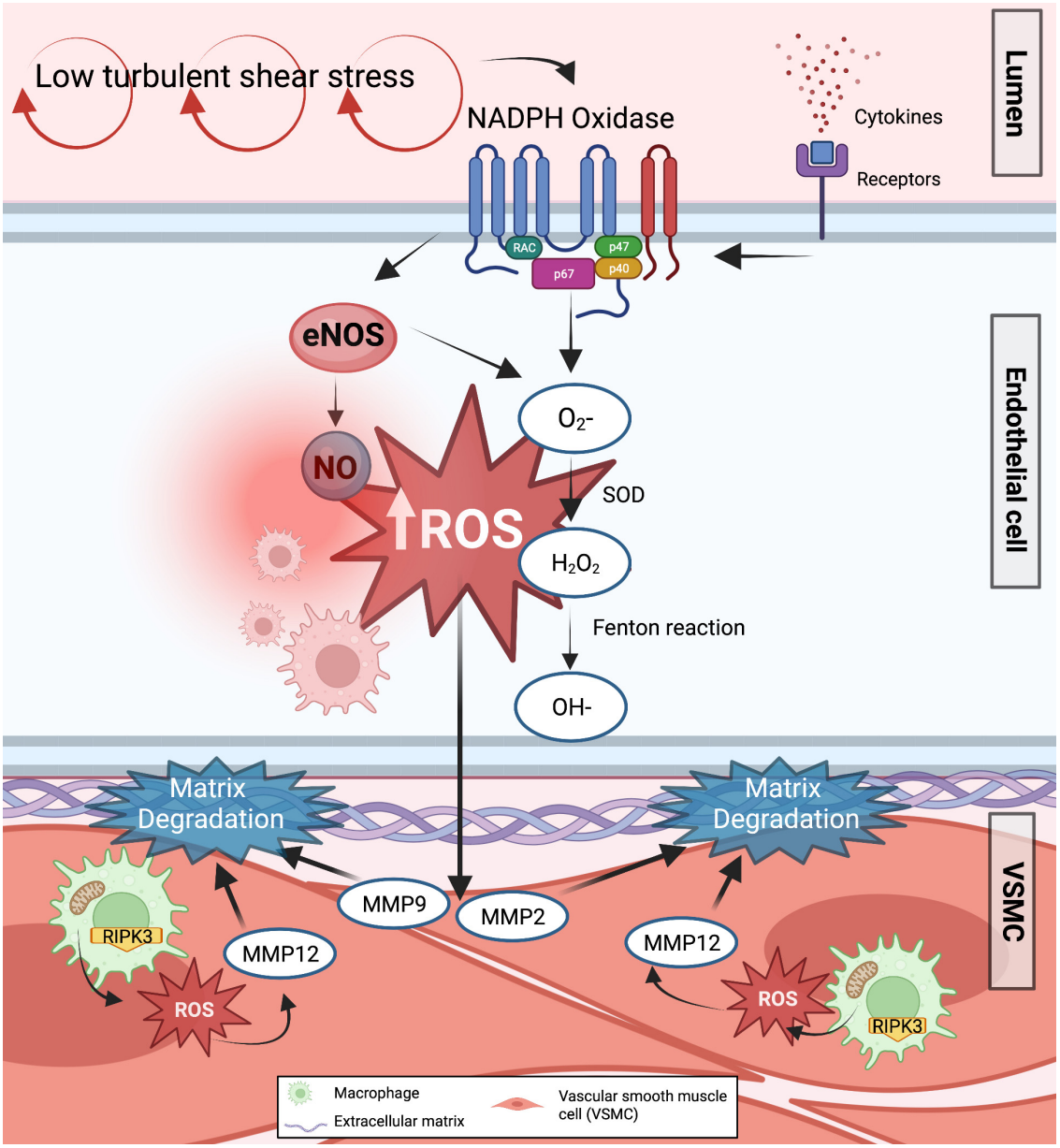

FIGURE 3
Formation of ROS in response to low shear stress in AAA. The majority of ROS primary sources, such as uncoupled eNOS and NADPH oxidase, are known to enhance ROS generation in response to low shear stress. As a result, various ROS are generated in the endothelium cells. Increased O_2^- and H_2O_2 inactivates endothelium-derived NO synthase and takes up any NO produced while augmenting the transcriptional factors involved in the activation of downstream effectors related to matrix degradation and inflammation. Furthermore, mitochondrial ROS are produced from pro-inflammatory aortic macrophages *via* RIPK3, further inducing matrix degradation and AAA expansion.

5.1. Tools to study mechanotransduction in AAA

Mimicking the cellular response to shear stress persists as the main challenge to study the mechanotransduction channels in AAA. Such studies require an appraisal of large animal or specific rodent models to observe vascular mechanical responsiveness while integrating several bioreactors and physical methods to apply flow to cells and specify the response of ECs from mass transport mechanisms (101). Bowden et al. (102) summarized the availability of *in vitro* and *in vivo* models to examine shear stress in AAA. Accordingly, porcine pancreatic elastase (PPE) infusion, along with partial ligation of the iliac artery in murine and rodent models, can increase mechanical stretch and shear stress and alter the morphology of AAA phenotypes (103, 104). However,

the difference in SS experienced between murine and human vasculature can lead to significant variation and bias in translating the results effectively. The porcine model can be a helpful alternative due to comparable vascular anatomy and mechanical rheology with humans (102, 105). Induction of elastase along with β-aminopropionitrile (BAPN) in the porcine model was successfully created and generated an additional analogous AAA model sharing similar hallmarks with human AAA (106). Thus, these large animal models seem adequate to test novel therapies targeting mechanotransduction signaling pathways to curb AAA development.

In order to understand the mechanism by which cells respond to mechanical stress and the mechanotransduction signaling that drives AAA at the subcellular level, a stringent *in vitro* system is necessary to mimic *in vivo* conditions, which remain a challenge considering cells in culture are not subjected to constant stress, ECM microenvironment and physical forces observed *in vivo* (107). Several studies have tackled such issues by creating a multi-layered 3D-vascular scaffold that can mimic the biological vasculature as opposed to the traditional 2D culture of SMCs or ECs (108–110). Organ-on-chip platforms have been utilized to characterize the interactions between ECs and SMCs. Using a platform bioprinted into a microfluidic device, SMCs and ECs can be cocultured on a porous, tensile membrane that underwent mechanical stretch and shear stress, making this system suitable to delve into the mechanical mechanisms in AAA and for the testing of high-throughput drug candidates (110). Using this model, Chen et al. replicated the cyclic stretch of human pluripotent stem cell-derived aortic smooth muscle cells (hPSC-HASMCs) to study the effect of metformin in aortic aneurysm development. They identified that metformin is capable of targeting NOTCH1 signaling, thereby rescuing the SMCs pathological switch that occurs in AAA (111).

Bogunovic et al. also developed a 3D-coculture model using primary ECs and SMCs derived from patients with AAA using poly-co-glycolide scaffolds that mimic the behavior of the medial aortic layer and exhibit mechanical properties and stiffness of AAA (112), thus serving as a promising model to understand the mechanobiology of AAA. To capture the dynamic stiffness and mechanosensing profile of SMCs, an ultrasound tweezers-based micromechanical system has been utilized to capture the mechanosensation of SMCs isolated from murine AAA (52). Transmission electron microscopy (TEM) and AFM can also be used to capture and map the structural and mechanical properties of viable human aortic SMCs (113, 114) and tissues. The recent advancement of the automatic patch-clamp system can also provide unlimited opportunities to directly measure the gating of ionic currents using an electrical force to induce cell stretching, thus allowing a recording in the membrane–matrix sites and the changes of physiological mechanosensors (98, 115, 116).

5.2. Clinical perspective: Monitoring disease progression and possible therapies

Multiple studies have shown that mechanical alterations within the AAA architecture can be utilized as a marker of the progressing phases of AAA, focusing on advanced imaging techniques and high-throughput computational methods. Previously, the changes in aortic pulse wave velocity (PWV), which allows the measurement of aortic stiffness, were reported as a promising imaging readout to monitor disease progression not only in mice but also for post-surgical prognosis of patients with AAA (117–119). However, the use of PWV to predict AAA risk needs to be evaluated in larger AAA cohorts in longitudinal studies in order to be able to be implemented clinically. Computational fluid dynamics (CFDs) is a widely used technique to investigate the potential risk of aneurysm rupture based on SS frequencies, blood flow, and changes in pressure (99, 120). However, CFD requires solid computational expertise to precisely and rigorously construct stimulations and perform numerical modeling (geometrical segmentation, fluid definition and domain) for each patient with AAA. Therefore, CFD is not yet clinically implemented and would necessitate concerted efforts from computational engineers to develop a platform using large-scale stimulations for the fast processing of geometry segmentation in a cost- and time-effective manner. Regardless, it was shown that maximum diameter and maximum wall stress were observed in the central aneurysm region, while regions with LSS (<0.4 Pa), larger curvature, and deposition of thrombus were associated with AAA expansion and higher risk of rupture (2, 3, 121). Using a CT angiography performed in 295 patients with AAA, LSS at baseline was associated with aortic expansion in a large clinical cohort, independent of any risk factors (3). It was also observed that 4D flow cardiovascular magnetic resonance images (MRIs) of the whole aorta were able to compute lower peak LSS in AAA compared to elderly controls and could be validated as a way to predict aneurysmal growth or rupture (4). Conversely, one retrospective clinical study reported greater aortic wall tension as a significant predictor of AAA rupture compared to the aortic diameter, even though this data has to be confirmed in larger prospective cohorts (122).

The Nobel-awarded study of David Julius and Ardem Patapoutian in 2021 (123) for the discovery of Piezo1 (51, 124) has further expanded its role in regulating vascular remodeling in AAA (52). Targeting Piezo1 is highly desirable as its expression peaks in established AAA, and its inhibition will likely break the cascade of signals responsible for promoting

matrix degradation in AAA (52). Recently, small molecules of Piezo1 mediators have been generated and reported in the literature. Yoda1, an activator of Piezo1, has been shown to selectively activate Piezo1 but not Piezo2 (125). Conversely, spider toxin GsMTx4 was shown to suppress Piezo1 (126) effects. However, previous studies have reported off-targets of GsMTx4 such as Piezo2 and the TRP channel (127). There is, therefore, the necessity to generate more-selective and specific compounds to inhibit Piezo1.

Other mechanical targets such as AT1R blocker, Losartan and Telmisartan, were shown to slow AAA growth in hypertensive and Marfan syndrome mice (69, 72). However, none of these discoveries have yet to been reproduced in clinical trials (45). The selectivity of these blockers also remains an issue as an *in vivo* study performed in Marfan mice treated with calcium channel blockers targeted extracellular AT1R-mediated ERK1/2 activation and resulted in deleterious effect on aortic SMCs, therefore, accelerating aneurysmal growth in the ascending aorta (128).

The availability of compounds targeting ROS and inflammation is another attractive future target for AAA treatment. Alpha-ketoglutarate, a pleitropic antioxidant, has been shown to reduce ROS generation in C57BL mice challenged with pancreatic elastase (129). Exogenous antioxidants such as folic acid, vitamin C, and vitamin E have been reported to inhibit ROS production in several animal models such as ApoE$^{-/-}$ mice and elastase-induced rat AAA models (130–132). However, no confirmatory studies have been performed in clinical subjects much needed to confirm the benefits of these agents in limiting AAA growth.

As the road to target mechanotransduction signaling pathways for therapeutic intervention remains an underdeveloped field, future works need to primarily address the exact contribution of key mechanosignaling pathways using available high-throughput systems that can replicate the microenvironment of the human aneurysm and precisely record the dynamic changes in both *in vitro* and *in vivo* models. The interrelated pathways between mechanosensors and other critical pathways in AAA may also hint that poly-pharmaceutical agents that can target both mechanosignaling and intrinsic cellular pathways are a more practical approach to prevent and limit AAA growth.

6. Concluding remarks

Mechanosensory and mechanotransduction machinery are typifying features inherent to AAA development. The formation of AAA is influenced by altered mechanical stress that amplifies pathological cellular signaling through the interaction between the stresses and mechanosensors present at the cell membrane of ECs and SMCs. In addition, increased ROS levels generally coincide with mechanotransduction during AAA, acting as critical second messengers that modulate several signaling pathways that participate in vascular remodeling, inflammation, and apoptosis. Further mapping of the mechano-behaviors in human AAA capable of capturing the dynamics of mechanical perturbation of the complex human aorta at critical phases of AAA development using sophisticated imaging and high-throughput technologies is still warranted. Further translational research is needed to test the relevance of the observations of defective mechanosensitive signals from murine to human disease. One critical step would be the use of large animal models such as porcine AAA models to test whether locally modulating mechanical signals during AAA onset would be of beneficial clinical interest. Importantly, strategies to intervene on these mechanical signals spatiotemporally are important factors to consider as most AAA are detected beyond their initial phase, bypassing an interventional window during the stages of AAA onset. Therefore, there is a dire need to discover novel druggable targets focused on altering mechanical signaling pathways during the progressing phases of AAA as the future of independent non-interventional therapies or in conjunction with current surgical approaches.

Author contributions

BR and MP conceptually developed and supervised the project and co-wrote the manuscript. AR, CL, PK, and MP did the literature search and wrote the specific sections. CR, RH, and JV edited the text, provided the feedback, and discussion. All authors contributed to the article and approved the submitted version.

Funding

BR's lab was supported by the National Institute of Health (R01HL146627 and R01HL149927). AR and CL were supported by the Department of Biomedicine, Indonesia International Institute for Life-Sciences (i3L).

Conflict of interest

The authors declare that the research was conducted in the absence of any commercial or financial relationships that could be construed as a potential conflict of interest.

Publisher's note

All claims expressed in this article are solely those of the authors and do not necessarily represent those of their affiliated organizations, or those of the publisher, the editors and the reviewers. Any product that may be evaluated in this article, or claim that may be made by its manufacturer, is not guaranteed or endorsed by the publisher.

References

1. Golledge J, Moxon J, Singh T, Bown M, Mani K, Wanhainen A. Lack of an effective drug therapy for abdominal aortic aneurysm. *J Intern Med.* (2020) 288:6–22. doi: 10.1111/joim.12958

2. Boyd A, Kuhn D, Lozowy R, Kulbisky G. Low wall shear stress predominates at sites of abdominal aortic aneurysm rupture. *J Vasc Surg.* (2016) 63:1613–9. doi: 10.1016/j.jvs.2015.01.040

3. Bappoo N, Syed M, Khinsoe G, Kelsey L, Forsythe R, Powell J, et al. Low shear stress at baseline predicts expansion and aneurysm-related events in patients with abdominal aortic aneurysm. *Circ Cardiovasc Imaging.* (2021) 14:1112–21. doi: 10.1161/CIRCIMAGING.121.013160

4. Trenti C, Ziegler M, Bjarnegård N, Ebbers T, Lindenberger M, Dyverfeldt P. Wall shear stress and relative residence time as potential risk factors for abdominal aortic aneurysms in males: a 4D flow cardiovascular magnetic resonance case–control study. *J Cardiovasc Magn Reson.* (2022) 24:18. doi: 10.1186/s12968-022-00848-2

5. Gimbrone M, Anderson K, Topper J. The critical role of mechanical forces in blood vessel development, physiology and pathology. *J Vasc Surg.* (1999) 29:1104–51. doi: 10.1016/S0741-5214(99)70252-1

6. Dabagh M, Jalali P, Butler P, Randles A, Tarbell J. Mechanotransmission in endothelial cells subjected to oscillatory and multi-directional shear flow. *J R Soc Interface.* (2017) 14:20170185. doi: 10.1098/rsif.2017.0185

7. Ramella M, Bertozzi G, Fusaro L, Talmon M, Manfredi M, Catoria M, et al. Effect of cyclic stretch on vascular endothelial cells and abdominal aortic aneurysm (AAA): role in the inflammatory response. *Int J Mol Sci.* (2019) 20:287. doi: 10.3390/ijms20020287

8. Xu J, Shi G. Vascular wall extracellular matrix proteins and vascular diseases. *Biochim Biophys Acta.* (2014) 1842:2106–19. doi: 10.1016/j.bbadis.2014.07.008

9. Kim D, Heo S, Kang Y, Shin J, Park S, Shin J. Shear stress and circumferential stretch by pulsatile flow direct vascular endothelial lineage commitment of mesenchymal stem cells in engineered blood vessels. *J Mater Sci Mater Med.* (2016) 27:60. doi: 10.1007/s10856-016-5670-0

10. Chatterjee S. Endothelial mechanotransduction, redox signaling and the regulation of vascular inflammatory pathways. *Front Physiol.* (2018) 9:524. doi: 10.3389/fphys.2018.00524

11. Martino F, Perestrelo A, Vinarský V, Pagliari S, Forte G. Cellular mechanotransduction: from tension to function. *Front Physiol.* (2018) 9:824. doi: 10.3389/fphys.2018.00824

12. Humphrey J, Schwartz M, Tellides G, Milewicz D. Role of mechanotransduction in vascular biology: focus on thoracic aortic aneurysms and dissections. *Circ Res.* (2015) 116:1448–61. doi: 10.1161/CIRCRESAHA.114.304936

13. Chiu J, Chien S. Effects of disturbed flow on vascular endothelium: pathophysiological basis and clinical perspectives. *Physiol Rev.* (2011) 91:327–87. doi: 10.1152/physrev.00047.2009

14. Krüger-Genge A, Blocki A, Franke R, Jung F. Vascular endothelial cell biology: an update. *Int J Mol Sci.* (2019) 20:4411. doi: 10.3390/ijms20184411

15. Chien S. Mechanotransduction and endothelial cell homeostasis: the wisdom of the cell. *Am J Physiol Heart Circ Physiol.* (2007) 292:H1209–24. doi: 10.1152/ajpheart.01047.2006

16. Culver J, Dickinson M. The effects of hemodynamic force on embryonic development. *Microcirculation.* (2010) 17:164–78. doi: 10.1111/j.1549-8719.2010.00025.x

17. Chen P, Qin L, Li G, Wang Z, Dahlman J, Malagon-Lopez J, et al. Endothelial TGF-β signalling drives vascular inflammation and atherosclerosis. *Nat Metab.* (2019) 1:912–26. doi: 10.1038/s42255-019-0102-3

18. Min E, Schwartz M. Translocating transcription factors in fluid shear stress-mediated vascular remodeling and disease. *Exp Cell Res.* (2019) 376:92–7. doi: 10.1016/j.yexcr.2019.01.005

19. Prahl Wittberg L, van Wyk S, Fuchs L, Gutmark E, Backeljauw P, Gutmark-Little I. Effects of aortic irregularities on blood flow. *Biomech Model Mechanobiol.* (2016) 15:345–60. doi: 10.1007/s10237-015-0692-y

20. Taguchi E, Nishigami K, Miyamoto S, Sakamoto T, Nakao K. Impact of shear stress and atherosclerosis on entrance-tear formation in patients with acute aortic syndromes. *Heart Vessels.* (2014) 29:78–82. doi: 10.1007/s00380-013-0328-z

21. Brähler S, Kaistha A, Schmidt V, Wölfle S, Busch C, Kaistha B, et al. Genetic deficit of SK3 and IK1 channels disrupts the endothelium-derived hyperpolarizing factor vasodilator pathway and causes hypertension. *Circulation.* (2009) 119:2323–32. doi: 10.1161/CIRCULATIONAHA.108.846634

22. Köhler R, Hoyer J. Role of TRPV4 in the mechanotransduction of shear stress in endothelial cells. In: Liedtke W, Heller S editors. *TRP ion channel function in sensory transduction and cellular signaling cascades.* Boca Raton, FL: CRC Press (2007). doi: 10.1201/9781420005844.ch27

23. Swain S, Liddle R. Piezo1 acts upstream of TRPV4 to induce pathological changes in endothelial cells due to shear stress. *J Biol Chem.* (2021) 296:100171. doi: 10.1074/jbc.RA120.015059

24. Kang H, Hong Z, Zhong M, Klomp J, Bayless K, Mehta D, et al. Piezo1 mediates angiogenesis through activation of MT1-MMP signaling. *Am J Physiol Cell Physiol.* (2019) 316:C92–103. doi: 10.1152/ajpcell.00346.2018

25. Lee H, Koh G. Shear stress activates Tie2 receptor tyrosine kinase in human endothelial cells. *Biochem Biophys Res Commun.* (2003) 304:399–404. doi: 10.1016/S0006-291X(03)00592-8

26. Woo K, Baldwin H. Role of Tie1 in shear stress and atherosclerosis. *Trends Cardiovasc Med.* (2011) 21:118–23. doi: 10.1016/j.tcm.2012.03.009

27. Chachisvilis M, Zhang Y, Frangos JA. G protein-coupled receptors sense fluid shear stress in endothelial cells. *Proc Natl Acad Sci USA.* (2006) 103:15463–8. doi: 10.1073/pnas.0607224103

28. Shyy J, Chien S. Role of integrins in endothelial mechanosensing of shear stress. *Circ Res.* (2002) 91:769–75. doi: 10.1161/01.RES.0000038487.19924.18

29. Tzima E, del Pozo M, Shattil S, Chien S, Schwartz M. Activation of integrins in endothelial cells by fluid shear stress mediates Rho-dependent cytoskeletal alignment. *EMBO J.* (2001) 20:4639–47. doi: 10.1093/emboj/20.17.4639

30. Loufrani L, Henrion D. Role of the cytoskeleton in flow (shear stress)-induced dilation and remodeling in resistance arteries. *Med Biol Eng Comput.* (2008) 46:451–60. doi: 10.1007/s11517-008-0306-2

31. Mazzag B, Tamaresis J, Barakat AIA. Model for shear stress sensing and transmission in vascular endothelial cells. *Biophys J.* (2003) 84:4087–101. doi: 10.1016/S0006-3495(03)75134-0

32. Xie X, Wang F, Zhu L, Yang H, Pan D, Liu Y, et al. Low shear stress induces endothelial cell apoptosis and monocyte adhesion by upregulating PECAM-1 expression. *Mol Med Rep.* (2020) 21:2580–8. doi: 10.3892/mmr.2020.11060

33. DeRoo E, Stranz A, Yang H, Hsieh M, Se C, Zhou T. Endothelial dysfunction in the pathogenesis of abdominal aortic aneurysm. *Biomolecules.* (2022) 12:509. doi: 10.3390/biom12040509

34. Meyrignac O, Bal L, Zadro C, Vavasseur A, Sewonu A, Gaudry M, et al. Combining volumetric and wall shear stress analysis from CT to assess risk of abdominal aortic aneurysm progression. *Radiology.* (2020) 295:722–9. doi: 10.1148/radiol.2020192112

35. Erhart P, Schiele S, Ginsbach P, Grond-Ginsbach C, Hakimi M, Böckler D, et al. Gene expression profiling in abdominal aortic aneurysms after finite element rupture risk assessment. *J Endovasc Ther.* (2017) 24:861–9. doi: 10.1177/1526602817729165

36. Chao Y, Yang H, Sun M, Sun J, Chen M. Elastin-derived peptides induce inflammatory responses through the activation of NF-κB in human ligamentum flavum cells. *Connect Tissue Res.* (2012) 53:407–14. doi: 10.3109/03008207.2012.679368

37. Liu L, Guo M, Lv X, Wang Z, Yang J, Li Y, et al. Role of transient receptor potential vanilloid 4 in vascular function. *Front Mol Biosci.* (2021) 8:677661. doi: 10.3389/fmolb.2021.677661

38. Sonkusare S, Bonev A, Ledoux J, Liedtke W, Kotlikoff M, Heppner T, et al. Elementary Ca2+ signals through endothelial TRPV4 channels regulate vascular function. *Science.* (2012) 336:597–601. doi: 10.1126/science.1216283

39. Sullivan M, Earley S. TRP channel Ca2+ sparklets: fundamental signals underlying endothelium-dependent hyperpolarization. *Am J Physiol Cell Physiol.* (2013) 305:C999–1008. doi: 10.1152/ajpcell.00273.2013

40. Freichel M, Suh S, Pfeifer A, Schweig U, Trost C, Weißgerber P, et al. Lack of an endothelial store-operated Ca2+ current impairs agonist-dependent vasorelaxation in TRP4-/- mice. *Nat Cell Biol.* (2001) 3:121–7. doi: 10.1038/35055019

41. Zhang J, Schmidt J, Ryschich E, Mueller-Schilling M, Schumacher H, Allenberg J. Inducible nitric oxide synthase is present in human abdominal aortic aneurysm and promotes oxidative vascular injury. *J Vasc Surg.* (2003) 38:360–7. doi: 10.1016/S0741-5214(03)00148-4

42. Shannon A, Elder C, Lu G, Su G, Mast A, Salmon M, et al. Pharmacologic inhibition of transient receptor channel vanilloid 4 attenuates abdominal aortic aneurysm formation. *FASEB J.* (2020) 34:9787–801. doi: 10.1096/fj.202000251R

43. Wang Y, Krishna S, Golledge J. The calcium chloride-induced rodent model of abdominal aortic aneurysm. *Atherosclerosis.* (2013) 226:29–39. doi: 10.1016/j.atherosclerosis.2012.09.010

44. Yamanouchi D, Morgan S, Stair C, Seedial S, Lengfeld J, Kent K, et al. Accelerated aneurysmal dilatation associated with apoptosis and inflammation in a newly created modified calcium chloride rodent AAA model. *J Vasc Surg.* (2011) 54:1544. doi: 10.1016/j.jvs.2011.09.029

45. Hofmann Bowman M, Eagle K, Milewicz D. Update on clinical trials of losartan with and without β-blockers to block aneurysm growth in patients with marfan syndrome: a review. *JAMA Cardiol.* (2019) 4:702–7. doi: 10.1001/jamacardio.2019.1176

46. Li J, Hou B, Tumova S, Muraki K, Bruns A, Ludlow M, et al. Piezo1 integration of vascular architecture with physiological force. *Nature.* (2014) 515:279–82. doi: 10.1038/nature13701

47. Muniappan L, Okuyama M, Javidan A, Thiagarajan D, Jiang W, Moorleghen J, et al. Inducible depletion of calpain-2 mitigates abdominal aortic aneurysm in mice. *Arterioscler Thromb Vasc Biol.* (2021) 41:1694–709. doi: 10.1161/ATVBAHA.120.315546

48. Subramanian V, Uchida H, Ijaz T, Moorleghen J, Howatt D, Balakrishnan A. Calpain inhibition attenuates angiotensin II–induced abdominal aortic aneurysms and atherosclerosis in low-density lipoprotein receptor–deficient mice. *J Cardiovasc Pharmacol.* (2012) 59:66–76. doi: 10.1097/FJC.0b013e318235d5ea

49. Fang X, Zhou T, Xu J, Wang Y, Sun M, He Y, et al. Structure, kinetic properties and biological function of mechanosensitive Piezo channels. *Cell Biosci.* (2021) 11:13. doi: 10.1186/s13578-020-00522-z

50. Albarrán-Juárez J, Iring A, Wang S, Joseph S, Grimm M, Strilic B, et al. Piezo1 and Gq/G11 promote endothelial inflammation depending on flow pattern and integrin activation. *J Exp Med.* (2018) 215:2655–72. doi: 10.1084/jem.20180483

51. Ranade S, Qiu Z, Woo S, Hur S, Murthy S, Cahalan S, et al. Piezo1, a mechanically activated ion channel, is required for vascular development in mice. *Proc Natl Acad Sci USA.* (2014) 111:10347–52. doi: 10.1073/pnas.1409233111

52. Qian W, Hadi T, Silvestro M, Ma X, Rivera C, Bajpai A, et al. Microskeletal stiffness promotes aortic aneurysm by sustaining pathological vascular smooth muscle cell mechanosensation via Piezo1. *Nat Commun.* (2022) 13:512. doi: 10.1038/s41467-021-27874-5

53. Qiu J, Zheng Y, Hu J, Liao D, Gregersen H, Deng X, et al. Biomechanical regulation of vascular smooth muscle cell functions: from in vitro to in vivo understanding. *J R Soc Interface.* (2014) 11:20130852. doi: 10.1098/rsif.2013.0852

54. Halka A, Turner N, Carter A, Ghosh J, Murphy M, Kirton J, et al. The effects of stretch on vascular smooth muscle cell phenotype in vitro. *Cardiovasc Pathol.* (2008) 17:98–102. doi: 10.1016/j.carpath.2007.03.001

55. Copp S, Kim J, Ruiz-Velasco V, Kaufman M. The mechano-gated channel inhibitor GsMTx4 reduces the exercise pressor reflex in rats with ligated femoral arteries. *Am J Physiol Heart Circ Physiol.* (2016) 310:H1233–41. doi: 10.1152/ajpheart.00974.2015

56. Hadi T, Boytard L, Silvestro M, Alebrahim D, Jacob S, Feinstein J, et al. Macrophage-derived netrin-1 promotes abdominal aortic aneurysm formation by activating MMP3 in vascular smooth muscle cells. *Nat Commun.* (2018) 9:5022. doi: 10.1038/s41467-018-07495-1

57. Wang Y, Miao H, Li S, Chen K, Li Y, Yuan S, et al. Interplay between integrins and FLK-1 in shear stress-induced signaling. *Am J Physiol Cell Physiol.* (2002) 283:C1540–7. doi: 10.1152/ajpcell.00222.2002

58. Conway D, Breckenridge M, Hinde E, Gratton E, Chen C, Schwartz M. Fluid shear stress on endothelial cells modulates mechanical tension across VE-cadherin and PECAM-1. *Curr Biol.* (2013) 23:1024–30. doi: 10.1016/j.cub.2013.04.049

59. Leiphart R, Chen D, Peredo A, Loneker A, Janmey P. Mechanosensing at cellular interfaces. *Langmuir.* (2019) 35:7509–19. doi: 10.1021/acs.langmuir.8b02841

60. Li S, Kim M, Hu Y, Jalali S, Schlaepfer D, Hunter T, et al. Fluid shear stress activation of focal adhesion kinase: linking to mitogen-activated protein kinases. *J Biol Chem.* (1997) 272:30455–62. doi: 10.1074/jbc.272.48.30455

61. Harada T, Yoshimura K, Yamashita O, Ueda K, Morikage N, Sawada Y, et al. Focal adhesion kinase promotes the progression of aortic aneurysm by modulating macrophage behavior. *Arterioscler Thromb Vasc Biol.* (2017) 37:156–65. doi: 10.1161/ATVBAHA.116.308542

62. Wang Q, Ren J, Morgan S, Liu Z, Dou C, Liu B. Monocyte chemoattractant protein-1 (MCP-1) regulates macrophage cytotoxicity in abdominal aortic aneurysm. *PLoS One.* (2014) 9:e92053. doi: 10.1371/journal.pone.0092053

63. Hunter E, Hamaia S, Gullberg D, Malcor J, Farndale R. Selectivity of the collagen-binding integrin inhibitors, TC-I-15 and obtustatin. *Toxicol Appl Pharmacol.* (2021) 428:115669. doi: 10.1016/j.taap.2021.115669

64. Cheuk B, Cheng S. Differential expression of integrin alpha5beta1 in human abdominal aortic aneurysm and healthy aortic tissues and its significance in pathogenesis. *J Surg Res.* (2004) 118:176–82. doi: 10.1016/S0022-4804(03)00351-2

65. Turlo K, Noel O, Vora R, LaRussa M, Fassler R, Hall-Glenn F, et al. An essential requirement for β1 integrin in the assembly of extracellular matrix proteins within the vascular wall. *Dev Biol.* (2012) 365:23–35. doi: 10.1016/j.ydbio.2012.01.027

66. Macek Jilkova Z, Deplano V, Verdier C, Toungara M, Geindreau C, Duperray A. Wall shear stress and endothelial cells dysfunction in the context of abdominal aortic aneurysms. *Comput Methods Biomech Biomed Eng.* (2013) 16:27–9. doi: 10.1080/10255842.2013.815959

67. Rosenbaum D, Rasmussen S, Kobilka B. The structure and function of G-protein-coupled receptors. *Nature.* (2009) 459:356–63. doi: 10.1038/nature08144

68. Wang J, Hanada K, Gareri C, Rockman H. Mechanoactivation of the angiotensin II type 1 receptor induces β-arrestin-biased signaling through Gαi coupling. *J Cell Biochem.* (2018) 119:3586–97. doi: 10.1002/jcb.26552

69. Hall S, Ward N, Patel R, Amin-Javaheri A, Lanford H, Grespin R, et al. Mechanical activation of the angiotensin II type 1 receptor contributes to abdominal aortic aneurysm formation. *JVS Vasc Sci.* (2021) 2:194–206. doi: 10.1016/j.jvssci.2021.07.001

70. Rateri D, Howatt D, Moorleghen J, Charnigo R, Cassis L, Daugherty A. Prolonged infusion of angiotensin II in apoE-/- mice promotes macrophage recruitment with continued expansion of abdominal aortic aneurysm. *Am J Pathol.* (2011) 179:1542–8. doi: 10.1016/j.ajpath.2011.05.049

71. Xie C, Ye F, Zhang N, Huang Y, Pan Y, Xie X. CCL7 contributes to angiotensin II-induced abdominal aortic aneurysm by promoting macrophage infiltration and pro-inflammatory phenotype. *J Cell Mol Med.* (2021) 25:7280–93. doi: 10.1111/jcmm.16757

72. Kaschina E, Schrader F, Sommerfeld M, Kemnitz U, Grzesiak A, Krikov M, et al. Telmisartan prevents aneurysm progression in the rat by inhibiting proteolysis, apoptosis and inflammation. *J Hypertens.* (2008) 26:2361–73. doi: 10.1097/HJH.0b013e328313e547

73. Golledge J, Pinchbeck J, Tomee S, Rowbotham S, Singh T, Moxon J, et al. Efficacy of telmisartan to slow growth of small abdominal aortic aneurysms: a randomized clinical trial. *JAMA Cardiol.* (2020) 5:1374–81. doi: 10.1001/jamacardio.2020.3524

74. Deng H, Min E, Baeyens N, Coon B, Hu R, Zhuang Z, et al. Activation of Smad2/3 signaling by low fluid shear stress mediates artery inward remodeling. *Proc Natl Acad Sci USA.* (2021) 118:e2105339118. doi: 10.1073/pnas.2105339118

75. Kigawa Y, Miyazaki T, Lei X, Nakamachi T, Oguchi T, Kim-Kaneyama J. NADPH oxidase deficiency exacerbates angiotensin II–induced abdominal aortic aneurysms in mice. *Arterioscler Thromb Vasc Biol.* (2014) 34:2413–20. doi: 10.1161/ATVBAHA.114.303086

76. Piechota-Polanczyk A, Goraca A, Demyanets S, Mittlboeck M, Domenig C, Neumayer C, et al. Simvastatin decreases free radicals formation in the human abdominal aortic aneurysm wall via NF-κB. *Eur J Vasc Endovasc Surg.* (2012) 44:133–7. doi: 10.1016/j.ejvs.2012.04.020

77. DiMusto P, Lu G, Ghosh A, Roelofs K, Sadiq O, McEvoy B, et al. Increased JNK in males compared with females in a rodent model of abdominal aortic aneurysm. *J Surg Res.* (2012) 176:687–95. doi: 10.1016/j.jss.2011.11.1024

78. Antoniades C, Antonopoulos A, Bendall J, Channon K. Targeting redox signaling in the vascular wall: from basic science to clinical practice. *Curr Pharm Des.* (2009) 15:329–42. doi: 10.2174/138161209787354230

79. Hsieh H, Liu C, Huang B, Tseng A, Wang D. Shear-induced endothelial mechanotransduction: the interplay between reactive oxygen species (ROS) and nitric oxide (NO) and the pathophysiological implications. *J Biomed Sci.* (2014) 21:3. doi: 10.1186/1423-0127-21-3

80. Guzik B, Sagan A, Ludew D, Mrowiecki W, Chwała M, Bujak-Gizycka B, et al. Mechanisms of oxidative stress in human aortic aneurysms — association with clinical risk factors for atherosclerosis and disease severity. *Int J Cardiol.* (2013) 168:2389–96. doi: 10.1016/j.ijcard.2013.01.278

81. Förstermann U, Xia N, Li H. Roles of vascular oxidative stress and nitric oxide in the pathogenesis of atherosclerosis. *Circ Res.* (2017) 120:713–35. doi: 10.1161/CIRCRESAHA.116.309326

82. Lubos E, Handy D, Loscalzo J. Role of oxidative stress and nitric oxide in atherothrombosis. *Front Biosci.* (2008) 13:5323–44. doi: 10.2741/3084

83. Boytard L, Hadi T, Silvestro M, Qu H, Kumpfbeck A, Sleiman R, et al. Lung-derived HMGB1 is detrimental for vascular remodeling of metabolically imbalanced arterial macrophages. *Nat Commun.* (2020) 11:4311. doi: 10.1038/s41467-020-18088-2

84. Guzik B, Cencora A, Chwala M, Korbut R, Guzik T, Żmudka K, et al. Abstract 2187: mechanisms of oxidative stress in human aortic abdominal aneurysms. Role of iNOS, NADPH oxidase and relationship to clinical features. *Circulation.* (2006) 114(Suppl. 18):II_445.

85. Gao L, Siu K, Chalupsky K, Nguyen A, Chen P, Weintraub N, et al. Role of uncoupled eNOS in abdominal aortic aneurysm formation: treatment with folic acid. *Hypertension.* (2012) 59:158–66. doi: 10.1161/HYPERTENSIONAHA.111.181644

86. Tarafdar A, Pula G. The role of NADPH oxidases and oxidative stress in neurodegenerative disorders. *Int J Mol Sci.* (2018) 19:3824. doi: 10.3390/ijms19123824

87. Xiong W, Mactaggart J, Knispel R, Worth J, Zhu Z, Li Y, et al. Inhibition of reactive oxygen species attenuates aneurysm formation in a murine model. *Atherosclerosis.* (2009) 202:128–34. doi: 10.1016/j.atherosclerosis.2008.03.029

88. Yip J, Shen Y, Berndt M, Andrews R. Primary platelet adhesion receptors. *IUBMB Life.* (2005) 57:103–8. doi: 10.1080/15216540500078962

89. Sun W, Zheng J, Gao Y. Targeting platelet activation in abdominal aortic aneurysm: current knowledge and perspectives. *Biomolecules.* (2022) 12:206. doi: 10.3390/biom12020206

90. Schrottmaier W, Mussbacher M, Salzmann M, Assinger A. Platelet-leukocyte interplay during vascular disease. *Atherosclerosis.* (2020) 307:109–20. doi: 10.1016/j.atherosclerosis.2020.04.018

91. Zhu C, Leach J, Wang Y, Gasper W, Saloner D, Hope M. Intraluminal thrombus predicts rapid growth of abdominal aortic aneurysms. *Radiology.* (2020) 294:707–13. doi: 10.1148/radiol.2020191723

92. Biasetti J, Gasser T, Auer M, Hedin U, Labruto F. Hemodynamics of the normal aorta compared to fusiform and saccular abdominal aortic aneurysms with emphasis on a potential thrombus formation mechanism. *Ann Biomed Eng.* (2010) 38:380–90. doi: 10.1007/s10439-009-9843-6

93. Ma X, Xia S, Liu G, Song C. The detrimental role of intraluminal thrombus outweighs protective advantage in abdominal aortic aneurysm pathogenesis: the implications for the anti-platelet therapy. *Biomolecules.* (2022) 12:942. doi: 10.3390/biom12070942

94. Chatzizisis Y, Coskun A, Jonas M, Edelman E, Feldman C, Stone P. Role of endothelial shear stress in the natural history of coronary atherosclerosis and vascular remodeling: molecular, cellular, and vascular behavior. *J Am Coll Cardiol.* (2007) 49:2379–93. doi: 10.1016/j.jacc.2007.02.059

95. Dua M, Dalman R. Hemodynamic influences on abdominal aortic aneurysm disease: application of biomechanics to aneurysm pathophysiology. *Vascul Pharmacol.* (2010) 53:11–21. doi: 10.1016/j.vph.2010.03.004

96. Di Achille P, Tellides G, Figueroa C, Humphrey JD. A haemodynamic predictor of intraluminal thrombus formation in abdominal aortic aneurysms. *Proc R Soc Math Phys Eng Sci.* (2014) 470:20140163. doi: 10.1098/rspa.2014.0163

97. Arzani A, Suh G, Dalman R, Shadden SC. A longitudinal comparison of hemodynamics and intraluminal thrombus deposition in abdominal aortic aneurysms. *Am J Physiol Heart Circ Physiol.* (2014) 307:H1786–95. doi: 10.1152/ajpheart.00461.2014

98. Li W, Luo X, Ulbricht Y, Wagner M, Piorkowski C, El-Armouche A, et al. Establishment of an automated patch-clamp platform for electrophysiological and pharmacological evaluation of hiPSC-CMs. *Stem Cell Res.* (2019) 41:101662. doi: 10.1016/j.scr.2019.101662

99. Soudah E, Ng E, Loong T, Bordone M, Pua U, Narayanan S. CFD modelling of abdominal aortic aneurysm on hemodynamic loads using a realistic geometry with CT. *Comput Math Methods Med.* (2013) 2013:472564. doi: 10.1155/2013/472564

100. Skov R, Eiberg J, Rouet L, Eldrup N, Zielinski A, Broda M, et al. Anticoagulants and reduced thrombus load in abdominal aortic aneurysms assessed with three-dimensional contrast-enhanced ultrasound examination. *J Vasc Surg.* (2022). [Epub ahead of print]. doi: 10.1016/j.jvs.2022.07.019

101. Muhamed I, Chowdhury F, Maruthamuthu V. Biophysical tools to study cellular mechanotransduction. *Bioengineering.* (2017) 4:12. doi: 10.3390/bioengineering4010012

102. Bowden N, Bryan M, Duckles H, Feng S, Hsiao S, Kim H, et al. Experimental approaches to study endothelial responses to shear stress. *Antioxid Redox Signal.* (2016) 25:389–400. doi: 10.1089/ars.2015.6553

103. Sangha G, Busch A, Acuna A, Berman A, Phillips E, Trenner M, et al. Effects of iliac stenosis on abdominal aortic aneurysm formation in mice and humans. *J Vasc Res.* (2019) 56:217–29. doi: 10.1159/000501312

104. Hoshina K, Sho E, Sho M, Nakahashi T, Dalman R. Wall shear stress and strain modulate experimental aneurysm cellularity. *J Vasc Surg.* (2003) 37:1067. doi: 10.1016/S0741-5214(03)70052-4

105. Wentland A, Wieben O, Shanmuganayagam D, Krueger C, Meudt J, Consigny D, et al. Measurements of wall shear stress and aortic pulse wave velocity in swine with familial hypercholesterolemia. *J Magn Reson Imaging.* (2015) 41:1475–85. doi: 10.1002/jmri.24681

106. Cullen J, Lu G, Shannon A, Su G, Sharma A, Salmon M, et al. A novel swine model of abdominal aortic aneurysm. *J Vasc Surg.* (2019) 70:252–60.e2. doi: 10.1016/j.jvs.2018.09.057

107. Gordon E, Schimmel L, Frye M. The importance of mechanical forces for in vitro endothelial cell biology. *Front Physiol.* (2020) 11:684. doi: 10.3389/fphys.2020.00684

108. Sarker M, Naghieh S, Sharma N, Chen X. 3D biofabrication of vascular networks for tissue regeneration: a report on recent advances. *J Pharm Anal.* (2018) 8:277–96. doi: 10.1016/j.jpha.2018.08.005

109. Chen E, Toksoy Z, Davis B, Geibel J. 3D bioprinting of vascularized tissues for in vitro and in vivo applications. *Front Bioeng Biotechnol.* (2021) 9:664188. doi: 10.3389/fbioe.2021.664188

110. Zhu K, Ma W, Li J, Zhang Y, Zhang W, Lai H, et al. Modeling aortic diseases using induced pluripotent stem cells. *Stem Cells Transl Med.* (2021) 10:190–7. doi: 10.1002/sctm.20-0322

111. Chen N, Abudupataer M, Feng S, Zhu S, Ma W, Li J, et al. Engineering a human pluripotent stem cell-based in vitro microphysiological system for studying the metformin response in aortic smooth muscle cells. *Front Bioeng Biotechnol.* (2021) 9:627877. doi: 10.3389/fbioe.2021.627877

112. Bogunovic N, Meekel J, Majolée J, Hekhuis M, Pyszkowski J, Jockenhövel S, et al. Patient-specific 3-dimensional model of smooth muscle cell and extracellular matrix dysfunction for the study of aortic aneurysms. *J Endovasc Ther.* (2021) 28:604–13. doi: 10.1177/15266028211009272

113. Jones B, Tonniges J, Debski A, Albert B, Yeung D, Gadde N, et al. Collagen fibril abnormalities in human and mice abdominal aortic aneurysm. *Acta Biomater.* (2020) 110:129–40. doi: 10.1016/j.actbio.2020.04.022

114. Petit C, Karkhaneh Yousefi A, Guilbot M, Barnier V, Avril S. Atomic force microscopy stiffness mapping in human aortic smooth muscle cells. *J Biomech Eng.* (2022) 144:081001. doi: 10.1115/1.4053657

115. Poole K, Moroni M, Lewin G. Sensory mechanotransduction at membrane-matrix interfaces. *Pflugers Arch.* (2015) 467:121–32. doi: 10.1007/s00424-014-1563-6

116. Annecchino L, Schultz S. Progress in automating patch clamp cellular physiology. *Brain Neurosci Adv.* (2018) 2:2398212818776561. doi: 10.1177/2398212818776561

117. Nandlall S, Konofagou E. Assessing the stability of aortic aneurysms with pulse wave imaging. *Radiology.* (2016) 281:772–81. doi: 10.1148/radiol.2016151407

118. Kadoglou N, Moulakakis K, Papadakis I, Ikonomidis I, Alepaki M, Lekakis J, et al. Changes in aortic pulse wave velocity of patients undergoing endovascular repair of abdominal aortic aneurysms. *J Endovasc Ther.* (2012) 19:661–6. doi: 10.1583/JEVT-12-3916MR.1

119. Paraskevas K, Kyriakides Z, Mikhailidis D. Aortic pulse wave velocity may have prognostic value not just for hypertension but also for abdominal aortic aneurysms. *Hypertension.* (2010) 55:e22–22. doi: 10.1161/HYPERTENSIONAHA.110.150110

120. Qiu Y, Wang J, Zhao J, Wang T, Zheng T, Yuan D. Association between blood flow pattern and rupture risk of abdominal aortic aneurysm based on computational fluid dynamics. *Eur J Vasc Endovasc Surg.* (2022) 64:155–64. doi: 10.1016/j.ejvs.2022.05.027

121. Wu J, Thabet S, Kirabo A, Trott D, Saleh M, Xiao L, et al. Inflammation and mechanical stretch promote aortic stiffening in hypertension through activation of p38 mitogen-activated protein kinase. *Circ Res.* (2014) 114:616–25. doi: 10.1161/CIRCRESAHA.114.302157

122. Hall A, Busse E, McCarville D, Burgess J. Aortic wall tension as a predictive factor for abdominal aortic aneurysm rupture: improving the selection of patients for abdominal aortic aneurysm repair. *Ann Vasc Surg.* (2000) 14:152–7. doi: 10.1007/s100169910027

123. Latorre R, Díaz-Franulic I. Profile of David Julius and Ardem Patapoutian: 2021 nobel laureates in physiology or medicine. *Proc Natl Acad Sci USA.* (2022) 119:e2121015119. doi: 10.1073/pnas.2121015119

124. Coste B, Xiao B, Santos J, Syeda R, Grandl J, Spencer K, et al. Piezo proteins are pore-forming subunits of mechanically activated channels. *Nature.* (2012) 483:176–81. doi: 10.1038/nature10812

125. Evans E, Cuthbertson K, Endesh N, Rode B, Blythe N, Hyman A, et al. Yoda1 analogue (Dooku1) which antagonizes Yoda1-evoked activation of Piezo1 and aortic relaxation. *Br J Pharmacol.* (2018) 175:1744–59. doi: 10.1111/bph.14188

126. Bae C, Sachs F, Gottlieb P. The mechanosensitive ion channel Piezo1 is inhibited by the peptide GsMTx4. *Biochemistry.* (2011) 50:6295–300. doi: 10.1021/bi200770q

127. Suchyna T. Piezo channels and GsMTx4: two milestones in our understanding of excitatory mechanosensitive channels and their role in pathology. *Prog Biophys Mol Biol.* (2017) 130:244–53. doi: 10.1016/j.pbiomolbio.2017.07.011

128. Doyle J, Doyle A, Wilson N, Habashi J, Bedja D, Whitworth R, et al. A deleterious gene-by-environment interaction imposed by calcium channel blockers in Marfan syndrome. *Elife.* (2015) 4:e08648. doi: 10.7554/eLife.08648

129. Liu J, Liu M, Feng J, Zhu H, Wu J, Zhang H, et al. Alpha-ketoglutarate ameliorates abdominal aortic aneurysm via inhibiting PXDN/HOCL/ERK signaling pathways. *J Transl Med.* (2022) 20:461. doi: 10.1186/s12967-022-03659-2

130. Siu K, Miao X, Cai H. Recoupling of eNOS with folic acid prevents abdominal aortic aneurysm formation in angiotensin ii-infused apolipoprotein E null mice. *PLoS One.* (2014) 9:e88899. doi: 10.1371/journal.pone.0088899

131. Shang T, Liu Z, Liu CJ. Antioxidant vitamin C attenuates experimental abdominal aortic aneurysm development in an elastase-induced rat model. *J Surg Res.* (2014) 188:316–25. doi: 10.1016/j.jss.2013.11.1105

132. Gavrila D, Li W, McCormick M, Thomas M, Daugherty A, Cassis L, et al. Vitamin E inhibits abdominal aortic aneurysm formation in angiotensin II–infused apolipoprotein E–deficient mice. *Arterioscler Thromb Vasc Biol.* (2005) 25:1671–7. doi: 10.1161/01.ATV.0000172631.50972.0f

frontiers | Frontiers in Cardiovascular Medicine

TYPE Original Research
PUBLISHED 23 February 2023
DOI 10.3389/fcvm.2023.1002832

Check for updates

OPEN ACCESS

EDITED BY
Wei Wang,
Central South University,
China

REVIEWED BY
Hanfei Tang,
Fudan University,
China
Niamh Hynes,
University of Galway,
Ireland
Droc Ionel,
Central Military Hospital Bucharest Romania,
Romania

*CORRESPONDENCE
Jinlin Wu
wujinlin@gdph.org.cn
Xin Li
lixin337000@163.com

†These authors have contributed equally to this work

SPECIALTY SECTION
This article was submitted to General Cardiovascular Medicine, a section of the journal Frontiers in Cardiovascular Medicine

RECEIVED 25 July 2022
ACCEPTED 31 January 2023
PUBLISHED 23 February 2023

CITATION
Wu J, Wu Y, Li F, Zhuang D, Cheng Y, Chen Z, Yang J, Liu J, Li X, Fan R and Sun T (2023) Natural history of isolated abdominal aortic dissection: A prospective cohort study. *Front. Cardiovasc. Med.* 10:1002832. doi: 10.3389/fcvm.2023.1002832

COPYRIGHT
© 2023 Wu, Wu, Li, Zhuang, Cheng, Chen, Yang, Liu, Li, Fan and Sun. This is an open-access article distributed under the terms of the Creative Commons Attribution License (CC BY). The use, distribution or reproduction in other forums is permitted, provided the original author(s) and the copyright owner(s) are credited and that the original publication in this journal is cited, in accordance with accepted academic practice. No use, distribution or reproduction is permitted which does not comply with these terms.

Natural history of isolated abdominal aortic dissection: A prospective cohort study

Jinlin Wu[1]*†, Yanfen Wu[1†], Fei Li[2†], Donglin Zhuang[1], Yunqing Cheng[1], Zerui Chen[1], Jue Yang[1], Jie Liu[1], Xin Li[1]*, Ruixin Fan[1] and Tucheng Sun[1]

[1]Department of Cardiac Surgery, Guangdong Cardiovascular Institute, Guangdong Provincial People's Hospital, Guangdong Academy of Medical Sciences, Guangzhou, China, [2]Department of Cardiac Surgery, Beijing Anzhen Hospital, Capital Medical University, Beijing, China

Objectives: Isolated abdominal aortic dissection (IAAD) is extremely rare, with its optimal treatment and intervention timing remaining poorly understood. We aimed to study the natural history of IAAD and facilitate better clinical decision.

Methods: Consecutive patients admitted to our institution from January 2016 to April 2021 were enrolled and followed up prospectively. All-cause death was taken as the primary endpoint.

Results: A total of 68 patients with IAAD were included. The mean age at presentation was 61.2±14.8 (Range: 26.0, 93.0) years and 55 (80.9%) were male. A total of 38 (55.9%) patients were treated conservatively, 27 (39.7%) received endovascular aneurysm repair (EVAR), and 3 (4.4%) underwent open surgery. After a mean follow-up of 2.4years (Range: 0.1, 5.5), 9 (13.2%) patients died, 8 of whom (21.0%) were treated conservatively and 1 EVAR (3.7%). Compared with EVAR/open surgery, patient treated conservatively had a much worse survival (p=0.043). There was no significant difference between different IAAD aortic sizes regarding mortality (p=0.220). Patients with completely thrombosed false lumen fared improved survival rate, followed by partial thrombosis and patency, respectively, although not significantly (p=0.190). No significant difference was observed between male and female concerning survival rate (p=0.970). Patients without symptoms had a significantly improved survival (p=0.048).

Conclusion: On the basis of patients' preference and surgeons' experience, a more aggressive treatment regimen for IAAD should be considered, with EVAR being the first choice, especially for those with persistent symptoms and patent false lumen, regardless of sex, age, or aortic size.

KEYWORDS

isolated abdominal aortic dissection, natural history, survival, treatment, aortic

Introduction

Aortic dissection (AD) is a notorious killer and is often known as Stanford type A or B (1). Isolated abdominal aortic dissection (IAAD), referring to AD limited to the abdominal aorta, is believed to be a unique entity (Figure 1). We have performed a meta-analysis enrolled only 491 IAAD patients worldwide previously, and the incidence is estimated to be about 5.1/1,000,000 per year, which is extremely rare (2). Currently, the best treatment modality for

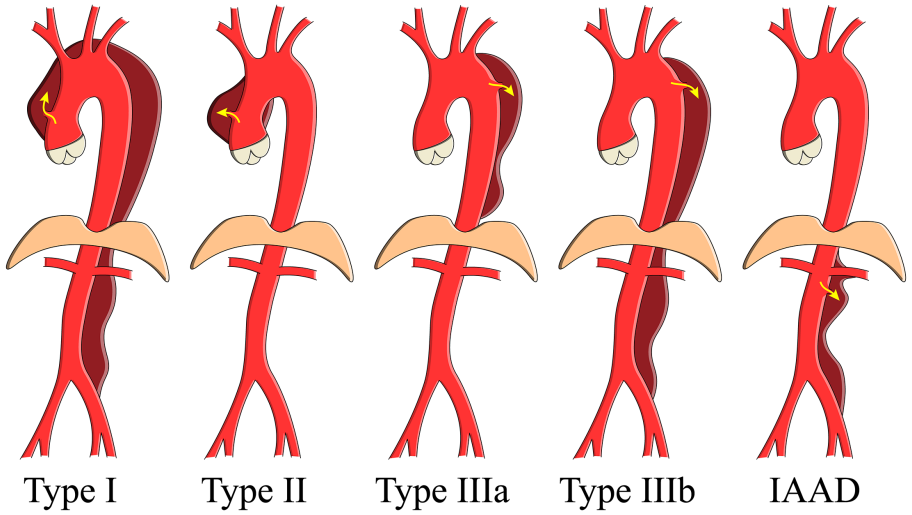

FIGURE 1
Schema showing the aortic dissection classification. IAAD, isolated abdominal aortic dissection.

IAAD, i.e., conservative or interventional [open surgery (OS) or endovascular aneurysm repair (EVAR)], remains controversial. For the timing of surgery, a natural history study is essential to select patients with a reasonable benefit to risk ratio for surgery, which is the key for both the doctor and patients to make a decision.

Unfortunately, due to the rarity of the disorder, there is a paucity of solid data on the natural history of IAAD. Importantly, Sen et al. (3) recently conducted a preliminary study of the natural history of IAAD. They found that the overall mortality of IAAD is similar to population controls. Unfortunately, as they pointed out that clinical recommendations or conclusions were hard to make with only 14 patients enrolled. In the present study, we aimed to study the natural history of IAAD with a relatively larger cohort, facilitating better clinical decision and providing more insights into this intriguing disorder.

Methods

The prospective cohort study was reported in line with Strengthening the Reporting of Observational Studies in Epidemiology (STROBE) (4). The study was approved by the Institutional Review Board (KY-Q-2021-073-01), with informed consent not required due to its observational nature.

All consecutive patients admitted to the Guangdong Provincial People's Hospital (Guangdong, China) from January 2016 to April 2021 were enrolled and followed up prospectively. Anthropometric, radiologic, laboratory, and operative data were manually accrued from individual electronic medical records and hospital charts. If there were missing values, we would check with the patient or relatives by phone. Computed Tomography Angiography (CTA) was used to confirm IAAD, demonstrating dissected intimal flap and double-lumen aorta below the diaphragm, with or without visible entry tear. Hypertension was diagnosed according to medical history as blood pressure measured at 140/90 mmHg or higher. Diameter was measured perpendicular to the centerline at the different levels in an outer-to-outer manner, and the maximum was noted. The thrombosis status of false lumen was classified as complete thrombosis (CT), partial thrombosis (PT, concurrent presence of both flow and thrombus), and patency (P) proposed by Tsai et al. (5). Accidental identification of IAAD indicated that the disease was diagnosed by chance such as routinely physical examination or undergoing imaging not specifically for aortic disease. Those patients usually had no symptoms and the aortic dissection was in chronic phase (6).

There was a lack of recognized protocol for the optimal management of IAAD. Patients were treated either conservatively with best medical therapy (BMT), or aggressively with OS or EVAR, based on attending surgeon's judgment and patients' preference. All-cause death was taken as the primary endpoint and surgical intervention for BMT cohort as the secondary endpoint. Patients were followed up either with clinical visits or phone calls.

Statistical analysis

And this study could be the largest prospective cohort investigating the natural history of IAAD based on our literature review. The potential variables were chosen based on expert opinion, clinical reasoning, availability, literature and plausibility without statistical pre-selection. Continuous variables were tested for normality distribution with the Kolmogorov–Smirnov test and were expressed as a mean with standard deviation (SD) and range (minimum, maximum). Categorical variables were presented as frequencies with percentages. We calculated the survival rate and freedom from death and intervention using the Kaplan–Meier (K-M) analytical method ("survival," "survivalAnalysis," and "survminer" packages in R) combined with the log-rank test. Univariable Cox proportional hazards regression was used to estimate the hazard ratios (HRs) with 95% confidence interval (CI). Loss of follow-up or end of the study period were treated as censors during the time-to-event analysis. R software (version 3.5.1) was used for data analysis. A two-tailed $p < 0.05$ indicated statistical significance.

Results

A total of 68 patients with IAAD were included in this study. Baseline information of these patients was shown in Table 1. The mean age at presentation was 61.2 ± 14.8 (Range: 26.0, 93.0) years and 55 (80.9%) were male. 38 (74.5%) had hypertension and 4 (7.8%) was complicated with diabetes mellitus. Thirteen (25.5%) suffered from hyperlipidemia and 10 (19.6%) developed chronic obstructive pulmonary disease. The incidence of coronary artery disease was 7 (13.7%), which was the same to the incidence of renal insufficiency. Thirty (58.8%) had a history of smoking and 5 (9.8%) had gout. Three (5.9%) had a history of cardiovascular surgery, and 1 (2.0%) reported a family history of aortic disease. Interestingly, up to 22 (32.8%) IAAD were identified accidentally without any perceivable symptoms. Further, the baseline characteristics of the conservatively treated cohort was shown in Table 2. A total of 38 (55.9%) patients received BMT with surveillance, 27 (39.7%) received EVAR, and 3 (4.4%) received OS. After a mean follow-up of 2.4 years (Range: 0.1, 5.5), a total of 9 (13.2%) patients died, 8 of whom received BMT (21.0%) and 1 of whom received EVAR (3.7%). Three patients in the BMT cohort underwent EVAR at 1.3, 1.7, and 1.9 years of follow-up, respectively, and all survived.

TABLE 1 Baseline characteristics of the overall cohort.

Variables	Mean±SD (Range)/Count (Percentage)
n	68
Age (year, mean ± SD)	61.2 ± 14.8 (Range: 26.0, 93.0)
Male (%)	55 (80.9)
Hypertension (%)	38 (74.5)
Diabetes (%)	4 (7.8)
Hyperlipidimia (%)	13 (25.5)
Chronic obstructive pulmonary disease (%)	10 (19.6)
Coronary artery disease (%)	7 (13.7)
Renal insufficiency (%)	7 (13.7)
Smoking (%)	30 (58.8)
Gout (%)	5 (9.8)
History of cardiovascular surgery (%)	3 (5.9)
Family history of aortic diseases (%)	1 (2.0)
Accidental identification (%)	22 (32.8)
Red blood cell (10^12/L, mean ± SD)	4.5 ± 0.9 (Range: 2.8, 8.1)
White blood cell (10^9/L, mean ± SD)	9.0 ± 4.4 (Range: 3.7, 28.5)
Platelet (10^9/L, mean ± SD)	243.5 ± 79.2 (Range: 120.0, 599.0)
D-dimer (ng/mL, mean ± SD)	1876.8 ± 2121.3 (Range: 220.0, 8790.0)
Below renal artery (%)	46 (67.6)
Diameter (mm, mean ± SD)	27.6 ± 9.9 (Range: 13.0, 57.0)
False lumen thrombosis (%)	
CT	19 (27.9)
P	25 (36.8)
PT	24 (35.3)
Treatment (%)	
BMT	38 (55.9)
EVAR	27 (39.7)
Open Surgery	3 (4.4)

SD, standard deviation; CT, complete thrombosis; P, patency, PT, partial thrombosis; BMT, best medical treatment; EVAR, endovascular aneurysm repair.

The survival rate of the overall cohort was shown in Figure 2. The survival rates at 1, 3, and 5 years were 91.2% (95% CI: 84.7–98.2%), 84.8% (95% CI: 75.7–94.9%), and 84.8% (95% CI: 75.7–94.9%), respectively. As was shown in Figure 3, Compared with EVAR/OS, patient treated conservatively had a worse survival ($p = 0.043$). The survival rates at 1, 3, and 5 years were 96.6% (95% CI: 90.4–100.0%), 96.6% (95% CI: 90.4–100.0%), and 96.6% (95% CI: 90.4–100.0%), respectively for EVAR/OS group, and 86.8% (76.7–98.2%), 76.3 (95% CI: 62.7–92.7%), and 76.3% (95% CI: 62.7–92.7%), respectively for BMT group. The HR of BMT versus EVAR/OS was 6.4 (95% CI: 0.8–51.3, $p = 0.079$). The natural history of the IAAD was then assessed based on the BMT cohort by aortic size, false lumen status, sex, and symptoms, respectively, as follows.

The BMT cohort was divided into four groups according to the quartiles of diameter: Q1: 13–20 mm ($n = 10$), Q2: 21–25 mm ($n = 8$), 26–32 mm ($n = 10$), 33–57 mm ($n = 10$). Figure 4 shows that there was no significant difference between IAAD of different sizes regarding mortality ($p = 0.220$). The survival rate at 1, 3, and 5 years of follow up were 90.0% (95% CI: 73.2–100.0%), 75.0% (95% CI: 49.6–100.0%), and 75.0% (95% CI: 49.6–100.0%) respectively for Q1 of aortic size, and 75.0% (95% CI: 50.3–100.0%), 56.2% (95% CI: 28.1–100.0%), and 56.2% (95% CI: 28.1–100.0%) respectively for Q2 of aortic size, and 100.0% (95% CI: 100.0–100.0%), 100.0% (95% CI: 100.0–100.0%), and 100.0% (95% CI: 100.0–100.0%) respectively for Q3 of aortic size, and 80.0% (95% CI: 58.7–100.0%), 68.6% (95% CI: 44.5–100.0%), and 68.6% (95% CI: 44.5–100.0%) respectively for Q4 of aortic size. Compared to Q1 of aortic size, the HR of mortality for Q2 and Q4 were 2.2 (95% CI: 0.3–13.6, $p = 0.372$), and 1.7 (95% CI: 0.2–10.7, $p = 0.526$), respectively. The HR for Q3 was not applicable because no events were observed in this sub-cohort.

As regards false lumen status, there were 9 cases of CT, 15 cases of P, and 14 cases of PT in the BMT cohort. Figure 5 shows that CT group fared improved survival rate, followed by group PT and P, respectively, although not significantly ($p = 0.190$). The survival rate at 1, 3, and 5 years of follow up were 100.0% (95% CI: 100.0–100.0%), 100.0% (95% CI: 100.0–100.0%), and 100.0% (95% CI: 100.0–100.0%) respectively for CT group, and 80.0% (95% CI: 62.1–100.0%), 61.1% (95% CI: 38.2–97.8%), and 61.1% (95% CI: 38.2–97.8%) respectively for P group, and 85.7% (95% CI: 69.2–100.0%), 76.2% (95% CI: 55.6–100.0%), and 76.2% (95% CI: 55.6–100.0%) respectively for PT group. Compared to group P, the HR of mortality for group PT was 0.6 (95% CI: 0.1–2.5, $p = 0.487$). The HR for group CT was not applicable because no events were observed in this sub-cohort.

There were 29 males and 9 females in the BMT cohort. As was demonstrated in Figure 6, no significant deference was observed between male and female concerning survival rate ($p = 0.970$). The survival rate at 1, 3, and 5 years of follow up were 86.2% (95% CI: 74.5–99.7%), 75.7% (95% CI: 59.6–96.2%), and 75.7% (95% CI: 59.6–96.2%), respectively for male, and 88.9% (95% CI: 70.6–100.0%), 76.2% (95% CI: 52.1–100.0%), and 76.2% (95% CI: 52.1–100.0%)

TABLE 2 Baseline characteristics of the conservatively treated cohort.

Variables	Mean±SD (Range)/Count (Percentage)
n	38
Age (year, mean ± SD)	63.4 ± 16.0 (Range: 26.0–93.0)
Male (%)	29 (76.3)
Hypertension (%)	20 (87.0)
Diabetes (%)	2 (8.7)
Hyperlipidimia (%)	4 (17.4)
Chronic obstructive pulmonary disease (%)	5 (21.7)
Coronary artery disease (%)	2 (8.7)
Renal insufficiency (%)	2 (8.7)
Smoking (%)	14 (60.9)
Gout (%)	1 (4.3)
History of cardiovascular surgery (%)	3 (13.0)
Family history of aortic diseases (%)	0 (0)
Accidental identification (%)	12 (32.4)
Red blood cell (10^12/L, mean ± SD)	4.7 ± 1.1 (Range: 2.8, 8.1)
White blood cell (10^9/L, mean ± SD)	9.2 ± 5.1 (Range: 3.7, 28.5)
Platelet (10^9/L, mean ± SD)	260.5 ± 103.7 (Range: 120.0, 599.0)
D-dimer (ng/mL, mean ± SD)	1592.1 ± 2005.9 (Range: 220.0, 8790.0)
Below renal artery (%)	24 (63.2)
Diameter (mm, mean ± SD)	28.5 ± 9.9 (Range: 13.0, 57.0)
False lumen thrombosis (%)	
CT	9 (23.7)
P	15 (39.5)
PT	14 (36.8)

SD, standard deviation; CT, complete thrombosis; P, patency, PT, partial thrombosis; BMT, best medical treatment.

respectively for female. Compared to female, the HR of mortality for male was 1.0 (95% CI: 0.2–5.1, $p = 0.963$).

For symptoms (abdominal pain or others), 12 cases were identified without any symptoms in the BMT cohort. As was demonstrated in Figure 7, patients without symptoms had better outcomes in terms of survival rate ($p = 0.048$). The survival rate at 1, 3, and 5 years of follow up were 80.7% (95% CI: 66.9–97.4%), 66.8% (95% CI: 50.0–89.1%), and 66.8% (95% CI: 50.0–89.1%), respectively for patients with symptoms, and 100.0% (95% CI: 100.0–100.0%), 100.0% (95% CI: 100.0–100.0%), and 100.0% (95% CI: 100.0–100.0%) respectively for patients without symptoms. The HR for patients without symptoms was not applicable because no events were observed in this sub-cohort.

Further, K-M curves (Supplementary Figures 1–4) with mortality and intervention as the combined endpoints were performed, demonstrating similar results as above.

Discussion

IAAD is a unique and extremely rare aortic disorder. It has long been neglected in almost all the guidelines or consensus for aortic diseases (7–11). Little was known for its natural history, rendering the clinical decision rather difficult. In the present study, we investigated the natural history of IAAD with a prospective cohort, revealing several interesting facts.

Reassuringly, compared to a 5-year survival of 65% for Type B aortic dissection (12), the prognosis of IAAD is pretty good, with survival rates of 91.2% (95% CI: 84.7–98.2%), 84.8% (95% CI: 75.7–94.9%), and 84.8% (75.7–94.9%), at 1, 3, and 5 years, respectively. It was found that patient treated conservatively had a worse survival ($p = 0.043$) compared to surgically intervened patients (either EVAR or OS). Strikingly, the HR of mortality for the BMT group is up to 6 times higher than that of the EVAR/OS group. Of note, only 2 patients received OS, demonstrating the increasing popularity and safety of EVAR, which is consistent to our previous finding that from 2002 to 2018, the prevalence of EVAR for the treatment of IAAD has been increasing, whereas that of OS has been declining (2). Our previous meta-analysis showed better outcomes for conservative treatment, which is contrary to the findings of this study. It is important to note that the patients included in this study were enrolled from 2016 to 2021, when EVAR techniques and devices were supposedly more sophisticated. In contrast, the previous meta-analysis spanned a wide range of years from 1990 to 2018, which may have a temporal bias that cannot be ignored. We speculated that because of the high intervention-related mortality in early days, the treatment regimen tended to be more conservative. Those who received OS or EVAR might have been intrinsically "sicker" and more urgent than conservatively managed patients.

So far, the diameter has always been the cornerstone for aortic aneurysm intervention. A diameter of or above 55.0 mm was recognized as the surgical indication for thoracic aortic aneurysm worldwide, owing to the pioneering work by Elefteriades et al. (13–16). According to the Laplace's law, wall tension is proportional to the vessel radius for a given blood pressure. Presumably, the larger an aortic aneurysm, the greater risk it will take for aortic dissection. Similarly, the larger an aortic dissection is, the greater risk it will take for rupture/death. However, we found that aortic size did not play a significant a role in the IAAD prognosis, suggesting that aortic size might not be taken as a surgical indication for IAAD. Note that we do not consider IAAD with large diameter to be less dangerous, but rather emphasize that IAAD with small diameter is equally dangerous. And we lack sufficient data for large diameter IAAD. Overall, the median diameter of IAAD was only 27.0 mm, far less than the current surgical recommendation of 55.0 mm. The mean aortic diameter for type A aortic dissection is 53.8 mm (17) and the median aortic size at type B aortic dissection is 41.0 mm (18). It's interesting to note that aorta dissects at smaller sizes progressively as it extends from ascending, descending to abdominal aorta. Even the fatality of aortic dissection decreases in the same way. And ascending aorta is more prone to dissection (hence the scarcity of ascending aortic rupture), the abdominal aorta is more susceptible to rupture (hence the rarity of IAAD), while the descending aorta behaves in the middle. These fascinating phenomena deserve further investigations.

PT of the false lumen was first brought into attention by Tsai et al. (5). They found that PT at discharge was a strong predictor of mortality in patients with type B aortic dissection compared with CT and P. It was reported that the mean 3-year mortality rate for patients with a patent false lumen was 13.7 ± 7.1%, for those with partial thrombosis was 31.6% ± 12.4, and for those with complete thrombosis was 22.6% ± 22.6 ($p = 0.003$). It was speculated that thrombosis at the

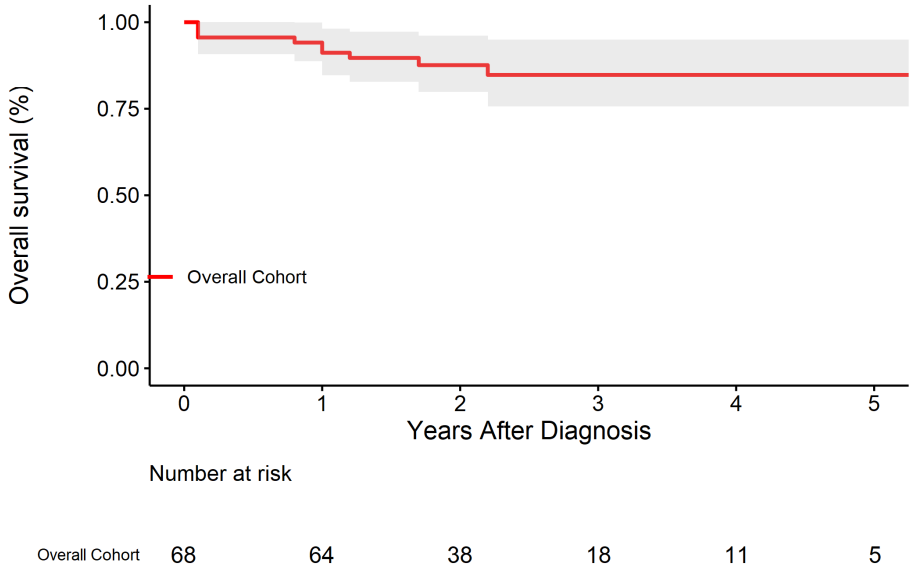

FIGURE 2
Kaplan–Meier survival curve for the overall cohort.

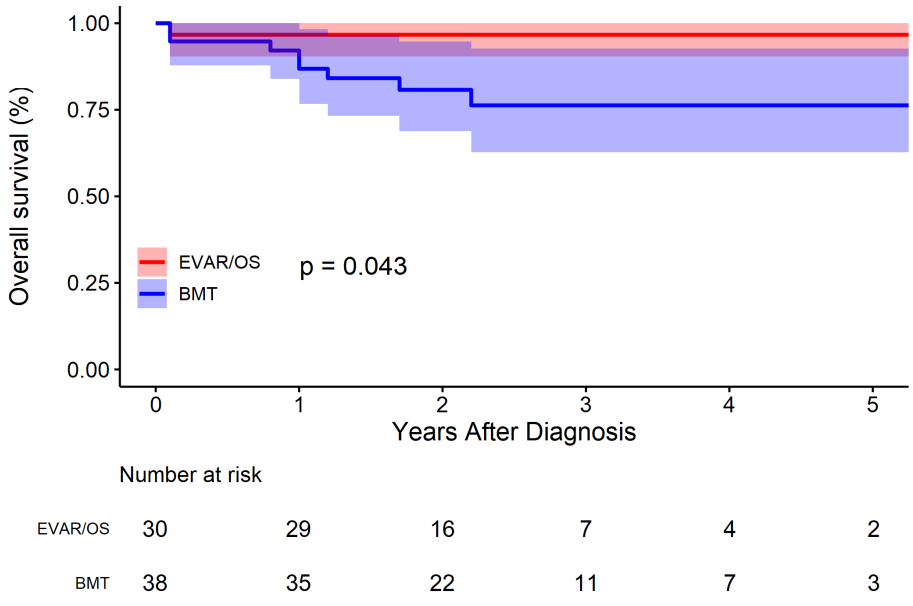

FIGURE 3
Kaplan–Meier survival curve by treatment for the overall cohort.

distal end of the false lumen may block the secondary entry tear to form a "blind sac" structure, increasing the pressure of the false lumen, or PT may increase the risk of rupture as a result of hypoxia of the arterial wall adjacent to the intraluminal thrombus, which leads to increased local inflammation, neovascularization, and localized wall weakening. However, the current study does not support the negative role of PT on the survival of IAAD. Figure 5 shows the trend that CT group fared improved survival rate, followed by group PT and P, respectively ($p = 0.190$), which is consistent with the clinical instinct that PT was merely a transitional phase between CT and Kudo et al. also found no difference in the survival rate among groups PT, P, and CT. The event-free rate was the greatest in group CT, with a 3-and 5-year event-free rate of 100 and 95.7%, respectively (19). Our recent study also demonstrated no significant differences in aortic growth between the three groups (20). Although no statistical difference was reached, the outcome was much worse in the P group in terms of trend, and an obvious gradient effect on the outcomes between P, PT, and CT sequentially was observed (Figure 5). Thus, the current evidence does not favor PT as a surgical indication for IAAD.

Sex differences in aortic disease is gaining increasing attention. The prevalence of thoracic aortic aneurysm/dissection in men and women is approximately 70%: 30% (21). This study also shows that

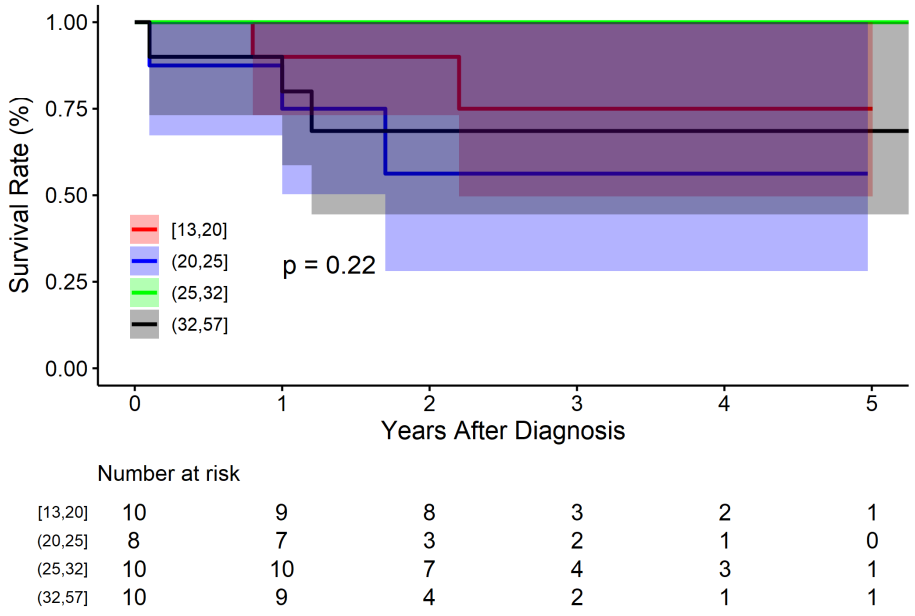

FIGURE 4
Kaplan–Meier survival curve by aortic size for the conservatively treated cohort.

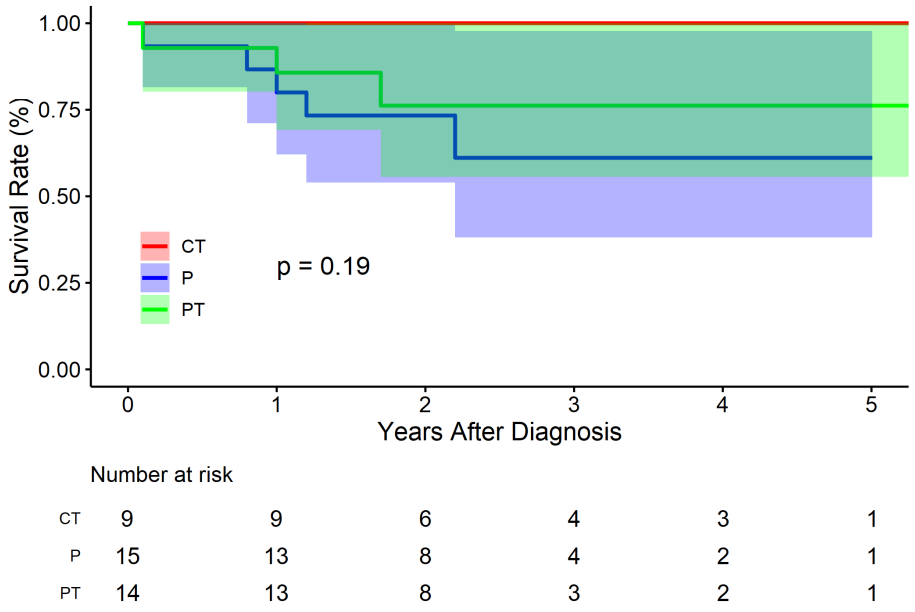

FIGURE 5
Kaplan–Meier survival curve by false lumen thrombosis status for the conservatively treated cohort. CT, complete thrombosis; PT, partial thrombosis; P, patency.

men are more susceptible to IAAD. Despite the low prevalence of aortic aneurysm, women may endure a higher risk of dissection or rupture (22). Although women seem to have a natural immunity to aortic disease, those who already develop this disease may bear a more severe burden of aortic wall lesions or be exposed to greater hemodynamic stress. Sokolis and colleagues reported higher levels of metaloproteinase-2 and-9 and reduced expression of tissue inhibitor of matrix metaloproteinase-1 and-2 in women than in men. This impairment for aortic wall homeostasis leads to enhanced degradation of the extracellular matrix, increased stiffness and reduced strength (23). Chunget al. found that despite the relatively uncomplicated procedure and shorter cardiopulmonary bypass time compared to men, women had a higher mortality rate (11% versus 7.4%; $p = 0.02$) (24). International Registry of Acute Aortic Dissection (IRAD) also reported that women had an older age of onset, a later diagnosis, a higher incidence of coma, hypotension, and tamponade, and a worse

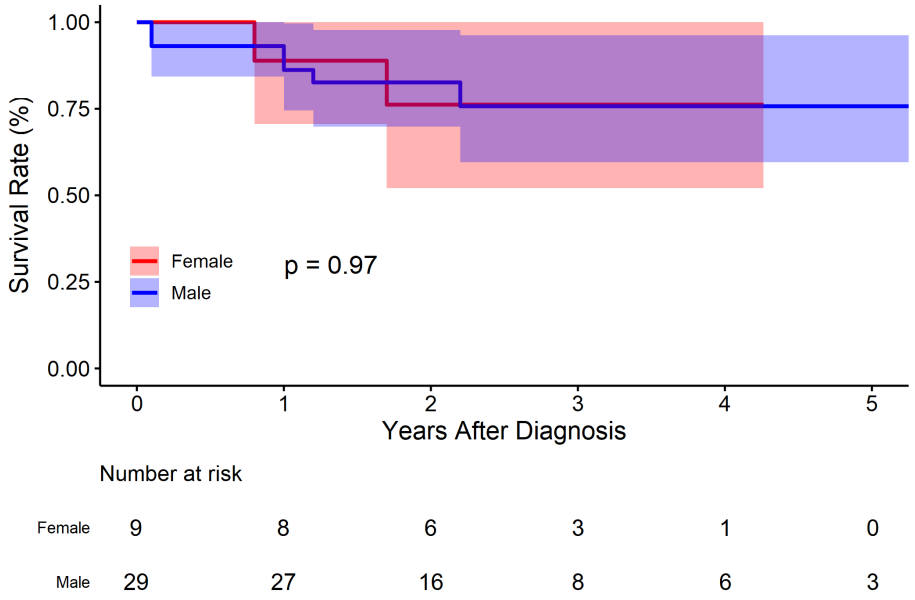

FIGURE 6
Kaplan–Meier survival curve by sex for the conservatively treated cohort.

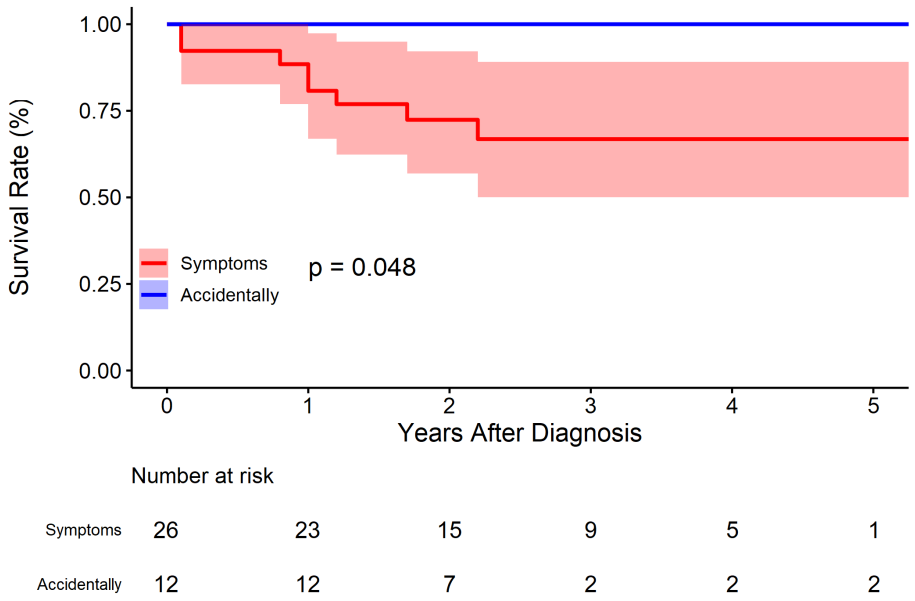

FIGURE 7
Kaplan–Meier survival curve by symptoms for the conservatively treated cohort.

surgical repair (21). Several epidemiological studies highlighting sexual dimorphism in the development and progression of abdominal aortic aneurysm have shown that women are at greater risk for aneurysm rupture and morbidity after surgical repair (25, 26). Data even suggest women are no longer protected from developing abdominal aortic aneurysm after menopause (27). However, current evidence on the effect of gender remain inconsistent. Some other studies have concluded that there is no outcomes difference in thoracic aortic disease between men and women (28, 29). Friedrich et al. argued that gender itself was no risk factor for mortality and the decision-making for surgical treatment should not depend on gender (28). Our data also demonstrated that no significant difference was observed between male and female concerning survival rate ($p = 0.970$) in IAAD. The survival rate at 1, 3, and 5 years of follow up were 86.2% (95% CI: 74.5–99.7%), 75.7% (95% CI: 59.6–96.2%), and 75.7% (95% CI: 59.6–96.2%), respectively for male, and 88.9% (95% CI: 70.6–100.0%), 76.2% (95% CI: 52.1–100.0%), and 76.2% (95% CI: 52.1–100.0%) respectively for female. Compared to female, the HR of mortality for male was 1.0 (95% CI: 0.2–5.1, $p = 0.963$). More in-depth research is needed on this conflicting issue.

In our previous study, symptoms were placed at the core of IAAD management based on literature reports (2). It was recommended that for cases of asymptomatic uncomplicated IAAD, conservative treatment with continuous monitoring and evaluation is preferred. For cases of asymptomatic complicated IAAD, invasive treatment should be considered, with EVAR as first-line therapy, followed by OS. In contrast, those with symptomatic IAAD should first receive conservative treatment and then be assessed if the symptoms persist. If the symptoms subside, the patients should be treated in accordance with the protocol for asymptomatic IAAD. If the symptoms persist, invasive treatment should be undertaken. Of note, the previous recommendations based on literature meta-analysis favored conservative treatment, which is challenged by the updated findings. In consistency to the aforementioned meta-analysis, the present study confirms the important role of symptoms in clinical decision for IAAD. As was demonstrated in Figure 7, patients without symptoms had better outcomes as regards survival rate ($p = 0.048$). The survival rate at 1, 3, and 5 years of follow up were 80.7% (95% CI: 66.9–97.4%), 66.8% (95% CI: 50.0–89.1%), and 66.8% (95% CI: 50.0–89.1%), respectively for patients with symptoms, and 100.0% (95% CI: 100.0–100.0%), 100.0% (95% CI: 100.0–100.0%), and 100.0% (95% CI: 100.0–100.0%) respectively for patients without symptoms.

Limitations

Our analysis should be interpreted in the context of several limitations. First, this study was based on single-center experience with a high volume of cardiovascular operations. The external validity of our results needs further investigation. Second, we reported a relatively short duration of follow-up. An ongoing follow-up and report are expected. Third, unfortunately, although the sample size of this study was acceptable considering the extreme rarity of IAAD, the statistical power was insufficient for us to perform a multi-variable analysis. Fourth, the exact cause of death cannot be confirmed, despite our best efforts. It may result in some bias.

Conclusion

On the basis of patients' preference and surgeons' experience, a more aggressive treatment regimen for IAAD should be considered, with EVAR being the most likely preferred choice, especially for those with persistent symptoms and patent false lumen, regardless of sex, age, or aortic size.

Data availability statement

The raw data supporting the conclusions of this article will be made available by the authors, without undue reservation.

Ethics statement

The studies involving human participants were reviewed and approved by the Institutional Review Board of GDPH. Written informed consent for participation was not required for this study in accordance with the national legislation and the institutional requirements.

Author contributions

JW had full access to all of the data in the study and takes responsibility for the integrity of the data and the accuracy of the data analysis. JW and YW: concept and design. JW and DZ: drafting of the manuscript. YC and ZC: critical revision of the manuscript for important intellectual content. JY and JL: statistical analysis. XL and TS: obtained funding. RF: administrative, technical, and material support. JW: supervision. JW, YW, FL, DZ, YC, ZC, JY, JL, XL, RF, and TS: acquisition, analysis, or interpretation of data. All authors contributed to the article and approved the submitted version.

Funding

This work was supported by the National Natural Science Foundation of China (82200518).

Acknowledgments

JW would like to extend his special gratitude to John Elefteriades, who guided him through the first research paper at the Yale Aortic Center, which was a meta-analysis on IAAD. That meta-analysis also inspired the current study. The natural history research methods and concepts learned at Yale were crucial to this study.

Conflict of interest

The authors declare that the research was conducted in the absence of any commercial or financial relationships that could be construed as a potential conflict of interest.

Publisher's note

All claims expressed in this article are solely those of the authors and do not necessarily represent those of their affiliated organizations, or those of the publisher, the editors and the reviewers. Any product that may be evaluated in this article, or claim that may be made by its manufacturer, is not guaranteed or endorsed by the publisher.

Supplementary material

The Supplementary material for this article can be found online at: https://www.frontiersin.org/articles/10.3389/fcvm.2023.1002832/full#supplementary-material

SUPPLEMENTARY FIGURE S1
Freedom from death and intervention by aortic size for the conservatively treated cohort.

SUPPLEMENTARY FIGURE S2
Freedom from death and intervention by aortic size for the conservatively treated cohort. CT, complete thrombosis; PT, partial thrombosis; P, patency.

SUPPLEMENTARY FIGURE S3
Freedom from death and intervention by sex for the conservatively treated cohort.

SUPPLEMENTARY FIGURE S4
Freedom from death and intervention by symptoms for the conservatively treated cohort.

References

1. Nienaber, CA, Clough, RE, Sakalihasan, N, Suzuki, T, Gibbs, R, Mussa, F, et al. Aortic dissection. *Nat Rev Dis Primers*. (2016) 2:16053. doi: 10.1038/nrdp.2016.53

2. Wu, J, Zafar, M, Qiu, J, Huang, Y, Chen, Y, Yu, C, et al. A systematic review and meta-analysis of isolated abdominal aortic dissection. *J Vasc Surg*. (2019) 70:2046–2053.e6. doi: 10.1016/j.jvs.2019.04.467

3. Sen, I, D'Oria, M, Weiss, S, Bower, TC, Oderich, GS, Kalra, M, et al. Incidence and natural history of isolated abdominal aortic dissection: a population-based assessment from 1995 to 2015. *J Vasc Surg*. (2021) 73:1198–1204.e1. doi: 10.1016/j.jvs.2020.07.090

4. Von Elm, E, Altman, DG, Egger, M, Pocock, SJ, Gøtzsche, PC, and Vandenbroucke, JP. The strengthening the reporting of observational studies in epidemiology (STROBE) statement: guidelines for reporting observational studies. *J Clin Epidemiol*. (2014):1495–9. doi: 10.1016/j.jclinepi.2007.11.008

5. Tsai, TT, Evangelista, A, Nienaber, CA, Myrmel, T, Meinhardt, G, Cooper, JV, et al. Partial thrombosis of the false lumen in patients with acute type B aortic dissection. *N Engl J Med*. (2007) 357:349–59. doi: 10.1056/NEJMoa063232

6. Wu, J, Xie, E, Qiu, J, Huang, Y, Jiang, W, Zafar, MA, et al. Subacute/chronic type A aortic dissection: a retrospective cohort study. *Eur J Cardio Thorac*. (2019) 57:388–96. doi: 10.1093/ejcts/ezz209

7. Hiratzka, LF, Bakris, GL, Beckman, JA, Bersin, RM, Carr, VF, Casey, DEJ, et al. ACCF/AHA/AATS/ACR/ASA/SCA/SCAI/SIR/STS/SVM guidelines for the diagnosis and management of patients with thoracic aortic disease. A report of the American College of Cardiology Foundation/American Heart Association task force on practice guidelines, American Association for Thoracic Surgery, American College of Radiology, American Stroke Association, Society of Cardiovascular Anesthesiologists, Society for Cardiovascular Angiography and Interventions, Society of Interventional Radiology, Society of Thoracic Surgeons, and Society for Vascular Medicine. *J Am Coll Cardiol*. (2010) 55:e27–e129.

8. Erbel, R, Aboyans, V, Boileau, C, Bossone, E, Bartolomeo, RD, Eggebrecht, H, et al. 2014 ESC guidelines on the diagnosis and treatment of aortic diseases: document covering acute and chronic aortic diseases of the thoracic and abdominal aorta of the adult. The task force for the diagnosis and treatment of aortic diseases of the European Society of Cardiology (ESC). *Eur Heart J*. (2014) 35:2873–926. doi: 10.1093/eurheartj/ehu281

9. Malaisrie, SC, Szeto, WY, Halas, M, Girardi, LN, Coselli, JS, Sundt, TMR, et al. 2021 the American Association for Thoracic Surgery expert consensus document: surgical treatment of acute type A aortic dissection. *J Thorac Cardiovasc Surg*. (2021) 162:735–758.e2. doi: 10.1016/j.jtcvs.2021.04.053

10. Boodhwani, M, Andelfinger, G, Leipsic, J, Lindsay, T, McMurtry, MS, Therrien, J, et al. Canadian cardiovascular society position statement on the management of thoracic aortic disease. *Can J Cardiol*. (2014) 30:577–89. doi: 10.1016/j.cjca.2014.02.018

11. Mac Gillivray, TE, Gleason, TG, Patel, HJ, Aldea, GS, Bavaria, JE, Beaver, TM, et al. The Society of Thoracic Surgeons/American Association for Thoracic Surgery clinical practice guidelines on the management of type B aortic dissection (2022) 163:1231–49. doi: 10.1016/j.jtcvs.2021.11.091,

12. Golledge, J, and Eagle, KA. Acute aortic dissection. *Lancet*. (2008) 372:55–66. doi: 10.1016/S0140-6736(08)60994-0

13. Coady, MA, Rizzo, JA, Hammond, GL, Mandapati, D, Darr, U, Kopf, GS, et al. What is the appropriate size criterion for resection of thoracic aortic aneurysms? *J Thorac Cardiovasc Surg*. (1997) 113:489–91.

14. Wu, J, Zafar, MA, Li, Y, Saeyeldin, A, Huang, Y, Zhao, R, et al. Ascending aortic length and risk of aortic adverse events. *J Am Coll Cardiol*. (2019) 74:1883–94. doi: 10.1016/j.jacc.2019.07.078

15. Zafar, MA, Li, Y, Rizzo, JA, Charilaou, P, Saeyeldin, A, Velasquez, CA, et al. Height alone, rather than body surface area, suffices for risk estimation in ascending aortic aneurysm. *J Thorac Cardiovasc Surg*. (2018) 155:1938–50. doi: 10.1016/j.jtcvs.2017.10.140

16. Ziganshin, BA, Zafar, MA, and Elefteriades, JA. Descending threshold for ascending aortic aneurysmectomy: is it time for a left-shift in guidelines? *J Thorac Cardiovasc Surg*. (2019) 157:37–42. doi: 10.1016/j.jtcvs.2018.07.114

17. Wu, J, Zhang, L, Qiu, J, and Yu, C. Morphological features of the thoracic aorta and supra-aortic branches in patients with acute type A aortic dissection in China. *Interact Cardiov Thorat*. (2018) 27:555–60. doi: 10.1093/icvts/ivy110

18. Zafar, MA, Chen, JF, Wu, J, Li, Y, Papanikolaou, D, Abdelbaky, M, et al. Natural history of descending thoracic and thoracoabdominal aortic aneurysms. *J Thorac Cardiovasc Surg*. (2021) 161:498–511.e1. doi: 10.1016/j.jtcvs.2019.10.125

19. Kudo, T, Mikamo, A, Kurazumi, H, Suzuki, R, Morikage, N, and Hamano, K. Predictors of late aortic events after Stanford type B acute aortic dissection. *J Thorac Cardiovasc Surg*. (2014) 148:98–104. doi: 10.1016/j.jtcvs.2013.07.047

20. Wu, J, Song, J, Li, X, Yang, J, Yu, C, Zhou, C, et al. Is partially thrombosed false lumen really a predictor for adverse events in uncomplicated type B aortic dissection: a systematic review and meta-analysis? *Front Cardiov Med*. (2022) 8:788541. doi: 10.3389/fcvm.2021.788541

21. Nienaber, CA, Fattori, R, Mehta, RH, Richartz, BM, Evangelista, A, Petzsch, M, et al. Gender-related differences in acute aortic dissection. *Circulation*. (2004) 109:3014–21. doi: 10.1161/01.CIR.0000130644.78677.2C

22. Davies, RR, Goldstein, LJ, Coady, MA, Tittle, SL, Rizzo, JA, Kopf, GS, et al. Yearly rupture or dissection rates for thoracic aortic aneurysms: simple prediction based on size. *Ann Thorac Surg*. (2002) 73:17–28. doi: 10.1016/S0003-4975(01)03236-2

23. Sokolis, DP, and Iliopoulos, DC. Impaired mechanics and matrix metalloproteinases/inhibitors expression in female ascending thoracic aortic aneurysms. *J Mech Behav Biomed*. (2014) 34:154–64. doi: 10.1016/j.jmbbm.2014.02.015

24. Chung, J, Stevens, L, Ouzounian, M, El-Hamamsy, I, Bouhout, I, Dagenais, F, et al. Sex-related differences in patients undergoing thoracic aortic surgery. *Circulation*. (2019) 139:1177–84. doi: 10.1161/CIRCULATIONAHA.118.035805

25. Katz, DJ, Stanley, JC, and Zelenock, GB. Gender differences in abdominal aortic aneurysm prevalence, treatment, and outcome. *J Vasc Surg*. (1997) 25:561–8. doi: 10.1016/S0741-5214(97)70268-4

26. Skibba, AA, Evans, JR, Hopkins, SP, Yoon, HR, Katras, T, Kalbfleisch, JH, et al. Reconsidering gender relative to risk of rupture in the contemporary management of abdominal aortic aneurysms. *J Vasc Surg*. (2015) 62:1429–36. doi: 10.1016/j.jvs.2015.07.079

27. Villard, C, Swedenborg, J, Eriksson, P, and Hultgren, R. Reproductive history in women with abdominal aortic aneurysms. *J Vasc Surg*. (2011) 54:341–345.e2. doi: 10.1016/j.jvs.2010.12.069

28. Friedrich, C, Salem, MA, Puehler, T, Hoffmann, G, Lutter, G, Cremer, J, et al. Sex-specific risk factors for early mortality and survival after surgery of acute aortic dissection type a: a retrospective observational study. *J Cardiothorac Surg*. (2020) 15:145. doi: 10.1186/s13019-020-01189-w

29. Suzuki, T, Asai, T, and Kinoshita, T. Clinical differences between men and women undergoing surgery for acute type A aortic dissection. *Interact Cardiov Thorat*. (2018) 26:944–50. doi: 10.1093/icvts/ivy005

Frontiers in
Cardiovascular Medicine

Innovations and improvements in cardiovascular treatment and practice

Focuses on research that challenges the status quo of cardiovascular care, or facilitates the translation of advances into new therapies and diagnostic tools.

Discover the latest Research Topics

See more →

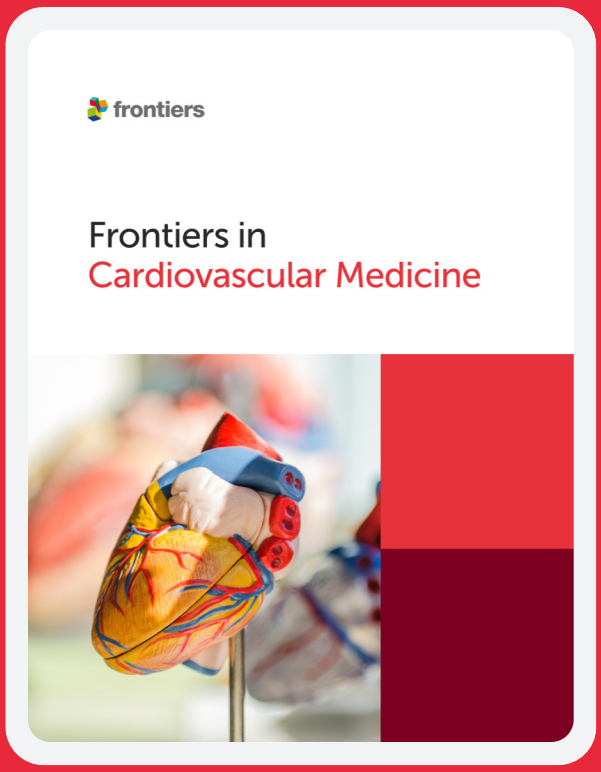

Frontiers

Avenue du Tribunal-Fédéral 34
1005 Lausanne, Switzerland
frontiersin.org

Contact us

+41 (0)21 510 17 00
frontiersin.org/about/contact